2019

# Characterization of Air Toxics and GHG Emission Sources and their Impacts on Community Scale Air Quality Levels in the Bay Area – sub report A

FluxSense

FINAL REPORT

FluxSense Inc

28 March 2019

**Date:** 28 March 2019
**Updated:** 24 August 2020, 1 December 2020

**Title:** Characterization of Air Toxics and GHG Emission Sources and their Impacts on Community Scale Air Quality Levels in the Bay Area - sub report A

**Authors:** Johan Mellqvist[1,3], Jerker Samuelsson[1], Brian Offerle[2] and Marianne Ericsson[1]

[1]FluxSense Inc, 113 W G Street # 757, San Diego, CA 92101
[2]FluxSense AB, Sven Hultins gata 9, SE-41288 Göteborg, Sweden
[3]Chalmers University of Technology, Hörsalsvägen 11, SE-41296, Göteborg, Sweden

**CARB contract no. 17RD021**
Principal Investigator: Johan Mellqvist,
October 2018, Bay Area survey
Prepared for the California Air Resources Board
and the California Environmental Protection Agency

[Cover: SOF measurement of alkane plumes in Richmond, California. Image mapped on Google Earth © 2019.]

## DISCLAIMER

## Executive summary

*Objective*

A two-year study is carried out by FluxSense Inc on behalf of California Air Resources Board (CARB). The objective is to provide ground-based flux measurements of VOCs, including methane and air toxics, and ammonia from various sources, e.g. refineries, petrochemical industry, oil storage, port activities, landfills, oil and gas production and Concentrated Animal Feeding Operation. The study also characterizes ground concentrations of the above-mentioned species at community scale to provide insights on exposure levels particularly in disadvantage communities near emission sources, and identify emissions sources and their contributions to high concentration levels. This project complements community monitoring efforts by CARB staff who have measured speciated VOCs and other toxics of concern.

*Background*

This sub-report corresponds to measurement results from a 4-week campaign in October 2018 carried out in the Bay Area, CA, with focus on industrial emissions from refineries, petrochemical industry, oil storage, port activities and landfills. It also includes investigating the impact of various sources on the concentration levels in Richmond. In addition to the above, some preliminary emission measurements (5 days) of VOCs were carried out in the central valley (Bakersfield) of oil and gas production and ammonia emissions from Concentrated Animal Feeding Operation (CAFOs). Here some general results are given for the latter measurements while details will be given in the report for a second campaign that will be carried out in May 2019 in the central valley. This report will include also emission results from a major brush fire near Travis airbase.

The emission fluxes (kg/h) of alkanes, ammonia, $SO_2$, $NO_2$ and formaldehyde were quantified using Solar Occultation Flux (SOF) and mobile SkyDOAS (Differential Optical Absorption Spectroscopy). MWDOAS (Mobile White Cell DOAS) and MeFTIR (Mobile extractive Fourier Transform Infrared) techniques were used to measure ground level concentrations of alkanes, BTEX and methane, which allowed to indirectly obtain emission fluxes when combined with measured SOF fluxes.

SOF is a proven technique that has been developed at Chalmers University of Technology in Sweden and further developed and applied by FluxSense in over 100 fugitive emission studies around the world. In Europe the SOF technique is considered Best Available Technology (BAT) for measurements of fugitive emission of VOCs from refineries, and in Sweden it is used in conjunction with tracer correlation and optical gas imaging to annually screen all larger refineries and petrochemical industries. The estimated uncertainty for SOF emission measurements is typically 30 % for total site emissions. The estimated measurement uncertainties have been verified in several (blind and non-blind) controlled source gas release and in side-by-side measurements with other measurement techniques.

The instrument systems above were operated in the FluxSense mobile laboratory and the measurement were conducted while driving outside the source site fence-lines along public roads. Background columns and concentrations were subtracted by encircling the sites, when possible, or by measuring upwind columns and concentrations, so that only emissions from within the facilities were quantified. Wind data were obtained from a mobile 10 m wind mast and a Light Detection and Ranging (LIDAR) instrument that measured the wind profile between 40 to 200 m altitude. The emission results are presented as daily and total survey averages. From the combination of the measured column and concentration values, respectively, the height of the plume could be derived to first order.

*Emission measurements*

The main results from the campaign are shown in Table E.1, including measured emissions of criteria pollutants from 5 refineries and the port of Richmond. For most sites, except Martinez E, around 20 transects through the plume were made over 3 - 4 days. More emission sources were studied during the campaign than presented in Table E.1. Those with limited repeated measurements are excluded from the summary but discussed in the report. This includes the Potrero Hills landfill in which emissions of 76 kg/h of alkanes and 860 kg/h of methane, respectively, were measured on one single day.

The emission results in Table E. 1 can be compared to emission inventory data from CARB for 2016 as given in Table E.2. Here the refinery capacity is also shown for each site, obtained from the *Energy Information Administration* (https://www.eia.gov/petroleum/).

In Table E.3 the difference between the measurements and the CARB 2016 inventory is shown, based on the data in Table E.1 and E.2. The table shows the discrepancy factors *D* for the different species, corresponding to the ratios of the measurements and inventory. In Table E.3 is also shown the emissions per crude oil capacity for each refinery (capacity specific VOC emission factor) for the inventory and measurement data, respectively.

The overall agreement between the CARB 2016 inventory and the measurements is shown in the SUM values in Table E.3. It can be seen that the measurements indicate that the VOC emissions on average are 2.5 times higher (150%) than the reported ones and even higher for the corresponding methane emissions (190%). The agreement appears to be excellent for $NO_x$ but here it should be noted that measured $NO_2$ is compared to $NO_x$ from the inventory. It is estimated that this causes a systematic negative bias in the $D_{NOx}$ factors of around 20 % based on a similar study (Rivera et al., 2010). Note that the inventory corresponds to annual average emission data while the measurements were acquired over 3-4 days during the 4-week campaign. Some of the observed positive discrepancies above can be explained by this, including that the SOF measurements are carried out only during sunny conditions (day time) and the fact that the average wind and temperature may differ from the annual average climatology. In a similar study (Johansson et al., 2014) it was shown that such effects could cause a positive bias in the measured emissions of 30-40%, compared to the annual average. In a recent study by AQMD (Pikelnaya 2019) long term, seasonal measurements were conducted using SOF on a single refinery in southern California. Here 7 separate measurement campaigns were carried out during each seasons from fall 2015 to summer 2018. The overall variability was 20 % with poor correlation ($r^2$=0.27) to season. The average ambient temperature in Bay area during the campaign month was close to the yearly average (Oct 2018: 16.1 C; Annual 2017: 14.7 °C) and therefore the measurements were representative for the annual average emissions wrt to this parameter. Slightly lower wind speeds than the annual average was observed in October 2018 which may lead to lower overall emissions from tank storage and open atmospheric sources.

In Table E.3. is also shown that the emissions relative to the refinery capacity varies between 0.016% to 0.037% with an average of 0.022 %. These refineries appear to be well operated since the emission factors for industries in Europe and Texas generally span between 0.03% to 0.15% (Mellqvist et al., 2010, Johansson et al., 2014).

Preliminary emission measurements of VOCs were carried out in the central valley of oil and gas production and ammonia emissions from Concentrated Animal Feeding Operation (CAFOs) during 5 days.

Several large-scale measurements with the mobile lab were carried out around the Elk Hills oil and gas production area in the central valley during 2 days. Here columns of VOCs and ground concentrations of VOCs and methane were detected (ratio of 1:2) but only small concentration amounts BTEX. The emission rate of alkanes was between 2000 - 5000 kg/h, and the methane emission approximately double. However, there is a large uncertainty in the wind, and more measurements are therefore needed under a range of wind conditions. Additional measurements are planned for the second field campaign in May 2019. Large-scale measurements of ammonia emitted from CAFOs were carried out using SOF in both Bakersfield and Merced. Here columns of ammonia were detected with fluxes up to 700 kg/h. Likewise there is a large uncertainty in the winds particularly near ground level where the emission sources are. Further measurements are therefore needed and planned for the second field campaign in May 2019.

Table E.1. Results of the emission measurements based on SOF, SkyDOAS, MeFTIR and MWDOAS. *Limited measurements.

| **Source** | **Alkane kg/h** | **95% CI kg/h** | **$SO_2$ kg/h** | **95% CI kg/h** | **$NO_2$ kg/h** | **95% CI kg/h** | **$H_2CO$ kg/h** | **BTEX kg/h** | **$C_6H_6$ kg/h** | **$CH_4$ kg/h** |
|---|---|---|---|---|---|---|---|---|---|---|
| **Martinez E refinery area** | 151 | 140 – 161 | 60 | 30 –90 | 69 | 60 –79 | <5 | - | - | 54 |
| **Richmond refinery area** | 291 | 248 – 335 | 105 | 34 – 175 | 113 | 83 – 142 | <5 | 40* | 6.1* | 105 |
| **Rodeo refinery area** | 143 | 118 – 168 | 11 | 8 –14 | 34 | 19 –49 | <5 | 17* | 2.0* | 44 |
| **Martinez W refinery area** | 334 | 249 – 419 | 200 | 159 – 240 | 104 | 85 – 122 | <10 | 31 | 3.3 | 157 |
| **Benicia refinery area** | 144 | 124 – 165 | 20 | 15 –25 | 84 | 66 – 102 | <5 | 12 | 1.0 | 69 |
| **SUM REFINERIES** | **1063** | | **395** | | **404** | | **-** | **100** | **12** | **430** |
| | | | | | | | | | | |
| **Richmond port area** | 90 | 78 – 102 | 4 | 1.5 –6 | 33 | 22 –44 | <5 | 9 | 0.6 | 12 |

Table E.2. CARB Inventory 2016 for primary refinery emissions in area and US Energy Information Administration refinery throughput data 2018.

| **Area** | **Crude capacity Barrels/day** | **VOC kg/h** | **$NO_x$ kg/h** | **$SO_2$ kg/h** | **$CH_4$ & $C_2H_6$ kg/h** |
|---|---|---|---|---|---|
| **Martinez E refinery** | 166000 | 111 | 84 | 46 | 43 |
| **Richmond refinery** | 245000 | 147 | 80 | 37 | 37 |
| **Rodeo refinery** | 120000 | 23 | 22 | 39 | 11 |
| **Martinez W refinery** | 156000 | 114 | 98 | 114 | 39 |
| **Benicia refinery** | 145000 | 36 | 123 | 8 | 16 |
| **SUM** | **832000** | **431** | **407** | **243** | **147** |

Table E.3. Crude capacity specific VOC emission factors (EF) and comparison between measurements and CARB 2016 inventory. Here the discrepancy factor D, i.e. ratio of the measurement and inventory, is shown for different species together with the capacity specific VOC emissions obtained from inventory and measurement, respectively. Note that $NO_2$ for the measurements is compared to $NO_x$ for inventory and methane for the measurements is compared to methane and ethane in inventory. Note also that the inventory values reference only the primary reported REFINERY emissions and the sites contain more emissions sources.

| | VOC EF inventory Capacity specific | VOC EF Survey Capacity specific | $D_{VOC}$ | $D_{NOx}$ | $D_{SO2}$ | $D_{CH4}$ |
|---|---|---|---|---|---|---|
| **Martinez E refinery area** | 0.012% | 0.016% | 1.36 | 0.82 | 1.30 | 1.26 |
| **Richmond refinery area** | 0.010% | 0.021% | 1.98 | 1.41 | 2.97 | 2.84 |
| **Rodeo refinery area** | 0.003% | 0.021% | 6.22 | 1.55 | 0.28 | 4.00 |
| **Martinez W refinery area** | 0.013% | 0.037% | 2.93 | 1.06 | 1.75 | 4.03 |
| **Benicia refinery area** | 0.004% | 0.017% | 4.00 | 0.68 | 2.50 | 4.31 |
| **SUM** | **0.009%** | **0.022%** | **2.47** | **0.99** | **1.64** | **2.93** |

### *Community monitoring*

Measurements with the mobile laboratory were carried out during 7 days and 2 evening/nights in the Richmond community and additionally 7 days of measurements at some of the other sites. Community monitoring was either done on preselected locations or by tracking identified emission plumes in the community. Targeted measured species included BTEX, various alkanes, and methane. In one case, strong concentrations of the solvent PCBTF (parachlorobenzotrifluoride) were identified in a domestic neighborhood. In Figure E.1 a compilation of all alkane measurements, excluding methane, carried out in Richmond are shown, similar data exists for BTEX and methane. Here the enhancement in concentration for each 50 x 50 m grid cell has been averaged.

Richmond has two major sources in the vicinity of the community that may influence the concentration levels, i.e. the refinery area in the west and the port in the south. The wind was generally southerly during the campaign thus the port activities affected the air quality in the Richmond community, together with the background from San Francisco. Winds were westerly on few occasions during the survey. Only at these times would the Richmond community be most affected by the emission plumes from the refinery area. The general impression is that the emissions from the port area affect the community more than the refinery does, since the former is placed in the prevalent upwind direction from the community, is closer and has predominantly non-elevated sources.

It is evident from Figure E.1. that most of the hotspots in the Richmond community are towards the port.

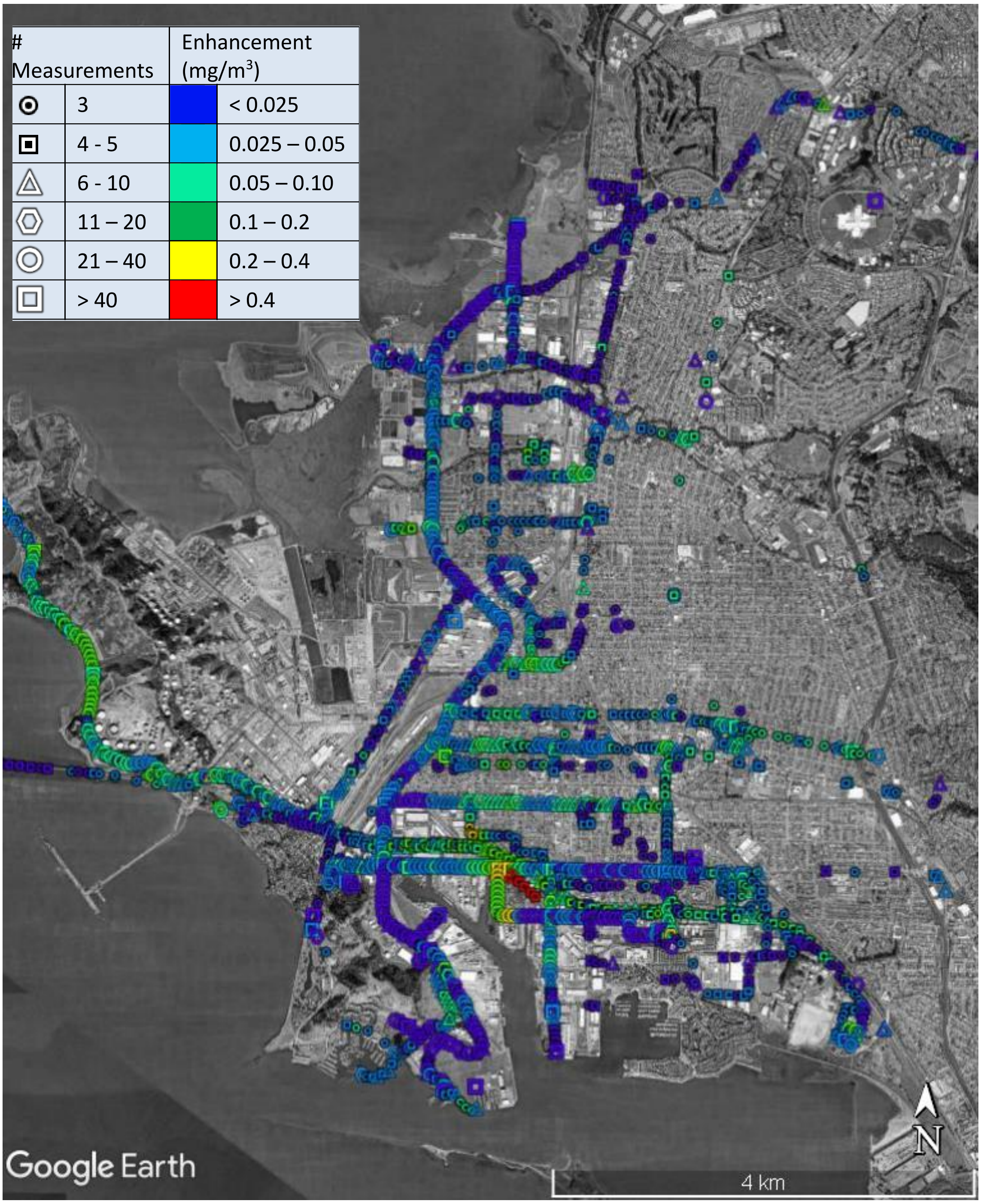

Figure E.1. Community monitoring in Richmond, number of measurements (minimum 3) within an approximately 50 x 50 m grid cell and mean alkane enhancement within the cell.

# Acronyms, Units and Definitions

## Acronyms used in this report

| | |
|---|---|
| BPD | Barrels per day |
| BTEX | Sum of Benzene, Toluene, Ethyl Benzene and Xylene |
| CARB | California Air Resources Board |
| CAFO | Concentrated Animal Feeding Operation |
| DOAS | Differential Optical Absorption Spectroscopy |
| EF | Emission factor |
| FTIR | Fourier Transform InfraRed |
| IME | Indirectly Measured Emission, combining direct emission with concentration ratios |
| LIDAR | Light Detection and Ranging |
| MWDOAS | Mobile White cell DOAS |
| MeFTIR | Mobile extractive FTIR |
| NMVOC | Non-methane volatile organic compound |
| PCBTF | Parachlorobenzotrifluoride |
| ROG | Reactive Organic Gases |
| SkyDOAS | Scattered Skylight DOAS |
| SOF | Solar Occultation Flux |
| VOC | Volatile organic compound, used interchangeably for non-methane VOC |

## Units

| | |
|---|---|
| Air temperature | degrees C |
| Atmospheric Pressure | mbar |
| Relative Humidity | % |
| Wind direction | degrees North |
| Wind speed | m/s |
| Column | $mg/m^2$ |
| Concentration | $mg/m^3$ |
| Flux | kg/h |

## Unit Conversions

1 lbs = 0.4536 kg
1 kg/h = 52.9 lbs/day
1 bbl = 159 l
1 bbl/day = 5.783 kg/h (crude oil)
1 (short) ton = 907.2 kg
1 kton/year = 104 kg/h
1 klbs/year=0.052 kg/h

### Definitions

Alkane or Alkanes are considered to be all non-methane alkane species.

# Table of Contents

## List of Figures

## List of Tables

# 1 Objective and Introduction

The objectives of this research are to characterize certain statewide GHGs and air toxics emission sources, to identify potential sources contributing to air pollution hotspots. This includes quantifying ground-based fluxes of VOCs, including methane and air toxics, and ammonia from various sources, e.g. refineries, petrochemical industry, oil storage, harbor activities, landfills, oil and gas production and Concentrated Animal Feeding Operations (CAFOs).

In the study also ground concentrations are characterized, of the above-mentioned species, at community scale to provide insights on exposure levels particularly in disadvantage communities near emission sources, and identify emissions sources and their contributions to high concentration levels. This project complements community monitoring efforts by CARB staff who has measured speciated VOCs and other toxics of concern. The study includes a comparison of the obtained methane emission estimations against airborne measurement for single sources.

The results from this study should provide useful screening information to identify high-risk communities for prioritizing air pollution mitigation efforts. The data should also potentially be useful to extrapolate community-level exposures and cancer risk to identify the highest impact sources. The data would also be useful to support enforcement efforts to address high BTEX (benzene, toluene, ethylbenzene and xylene) sources, and may be useful to conduct real-world verification of the impact of the oil and gas regulation (effective Jan 1, 2018) on $CH_4$ emissions.

This sub report corresponds to measurement results from a 5-week campaign in October 2018 carried out in the Bay Area, CA, with focus on industrial emissions from refineries, petrochemical industry, oil storage, harbor activities and landfills. It also includes investigating the impact of various sources on the concentration levels in Richmond.

In addition to the above, some preliminary emission measurements (4 days) were carried out in the central valley (Bakersfield) of oil and gas production and ammonia emissions from CAFOs (Bakersfield and Merced area). The latter results will be reported with results from a second campaign in May 2019 in which we will focus on oil and gas and CAFO emissions in the central valley. This includes also results from a major brush fire.

## 2 Background

Industrial volatile organic compounds (VOC) emissions may contribute to significant formation of ground level ozone, which is formed through atmospheric chemical reactions of volatile organic compounds (VOCs) and nitrogen oxides ($NO_x$) in the presence of sunlight, often called photo chemical smog. Elevated ozone concentrations are known to reduce crop yields and constitute a public health concern. Larger metropolitan areas in the US have trouble meeting ozone standards since anthropogenic sources tend to be concentrated in urban areas, including both mobile and stationary sources. For instance, in order to meet current and future more stringent ozone standards in Los Angeles, reductions in VOC emissions are foreseen [Downey et. al. 2015]. Stationary sources such as refineries, storage depots, petrochemical industries are the largest point sources of VOC emissions. The emissions are typically dominated by evaporative losses from storage tanks and process equipment, so-called fugitive emissions. Several VOCs are also toxic with direct impact on health. Methane causes climate change. Ammonia emissions cause production of particles of concern for health and climate.

In 2015, the Governor approved Assembly Bill 1496 (AB 1496), which requires the California Air Resources Board (CARB) to monitor and measure high methane emission hotspots within the state using the best available scientific and technical methods. In order to meet the requirements under AB 1496, CARB, in conjunction with CEC, has funded a large-scale statewide aerial methane survey conducted by NASA Jet Propulsion Laboratory (JPL) to detect and identify methane super emitters which may be a large contributor to the regional methane hotspots. CARB has also funded Scientific Aviation to quantify emission fluxes from various methane sources (including super emitters) with airborne measurement. Furthermore, certain emissions from oil and gas facilities, which are also major methane emitters, are known to have potential adverse health effects. Oil and gas operations are located in a variety of areas in California, including in densely populated areas and near disadvantaged communities. In order to meet CARB’s mission to protect the public from harmful effects of air pollution, there have been efforts to enhance the community monitoring for air toxics and methane, particularly in the communities near oil and gas facilities, which are primarily disadvantage communities. The recently approved AB 617 will also require CARB to develop a community monitoring plan to identify disadvantaged communities for community monitoring deployment. It will also require CARB to develop a cumulative impact state strategy to identify communities with high cumulative risk so air districts can develop Community Action Plans.

## 3 Instrumentation and Methods

The FluxSense measurement vehicle or “mobile lab” is equipped with four instruments optical for gas monitoring and they were all used during the survey: SOF (Solar Occultation Flux), SkyDOAS (Differential Optical Absorption Spectroscopy), MeFTIR (Mobile extractive Fourier Transformed Infrared spectrometer) and MWDOAS (Mobile White cell DOAS). The individual measurement methods are described in the subsections below. SOF and SkyDOAS both measure gas columns through the atmosphere by means of light absorption. SOF utilizes infrared light from the direct sun whereas SkyDOAS measures scattered ultraviolet light from the sky. MeFTIR and MWDOAS both measure ground level concentrations of alkanes and

BTEX respectively. Accurate wind data is necessary in order to compute emission fluxes. Wind information for the survey was derived from several different sources. A wind LIDAR was used to measure vertical profiles of wind speed and wind direction from 50-200 m height. The LIDAR data was combined with data from several wind masts from fixed met network- and mobile stations. Figure 1 gives a general overview of the measurement setup and the data flow and pictures of the FluxSense mobile lab is found in Figure 2.

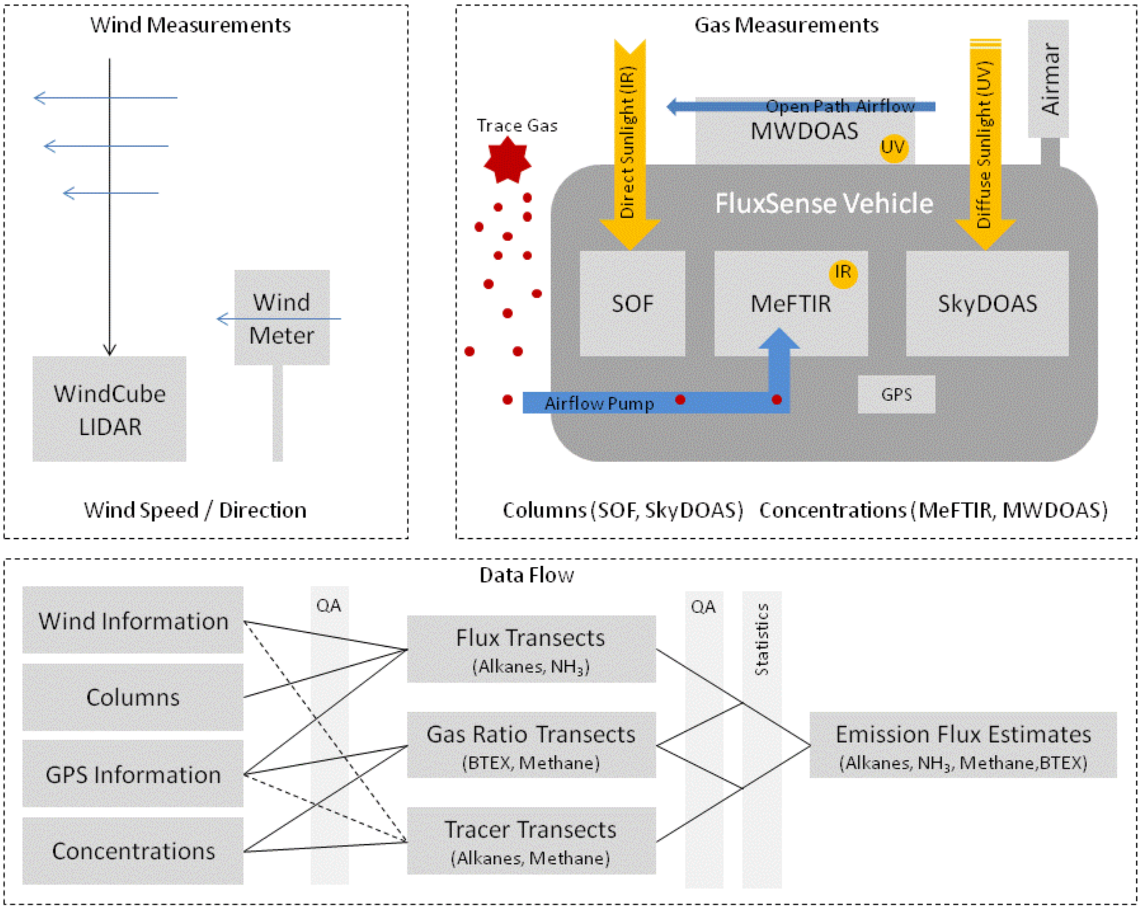

Figure 1. Overview of the FluxSense mobile lab main instruments; SOF, MeFTIR, MWDOAS and SkyDOAS (upper right panel) and wind measurements (upper left panel) and simplified data flow diagram (lower panel). SOF and SkyDOAS are column integrating passive techniques using the Sun as the light source while MeFTIR and SkyDOAS sample local air concentrations using active internal light sources. The data flow describes what information that goes into the flux emission estimates. Direct flux emissions are given from measured columns (SOF and SkyDOAS) of alkanes, $SO_2$ and $NO_2$, while inferred fluxes are calculated via gas concentration ratios (MeFTIR and MWDOAS) of BTEX and $CH_4$. See section 4.1 for principal equations. All emission flux estimates are based on statistical analysis of measured data. Q.C. = Quality Control, S.A.= Statistical Analysis (see Appendix for details).

In order to derive final emission flux estimates, the GPS-tagged gas column measurements by SOF and SkyDOAS are combined with wind data and integrated across plume transects at the various source locations. Gas mass ratio measurements by MeFTIR and MWDOAS are then used to indirectly estimate the emissions also for methane and BTEX.

Figure 2. Internal and external view of the FluxSense mobile lab.

Table 1.Summary of FluxSense gas measurement techniques. *For typical wind conditions at an optimal distance from the source.

| **Method** | **SOF** | **Sky DOAS** | **MeFTIR** | **MWDOAS** |
|---|---|---|---|---|
| Compounds | **Alkanes:** ($C_nH_{2n+2}$)<br>**Alkenes:**$C_2H_4$, $C_3H_6$<br>**$NH_3$** | **$SO_2$**<br>**$NO_2$**<br>**$H_2CO$** | **$CH_4$**<br>**Alkanes:** ($C_nH_{2n+2}$)<br>**Alkenes:** $C_2H_4$, $C_3H_6$<br>**$NH_3$**<br>**$N_2O$** (tracer) | **BTEX** |
| Detection limit Column | 0.1-5 mg/m$^2$ | 0.1-5 mg/m$^2$ | 1-10 ppbv | 0.5-3 ppbv |
| Detection limit Flux* | 0.2-1 kg/h | 1 kg/h | 0.2-2 kg/h | 0.2-2 kg/h |
| Wind Speed Tolerance | 1.5-12 m/s | 1.5-12 m/s | | |
| Sampling Time Resolution | 1-5 s | 1-5 s | 5-15 s | 8-10 s |
| Measured Quantity [unit] | Integrated vertical column mass [mg/m$^2$] | Integrated vertical column mass [mg/m$^2$] | Mass concentration at Vehicle height [mg/m$^3$] | Concentration at Vehicle height [mg/m$^3$] |
| Inferred Quantity [unit] | Mass Flux [kg/h] | Mass Flux [kg/h] | 1) Alkane ratio of ground plume combined with SOF gives mass flux [kg/h] and plume height information [m]<br>2) Alkane and $CH_4$ flux [kg/h] via tracer release | Combined with MeFTIR and SOF gives Mass Flux [kg/h] |
| Complementary data | Vehicle GPS-coordinates, Plume wind speed and direction | Vehicle GPS-coordinates, Plume wind speed and direction | Vehicle GPS-coordinates<br>Plume wind direction | Vehicle GPS-coordinates, Plume wind direction |

## 3.1 The SOF method

The SOF method [Mellqvist 1999, 2008a, 2008b, 2009, 2010; Kihlman 2005a; Johansson 2014] is based on the recording of broadband infrared spectra of the sun with a Fourier transform infrared spectrometer (FTIR) that is connected to a solar tracker. The latter is a telescope that tracks the sun and reflects the light into the spectrometer independent of the orientation of the vehicle. Using multivariate optimization, it is possible from these solar spectra to retrieve the path-integrated concentrations (referred to as column concentrations), in the unit mg/m$^2$, of various species between the sun and the spectrometer. The system used in this project consists of a custom-built solar tracker, transfer optics and a Bruker IRCube FTIR spectrometer with a spectral resolution of 0.5 cm$^{-1}$, equipped with a dual InSb (Indium Antimonide) / MCT (Mercury Cadmium Telluride) detector. A reference spectrum is taken outside the plume so that atmospheric background concentrations are removed. This means that all measured SOF columns are analyzed relative to the background column concentrations.

The system is installed in a measurement vehicle which allows consecutive column concentration measurements to be performed while driving. The flux of a species in a plume from an industry is measured by collecting spectra while driving the vehicle so that the light path from the sun to the instrument gradually cuts through the whole plume, preferably as orthogonally as possible to the wind direction, see Figure 3.

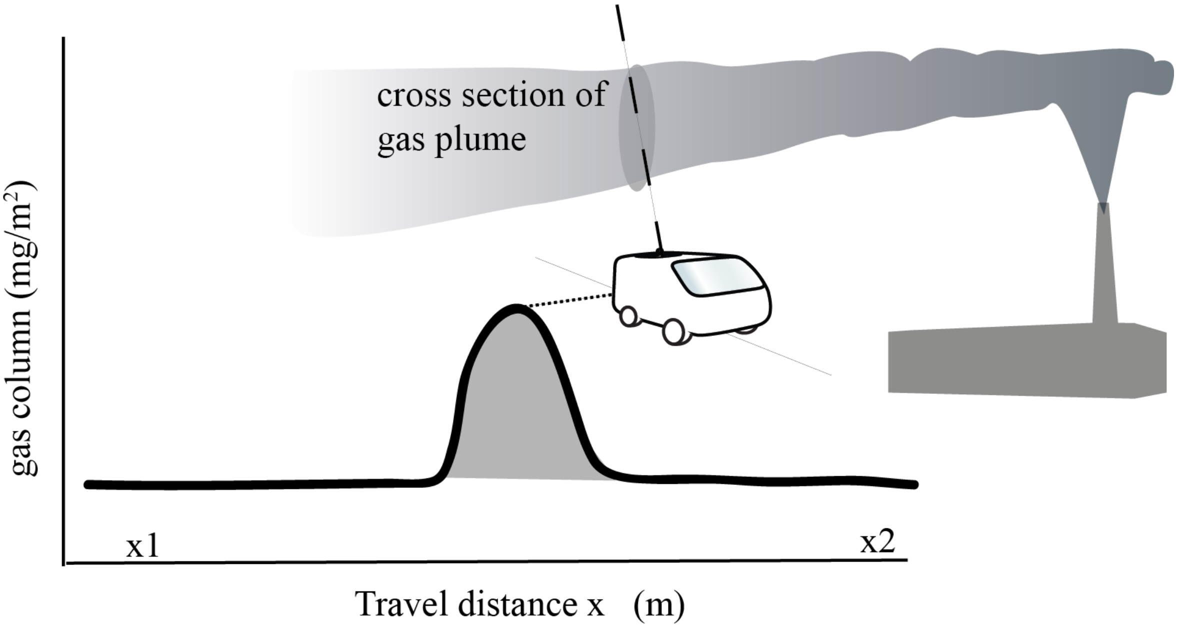

Figure 3. Schematic of the SOF measurement where the vehicle is driven across the prevailing wind so that the solar beam cuts through the emission plume while the sun is locked into the FTIR spectrometer by the solar tracking device on the roof. The VOC mass (or other compound of interest) is integrated through the plume cross section. See section 4.1 for complete equations.

For each spectrum a column concentration of the species is retrieved using custom software (QESOF, i.e. *Quantitative evaluation of SOF*) [Kihlman 2005b]. These column concentrations, together with positions recorded with a GPS (Global Positioning System) receiver and the solar angle calculated from the time of the measurements, are used to calculate the area integrated column of the species in the intersection area between the plume and the light path. The flux of the species is then obtained by multiplying this area integrated concentration with the orthogonal wind speed vector component.

The IR spectra recorded by the SOF instrument are analyzed in QESOF by fitting a set of spectra from the HITRAN infrared database [Rothman 2003] and the PNNL (Pacific Northwest National Laboratory) database [Sharpe 2004] in a least-squares fitting procedure. Calibration data from the HITRAN database is used to simulate absorption spectra for atmospheric background compounds present in the atmosphere with high enough abundance to have detectable absorption peaks in the wavelength region used by SOF. Spectra, including water vapor, carbon dioxide and methane, are calibrated at the actual pressure and temperature and degraded to the instrumental resolution of the measurements. The same approach is applied for several retrieval codes for high resolution solar spectroscopy developed within Network for the Detection of Atmospheric Composition Change (NDACC) [Rinsland 1991; Griffith 1996] and QESOF has been tested against these with good agreement, better than 3%. For the retrievals, high resolution spectra of ethylene, propene, propane, n-butane and n-octane were obtained from the PNNL database and these are degraded to the spectral resolution of the instrument by convolution with the instrument line shape. The uncertainty in the absorption strength of the calibration spectra is about 3.5% for all five species.

In this project, the SOF method was used to measure VOCs in two different modes. Most VOCs with C-H-bonds absorb strongly in the 3.3-3.7 µm (2700-3005 $cm^{-1}$) spectral region. This region is mainly used for alkane measurements using a spectral resolution of 8 $cm^{-1}$. Alkenes (including ethylene and propylene) and ammonia are instead measured in the spectral region between 910 and 1000 $cm^{-1}$ using a spectral resolution of 0.5 $cm^{-1}$. In the alkane mode – the IR light absorption is essentially sensitive to the total alkane mass (number of alkane C-H bonds) present in the plume. The absorption structures (cross sections) for the various alkane compounds are rather similar, with the absorption strength scaling to the mass of the alkane species. Hence, the actual mix of alkanes in the plume does not affect the retrieved total alkane mass flux much, although only cross sections from a subset of all alkanes (propane, n-butane and octane) are fitted in the spectral analysis. Typically, the rare event of significant absorption from other species in the plume shows up as elevated residuals and is further investigated in the re-analysis. For the alkene mode the specificity of the measurements is good, since the absorption of different species is rather unique in this so called “fingerprint region” and absorption features are often sharp and well separable from each other at 0.5 $cm^{-1}$ resolution.

SOF is a proven technique employed by FluxSense in over 100 fugitive emission studies around the world. In Europe the SOF technique is considered one of the Best Available Technology [European Commission 2015] for measurements of fugitive emission of VOCs from refineries; and in Sweden it is used together with tracer correlation and optical gas imaging for annual screening of all larger refineries and petrochemical plants. The estimated uncertainty for the SOF emissions measurements is typically 30 % for the total site emissions. This uncertainty has been calculated from several controlled release experiments (blind and non-blind) and side-by-side measurements with other measurement techniques.

## 3.2 Mobile SkyDOAS

The principle for Mobile SkyDOAS (Mobile Differential Optical Absorption Spectroscopy) measurements is very similar to that of SOF. Instead of measuring direct sun light in the infrared region, scattered light in the UV and visible region is measured in zenith angle with a telescope connected with an optical fiber to a Czerny-Turner spectrometer with a CCD camera. Column concentrations are retrieved from spectra in a similar way as with the SOF, although absorption is generally weaker. The system that was used for this project consists of a quartz telescope (20 mrad field of view, diameter 7.5 cm) connected with an optical fiber (liquid guide, diameter 3 mm) to a 303 mm focal length Czerny-Turner spectrometer with a 1024 by 255 pixels, thermoelectrically cooled CCD camera, see Figure 4.

Figure 4. The mobile SkyDOAS system: Telescope, optical fibre, spectrometer and control computer.

The system was installed in the same measurement vehicle as the SOF system. Plumes were transected in the same way as with the SOF system and the retrieved column concentrations used to calculate fluxes exactly the same way, except that the SkyDOAS measurement direction is always zenith.

In this project, mobile SkyDOAS was used to measure $SO_2$, $NO_2$ and $H_2CO$. $NO_2$ is retrieved in the wavelength region between 324 and 350 nm and $SO_2$ in the region 310-325 nm. $H_2CO$ is measured in the region 322-350 nm. Apart from $SO_2$, $NO_2$ and $H_2CO$ the spectral analysis also includes other atmospheric compounds such as $O_3$ and $O_4$. The rare event of significant absorption from other species in the plume than those included in the spectral fit shows up as elevated residuals and is further investigated in the re-analysis. The absorption line parameters of the retrieved compounds are well established in published databases, stating an uncertainty of 4% (Vandaele *et al.* 1998) for the UV cross section of $NO_2$ and less than 2% for the $SO_2$ cross sections (Bogumil *et al.* 2003).

The DOAS technique was introduced in the 1970's (Platt *et al.* 1979) and has since then become an increasingly important tool in atmospheric research and monitoring both with artificial light sources and in passive mode utilizing the scattered solar light. In recent time the multi axis DOAS technique (scanning passive DOAS) has been applied in tropospheric research for instance measuring formaldehyde (Heckel *et al.* 2005; Pikelnaya *et al.* 2007).

Passive DOAS spectroscopy from mobile platforms has also been quite extensively applied in volcanic gas monitoring (Galle *et al.* 2003) for $SO_2$ flux measurements and for mapping of formaldehyde flux measurements in megacities (Johansson *et al.* 2009), . Mobile SkyDOAS has been used in several studies for measurements of industries i.e. $SO_2$, $NO_2$ and $H_2CO$ for several campaigns in Texas including $NO_2$ measurements at Longview in 2012 (Johansson *et al.* 2014a; Johansson & Mellqvist 2013). (Rivera 2009) did $SO_2$ measurements on a power plant in Spain for validation purposes. They also made measurements at an industrial conglomerate in Tula in Mexico (Rivera *et al.* 2009a) and measurements of $SO_2$, $NO_2$ and $H_2CO$ during the TexAQS 2006 campaign (Rivera *et al.* 2009b; Rivera *et al.* 2010). There are also groups in both China and Spain working with mobile mini-DOAS.

## 3.3 Mobile extractive FTIR (MeFTIR)

Mobile Extractive FTIR (MeFTIR) [Galle 2001, Börjesson 2009] in combination with tracers has been used to quantify VOC emissions from refinery and petrochemical sources in Europe and in the U.S. alkanes and alkenes are typically measured, but also methane and other climate gases can be retrieved. MeFTIR is an optical technique capable of monitoring gas concentrations at ppb-sensitivity in mobile field operations. It is used both independently for concentration mapping and flux measurements, but often combined together with simultaneous SOF flux measurements to provide more detailed VOC speciation of plumes and for plume height assessments [Johansson et. al. 2013a]. The plume height can be estimated by dividing measured columns (mg/m$^2$) with ground concentrations (mg/m$^3$), assuming that the plume is evenly distributed up to the plume height (and zero above).

The MeFTIR system contains a mid-infrared spectrometer with medium resolution (0.5 cm$^{-1}$). It utilizes an internal glow bar as an infrared radiation source, and by customized optics this light is transmitted through an optical multi-pass measurement cell with path-length of 56 meters. The system is mounted on a vibration dampening platform to allow for real time plume mapping from a mobile platform, such as a vehicle or boat, see Figure 5.

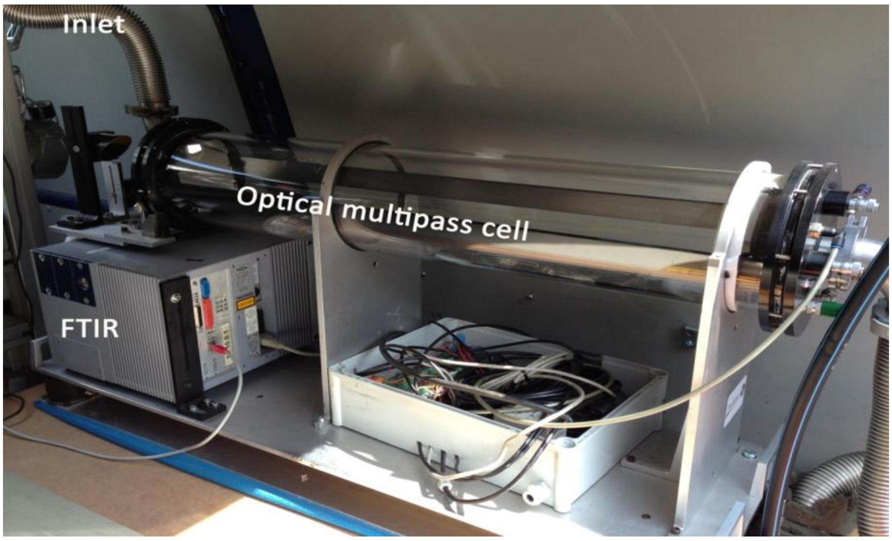

Figure 5. The MeFTIR instrumentation consisting of a Bruker FTIR spectrometer connected to an optical multi-pass cell.

The transmitted light is detected simultaneously with an InSb-detector in the 2.5–5.5 µm (1800–4000 cm$^{-1}$) region and an MCT detector in the 8.3–14.3 µm (700–1200 cm$^{-1}$) region. Temperature and pressure in the cell are averaged over the duration of each measurement. Atmospheric air is continuously pumped at high flow rate through the optical cell from the outside, taking in plume air from the roof of the vehicle (2.5 m height) through a Teflon tube. A high flow pump is used to ensure that the gas volume in the cell is fully replaced within a few seconds. Spectra are typically recorded with an integration time of 10-15 seconds. A GPS-receiver is used to register the position of the vehicle every second.

The concentration in the spectra is analyzed in real time by fitting a set of calibrated spectra from the HITRAN infrared database [Rothman 2003] and the PNNL database [Sharpe 2004] in a least-squares fitting procedure. Compounds being analyzed include ethylene, propylene, total alkane mass (based on fitting cross sections of ethane, propane, n-butane, i-pentane, n-octane), water, methane, CO, $CO_2$ and $N_2O$. The analysis routines are very similar to the ones for SOF, but less complex because strong absorption by atmospheric trace gases (water, methane, $CO_2$) has less consequence at the shorter path length in the MeFTIR measurement cell.

The MeFTIR tracer approach has been tested in a so-called gas release “blind test” together with other techniques in U.S. [EREF 2011]. In that test, methane was released from an area-distributed source in four different configurations and flow rates ranging from 1.1-3.3 g/s. At a downwind distance of 400 meters MeFTIR retrieved the fluxes within 6% in 3 cases and 19% in the fourth. This is consistent with other validation experiments, showing a flux estimate accuracy of better than 20%. Concentration measurement by FTIR is a widely used procedure, and the main uncertainties are associated with the absorption cross sections (typically < 3.5%) and spectral retrieval, with an aggregate uncertainty better than 10% in the analysis.

Concentrations are monitored in real time in order to detect emission plumes and to judge whether any interfering sources are being sampled. Unwanted signals from local traffic exhaust or from the measurement vehicle itself could be filtered out by looking at exhaust compound signatures like carbon monoxide concentrations. A stationary source is, on the contrary to any local traffic plumes, characterized by recurrent downwind plumes. Transient and non-repeatable observations are therefore excluded from the results. Furthermore, measurements of ambient concentrations of methane and carbon dioxide (with known atmospheric concentrations) are used for consistency check.

## 3.4 Mobile White Cell DOAS (MWDOAS)

The ground level mass concentration of benzene, toluene, ethylbenzene, m- and p-xylene (BTEX) was measured using a mobile real-time system: Mobile White cell DOAS (MWDOAS). The MWDOAS system consists of an open, 2.5 m long optical White cell that is mounted on the roof of the measurement vehicle (see Figure 6). By multiple reflections in the White cell mirror system an overall path length of 210 m is obtained, resulting in low detection limits (ppb). The light from the internal lamp is transmitted through the White cell and then analyzed in a DOAS spectrometer, using the UV wavelength region 255 - 285 nm.

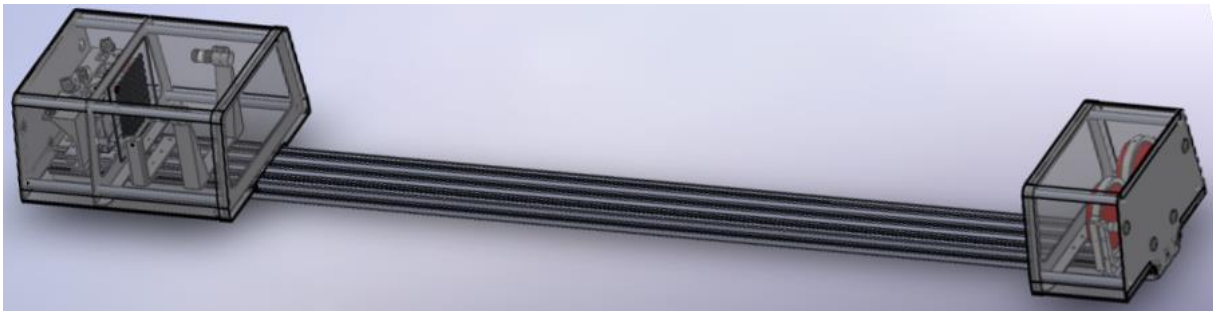

Figure 6. The open path MWDOAS cell having an overall optical path-length of 210 m.

A measurement begins by acquiring a reference spectrum outside the plume, usually upwind of the facility. Spectra are then sampled and averaged continuously while driving through emission plumes. The averaging time is set to around 8 seconds in order to achieve acceptable SNR (see below). This is the lower limit of the temporal sampling between independent measurements, but the spatial sampling is also dependent by the vehicle's velocity. A typical driving speed for MWDOAS measurements is 10-20 km/h for sufficient plume sampling. The spectra are geo-tagged and evaluated online using the standard DOAS technique, giving information of plume locations and constituents. Cross-sections included in the evaluation are tabulated in Table 2.

The MWDOAS data is later post evaluated and merged with the corresponding MeFTIR data to produce a plume specific BTEX/Alkane mass ratio. The mass ratio of BTEX/Alkanes is then used to calculate the aromatic flux from individual sub areas where alkane fluxes have been measured by SOF, assuming they have the same source. Specific area plumes are ideally probed at several times, and an overall average of all plume transect BTEX/Alkane ratios is then made. The method requires in situ access to the plume of the studied source, and as instrumentation typically are mounted on a truck, highly elevated sources with a strong plume lift like hot flares, chimneys and high process towers will not be possible to survey at close distance.

Table 2. The UV-cross-sections used in the evaluation of the MWDOAS spectra.

| Chemical compound | Origin of reference spectrum |
|---|---|
| $O_3$ | [Burrows 1999] |
| $SO_2$ | [Bogumil 2003] |
| $O_2$ | [Bogumil 2003] |
| Toluene | [Fally 2009] |
| Benzene | [Etzkorn 1999] |
| 1,3,5-Trimethylbenzene | [Etzkorn 1999] |
| 1,2,4-Trimethylbenzene | [Etzkorn 1999] |
| Styrene | [Etzkorn 1999] |
| Phenol | [Etzkorn 1999] |
| p-Xylene | [Etzkorn 1999] |
| m-Xylene | [Etzkorn 1999] |
| Ethylbenzene | [Etzkorn 1999] |

The MWDOAS technique has been validated in various surveys by comparison with canister samples acquired at several different locations and which were subsequently analyzed by gas chromatography (GC-FID). The validation shows that the result from MWDOAS lies well within 10% of the result of the certified canister results for BTEX. Due to an absorption cross-section too weak to be used with reliability in the MWDOAS analysis, the ortho isomer of the xylene has been omitted in this comparison. When total xylene is presented in the present survey, the sum of m- and p-xylenes from the MWDOAS measurement is multiplied by 1.32. This number comes from a ratio comparison of xylene isomers in 49 canister samples analyzed by GC/FID and taken from eight refineries and tank parks from two countries. The standard deviation in this comparison was 0.07 and adds a 4.5% uncertainty to the total xylene concentration. Hence, the xylene concentration from MWDOAS is defined as the sum of the measured m- and p-isomers and the inferred o-isomer.

The MWDOAS system has been used in previous campaigns in USA during 2013 with good results. During the 2013 DISCOVER-AQ campaign [Johansson, 2013b] in Houston, Texas, the system was run in parallel to a mobile Proton Transfer Mass spectrometer (PtrMS) lab as a validation check. The results of benzene, toluene and styrene was compared and showed good agreement, with the PtrMS showing slightly elevated benzene concentrations compared to the MWDOAS. The sensitivity of MWDOAS is better than 1 ppb for benzene, better than 3 ppb for toluene, ethylbenzene and m-xylene and 0.5 ppb for p-xylene.

Since the distribution of the BTEX constituents varies with source we will also present the benzene to alkane ratio to facilitate the calculation of benzene flux and identify specific benzene sources.

Unwanted BTEX signals from local traffic exhausts are generally only significant in congestions (at traffic lights etc.) or in confined spaces, e.g. tunnels. Apart from this, large emitters are also occasionally seen elsewhere. They are generally recognized, partly by their typical gasoline composition signature and partly by their transient nature. A stationary BTEX source is, on the other hand, characterized by recurrent downwind plumes. Transient and non-repeatable BTEX observations are therefore excluded from the result. Note that all concentrations are enhancements above the reference/background.

## 3.5 Wind Measurements and Auxiliary Data

### ***Wind LIDAR***

A wind LIDAR (LIght Detetction and Ranging, Leosphere WindCube v2) was used to measure vertical wind profiles of wind speed and direction. The LIDAR provided wind profiles in the vertical range of 40 m to up to 300 m above ground, with 20 m vertical resolution, and wind speed accuracy of 0.1 m/s. The system records 1-s data, and 1-minute averages were used for flux calculations in this study. The principle of detection is based on the Doppler shift of the infrared pulse that the instrument sends out and retrieves. Numerous validation surveys attesting the accuracy of the WindCube LIDARs are publicly available at www.leosphere.com.

Figure 7. Wind measurements with portable wind LIDAR profiler (40-200+ m).

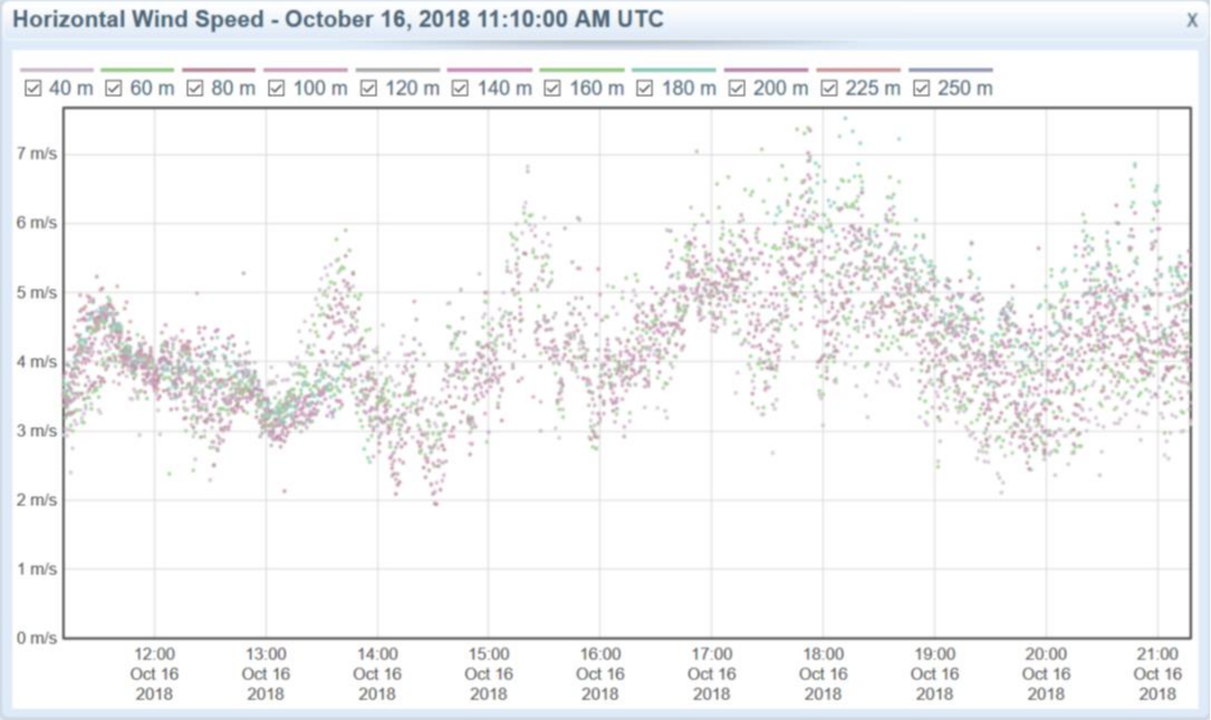

Figure 8. Data example, LIDAR wind profiler, October 16, 2018.

### *Wind Masts*

Meteorological parameters were measured at selected sites using a portable 3-10 m mast. This mast was equipped with a calibrated RM Young 05108 “prop and vane” anemometer and a Campbell Scientific CR5000 data-logger, see  Figure 7. Wind data from the measurement period are also collected from nearby ASOS (typically airport stations) and NOAA weather station network. Typically wind mast measurement height is 10 m but varies for NOAA weather stations.

Figure 9. The FluxSense mobile wind mast used in the 2018 CARB survey with an RM Young anemometer mounted on top. The mast could be erected from 3 to 10 m.

### *Airmar (Mobile Weather Station)*

A sonic wind meter (Airmar WeatherStation 200 WX) was installed on the roof of the measurement vehicle to complement the other wind measurements and give local ground winds at the vehicle. The wind information from the car-based Airmar was not used for flux calculation since the wind field at street level can be heavily disturbed and turbulent. The Airmar was only used as a real-time aid to keep track of the plume directions when making the gas emission measurements.  The Airmar provides wind speed and direction relative to true north (compensating for vehicle position), as well as air temperature, pressure and relative humidity. It also provides GPS positions that may be used as a backup for the other GPS-antenna.

### *GPS*

The FluxSense vehicle is equipped with two standard USB GPS-L1 receivers (GlobalSat BU-353S4) hooked up to the SOF and MWDOAS-computers. They are placed horizontally on the roof and by the windscreen for optimal reception. The receivers give the position at a rate of 1 Hz.

## 3.6 Additional sensors from CARB

This project complements community monitoring efforts by CARB, who have been running mobile measurements with smaller sensors, including on photo ionization (ppbRae3000 and Falco PID) for VOCs and optical measurements for particulate matter and black carbon.

In order to investigate the sensitivity and accuracy of the sensors they were mounted on the FluxSense mobile lab and run in parallel with the FluxSense equipment during most of the survey duration.

Figure 10. The CARB measurement box with smaller sensors for VOCs and particles installed on the FluxSense measurement van.

# 4 Measurement Methodology

## 4.1 Principal Equations

This report includes three different techniques to measure emission mass fluxes as specified below. The primary method in this project is the direct flux measurements of alkanes from SOF. In the secondary method BTEX and methane fluxes are measured indirectly from MWDOAS/MeFTIR gas mass ratios.

### *4.1.1 DIRECT FLUX MEASUREMENTS:*

The emission mass flux ($Q$) of species (*j*) measured by SOF for a single transect (*T*) across the plume ($P$) along path ($l$) can be expressed by the following integral (Si-units in gray brackets):

$$Q_T^j[\mathrm{kg/s}] = \bar{v}_T[\mathrm{m/s}] \cdot \int_P C_l^j[\mathrm{kg/m^2}] \cdot \cos(\theta_l) \cdot \sin(\alpha_l)\ dl\ [\mathrm{m}]$$

Where,

$\bar{v}_T$ = the average wind speed at plume height for the transect,

$C_l^j$ = the measured slant column densities for the species *j* as measured by SOF or SkyDOAS,

$\theta_l$ = the angles of the light path from zenith ($\cos(\theta_l)$ gives vertical columns),

$\alpha_l$ = the angles between the wind directions and driving directions

$dl$ = the driving distance across the plume

Note that SOF and SkyDOAS have different light paths, where the SkyDOAS telescope is always looking in the zenith direction while the SOF solar tracker is pointing toward the Sun. Hence, the measured SOF slant column densities will vary with latitude, season and time of day.

To isolate emissions from a specific source, the incoming/upwind background flux must be either insignificant or subtracted. If the source is encircled or "boxed", the integral along *l* is a closed loop and the flux calculations are done with sign. This is taken care of by the FluxSense software.

### *4.1.2 INDIRECT FLUX MEASUREMENTS:*

The indirectly measured flux (indirectly measured emission, IME) is computed using a combination of SOF and MeFTIR/MWDOAS measurements. The inferred mass flux ($\hat{Q}^i$) for species (*i*) are calculated from MeFTIR and/or MWDOAS ground level gas ratios integrated over the plume ($P$) along path ($l$) are given by (Si-units in gray brackets):

$$\hat{Q}^i[\mathrm{kg/s}] = \bar{Q}^j[\mathrm{kg/s}] \cdot \frac{1}{k}\sum_k \frac{\int_P N_l^i[\mathrm{kg/m^3}]\ dl[\mathrm{m}]}{\int_P N_l^j[\mathrm{kg/m^3}]\ dl[\mathrm{m}]}$$

Where,

$\bar{Q}^j$ = the average flux of species *j* from multiple transects as measured by SOF,
$N_l^i$ = the number density concentrations of species *i* as measured by MWDOAS or MeFTIR,
$N_l^j$ = the number density concentrations of species *j* as measured by MeFTIR,
$k$ = the number of gas ratio measurements

Note that the IME operates on average values since simultaneous SOF, MWDOAS and MeFTIR measurements are generally not performed and because individual gas ratios are more uncertain than the average. Although not necessarily simultaneously measured, SOF and MeFTIR/MWDOAS measurements must represent the same source plumes. Note also that gas ratios do not intrinsically depend on complete plume transects (like for direct flux methods) as long as the emission plume is well mixed at the sampling distance. Additionally, it is not necessary that the source of the tracer and measured gas be identical, merely that they are co-located at the measurement distance and uniform in time.

### *4.1.3 TRACER GAS FLUX MEASUREMENTS:*

The third method to conduct flux measurements is by tracer correlations using only MeFTIR measurements or simultaneous MeFTIR and MWDOAS measurement and a known tracer gas release. Note that this method was not applied during the first campaign in October 2018, although it will be used on later studies. These fluxes are given for each transect (*T*) by the following equation (Si-units in gray brackets):

$$Q_T^j[\mathrm{kg/s}] = Q^{tracer}[\mathrm{kg/s}]\,\frac{\int_P \; N_l^j[\mathrm{kg/m^3}]\;dl[\mathrm{m}]}{\int_P \; N_l^{tracer}[\mathrm{kg/m^3}]\;dl[\mathrm{m}]}$$

Where,

$Q^{tracer}$ = the release mass flux of the tracer gas from bottle,
$N_l^{tracer}$ = the number density concentrations of the tracer as measured by MeFTIR,
$N_l^j$ = the number density concentrations of species *j* from MeFTIR or MWDOAS,

Note that tracer gas correlation fluxes do not intrinsically depend on complete plume transects (like for direct flux methods) as long as the emission plume and the tracer gas is well mixed at the sampling distance. Complete plume transects are, however, recommended since the tracer gas release point might not completely match at the sampling distance

## 4.2 Uncertainties and Error Budget

A summary of the typical performance of the FluxSense measurements is presented in Table 3.

In addition, for each site the statistical error is calculated. It corresponds to the random error but in addition there could be systematic errors. For instance, in the used wind speed due to the errors in estimated height of the plume and spectral calibration errors. The statistical error is given by the 95 % Confidence Interval (CI) for the mean, $\bar{x}$, according to:

$$CI = \bar{x} \pm t_{.025} \frac{s}{\sqrt{N}}$$

Here t is Student’s T distribution and s corresponds to sample standard deviation:

$$s_x = \sqrt{\frac{\sum_{i=1}^{N}(x - \bar{x})^2}{N - 1}}$$

Table 3. Performance of FluxSense measurement methods.

| Measurement Parameter | Analysis Method | Accuracy | Precision |
|---|---|---|---|
| SOF column concentrations alkanes, alkenes, $NH_3$ | QESOF spectral retrieval | ±10% | ±5% |
| SkyDOAS column concentrations $NO_2$, $SO_2$, $H_2CO$ | DOAS spectral retrieval | ±10% | ±5% |
| MeFTIR concentrations $CH_4$, VOC, $NH_3$, $N_2O$ | QESOF spectral retrieval | ±10% | ±5% |
| MWDOAS concentrations BTEX, Benzene | MWDOAS spectral retrieval | ±10% | ±5% |
| Wind Speed (10 m) | R.M. Young Wind monitor | ±0.3 m/s or 1% | ±0.3 m/s |
| Wind Direction (10 m) | R.M. Young Wind monitor | ±5° | ±3° |
| LIDAR Wind Speed (40-300 m) | Leosphere Windcube V 2 | ±0.1 m/s | - |
| GPS position | USB GPS receiver | ±2m | ±2m |
| SOF mass flux Alkanes, alkenes, $NH_3$ | SOF-Report flux calculations | ±30% | ±10% |
| SkyDOAS mass flux $NO_2$, $SO_2$, $H_2CO$ | SkyDOAS flux calculations | ±30% | ±10% |

# 5 Survey Setup & Complementary Measurements

Mobile measurements with SOF, SkyDOAS, MWDOAS, and MeFTIR were carried out during 18 measurement days between October 4 and October 24, 2018 in the Bay Area, California, Figure 11. The focus was on industrial VOC emissions from refineries, petrochemical industry, oil storage, harbor activities and landfills. It also included investigating the impact of various sources on the concentration levels in Richmond. Because measurements were carried out on the nearest traversable roads to the fenceline of the facilities, refinery areas in particular may include more industries than the refinery. The emissions are therefore designated as from the area incorporating the refinery and nearby inseparable sources. These are defined cartographically in the following section.

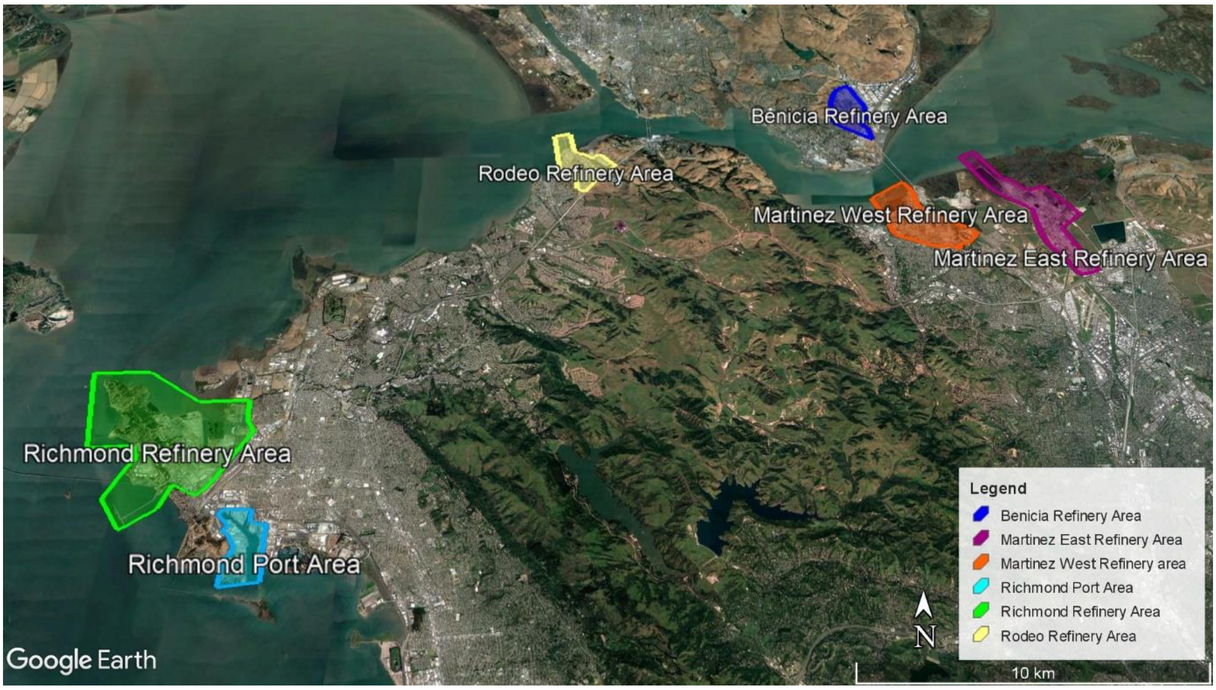

Figure 11. The primary sites in the Bay Area that were studied in the emissions survey during October 2018. Refinery areas typically included additional industries that were inseparable from the primary refinery source during the emissions survey. Emissions measurement areas are defined in Section 5.1.

In addition to the above, some preliminary emission measurements (5 days, 30 September - 2 October and 25-26 October) were carried out in the San Joaquin valley (Bakersfield) of oil and gas production and ammonia emissions from Concentrated Animal Feeding Operations (CAFOs) (Bakersfield and Merced). An additional emission source studied was a major brush fire. The results from latter measurements are only briefly shown in this report and these gas fluxes will instead be reported together with the results from the second campaign in May 2019 in which the main focus will be on impact of oil and gas production and CAFO emissions in the central valley.

The gas measurements were combined with wind data, primarily from a mobile wind LIDAR but also from adjacent stationary meteorological stations, to calculate fluxes and identify sources. During the measurement campaign the wind LIDAR, which was installed on the back of a measurement van, was positioned in proximity to the emission sources.

All measurements have been subjected to quality control and assurance. This include following standard protocols for SOF, MEFTIR, and MWDOAS, ocular examination of instruments and data, daily instrument calibration and statistical measures of data quality. The number of accepted measurements varied substantially from day to day and from source to source depending on weather conditions, local measurement conditions (accessibility, state of the roads, obstacles etc.) and time sharing between different projects, objects and instruments. Statistical estimates of the flux emissions (kg/h) from the various sources were computed for each measurement day and for the entire survey, including the statistical error.

## 5.1 Sites

All measurements during the survey were made publicly accessible roads. Approximate area boundaries for the emissions survey are shown in Figures 12 to 17.

Figure 12. Approximate boundary for Richmond refinery area and pier/terminal in Point Richmond.

Figure 13. Approximate boundary for Rodeo refinery area. The tank park east of Hwy 80 belongs to the refinery but could not be included in the measurements with the prevailing wind direction during the survey days.

Figure 14. Approximate boundary for Martinez West refinery area.

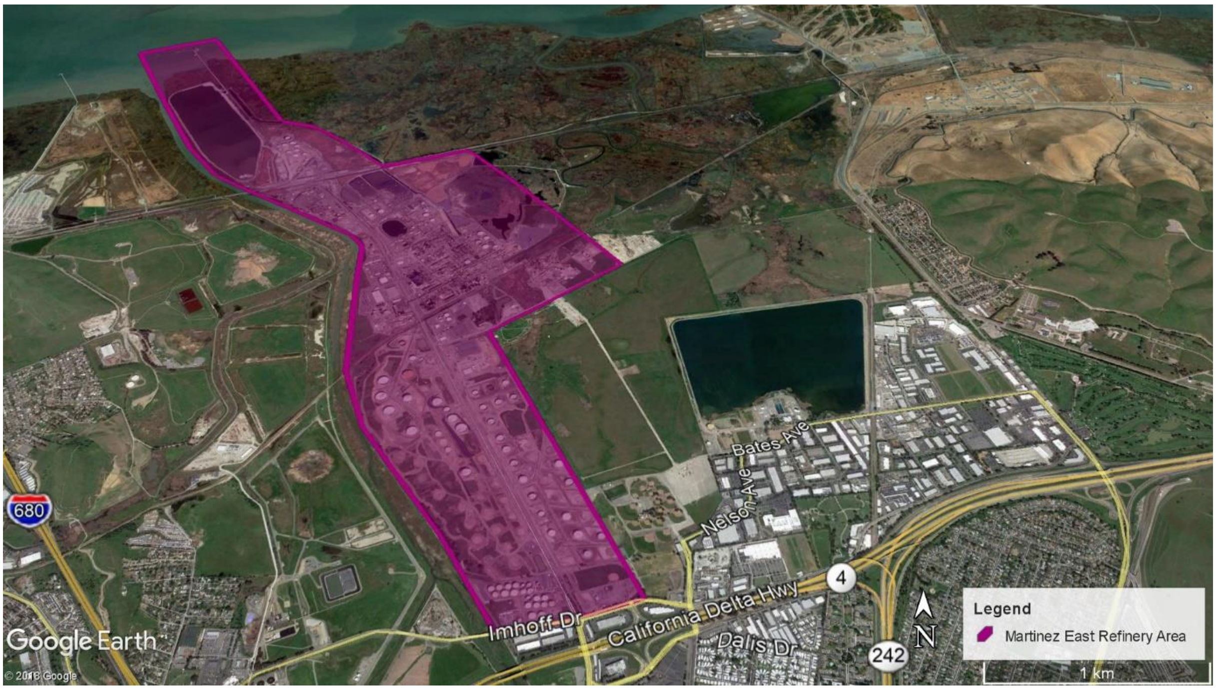

Figure 15. Approximate boundary for Martinez East refinery area.

Figure 16. Approximate boundary for Benicia refinery area.

Figure 17. Approximate boundary for the Richmond Port area.

Table 4. Measurement days carried out during the campaign.

| Date | Region | Lidar Location | Survey Area |
|---|---|---|---|
| 30-Sep-2018 | San Joaquin Valley | Taft Highway<br>35.267083N, 119.254905W | Elk Hills |
| 1-Oct-2018 | San Joaquin Valley | Taft Highway<br>35.267083N, 119.254905W | Elk Hills |
| 2-Oct-2018 | San Joaquin Valley | Taft Highway<br>35.267083N, 119.254905W | Elk Hills, Lost Hills |
| 4-Oct-2018 | Bay Area | Martinez,<br>38.004572N, 122.043652W | Instrumentation service & QA, Martinez |
| 5-Oct-2018 | Bay Area | Richmond North,<br>37.982553N, 122.326700W | Richmond |
| 6-Oct-2018 | Bay Area | Richmond North,<br>37.982553N, 122.326700W | Richmond, Rodeo |
| 7-Oct-2018 | Bay Area | Martinez,<br>37.996165N, 122.108130W | Martinez, Travis AFB fire |
| 10-Oct-2018 | Bay Area | Martinez,<br>38.025336N, 122.098101W | Benicia, Martinez |
| 11-Oct-2018 | Bay Area | Richmond N, Laurie Ln,<br>37.965089N, 122.343991W | Richmond |
| 12-Oct-2018 | Bay Area | Rodeo, Springwood St<br>38.030437N, 122.254275W | Rodeo |
| 13-Oct-2018 | Bay Area | Martinez,<br>38.025336N, 122.098101W | Benicia, Martinez |
| 14-Oct-2018 | Bay Area | Rodeo, Springwood St<br>38.030437N, 122.254275W | Rodeo |
| 15-Oct-2018 | Bay Area | Martinez,<br>37.996165N, 122.108130W | Benicia, Martinez |
| 16-Oct-2018 | Bay Area | Richmond S, Marina Way,<br>37.919250N, 122.356733W | Richmond |
| 17-Oct-2018 | Bay Area | Martinez,<br>38.004572N, 122.043652W | Martinez East |
| 18-Oct-2018 | Bay Area | Richmond S, Meeker Ave,<br>37.919948N, 122.348483W | Richmond |
| 19-Oct-2018 | Bay Area | Richmond S, Meeker Ave,<br>37.919948N, 122.348483W | Richmond |
| 20-Oct-2018 | Bay Area | Richmond S, Meeker Ave,<br>37.919948N, 122.348483W | Richmond |
| 21-Oct-2018 | Inland | West McDonald Rd, Stockton<br>37.977300N, 121.473324W<br>Fresno Ave, Stockton<br>37.937212N, 121.312043W | McDonald Island Gas Storage, Port of Stockton |
| 22-Oct-2018 | Bay Area | Richmond S, Meeker Ave,<br>37.919948N, 122.348483W | Richmond |
| 23-Oct-2018 | Bay Area | Martinez<br>37.976673N, 122.083369W | Martinez West, Rodeo, Richmond |
| 25-Oct-2018 | San Joaquin Valley | Merced<br>37.297977N, 120.483480W | Cattle Farms |
| 26-Oct-2018 | San Joaquin Valley | Taft Highway<br>35.267083N, 119.254905W | Elk Hills |

## 5.2 Wind measurements

The largest source of error in SOF and SkyDOAS measurements of emission fluxes is typically the wind measurements. The flux is directly proportional to the wind speed (at average plume height) and to the cosine of the wind direction relative to the driving direction. The wind error is a combination of errors in the wind measurements themselves and errors due to the assumption that the measured wind or wind profile is representative of the average plume velocity.

The vector from the plume source to where it is encountered in the measurement vehicle is essentially a measure of integrated wind direction over the plume path. Hence errors in wind direction are usually apparent in the measurements and large errors can be corrected or avoided. Plume speed in the measurement plane is not directly measured, and plume height is only partially known so wind speed errors are typically more problematic.

Wind profile data, as supplied by a LIDAR, has the major advantage of allowing an average wind for an arbitrary height interval to be calculated. Given some approximate information about the mixing height of the plume, a suitable averaging interval can be chosen, and the LIDAR data can also be used to estimate the sensitivity of the wind error to the error in the mixing height. Hence, LIDAR data was main source of wind information in these measurements complemented with local winds and AIRMAR sonic sensor, mounted on the top of the measurement car, see Figure 18.

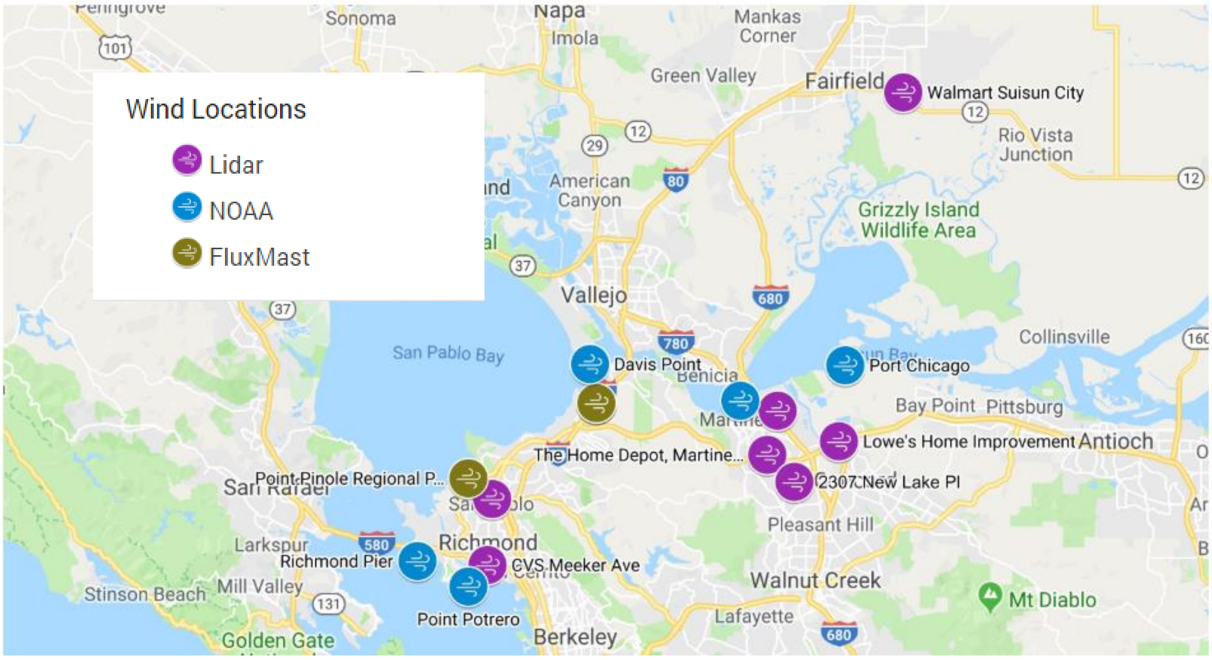

Figure 18. Locations of wind measurements for the emissions survey.

As the wind speed can vary significantly with height it is worth exploring how these choices may affect the measured fluxes. Ground level winds are particularly affected by topography and vicinity to coast, bays and large water ways. In the Bay Area when winds are light the complications due to water and topography are more evident. Here we examine three cases from the survey:

Figure 19 shows the wind profile on a typical sunny day with moderate winds during SOF measurements inland near Martinez. Both the wind speed and direction vary with time but are similar through at least the first few hundred meters of the boundary layer.

Figure 20 shows the wind profile on a typical sunny day with light winds during SOF measurements in Richmond at the Hilltop Mall site. The wind direction turns only slightly to the ground and the speed profile is near vertical. Some speeds may be too light for SOF measurements (< 1.5 m/s) but wind direction is consistent so this is less of an issue. When the wind shifts late in the day it does so throughout the boundary layer.

Figure 21 shows how the wind profile develops on a day with light wind in Richmond near the port. High level winds are north-westerly throughout the day while low level winds are southerly with the exception of midday. During much of this time period winds were too light (< 1.5 m/s) for SOF measurements and otherwise during SOF hours there is a larger uncertainty in the wind direction. This is problematic for sites with both elevated and ground sources. SOF measurements of Richmond refinery area for the entire day (October 18) were excluded because of the wind uncertainty.

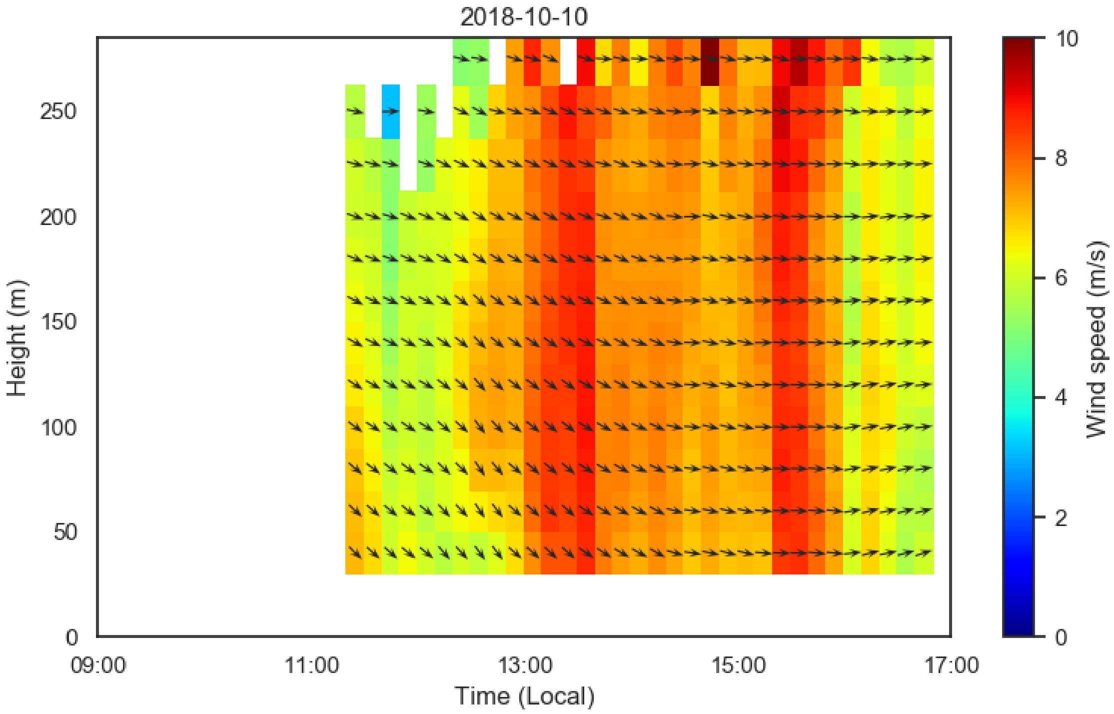

Figure 19 Wind LIDAR data October 10 showing wind speed (color) and horizontal wind direction (arrows) with height.

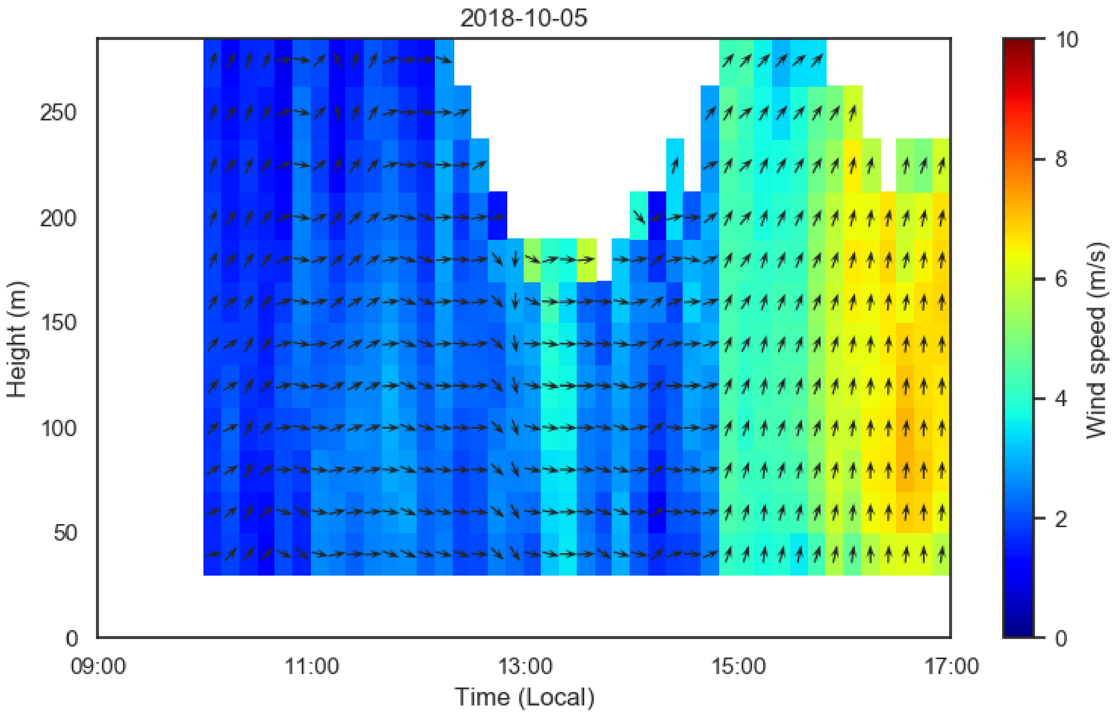

Figure 20. Wind LIDAR data October 5 showing wind speed (color) and horizontal wind direction (arrows) with height.

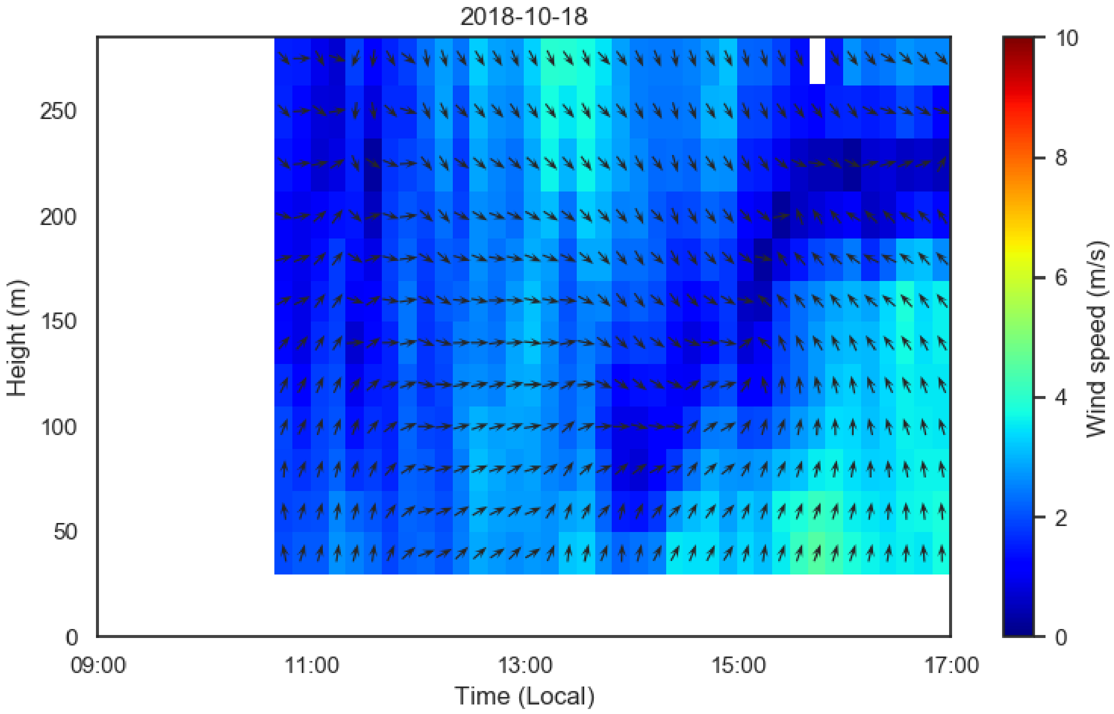

Figure 21. Wind LIDAR data October 18 showing wind speed (color) and horizontal wind direction (arrows) with height.

Profiles for all days are included with the digital data.

In order to assess the sensitivity of the flux calculations to deviations from the assumed plume mixing height, wind LIDAR data (10 min average) have been compared for several height intervals. For the entire measurement period and all LIDAR locations, the wind speed average from 40 – 200m were only slightly higher (1.4%) than the wind from 40 – 100m (Figure 22). The wind direction was nearly always within 30°. Even the 50 m winds differed only slightly from the 40 – 100m winds with speed being a 6 % lower but direction well within 30° (Figure 23). These results indicate that plume height misestimation should have only small effect on measured fluxes.

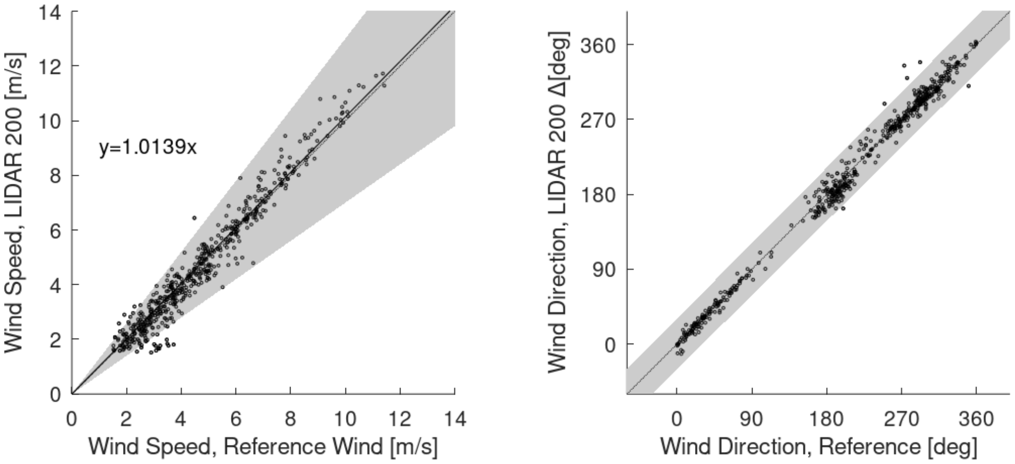

Figure 22. Wind LIDAR data comparison for 40 – 200m (10 min average from 9AM to 5PM) versus the reference 40 – 100m wind over the measurement period 4-23 October 2018 at all measurement locations. The shaded areas indicate ±30% relative deviation from reference wind speed (left panel) and ±30° deviation from reference wind direction (right panel). Fitted least squares are shown as solid line.

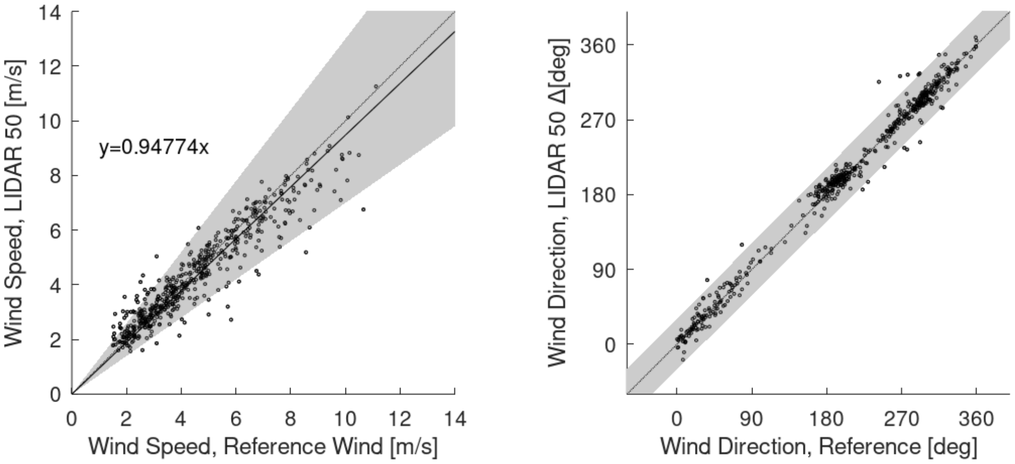

Figure 23. Wind LIDAR data comparison for 50 m (10 min average from 9AM to 5PM) versus the reference 40 – 100m wind over the measurement period 4-23 October 2018 at all measurement locations. The shaded areas indicate ±30% relative deviation from reference wind speed (left panel) and ±30° deviation from reference wind direction (right panel). Fitted least squares are shown as solid line.

For some days or times of day LIDAR data was not available for all sites. This was due to distances between survey sites and instrument setup time. In these cases suitable 10 m mast winds were applied with the wind speeds scaled to the appropriate LIDAR profile based on statistical analysis of data when LIDAR was available or the site.

An example is the Benicia refinery area for the 6 October 2018. The wind LIDAR was positioned at the Richmond Hilltop Mall (see Table 4) for measurements at both Richmond and Rodeo on that day. Additional measurements were later made at the Benicia refinery area for which no nearby LIDAR data are available. Figure 24 shows the relationship between the 40-100m LIDAR reference wind and the NOAA Port Chicago wind on 10 October 2018 with WNW winds.

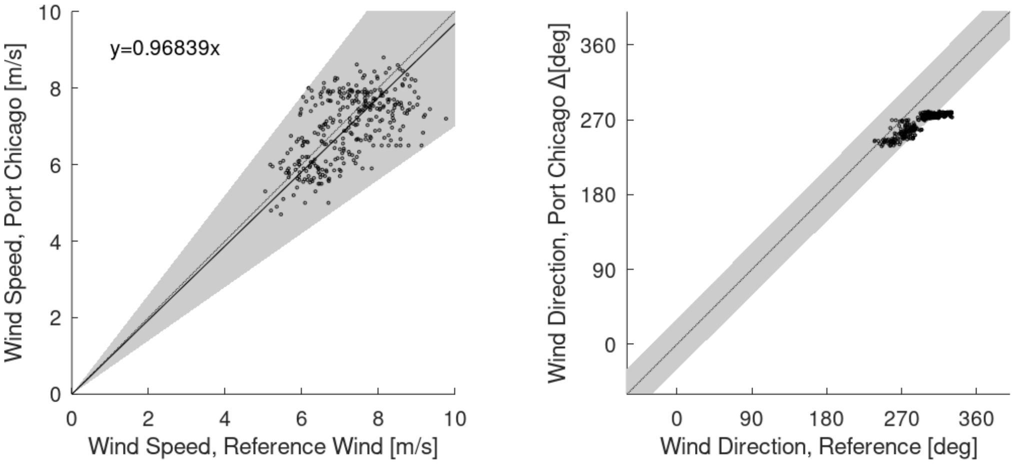

Figure 24. NOAA Port Chicago station versus the reference 40 – 100m wind at Waterbird national preserve 10 October 2018.

Table 5. Replacement winds when nearby LIDAR data were unavailable

| Date Time | Site | Replacement for Lidar Data |
|---|---|---|
| 6-Oct-2018 | Benicia | Port Chicago |

## 5.3 Plume height

The height of the plume influences which wind speed and direction to apply in the flux calculation.

A first order estimate of the plume mixing height can be retrieved from simultaneous concentration measurements and SOF column measurements. The method assumes a homogenous and uniformly distributed plume from ground level to the top of the plume i.e. zero above, and results are used to indicate if the plume is close to ground or aloft where the wind speed changes less rapidly with height compared to close to ground. Results for the different sources are shown in Figure 25. In the figure the upper height of the plume (vertical extent) is shown and varies from within a few meters of the ground to over several hundred meters depending on the source height and plume travel time. Note that since it is assumed that the plume starts from the ground, elevated sources generally give a much higher plume top, as ground concentrations will be very low or even non-existent with nearby elevated sources.

Another way to estimate the plume height is to apply a certain vertical mixing to a plume transport time from the source to the SOF measurement column. Here a vertical mixing speed of 0.5 m/s is used based on measurements from Texas (Mellqvist, 2009). The results are also shown in Figure 25.

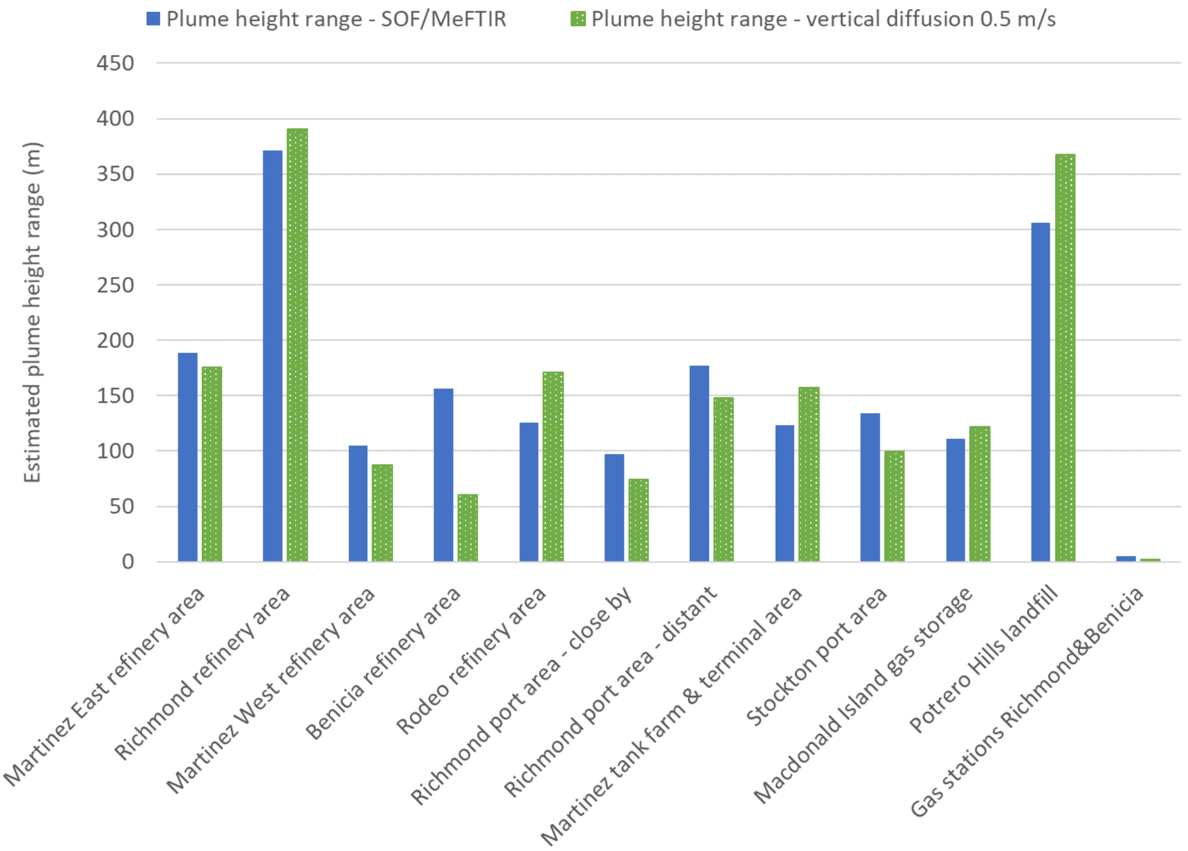

Figure 25. The median upper plume height at the different measurement sites. Estimated (a) from SOF and MeFTIR and (b) from applying a vertical mixing height speed of 0.5 m/s to the plume transport time. These estimates provide the basis for which height interval to average over using the LIDAR.

Very similar results are obtained from both methods, and more importantly both indicate plume heights where winds speeds vary less with height. The exception to this being nearby ground level sources such as gas stations which were not primary objects of the survey. Based on these results the average wind from 40 – 100 m was used for flux calculations for the primary sites, with the only exceptions being the Richmond and Martinez East refinery sites and the Potrero Hills landfill for which the highest reliably measured profile, 40 – 200 m, was used. Other sites, for which plume height analysis was not carried out or lack robustness, were evaluated on a case by case basis. For known ground level point sources this is uncomplicated and a nearby mast wind was used. Unknown sources and those without nearby masts used lidar data up to 50 m. A full listing of emission measurement wind data for sites in the survey is given in Table 6. Winds for other measurements (concentration mapping, concentration ratios) have no impact on measured or calculated emissions and are important only for source attribution and visualisation.

Table 6 Selected wind based on plume heights for emission measurements in the survey.

| *Site or Area* | *Primary Wind* | *Determination* |
|---|---|---|
| Richmond Refinery | LIDAR 40-200 m | Plume height |
| Rodeo Refinery | LIDAR 40-100 m | Plume height |
| Martinez West Refinery | LIDAR 40-100 m | Plume height |
| Martinez East Refinery | LIDAR 40-200 m | Plume height |
| Benicia Refinery | LIDAR 40-100 m | Plume height |
| Potrero Hills Landfill | LIDAR 40-200 m | Plume height |
| Richmond Port | LIDAR 40-100 m | Plume height |
| Port of Stockton | LIDAR 40-100 m | Plume height |
| McDonald Island Gas Storage | LIDAR 40-100 m | Plume height |
| Martinez Sulfuric Acid Regen | Martinez-Amorco Pier | Ground level |
| Propane facility, Richmond | LIDAR 40-50 m | Plume height |

## 5.4 Wind Climatology

For the purposes of examining potential impacts of VOC sources on the community of Richmond, the wind climatology was examined based on data from Point Potrero (https://mesonet.agron.iastate.edu/sites/dyn_windrose.phtml?station=PPXC1&network=CA_DCP). As seen in Figure 26, the survey month did not deviate substantially from the annual climatology in terms of wind direction and winds from the South-Southwest predominate. Slightly lower wind speeds than the annual average were seen in October 2018 (wind speeds here are typically lower than the annual average in October) which may lead to lower overall emissions from tank storage and open atmospheric sources.

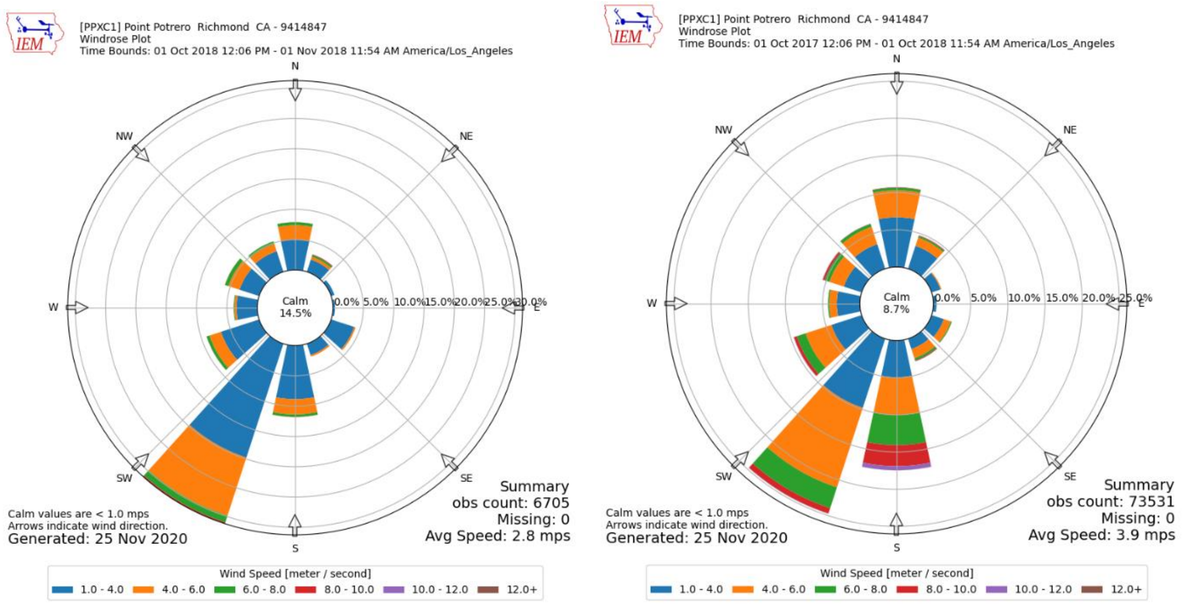

Figure 26. Wind roses for Point Potrero, Richmond, October 2018 (left) and annual, Oct 2017 - Oct 2018 (right). MPS is meters per second.

URL: https://mesonet.agron.iastate.edu/sites/dyn_windrose.phtml?station=PPXC1&network=CA_DCP

# 6 Results

Quantitative results for the main emission measurements in the Bay Area are presented in section 6.1, whereas concentration measurements in communities and along site fencelines are included in section 6.2. Section 6.3 handles results and observations for complementary emission sources in both San Joaquin valley and the Bay area.

SOF measured direct emissions of alkanes, and SkyDOAS measured direct emissions of $SO_2$, $NO_2$ and $H_2CO$. MeFTIR and MWDOAS was used to measure mass concentration ratios of methane to alkanes and BTEX to alkanes at the site fence-lines. These plume mass ratios were combined with the direct alkane flux from SOF measurements to obtain indirect emission estimates of methane and BTEX, respectively.

## 6.1 Emission measurements and gas fluxes – Bay Area

Bay Area sources were surveyed on a total of 19 days in the period 5-24 October, 2018. Primary sites were the five refinery areas located in Martinez, Benicia and Richmond along with the Richmond port area. For these sites, measurements were conducted on multiple days throughout the period, and with more repetitions compared to other sources targeted in the survey. The surveyed areas are described in Figures 12 to 17. It should be noted that the areas can comprise several facilities.

Emission measurements of alkanes, sulfur dioxide, nitrogen dioxide and formaldehyde are summarized for the five refinery areas and the Richmond port area in Table 7 and Table 8, respectively. Figure 27 shows the measured emissions of alkanes and Figure 28 and Figure 29 the corresponding for $NO_2$ and $SO_2$, respectively. Formaldehyde was generally at detection limit indicated by a "less than" mark (<) in the tables and figures.

Table 7. The overall measured emission data for the refinery areas. *Limited samples.

| **Source** | **Alkane kg/h** | **95% CI kg/h** | **$SO_2$ kg/h** | **95% CI kg/h** | **$NO_2$ kg/h** | **95% CI kg/h** | **$H_2CO$ kg/h** | **BTEX kg/h** | **$C_6H_6$ kg/h** | **$CH_4$ kg/h** |
|---|---|---|---|---|---|---|---|---|---|---|
| **Martinez E refinery area** | 151 | 140 - 161 | 60 | 30 - 90 | 69 | 60 - 79 | <5 | - | - | 54 |
| **Richmond refinery area** | 291 | 248 - 335 | 105 | 34 - 175 | 113 | 83 - 142 | <5 | 40* | 6.1* | 105 |
| **Rodeo refinery area** | 143 | 118 - 168 | 11 | 8 - 14 | 34 | 19 - 49 | <5 | 17* | 2.0* | 44 |
| **Martinez W refinery area** | 334 | 249 - 419 | 200 | 159 - 240 | 104 | 85 - 122 | <10 | 31 | 3.3 | 157 |
| **Benicia refinery area** | 144 | 124 - 165 | 20 | 15 - 25 | 84 | 66 - 102 | <5 | 12 | 1.0 | 69 |
| **SUM REFINERIES** | **1063** | | **395** | | **404** | | **-** | **100** | **12** | **430** |

Overall average emissions of 1063 kg/h of alkanes were measured for the five refinery areas. The Martinez West refinery area and Richmond refinery area were found to have emissions of 334 kg/h and 291 kg/h, respectively. Benicia, Martinez East, and Rodeo all had emissions of about 140-150 kg/h each.

The span of the 95% confidence interval for the mean as compared to the mean emission was within 35% for all sites but for Martinez West refinery (51%) where a larger variability in the measured emissions were observed.

The average alkane emission of the Richmond port area was 90 kg/h, with a 95% confidence interval span of 27%, see Table 8.

Table 8. The overall measured emission data for the Richmond port area.

| Source | Alkane kg/h | 95% CI kg/h | $SO_2$ kg/h | 95% CI kg/h | $NO_2$ kg/h | 95% CI kg/h | $H_2CO$ kg/h | BTEX kg/h | $C_6H_6$ kg/h | $CH_4$ kg/h |
|---|---|---|---|---|---|---|---|---|---|---|
| **Richmond port area** | 90 | 78 - 102 | 4 | 1.5 - 6 | 33 | 22 - 44 | <5 | 8.7 | 0.6 | 12 |

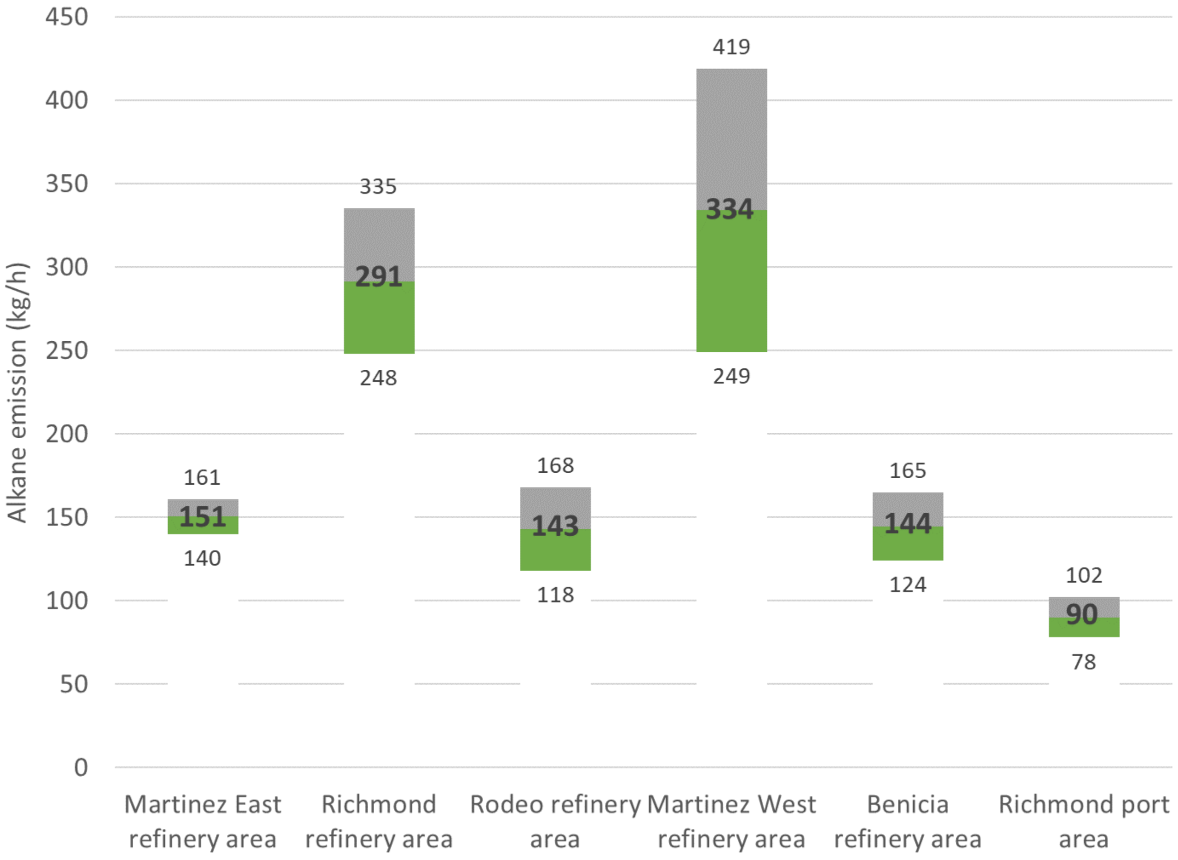

Figure 27. Measured alkane emissions (SOF) from the five refinery areas and the Richmond port area. **Mean** and 95% CI.

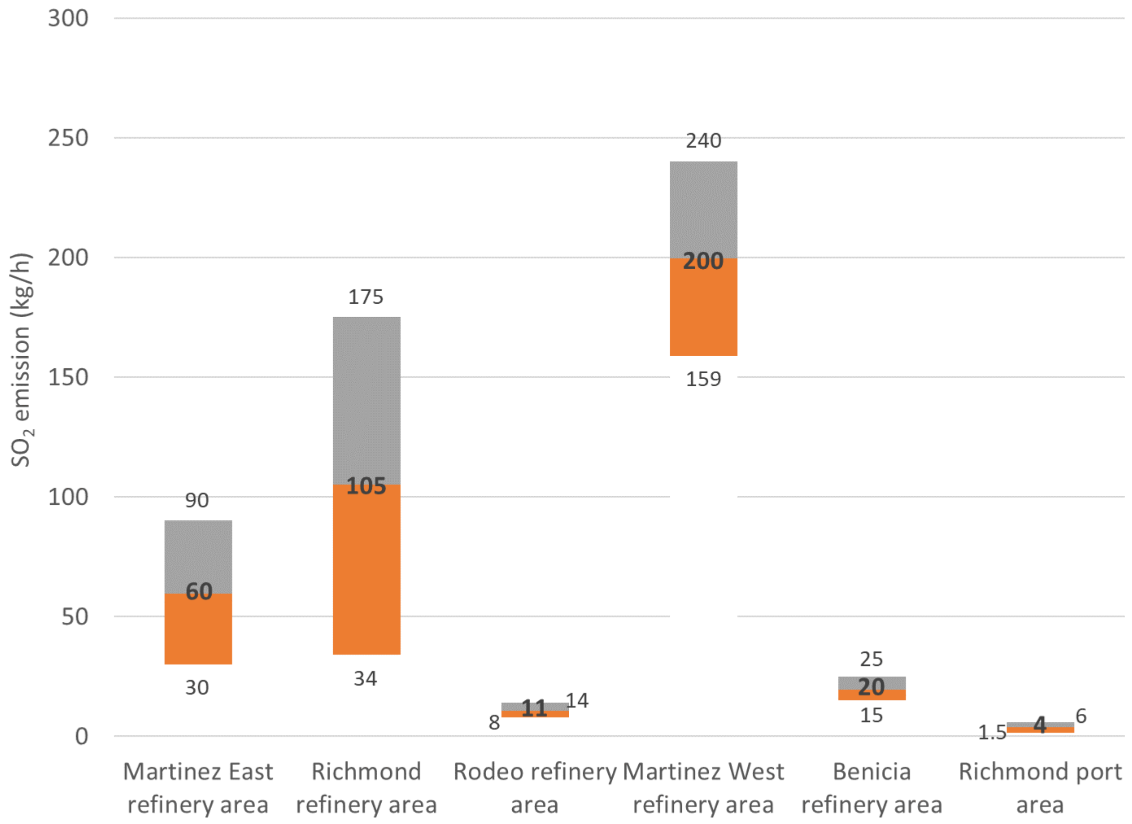

Figure 28. Measured SO$_2$ emissions (SkyDOAS) from the five refinery areas and the Richmond port area. **Mean** and 95% CI.

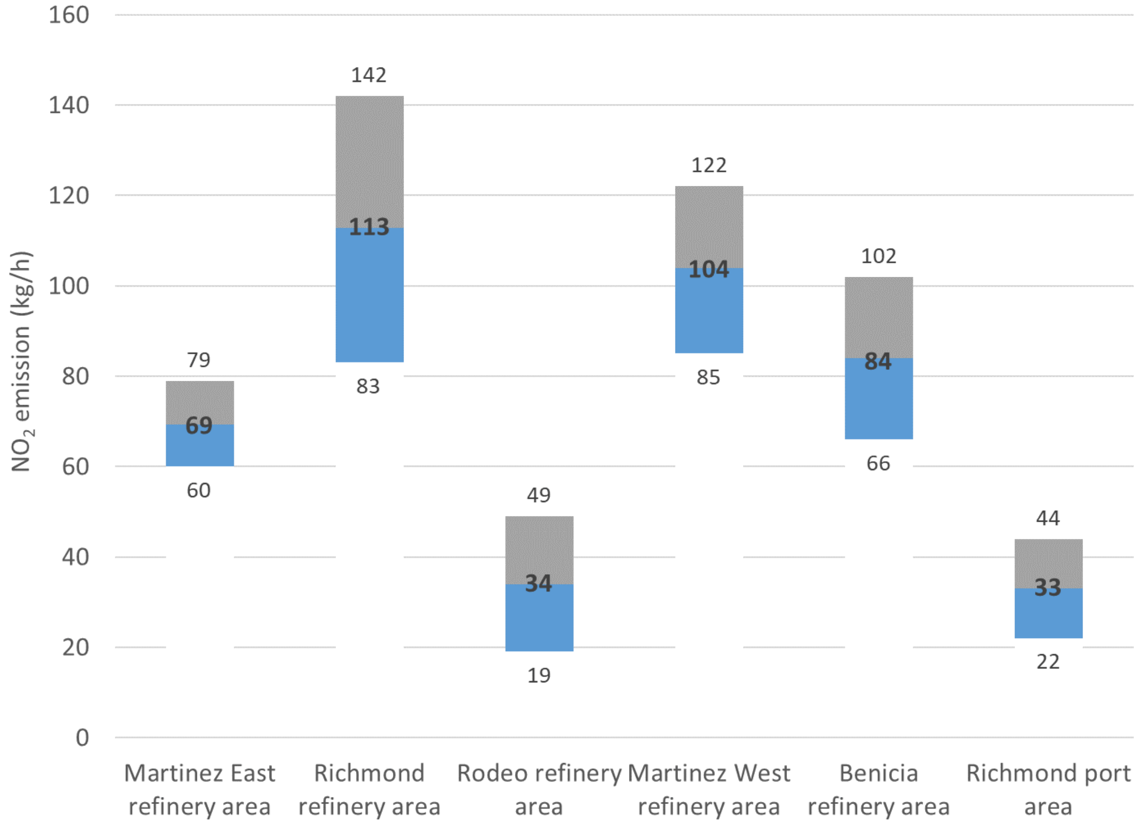

Figure 29. Measured NO$_2$ emissions (SkyDOAS) from the five refinery areas and the Richmond port area. **Mean** and 95% CI.

The overall $SO_2$ emission from the refinery areas were 395 kg/h, of which half was observed at the Martinez West refinery area. It should be noted that the Richmond refinery area comprise both the refinery area and a sulfur acid regeneration plant. As detailed in Table 12 and Table 13, the refinery part and the regeneration plant each made up about 50% of the combined, for times when the two emission plumes could be separated. However, the $SO_2$ emission from the regeneration plant showed a large span in the emissions.

For $NO_2$, the overall emissions from the refinery areas were 404 kg/h. Both for $SO_2$ and $NO_2$, Rodeo stood out with the lowest emissions, being a factor of two less than the next in order. Measurements were done at fence-line or beyond, so in terms of $NO_x$ the observed $NO_2$ emissions would constitute a lower end estimate as a fraction of the $NO_x$ would still be in the form of NO. Similar measurements in Texas showed that approximately 80 % of the NOx was present as $NO_2$ at the fenceline of the industries (Rivera et al, 2010).

The methane to alkane mass concentration ratios were measured by MeFTIR, integrating through the emission plume at ground level along the fence-line, downwind of the site areas. Figure 30 summarizes the observations. For the refinery areas, the measured $CH_4$/alkane mass ratio median were in the range 31-48 %, whereas for the Richmond port area the median ratio was 13%. The interquartile span relative the median was on average 71%.

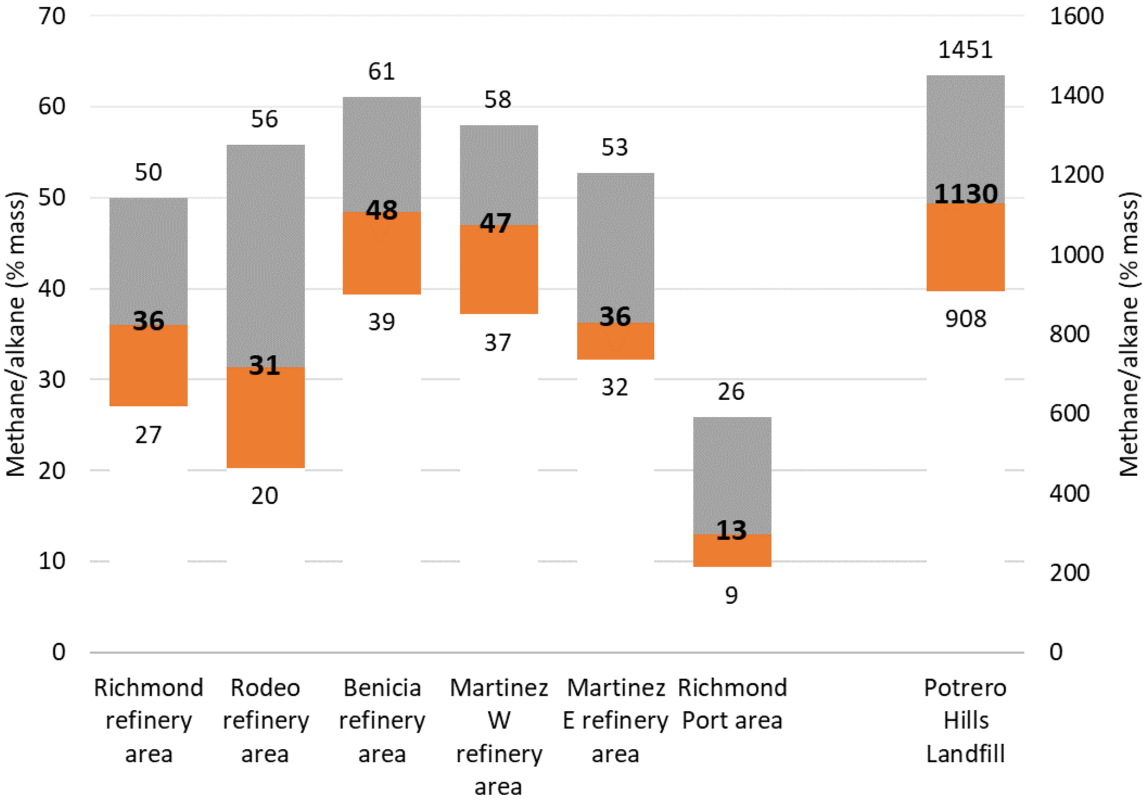

Figure 30. The relative amount of methane compared to alkanes is shown here by **median**, 25th and 75th percentile. The five refineries and the Richmond port area are plotted on the left axis while the Potrero landfill is on the right. These relative amounts are used to obtain the indirectly measured emissions of methane by multiplication with the SOF alkane emission in Figure 27.

Combining the observed methane to alkane mass ratios in Figure 30 with the measured alkane emissions by SOF (Table 7) give an indirect emission estimate for methane, Figure 31. As this is a combined measure, associated uncertainties are larger than for the direct measurements. The overall methane emission from the five refinery areas was 430 kg/h, with a span of 44-157 kg/h among the sites. The Richmond port area had a comparably lower methane emission of 12 kg/h.

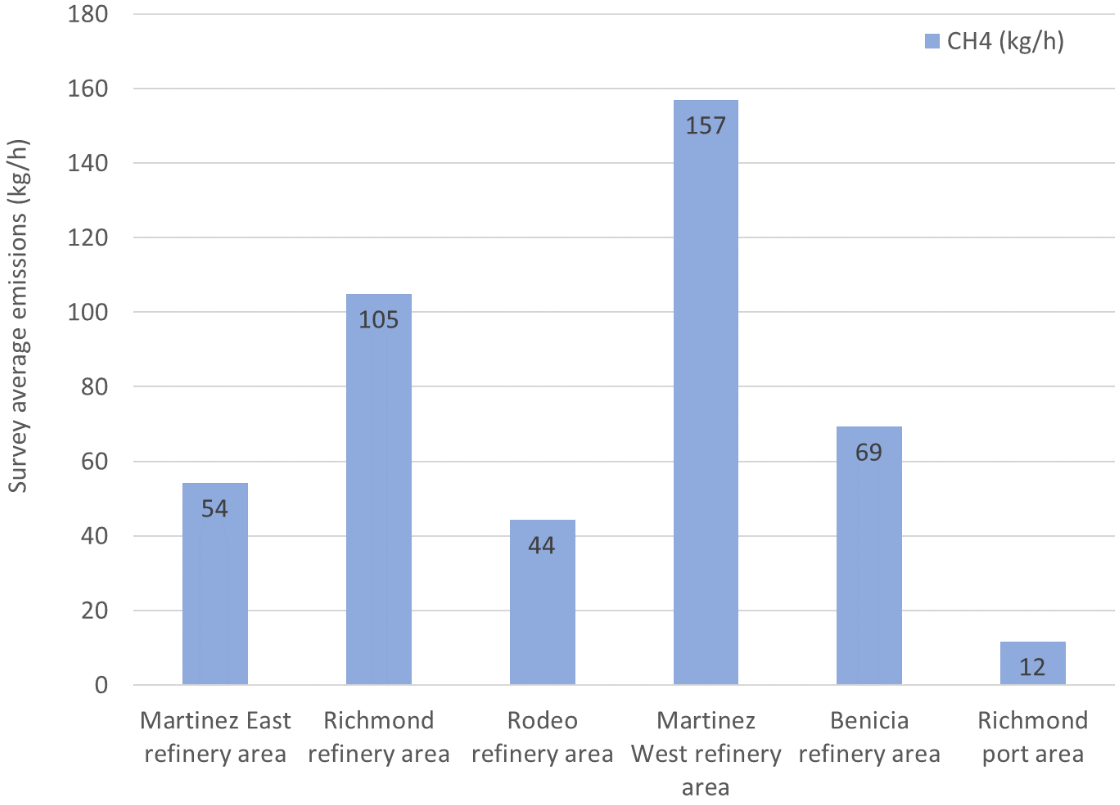

Figure 31. Methane emissions for the survey measured indirectly from the ground ratio of methane and alkanes as shown in Figure 30, multiplied with the SOF alkane emission as shown in Figure 27.

As for methane, the BTEX and benzene emissions from the main sites were obtained from mass ratios to alkanes, integrated at fence-line by MWDOAS and MeFTIR combined. The median mass ratio of the measurements at each site was then applied to the directly measured alkane emission by SOF in order to derive the BTEX and benzene emission, respectively.

The number of samples for the BTEX (and benzene) mass ratios are few, due to prevailing winds, survey duration and instrumentation priorities. This is especially true for the Richmond, Rodeo and Martinez East refinery area (missing) sites. The measured median BTEX to alkane mass ratios ranged 8.2-13.7 % for the main refinery and port sites, Figure 32 and Table 9. The corresponding range for benzene was 0.7-2.1 %, Figure 33 and Table 10.

The overall BTEX emission from four of the refinery areas was 100 kg/h, of which 12 kg/h as benzene, Table 7 and Figure 34. Benzene concentrations at fence-line were generally low, often at detection limit (~1 ppb). The Richmond port area BTEX emission was 8.7 kg/h, of which benzene 0.6 kg/h (Table 8).

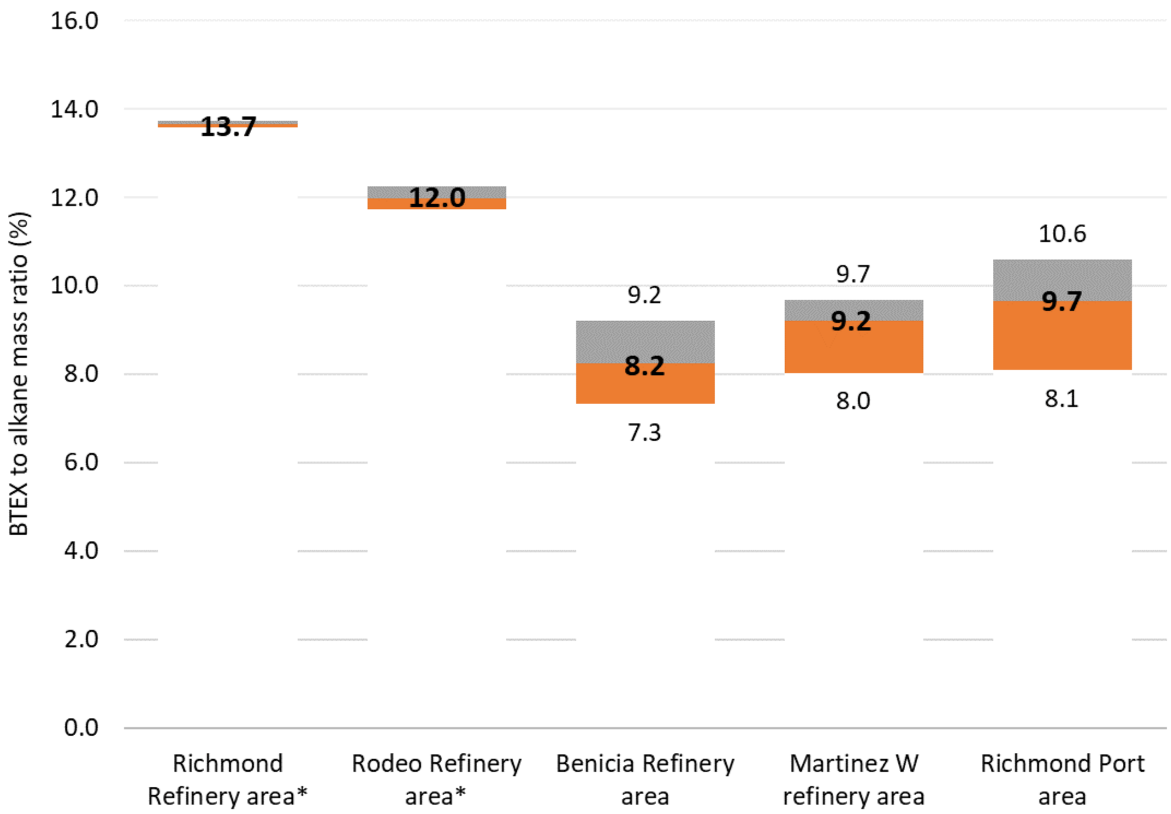

Figure 32. The relative amount of BTEX compared to alkanes is shown here by **median**, 25th and 75th percentile. These relative amounts are used to obtain the indirectly measured emissions of BTEX by multiplication with the SOF alkane emission in Figure 27. *Few measurements. (Note that data is lacking for Martinez E refinery area).

Table 9. BTEX to alkane mass ratio measurements. D = number of days, N = number of samples. *Limited samples.

| Area | D | N | 1-Quartile | Median | 3-Quartile |
|---|---|---|---|---|---|
| Richmond Refinery area* | 2 | 2 | - | **13.7** | - |
| Rodeo Refinery area* | 1 | 2 | - | **12.0** | - |
| Benicia Refinery area | 2 | 6 | 7.3 | **8.2** | 9.2 |
| Martinez W refinery area | 3 | 7 | 8.0 | **9.2** | 9.7 |
| Richmond Port area | 3 | 10 | 8.1 | **9.7** | 10.6 |

Table 10. Benzene to alkane mass ratio measurements. *Limited samples.

| Area | D | N | 1-Quartile | Median | 3-Quartile |
|---|---|---|---|---|---|
| Richmond Refinery area* | 2 | 2 | - | **2.1** | - |
| Rodeo Refinery area* | 1 | 2 | - | **1.4** | - |
| Benicia Refinery area | 2 | 8 | 0.4 | **0.7** | 1.6 |
| Martinez W refinery area | 3 | 6 | 0.5 | **1.0** | 1.6 |
| Richmond Port area | 3 | 12 | 0.5 | **0.7** | 1.3 |

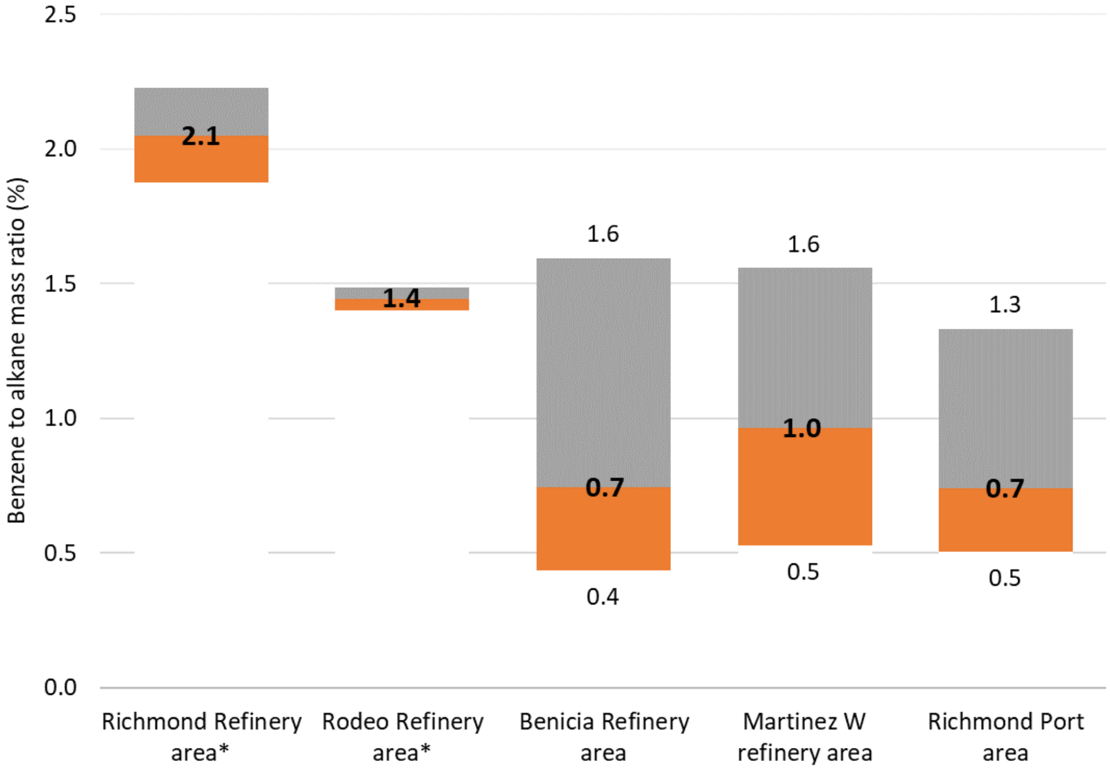

Figure 33. The relative amount of benzene compared to alkanes is shown here, **median**, 25th and 75th percentile. These relative amounts are used to obtain the indirectly measured emissions of benzene by multiplication with the SOF alkane emission in Figure 27. *Limited number of measurements. (Note that data is lacking for Martinez E refinery area).

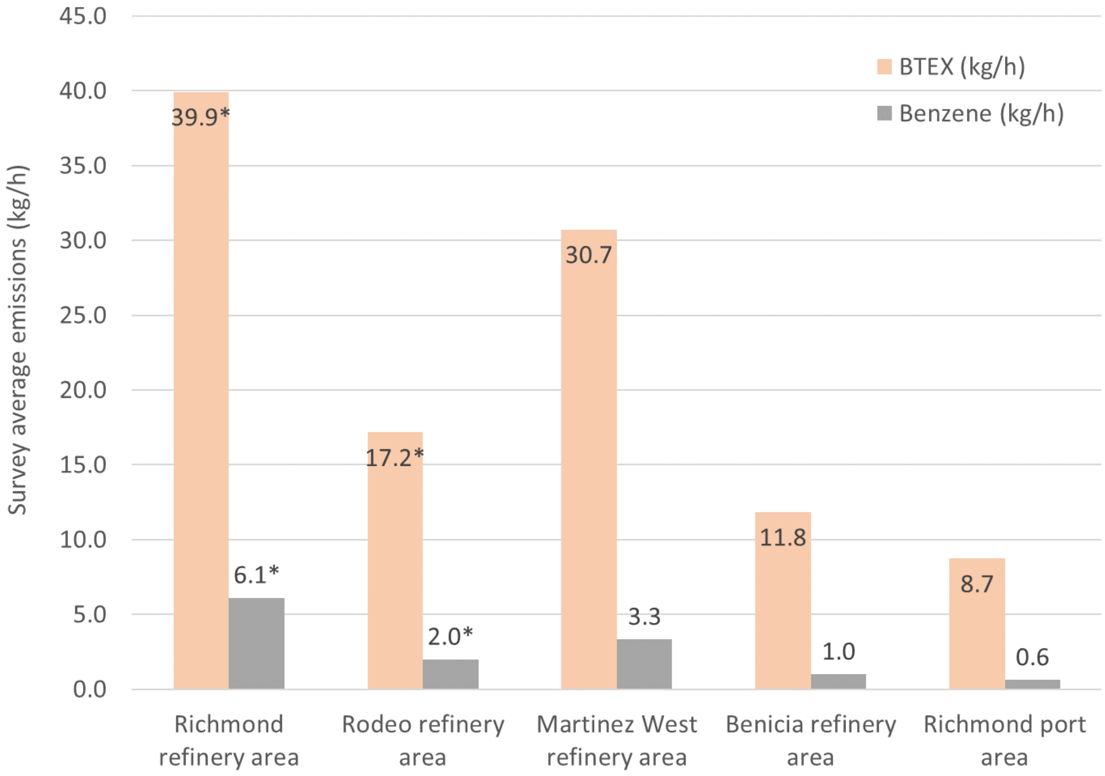

Figure 34. BTEX and benzene emissions for the survey measured indirectly from the ground ratio of BTEX (benzene, toluene, ethylbenzene and xylene) and benzene versus alkanes as shown in Figure 30, multiplied with the SOF alkane flux as shown in Figure 27. *Limited number of samples.

### 6.1.1 Richmond refinery area

Alkane emissions from the Richmond refinery area were measured on 4 days and $SO_2$, $NO_2$ and $H_2CO$ emissions were measured on 3 days. Figures 35 to 37 show examples of these measurements. Winds were generally within the SW-NW sector, and in the 2-5 m/s wind speed range during the measurements. Tables 11 to 19 summarize results from the individual survey days for the site and mean emissions and confidence intervals over the duration of the survey.

The alkane survey average emission was 291 kg/h, with a 95% CI of 248-335 kg/h, e.g. 30% relative the mean (Table 11). Three to five measurements were done on each of the four survey days, and the daily mean emission span was 249-360 kg/h, where the day with the highest mean also showed the largest daily standard deviation.

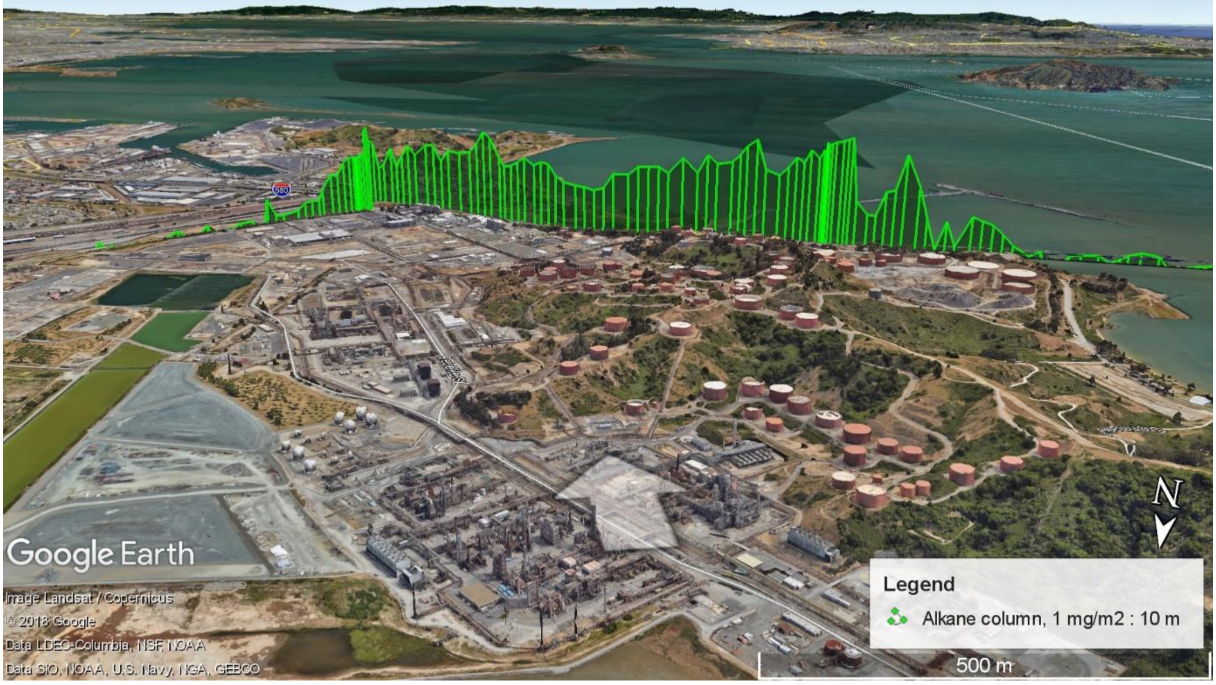

Figure 35. Example of SOF measurement of alkanes at Richmond refinery area, October 6, 2018, 11 AM Map from Google Earth™ 2019.

Emissions of $SO_2$ were measured on three days and a total of nine plume transects, Table 12. For the whole area the emission mean was 105 kg/h, with a 95% CI of 34-175 kg/h. The median emission was only 57 kg/h further emphasizing the skew emission distribution here. The Richmond refinery area, as defined, comprises both the refinery itself and a sulfuric acid regeneration plant located towards the eastern border of the area. For a subset of the measurements the emissions from the refinery part and the regeneration plant part could be separated, Table 13 and Table 14. The refinery part $SO_2$ mean was then 52 kg/h with a 95% CI of 37-68 kg/h. The regeneration plant showed much larger variability compared to the mean of 55 kg/h, with the upper end of the 95% confidence interval reaching 146 kg/h.

The $NO_2$ emissions from the whole area where less variable, with a mean emission of 113 kg/h and a 95% CI of 83-143 kg/h, based on 8 measurements over 3 days, Table 15. Formaldehyde was generally at or below detection limit and less than 5 kg/h of $H_2CO$ was concluded for the Richmond refinery area (Table 16).

Figure 36. Example of SkyDOAS $SO_2$ measurement at Richmond refinery area. Map from Google Earth™ 2019.

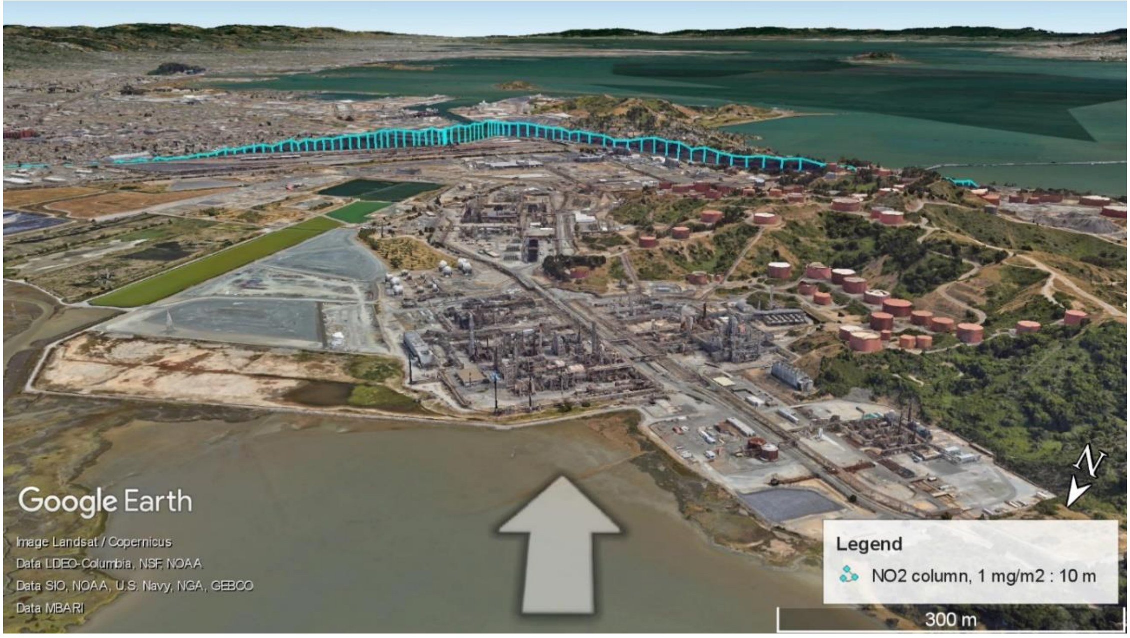

Figure 37. Example of SkyDOAS $NO_2$ measurement at Richmond refinery area. Map from Google Earth™2019.

Concentrations of methane, BTEX, and alkanes outside the facilities for determining emissions of methane and BTEX indirectly are shown in Figure 38 and Figure 39. A landfill and water treatment site are located northeast of the refinery area, and strong methane plumes were observed from this part. For occasions when the landfill/water treatment plume got mixed into the refinery plume, refinery area methane data had to be omitted. The median methane to alkane mass ratio for the refinery area plume was 36%, based on 4 days of sampling and ten observations, Table 17. Combined with the directly measured (SOF) alkane emission of 291 kg/h, the indirect methane emission obtained was 105 kg/h.

Figure 38. Concentration measurements of methane and alkanes at Richmond refinery area. Apparent vertical scale 1 m : 1 µg/m³. Map from Google Earth™ 2019.

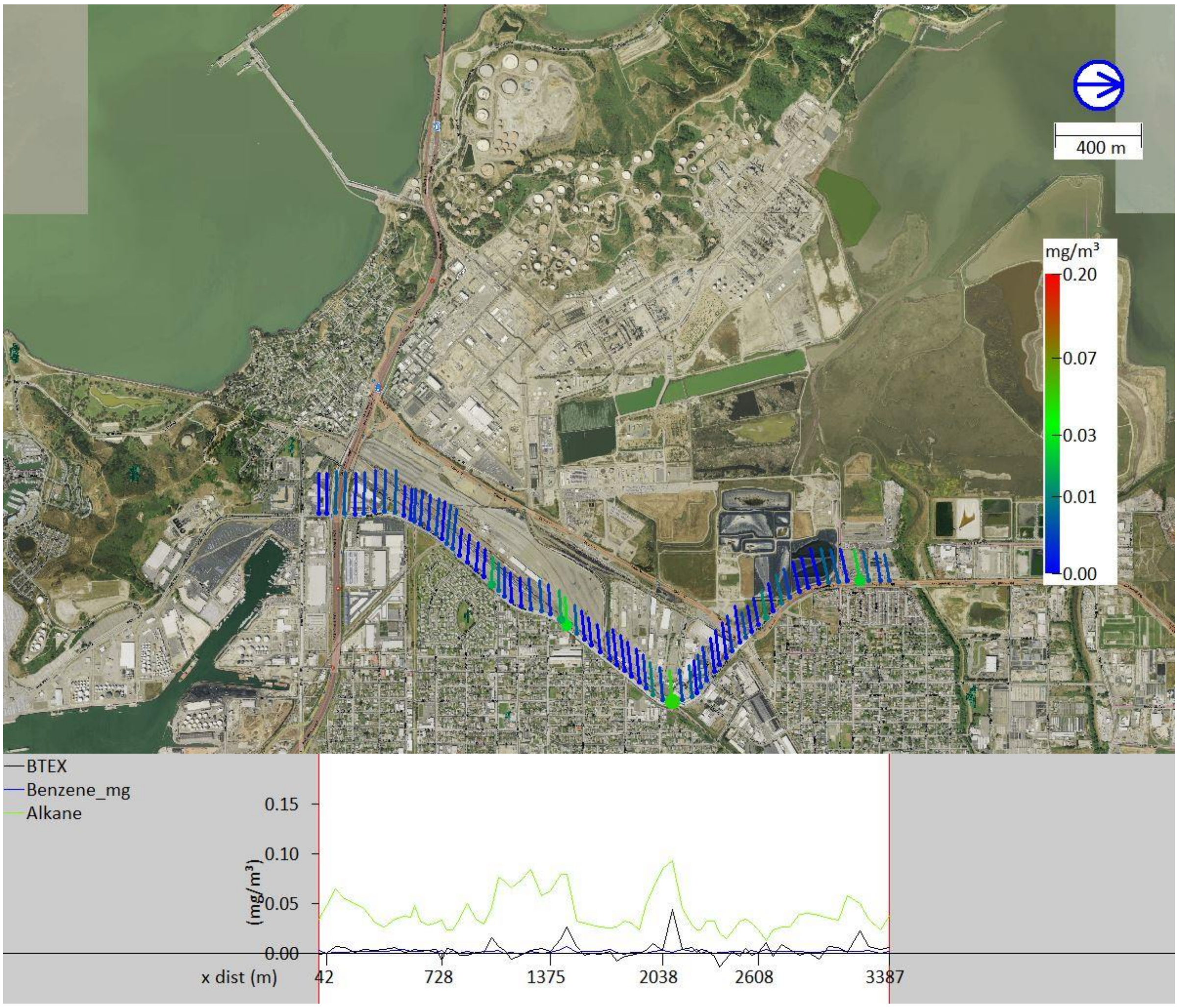

Figure 39. Concentration measurements of BTEX and alkanes at Richmond refinery area.

Table 11. Richmond refinery area, alkanes.

| Day [yymmdd] | Time span [hhmmss-hhmmss] | Num Meas | Emission avg [kg/h] | Emission SD [kg/h] | Wind Speed Min-Max [m/s] | Wind Dir Span [deg] |
|---|---|---|---|---|---|---|
| **181005** | 111422-145657 | 4 | 360 | 99.9 | 2.1-3.4 | 223-288 |
| **181006** | 100152-115259 | 4 | 329 | 48.8 | 3.3-5.0 | 314-330 |
| **181011** | 121530-152645 | 5 | 233 | 57.8 | 1.8-2.8 | 283-339 |
| **181019** | 135411-143937 | 3 | 249 | 33.1 | 1.7-2.2 | 319-355 |
| **Total # of Meas.** | | **16** | | | | |
| **Median** | | | **273.8** | | | |
| **Mean** | | | **291.4** | | | |
| **SD** | | | **81.5** | | | |
| **95% CI** | | | **248.0 - 334.9** | | | |

Table 12. Richmond refinery area, $SO_2$.

| Day [yymmdd] | Time span [hhmmss-hhmmss] | Num Meas | Emission avg [kg/h] | Emission SD [kg/h] | Wind Speed Min-Max [m/s] | Wind Dir Span [deg] |
|---|---|---|---|---|---|---|
| **181006** | 100338-115146 | 4 | 169 | 107.4 | 2.6-4.9 | 320-329 |
| **181011** | 144103-152537 | 2 | 77.3 | 35.9 | 2.5-2.8 | 296-313 |
| **181018** | 131131-145453 | 3 | 36.9 | 7.5 | 2.0-2.3 | 256-281 |
| **Total # of Meas.** | | **9** | | | | |
| **Median** | | | **57.0** | | | |
| **Mean** | | | **104.6** | | | |
| **SD** | | | **92.1** | | | |
| **95% C.I.** | | | **33.8 - 175.4** | | | |

Table 13. Richmond refinery area (sulfuric acid regen sub area), $SO_2$.

| Day [yymmdd] | Time span [hhmmss-hhmmss] | Num Meas | Emission avg [kg/h] | Emission SD [kg/h] | Wind Speed Min-Max [m/s] | Wind Dir Span [deg] |
|---|---|---|---|---|---|---|
| **181006** | 100506-110232 | 3 | 56.7 | 69.7 | 1.9-4.9 | 315-342 |
| **181011** | 141523-141635 | 1 | 50.3 | N/A | 3.1-3.1 | 322-322 |
| **Total # of Meas.** | | **4** | | | | |
| **Median** | | | **35.9** | | | |
| **Mean** | | | **55.1** | | | |
| **SD** | | | **57.0** | | | |
| **95% C.I.** | | | **-35.7 - 145.8** | | | |

Table 14. Richmond refinery area (except sulfuric acid regen sub area), $SO_2$.

| Day [yymmdd] | Time span [hhmmss-hhmmss] | Num Meas | Emission avg [kg/h] | Emission SD [kg/h] | Wind Speed Min-Max [m/s] | Wind Dir Span [deg] |
|---|---|---|---|---|---|---|
| **181006** | 100454-114808 | 4 | 70.5 | 13.0 | 2.7-4.8 | 316-329 |
| **181011** | 144103-152537 | 2 | 37.3 | 16.5 | 2.6-2.8 | 309-321 |
| **181018** | 131131-145357 | 3 | 37.5 | 4.1 | 2.0-2.4 | 256-282 |
| **Total # of Meas.** | | **9** | | | | |
| **Median** | | | **49.0** | | | |
| **Mean** | | | **52.1** | | | |
| **SD** | | | **20.1** | | | |
| **95% CI** | | | **36.6 - 67.6** | | | |

Table 15. Richmond refinery area, $NO_2$.

| Day [yymmdd] | Time span [hhmmss-hhmmss] | Num Meas | Emission avg [kg/h] | Emission SD [kg/h] | Wind Speed Min-Max [m/s] | Wind Dir Span [deg] |
|---|---|---|---|---|---|---|
| **181006** | 100514-115031 | 4 | 140 | 24.4 | 2.5-4.5 | 314-332 |
| **181011** | 143809-152601 | 2 | 103 | 2.3 | 2.6-2.8 | 294-314 |
| **181018** | 131122-134041 | 2 | 68.7 | 0.4 | 2.0-2.3 | 257-270 |
| **Total # of Meas.** | | **8** | | | | |
| **Median** | | | **109.0** | | | |
| **Mean** | | | **112.9** | | | |
| **SD** | | | **35.4** | | | |
| **95% CI** | | | **83.3 - 142.5** | | | |

Table 16. Richmond refinery area, $H_2CO$.

| Day [yymmdd] | Time span [hhmmss-hhmmss] | Num Meas | Emission avg [kg/h] | Emission SD [kg/h] | Wind Speed Min-Max [m/s] | Wind Dir Span [deg] |
|---|---|---|---|---|---|---|
| **181006** | 110148-115042 | 2 | 3.4 | 1.8 | 4.0-4.6 | 318-331 |
| **181011** | 144327-152601 | 2 | 2.9 | 0.5 | 2.6-2.8 | 309-314 |
| **181018** | 131240-145654 | 3 | 1.7 | 1.5 | 1.9-2.3 | 255-270 |
| **Total # of Meas.** | | **7** | | | | |
| **Median** | | | **<5** | | | |
| **Mean** | | | **<5** | | | |

Table 17. Richmond refinery area, Methane/Alkane mass ratios.

| Day [yymmdd] | Time span [hhmmss-hhmmss] | Num Meas | Mass Ratio avg [%] | Mass Ratio SD [%] | Wind Speed Min-Max [m/s] | Wind Dir Span [deg] |
|---|---|---|---|---|---|---|
| **181005** | 111822-145537 | 4 | 36.8 | 13.9 | 2.1-4.0 | 208-297 |
| **181006** | 100314-115450 | 3 | 29.6 | 10.2 | 2.1-4.8 | 318-332 |
| **181011** | 125658-130517 | 1 | 56.7 | N/A | 2.7-2.7 | 336-336 |
| **181023** | 194002-201058 | 2 | 42.9 | 16.8 | 4.0-4.1 | 266-302 |
| **Total # of Meas.** | | **10** | | | | |
| **Median** | | | **36.0** | | | |
| **IQR** | | | **27.0 - 50.0** | | | |
| **Mean** | | | **37.8** | | | |
| **SD** | | | **13.7** | | | |

Table 18. Richmond refinery area, BTEX/Alkane mass ratios.

| Day [yymmdd] | Time span [hhmmss-hhmmss] | Num Meas | Mass Ratio avg [%] | Mass Ratio SD [%] | Wind Speed Min-Max [m/s] | Wind Dir Span [deg] |
|---|---|---|---|---|---|---|
| **181011** | 130329-130841 | 1 | 13.5 | N/A | 3.2-3.2 | 336-336 |
| **181023** | 193813-194554 | 1 | 13.8 | N/A | 4.3-4.3 | 267-267 |
| **Total # of Meas.** | | **2** | | | | |
| **Median** | | | **13.7** | | | |
| **Mean** | | | **13.7** | | | |
| **SD** | | | **0.2** | | | |

Table 19. Richmond refinery area, Benzene/Alkane mass ratios.

| Day [yymmdd] | Time span [hhmmss-hhmmss] | Num Meas | Mass Ratio avg [%] | Mass Ratio SD [%] | Wind Speed Min-Max [m/s] | Wind Dir Span [deg] |
|---|---|---|---|---|---|---|
| **181011** | 125151-125614 | 1 | 1.7 | N/A | 1.8-1.8 | 359-359 |
| **181023** | 193813-194502 | 1 | 2.4 | N/A | 4.2-4.2 | 266-266 |
| **Total # of Meas.** | | **2** | | | | |
| **Median** | | | **2.1** | | | |
| **Mean** | | | **2.1** | | | |
| **SD** | | | **0.5** | | | |

### *6.1.2 Rodeo refinery area*

Alkane and $SO_2$ emissions from the Rodeo refinery area were measured on 2 days, $NO_2$ and $H_2CO$ emissions on 3 days. Winds were in the 1.5-8 m/s from west for all measurements here. This wind direction worked well for assessing the emissions for the refinery area, but for the tank farm east of Hwy 80, so presented results are excluding this tank farm part. Tables 20 to Table 26 summarize results from the individual survey days for the site and mean emissions and confidence intervals over the duration of the survey.

The alkane survey average emission was 143 kg/h, with a 95% CI of 118-168 kg/h, e.g. 35% relative the mean (Table 20). Six to eleven measurements were done on each of the two survey days, and the daily mean emission span was very confined, 141-146 kg/h. Figure 40 shows a SOF transect at Rodeo on October 6. One can see some contribution from tank farms at the edges, although the core of the plume seems to originate from the central part of the refinery area.

Figure 41 and 42 show examples of $SO_2$ and $NO_2$ measurements, respectively. $SO_2$ were at or near detection limits, with a mean of 11 kg/h (Table 21). The NO2 survey mean emission was 34 kg/h, Table 22. The formaldehyde emissions were at or below detection limit, with less than 5 kg/h being emitted, Table 23.

Concentrations of methane, BTEX, and alkanes outside the facilities for determining emissions of methane and BTEX indirectly are shown in Figures 43 and Figure 44. The tank storage area at the north end of the site shows some indication of enhanced methane emissions relative to the site as a whole (Figure 45). This is a separate facility from the refinery. However, its emissions cannot be separated from the area as a whole from publicly accessible roads.

The median methane to alkane mass ratio was 36%, based on 4 days of sampling and seventeen observations, Table 24. Combined with the directly measured (SOF) alkane emission of 143 kg/h, the indirect methane emission obtained was 44 kg/h.

For BTEX and benzene specifically, the emissions were estimated at 17 and 2 kg/h, respectively. As noted in Table 25 and Table 26, samples are few and uncertainties therefore larger here.

Figure 40. Example of SOF measurement at Rodeo refinery area, October 6, 2018, 11 AM Map from Google Earth™ 2019.

Figure 41. Example of SkyDOAS $SO_2$ measurement at Rodeo refinery area. Map from Google Earth™ 2019.

Figure 42. Example of SkyDOAS $NO_2$ measurement at Rodeo refinery area. Map from Google Earth™ 2019.

Figure 43. Concentration measurements of methane and alkanes at Rodeo refinery area. Apparent vertical scale 1 m : 1 µg/m³. Map from Google Earth™ 2019.

Figure 44. Concentration measurements of BTEX and alkanes at Rodeo refinery area.

Table 20. Rodeo refinery area, alkanes.

| Day [yymmdd] | Time span [hhmmss-hhmmss] | Num Meas | Emission avg [kg/h] | Emission SD [kg/h] | Wind Speed Min-Max [m/s] | Wind Dir Span [deg] |
|---|---|---|---|---|---|---|
| **181012** | 123713-154536 | 11 | 141 | 57.4 | 1.6-2.6 | 258-295 |
| **181014** | 135140-152110 | 6 | 146 | 28.2 | 1.9-2.3 | 293-308 |
| **Total # of Meas.** | | **17** | | | | |
| **Median** | | | **123.9** | | | |
| **Mean** | | | **143.0** | | | |
| **SD** | | | **48.1** | | | |
| **95% CI** | | | **118.3 - 167.8** | | | |

Table 21. Rodeo refinery area, $SO_2$.

| Day [yymmdd] | Time span [hhmmss-hhmmss] | Num Meas | Emission avg [kg/h] | Emission SD [kg/h] | Wind Speed Min-Max [m/s] | Wind Dir Span [deg] |
|---|---|---|---|---|---|---|
| **181006** | 121308-132753 | 4 | 10.0 | 3.7 | 5.1-8.2 | 309-309 |
| **181014** | 132957-152057 | 5 | 11.3 | 4.9 | 1.4-2.4 | 286-317 |
| **Total # of Meas.** | | **9** | | | | |
| **Median** | | | **9.2** | | | |
| **Mean** | | | **10.7** | | | |
| **SD** | | | **4.2** | | | |
| **95% CI** | | | **7.5 - 13.9** | | | |

Table 22. Rodeo refinery area, $NO_2$.

| Day [yymmdd] | Time span [hhmmss-hhmmss] | Num Meas | Emission avg [kg/h] | Emission SD [kg/h] | Wind Speed Min-Max [m/s] | Wind Dir Span [deg] |
|---|---|---|---|---|---|---|
| **181006** | 121308-132652 | 4 | 58.0 | 18.9 | 5.1-8.2 | 309-309 |
| **181012** | 121602-124000 | 3 | 24.1 | 8.5 | 1.6-1.9 | 274-278 |
| **181014** | 132936-151117 | 4 | 17.4 | 7.8 | 1.5-2.3 | 285-326 |
| **Total # of Meas.** | | **11** | | | | |
| **Median** | | | **27.0** | | | |
| **Mean** | | | **34.0** | | | |
| **SD** | | | **22.6** | | | |
| **95% CI** | | | **18.8 - 49.1** | | | |

Table 23. Rodeo refinery area, $H_2CO$.

| Day [yymmdd] | Time span [hhmmss-hhmmss] | Num Meas | Emission avg [kg/h] | Emission SD [kg/h] | Wind Speed Min-Max [m/s] | Wind Dir Span [deg] |
|---|---|---|---|---|---|---|
| **181006** | 131143-132652 | 3 | 4.2 | 0.6 | 7.6-8.2 | 309-309 |
| **181012** | 121503-124000 | 3 | 2.0 | 1.0 | 1.5-2.0 | 274-277 |
| **181014** | 132936-151146 | 4 | 3.7 | 2.2 | 1.5-2.4 | 285-313 |
| **Total # of Meas.** | | **10** | | | | |
| **Median** | | | **<5** | | | |
| **Mean** | | | **<5** | | | |

Table 24. Rodeo refinery area, Methane/Alkane ratio.

| Day [yymmdd] | Time span [hhmmss-hhmmss] | Num Meas | Mass Ratio avg [%] | Mass Ratio SD [%] | Wind Speed Min-Max [m/s] | Wind Dir Span [deg] |
|---|---|---|---|---|---|---|
| **181006** | 131119-131859 | 2 | 39.7 | 34.4 | 6.0-6.1 | 294-295 |
| **181012** | 121415-154508 | 10 | 31.4 | 16.4 | 1.4-3.5 | 238-336 |
| **181014** | 142135-152016 | 3 | 59.2 | 5.4 | 2.1-2.4 | 287-295 |
| **181023** | 142116-144155 | 2 | 21.6 | 13.9 | 3.0-4.7 | 294-297 |
| **Total # of Meas.** | | **17** | | | | |
| **Median** | | | **31.4** | | | |
| **IQR** | | | **20.3 - 55.8** | | | |
| **Mean** | | | **36.1** | | | |
| **SD** | | | **19.6** | | | |

Table 25. Rodeo refinery area, BTEX/Alkane mass ratios.

| Day [yymmdd] | Time span [hhmmss-hhmmss] | Num Meas | Mass Ratio avg [%] | Mass Ratio SD [%] | Wind Speed Min-Max [m/s] | Wind Dir Span [deg] |
|---|---|---|---|---|---|---|
| **181012** | 152111-153944 | 2 | 12.0 | 0.7 | 1.8-2.0 | 252-264 |
| **Total # of Meas.** | | **2** | | | | |
| **Median** | | | **12.0** | | | |
| **Mean** | | | **12.0** | | | |
| **SD** | | | **0.7** | | | |

Table 26. Rodeo refinery area, Benzene/Alkane mass ratios.

| Day [yymmdd] | Time span [hhmmss-hhmmss] | Num Meas | Mass Ratio avg [%] | Mass Ratio SD [%] | Wind Speed Min-Max [m/s] | Wind Dir Span [deg] |
|---|---|---|---|---|---|---|
| **181012** | 152111-153920 | 2 | 1.4 | 0.1 | 1.8-1.8 | 243-252 |
| **Total # of Meas.** | | **2** | | | | |
| **Median** | | | **1.4** | | | |
| **Mean** | | | **1.4** | | | |
| **SD** | | | **0.1** | | | |

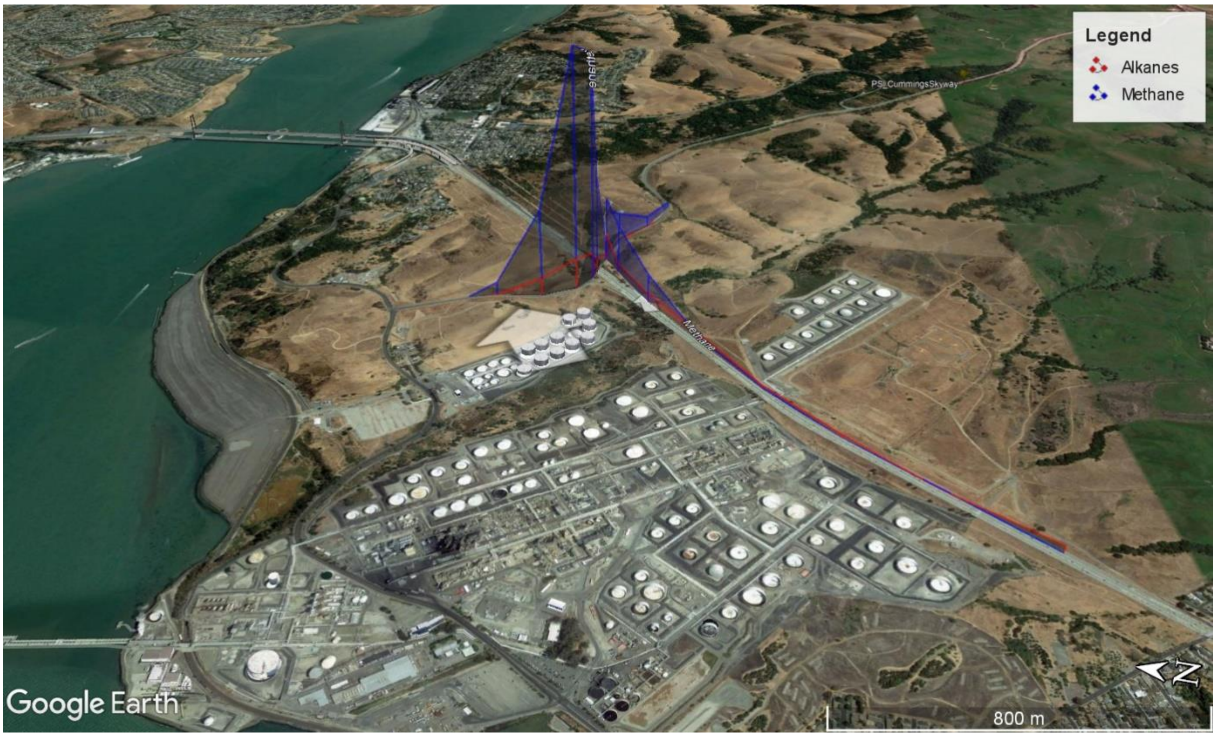

Figure 45. Concentration measurements of methane and alkanes at Rodeo refinery area, showing typical and temporary increase in methane emissions in the vicinity of the tank park to the north of the site. Apparent vertical scale 1 m : 1 µg/m³. Map from Google Earth™ 2019.

### 6.1.3 Martinez W refinery area

Alkane emissions from the Martinez W refinery area were measured on 4 days. $SO_2$ and $NO_2$ emissions were measured on 3 days, while $H_2CO$ could be sampled on two days. Wind speed for the survey days was in the 2-10 m/s range, and the site was measured with both north-easterly and westerly winds. Tables 27 to Table 33 summarize results from the individual survey days for the site and mean emissions and confidence intervals over the duration of the survey.

The alkane survey average emission was 334 kg/h, with a 95% CI of 249-419 kg/h, e.g. 51% relative the mean (Table 27). Figure 46 shows an alkane measurement with SOF on October 6, 2018. One of the days (October 15) showed comparably large variability in the emissions.

Figure 47 to 48 show examples of $SO_2$ and $NO_2$ measurements. For $SO_2$ the mean emission based on 14 measurements were 200 kg/h, with a 95% CI of 159-240 kg/h (Table 28). Corresponding for $NO_2$ was 104 kg/h (95% CI 85-122 kg/h) based on 13 measurements (Table 29). Formaldehyde emissions were generally at or below detection limit and set to less than 10 kg/h, Table 30.

Concentrations of methane, BTEX, and alkanes outside the facilities for determining emissions of methane and BTEX are shown in Figures 49 and 50. The median methane to alkane mass ratio was 47%, based on 5 days of sampling and seventeen observations, Table 31. Combined with the directly measured (SOF) alkane emission of 334 kg/h, the indirect methane emission obtained was 157 kg/h.

For BTEX and benzene specifically the indirectly measured emission was 31 and 3 kg/h, respectively, based on a BTEX to alkane mass ratio of 9.2% and benzene to alkane mass ratio of 1.0%, Table 32 and Table 33.

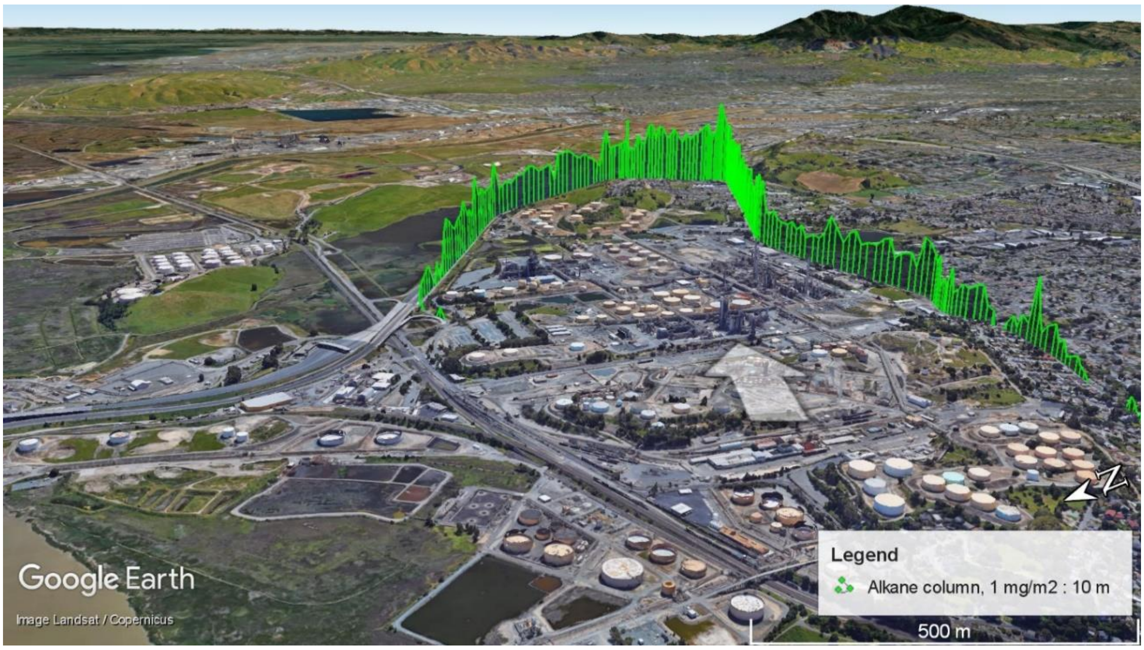

Figure 46. Example of SOF measurement at Martinez W refinery area, October 6, 2018, 11 AM. Map from Google Earth™ 2019.

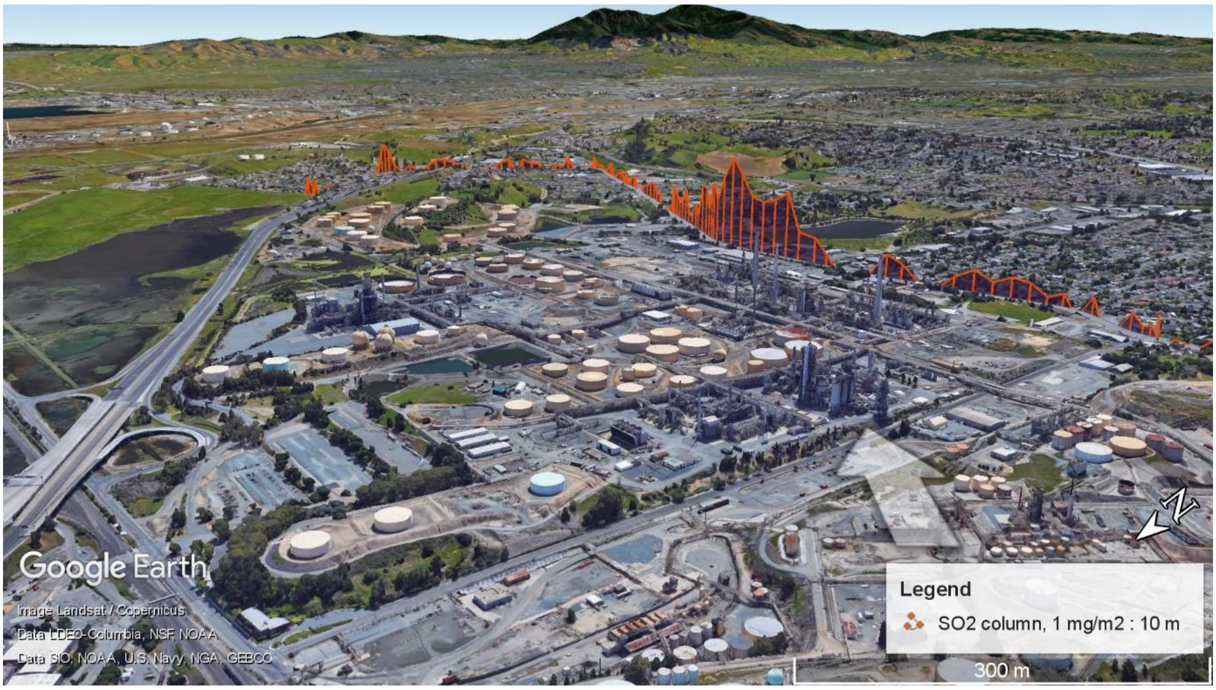

Figure 47. Example of SkyDOAS $SO_2$ measurement at Martinez W refinery area. Map from Google Earth™ 2019.

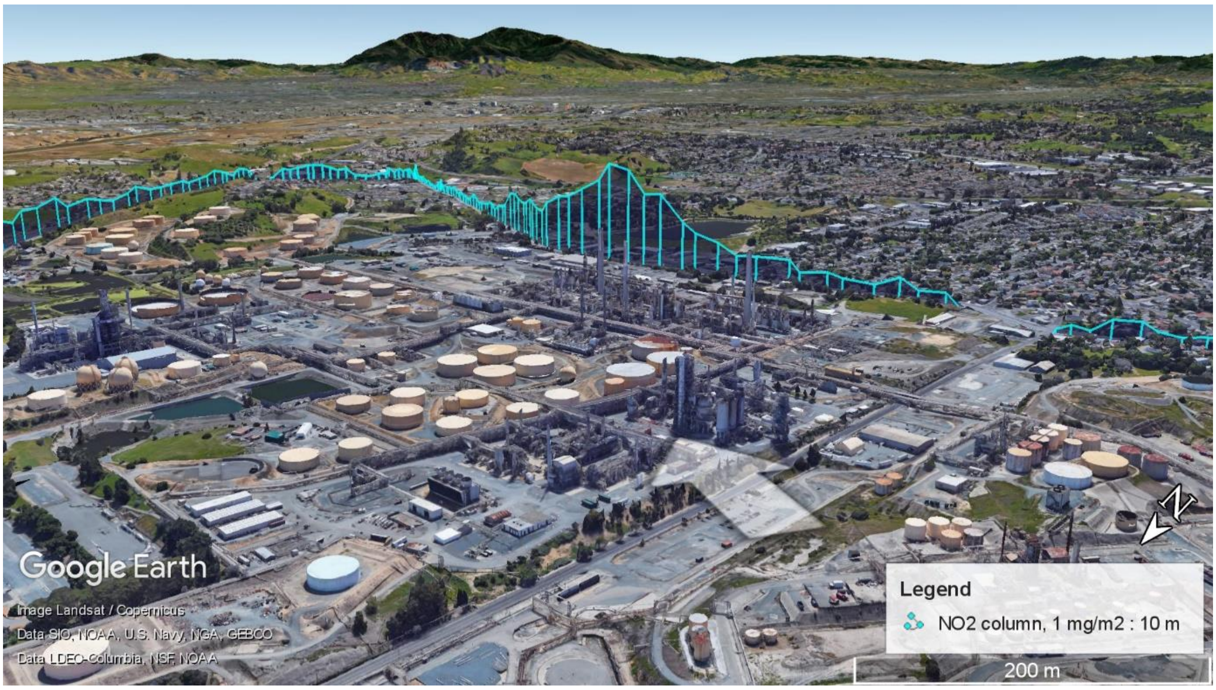

Figure 48. Example of SkyDOAS $NO_2$ measurement at Martinez W refinery area. Map from Google Earth™ 2019.

Figure 49. Concentration measurements of $CH_4$ and alkanes at Martinez W refinery area. Map from Google Earth™ 2019.

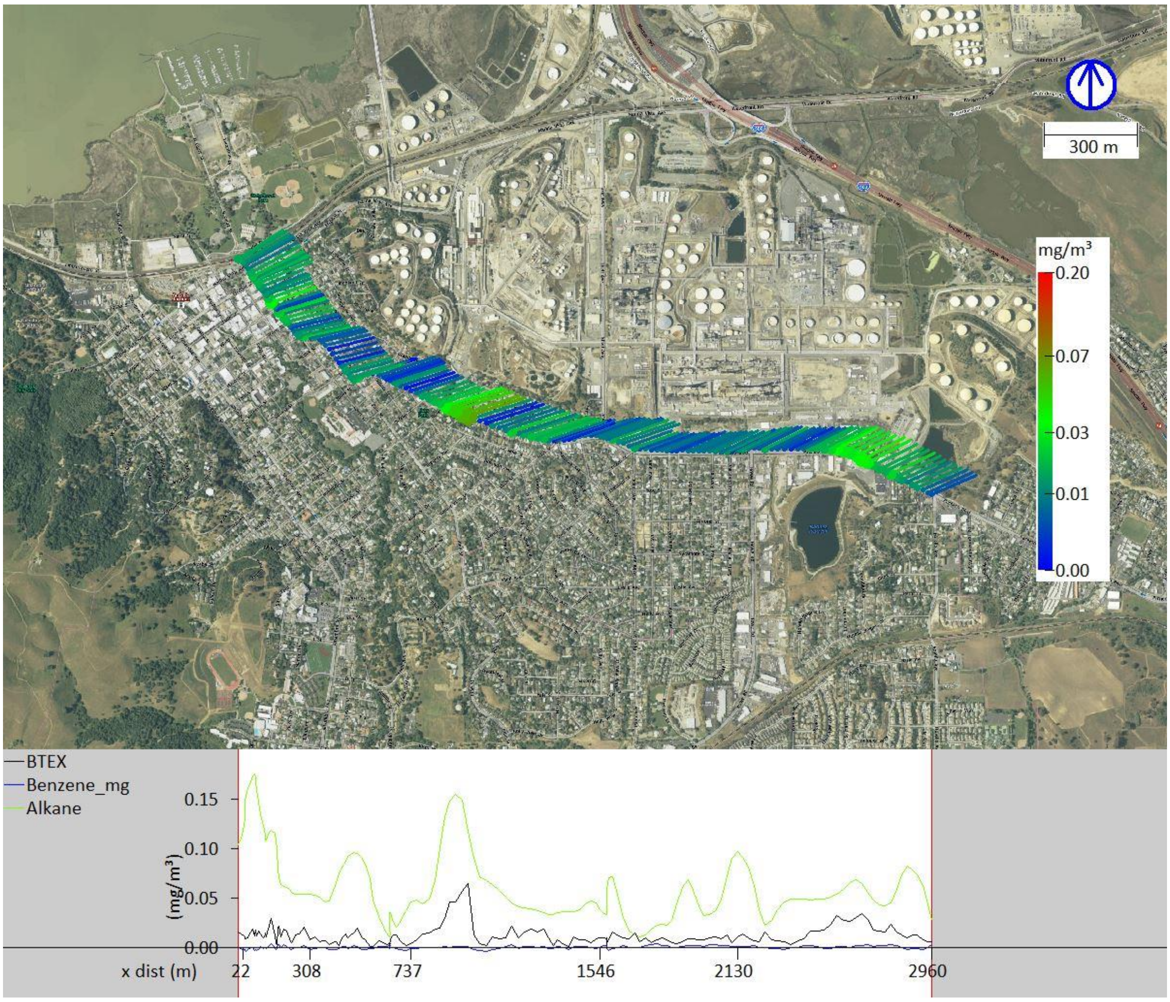

Figure 50. Concentration measurements of BTEX and alkanes at Martinez W refinery area.

Table 27. Martinez W refinery area, alkanes.

| Day [yymmdd] | Time span [hhmmss-hhmmss] | Num Meas | Emission avg [kg/h] | Emission SD [kg/h] | Wind Speed Min-Max [m/s] | Wind Dir Span [deg] |
|---|---|---|---|---|---|---|
| **181007** | 151854-152756 | 1 | 451 | N/A | 9.9-9.9 | 38-38 |
| **181010** | 115656-154146 | 4 | 253 | 37.2 | 5.9-8.1 | 274-308 |
| **181013** | 112531-153727 | 7 | 392 | 198.9 | 1.9-4.1 | 271-293 |
| **181015** | 113450-132523 | 3 | 269 | 86.8 | 4.9-7.6 | 61-73 |
| **Total # of Meas.** | | **15** | | | | |
| **Median** | | | **294.5** | | | |
| **Mean** | | | **334.0** | | | |
| **SD** | | | **154.3** | | | |
| **95% CI** | | | **248.5 - 419.4** | | | |

Table 28. Martinez W refinery area, $SO_2$.

| Day [yymmdd] | Time span [hhmmss-hhmmss] | Num Meas | Emission avg [kg/h] | Emission SD [kg/h] | Wind Speed Min-Max [m/s] | Wind Dir Span [deg] |
|---|---|---|---|---|---|---|
| **181007** | 125936-162926 | 6 | 198 | 37.0 | 8.8-10.2 | 16-40 |
| **181013** | 124403-155106 | 7 | 213 | 90.3 | 3.6-6.5 | 284-293 |
| **181023** | 110944-112241 | 1 | 116 | N/A | 5.4-5.4 | 308-308 |
| **Total # of Meas.** | | **14** | | | | |
| **Median** | | | **187.1** | | | |
| **Mean** | | | **199.7** | | | |
| **SD** | | | **70.1** | | | |
| **95% CI** | | | **159.2 - 240.2** | | | |

Table 29. Martinez W refinery area, $NO_2$.

| Day [yymmdd] | Time span [hhmmss-hhmmss] | Num Meas | Emission avg [kg/h] | Emission SD [kg/h] | Wind Speed Min-Max [m/s] | Wind Dir Span [deg] |
|---|---|---|---|---|---|---|
| **181007** | 125936-163014 | 5 | 97.4 | 14.8 | 8.8-10.4 | 16-38 |
| **181013** | 124409-155026 | 7 | 114 | 36.8 | 3.6-6.5 | 285-293 |
| **181023** | 104416-105040 | 1 | 65.6 | N/A | 2.2-2.2 | 265-265 |
| **Total # of Meas.** | | **13** | | | | |
| **Median** | | | **96.3** | | | |
| **Mean** | | | **103.9** | | | |
| **SD** | | | **30.8** | | | |
| **95% CI** | | | **85.3 - 122.5** | | | |

Table 30. Martinez W refinery area, $H_2CO$.

| Day [yymmdd] | Time span [hhmmss-hhmmss] | Num Meas | Emission avg [kg/h] | Emission SD [kg/h] | Wind Speed Min-Max [m/s] | Wind Dir Span [deg] |
|---|---|---|---|---|---|---|
| **181007** | 125936-160031 | 4 | 4.2 | 3.3 | 6.2-10.1 | 16-38 |
| **181013** | 124418-155110 | 7 | 11.7 | 18.5 | 3.0-6.5 | 284-297 |
| **Total # of Meas.** | | **11** | | | | |
| **Median** | | | **<10** | | | |
| **Mean** | | | **<10** | | | |

Table 31. Martinez W refinery area, methane/alkane ratios.

| Day [yymmdd] | Time span [hhmmss-hhmmss] | Num Meas | Mass Ratio avg [%] | Mass Ratio SD [%] | Wind Speed Min-Max [m/s] | Wind Dir Span [deg] |
|---|---|---|---|---|---|---|
| **181007** | 162537-163013 | 1 | 55.8 | N/A | 10.0-10.0 | 31-31 |
| **181010** | 144810-162557 | 4 | 66.4 | 34.9 | 6.1-8.3 | 263-287 |
| **181014** | 083409-101309 | 4 | 48.0 | 9.0 | 4.5-5.1 | 258-298 |
| **181015** | 114216-130310 | 3 | 31.2 | 6.3 | 4.4-7.0 | 68-74 |
| **181023** | 111910-130910 | 5 | 45.9 | 23.1 | 3.1-5.0 | 269-296 |
| **Total # of Meas.** | | **17** | | | | |
| **Median** | | | **47.0** | | | |
| **IQR** | | | **37.2 - 58.0** | | | |
| **Mean** | | | **49.2** | | | |
| **SD** | | | **22.9** | | | |

Table 32. Martinez W refinery area, BTEX/alkane mass ratios.

| Day [yymmdd] | Time span [hhmmss-hhmmss] | Num Meas | Mass Ratio avg [%] | Mass Ratio SD [%] | Wind Speed Min-Max [m/s] | Wind Dir Span [deg] |
|---|---|---|---|---|---|---|
| **181010** | 115617-162855 | 3 | 8.9 | 0.9 | 5.8-7.4 | 256-310 |
| **181014** | 083232-085132 | 1 | 14.9 | N/A | 4.5-4.5 | 261-261 |
| **181015** | 114218-130542 | 3 | 7.5 | 2.6 | 4.5-7.0 | 70-73 |
| **Total # of Meas.** | | **7** | | | | |
| **Median** | | | **9.2** | | | |
| **IQR** | | | **8.0 - 9.7** | | | |
| **Mean** | | | **9.2** | | | |
| **SD** | | | **3.1** | | | |

Table 33. Martinez W refinery area, benzene/alkane mass ratios.

| Day [yymmdd] | Time span [hhmmss-hhmmss] | Num Meas | Mass Ratio avg [%] | Mass Ratio SD [%] | Wind Speed Min-Max [m/s] | Wind Dir Span [deg] |
|---|---|---|---|---|---|---|
| **181010** | 115617-145214 | 2 | 0.62 | 0.3 | 6.4-6.8 | 287-310 |
| **181014** | 083232-085132 | 1 | 1.7 | N/A | 4.5-4.5 | 261-261 |
| **181015** | 114218-130448 | 3 | 1.3 | 1.0 | 4.5-7.0 | 70-74 |
| **Total # of Meas.** | | **6** | | | | |
| **Median** | | | **1.0** | | | |
| **IQR** | | | **0.5 - 1.6** | | | |
| **Mean** | | | **1.1** | | | |
| **SD** | | | **0.8** | | | |

### *6.1.4 Benicia refinery area*

Alkane emissions from the Benicia refinery area were measured on 4 days and $SO_2$, $NO_2$ and $H_2CO$ emissions were measured on 3 days. Figures 51 to 53 show examples of these measurements, and Tables 34 to Table 40 summarize results from the individual survey days for the site and mean emissions and confidence intervals over the duration of the survey.

The wind speed during the measurements at Benicia was in the 1.5-9 m/s range, and measurements were done with winds coming both from west and northeast. The mean alkane emissions were 144 kg/h, with a 95% CI of 124-165 kg/h, e.g. 28% relative the mean. Overall

20 measurements were made, distributed over four days, and the daily average emissions had a span of 115-181 kg/h.

Concentrations of methane, BTEX, and alkanes outside the facilities for determining emissions of methane and BTEX indirectly are shown in Figures 54 and 55.

Figure 51. Example of SOF measurement at Benicia refinery area. Map from Google Earth™ 2019.

Figure 52. Example of SkyDOAS $SO_2$ measurement at Benicia refinery area. Map from Google Earth™ 2019.

Figure 53. Example of SkyDOAS $NO_2$ measurement at Benicia refinery area. Map from Google Earth™ 2019.

Figure 54. Concentration measurements of methane and alkanes at Benicia refinery area. Map from Google Earth™ 2019.

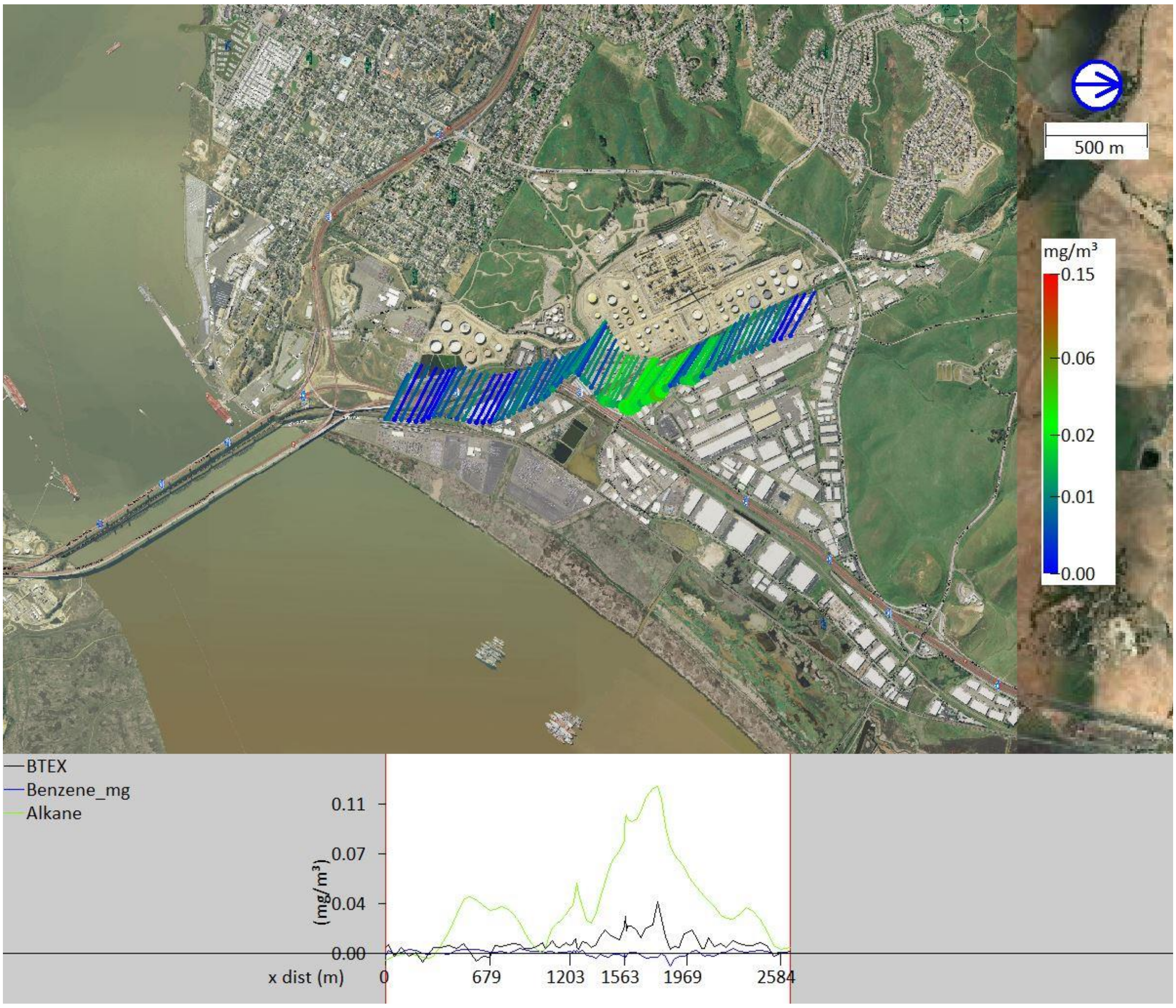

Figure 55. Concentration measurements of BTEX and alkanes at Benicia refinery area.

Table 34. Benicia refinery area, alkanes.

| Day [yymmdd] | Time span [hhmmss-hhmmss] | Num Meas | Emission avg [kg/h] | Emission SD [kg/h] | Wind Speed Min-Max [m/s] | Wind Dir Span [deg] |
|---|---|---|---|---|---|---|
| **181006** | 143148-145913 | 2 | 160 | 44.8 | 2.4-3.0 | 267-272 |
| **181010** | 131823-153555 | 5 | 181 | 25.5 | 7.4-8.7 | 272-309 |
| **181013** | 104250-152150 | 7 | 139 | 53.1 | 1.5-6.3 | 273-311 |
| **181015** | 133605-152456 | 6 | 115 | 19.6 | 3.3-4.2 | 61-96 |
| **Total # of Meas.** | | **20** | | | | |
| **Median** | | | **133.6** | | | |
| **Mean** | | | **144.4** | | | |
| **SD** | | | **43.4** | | | |
| **95% CI** | | | **124.1 - 164.7** | | | |

Table 35. Benicia refinery area, $SO_2$.

| Day [yymmdd] | Time span [hhmmss-hhmmss] | Num Meas | Emission avg [kg/h] | Emission SD [kg/h] | Wind Speed Min-Max [m/s] | Wind Dir Span [deg] |
|---|---|---|---|---|---|---|
| **181006** | 140220-152254 | 4 | 12.7 | 5.2 | 2.3-4.8 | 253-270 |
| **181013** | 135120-152225 | 7 | 22.6 | 9.0 | 4.4-6.4 | 283-293 |
| **181015** | 145705-152243 | 2 | 22.6 | 2.6 | 3.4-4.2 | 65-101 |
| **Total # of Meas.** | | **13** | | | | |
| **Median** | | | **17.9** | | | |
| **Mean** | | | **19.6** | | | |
| **SD** | | | **8.4** | | | |
| **95% CI** | | | **14.5 - 24.7** | | | |

Table 36. Benicia refinery area, $NO_2$.

| Day [yymmdd] | Time span [hhmmss-hhmmss] | Num Meas | Emission avg [kg/h] | Emission SD [kg/h] | Wind Speed Min-Max [m/s] | Wind Dir Span [deg] |
|---|---|---|---|---|---|---|
| **181006** | 134105-152401 | 7 | 98.4 | 56.7 | 2.3-4.7 | 253-272 |
| **181007** | 125656-162538 | 3 | 61.3 | 6.3 | 7.9-10.7 | 23-35 |
| **181013** | 135023-152044 | 7 | 84.1 | 25.3 | 4.4-6.4 | 282-294 |
| **181015** | 145632-152450 | 3 | 72.1 | 9.6 | 3.1-4.2 | 74-99 |
| **Total # of Meas.** | | **20** | | | | |
| **Median** | | | **72.9** | | | |
| **Mean** | | | **83.9** | | | |
| **SD** | | | **37.6** | | | |
| **95% CI** | | | **66.3 - 101.5** | | | |

Table 37. Benicia refinery area, $H_2CO$.

| Day [yymmdd] | Time span [hhmmss-hhmmss] | Num Meas | Emission avg [kg/h] | Emission SD [kg/h] | Wind Speed Min-Max [m/s] | Wind Dir Span [deg] |
|---|---|---|---|---|---|---|
| **181006** | 140317-152313 | 5 | 1.4 | 1.5 | 2.2-4.7 | 253-274 |
| **181013** | 143423-145642 | 2 | 1.5 | 2.1 | 6.2-6.4 | 286-288 |
| **181015** | 150735-152437 | 2 | 1.8 | 0.1 | 3.1-3.3 | 74-85 |
| **Total # of Meas.** | | **9** | | | | |
| **Median** | | | **<5** | | | |
| **Mean** | | | **<5** | | | |

Table 38. Benicia refinery area, methane/alkane ratios

| Day [yymmdd] | Time span [hhmmss-hhmmss] | Num Meas | Mass Ratio avg [%] | Mass Ratio SD [%] | Wind Speed Min-Max [m/s] | Wind Dir Span [deg] |
|---|---|---|---|---|---|---|
| **181006** | 134000-145804 | 3 | 46.2 | 5.8 | 2.3-5.5 | 262-290 |
| **181010** | 125836-153534 | 6 | 44.5 | 12.6 | 6.9-9.0 | 271-312 |
| **181015** | 133554-152434 | 7 | 75.0 | 43.9 | 2.5-3.8 | 54-101 |
| **Total # of Meas.** | | **16** | | | | |
| **Median** | | | **48.4** | | | |
| **IQR** | | | **39.4 - 61.1** | | | |
| **Mean** | | | **58.2** | | | |
| **SD** | | | **32.6** | | | |

Table 39. Benicia refinery area, BTEX/alkane mass ratios.

| Day [yymmdd] | Time span [hhmmss-hhmmss] | Num Meas | Mass Ratio avg [%] | Mass Ratio SD [%] | Wind Speed Min-Max [m/s] | Wind Dir Span [deg] |
|---|---|---|---|---|---|---|
| **181010** | 121306-140700 | 4 | 7.9 | 2.6 | 5.7-8.3 | 300-330 |
| **181015** | 133457-142212 | 2 | 8.8 | 1.0 | 2.9-3.3 | 59-87 |
| **Total # of Meas.** | | **6** | | | | |
| **Median** | | | **8.2** | | | |
| **IQR** | | | **7.3 - 9.2** | | | |
| **Mean** | | | **8.2** | | | |
| **SD** | | | **2.1** | | | |

Table 40. Benicia refinery area, benzene/alkane mass ratios.

| Day [yymmdd] | Time span [hhmmss-hhmmss] | Num Meas | Mass Ratio avg [%] | Mass Ratio SD [%] | Wind Speed Min-Max [m/s] | Wind Dir Span [deg] |
|---|---|---|---|---|---|---|
| **181010** | 124242-153550 | 7 | 1.3 | 1.0 | 6.2-8.3 | 255-324 |
| **181015** | 133457-134039 | 1 | 0.34 | N/A | 3.3-3.3 | 88-88 |
| **Total # of Meas.** | | **8** | | | | |
| **Median** | | | **0.7** | | | |
| **IQR** | | | **0.4 - 1.6** | | | |
| **Mean** | | | **1.2** | | | |
| **SD** | | | **1.0** | | | |

### 6.1.5 Martinez E refinery area

Alkane emissions from the Martinez E refinery area were measured on 2 days and $SO_2$, $NO_2$ and $H_2CO$ emissions were measured on 3 days. The fenceline of the site is not well accessible by public road and measurements were generally made from at least 1 km distance. Additionally, due to the site layout and dominant wind direction during the survey, the emissions plume is extensive rather than concentrated spatially. On one day northerly winds gave a more concentrated plume. Figure 56 to Figure 58 show examples of these measurements. Interference sources exist for both methane and $SO_2$ in particular.

Concentrations of methane and alkanes outside the facilities for determining emissions of methane indirectly are shown in Figure 59. Tables 41 to 45 summarize results from the individual survey days for the site and mean emissions and confidence intervals over the duration of the survey.

Figure 56. Example of SOF measurement at Martinez E refinery area. Map from Google Earth™ 2019.

Figure 57. Example of SkyDOAS $SO_2$ measurement at Martinez E refinery area. Map from Google Earth™ 2019.

Figure 58. Example of SkyDOAS $NO_2$ measurement at Martinez E refinery area. Map from Google Earth™ 2019.

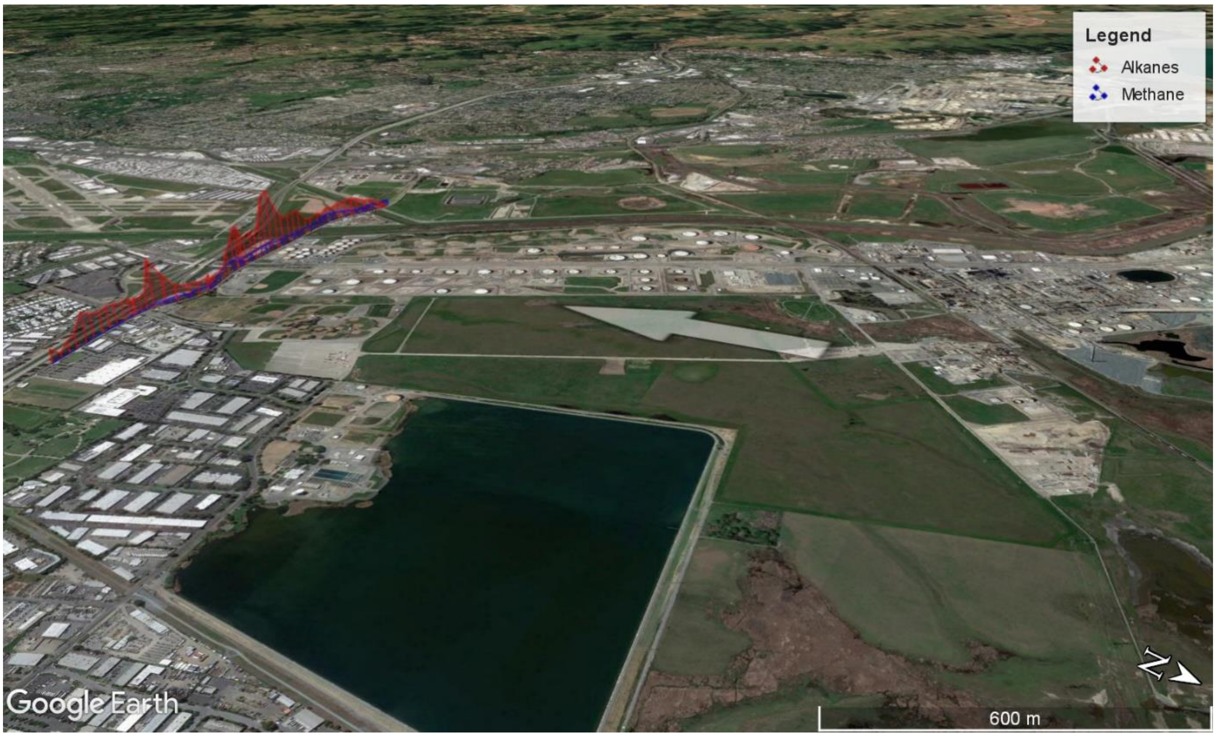

Figure 59. Concentration measurements of methane and alkanes at Martinez E refinery area. Map from Google Earth™ 2019.

Table 41. Martinez E refinery area, alkanes.

| Day [yymmdd] | Time span [hhmmss-hhmmss] | Num Meas | Emission avg [kg/h] | Emission SD [kg/h] | Wind Speed Min-Max [m/s] | Wind Dir Span [deg] |
|---|---|---|---|---|---|---|
| **181007** | 130349-130647 | 1 | 155 | N/A | 7.8-7.8 | 20-20 |
| **181015** | 131701-160745 | 4 | 143 | 14.5 | 2.5-5.6 | 45-84 |
| **181017** | 143956-152400 | 3 | 159 | 5.0 | 2.6-3.0 | 8-350 |
| **Total # of Meas.** | | **8** | | | | |
| **Median** | | | **154.5** | | | |
| **Mean** | | | **150.6** | | | |
| **SD** | | | **12.8** | | | |
| **95% CI** | | | **139.8 - 161.3** | | | |

Table 42. Martinez E refinery area, $SO_2$.

| Day [yymmdd] | Time span [hhmmss-hhmmss] | Num Meas | Emission avg [kg/h] | Emission SD [kg/h] | Wind Speed Min-Max [m/s] | Wind Dir Span [deg] |
|---|---|---|---|---|---|---|
| **181007** | 134658-163220 | 4 | 51.2 | 20.9 | 8.2-11.0 | 28-39 |
| **181015** | 152834-160704 | 3 | 99.6 | 74.4 | 2.5-3.6 | 37-46 |
| **181017** | 143824-162058 | 4 | 37.8 | 6.2 | 2.4-2.9 | 2-350 |
| **Total # of Meas.** | | **11** | | | | |
| **Median** | | | **40.5** | | | |
| **Mean** | | | **59.5** | | | |
| **SD** | | | **44.1** | | | |
| **95% CI** | | | **29.8 - 89.1** | | | |

Table 43. Martinez E refinery area, $NO_2$.

| Day [yymmdd] | Time span [hhmmss-hhmmss] | Num Meas | Emission avg [kg/h] | Emission SD [kg/h] | Wind Speed Min-Max [m/s] | Wind Dir Span [deg] |
|---|---|---|---|---|---|---|
| **181007** | 130148-171105 | 7 | 66.9 | 16.0 | 7.4-11.1 | 20-36 |
| **181015** | 152834-160848 | 3 | 75.0 | 4.3 | 2.5-3.6 | 35-40 |
| **Total # of Meas.** | | **10** | | | | |
| **Median** | | | **71.1** | | | |
| **Mean** | | | **69.3** | | | |
| **SD** | | | **13.8** | | | |
| **95% CI** | | | **59.5 - 79.2** | | | |

Table 44. Martinez E refinery area, $H_2CO$.

| Day [yymmdd] | Time span [hhmmss-hhmmss] | Num Meas | Emission avg [kg/h] | Emission SD [kg/h] | Wind Speed Min-Max [m/s] | Wind Dir Span [deg] |
|---|---|---|---|---|---|---|
| **181007** | 130345-155409 | 5 | 4.4 | 1.4 | 6.7-10.6 | 27-36 |
| **181015** | 152834-162453 | 4 | 4.2 | 1.7 | 2.2-3.6 | 37-117 |
| **181017** | 144021-145426 | 2 | 2.4 | 1.7 | 2.8-2.8 | 353-360 |
| **Total # of Meas.** | | **11** | | | | |
| **Median** | | | **<5** | | | |
| **Mean** | | | **<5** | | | |

Table 45. Martinez E refinery area, methane/alkanes ratios.

| Day [yymmdd] | Time span [hhmmss-hhmmss] | Num Meas | Mass Ratio avg [%] | Mass Ratio SD [%] | Wind Speed Min-Max [m/s] | Wind Dir Span [deg] |
|---|---|---|---|---|---|---|
| **181007** | 151138-155428 | 2 | 91.2 | 47.2 | 7.6-8.1 | 43-49 |
| **181017** | 144107-161902 | 3 | 31.2 | 3.8 | 2.6-3.1 | 8-19 |
| **181021** | 174402-174552 | 1 | 37.5 | N/A | 6.7-6.7 | 285-285 |
| **Total # of Meas.** | | **6** | | | | |
| **Median** | | | **36.3** | | | |
| **IQR** | | | **32.2 - 52.7** | | | |
| **Mean** | | | **52.3** | | | |
| **SD** | | | **37.0** | | | |

### 6.1.6 *Richmond port area*

The Richmond port area (Figure 60) is located immediately south of the Richmond community, and comprise both tank storage, terminals as well as other industrial operations.

Figure 60. View towards east over the Richmond port area.

The prevalent wind direction during the survey in this area was southerly, and the wind speed range for the main 5 days of measurements here were 2-7 m/s.

Alkane emissions from the Richmond port area were measured on 5 days, with a total of 40 SOF measurement transects, Table 46. The mean alkane emission for the survey was 90 kg/h, with a 95% CI of 78-102 kg/h, e.g. 27% relative the mean. Each survey day had 3-16 measurements, and the daily means were very similar with a span of 80-98 kg/h, suggesting persisting emissions from the port, although with intermittent enhancements. Figure 61 and Figure 62 show two examples of SOF alkane measurements at extended distances towards north downwind of the port, further and further into the Richmond community. It's evident how the port emission plume is being transported and dispersed over Richmond.

$SO_2$, $NO_2$ and $H_2CO$ emissions were measured on 2 days. Figure 63 to 64 show examples of these measurements. Sulfur dioxide emissions were low, with a mean of 3.7 kg/h, based on 6 observations, Table 47. Nitrogen dioxide emissions were measured on same two days as SO2, with a mean emission of 33 kg/h, Table 48. Formaldehyde was at or below detection limit with emissions being less than 5 kg/h (Table 49). Figure 63 and Figure 64 show examples of $SO_2$ and $NO_2$ measurements at the Richmond port area, respectively.

Concentrations of methane, BTEX, and alkanes outside the facilities for determining emissions of methane and BTEX indirectly are shown in Figure 65 and Figure 66. Based on 33 mass concentration ratio measurements over six days, the median $CH_4$ to alkane ratio was 13% with the interquartile range being 9-26% (Table 50). Combined with the mean alkane emission of 90 kg/h this methane to alkane mass ration give a port area methane emission estimate of 12 kg/h.

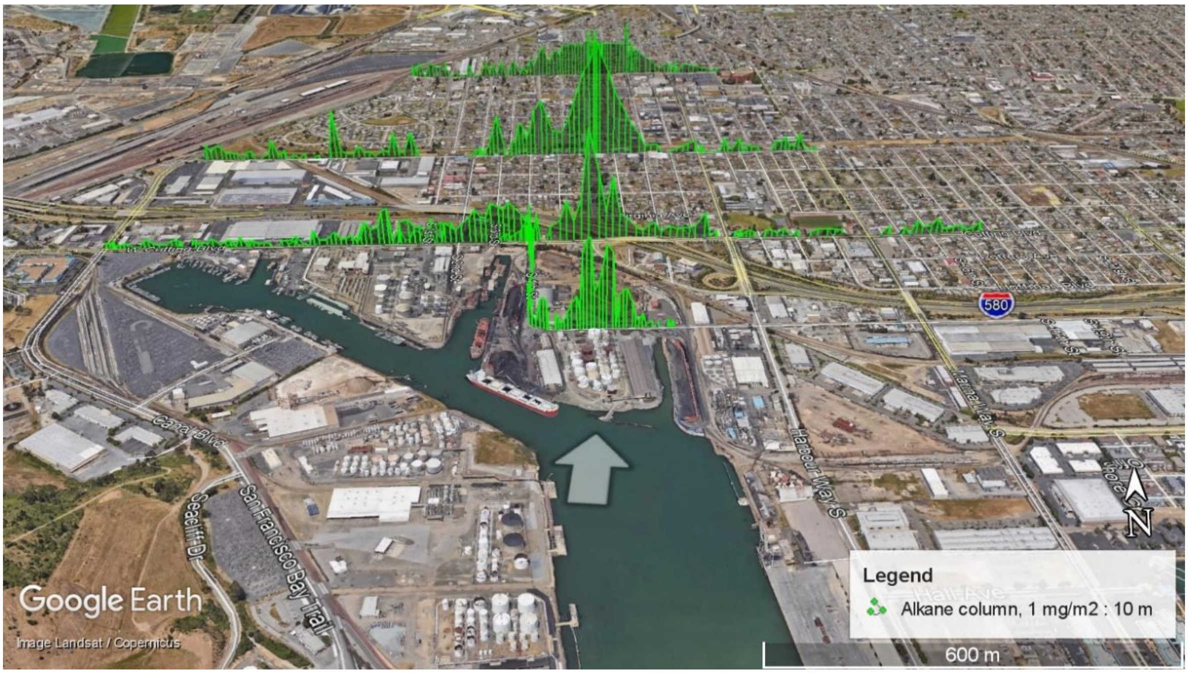

Figure 61. Example of SOF measurement at Richmond port area. Map from Google Earth™ 2019.

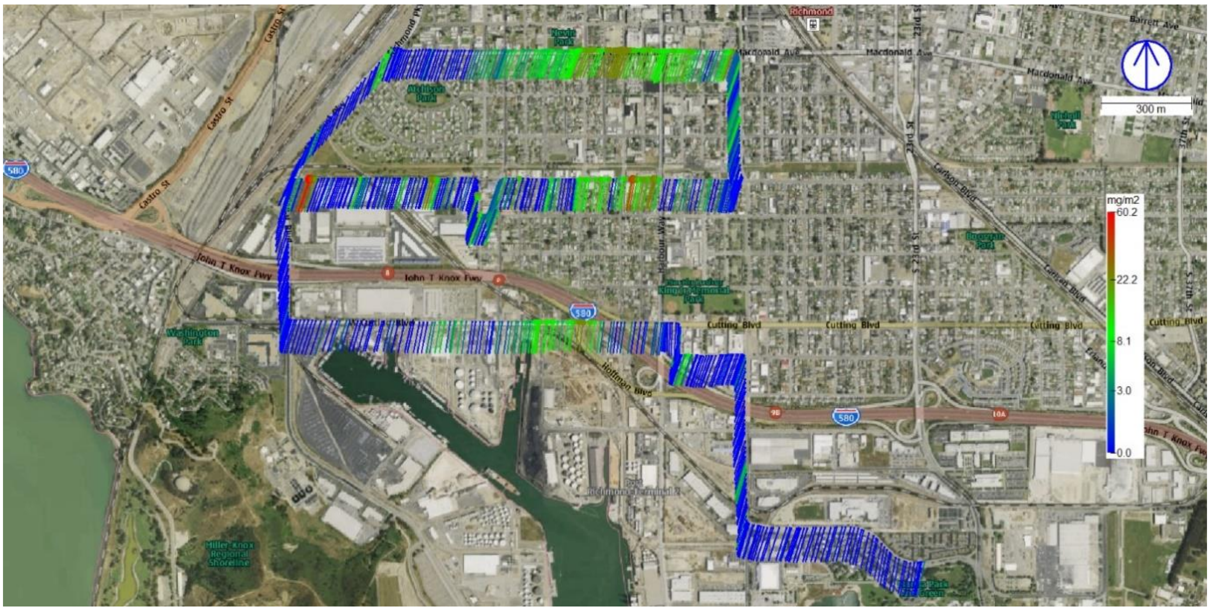

Figure 62. Tracking the VOC plume from the Port of Richmond into the community using SOF, October 20.

Figure 63. Example of SkyDOAS $SO_2$ measurement at Richmond port area. Map from Google Earth™ 2019.

Figure 64. Example of SkyDOAS $NO_2$ measurement at Richmond port area. Map from Google Earth™ 2019.

The BTEX emission from the Richmond port area was measured to be 8.7 kg/h, of which benzene 0.6 kg/h (Table 8). This was based on a BTEX and benzene to alkane mass ratio of 9.7% and 0.7% respectively, Table 51 and Table 52. A measurement example of BTEX, benzene and alkanes are shown in Figure 66.

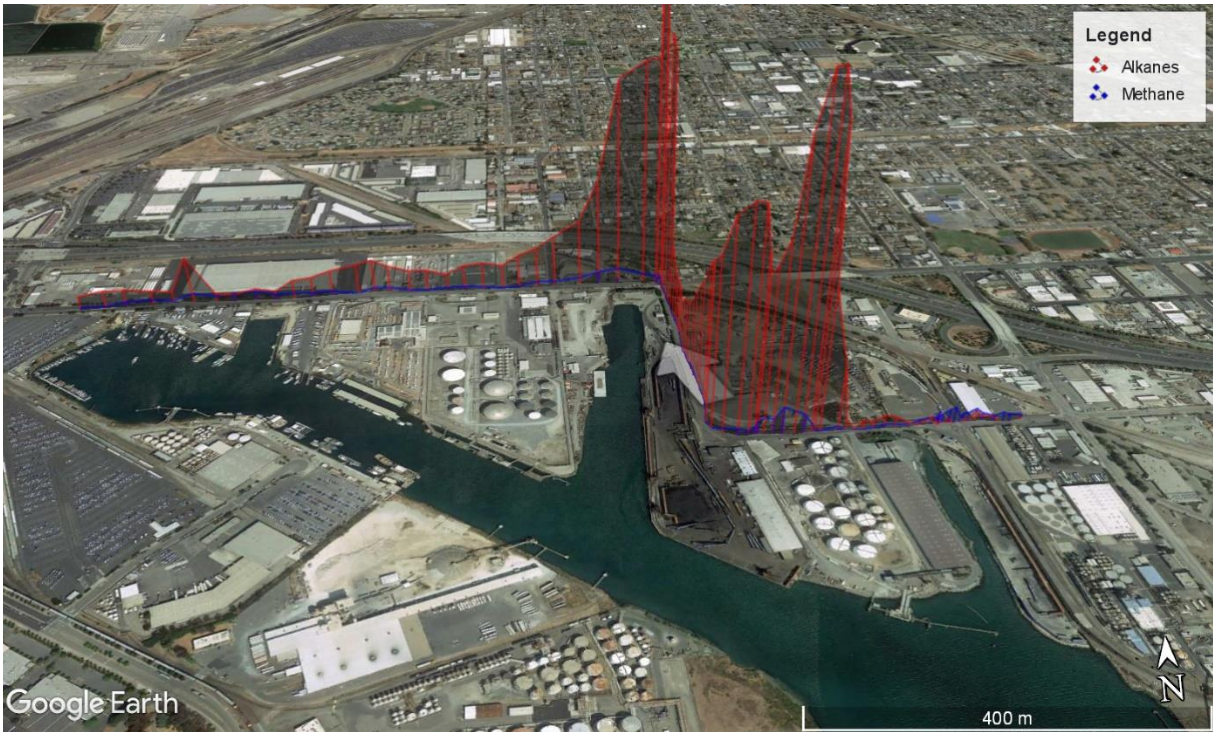

Figure 65. Concentration measurements of methane and alkanes at Richmond port area. Map from Google Earth™ 2019.

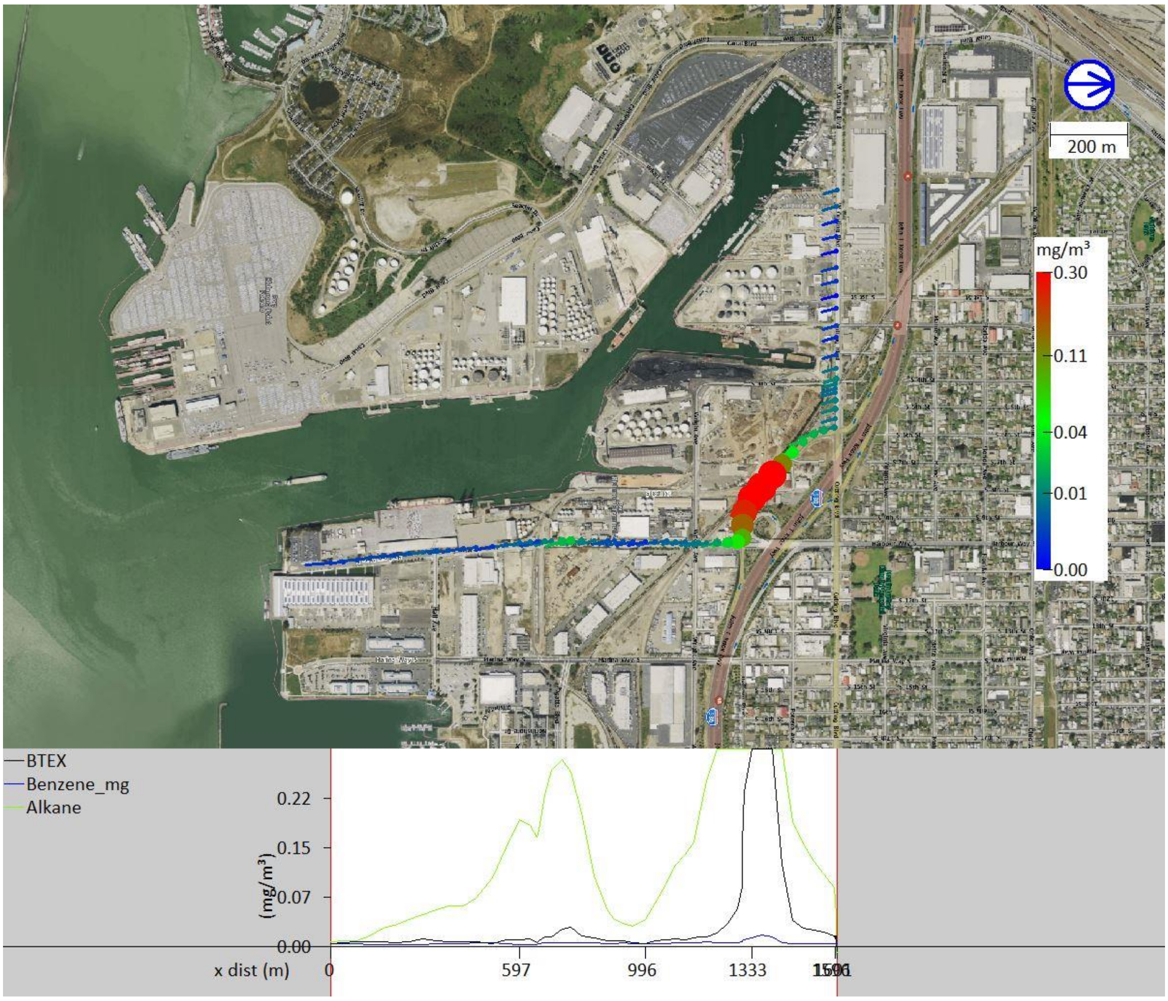

Figure 66. Concentration measurements of BTEX, benzene and alkanes at the Richmond port area.

Table 46. Richmond port area, alkanes.

| Day [yymmdd] | Time span [hhmmss-hhmmss] | Num Meas | Emission avg [kg/h] | Emission SD [kg/h] | Wind Speed Min-Max [m/s] | Wind Dir Span [deg] |
|---|---|---|---|---|---|---|
| **181016** | 113617-155119 | 8 | 97.8 | 40.1 | 3.5-5.7 | 172-202 |
| **181018** | 130304-165510 | 3 | 88.4 | 9.8 | 2.7-3.7 | 171-246 |
| **181019** | 151139-154126 | 3 | 79.8 | 40.5 | 1.8-2.8 | 177-186 |
| **181020** | 114435-160625 | 16 | 88.9 | 34.1 | 2.6-6.7 | 184-211 |
| **181022** | 120911-162802 | 10 | 89.3 | 49.6 | 1.7-5.1 | 163-210 |
| **Total # of Meas.** | | **40** | | | | |
| **Median** | | | **82.5** | | | |
| **Mean** | | | **90.0** | | | |
| **SD** | | | **37.6** | | | |
| **95% CI** | | | **78.0 - 102.1** | | | |

Table 47. Richmond port area, $SO_2$.

| Day [yymmdd] | Time span [hhmmss-hhmmss] | Num Meas | Emission avg [kg/h] | Emission SD [kg/h] | Wind Speed Min-Max [m/s] | Wind Dir Span [deg] |
|---|---|---|---|---|---|---|
| **181016** | 124849-155234 | 5 | 3.0 | 1.4 | 3.3-5.0 | 169-191 |
| **181018** | 130549-131225 | 1 | 7.0 | N/A | 2.6-2.6 | 242-242 |
| **Total # of Meas.** | | **6** | | | | |
| **Median** | | | **3.1** | | | |
| **Mean** | | | **3.7** | | | |
| **SD** | | | **2.1** | | | |
| **95% CI** | | | **1.5 - 5.9** | | | |

Table 48. Richmond port area, $NO_2$.

| Day [yymmdd] | Time span [hhmmss-hhmmss] | Num Meas | Emission avg [kg/h] | Emission SD [kg/h] | Wind Speed Min-Max [m/s] | Wind Dir Span [deg] |
|---|---|---|---|---|---|---|
| **181016** | 124849-155128 | 6 | 35.2 | 11.1 | 3.5-5.2 | 178-192 |
| **181018** | 130246-130940 | 1 | 20.5 | N/A | 2.8-2.8 | 252-252 |
| **Total # of Meas.** | | **7** | | | | |
| **Median** | | | **28.5** | | | |
| **Mean** | | | **33.1** | | | |
| **SD** | | | **11.6** | | | |
| **95% CI** | | | **22.4 - 43.8** | | | |

Table 49. Richmond port area, $H_2CO$.

| Day [yymmdd] | Time span [hhmmss-hhmmss] | Num Meas | Emission avg [kg/h] | Emission SD [kg/h] | Wind Speed Min-Max [m/s] | Wind Dir Span [deg] |
|---|---|---|---|---|---|---|
| **181016** | 124849-155128 | 5 | 1.2 | 0.8 | 3.5-5.0 | 179-192 |
| **181018** | 125517-130940 | 3 | 0.63 | 0.2 | 2.8-2.9 | 221-252 |
| **Total # of Meas.** | | **8** | | | | |
| **Median** | | | **<5** | | | |
| **Mean** | | | **<5** | | | |

Table 50. Richmond port area, methane/alkane ratios

| Day [yymmdd] | Time span [hhmmss-hhmmss] | Num Meas | Mass Ratio avg [%] | Mass Ratio SD [%] | Wind Speed Min-Max [m/s] | Wind Dir Span [deg] |
|---|---|---|---|---|---|---|
| **181016** | 113132-211012 | 10 | 12.8 | 7.0 | 2.9-5.6 | 142-207 |
| **181018** | 130520-164741 | 2 | 26.6 | 15.5 | 2.8-3.6 | 175-236 |
| **181019** | 160113-170414 | 4 | 18.6 | 12.3 | 3.0-3.4 | 191-200 |
| **181020** | 123544-155107 | 6 | 24.5 | 24.3 | 2.9-5.5 | 192-208 |
| **181022** | 113303-134726 | 7 | 17.5 | 18.3 | 1.6-3.9 | 125-208 |
| **181023** | 211735-231532 | 4 | 41.2 | 30.6 | 1.1-3.4 | 184-312 |
| **Total # of Meas.** | | **33** | | | | |
| **Median** | | | **13.0** | | | |
| **IQR** | | | **9.4 - 25.8** | | | |
| **Mean** | | | **20.9** | | | |
| **SD** | | | **18.9** | | | |

Table 51. Richmond port area, BTEX/alkane mass ratios.

| Day [yymmdd] | Time span [hhmmss-hhmmss] | Num Meas | Mass Ratio avg [%] | Mass Ratio SD [%] | Wind Speed Min-Max [m/s] | Wind Dir Span [deg] |
|---|---|---|---|---|---|---|
| **181016** | 113300-210758 | 5 | 9.7 | 3.2 | 2.8-4.0 | 147-206 |
| **181018** | 163806-164330 | 1 | 10.5 | N/A | 3.6-3.6 | 173-173 |
| **181023** | 210927-231608 | 4 | 9.9 | 4.0 | 1.5-2.3 | 165-265 |
| **Total # of Meas.** | | **10** | | | | |
| **Median** | | | **9.7** | | | |
| **IQR** | | | **8.1 - 10.6** | | | |
| **Mean** | | | **9.9** | | | |
| **SD** | | | **3.1** | | | |

Table 52. Richmond port area, benzene/alkane mass ratios.

| Day [yymmdd] | Time span [hhmmss-hhmmss] | Num Meas | Mass Ratio avg [%] | Mass Ratio SD [%] | Wind Speed Min-Max [m/s] | Wind Dir Span [deg] |
|---|---|---|---|---|---|---|
| **181016** | 113300-210758 | 4 | 1.2 | 0.5 | 2.8-4.0 | 147-206 |
| **181018** | 163806-170259 | 3 | 0.87 | 1.1 | 3.6-3.9 | 173-187 |
| **181023** | 210927-231653 | 5 | 0.74 | 0.3 | 2.0-2.3 | 165-265 |
| **Total # of Meas.** | | **12** | | | | |
| **Median** | | | **0.7** | | | |
| **IQR** | | | **0.5 - 1.3** | | | |
| **Mean** | | | **0.9** | | | |
| **SD** | | | **0.6** | | | |

### *6.1.7 Stockton port area*

Alkane emissions from the Stockton port area were measured on 21 October along with $SO_2$, $NO_2$, $H_2CO$ and ethanol emissions. Figure 67 shows an example of the SOF alkane measurements, while the $SO_2$ and $NO_2$ measurements are given in Figure 68 and Figure 69, respectively. An alkane emission of 84 kg/h was measured, along with $SO_2$ and $NO_2$ emissions of 18 and 65 kg/h, respectively. The port’s ethanol facility was surveyed with SOF and the ethanol emissions averaged 48 kg/h, Figure 71 and Table 57.

Concentrations of methane and alkanes are shown in Figure 70. Methane was detected downwind the water treatment plant, the ethanol facility as well as some from the northern part of the port. Tables 53 through 57 summarize the results from the individual survey day at Stockton port with mean emissions and confidence intervals.

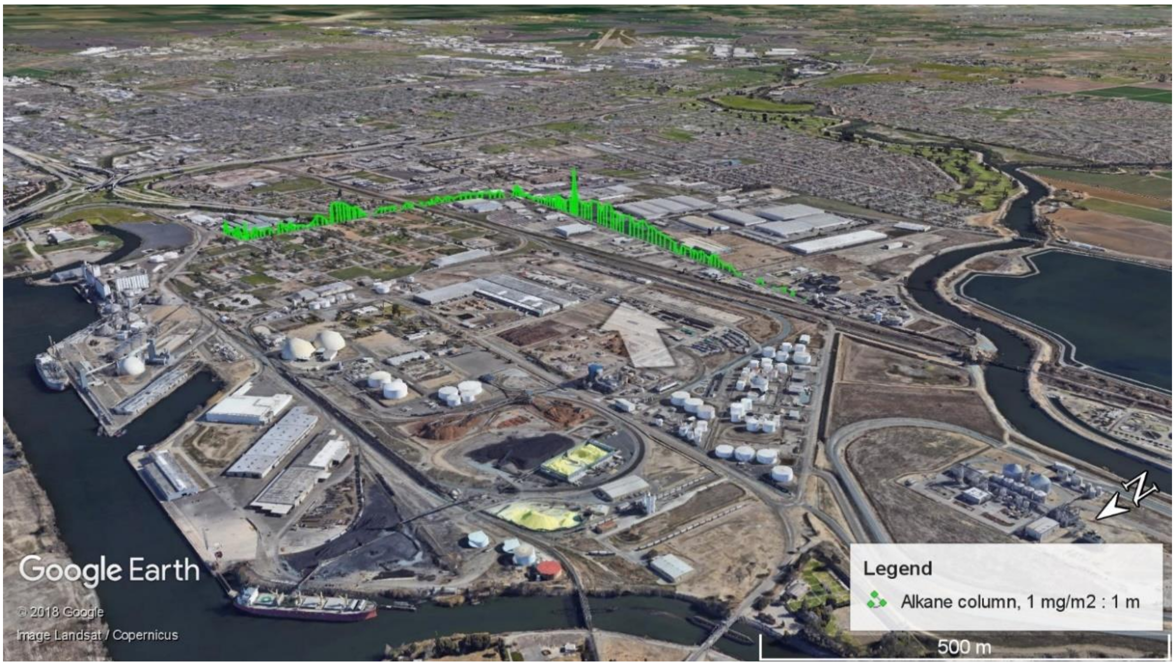

Figure 67. Example of SOF measurement of alkanes at Stockton port area, October 6, 2018, 11 AM Map from Google Earth™ 2019.

Figure 68. Example of SkyDOAS $SO_2$ measurement at Stockton port area. Emissions are near detection limits. Map from Google Earth™ 2019.

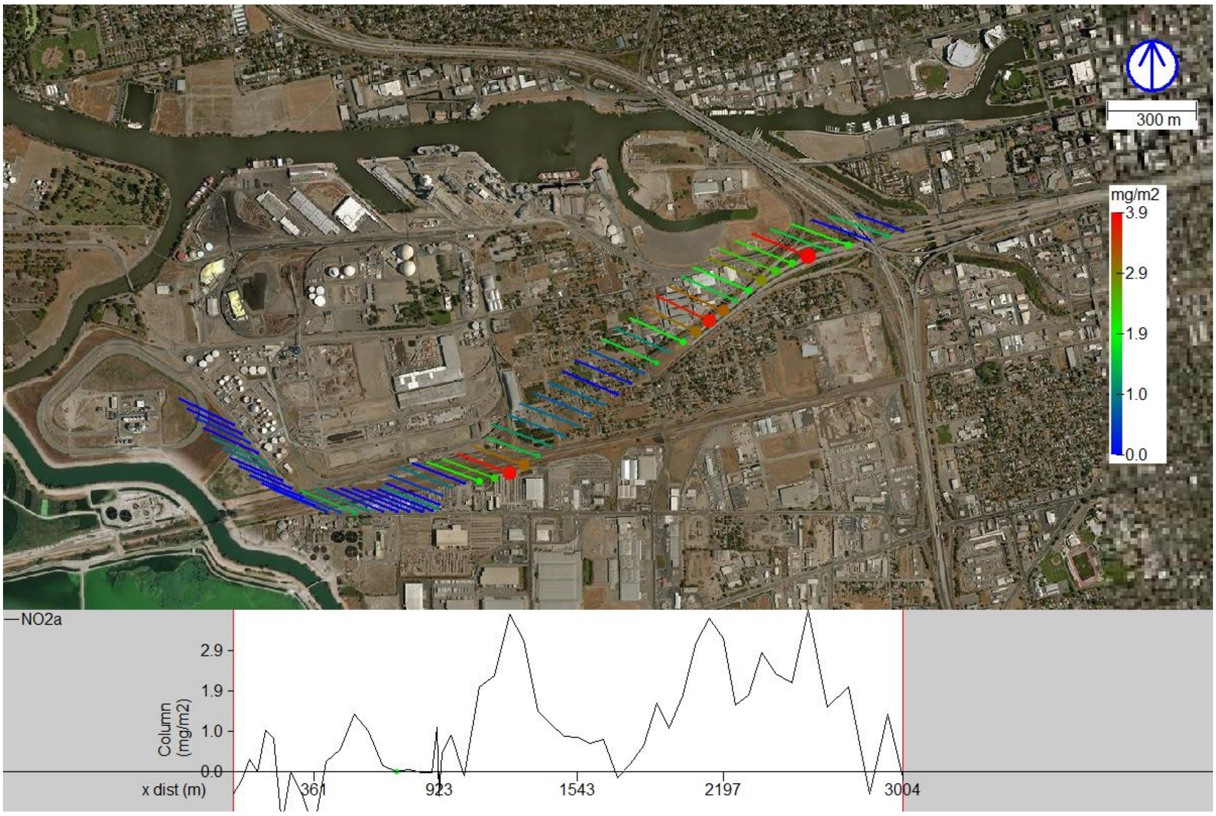

Figure 69. Example of SkyDOAS $NO_2$ measurement at Stockton port area.

Figure 70. Concentration measurements of methane and alkanes at Stockton port area, excluding and including plume from water treatment. Map from Google Earth™ 2019.

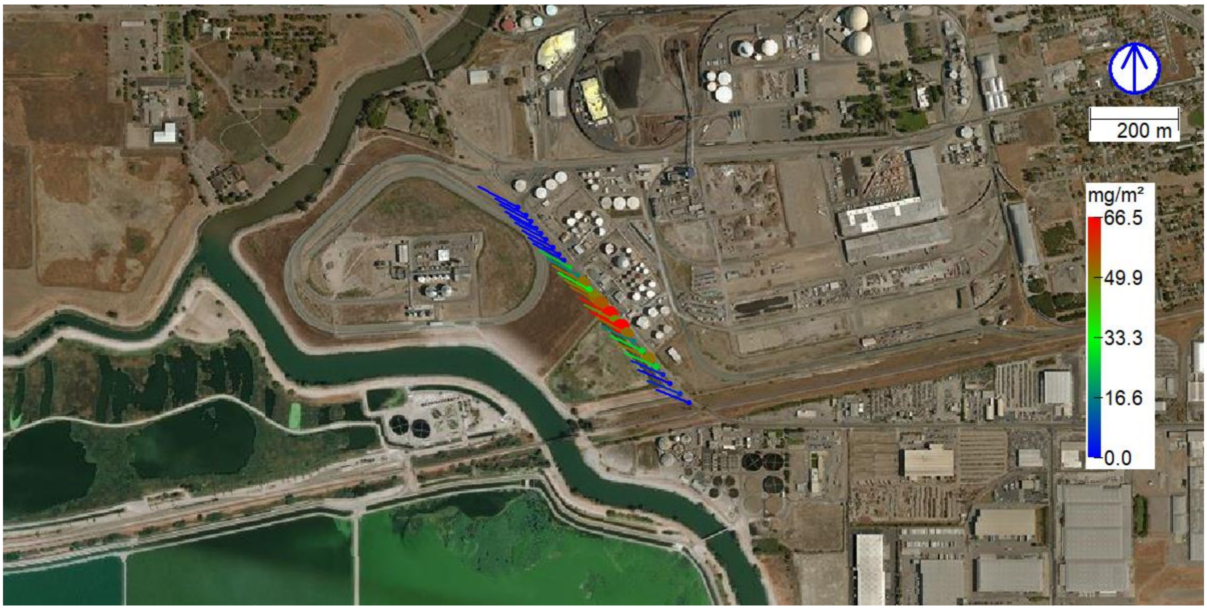

Figure 71. Ethanol measurement at Port of Stockton, October 21, 2018.

Table 53. Stockton port area, alkanes.

| Day [yymmdd] | Time span [hhmmss-hhmmss] | Num Meas | Emission avg [kg/h] | Emission SD [kg/h] | Wind Speed Min-Max [m/s] | Wind Dir Span [deg] |
|---|---|---|---|---|---|---|
| **181021** | 150524-154049 | 3 | 83.8 | 17.0 | 4.8-5.1 | 293-301 |
| **Total # of Meas.** | | **3** | | | | |
| **Median** | | | **93.0** | | | |
| **Mean** | | | **83.8** | | | |
| **SD** | | | **17.0** | | | |
| **95% CI** | | | **41.5 - 126.2** | | | |

Table 54. Stockton port area, $SO_2$.

| Day [yymmdd] | Time span [hhmmss-hhmmss] | Num Meas | Emission avg [kg/h] | Emission SD [kg/h] | Wind Speed Min-Max [m/s] | Wind Dir Span [deg] |
|---|---|---|---|---|---|---|
| **181021** | 162342-162627 | 1 | 18.5 | N/A | 5.8-5.8 | 292-292 |
| **Total # of Meas.** | | **1** | | | | |
| **Median** | | | **18.5** | | | |
| **Mean** | | | **18.5** | | | |
| **SD** | | | **NaN** | | | |
| **95% CI** | | | **nan - nan** | | | |

Table 55. Stockton port area, $NO_2$.

| Day [yymmdd] | Time span [hhmmss-hhmmss] | Num Meas | Emission avg [kg/h] | Emission SD [kg/h] | Wind Speed Min-Max [m/s] | Wind Dir Span [deg] |
|---|---|---|---|---|---|---|
| **181021** | 162257-162632 | 1 | 64.8 | N/A | 5.8-5.8 | 291-291 |
| **Total # of Meas.** | | **1** | | | | |
| **Median** | | | **64.8** | | | |
| **Mean** | | | **64.8** | | | |
| **SD** | | | **NaN** | | | |
| **95% CI** | | | **nan - nan** | | | |

Table 56. Stockton port area, $H_2CO$ (at detection limit).

| Day [yymmdd] | Time span [hhmmss-hhmmss] | Num Meas | Emission avg [kg/h] | Emission SD [kg/h] | Wind Speed Min-Max [m/s] | Wind Dir Span [deg] |
|---|---|---|---|---|---|---|
| **181021** | 164817-165423 | 1 | 0.5 | N/A | 3.2-3.2 | 323-323 |
| **Total # of Meas.** | | **1** | | | | |
| **Median** | | | **0.5** | | | |
| **Mean** | | | **0.5** | | | |
| **SD** | | | **NaN** | | | |
| **95% CI** | | | **nan - nan** | | | |

Table 57. Stockton port area, ethanol.

| Day [yymmdd] | Time span [hhmmss-hhmmss] | Num Meas | Emission avg [kg/h] | Emission SD [kg/h] | Wind Speed Min-Max [m/s] | Wind Dir Span [deg] |
|---|---|---|---|---|---|---|
| **181021** | 150313-153715 | 6 | 47.7 | 13.2 | 3.9-5.0 | 289-296 |
| **Total # of Meas.** | | **6** | | | | |
| **Median** | | | **51.7** | | | |
| **Mean** | | | **47.7** | | | |
| **SD** | | | **13.2** | | | |
| **C.I. 95%** | | | **33.8 - 61.6** | | | |

### *6.1.8 Gas storage McDonald Island, Stockton*

Alkane emissions from the Gas storage McDonald Island, Stockton were measured on 21 October. Figure 72 shows an example of these measurements. Primary emissions from the natural gas storage site are expected to be methane. Concentrations of methane and alkanes outside the facilities for determining emissions of methane indirectly are shown in Figure 73. Table 58 summarize results from the individual survey days for the site and mean emissions and confidence intervals over the duration of the survey.

Access to the island is controlled so that measurements were made just off the island. This had the disadvantage of being downwind of a small motorboat marina. There were numerous episodes of plumes from several boats for the concentration measurements which could interfere with the extractive ratio measurements, however too small for significant impacts in the SOF readings. Alkane and methane plumes in the near-field were thus not so well correlated to be sufficient for indirect flux of methane. However, in the far-field there is both a larger methane plume and good correlation with an alkane plume (Figure 88), but to exclude interfering sources along the plume transport, a revisit for repeated sampling would be needed.

Figure 72. Example of SOF measurements at Gas storage McDonald Island Stockton, October 21, 2018, 1 PM Map from Google Earth™ 2019.

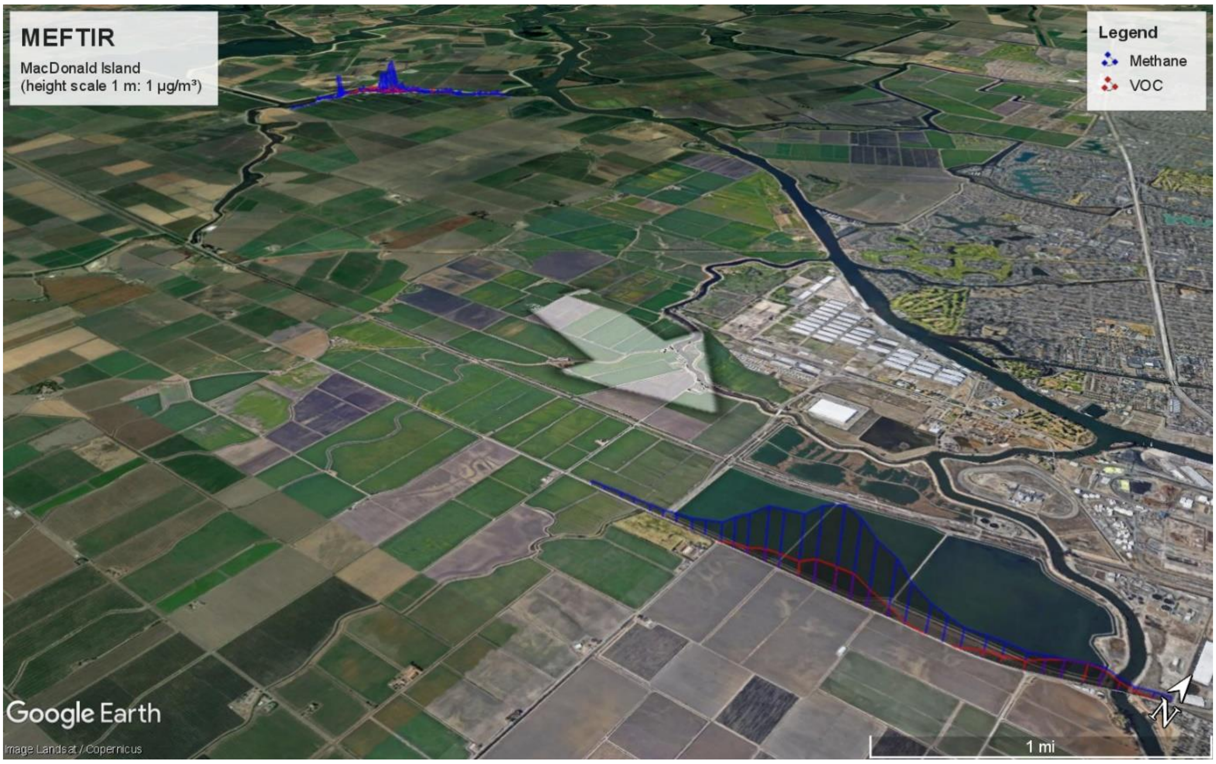

Figure 73. Concentration measurements of $CH_4$ and alkanes near and far-field, Gas storage McDonald Island Stockton. Map from Google Earth™ 2019.

Table 58. McDonald Island Gas Storage, alkanes.

| Day [yymmdd] | Time span [hhmmss-hhmmss] | Num Meas | Emission avg [kg/h] | Emission SD [kg/h] | Wind Speed Min-Max [m/s] | Wind Dir Span [deg] |
|---|---|---|---|---|---|---|
| **181021** | 114724-132355 | 4 | 26.3 | 7.3 | 4.5-5.1 | 298-300 |
| **Total # of Meas.** |  | **4** |  |  |  |  |
| **Median** |  |  | **26.6** |  |  |  |
| **Mean** |  |  | **26.3** |  |  |  |
| **SD** |  |  | **7.3** |  |  |  |
| **95% CI** |  |  | **14.7 - 38.0** |  |  |  |

### *6.1.9 Martinez tank farm & terminal area*

Alkane emissions from the Martinez tank farm & terminal area were measured on 4 days. Figure 74 shows an example of these measurements. Measurements may even include emissions from further afield at the Martinez East Refinery terminal. Table 59 summarize results from the individual survey days for the site and mean emissions and confidence intervals over the duration of the survey.

The survey mean alkane emission was 86 kg/h, but very variable emissions were seen at this site, reflected by the broad 95% CI for the mean of 28-143 kg/h.

Figure 74. Example of SOF measurement at Martinez tank farm & terminal area.

Table 59. Martinez tank farm and terminal area, alkane emissions.

| Day [yymmdd] | Time span [hhmmss-hhmmss] | Num Meas | Emission avg [kg/h] | Emission SD [kg/h] | Wind Speed Min-Max [m/s] | Wind Dir Span [deg] |
|---|---|---|---|---|---|---|
| **181007** | 143917-144103 | 1 | 118 | N/A | 10.1-10.1 | 32-32 |
| **181013** | 155138-155738 | 2 | 9.1 | 3.2 | 3.2-3.3 | 268-268 |
| **181015** | 132156-162230 | 4 | 118 | 95.1 | 2.3-5.1 | 40-103 |
| **181017** | 152351-154154 | 2 | 82.2 | 20.2 | 2.5-2.7 | 5-10 |
| **Total # of Meas.** | | **9** | | | | |
| **Median** | | | **82.8** | | | |
| **Mean** | | | **86.0** | | | |
| **SD** | | | **74.7** | | | |
| **95% CI** | | | **28.6 - 143.4** | | | |

### 6.1.10 *Smaller sites*

Emissions from a number of smaller sites were also measured when they were encountered. This includes individual facilities within certain areas or industrial sites as well as individual or isolatable sites. Emissions at these smaller sites generally were only measured or tabulated for the dominant emitter.

#### *6.1.10.1 Propane management facility Richmond*

A propane facility was a repeated source for alkanes within the Stege Area of Richmond. Figure 75 shows an example of a SOF measurement of the facility. A mean emission of 9.5 kg/h alkanes was measured, Table 60.

Figure 75. Example of SOF measurement at a Propane management facility Richmond.

Table 60. Propane management facility, Richmond, alkane emissions.

| Day [yymmdd] | Time span [hhmmss-hhmmss] | Num Meas | Emission avg [kg/h] | Emission SD [kg/h] | Wind Speed Min-Max [m/s] | Wind Dir Span [deg] |
|---|---|---|---|---|---|---|
| **181016** | 151135-151257 | 1 | 16.6 | N/A | 5.2-5.2 | 196-196 |
| **181022** | 124436-130122 | 4 | 7.8 | 6.0 | 2.5-2.9 | 172-192 |
| **Total # of Meas.** | | **5** | | | | |
| **Median** | | | **8.1** | | | |
| **Mean** | | | **9.5** | | | |
| **SD** | | | **6.5** | | | |
| **95% CI** | | | **1.4 - 17.7** | | | |

#### *6.1.10.2 Martinez sulfuric acid regeneration plant*

Just next to the Benicia-Martinez bridge, on the eastern side of the southern shore, a sulfuric acid regeneration plant is located. $SO_2$ emissions from this plant were measured on a single day, October 15, with a mean emission of 102 kg/h based on five measurements, Table 61. Figure 76 shows a SkyDOAS measurement example of $SO_2$ at the site.

Figure 76. Example of $SO_2$ measurement at Martinez sulfuric acid regeneration plant. Map from Google Earth™ 2019.

Table 61. Martinez sulfuric acid regeneration plant, $SO_2$.

| Day [yymmdd] | Time span [hhmmss-hhmmss] | Num Meas | Emission avg [kg/h] | Emission SD [kg/h] | Wind Speed Min-Max [m/s] | Wind Dir Span [deg] |
|---|---|---|---|---|---|---|
| **181015** | 152708-162225 | 5 | 102 | 29.5 | 2.2-4.2 | 35-116 |
| **Total # of Meas.** | | **5** | | | | |
| **Median** | | | **97.4** | | | |
| **Mean** | | | **102.3** | | | |
| **SD** | | | **29.5** | | | |
| **95% CI** | | | **65.6 - 139.0** | | | |

The $NO_2$ emissions were measured on a total of four transects with a mean emission of 5 kg/h, Table 62.

Table 62. Martinez sulfuric acid regeneration plant, $NO_2$.

| Day [yymmdd] | Time span [hhmmss-hhmmss] | Num Meas | Emission avg [kg/h] | Emission SD [kg/h] | Wind Speed Min-Max [m/s] | Wind Dir Span [deg] |
|---|---|---|---|---|---|---|
| **181015** | 152705-161032 | 4 | 4.8 | 1.1 | 2.2-4.2 | 35-88 |
| **Total # of Meas.** | | **4** | | | | |
| **Median** | | | **5.2** | | | |
| **Mean** | | | **4.8** | | | |
| **SD** | | | **1.1** | | | |
| **95% CI** | | | **3.1 - 6.5** | | | |

### *6.1.10.3 Richmond Chevron Long Wharf Terminal/Point Richmond*

Alkane emissions from the terminal at Point Richmond were measured over several days but only a few total measurements. The measurements indicate significant emissions however the wind angle is non-ideal for flux measurements, and even makes source attribution uncertain. Figure 77 shows the measurements where the wind crosses the transects, in all cases but the bridge transect, very obliquely. Thus, small errors in wind direction lead to rather large changes in emissions and even possibly source attribution. The area source attribution of the SOF measurements is supported by community monitoring measurements which indicated significant leakage just onshore by the terminal (Figure 79) as well as observations during the measurements of both wind direction and the presence of ships at the pier or offshore (Figure 80).

Figure 77. SOF measurements of Richmond Chevron Long Wharf Terminal/Point Richmond over 3 days. Wind arrows point to the respective maximum column for each transect however, the wind was approximately the same (southerly) on all measurements. Map from Google Earth™ 2019.

Figure 78. Concentration mapping of plume from Chevron Long Wharf/Point Richmond on 2 days, October 16 (S wind) and October 19 (SSW wind).

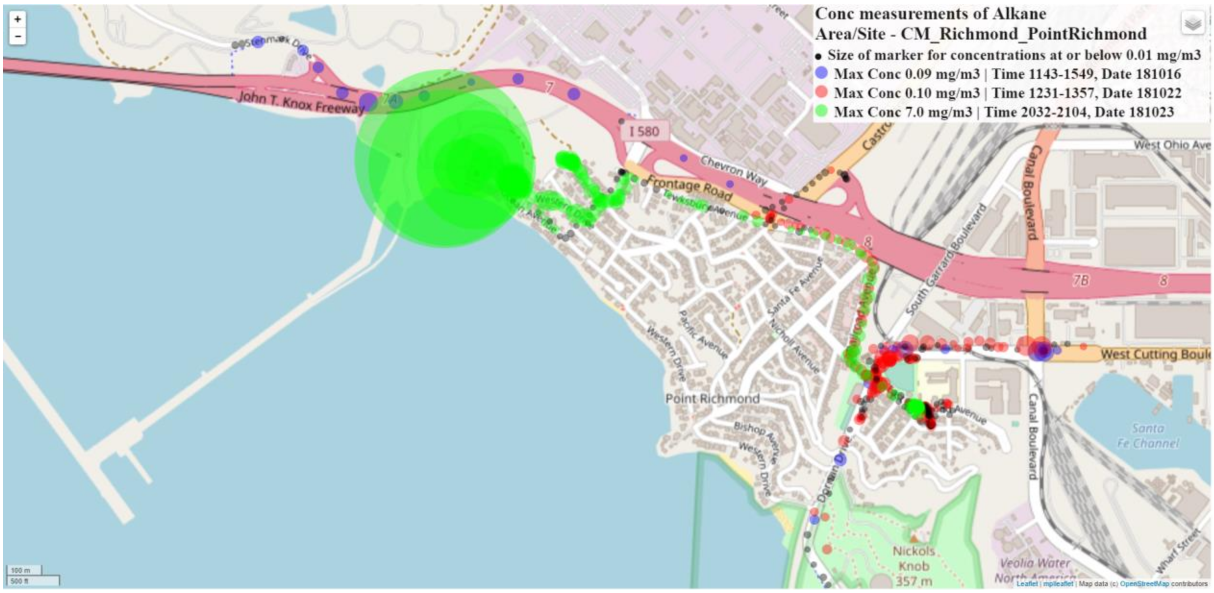

Figure 79. Community Monitoring of VOC at Point Richmond. Plume found near ship terminal pipeline.

Figure 80. Oil Tankers docked (red squares) at Richmond, October 16, 2018, 15:03. Blue arrow shows FluxSense Mobile Lab. Source: Marine Traffic.

### *6.1.11 Potrero Hills landfill*

Alkane emissions from the Potrero Hills landfill were measured on 24 October. Figure 81 shows an example of these measurements. Primary emissions from the site are expected to be methane and smaller emissions of alkanes, aldehydes, alcohols and other gases can be expected. Concentrations of methane and alkanes outside the facilities for determining emissions of methane indirectly are shown in Figure 82. Here the correlation of the methane and alkane plume is good despite the low concentrations of alkanes during these daytime measurements. Still the methane/alkane ratios could be made with greater precision at this site during the evening or night.

Table 63 summarizes the alkane emission measurements and Table 64 summarizes the ratio measurements for IME determination for methane. A methane emission of 860 kg/h was obtained from the measurements. It should be noted that the plume mass ratio measurements would benefit from evening or night-time measurements when concentrations at ground are higher (VOC concentration limiting factor for the uncertainty).

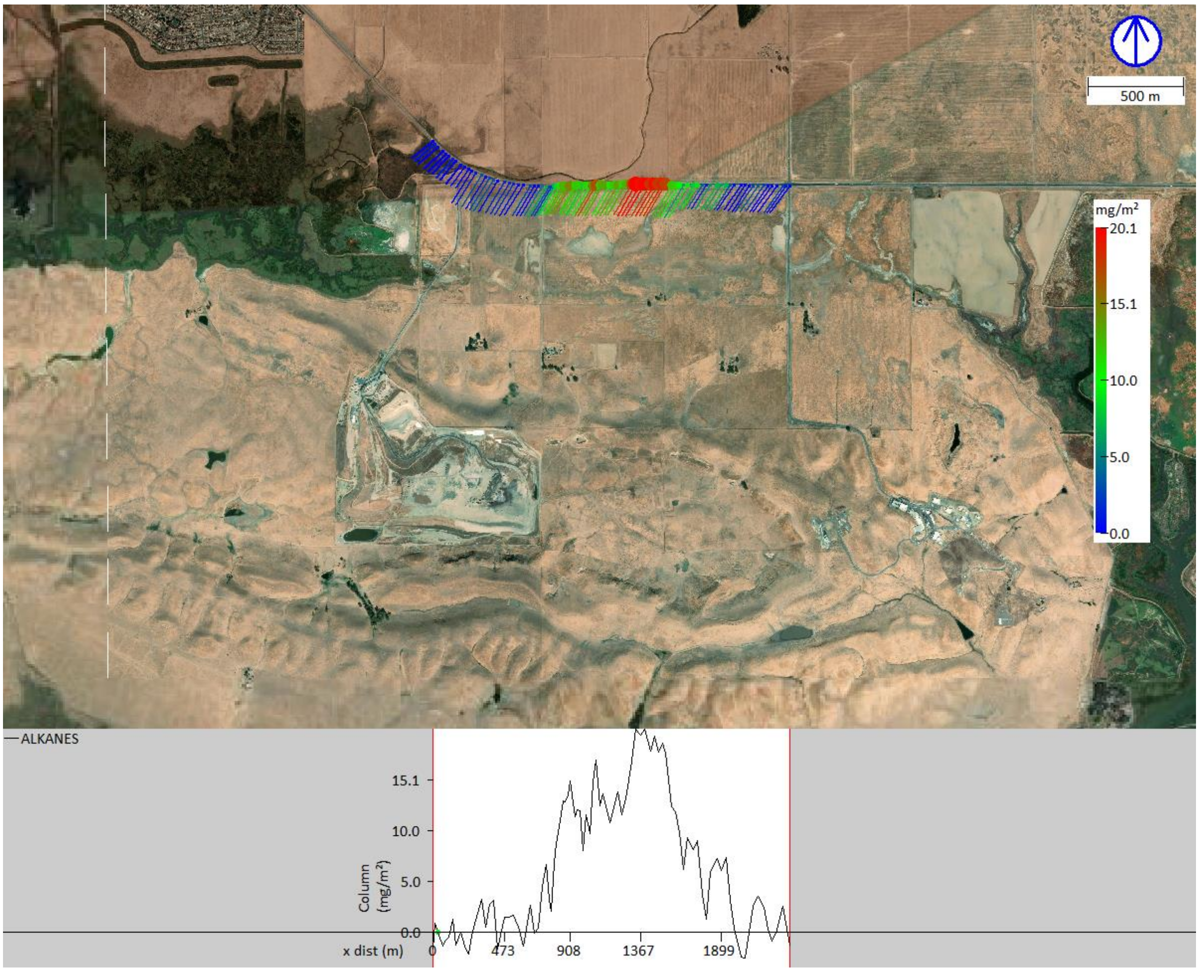

Figure 81. Example of SOF measurement of VOC signatures at Potrero Hills landfill. Map from Google Earth™ 2019.

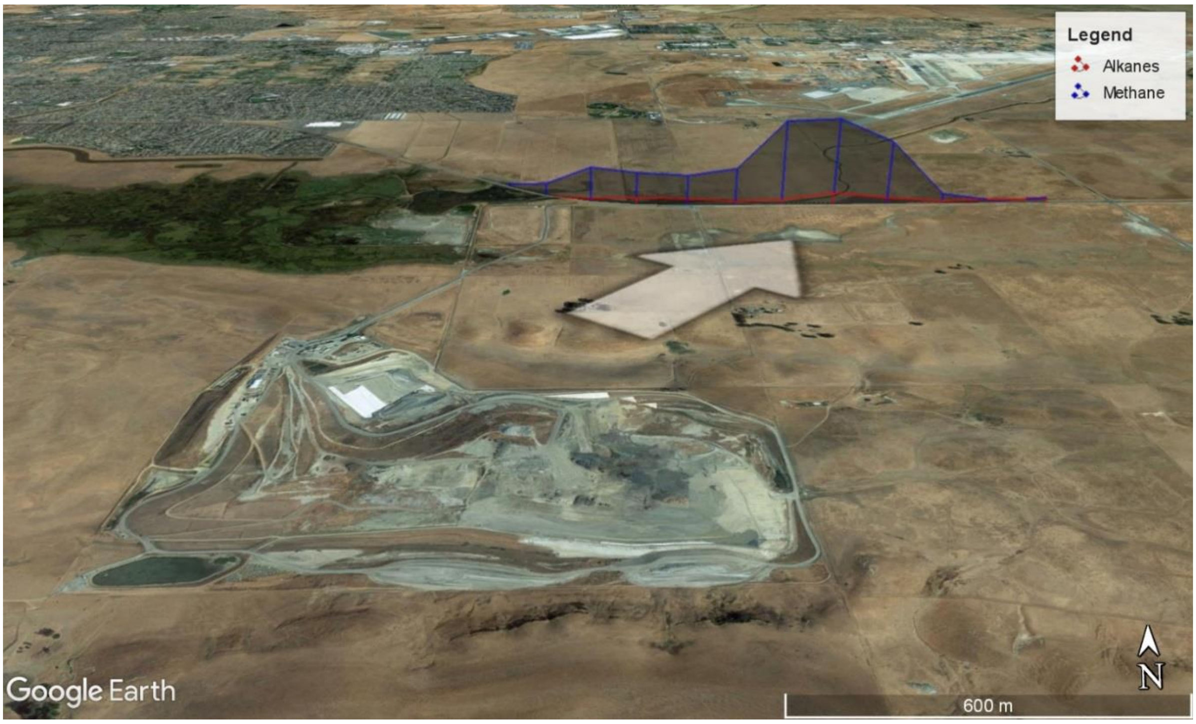

Figure 82. Concentration measurements of methane and alkanes at Potrero Hills landfill, 24 October 1-4 PM, 2018. Map from Google Earth™ 2019.

Table 63. Potrero Hills, SOF VOC measurements.

| Day [yymmdd] | Time span [hhmmss-hhmmss] | Num Meas | Emission avg [kg/h] | Emission SD [kg/h] | Wind Speed Min-Max [m/s] | Wind Dir Span [deg] |
|---|---|---|---|---|---|---|
| **181024** | 130852-161132 | 7 | 75.9 | 19.0 | 2.5-3.3 | 189-226 |
| **Total # of Meas.** | | **7** | | | | |
| **Median** | | | **70.3** | | | |
| **Mean** | | | **75.9** | | | |
| **SD** | | | **19.0** | | | |
| **95% CI** | | | **58.3 - 93.5** | | | |

Table 64. Potrero Hills, Methane to VOC concentration ratio.

| Day [yymmdd] | Time span [hhmmss-hhmmss] | Num Meas | Mass Ratio avg [%] | Mass Ratio SD [%] | Wind Speed Min-Max [m/s] | Wind Dir Span [deg] |
|---|---|---|---|---|---|---|
| **181024** | 132948-161045 | 10 | 1039 | 680.6 | 1.9-3.5 | 192-270 |
| **Total # of Meas.** | | **10** | | | | |
| **Median** | | | **1129.6** | | | |
| **Mean** | | | **1038.5** | | | |
| **SD** | | | **680.6** | | | |
| **95% CI** | | | **551.6 - 1525.4** | | | |

## 6.2 Community monitoring

One of the main objectives in the campaign was to investigate the impacts of various emission sources on community scale air quality, with special focus on disadvantaged communities. This was partly done to complement community monitoring efforts by CARB, who have been running mobile measurements in the Richmond area with smaller sensors as described in section 3. CARB carried out these mobile concentration measurements over several months. The data have been spatially gridded, averaged and mapped.

FluxSense used the concentration maps during the emissions survey and an effort was made to revisit highlighted areas on several occasions and most often over a number of days. It was immediately obvious given the resources available that this would not be possible for all areas so a number of areas were purposely excluded from the monitoring efforts. Sources of VOCs were prioritized along with vicinity to major sources. Both area 6 – Riverside and area 9 – Korematsu (see Figure 83) were excluded both due to a lack of obvious sources and distance from other areas.

The main product of the community monitoring measurements is the digital data. In our analysis we have focused on large sources, unknown sources, and a comparison with earlier monitoring efforts by CAR, and the impact of the sources on community air quality. However, note that even smaller emission sources not focused on here can impact nearby surroundings.

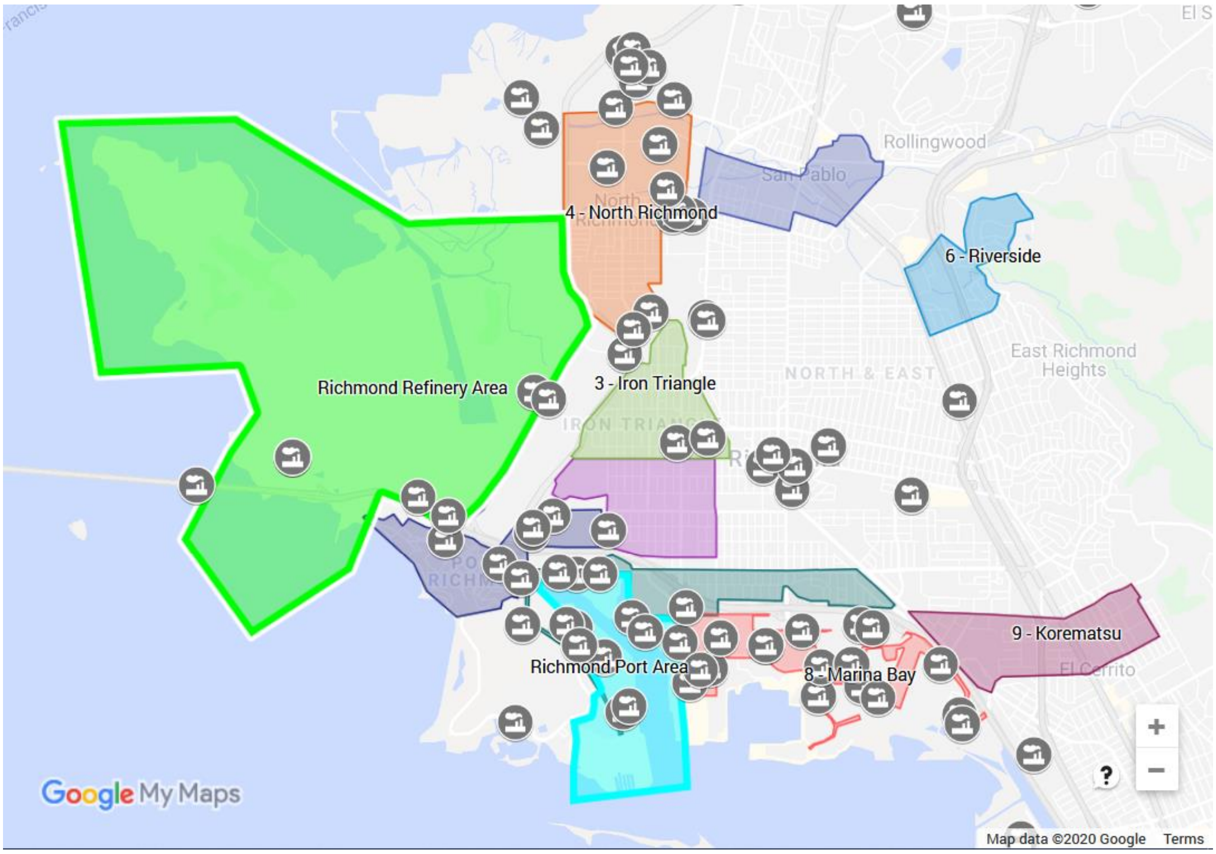

Figure 83 CEIDARS sources in the Richmond Area.

### *6.2.1 Measurement overview*

The community measurements were carried out both night and day following the main streets of Richmond and similar measurements were made at some of the other areas and sites. In addition, measurements were carried out by following emission plumes downwind into the community. This 'plume tracking' approach has the advantage of more sampling of big sources and better identification of large sources much further afield which, because of the plume size, may otherwise be removed as background. The disadvantage of this is that no regular grid pattern is driven and thus spatial and statistical analysis becomes more cumbersome. Measurements were also specifically made in the near vicinity of monitoring stations for later comparison. However, it was noted that instrumentation at these stations is not typically sensitive enough to be used for comparison with the exception of high concentration events.

To give a better idea of the monitoring the totality of the alkane measurements, level 1 evaluation is shown in Figures 84 to 86. In level 1 data the background is adjusted to the 5th percentile of the scan and thus may show some increase in enhancement for longer time series. In Figure 84, main sources in Richmond (e.g. port, refinery storage areas, terminal) can be seen along with numerous small sources, many corresponding to areas highlighted in CARBs community monitoring efforts. In contrast, in Figure 86, Rodeo, the refinery area dominates, although again some small sources can be seen. However, how the refinery emissions affect the community of Rodeo is uncertain. Because of the prevailing wind direction few measurements were made just outside the south fenceline of the Rodeo refinery area, hence not shown in Figure 86. The predominant wind in this area is westerly so most probably the times when the refinery area affects the community are fewer. At issue here is the number and when the measurements that were made. All Rodeo measurements during the survey were made during the daytime and all with westerly winds. The single measurement nearest the community fenceline showed relatively low concentrations just south refinery area (Figure 87).

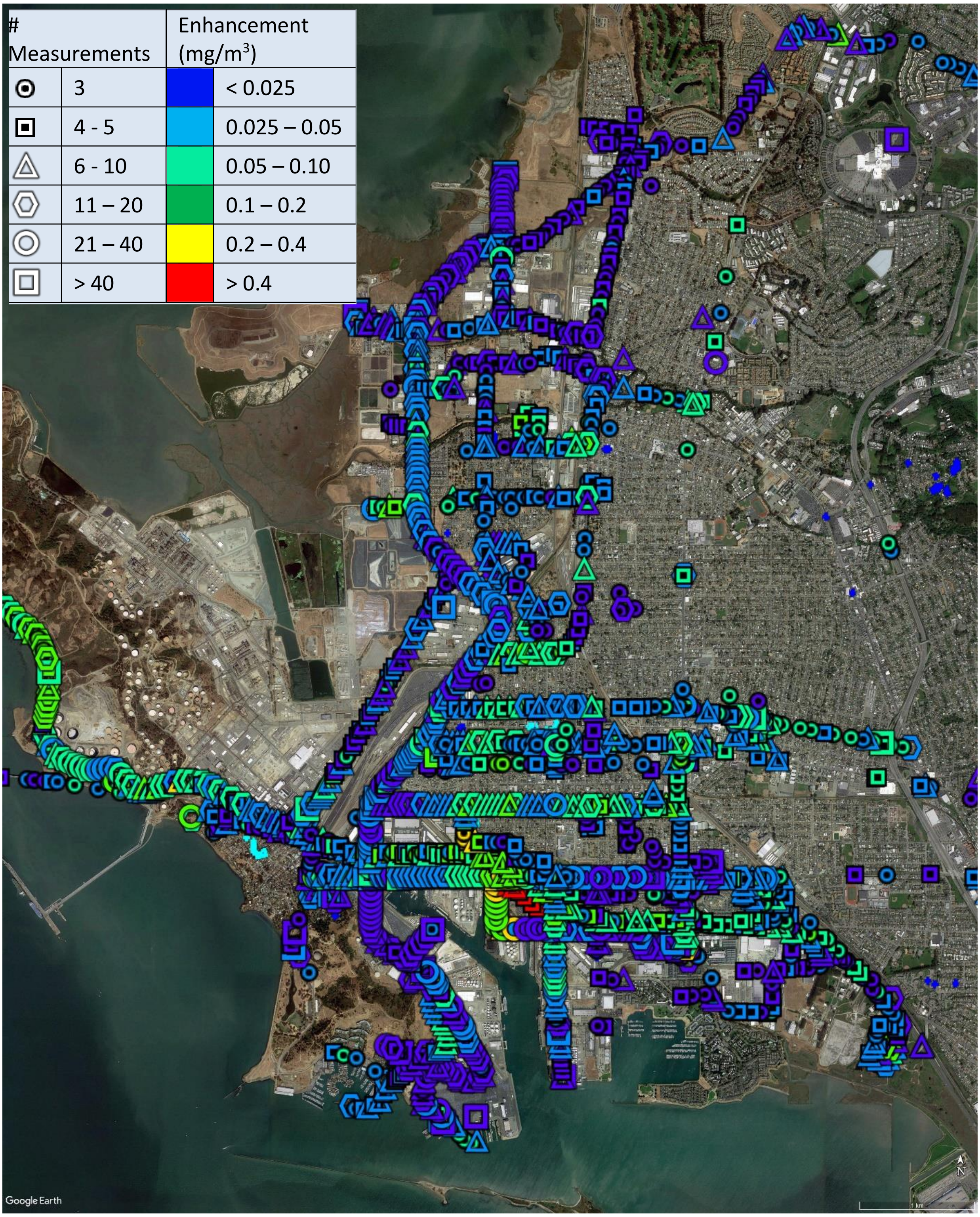

Figure 84 Community monitoring of alkanes in Richmond, number of measurements (min. 3) within an approximately 50 x 50 m grid cell and mean alkane enhancement within the cell.

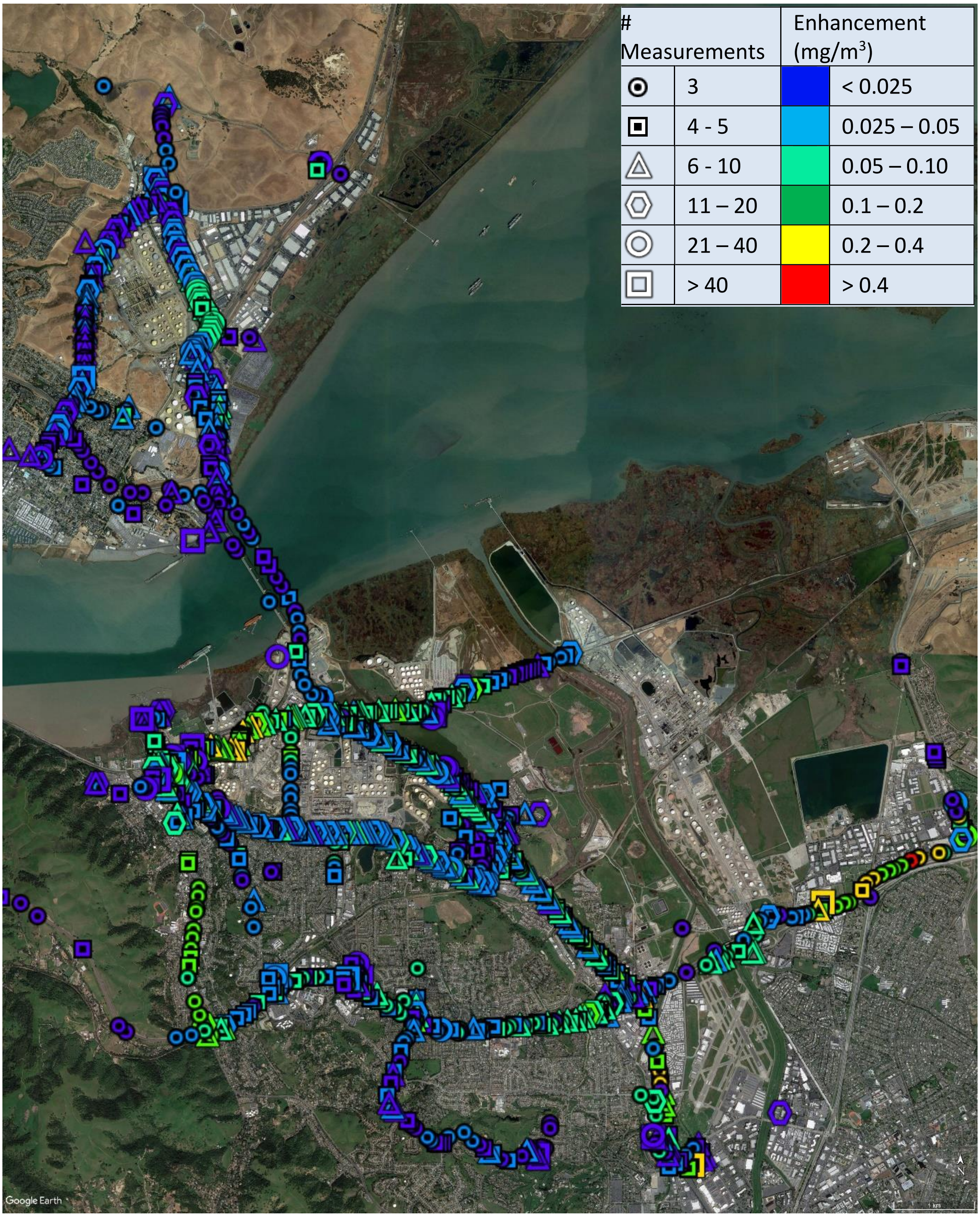

Figure 85 Community monitoring of alkanes in Benicia and Martinez, number of measurements (min. 3) within an approximately 50 x 50 m grid cell and mean alkane enhancement within the cell.

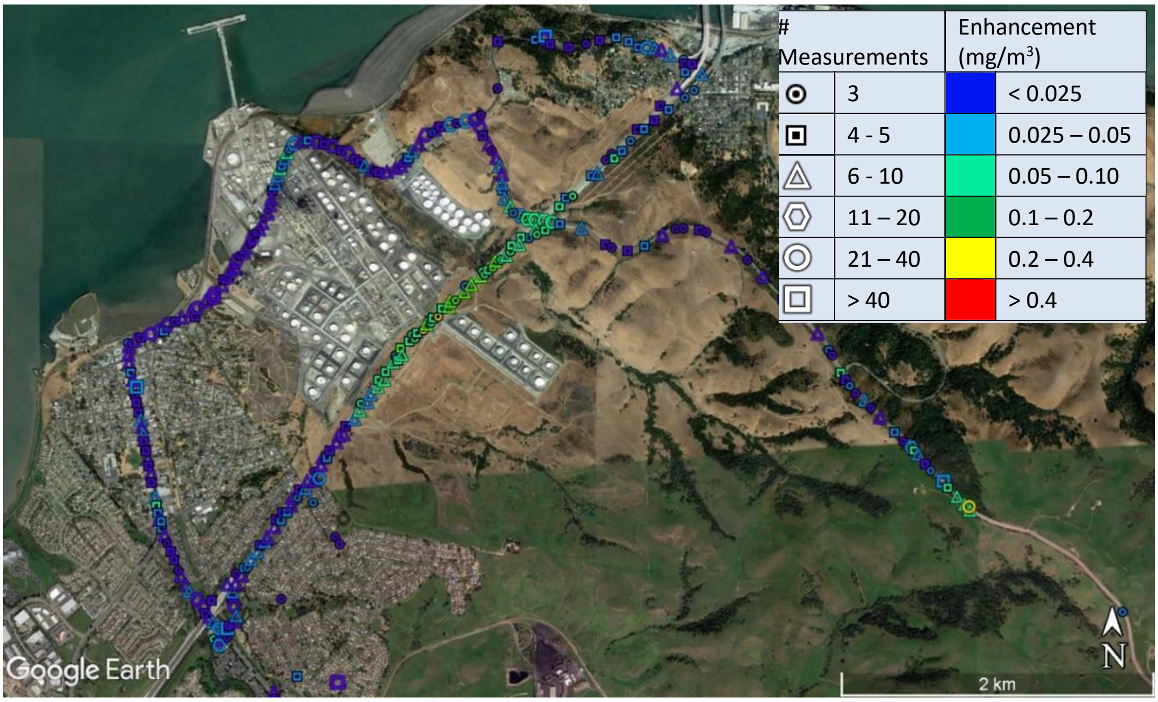

Figure 86 Community monitoring of alkanes in Rodeo, number of measurements (minimum of 3) within an approximately 50 x 50 m grid cell and mean alkane enhancement within the cell.

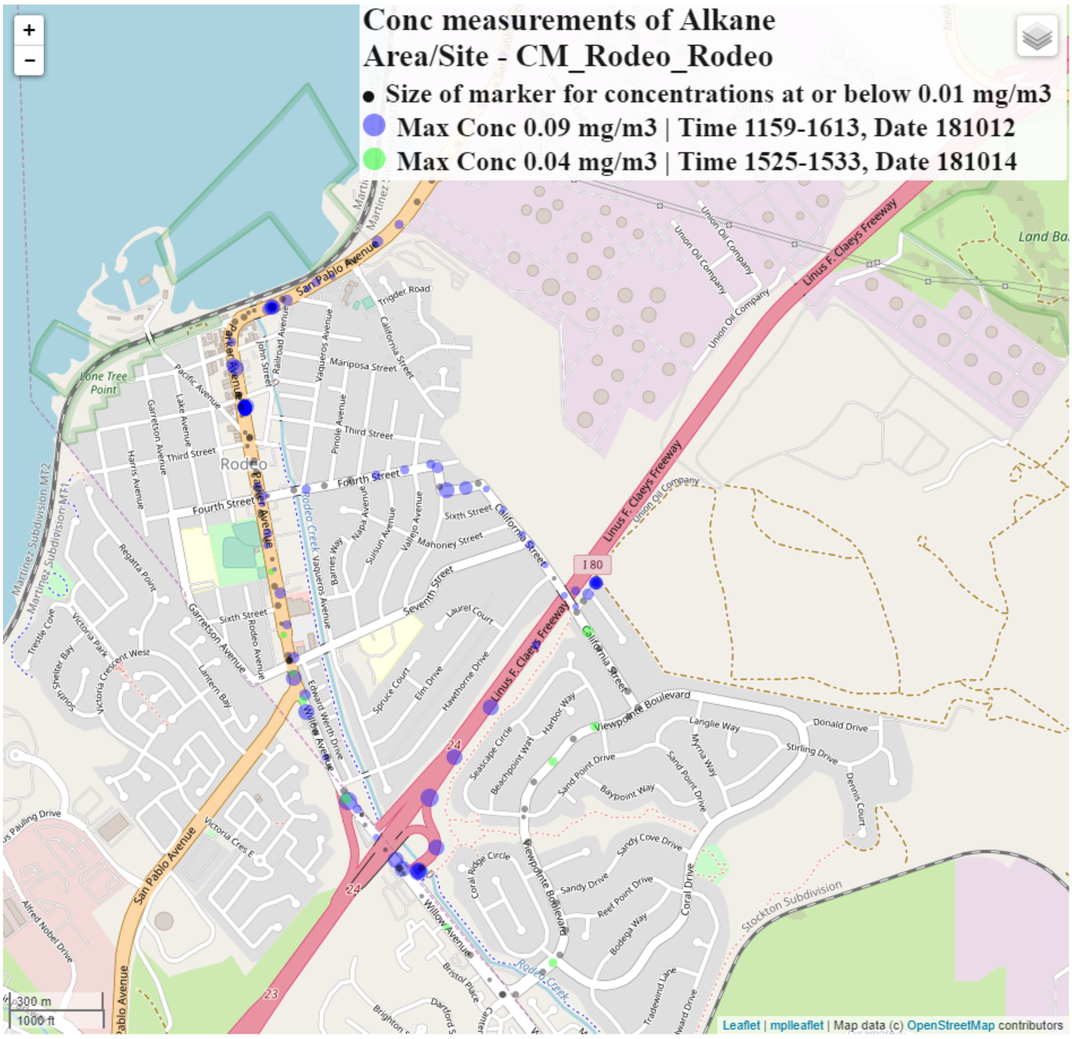

Figure 87 CM in Rodeo just south of the refinery area fenceline, October 12, 12PM, SW wind.

Table 65 shows the measurements locations and dates for community monitoring.

Table 65. Summary of all days with community monitoring.

| Date | Region | Other | CM |
|---|---|---|---|
| 30-sep-2018 | San Joaquin Valley | DAY | Elk Hills |
| 1-okt-2018 | San Joaquin Valley | DAY | Elk Hills |
| 2-okt-2018 | San Joaquin Valley | DAY | Midway Sunset, Lost Hills, Elk Hills |
| 10-okt-2018 | Bay Area | DAY | Benicia |
| 11-okt-2018 | Bay Area | DAY | Richmond |
| 15-okt-2018 | Bay Area | DAY | Martinez |
| 16-okt-2018 | Bay Area | DAY | Richmond |
| 18-okt-2018 | Bay Area | DAY/NIGHT | Richmond |
| 19-okt-2018 | Bay Area | DAY | Richmond |
| 20-okt-2018 | Bay Area | DAY | Richmond |
| 21-okt-2018 | Inland | DAY | McDonald Island Gas Storage |
| 22-okt-2018 | Bay Area | DAY | Richmond |
| 23-okt-2018 | Bay Area | DAY/NIGHT | Richmond |

### *6.2.2 Richmond*

One of the challenges of the community monitoring was to examine the largest potential sources affecting the community, obviously it was thought the refinery area would be among these. As it were, the winds were westerly on only a few occasions during the Richmond portion of the survey, when the Richmond community would be most affected by the emission plumes from the refinery area. Additionally, these few occasions were during the daytime, continuing to early evening only once. On most occasions the wind was southerly, and at such times port activities are a stronger influence on the air quality in the Richmond community, together with the background from San Francisco.

Thus, the general impression during the campaign is that the emissions from the Port of Richmond affects the community more than the refinery area does, since the former is placed in the prevalent upwind direction from the community, is closer and is more dominated by non-elevated (near ground level) sources than the latter. As was seen in 5.4 Wind Climatology, this is the predominant upwind source even annually. We also found that some of the locations identified in CARBs monitoring coincided with sources in the Port of Richmond, even if they were not immediately adjacent the port area. This is illustrated rather well in Figure 88 where the alkane concentration at near ground level (2 m) is measured with MeFTIR during the afternoon with southerly winds and the vehicle tracking the plume into the community. It is evident that many areas of Richmond, even well downwind, can be affected by the emissions from the port. Multiple such measurements were made in which ship loading was also identified as an important source in addition to tank storage. Figure 89 shows the subsequent measurement transect. For methane, the port is not as strong a source and small local sources dominate along with the plume from the water treatment on Canal Blvd. The port alkane source was traversed twice on Cutting Blvd. on this transect (14:50 & 17:00) with similar results.

Figure 90 shows the totality of BTEX measurements in Richmond by the port, Easter Hill and central Richmond. With the exception of the port no strong sources could be identified. The port sources confirm also the same hotspot as the alkane measurements. Even some of the hotspots further afield are probably attributable to this source. Occasional plumes can be found in residential areas, likely from nearby temporary residential sources, such as the one near Seacliff Drive. Figure 91 shows BTEX measurements in North Richmond. Here there appear to be a number of smaller sources that correspond to those previously indicated in community monitoring. These and alkane and methane and BTEX sources and hotspots are addressed in the following section, *6.2.3 Other point and area sources in Richmond*.

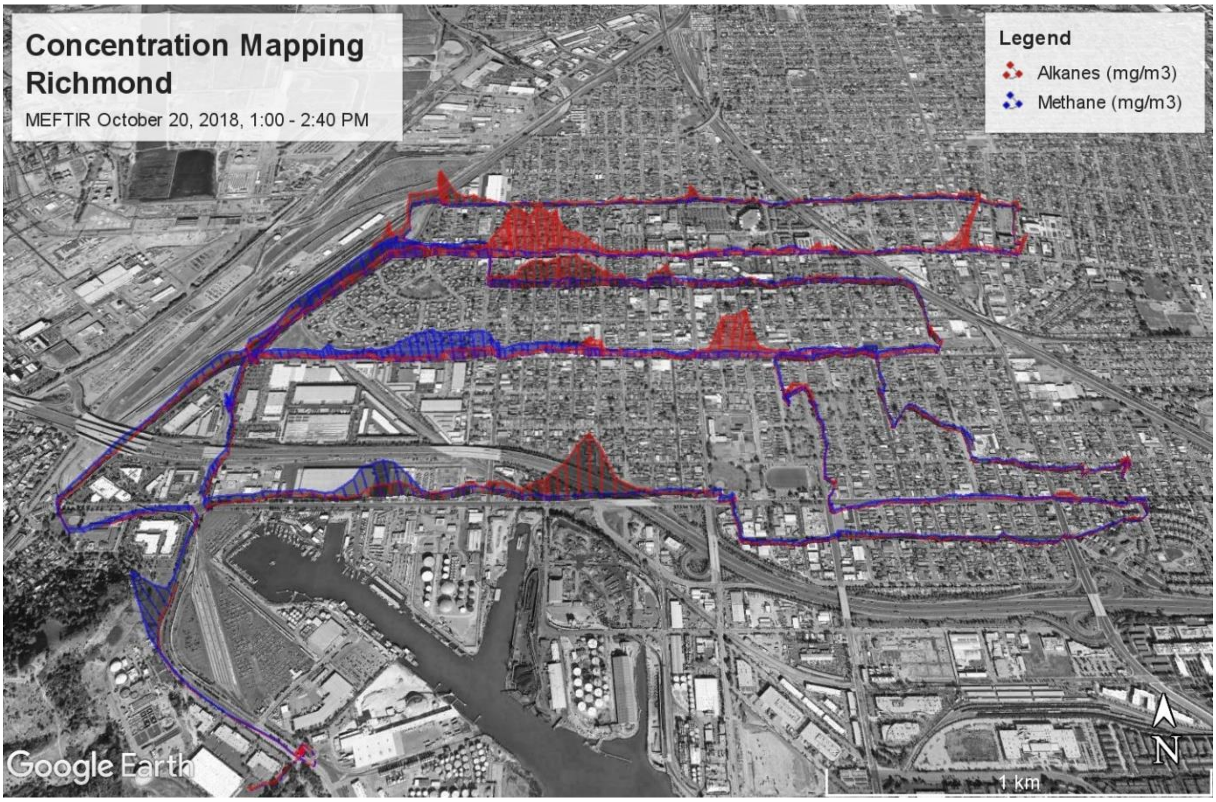

Figure 88. Tracking the VOC (alkane) plume from the Port of Richmond into the community using MeFTIR. Daytime measurement, October 20.

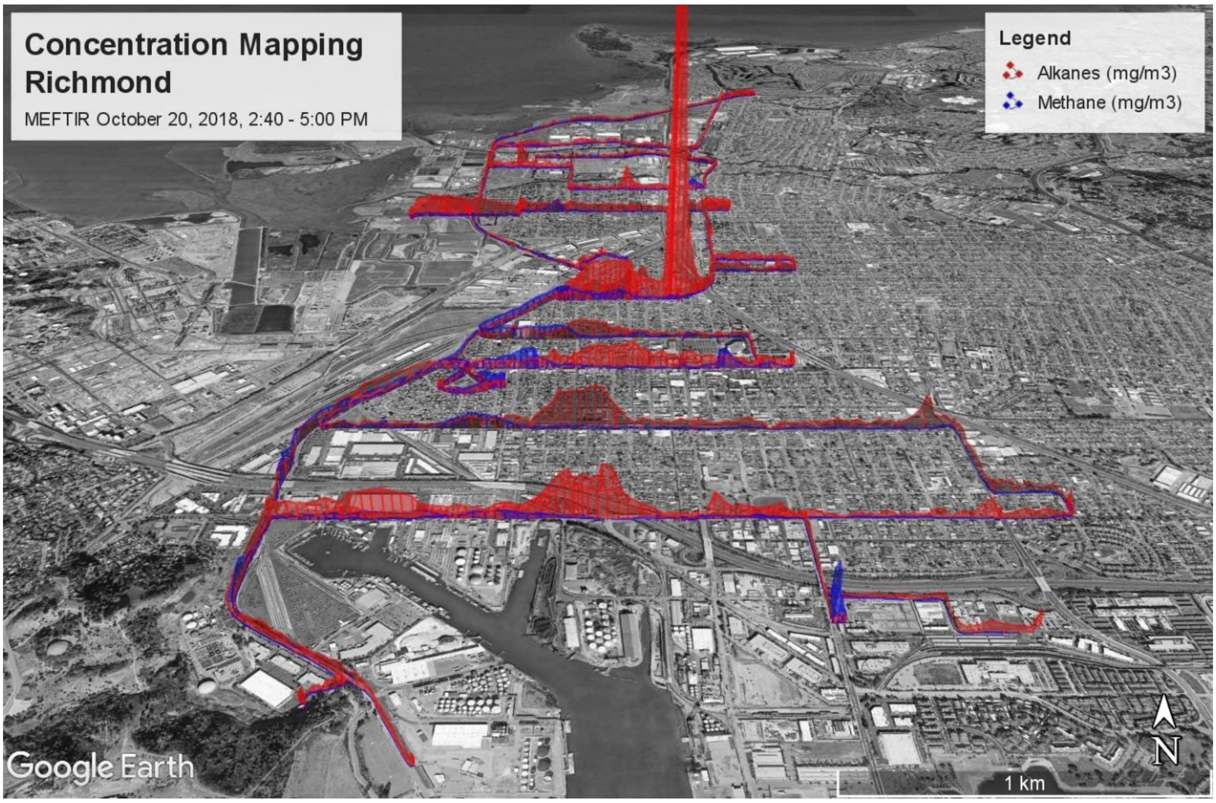

Figure 89. Concentration of methane and alkanes in Richmond, October 20, 2018, 14:43 – 17:06. The subsequent transect to Figure 88.

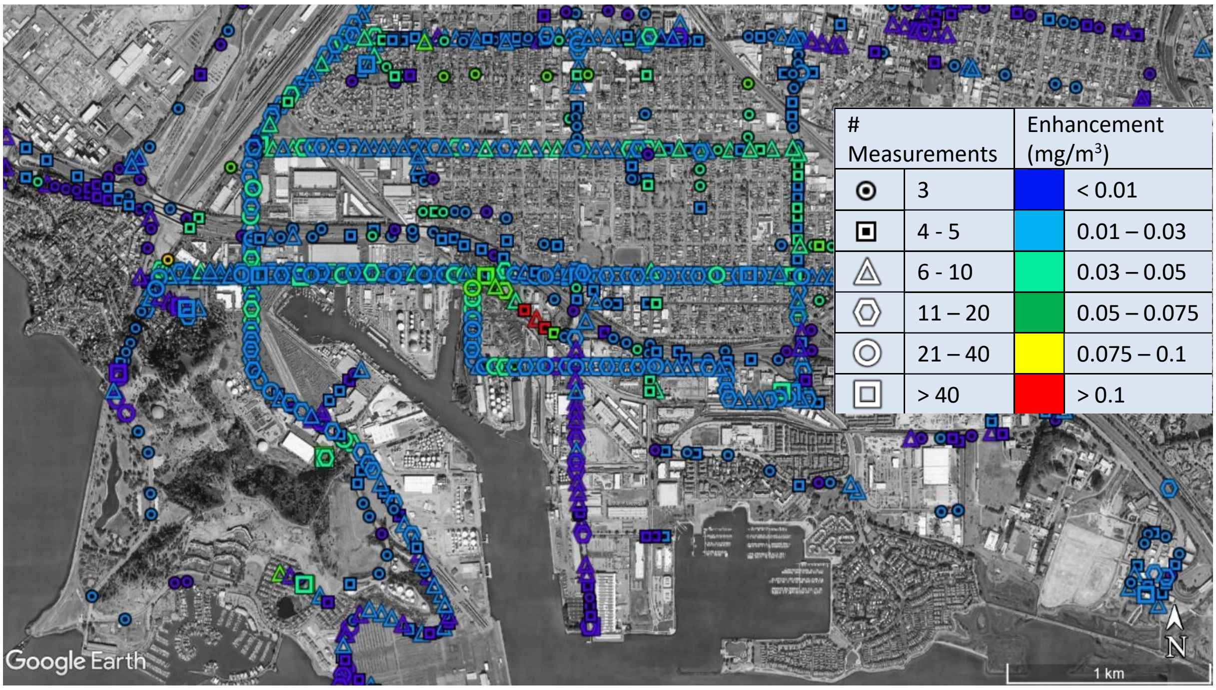

Figure 90. Community monitoring of BTEX in Richmond, number of measurements (min 3) within an approximately 50 x 50 m grid cell and mean BTEX enhancement within the cell.

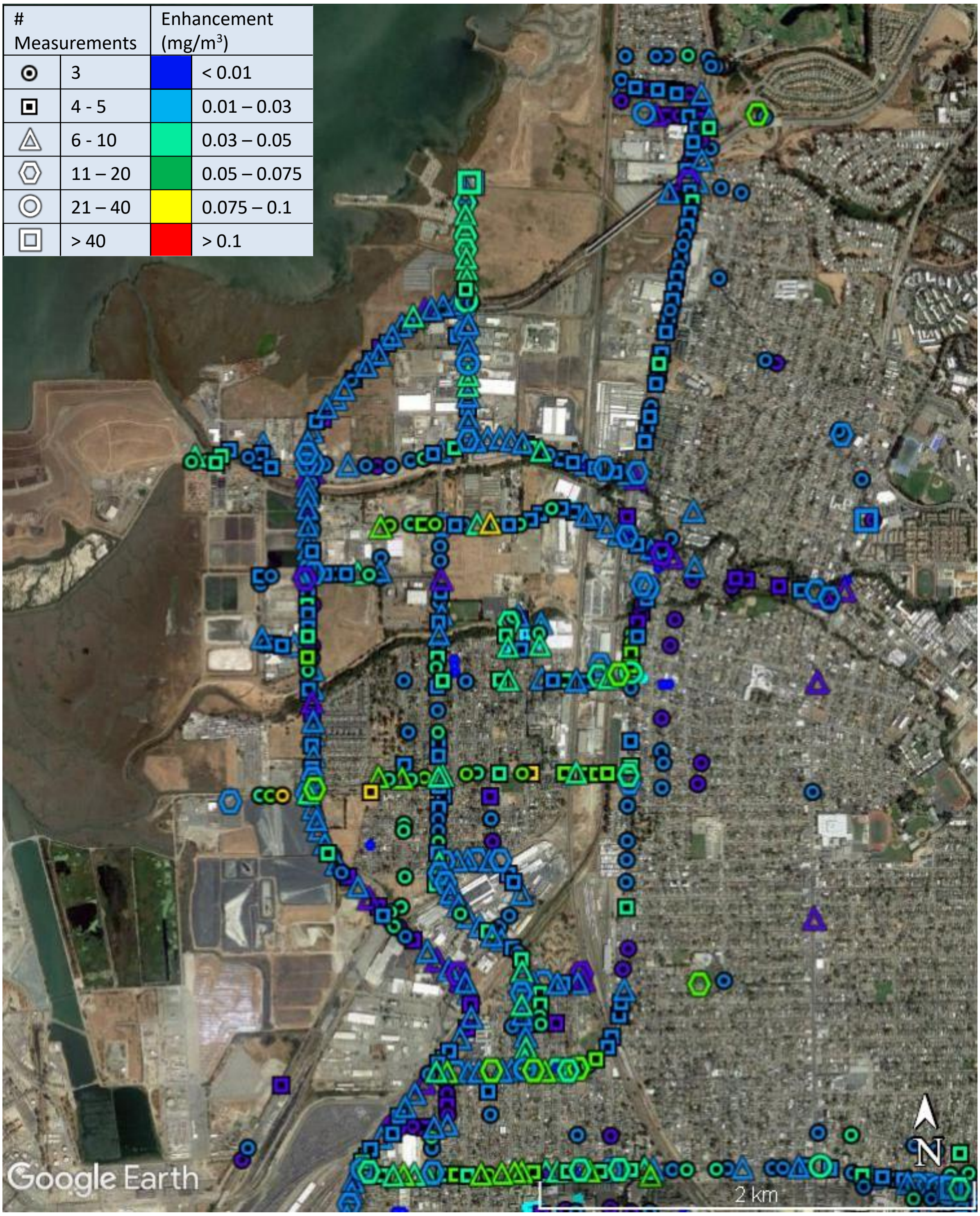

Figure 91. Community monitoring of BTEX in North Richmond, number of measurements (min 3) within an approximately 50 x 50 m grid cell and mean BTEX enhancement within the cell.

### *6.2.3 Other point and area sources in Richmond*

Apart from the major sources and smaller sites for which emissions have already been presented, other point and area sources (repeatable hot spots) found within the Richmond area during the survey are presented here. An area source may be diffuse emissions or aggregated point sources from a distance that they are inseparable from one another in the measurements. Many of these sources may be more specific in terms of gas emissions, e.g. dominated by methane for water treatment, and therefore these sources are gas specific. In other words, an identified alkane hotspot may not have the same source as the methane hotspot at the same location. These sources are therefore presented under separate headings: NMVOCs (alkane and BTEX) and methane specific. For alkane sources typically even SOF emission measurements are available. Therefore, indirectly measured emissions for BTEX or methane can be determined for these sources.

Although numerous ephemeral plumes occur for which no source attribution is possible, recurring plumes with winds suggesting the same source have been attributed.

#### *6.2.3.1 NMVOC hotspots, Alkane and BTEX point and area sources*

Apart from the refinery areas, the primary point sources of alkane emissions were either located in the port or were gas stations with temporarily large emissions. One unattributed plume in the area of Pittsburg Ave intersection with Richmond Parkway but closer to De Carlo Ave stands out for its sheer magnitude (Figure 92). Several CEIDARS sources exist in the area. No visual confirmation could be made of related activity and the plume was not captured again during later measurements on the same day. This is a minor industrial area and frequently measured emissions with SOF from this area. Besides alkanes the plume also had a BTEX signature. Figure 93 shows the spectral retrieval for one of the peak concentrations. Methane was also consequently high at the time but consists of a much wider plume so unlikely all could be from the same source.

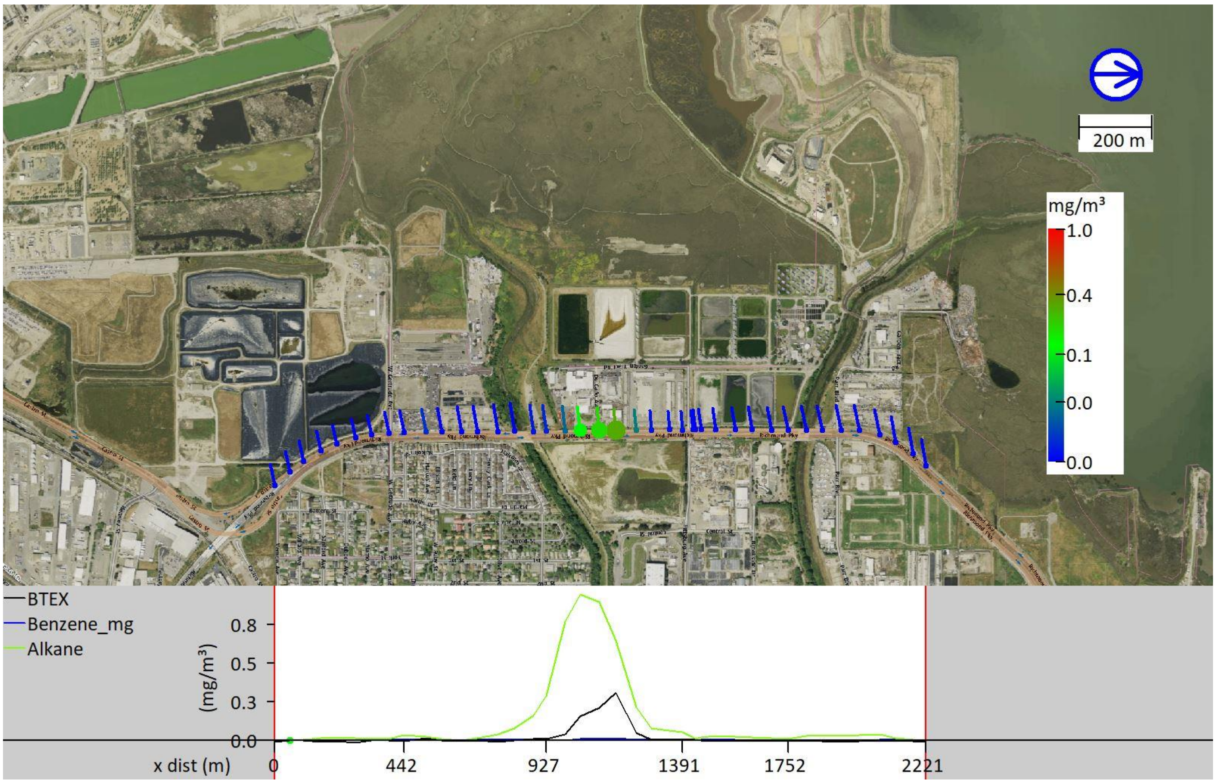

Figure 92. Temporary but unusually large VOC plume from the vicinity of the Pittsburg Ave intersection with Richmond Parkway, October 23, 6PM. Image shows total BTEX in logarithmic color scale with lines point upwind in the direction of the source. The plot below the image shows BTEX (0.31 mg/m$^3$), benzene, and

Alkane concentrations (1 mg/m$^3$). Note the ratio of BTEX/Alkane is approximately 30%. North is to the right in the image.

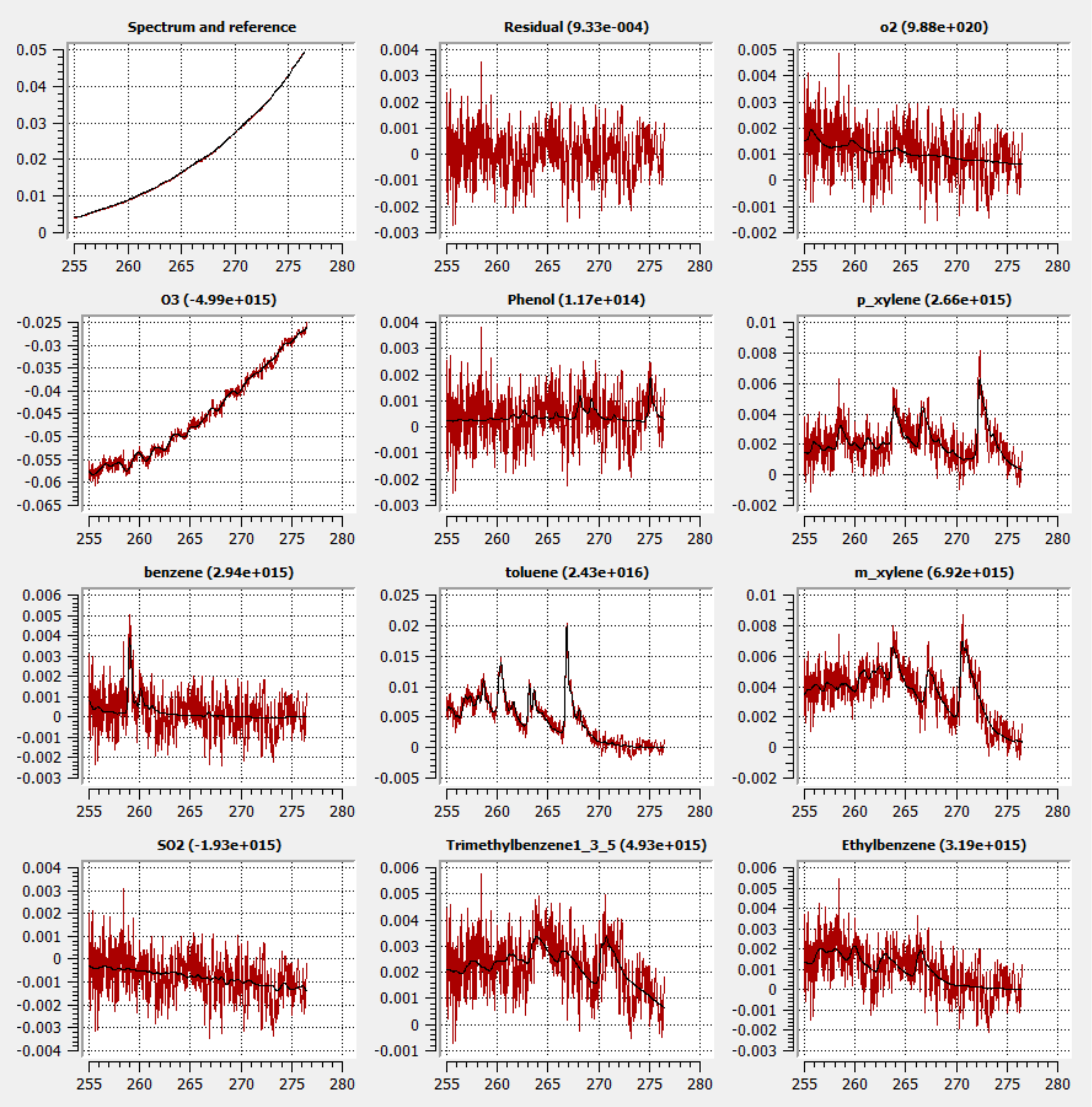

Figure 93 Spectral retrieval with QDOAS of measurement 7:37:27 PM October 23. BTEX concentration was 0.31 mg/m$^3$. Black shows the fitted species to the measured spectra in red. X axis in wavelength in nm. Toluene was the dominant BTEX specie.

Gas stations routinely showed emissions of alkanes and occasionally large emissions. The largest is shown in Figure 94 where a tanker truck was observed leaving the site.

Another temporary unknown occurred October 18 in a residential neighbourhood on 7th St between Lincoln and Lucas Avenues (Figure 95). The location corresponds to no hot spots and the nearest sources are to the north, or upwind at the time.

Figure 94. Alkane and BTEX plume from a Gas station at Pennsylvania and Harbor Way. Image shows total BTEX in logarithmic color scale with lines point upwind in the direction of the source. The plot below the image shows BTEX (0.61 mg/m$^3$), benzene, and alkane concentrations (2.5 mg/m$^3$). Here it is easy to see the different response times of the instruments: the open path DOAS for BTEX is almost instantaneous while the extractive IR instrument response is somewhat delayed and the plume appears wider.

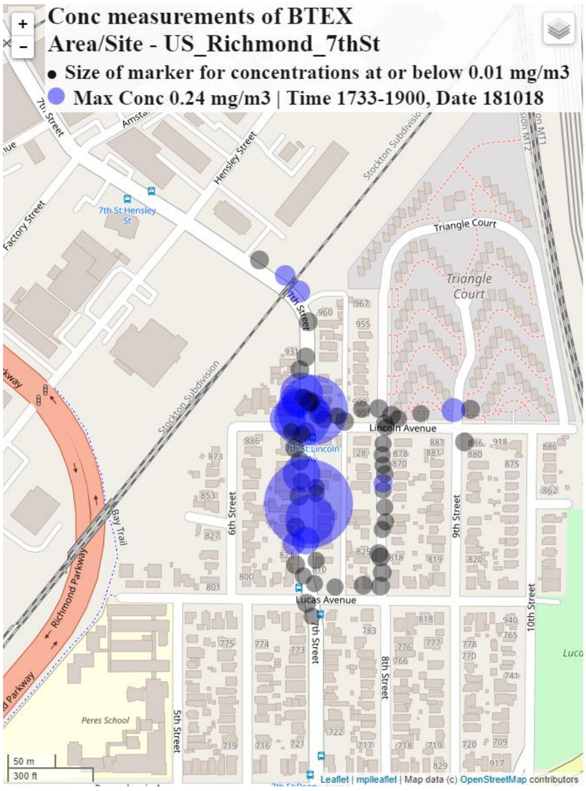

Figure 95. Unknown BTEX (up to 0.24 mg/m$^3$) and alkane source 18 October 6PM, 2018. The source was in a residential neighborhood and a large truck was parked in the alley way and empty lot. BTEX measurements show that the plume did not exist before 6PM. No benzene was detected in the plume.

Within the area of North Richmond there are many small industries. Figure 96 shows an example of community monitoring within North Richmond confirming many of these as probable hot spots.

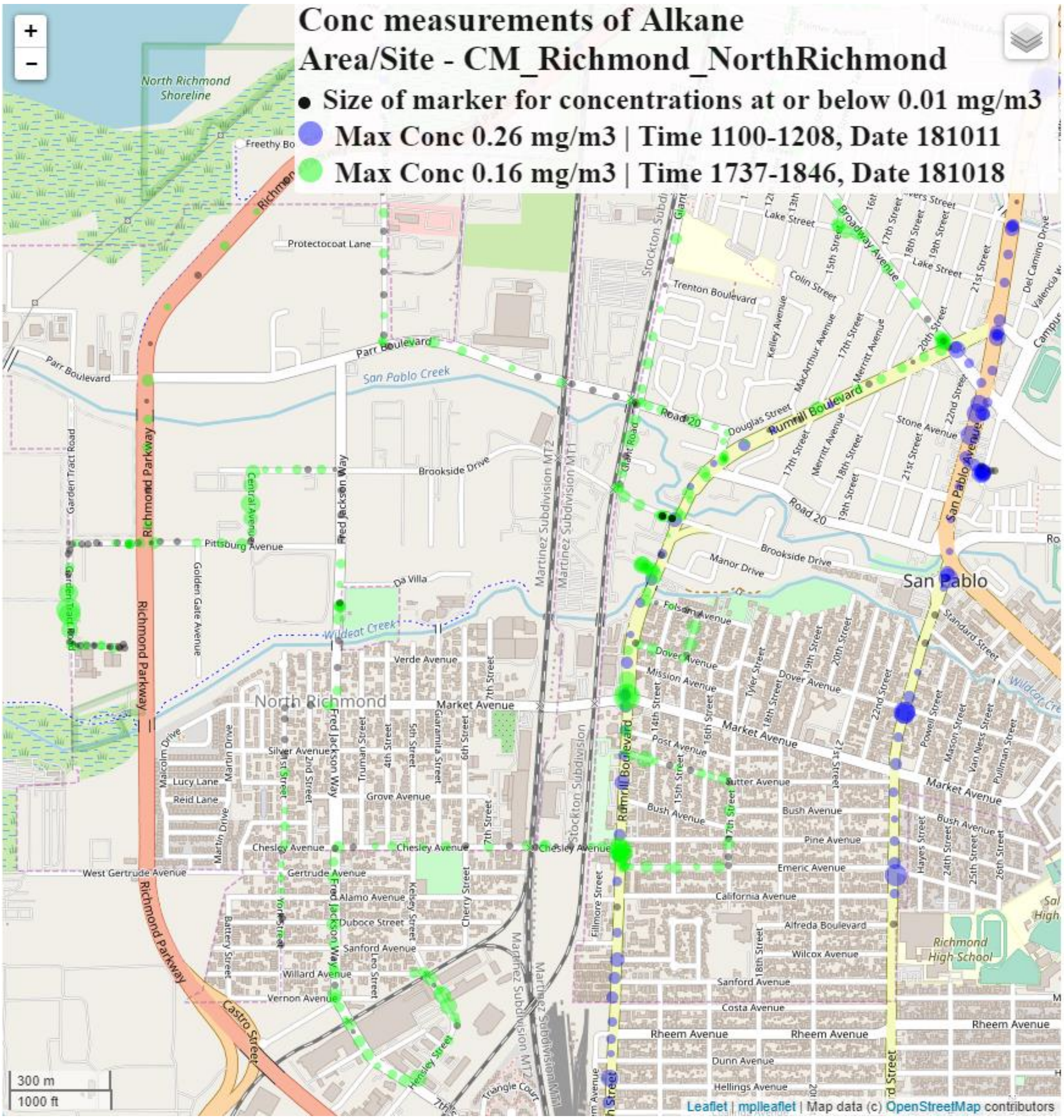

Figure 96. Example of community monitoring in North Richmond, alkanes.

#### 6.2.3.2 *Methane point and area sources*

Figure 97 shows an overview of the ground level methane plumes encountered in the Richmond area during the survey. This excludes occasions of high concentrations from the refinery and the port to . Plumes correspond to these sources: the 2 water treatment facilities, the landfill, and some facilities in Marina Bay. This is particularly evident in Figure 98 where a large methane plume is sourced from the area in North Richmond that includes a landfill, water treatment and other industries. Secondary smaller sources exist, a number of these within the Marina Bay area. Most of the apparent hot spots that have no nearby source but are downwind of larger sources are probably due to these large sources farther afield. Figure 99 shows an example of how plumes from the water treatment and Port of Richmond migrate into Richmond with southerly winds. Other small methane sources are numerous and even residential and commercial (non-industrial) can be identified as hot spots.

Figure 97. Community monitoring for possible methane sources in Richmond with MeFTIR measurements, apparent height scale 1 m : 1 µg/m$^3$.

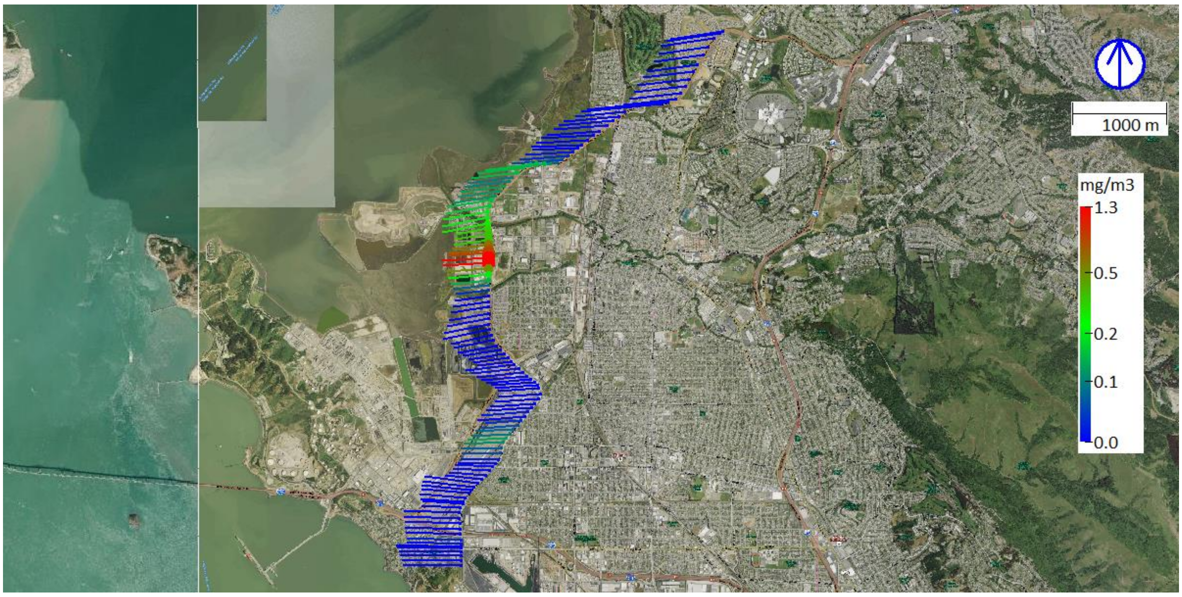

Figure 98. Methane mapping – landfill and water treatment and refinery, Richmond. $CH_4$, 23 October 2018, 7:30 PM. Logarithmic color scale showing methane enhancement in mg/m$^3$. Landfill plume is dominant but refinery area plume is very apparent. This was an unusual occurrence during the survey both westerly winds and when a methane plume from the refinery area was so distinct.

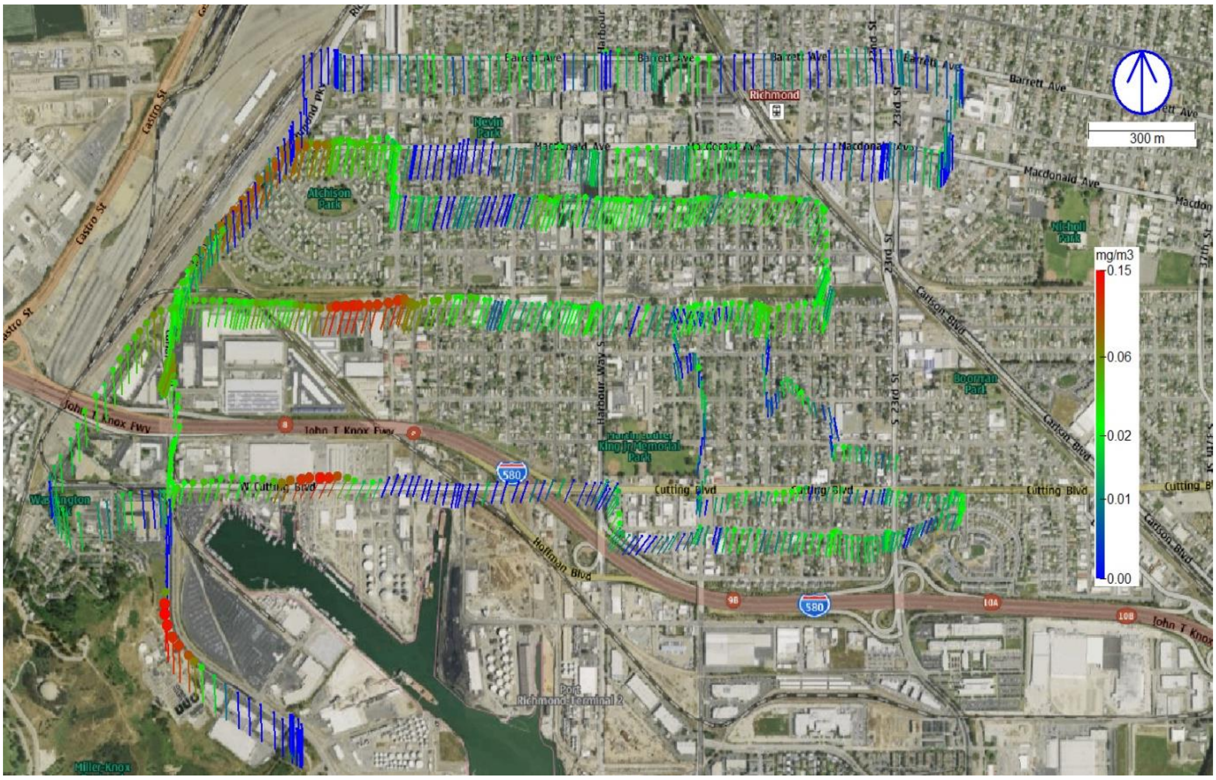

Figure 99. $CH_4$ concentration mapping. Tracking plumes from Port of Richmond and Water treatment (SW corner) into the Richmond community.

Within the survey there were many other measurements of methane plumes from water treatments facilities and even another landfill (Keller Canyon). Figure 100 shows one such measurement of a water treatment plant outside of Richmond. While no emissions calculations have been made for these facilities within the current survey because a lack of alkane emissions from the sites, emission measurements are possible and could be conducted at a future date.

Figure 100. Methane mapping – Central Contra Costa sanitary water treatment, 15 October 1PM, 2018.

### 6.2.4 *Unknown domestic VOC source of PCBTF*

A strong VOC hotspot was identified at street level at a domestic neighborhood at 29th Street and Barrett (Figure 101). The specific compound could not be identified in the real time VOC analysis but it was later identified as Parachlorobenzotrifluoride (PCBTF) from the measured infrared absorption spectra by the MeFTIR (Figure 102). This species also has a strong absorption feature in the UV/visible region, interfering with the BTEX retrieval in the MWDOAS if not taken into account.

PCBTF is a lower volatility solvent which is used in place of toluene in some applications, but which may have health impacts. It has a vapor pressure about ¼ that of toluene at 20 C (Maul et al. 2008).

We have only qualitative calibration spectra for PCBTF (Figure 102). To estimate the concentration enhancement of PCBTF, the absorption sensitivity of a similar species (fluorine containing PCB was used as a proxy. We estimate this causes an uncertainty of 30 - 50% in the concentration estimate based on how much several similar species vary.

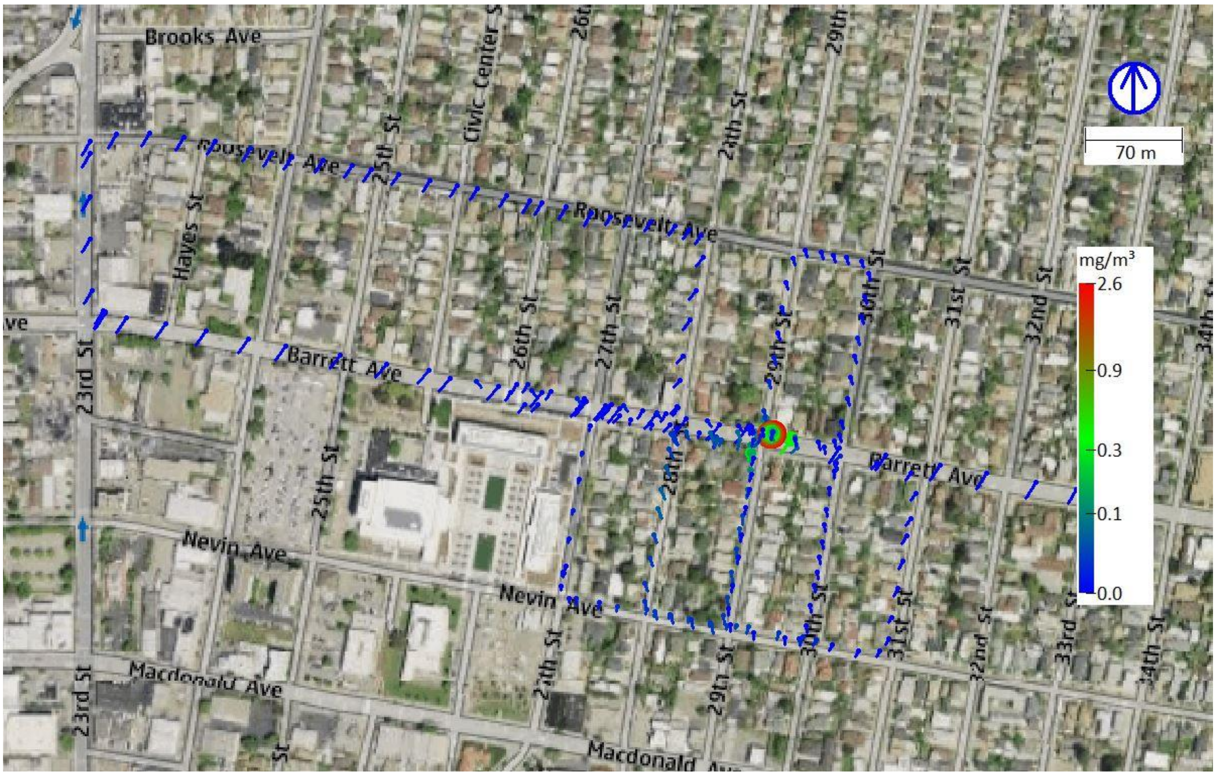

Figure 101. Unknown domestic VOC source of PCBTF at 29th and Barrett, measured October 23 between 22:00 - 22:35. The concentration is in equivalent PCTBF units (mg/m$^3$.)

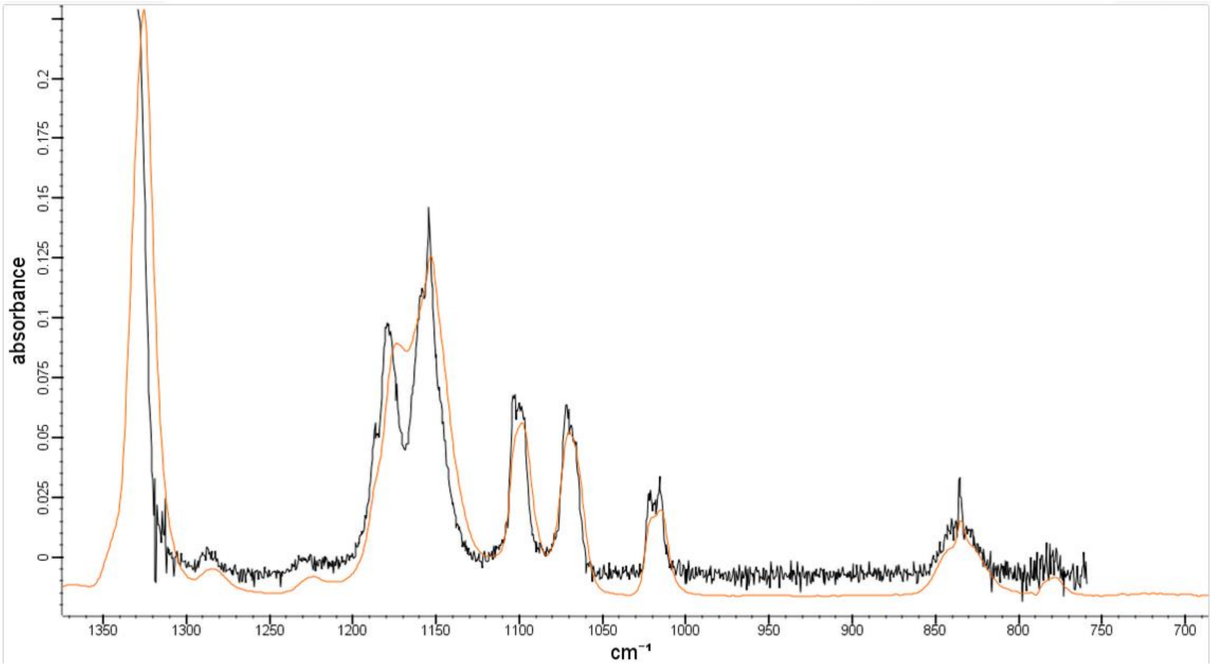

Figure 102. Comparison of the measured absorption spectra at 29th and Barret with an absorption cross section of PCBTF.

## 6.3 Other emission sources

Measurements of VOC emissions from oil and gas production and ammonia emissions from Concentrated Animal Feeding Operations (CAFOs) were carried out during 5 days in the San Joaquin valley. An additional emission source studied was a major brush fire.

The main results from these measurements, including gas fluxes, will be reported together with the results from the second campaign in May 2019 in which the focus will be on impact of oil and gas production and CAFO emissions in the central valley. During the campaign only a few large-scale measurements were carried out and since the wind patterns were complex with turning wind we want to analyze this further. The quantitative results given below should only be considered as examples at this stage.

### *6.3.1 Oil and Gas Elk Hills (St Joaquin Valley)*

Several large-scale measurements with SOF, MeFTIR and MWDOAS were carried out around the Elk Hills oil and gas production area over 2 Days. Here distinct columns of VOCs and methane were detected (1:2 alkane to methane mass) but only small amounts BTEX. In Figure 103 such a measurement is shown of alkanes. The emissions rate of alkanes inside the area encircled by the measurement was here around 5000 kg/h, and the methane emission approximately double. However, we are uncertain of the persistence of the wind, measured in the middle of the figure and further measurements are therefore needed, also in other wind directions.

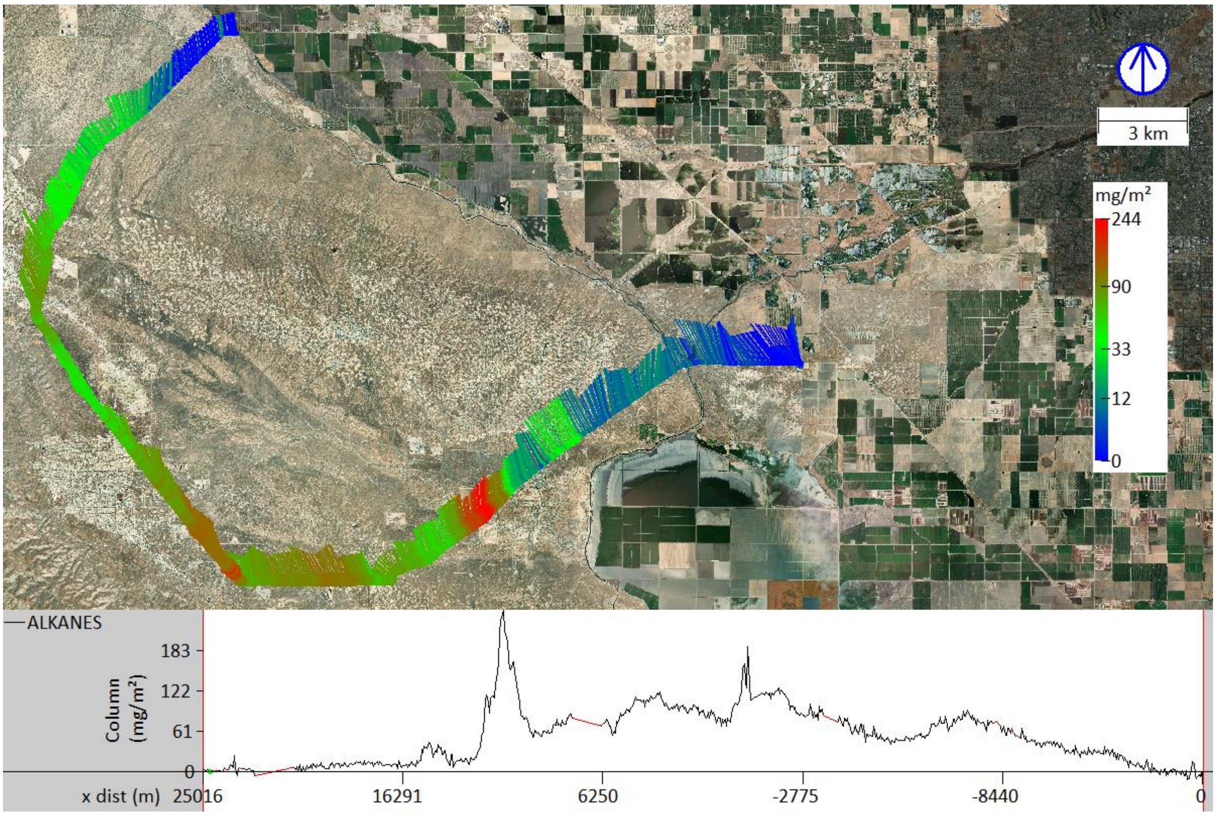

Figure 103. SOF alkane measurements (NMVOC) from Elk Hills. The typical mass ratio between $CH_4$ and the alkanes was 2:1.

### 6.3.2 *CAFOs Bakersfield and Merced*

Large-scale measurements of ammonia were carried out using SOF in both Bakersfield, Figure 104 and Figure 105, and Merced, Figure 106. Here distinct columns of ammonia were detected. The emissions rate of ammonia inside the area encircled by the measurement was here around 700 kg/h, but it is uncertain whether the wind shifted direction during the scan since the wind was measured in the top left corner, and further measurements are therefore needed.

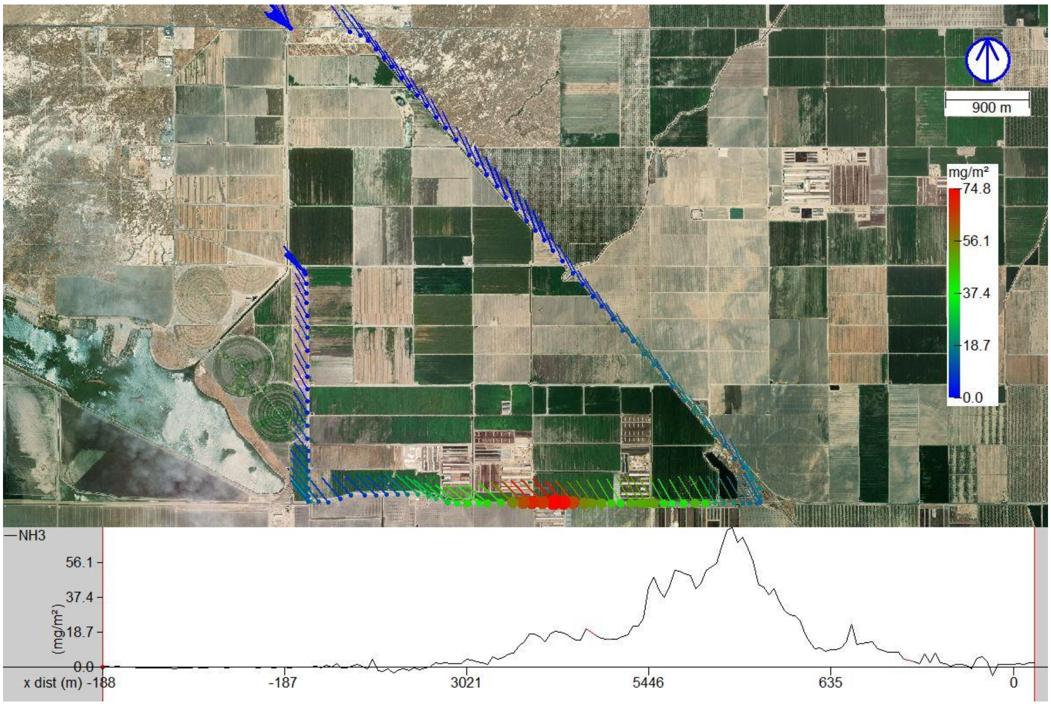

Figure 104. Measurements of ammonia downwind of several CAFOs and other agriculture operations near Bakersfield.

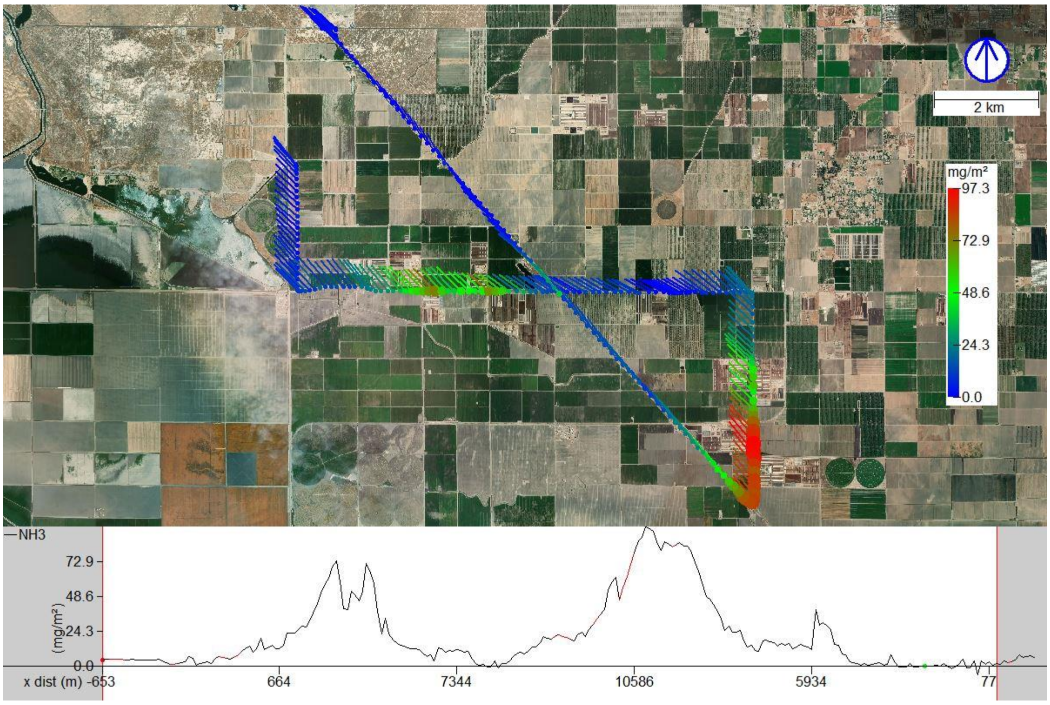

Figure 105. SOF measurements of ammonia downwind of several CAFOs and other agriculture operations near Bakersfield.

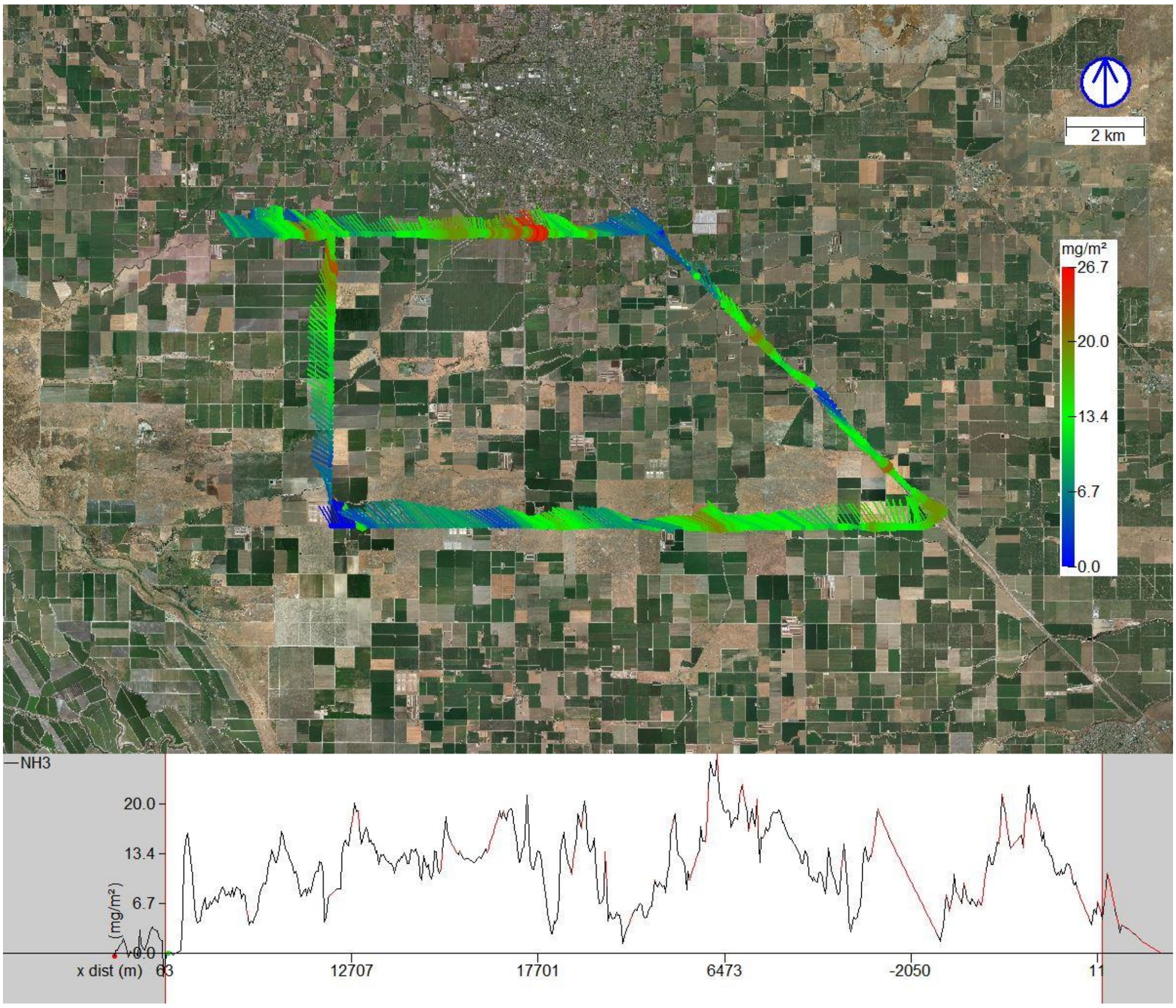

Figure 106. SOF measurements of ammonia downwind of several CAFOs and other agriculture operations near Merced. Color scale in image shows $NH_3$ column in mg/m$^2$ with a line pointing upwind in the direction of the source. Note the high background.

### *6.3.3 Brush fire*

On October 7 a brush Fire near Travis air force base occurred in which about 4500 acres were burning over one day. Measurements of SOF, SkyDOAS, MeFTIR, and MWDOAS were carried out 4 times at a distance of approximately 25 km downwind the fire. In Figure 108 such column measurements of $SO_2$, $NO_2$ and $H_2CO$ are shown obtained with SkyDOAS.

The analysis shows emissions of several species, Table 66, obtained from either SkyDOAS or SOF. The spectral analysis is still on-going and here are several more species, including VOCs that will be obtained from this measurement.

Table 66. Emission rates obtained during 4 transects through the brush fire plume at 25 km distance from the source.

| Species | Emission kg/h |
|---|---|
| $NH_3$ | 500 - 900 |
| $SO_2$ | 3000 – 4000 |
| $NO_2$ | 1100 – 1600 |
| $H_2CO$ | 1400 – 4900 |

Figure 107. Brush Fire near Travis AFB. About 4500 acres burning in late afternoon. Photo with courtesy to Peter Da Silva, SF Gate The Chronicle, Oct 8 2018.

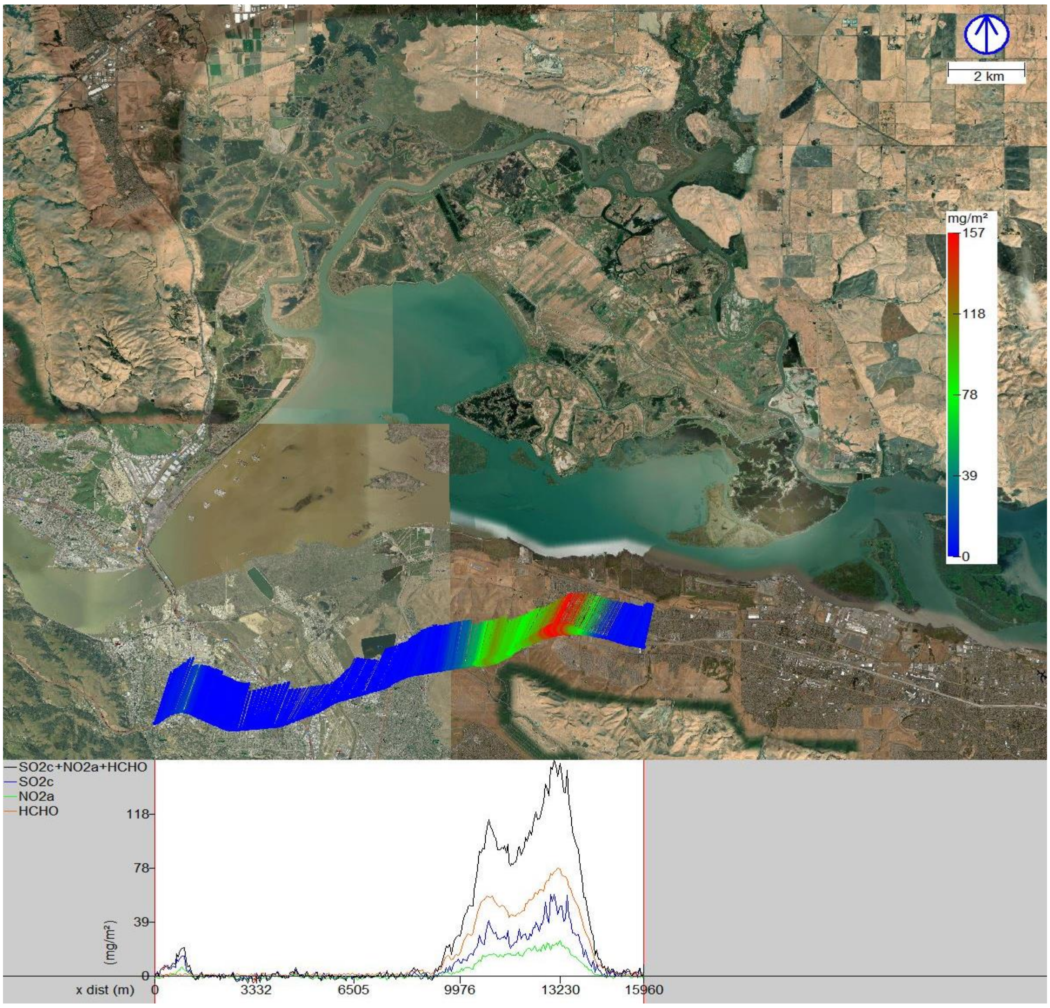

Figure 108. $SO_2$, $NO_2$ and HCHO measurements by SkyDOAS downwind a brush fire near Travis AFB. About 4500 acres burning in late afternoon. The color-coded values correspond to the sum of all three species in the unit mg/m$^2$.

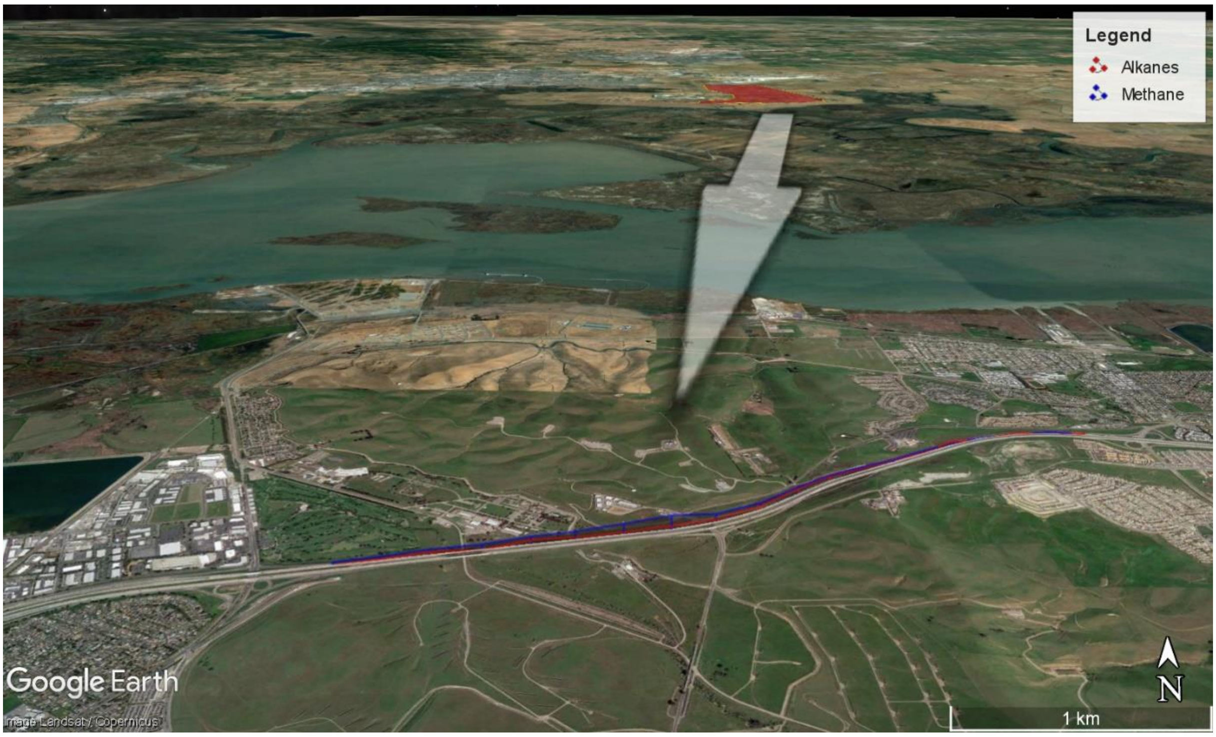

Figure 109. Ground-level concentration measurements of methane and alkane downwind a brush fire near Travis AFB (orange shading). Approximate vertical scale 1 m: 1 µg/m³.

# 7 Discussion and Conclusions

Emissions from the sites in this survey can be assessed by comparison with historical measurements, reported inventories, and emission factors based on throughput for similar industries, which in this case for the major sites, petroleum refineries, much data exist. Although generally historical data is difficult to obtain, the main emission results in

Table 7 for 2018 can be compared to emission data from a Bay Area refinery emissions survey conducted by FluxSense in 2013 albeit with fewer measurements and sites (Mellqvist et al., 2013a). As seen in Table 67 the alkane emissions were reduced by 30-35% for the Benicia and Martinez W refinery areas, while remaining about the same for the Rodeo refinery area.

The overall emission results in Table 7 can be compared to emission inventory data from CARB for 2016 as given in Table 68. Here the refinery capacity is also shown for each site, obtained from the *US Energy Information Administration* for 2018.

In Table 69 the difference between the measurements and the CARB 2016 inventory is shown, based on the data in Table 7 and Table 69. The table shows the discrepancy factors *D* for the different species, corresponding to the ratios of the measurements and inventory. In Table 69 is also shown the emissions per crude oil capacity for each refinery (capacity specific VOC emission factor) for the inventory and measurement data, respectively.

The overall agreement between the CARB 2016 inventory and the measurements is shown in the SUM values in Table 69. It can be seen that the measurements indicate that the VOC emissions on average are 2.5 times higher (150%) than the reported ones and even higher for the corresponding methane emissions (190%). The agreement appears to be excellent for $NO_x$ but here it should be noted that measured $NO_2$ is compared to $NO_x$ from the inventory. It is estimated that this causes a systematic negative bias in the $D_{NOx}$ factors of around 20% based on a similar study (Rivera et al., 2010).

For the $SO_2$ the measurements indicate 60% higher emissions than reported. It can be seen that the discrepancies are larger for some of the individual refinery areas. In the instance of the Richmond refinery area, an source separate from the refinery but within the area had emissions of 55 kg/h. The $D_{SO2}$ for just the refinery is then 1.4. Note that the inventory corresponds to annual average emission data while the measurements were acquired over 3-4 days during the 4-week campaign. Some of the observed positive discrepancies above can be explained by this, including that the SOF measurements are carried out only during sunny conditions and the fact that the average wind and temperature may differ from the annual average climatology. In a similar study (Johansson et al., 2014) it was shown that such effects could cause a positive bias in the measured emissions of 30-40%, compared to the annual average. In a recent study by AQMD (Pikelnaya 2019) long term, seasonal measurements were conducted using SOF on a single refinery in southern California. Here 7 separate measurement campaigns were carried out during each seasons from fall 2015 to summer 2018. The overall variability was 20 % with poor correlation ($r^2$=0.27) to season.

In Table 69 is also shown that the emissions relative to the refinery capacity varies between 0.016% to 0.037% with an average of 0.022%. The refineries in the Bay area hence appears to be well maintained and operated since the emission factors for industries in Europe and Texas generally span between 0.03% to 0.15% (Mellqvist et al., 2010, Johansson et al., 2014).

The community monitoring measurements performed over 7 days and 2 nights in Richmond showed many hotspots. Since the general approach was done by 'plume tracking' the influence of the big sources in the community could be assessed. The disadvantage of this was that no regular grid pattern was driven and thus spatial and statistical analysis becomes more cumbersome.

Richmond has two major sources in the vicinity of the community that may influence the concentration levels, i.e. the refinery area in the west and the port in the south. The wind was generally southerly during the campaign thus the port activities affected the air quality in the Richmond community, together with the background from San Francisco. Only a few times were the winds westerly during which the refinery area impacted the Richmond community. The general impression is that the emissions from the port area frequently affects the community and in a stronger way than for the refinery, since the former is placed in the prevalent upwind direction from the community, is closer and have lower sources than the latter. We also found that some of the locations highlighted in CARBs community monitoring coincided with sources in the port area.

An unexpected VOC hotspot was the one found in a domestic neighborhood. It was observed from a strong apparent aromatic response in the MWDOAS sensor. A spectral post analysis using both the DOAS and FTIR spectra showed that the species was PCBTF (parachlorobenzotrifluoride) instead of aromatics and this is a solvent. The concentrations were estimated as high as 2000 µg/m$^3$ at a street corner (29th and Barret) and the high concentration remained for several hours. We suspect this could be caused by some illegal activity since there was not industrial nor commercial facilities in this residential neighborhood.

Table 67. Results of the emission measurements in this study and a similar one in 2013.

| **Source** | **Alkane 2013** kg/h | **Alkane 2018** kg/h | **$NO_2$ 2013** kg/h | **$NO_2$ 2018** kg/h | **BTEX 2013** kg/h | **BTEX 2018** kg/h |
|---|---|---|---|---|---|---|
| **Martinez E refinery area** | | 151 | | 69 | | |
| **Richmond refinery area** | | 291 | | 113 | | |
| **Rodeo refinery area** | 156 | 143 | | 34 | | |
| **Martinez W refinery area** | 513 | 334 | | 104 | | |
| **Benicia refinery area** | 208 | 144 | 66 | 84 | 11* | 12 |

*Only benzene and toluene in 2013.

Table 68. CARB Inventory 2016 for primary refinery emissions in area and US Energy Information Administration refinery throughput data 2018.

| | Crude capacity Barrels/day | VOC kg/h | $NO_x$ kg/h | $SO_2$ kg/h | $CH_4$ & $C_2H_6$ kg/h |
|---|---|---|---|---|---|
| **Martinez E refinery area** | 166000 | 111 | 84 | 46 | 43 |
| **Richmond refinery area** | 245000 | 147 | 80 | 37 | 37 |
| **Rodeo refinery area** | 120000 | 23 | 22 | 39 | 11 |
| **Martinez W refinery area** | 156000 | 114 | 98 | 114 | 39 |
| **Benicia refinery area** | 145000 | 36 | 123 | 8 | 16 |
| **SUM** | **832000** | **431** | **407** | **243** | **147** |

Table 69. Crude capacity specific VOC emission factors (EF) and comparison between measurements and CARB 2016 inventory. Here the discrepancy factor D, i.e. ratio of the measurement and inventory, is shown for different species together with the capacity specific VOC emissions obtained from inventory and measurement, respectively. Note that $NO_2$ for the measurements is compared to $NO_x$ for inventory and methane for the measurements is compared to methane and ethane in inventory. Note also that the inventory values reference only the primary reported REFINERY emissions and the sites contain more emissions sources.

| | VOC EF inventory Capacity specific | VOC EF Survey Capacity specific | $D_{VOC}$ | $D_{NOx}$ | $D_{SO2}$ | $D_{CH4}$ |
|---|---|---|---|---|---|---|
| **Martinez E refinery area** | 0.012% | 0.016% | 1.36 | 0.82 | 1.30 | 1.26 |
| **Richmond refinery area** | 0.010% | 0.021% | 1.98 | 1.41 | 2.97 | 2.84 |
| **Rodeo refinery area** | 0.003% | 0.021% | 6.22 | 1.55 | 0.28 | 4.00 |
| **Martinez W refinery area** | 0.013% | 0.037% | 2.93 | 1.06 | 1.75 | 4.03 |
| **Benicia refinery area** | 0.004% | 0.017% | 4.00 | 0.68 | 2.50 | 4.31 |
| **SUM** | **0.009%** | **0.022%** | **2.47** | **0.99** | **1.64** | **2.93** |

# 8 Acknowledgements

This Report was submitted in fulfilment of 17RD021 “Characterization of Air Toxics and GHG Emission Sources and their Impacts on Community -Scale Air Quality Levels in Disadvantaged Communities” By FluxSense Inc under the sponsorship of the California Air Resources Board. Work was completed as of 27 March 2019.

# 9 References

Bogumil K., et al, 2003. Measurements of molecular absorption spectra with the SCIAMACHY pre-flight model: instrument characterization and reference data for atmospheric remote-sensing in the 230-2380 nm region, *Journal of Photochemistry and Photobiology A: Chemistry*, 157(2-3):167-184 5/5, 2003.

Burrows J.P., A. Richter, A. Dehn, B. Deters, S. Himmelmann, S. Voigt, and J. Orphal, 1999. "Atmospheric remote-sensing reference data from GOME: Part 2. Temperature-dependent absorption cross-sections of $O_3$ in the 231-794 nm range," J. Quant. Spectrosc. Radiat. Transfer 61, 509-517, 1999.

Börjesson, G., Samuelsson, J., Chanton, J., Adolfsson, R., Galle, B., Svensson, B.H., 2009. A national landfill methane budget for Sweden based on field measurements, and an evaluation of IPCC models.Tellus B, 61, 424–435.

DOGGR, 2016. Division of Oil, Gas & Geothermal Resources, at Department of Conservation, CA. http://maps.conservation.ca.gov/doggr/#close .

Downey N., Emery C., Jung J., Sakulyanontvittaya T., Hebert L., Blewitt D., Yarwood G., 2015. Emission reductions and urban ozone responses under more stringent US standards. Atmospheric Environment, 101, pp 209-216, 2015.

Environmental Research & Education Foundation (EREF), 2011. Field comparison of methods for assessment of fugitive emissions from landfills. Available at https://erefdn.org/wp-content/uploads/2015/12/FugitiveEmissions_FinalReport.pdf

Etzkorn T., B. Klotz, S. Sørensen, I.V. Patroescu, I. Barnes, K.H. Becker, and U. Platt, 1999. "Gas-phase absorption cross sections of 24 monocyclic aromatic hydrocarbons in the UV and IR spectral ranges," Atmos. Environ. 33, 525-540, 1999.

European Commission, 2015, Best Available Techniques (BAT) Reference Document for the Refining of Mineral Oil and Gas: Joint Research Centre, Institute for Prospective Technological Studies, ISBN 978-92-79-46198-9 (PDF)ISSN 1831-9424 (online)doi:10.2791/010758, http://eippcb.jrc.ec.europa.eu/reference/BREF/REF_BREF_2015.pdf

Fally S., M. Carleer, and A. C. Vandaele, "UV Fourier transform absorption cross sections of benzene, toluene, meta-, ortho-, and para-xylene," J. Quant. Spectrosc. Radiat. Transfer 110, 766-782, 2009.

Galle, B., J. Samuelsson, B.H. Svensson, G. Börjesson, "Measurements of methane emissions from landfills using a time correlation tracer method based on FTIR absorption spectroscopy." Environ. Sci. Technol. 35: 21–25. 2001.

Griffith D.W.T., Synthetic calibration and quantitative analysis of gas-phase FT-IR spectra. Applied Spectroscopy, 1996. 50(1): p. 59-70.

Johansson, J., et al., 2013a, Quantitative Measurements and Modeling of Industrial Formaldehyde Emissions in the Greater Houston Area during Campaigns in 2009 and 2011, Journal of Geophysical Research – Atmospheres, 2013JD020159R.

Johansson, J., Mellqvist, J., et al., 2013b. Quantification of industrial emissions of VOCs, $NO_2$ and $SO_2$ by SOF and Mobile DOAS during DISCOVER-AQ, AQRP project 13-0051, AQRP report, Dec 7 2013.

Johansson, J. K. E., J. Mellqvist, J. Samuelsson, B. Offerle, B. Lefer, B. Rappenglück, J. Flynn, and G. Yarwood, 2014. Emission measurements of alkenes, alkanes, $SO_2$, and $NO_2$ from stationary sources in Southeast Texas over a 5 year period using SOF and mobile DOAS, Journal of Geophysical Research, 118, doi:10.1002/2013JD020485.

Kihlman, M., 2005a. Application of solar FTIR spectroscopy for quantifying gas emissions, Technical report No. 4L, ISSN 1652-9103, Department of Radio and Space Science, Chalmers University of Technology, Gothenburg, Sweden.

Kihlman, M., J. Mellqvist, and J. Samuelsson (2005b), Monitoring of VOC emissions from three refineries in Sweden and the Oil harbor of Göteborg using the Solar Occultation Flux method, Technical report, ISSN 1653 333X, Department of Radio and Space, Chalmers University of Technology, Gothenburg, Sweden.

Maul J., James & J. Ostrowski, Philip & A. Ublacker, Gregg & Linclau, Bruno & P. Curran, Dennis. (2008). Benzotrifluoride and Derivatives: Useful Solvents for Organic Synthesis and Fluorous Synthesis. 10.1007/3-540-48664-X_4.

Mellqvist, J., et al. (2013a), Pilot study to quantify industrial emissions of VOCs, $NO_2$ and $SO_2$ by SOF and mobile DOAS in the Bay Area, Fluxsense AB, 2013.

Mellqvist, J., et al. (2013b), Pilot study to quantify industrial emissions of VOCs, $NO_2$ and $SO_2$ by SOF and mobile DOAS in the Carson Area, Fluxsense AB, 2013.

Mellqvist, J. (1999), Application of infrared and UV-visible remote sensing techniques for studying the stratosphere and for estimating anthropogenic emissions, doktorsavhandling, Chalmers tekniska högskola, Göteborg, Sweden, 1999.

Mellqvist, J., Johansson J., Samuelsson J. And Offerle B. (2008a), Emission Measurements of Volatile Organic Compounds with the SOF method in Normandy 2008. available at www.fluxsense.se

Mellqvist, J., Johansson, J., Samuelsson, J., Rivera, C., Lefer, B. and S. Alvarez (2008b), Comparison of Solar Occultation Flux Measurements to the 2006 TCEQ Emission Inventory and Airborne Measurements for the TexAQS II, Project No. 582-5-64594-FY08-06, TCEQ report., Texas. (available at http://www.tceq.state.tx.us/assets/public/implementation/air/am/contracts/reports/da/20081108-comparison_solar_occultation_flux_measurements.pdf)

Mellqvist, J., et al. (2009), Emission Measurements of Volatile Organic Compounds with the SOF method in the Rotterdam Harbor 2008, available at www.fluxsense.se

Mellqvist, J., J. Samuelsson, J. K. E. Johansson, C. Rivera, B. Lefer, S. Alvarez, and J. Jolly (2010), Measurements of industrial emissions of alkenes in Texas using the solar occultation flux method, Journal of Geophysical Research: Atmospheres, 115(D7), doi:10.1029/2008JD011682.

Pikelnaya, O et al., Understanding seasonal variations in refinery VOC emissions using quarterly optical remote sensing mobile surveys, Proceedings of " AWMA, AIR QUALITY MEASUREMENT METHODS AND TECHNOLOGY, APRIL 2 – 4, 2019 • DURHAM, NC Durham, 2019

Rinsland, C. P., R. Zander, and P. Demoulin (1991), Ground-based infrared measurements of $HNO_3$ total column abundances: long-term trend and variability. *J. Geophys. Res.*, *96*, 9379–9389.

Rivera, C., Mellqvist, J., Samuelsson, J., Lefer, B., Alvarez, S. & Patel, M. (2010) Quantification of NO2 and SO2 emissions from the Houston Ship Channel and Texas City industrial areas during the 2006 Texas Air Quality Study. Journal of Geophysical Research - Atmospheres 115. DOI: 10.1029/2009JD012675.

Rothman et al. (2003), HITRAN 2000, Journal of Quantitative Spectroscopy and Radiative Transfer, vol. 82, pp. 5-44.

Sharpe, S., et al. (2004), Gas-Phase Databases for Quantitative Infrared Spectroscopy, *Applied Optics*, 58(12).

2019

# VOC Emissions from Oil and Gas Production in San Joaquin Valley - Sub Report B

FINAL REPORT

FluxSense Inc

24 January 2020

**Date:** 24 January 2020
**Updated**: 1 December 2020

**Title:** VOC Emissions from Oil and Gas Production in San Joaquin Valley - Sub Report B

**Authors:** Johan Mellqvist[1,3], Jerker Samuelsson[1], Brian Offerle[2], Nathalia dos Reis Vechi[3] and Marianne Ericsson[1]

[1]FluxSense Inc, 113 W G Street # 757, San Diego, CA 92101
[2]FluxSense AB, Sven Hultins gata 9, SE-41288 Göteborg, Sweden
[3]Chalmers University of Technology, Hörsalsvägen 11, SE-41296, Göteborg, Sweden

**CARB contract no. 17RD021**
Principal Investigator: Johan Mellqvist,
October 2018 and May 2019, San Joaquin Valley survey
Prepared for the California Air Resources Board
and the California Environmental Protection Agency

[Cover: FluxSense MobileLab © 2019.]

## DISCLAIMER

# Executive summary

*Objective*

A two-year study is carried out by FluxSense Inc on behalf of California Air Resources Board (CARB). The objective is to provide ground-based flux measurements of VOCs, methane, air toxics and ammonia from various sources, e.g. refineries, petrochemical facilities, oil storage, port activities, landfills, oil and gas production and Concentrated Animal Feeding Operations (CAFOs). The study also characterizes ground concentrations of the above-mentioned species at community scale to provide insights on concentration levels particularly in disadvantaged communities near emission sources and to identify emissions sources and their contributions to observed levels. This project complements community monitoring efforts by CARB staff who have measured speciated VOCs and air toxics of concern.

*Background*

This sub-report consists of measurement results from 5 days in October 2018 and a 5-week campaign in May 2019 carried out in the San Joaquin Valley, CA, with focus on methane and NMVOC emissions from oil and gas production. This report also includes measurements of the impact of various sources on the concentration levels in some of the communities within the oil and gas production area. As part of the same campaign, methane, ammonia and other VOC emissions from Concentrated Animal Feeding Operation (CAFOs) were also measured (CAFO emissions are reported in Sub Report C).

The emission fluxes (kg/h) of alkanes, ammonia, $SO_2$, $NO_2$ and formaldehyde were quantified using Solar Occultation Flux (SOF) and mobile SkyDOAS (Differential Optical Absorption Spectroscopy). MWDOAS (Mobile White Cell DOAS) and MeFTIR (Mobile extractive Fourier Transform Infrared) techniques were used to measure ground level concentrations of alkanes, BTEX and methane, which allowed to indirectly obtain emission fluxes when combined with measured SOF fluxes.

SOF is a proven technique that has been developed at Chalmers University of Technology in Sweden and further developed and applied by FluxSense in over 100 fugitive emission studies around the world. In Europe the SOF technique is considered Best Available Technology (BAT) for measurements of fugitive emission of VOCs from refineries, and in Sweden it is used in conjunction with tracer correlation and optical gas imaging to annually screen all larger refineries and petrochemical facilities. The estimated uncertainty for SOF emission measurements is typically 30 % for total site emissions. The estimated measurement uncertainties have been verified in several (blind and non-blind) controlled source gas release and in side-by-side measurements with other measurement techniques.

The instrument systems above were operated in the FluxSense mobile laboratory and the measurement were conducted while driving outside the source area fence-lines along public roads. Background columns and concentrations were subtracted by encircling the sites, when possible, or by measuring upwind columns and concentrations, so that only emissions from within the facilities were quantified. Wind data were obtained from a Light Detection and Ranging (LIDAR) instrument that measured the wind profile between 10 to 300 m altitude. From the combination of the measured column and concentration values, the height of the plume could be derived to first order.

*Emission measurements*

Table E.1 shows the main results from the two campaigns in 2018 and 2019, including measured emissions of alkanes and methane from 8 oil and gas fields in Kern County, California. The large geographical extent of the oil fields and challenging wind meteorology limited the number of measurements that could be accomplished during a measurement day and aggregated for the survey. Multiple measurements were made over a number of days for the main fields listed in the table. In addition to the sites presented in Table E.1, point- or smaller area sources within the oil and gas fields, were also measured repeatedly during the campaign. Additional oil and gas fields with few repeated measurements are excluded from the summary but discussed in the report.

Cumulative emissions for the fields, wholly or partially measured, amount to about 7600 kg/h NMVOCs and 8000 kg/h methane.

Table E.1. Results of the alkane and methane emission measurements based on SOF and MeFTIR. *Limited number measurements meeting acceptance criteria.

| *Area (oil and gas fields and associated facilities)* | Days | $N_{MEASUREMENTS}$ | Alkane (kg/h) | $SD_{alkane}$ (kg/h) | $CH_4$ / Alkane mass concentration ratio | | $CH_4$ (kg/h) |
|---|---|---|---|---|---|---|---|
| | | | | | 1Q | 3Q | |
| Elk Hills | 8 | 13 | 3470 | 810 | 1.25 | 1.49 | 4820 |
| Poso Creek & Kern Front | 3 | 5 | 440 | 190 | 0.71 | 1.42 | 470 |
| Coles Levee North | 3 | 5 | 250 | 43 | * | * | |
| Cymric & McKittrick | 3 | 7 | 1230 | 480 | 1.06 | 1.35 | 1470 |
| Lost Hills | 4 | 6 | 780 | 310 | 0.38 | 0.46 | 330 |
| Belridge | 2 | 4 | 1480 | 340 | 0.43 | 0.71 | 860 |
| McKittrick | 3 | 4 | 320 | 120 | * | * | |

The measured methane emissions in this study were compared with airborne emission measurements by Scientific Aviation and JPL from the same area and incorporating similar sources, as well as emissions from inventories and from application of standard emission factors. JPL measured point sources from 2016 - 2018 which were aggregated to provide total emissions, whereas FluxSense and Scientific Aviation measured diffuse emissions concurrently during the present study. For methane it was found that the airborne measurements by JPL and Scientific Aviation were 25% and 30-100 % higher, respectively, than the survey measurements. It was also found that the inventory data for methane and emission factor calculations showed 20% and 50 % lower values respectively, than the current survey measurements. For NMVOCs the emission factor based calculations resulted in an order of magnitude lower values than the measurements in this survey. It should be noted that these production based emission factor calculations may be biased too low.

In addition to the alkane and methane emissions presented in Table E.1., several other species were measured in the survey. BTEX (benzene, toluene, ethylbenzene, xylene) concentrations were generally below detection limits for the large-scale oil and gas field measurements although they were measurable for a number of point sources within the fields. The point sources measured indicated that BTEX emissions on the whole are less than 1% of the total emissions. Large scale fenceline measurements of $NO_2$, $SO_2$ and $H_2CO$ by SkyDOAS showed no significant emissions from the surveyed oil fields at the time of the study.

*Community monitoring*

Measurements with the mobile laboratory were carried out during 2 evening/nights in the northeast Bakersfield communities Highland Park and Meadow View and additionally 7 days of measurements at some of the other sites, i.e. Lost Hills, Derby Acres, Port of Stockton, Alon refinery. Targeted measured species included BTEX, various alkanes, and methane. For alkanes several hotspots were found while for aromatic VOCs the concentrations were low but measurable in Meadow View, Highland Knolls, Derby Acres and Port of Stockton while below detection limit in Lost Hills, Quailwood and Park Stockdale.

# Acronyms, Units and Definitions

## Acronyms used in this report

| | |
|---|---|
| BPD | Barrels per day |
| BTEX | Sum of Benzene, Toluene, Ethyl Benzene and Xylene |
| CARB | California Air Resources Board |
| CAFO | Concentrated Animal Feeding Operation |
| CEC | The California Energy Commission |
| DOAS | Differential Optical Absorption Spectroscopy |
| DOGGR | California Department of Conservation Division of Oil, Gas, and Geothermal Resources |
| EF | Emission factor |
| FTIR | Fourier Transform InfraRed |
| IME | Indirectly Measured Emission, combining direct emission with concentration ratios |
| LIDAR | Light Detection and Ranging |
| MWDOAS | Mobile White cell DOAS |
| MeFTIR | Mobile extractive FTIR |
| NMVOC | Non-methane volatile organic compound |
| ROG | Reactive Organic Gases |
| SkyDOAS | Scattered Skylight DOAS |
| SOF | Solar Occultation Flux |
| VOC | Volatile organic compound, used interchangeably for non-methane VOC |

## Units

| | |
|---|---|
| Air temperature | degrees C |
| Atmospheric Pressure | mbar |
| Relative Humidity | % |
| Wind direction | degrees North |
| Wind speed | m/s |
| Column | mg/m$^2$ |
| Concentration | mg/m$^3$ |
| Flux | kg/h |

## Unit Conversions

1 lbs = 0.4536 kg
1 kg/h = 52.9 lbs/day
1 bbl = 159 l
1 bbl/day = 5.783 kg/h (crude oil)
1 (short) ton = 907.2 kg
1 kton/year = 104 kg/h
1 klbs/year=0.052 kg/h

### Definitions

**Alkane** or **Alkanes** are considered to be all non-methane alkane species.

**Treatment Site** is an unspecified or unknown facility or unit for processing, treatment, temporary storage, etc. of oil and gas.

# Table of Contents

## List of Figures

## List of Tables

# 1 Objective and Introduction

The objectives of this research are to characterize certain statewide GHGs and air toxics emission sources, to identify potential sources contributing to air pollution hotspots. This includes quantifying ground-based fluxes of VOCs, including methane and air toxics, and ammonia from various sources, e.g. refineries, petrochemical industry, oil storage, harbor activities, landfills, oil and gas production and Concentrated Animal Feeding Operations (CAFOs).

In the study also ground concentrations are characterized, of the above-mentioned species, at community scale to provide insights on concentration levels particularly in disadvantage communities near emission sources and identify emissions sources and their contributions to high concentration levels. This project complements community monitoring efforts by CARB staff who has measured speciated VOCs and other toxics of concern. The study includes a comparison of the obtained methane emission estimations against airborne measurement for single sources.

The results from this study should provide useful screening information to identify high-risk communities for prioritizing air pollution mitigation efforts. The data would also be useful to support enforcement efforts to address high BTEX (benzene, toluene, ethylbenzene and xylene) sources, and may be useful to conduct real-world verification of the impact of the oil and gas regulation (implemented Jan 1, 2018) on $CH_4$ emissions.

This sub-report consists of measurement results from 2 campaigns in October 2018 and May 2019 carried out in the San Joaquin Valley, CA, with focus on methane and NMVOC emissions from oil and gas production. This report also includes investigations of the impact of various sources on the concentration levels in some of the communities within the oil and gas production area.

As part of the same campaign, methane, ammonia and other VOC emissions from Concentrated Animal Feeding Operation (CAFOs) were also measured (CAFO emissions are reported in Sub Report C).

# 2 Background

Industrial volatile organic compounds (VOC) emissions may contribute to significant formation of ground level ozone, which is formed through atmospheric chemical reactions of volatile organic compounds (VOCs) and nitrogen oxides ($NO_x$) in the presence of sunlight, often called photo chemical smog. Elevated ozone concentrations are known to reduce crop yields and constitute a public health concern. Larger metropolitan areas in the US have trouble meeting ozone standards since anthropogenic sources tend to be concentrated in urban areas, including both mobile and stationary sources. For instance, in order to meet current and future more stringent ozone standards in Los Angeles, reductions in VOC emissions are foreseen [Downey et. al. 2015]. Stationary sources such as refineries, storage depots, petrochemical facilities are the largest point sources of VOC emissions. The emissions are typically dominated by evaporative losses from storage tanks and process equipment, so-called fugitive emissions. Several VOCs are also toxic with direct impact on health.  Methane causes climate change. Ammonia emissions cause production of particles of concern for health and climate.

In 2015, the Governor approved Assembly Bill 1496 (AB 1496), which requires the California Air Resources Board (CARB) to monitor and measure high methane emission hotspots within the state using the best available scientific and technical methods. In order to meet the requirements under AB 1496, CARB, in conjunction with the California Energy Commission (CEC), has funded a large-scale statewide aerial methane survey conducted by NASA Jet Propulsion Laboratory (JPL) to detect and identify methane super emitters which may be a large contributor to the regional methane hotspots. CARB has also funded Scientific Aviation to quantify emission fluxes from various methane sources (including super emitters) with airborne measurements. Furthermore, certain emissions from oil and gas facilities, which are also major methane emitters, are known to have potential adverse health effects. Oil and gas operations are located in a variety of areas in California, including densely populated areas and in proximity of disadvantaged communities. In order to meet CARB's mission to protect the public from harmful effects of air pollution, there have been efforts to enhance the community monitoring for air toxics and methane, particularly in the communities near oil and gas facilities, which are primarily disadvantaged communities. The recently approved AB 617 will also require CARB to develop a community monitoring plan to identify disadvantaged communities for community monitoring deployment. It will also require CARB to develop a cumulative impact state strategy to identify communities with high cumulative risk so air districts can develop Community Action Plans.

# 3 Instrumentation and Methods

The FluxSense measurement vehicle or "mobile lab" is equipped with four optical instruments for gas monitoring which were used during the survey: SOF (Solar Occultation Flux), SkyDOAS (Differential Optical Absorption Spectroscopy), MeFTIR (Mobile extractive Fourier Transformed Infrared spectrometer) and MWDOAS (Mobile White cell DOAS). The individual measurement methods are described in the subsections below. SOF and SkyDOAS both measure gas columns through the atmosphere by means of light absorption. SOF utilizes infrared light from the direct sun whereas SkyDOAS measures scattered ultraviolet light from the sky. MeFTIR and MWDOAS both measure ground level concentrations (vehicle roof height, approx. 2 m) of alkanes and BTEX (benzene, toluene, ethylbenzene, and xylene) respectively. Accurate wind data is necessary in order to compute gas emission fluxes. Wind information for the survey was derived from several different sources. A wind LIDAR was used to measure vertical profiles of wind speed and wind direction from 10-300 m height. This was re-located for each measurement day and measurement area to a suitable site within the vicinity downwind (ideally with same elevation, no intervening terrain or geographic features) of the measured oil and gas production areas. However due to the large-scale nature of the measurements (for example, the perimeter of Elk Hills is over 60 km with hilly terrain) such requirements could not be met. The LIDAR data was compared with data from several wind masts from fixed met network- and mobile stations to extend the measurements to times when LIDAR was unavailable. This includes measurements begun before LIDAR setup each day and those after shutdown. Figure 1 gives a general overview of the measurement setup and the data flow and pictures of the FluxSense mobile lab is found in Figure 2.

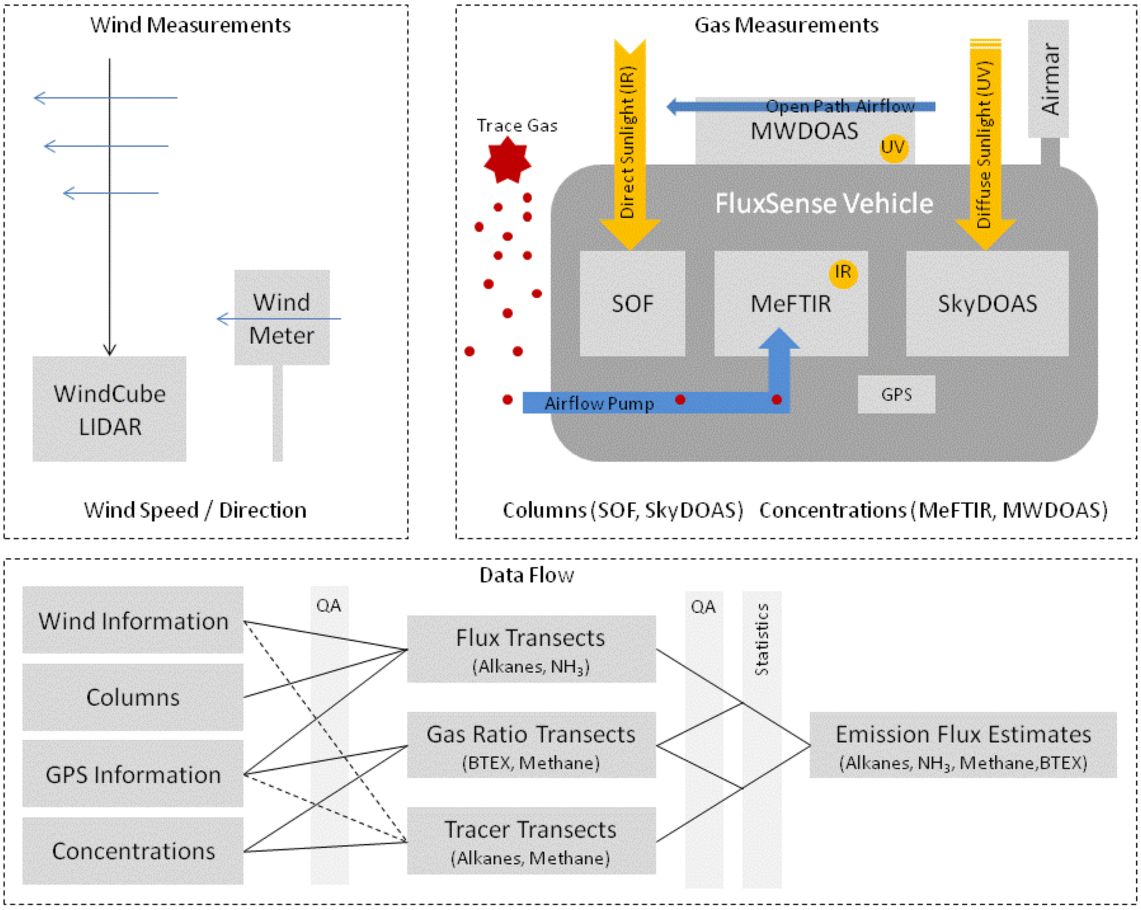

Figure 1. Overview of the FluxSense mobile lab main instruments; SOF, MeFTIR, MWDOAS and SkyDOAS (upper right panel) and wind measurements (upper left panel) and simplified data flow diagram (lower panel). SOF and SkyDOAS are column integrating passive techniques using the Sun as the light source while MeFTIR and SkyDOAS sample local air concentrations using active internal light sources. The data flow describes what information that goes into the flux emission estimates. Direct flux emissions are given from measured columns (SOF and SkyDOAS) of alkanes, $SO_2$ and $NO_2$, while indirectly measured emissions are calculated via gas concentration ratios (MeFTIR and MWDOAS) of BTEX and $CH_4$. See section 4.1 for principal equations. All emission flux estimates are based on statistical analysis of measured data. Q.C. = Quality Control, S.A.= Statistical Analysis (see Appendix for details).

In order to derive final emission flux estimates, the GPS-tagged gas column measurements by SOF and SkyDOAS are combined with wind data and integrated across plume transects at the various source locations. Gas mass ratio measurements by MeFTIR and MWDOAS are then used to indirectly estimate the emissions also for methane and BTEX.

Figure 2. Internal and external view of the FluxSense mobile lab.

Table 1.Summary of FluxSense gas measurement techniques. *For typical wind conditions at an optimal distance from the source.

| **Method** | **SOF** | **Sky DOAS** | **MeFTIR** | **MWDOAS** |
|---|---|---|---|---|
| Compounds | **Alkanes**: ($C_nH_{2n+2}$)<br>**Alkenes:**$C_2H_4$, $C_3H_6$<br>**$NH_3$** | **$SO_2$**<br>**$NO_2$**<br>**$H_2CO$** | **$CH_4$**<br>**Alkanes:** ($C_nH_{2n+2}$)<br>**Alkenes:** $C_2H_4$, $C_3H_6$<br>**$NH_3$**<br>**$N_2O$** (tracer) | **BTEX** |
| Detection limit Column | 0.1-5 mg/m$^2$ | 0.1-5 mg/m$^2$ | 1-10 ppbv | 0.5-3 ppbv |
| Detection limit Flux* | 0.2-1 kg/h | 1 kg/h | 0.2-2 kg/h | 0.2-2 kg/h |
| Wind Speed Tolerance | 1.5-12 m/s | 1.5-12 m/s | | |
| Sampling Time Resolution | 1-5 s | 1-5 s | 5-15 s | 8-10 s |
| Measured Quantity [unit] | Integrated vertical column mass [mg/m$^2$] | Integrated vertical column mass [mg/m$^2$] | Mass concentration at Vehicle height [mg/m$^3$] | Concentration at Vehicle height [mg/m$^3$] |
| Derived Quantity [unit] | Mass Flux [kg/h] | Mass Flux [kg/h] | 1) Alkane and methane mass concentration ratio of ground plume combined with SOF gives mass flux [kg/h] and plume height information [m]<br>2) Alkane and $CH_4$ flux [kg/h] via tracer release | Combined with MeFTIR and SOF gives Mass Flux [kg/h] |
| Complementary data | Vehicle GPS-coordinates, Plume wind speed and direction | Vehicle GPS-coordinates, Plume wind speed and direction | Vehicle GPS-coordinates<br>Plume wind direction | Vehicle GPS-coordinates, Plume wind direction |

## 3.1 The SOF method

The SOF method [Mellqvist 1999, 2008a, 2008b, 2009, 2010; Kihlman 2005a; Johansson 2014] is based on the recording of broadband infrared spectra of the sun with a Fourier transform infrared spectrometer (FTIR) that is connected to a solar tracker. The latter is a telescope that tracks the sun and reflects the light into the spectrometer independent of the orientation of the vehicle. Using multivariate optimization, it is possible from these solar spectra to retrieve the path-integrated concentrations (referred to as column concentrations), in the unit $mg/m^2$, of various species between the sun and the spectrometer. The system used in this project consists of a custom-built solar tracker, transfer optics and a Bruker IRCube FTIR spectrometer with a spectral resolution of 0.5 $cm^{-1}$, equipped with a dual InSb (Indium Antimonide) / MCT (Mercury Cadmium Telluride) detector. A reference spectrum is taken outside the plume so that atmospheric background concentrations are removed. This means that all measured SOF columns are analyzed relative to the background column concentrations.

The system is installed in a measurement vehicle which allows consecutive column concentration measurements to be performed while driving. The flux of a species in a plume from an industry is measured by collecting spectra while driving the vehicle so that the light path from the sun to the instrument gradually cuts through the whole plume, preferably as orthogonally as possible to the wind direction, see Figure 3.

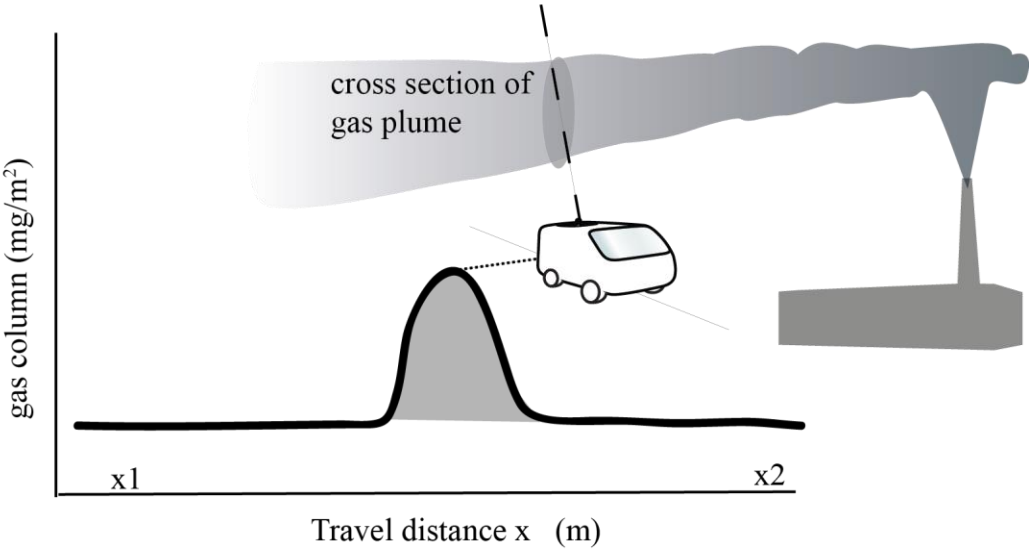

Figure 3. Schematic of the SOF measurement where the vehicle is driven across the prevailing wind so that the solar beam cuts through the emission plume while the sun is locked into the FTIR spectrometer by the solar tracking device on the roof. The VOC mass (or other compound of interest) is integrated through the plume cross section. See section 4.1 for complete equations.

For each spectrum a column concentration of the species is retrieved using custom software (QESOF, i.e. *Quantitative evaluation of SOF*) [Kihlman 2005b]. These column concentrations, together with positions recorded with a GPS (Global Positioning System) receiver and the solar angle calculated from the time of the measurements, are used to calculate the area integrated column of the species in the intersection area between the plume and the light path. The flux of the species is then obtained by multiplying this area integrated concentration with the orthogonal wind speed vector component.

The IR spectra recorded by the SOF instrument are analyzed in QESOF by fitting a set of spectra from the HITRAN infrared database [Rothman 2003] and the PNNL (Pacific Northwest National Laboratory) database [Sharpe 2004] in a least-squares fitting procedure. Calibration data from the HITRAN database is used to simulate absorption spectra for atmospheric background compounds present in the atmosphere with high enough abundance to have detectable absorption peaks in the wavelength region used by SOF. Spectra, including water vapor, carbon dioxide and methane, are calibrated at the actual pressure and temperature and degraded to the instrumental resolution of the measurements. The same approach is applied for several retrieval codes for high resolution solar spectroscopy developed within Network for the Detection of Atmospheric Composition Change (NDACC) [Rinsland 1991; Griffith 1996] and QESOF has been tested against these with good agreement, better than 3%. For the retrievals, high resolution spectra of ethylene, propene, propane, n-butane and n-octane were obtained from the PNNL database and these are degraded to the spectral resolution of the instrument by convolution with the instrument line shape. The uncertainty in the absorption strength of the calibration spectra is about 3.5% for all five species.

In this project, the SOF method was used to measure VOCs in two different modes. Most VOCs with C-H-bonds absorb strongly in the 3.3-3.7 µm (2700-3005 $cm^{-1}$) spectral region. This region is mainly used for alkane measurements using a spectral resolution of 8 $cm^{-1}$. Alkenes (including ethylene and propylene) and ammonia are instead measured in the spectral region between 910 and 1000 $cm^{-1}$ using a spectral resolution of 0.5 $cm^{-1}$. In the alkane mode – the IR light absorption is essentially sensitive to the total alkane mass (number of alkane C-H bonds) present in the plume. The absorption structures (cross sections) for the various alkane compounds are rather similar, with the absorption strength scaling to the mass of the alkane species. Hence, the actual mix of alkanes in the plume does not affect the retrieved total alkane mass flux much, although only cross sections from a subset of all alkanes (propane, n-butane and octane) are fitted in the spectral analysis. Typically, the rare event of significant absorption from other species in the plume shows up as elevated residuals and is further investigated in the re-analysis. For the alkene mode the specificity of the measurements is good, since the absorption of different species is rather unique in this so called “fingerprint region” and absorption features are often sharp and well separable from each other at 0.5 $cm^{-1}$ resolution.

SOF is a proven technique employed by FluxSense in over 100 fugitive emission studies around the world. In Europe the SOF technique is considered one of the Best Available Technology [European Commission 2015] for measurements of fugitive emission of VOCs from refineries; and in Sweden it is used together with tracer correlation and optical gas imaging for annual screening of all larger refineries and petrochemical plants. The estimated uncertainty for the SOF emission measurements is typically 30 % for the total site emissions. This uncertainty has been calculated from several controlled release experiments (blind and non-blind) and side-by-side measurements with other measurement techniques.

## 3.2 Mobile SkyDOAS

The principle for Mobile SkyDOAS (Mobile Differential Optical Absorption Spectroscopy) measurements is very similar to that of SOF. Instead of measuring direct sun light in the infrared region, scattered light in the UV and visible region is measured in zenith angle with a telescope connected with an optical fiber to a Czerny-Turner spectrometer with a CCD camera. Column concentrations are retrieved from spectra in a similar way as with the SOF, although absorption is generally weaker. The system that was used for this project consists of a quartz telescope (20 mrad field of view, diameter 7.5 cm) connected with an optical fiber (liquid guide, diameter 3 mm) to a 303 mm focal length Czerny-Turner spectrometer with a 1024 by 255 pixels, thermoelectrically cooled CCD camera, see Figure 4.

Figure 4. The mobile SkyDOAS system: Telescope, optical fibre, spectrometer and control computer.

The system was installed in the same measurement vehicle as the SOF system. Plumes were transected in the same way as with the SOF system and the retrieved column concentrations used to calculate fluxes exactly the same way, except that the SkyDOAS measurement direction is always zenith.

In this project, mobile SkyDOAS was used to measure $SO_2$, $NO_2$ and $H_2CO$. $NO_2$ is retrieved in the wavelength region between 324 and 350 nm and $SO_2$ in the region 310-325 nm. $H_2CO$ is measured in the region 322-350 nm. Apart from $SO_2$, $NO_2$ and $H_2CO$ the spectral analysis also includes other atmospheric compounds such as $O_3$ and $O_4$. The rare event of significant absorption from other species in the plume than those included in the spectral fit shows up as elevated residuals and is further investigated in the re-analysis. The absorption line parameters of the retrieved compounds are well established in published databases, stating an uncertainty of 4% (Vandaele *et al.* 1998) for the UV cross section of $NO_2$ and less than 2% for the $SO_2$ cross sections (Bogumil *et al.* 2003).

The DOAS technique was introduced in the 1970's (Platt *et al.* 1979) and has since then become an increasingly important tool in atmospheric research and monitoring both with artificial light sources and in passive mode utilizing the scattered solar light. In recent time the multi axis DOAS technique (scanning passive DOAS) has been applied in tropospheric research for instance measuring formaldehyde (Heckel *et al.* 2005; Pikelnaya *et al.* 2007).

Passive DOAS spectroscopy from mobile platforms has also been quite extensively applied in volcanic gas monitoring (Galle *et al.* 2003) for $SO_2$ flux measurements and for mapping of formaldehyde flux measurements in megacities (Johansson *et al.* 2009), . Mobile SkyDOAS has been used in several studies for measurements of industrial facilities i.e. $SO_2$, $NO_2$ and $H_2CO$ for several campaigns in Texas including $NO_2$ measurements at Longview in 2012 (Johansson *et al.* 2014a; Johansson & Mellqvist 2013). (Rivera 2009) did $SO_2$ measurements on a power plant in Spain for validation purposes. They also made measurements at an industrial conglomerate in Tula in Mexico (Rivera *et al.* 2009a) and measurements of $SO_2$, $NO_2$ and $H_2CO$ during the TexAQS 2006 campaign (Rivera *et al.* 2009b; Rivera *et al.* 2010). There are also groups in both China and Spain working with mobile mini-DOAS.

## 3.3 Mobile extractive FTIR (MeFTIR)

Mobile Extractive FTIR (MeFTIR) [Galle 2001, Börjesson 2009] in combination with tracers has been used to quantify VOC emissions from refinery and petrochemical sources in Europe and in the U.S. Alkanes and alkenes are typically measured, but also methane and other climate gases can be retrieved. MeFTIR is an optical technique capable of monitoring gas concentrations at ppb-sensitivity in mobile field operations. It is used both independently for concentration mapping and flux measurements, but often combined together with simultaneous SOF flux measurements to provide more detailed VOC speciation of plumes and for plume height assessments [Johansson et. al. 2013a]. The plume height can be estimated by dividing measured columns ($mg/m^2$) with ground concentrations ($mg/m^3$), assuming that the plume is evenly distributed up to the plume height (and zero above).

The MeFTIR system contains a mid-infrared spectrometer with medium resolution ($0.5\ cm^{-1}$). It utilizes an internal glow bar as an infrared radiation source, and by customized optics this light is transmitted through an optical multi-pass measurement cell with path-length of 68 meters. The system is mounted on a vibration dampening platform to allow for real time plume mapping from a mobile platform, such as a vehicle or boat, see Figure 5. Additionally, for ammonia measurements, the inlet and the cell are heated and insulated so that the sample air and cell temperature is above 40 ºC. Heating the sample is desirable since ammonia is a “sticky” gas, therefore heating the inlet and cell minimizes the risk of ammonia adhering to the tubing or cell surface and the residence time in the cell increasing. Temperature stability is also necessary to minimize instrumental drift. Internal cell temperature and pressure are sampled each second and logged every minute.

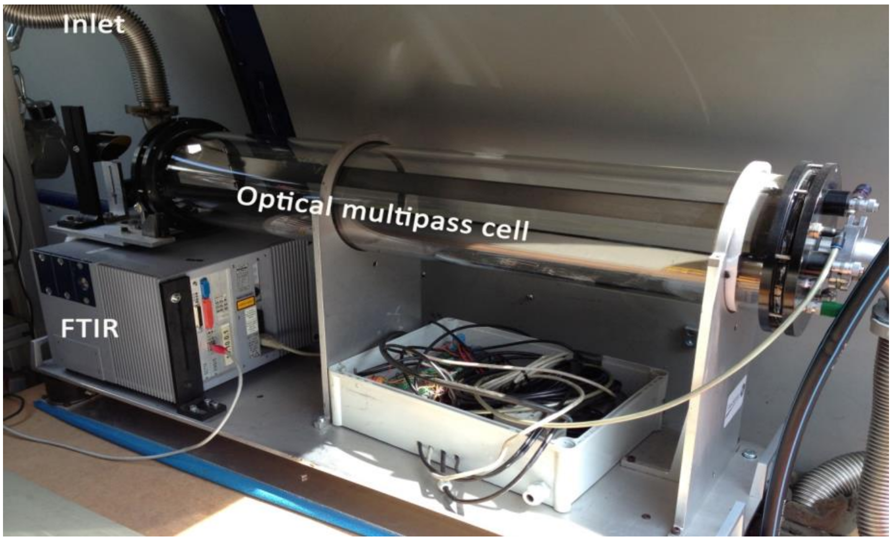

Figure 5. The MeFTIR instrumentation consisting of a Bruker FTIR spectrometer connected to an optical multi-pass cell.

The transmitted light is detected simultaneously with an InSb-detector in the 2.5–5.5 µm (1800–4000 cm$^{-1}$) region and an MCT detector in the 8.3–14.3 µm (700–1200 cm$^{-1}$) region. Temperature and pressure in the cell are averaged over the duration of each measurement. Atmospheric air is continuously pumped at high flow rate through the optical cell from the outside, taking in plume air from the roof of the vehicle (2.5 m height) through a Teflon tube. A high flow pump (> 120 lpm, Vacuubrand ME 8 NT) is used to ensure that the gas volume in the cell (16 l) has a flushing time of less than 8 seconds. Spectra are typically recorded with an integration time of 8-12 seconds. A GPS-receiver is used to register the position of the vehicle every second.

The concentration in the spectra is analyzed in real time by fitting a set of calibrated spectra from the HITRAN infrared database [Rothman 2003] and the PNNL database [Sharpe 2004] in a least-squares fitting procedure. Compounds being analyzed include ethylene, propylene, total alkane mass (based on fitting cross sections of ethane, propane, n-butane, i-pentane, n-octane), water, methane, CO, $CO_2$ and $N_2O$. The analysis routines are very similar to the ones for SOF, but less complex because strong absorption by atmospheric trace gases (water, methane, $CO_2$) has less consequence at the shorter path length in the MeFTIR measurement cell.

The MeFTIR tracer approach has been tested in a so-called gas release “blind test” together with other techniques in U.S. [EREF 2011]. In that test, methane was released from an area-distributed source in four different configurations and flow rates ranging from 1.1-3.3 g/s. At a downwind distance of 400 meters MeFTIR retrieved the fluxes within 6% in 3 cases and 19% in the fourth. This is consistent with other validation experiments, showing a flux estimate accuracy of better than 20%. Concentration measurement by FTIR is a widely used procedure, and the main uncertainties are associated with the absorption cross sections (typically < 3.5%) and spectral retrieval, with an aggregate uncertainty better than 10% in the analysis.

Concentrations are monitored in real time in order to detect emission plumes and to judge whether any interfering sources are being sampled. Unwanted signals from local traffic exhaust or from the measurement vehicle itself could be filtered out by looking at exhaust compound signatures like carbon monoxide concentrations. A stationary source is, on the contrary to any local traffic plumes, characterized by recurrent downwind plumes. Transient and non-repeatable observations are therefore excluded from the results. Furthermore, measurements of ambient concentrations of methane and carbon dioxide (with known atmospheric concentrations) are used for consistency check.

## 3.4 Mobile White Cell DOAS (MWDOAS)

The ground level mass concentration of benzene, toluene, ethylbenzene, m- and p-xylene (BTEX) was measured using a mobile real-time system: Mobile White cell DOAS (MWDOAS). The MWDOAS system consists of an open, 2.5 m long optical White cell that is mounted on the roof of the measurement vehicle (see Figure 6). By multiple reflections in the White cell mirror system an overall path length of 210 m is obtained, resulting in low detection limits (ppb). The light from the internal lamp is transmitted through the White cell and then analyzed in a DOAS spectrometer, using the UV wavelength region 255 - 285 nm.

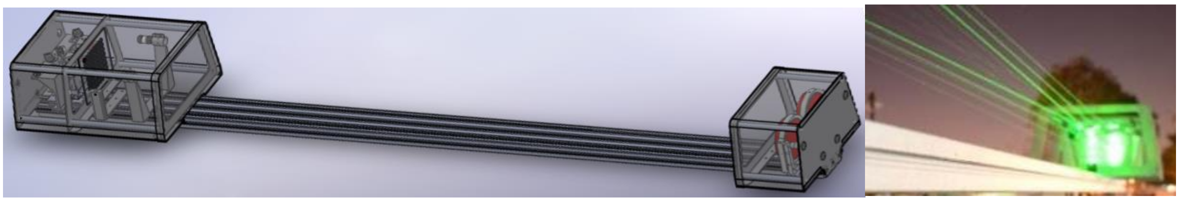

Figure 6. The open path MWDOAS cell having an overall optical path-length of 210 m.

A measurement begins by acquiring a reference spectrum outside the plume, usually upwind of the facility. Spectra are then sampled and averaged continuously while driving through emission plumes. The averaging time is set to around 8 seconds in order to achieve acceptable SNR (see below). This is the lower limit of the temporal sampling between independent measurements, but the spatial sampling is also dependent by the vehicle’s velocity. A typical driving speed for MWDOAS measurements is 10-20 km/h for sufficient plume sampling. The spectra are geo-tagged and evaluated online using the standard DOAS technique, giving information of plume locations and constituents. Cross-sections included in the evaluation are tabulated in Table 2.

The MWDOAS data is later post evaluated and merged with the corresponding MeFTIR data to produce a plume specific BTEX/Alkane mass ratio. The mass ratio of BTEX/Alkanes is then used to calculate the aromatic flux from individual sub areas where alkane fluxes have been measured by SOF, assuming they have the same source. Specific area plumes are ideally probed at several times, and an overall average of all plume transect BTEX/Alkane ratios is then made. The method requires in situ access to the plume of the studied source, and as instrumentation typically are mounted on a truck, highly elevated sources with a strong plume lift like hot flares, chimneys and high process towers will not be possible to survey at close distance.

Table 2. The UV-cross-sections used in the evaluation of the MWDOAS spectra.

| **Chemical compound** | **Origin of reference spectrum** |
|---|---|
| **$O_3$** | [Burrows 1999] |
| **$SO_2$** | [Bogumil 2003] |
| **$O_2$** | [Bogumil 2003] |
| **Toluene** | [Fally 2009] |
| **Benzene** | [Etzkorn 1999] |
| **1,3,5-Trimethylbenzene** | [Etzkorn 1999] |
| **1,2,4-Trimethylbenzene** | [Etzkorn 1999] |
| **Styrene** | [Etzkorn 1999] |
| **Phenol** | [Etzkorn 1999] |
| **p-Xylene** | [Etzkorn 1999] |
| **m-Xylene** | [Etzkorn 1999] |
| **Ethylbenzene** | [Etzkorn 1999] |

The MWDOAS technique has been validated in various surveys by comparison with canister samples acquired at several different locations and which were subsequently analyzed by gas chromatography (GC-FID). The validation shows that the result from MWDOAS lies well within 10% of the result of the certified canister results for BTEX. Due to an absorption cross-section too weak to be used with reliability in the MWDOAS analysis, the ortho isomer of the xylene has been omitted in this comparison. When total xylene is presented in the present survey, the sum of m- and p-xylenes from the MWDOAS measurement is multiplied by 1.32. This number comes from a ratio comparison of xylene isomers in 49 canister samples analyzed by GC/FID and taken from eight refineries and tank parks from two countries. The standard deviation in this comparison was 0.07 and adds a 4.5% uncertainty to the total xylene concentration. Hence, the xylene concentration from MWDOAS is defined as the sum of the measured m- and p-isomers and the inferred o-isomer.

The MWDOAS system has been used in previous campaigns in USA during 2013 with good results. During the 2013 DISCOVER-AQ campaign [Johansson, 2013b] in Houston, Texas, the system was run in parallel to a mobile Proton Transfer Mass spectrometer (PtrMS) lab as a validation check. The results of benzene, toluene and styrene was compared and showed good agreement, with the PtrMS showing slightly elevated benzene concentrations compared to the MWDOAS. The sensitivity of MWDOAS is better than 1 ppb for benzene, better than 3 ppb for toluene, ethylbenzene and m-xylene and 0.5 ppb for p-xylene.

Since the distribution of the BTEX constituents varies with source we will also present the benzene to alkane ratio to facilitate the calculation of benzene flux and identify specific benzene sources.

Unwanted BTEX signals from local traffic exhausts are generally only significant in congestions (at traffic lights etc.) or in confined spaces, e.g. tunnels. Apart from this, large emitters are also occasionally seen elsewhere. They are generally recognized, partly by their typical gasoline composition signature and partly by their transient nature. A stationary BTEX source is, on the other hand, characterized by recurrent downwind plumes. Transient and non-repeatable BTEX observations are therefore excluded from the result. Note that all concentrations are enhancements above the reference/background.

## 3.5 Wind Measurements and Auxiliary Data

***Wind LIDAR***

A wind LIDAR (LIght Detection and Ranging, Zephyr ZX-300) was used to measure vertical wind profiles of wind speed and direction in 2019. For the wind measurements in 2018 a Leosphere WindCubeV2 was used. The LIDAR provided wind profiles in the vertical range of 10 m to up to 300 m above ground and the measurements are integrated with a sonic anemometer at around 2 m height to provide coverage down to ground level. The system records 1-s data, and 5-minute averages were used for flux calculations in this study. The principle of detection is based on the Doppler shift of the infrared pulse that the instrument sends out and retrieves.

Figure 7. Wind measurements with portable wind LIDAR (10 - 300 m) mounted in pickup. The instrument is integrated with a sonic anemometer at around 2 m height.

***Portable Wind Masts***

Winds were also measured using a portable 10 m mast for suitable sites. This mast was equipped with a calibrated RM Young 05108 “prop and vane” anemometer, sampled every second and logged over 1 minute averages with a Campbell Scientific CR200 data-logger. Wind data from the measurement period are also collected from nearby ASOS (automated airport stations) Typical ASOS measurement height is 10 m.

Figure 8. The FluxSense mobile wind setup with wind LIDAR measurement truck and portable 10 m mast. The LIDAR instrument is integrated with a sonic anemometer placed on a small mast on the roof of the car.

### *Airmar (Mobile Weather Station)*

A sonic wind meter (Airmar WeatherStation 200 WX) was installed on the roof of the measurement vehicle to complement the other wind measurements and give local ground winds at the vehicle. The wind information from the vehicle mounted Airmar was not used for flux calculation since the wind field at street level can be heavily disturbed and turbulent. The Airmar was only used as a real-time aid to keep track of the plume directions when making the gas emission measurements. The Airmar provides wind speed and direction relative to true north (compensating for vehicle position), as well as air temperature, pressure and relative humidity. It also provides GPS positions that may be used as a backup for the other GPS-antenna.

### *GPS*

The FluxSense vehicle is equipped with two standard USB GPS-L1 receivers (GlobalSat BU-353S4) hooked up to the SOF and MWDOAS-computers. They are placed horizontally on the roof and by the windscreen for optimal reception. The receivers give the position at a rate of 1 Hz.

# 4 Measurement Methodology

## 4.1 Principal Equations

This report includes three different techniques to measure emission mass fluxes as specified below. The primary method in this project is the direct flux measurements of alkanes from SOF. In the secondary method BTEX and methane fluxes are measured indirectly from MWDOAS/MeFTIR gas mass ratios.

### 4.1.1 *DIRECT FLUX MEASUREMENTS:*

The emission mass flux ($Q$) of species (*j*) measured by SOF for a single transect (*T*) across the plume ($P$) along path (*l*) can be expressed by the following integral (units in gray brackets):

$$Q_T^j[\mathrm{g/s}] = \bar{v}_T[\mathrm{m/s}] \cdot \int_P C_l^j[\mathrm{mg/m^2}] \cdot \cos(\theta_l) \cdot \sin(\alpha_l)\ dl\,[\mathrm{m}]$$

Where,

$\bar{v}_T$ = the average wind speed at plume height for the transect,

$C_l^j$ = the measured slant column densities for the species *j* as measured by SOF or SkyDOAS,

$\theta_l$ = the angles of the light path from zenith ($\cos(\theta_l)$ gives vertical columns),

$\alpha_l$ = the angles between the wind directions and driving directions

$dl$ = the driving distance across the plume

Note that SOF and SkyDOAS have different light paths, where the SkyDOAS telescope is always looking in the zenith direction while the SOF solar tracker is pointing toward the Sun. Hence, the measured SOF slant column densities will vary with latitude, season and time of day.

To isolate emissions from a specific source, the incoming/upwind background flux must be either insignificant or subtracted. If the source is encircled or "boxed", the integral along *l* is a closed loop and the flux calculations are done with sign. This is taken care of by the FluxSense software.

### 4.1.2 *INDIRECT FLUX MEASUREMENTS:*

The indirectly measured flux (indirectly measured emission, IME) is computed using a combination of SOF and MeFTIR/MWDOAS measurements. The inferred mass flux ($\hat{Q}^i$) for species (*i*) are calculated from MeFTIR and/or MWDOAS ground level gas ratios integrated over the plume ($P$) along path (*l*) are given by (Si-units in gray brackets):

$$\hat{Q}^i[\mathrm{g/s}] = \bar{Q}^j[\mathrm{g/s}] \cdot \frac{1}{k}\sum_k \frac{\int_P N_l^i[\mathrm{mg/m^3}]\, dl[\mathrm{m}]}{\int_P N_l^j[\mathrm{mg/m^3}]\, dl[\mathrm{m}]}$$

Where,

$\bar{Q}^j$ = the average flux of species *j* from multiple transects as measured by SOF,
$N_l^i$ = the number density concentrations of species *i* as measured by MWDOAS or MeFTIR,
$N_l^j$ = the number density concentrations of species *j* as measured by MeFTIR,
$k$ = the number of gas ratio measurements

Note that the IME operates on average values since simultaneous SOF, MWDOAS and MeFTIR measurements are generally not performed and because individual gas ratios are more uncertain than the average. Although not necessarily simultaneously measured, SOF and MeFTIR/MWDOAS measurements must represent the same source plumes. Note also that gas ratios do not intrinsically depend on complete plume transects (like for direct flux methods) as long as the emission plume is well mixed at the sampling distance. Additionally, it is not necessary that the source of the tracer and measured gas be identical, merely that they are co-located at the measurement distance and uniform in time.

### *4.1.3 TRACER GAS FLUX MEASUREMENTS:*

The third method to conduct flux measurements is by tracer correlations using only MeFTIR measurements or simultaneous MeFTIR and MWDOAS measurement and a known tracer gas release. Note that this method was not applied during the first campaign in October 2018, although it will be used on later studies. These fluxes are given for each transect (*T*) by the following equation (Si-units in gray brackets):

$$Q_T^j[\mathrm{g/s}] = Q^{tracer}[\mathrm{g/s}]\,\frac{\int_P N_l^j[\mathrm{mg/m^3}]\,dl[\mathrm{m}]}{\int_P N_l^{tracer}[\mathrm{mg/m^3}]\,dl[\mathrm{m}]}$$

Where,

$Q^{tracer}$ = the release mass flux of the tracer gas from bottle,
$N_l^{tracer}$ = the number density concentrations of the tracer as measured by MeFTIR,
$N_l^j$ = the number density concentrations of species *j* from MeFTIR or MWDOAS,

Note that tracer gas correlation fluxes do not intrinsically depend on complete plume transects (like for direct flux methods) as long as the emission plume and the tracer gas is well mixed at the sampling distance. Complete plume transects are, however, recommended since the tracer gas release point might not completely match at the sampling distance

## 4.2 Uncertainties and Error Budget

A summary of the typical performance of the FluxSense measurements is presented in Table 3. In addition, for each site the statistical error is calculated. It corresponds to the random error but in addition there could be systematic errors. For instance, in the used wind speed due to the errors in estimated height of the plume and spectral calibration errors. The statistical error is given by the 95 % Confidence Interval (CI) for the mean, $\bar{x}$, according to:

$$CI = \bar{x} \pm t_{.025} \frac{s}{\sqrt{N}}$$

Here t is Student's T distribution and s corresponds to sample standard deviation:

$$s_x = \sqrt{\frac{\sum_{i=1}^{N}(x - \bar{x})^2}{N - 1}}$$

Table 3. Performance of FluxSense measurement methods.

| Measurement Parameter | Analysis Method | Accuracy | Precision |
|---|---|---|---|
| SOF column concentrations alkanes, alkenes, $NH_3$ | QESOF spectral retrieval | ±10% | ±5% |
| SkyDOAS column concentrations $NO_2$, $SO_2$, $H_2CO$ | DOAS spectral retrieval | ±10% | ±5% |
| MeFTIR concentrations $CH_4$, VOC, $NH_3$, $N_2O$ | QESOF spectral retrieval | ±10% | ±5% |
| MWDOAS concentrations BTEX, Benzene | MWDOAS spectral retrieval | ±10% | ±5% |
| Wind Speed (10 m) | R.M. Young Wind monitor | ±0.3 m/s or 1% | ±0.3 m/s |
| Wind Direction (10 m) | R.M. Young Wind monitor | ±5° | ±3° |
| LIDAR Wind Speed (10-300 m) | Zephyr Zx-3000 Wind LIDAR | ±0.1 m/s | - |
| GPS position | USB GPS receiver | ±2m | ±2m |
| SOF mass flux Alkanes, alkenes, $NH_3$ | SOF-Report flux calculations | 30%-40% 95 CI | ±10%-30% |
| SkyDOAS mass flux $NO_2$, $SO_2$, $H_2CO$ | SkyDOAS flux calculations | ±30% | ±10% |

## 5 Survey Setup & Complementary Measurements

Mobile measurements with SOF, SkyDOAS, MWDOAS, and MeFTIR were carried out during 4 measurements days in 2018 (September 30-October 2 and October 25-October 26) and 18 measurement days in 2019 (April 27-May 19) in Kern County, California (Figure 9). The focus of these measurements was methane and NMVOC emissions from oil and gas production as well as investigating the impact of various sources on communities within the vicinity. Two additional days' (26-27 May) measurement of industrial sources were made within the Port of Stockton.

The gas measurements were combined with wind data, primarily from a mobile wind LIDAR but also from adjacent stationary meteorological stations, to calculate fluxes and identify sources. During the measurement campaign the wind LIDAR, which was installed on the back of a measurement van, was positioned in proximity to the emission sources.

Figure 9. The primary oil and gas areas in the San Joaquin Valley that were studied in the emissions survey during May 2019 and October 2018. The polygon to the left incorporates the fields of Lost Hills, Belridge, Cymric, McKittrick, Elk Hills, Midway-Sunset and Buena Vista. The polygon to the right incorporates Poso Creek, Kern Front, Kern River, Round Mountain and Mount Poso. "O & G Super emitter" refers to "high-emission methane hot spots" from AB1496 identified by JPLduring the California Methane Survey. (see https://ww2.arb.ca.gov/sites/default/files/2020-07/ca_ch4_survey_phase1_report_2017.pdf)

The objective was to quantify VOC emissions from individual oil fields, to be able to relate the measured emissions to oil production and to emission inventory data. However, it was generally difficult to find suitable roads for measuring around the full perimeter of the individual oil fields and therefore emission plumes from several oil fields occasionally overlapped. This is evident studying the most current information on active wells from DOGGR (October 2019) which shows that wells with attribute info identifying one field could have geographic coordinates within boundaries of another field. Unknown if this is intentional or due to a registration error.

The emissions are designated as from the geographic areas coinciding with this latest listing of active wells and these are defined cartographically in the following section. Note that in some cases there is some field overlap.

All measurements have been subjected to quality control and assurance. This include following the standard protocols for SOF, MEFTIR, and MWDOAS, ocular examination of instruments and data, daily instrument calibration and statistical measures of data quality. The number of accepted measurements varied substantially from day to day and from source to source depending on weather conditions, local measurement conditions (accessibility, state of the roads, obstacles etc.) and time sharing between different projects, objects and instruments. Statistical estimates of the flux emissions (kg/h) from the various sources were computed for each measurement day and for the entire survey, including the statistical error.

## 5.1 Sites – Oil and Gas Fields

Table 4 and

Table 5 present the top ten oil producing fields and gas producing fields in California 2018, respectively. Kern county includes 78% of the state's active wells (41332 wells) contributing to 70 % (113,141,827 barrels) of the state oil production and 78 % (140,562,397 Mcf) of the state gas production.

The primary targets for the campaign were Elk Hills Field and the Kern Front-Kern River area but we also investigated the other major oil fields in Kern County in the vicinity of Bakersfield. The oil fields, listed in Figure 10, ranged from Lost Hills in the north, Round Mountain in the east, to Midway Sunset and Elk Hills in the west and south. As can be seen in Table 4 and 5 this represents seven of the top ten oil producing fields in California. More specific information of the oil fields is provided in the discussion section.

Table 4 Top ten oil producing fields in California. Fields in current study in boldface. Source: 2018 Annual Report of California Oil and Gas Production Statistics, DOGGR 2019.

| | **Oil Production (M m$^3$)** | | | | |
|---|---|---|---|---|---|
| **Field** | **2018** | **2017** | **2016** | **2015** | **2014** |
| **Belridge, South** | **3.32** | **3.37** | **3.59** | **3.64** | **3.75** |
| **Midway-Sunset** | **3.29** | **3.51** | **3.93** | **4.48** | **4.66** |
| **Kern River** | **2.61** | **3.48** | **3.86** | **4.09** | **4.02** |
| **Cymric** | **2.07** | **2.58** | **2.69** | **2.62** | **2.50** |
| Wilmington | 1.72 | 1.84 | 2.00 | 1.54 | 1.59 |
| **Lost Hills** | **1.54** | **1.51** | **1.64** | **1.78** | **1.78** |
| **Elk Hills** | **1.37** | **1.45** | **1.61** | **1.80** | **1.91** |
| San Ardo | 1.30 | 1.14 | 1.26 | 1.24 | 1.22 |
| Coalinga | 1.00 | 1.05 | 1.02 | 1.08 | 0.97 |
| **Poso Creek** | **0.81** | **0.70** | **0.67** | **0.64** | **0.57** |

Table 5 Top ten gas producing fields in California. Fields in current study in boldface. Source: 2018 Annual Report of California Oil and Gas Production Statistics, DOGGR 2019.

| **Field** | **Gas production 2018 (M m$^3$)** |
|---|---|
| **Elk Hills** | **2526** |
| **Buena Vista** | **408** |
| **Belridge, South** | **229** |
| **Lost Hills** | **147** |
| **Asphalto** | **139** |
| **Midway-Sunset** | **122** |
| Wilmington | 96 |
| **Cymric** | **68** |
| **Belridge, North** | **65** |
| Ventura | 65 |

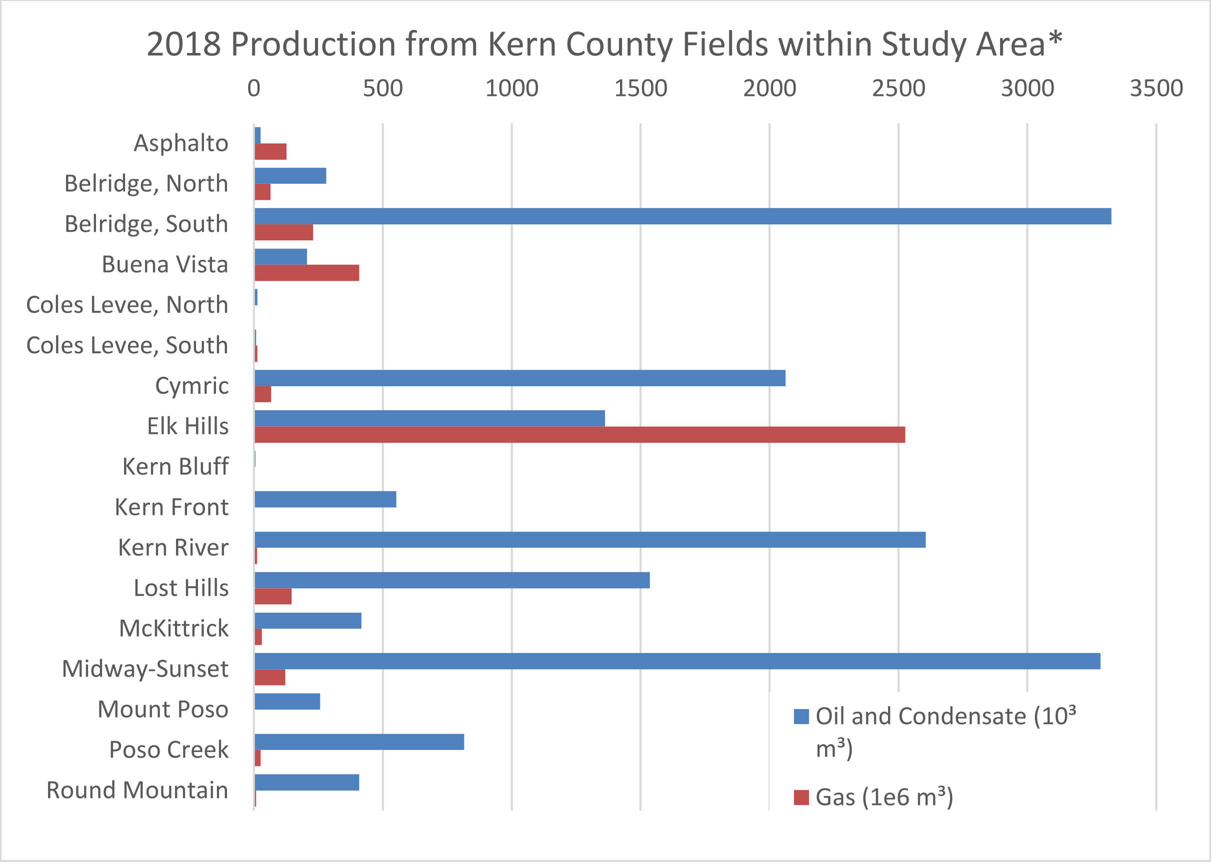

Figure 10 2018 Oil and Gas production from the major fields within the study area (same information as Table 4 and 5 above. *some smaller fields are not included.

All measurements during the survey were made on publicly accessible roads, thus fenceline measurements, measuring the full perimeter, were not possible of all fields. Active oil and gas wells within the major fields of the study along with approximate area boundaries for the emissions survey are shown highlighted in Figures 11 to Figure 15. Boundaries and measurement perimeters therefore follow accessible roads rather than field boundaries. This is most notable for measurements around and near Midway-Sunset and Belridge where the only north-south thoroughfare bisects the fields. In addition, due to its shape and extent Midway-Sunset is only measurable in its northern or southern sections and not in its entirety in a single measurement.

Table 6 shows the measurements days that were carried out during the two campaigns in 2018 and 2019.

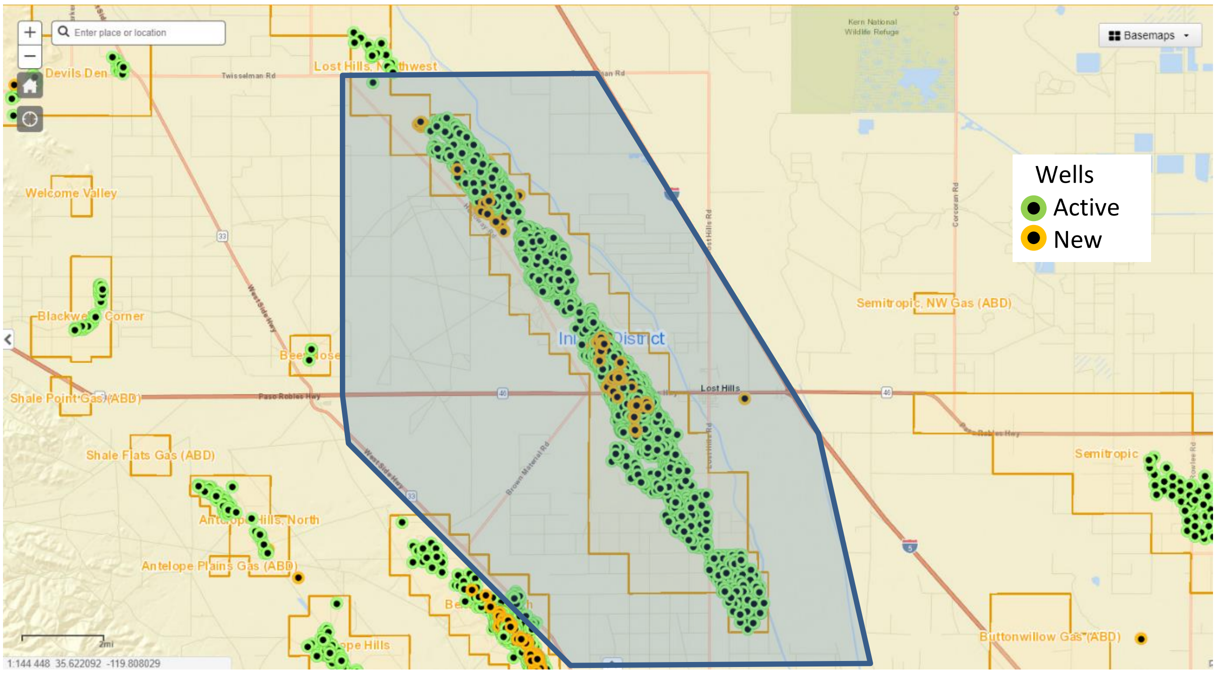

Figure 11. SOF measurement box in blue defining the measurement area for Lost Hills region. The figure also shows new and active wells (DOGGR, December 2019).

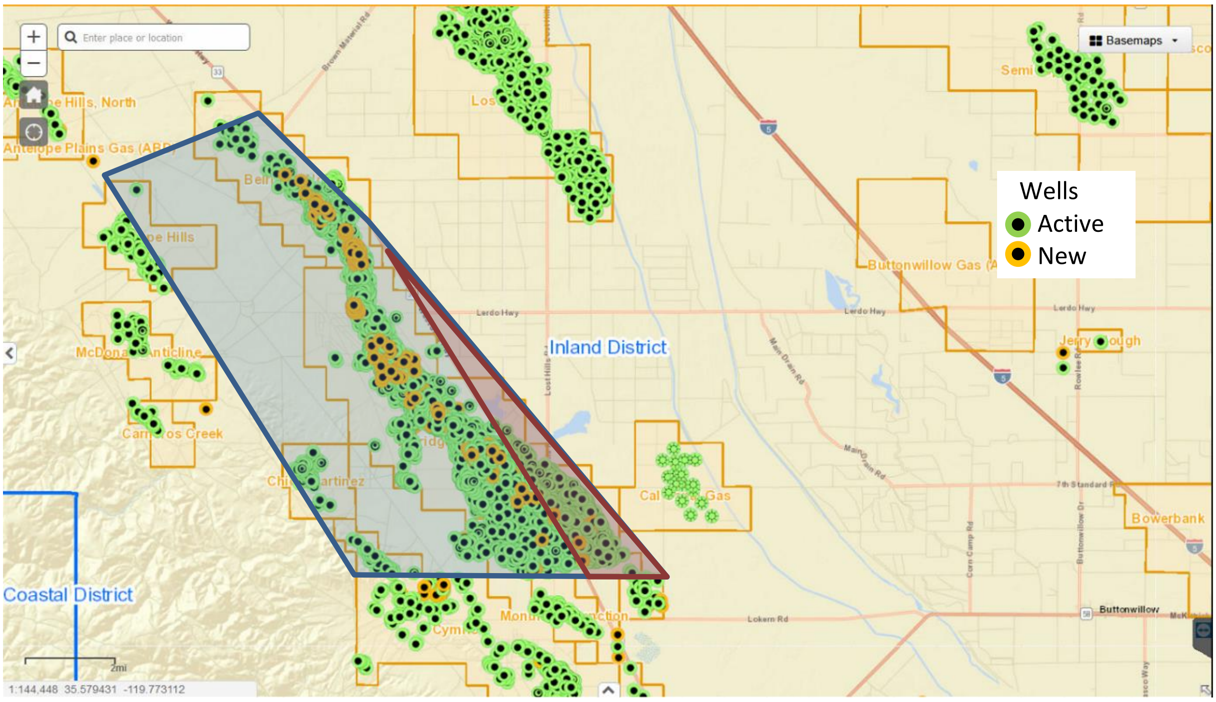

Figure 12. SOF measurement box in blue defining the measurement area for Belridge North and South . The figure also shows new and active wells (DOGGR, December 2019). Note that wells in Belridge South east of Highway 33 (highlight in red) have been included occasionally.

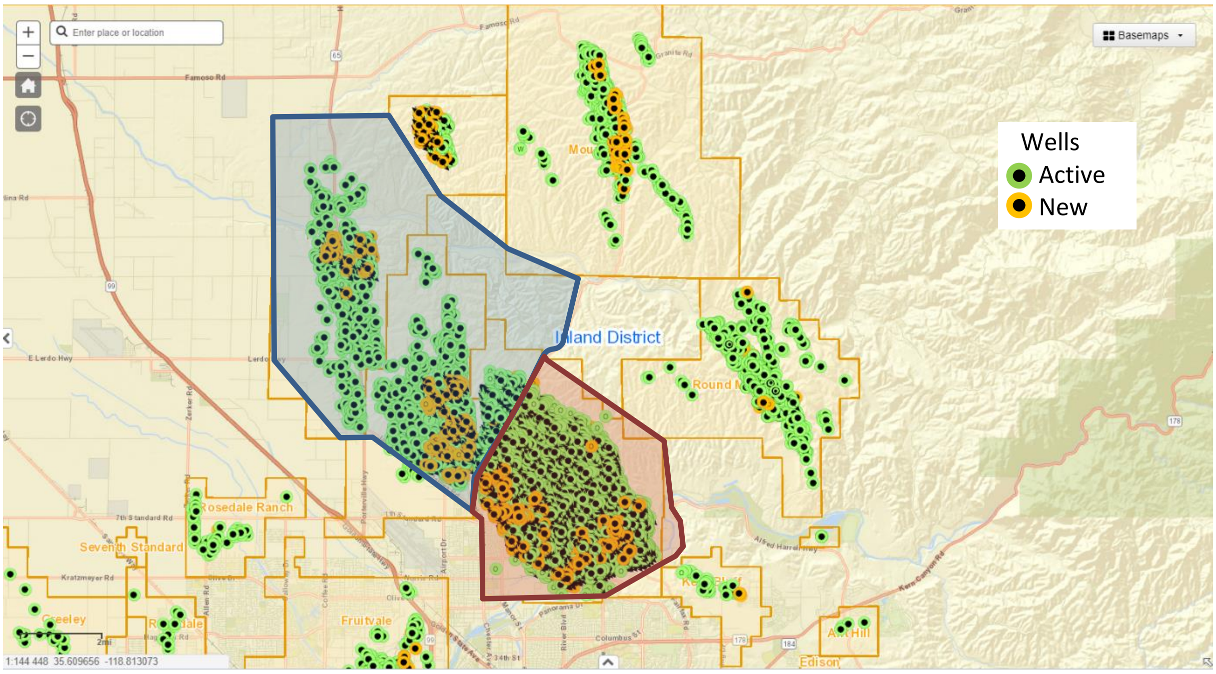

Figure 13. SOF measurement boxes defining the measurement area for the fields of Poso Creek & Kern Front (blue) and Kern River (red). Note that the northwesternmost wells in Kern River are incorporated in Kern Front due to the bisecting road. The figure also shows new and active wells (DOGGR, December 2019). Round Mountain and Mount Poso were measured but with an insufficient number of measurements to be incorporated in the report.

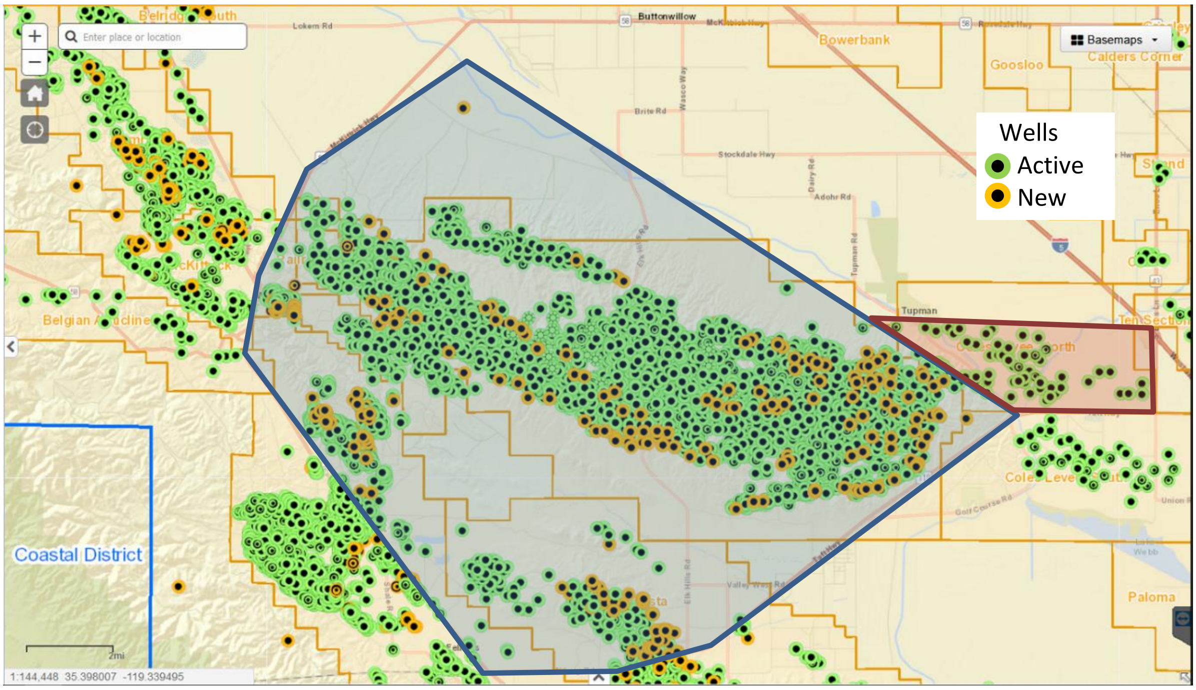

Figure 14. SOF measurement box in blue defining the Elk Hills measurement area includes the fields of Elk Hills, Asphalto, and northern portions of Buena Vista and Midway-Sunset. Occasionally this unavoidably included Coles Levee North (in red). The figure also shows new and active wells (DOGGR, December 2019).

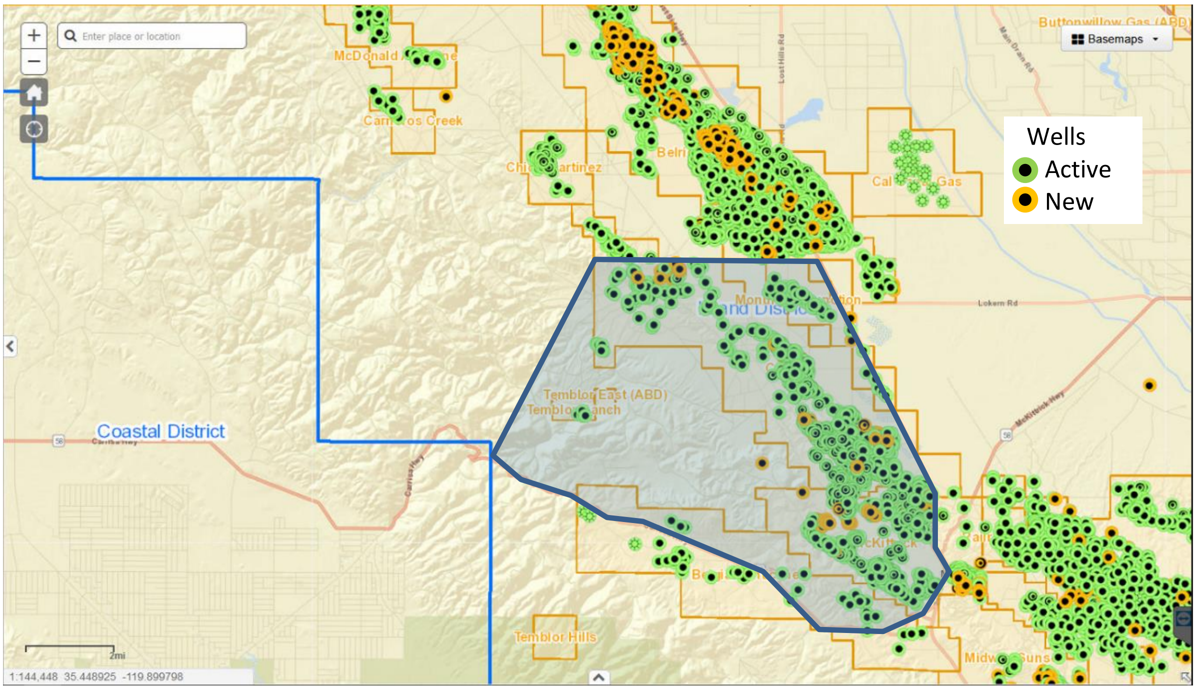

Figure 15. SOF measurement box in blue defining the measurement area for the fields Cymric-McKittrick. The figure also shows new and active wells (DOGGR, December 2019).

Table 6. Measurement days carried out during the campaign.

| Date | LIDAR Location | Survey Area | |
|---|---|---|---|
| | | Emissions | Concentration Mapping/Monitoring |
| 29 Sep 2018 | Shell, Taft Highway | Elk Hills | |
| 30 Sep 2018 | Shell, Taft Highway | Elk Hills | |
| 1 Oct 2018 | Shell, Taft Highway | Elk Hills, Midway sunset | Midway Sunset |
| 26 Oct 2018 | Shell, Taft Highway | Shell, Taft Highway | |
| 27-Apr 2019 | Shell, Taft Highway; late afternoon Fellows Park | Sunset Midway & Elk Hills | Sunset Midway |
| 28 Apr 2019 | Fellows Park | Elk Hills | Elk Hills |
| 29 Apr 2019 | No LIDAR | | Midway Sunset, Elk Hills, Buttonwillow |
| 30 Apr 2019 | Valley Acres Park | Sunset Midway, Elk Hills, McKittrick | Midway Sunset, Elk Hills |
| 1 May 2019 | Derby Acres Park | Sunset Midway, Elk Hills, McKittrick | Midway Sunset, Elk Hills |
| 2 May 2019 | N Chester Ave Ext | Kern Front, Kern River | Meadowview, Highland Park |
| 3 May 2019 | N Chester Ave Ext | Kern Front, Kern River | |
| 4 May 2019 | Hwy58, N of McKittrick | Lost Hills, Cymric, McKittrick, Belridge S | |
| 5 May 2019 | Lost Hills Rd<br>(Missouri Triangle) | Lost Hills, Cymric, Belridge, McKittrick, Buena Vista | |
| 8 May 2019 | Elk Hills Rd + Valley West | Sunset Midway, Elk Hills, McKittrick | Midway Sunset, Elk Hills |
| 8 May 2019 | Derby Acres | Sunset Midway, Elk Hills, McKittrick | Midway Sunset, Elk Hills |
| 1-May 2019 | Wonderful park, Lost Hills | Lost Hills | |
| 12-May 2019 | Derby Acres Park | Produced water ponds | Derby Acres, Taft main road |
| 14-May 2019 | Herring Rd x Old Rd until 7PM | | Lost Hills, Lost Hills to Maricopa late night |
| 15-May 2019 | Taft Ponds FM, then McKittrick field 35.329907°, -119.627240° | Taft ponds, McKittrick E pond, McKittrick field mapping | Main road Taft-McKittrick |
| 17-May 2019 | N Chester Ave Ext | Leases between Hwy65-FamosoRd-Zeker, and S Kern Front. | Round Mountain, late night HighlandKnolls & Meadow View, Airport Rd daytime and nighttime, GraniteRd Kern Front, Hwy65+Zeker |
| 18-May 2019 | Hilton Doubletree, Bakersfield | Bakersfield refineries | Quailwood & Park Stockdale Bakersfield |
| 19-May 2019 | Maricopa ponds | Maricopa ponds | |

## 5.2 Wind measurements

The wind speed and direction of the gas plume are to calculate the gas flux from the geospatial columns measured by SOF and SkyDOAS, as described in section 4. The wind constitutes the largest source of error in the emission measurements, since the flux is directly proportional to the wind speed and to the cosine of the wind direction relative to the driving direction. The wind error is a combination of errors in the wind measurements themselves and errors due to the assumption that the measured wind or wind profile is representative of the average plume velocity.

The vector from the plume source to where it is encountered in the measurement vehicle is essentially a measure of integrated wind direction over the plume path. Hence errors in wind direction are usually apparent in the measurements, given that the location of the leakage point is known, and large errors can then be corrected or avoided. Plume speed in the measurement plane is not directly measured, and plume height is only partially known so wind speed errors are typically more problematic. Note that actual wind or plume speeds only affect emission measurements and not integrated concentration ratios.

Wind profile data, as supplied by a LIDAR, has the major advantage of allowing an average wind for an arbitrary height interval to be calculated. Given some approximate information about the mixing height of the plume, a suitable averaging interval can be chosen, and the LIDAR data can also be used to estimate the sensitivity of the wind error to the error in the mixing height. Hence, LIDAR data was main source of wind information in these measurements complemented with local winds and AIRMAR sonic sensor, mounted on the top of the measurement car. In general, the LIDAR vehicle was stationed in one location per day with the location selected to be close to the downwind measurement perimeter from the day’s primary target based on the morning forecast. Figure 16 shows wind measurement locations are and Table 6 presents the specific days for each location.

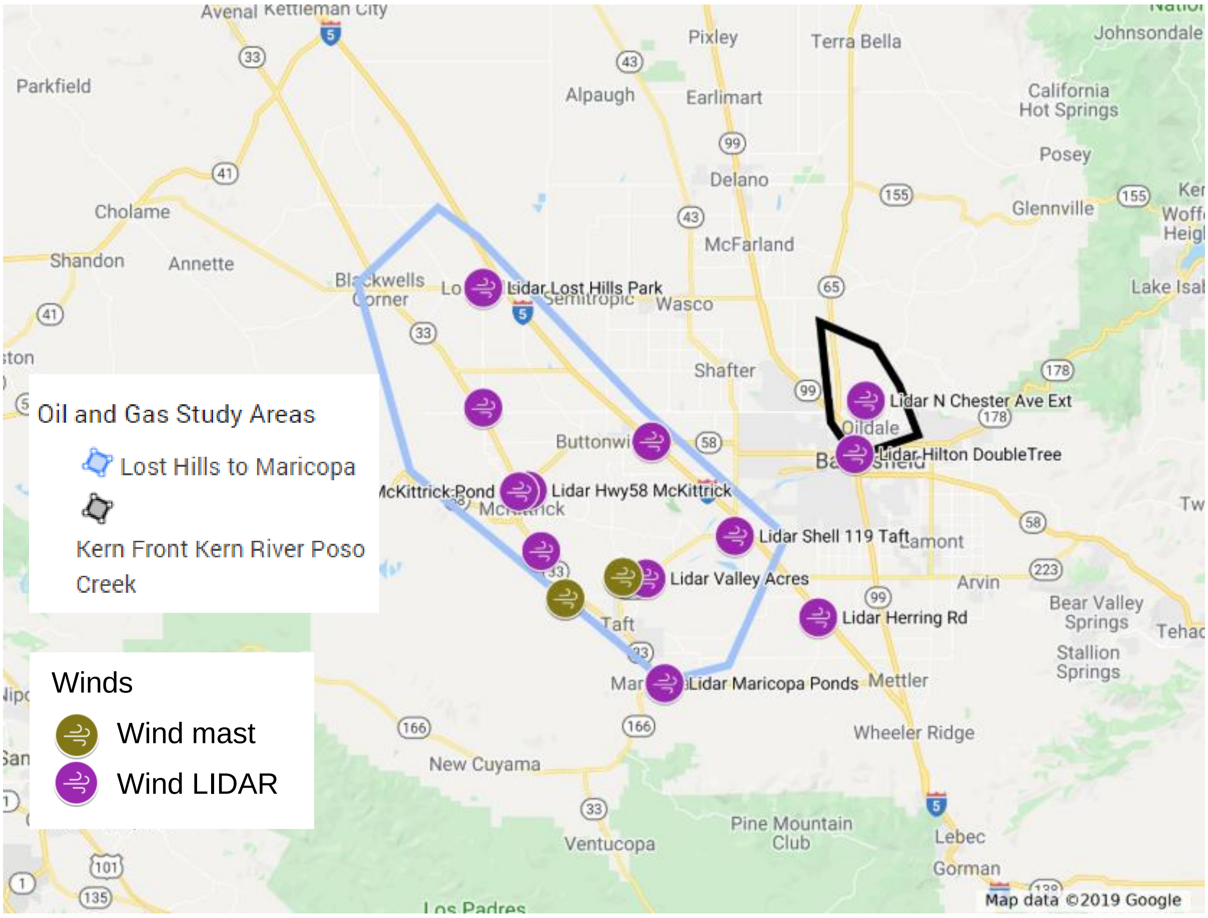

Figure 16. Locations of wind measurements for the emissions survey.

For near-field measurements and point sources it is worthwhile to investigate wind profiles with height to determine how variations in plume height could affect measured emissions. In general, SOF measurement days have vertical profiles with relatively constant wind speed with height and invariant direction up to the max height of the plume due to turbulent mixing. Figure 17 and Figure 18 show typical profiles of the wind.

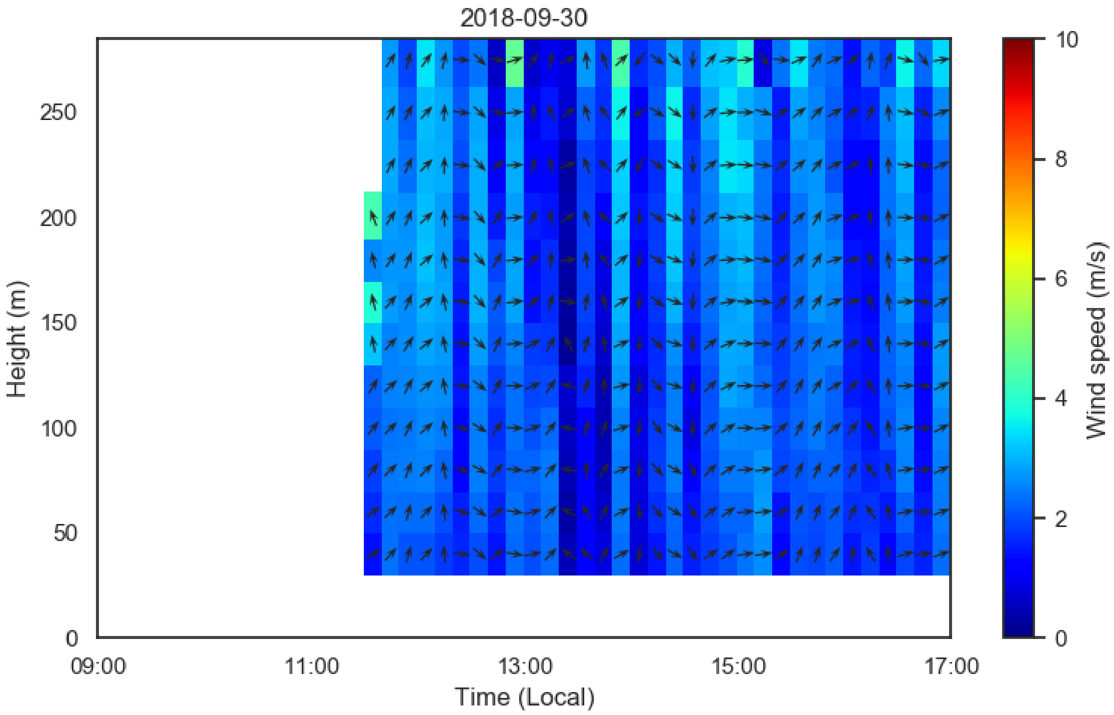

Figure 17 Wind LIDAR data September 30, 2018 showing wind speed (color) and horizontal wind direction (arrows) with height.

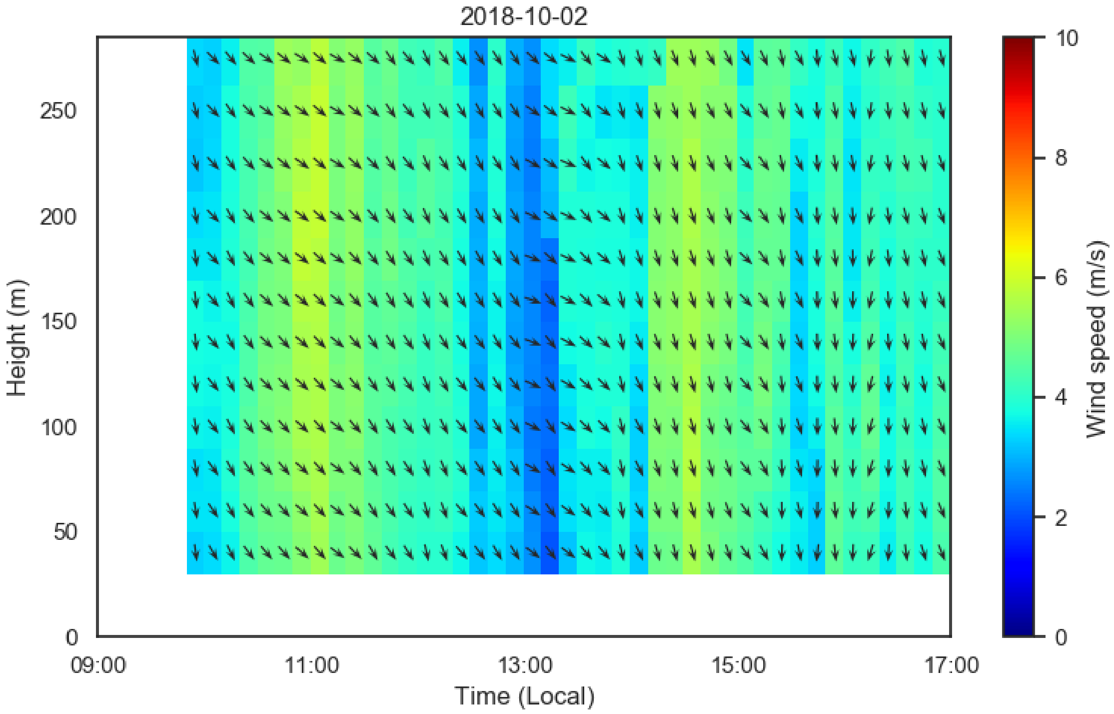

Figure 18. Wind LIDAR data October 2, 2018 showing wind speed (color) and horizontal wind direction (arrows) with height.

In order to assess the sensitivity of the flux calculations to deviations from the assumed plume mixing height, wind LIDAR data (5 min average) have been compared for several height intervals. For the entire measurement period and all LIDAR locations, the wind speed average from 2 – 300m were only slightly higher (2.8 %) than the wind from 2 – 100m (Figure 19). The wind direction was always within 30°. Even the 2 - 50 m winds differed only slightly from the 2 – 100m winds with speed being a 3 % lower but direction well within 30° (Figure 20). These results indicate that plume height misestimation should have only small effect on measured fluxes.

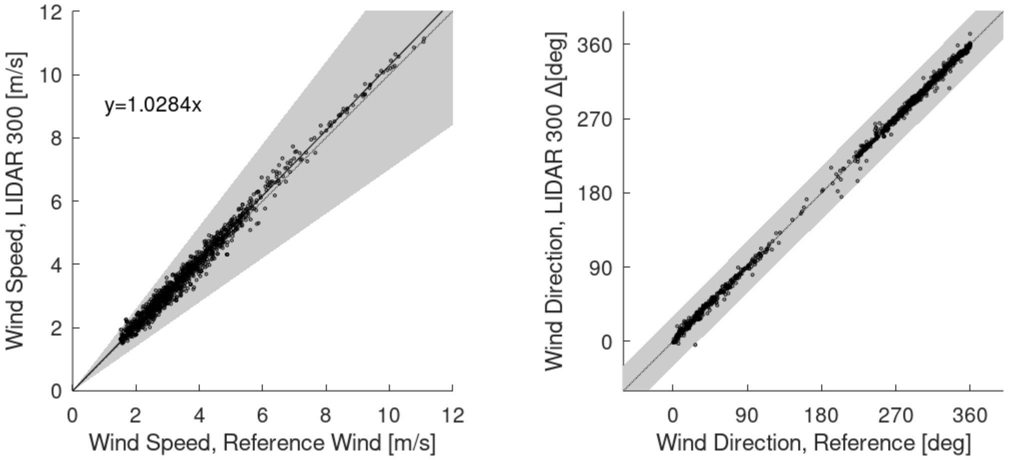

Figure 19. Wind LIDAR data comparison for 2 – 300m (5 min average from 9AM to 5PM) versus the reference 2 – 100 m wind over the measurement period 30 April - 19 May 2019 at all measurement locations. The shaded areas indicate ±30% relative deviation from reference wind speed (left panel) and ±30° deviation from reference wind direction (right panel). Fitted least squares are shown as solid line.

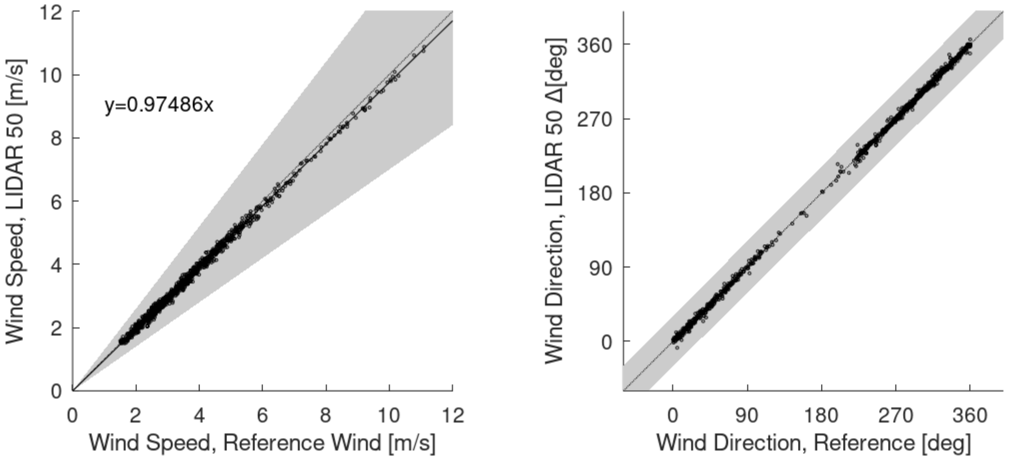

Figure 20. Wind LIDAR data comparison for 2 - 50 m (5 min average from 9AM to 5PM) versus the LIDAR reference (2 – 100m) over the measurement period 30 April - 19 May 2019 at all measurement locations. The shaded areas indicate ±30% relative deviation from reference wind speed (left panel) and ±30° deviation from reference wind direction (right panel). Fitted least squares are shown as solid line.

In the current study the variations with height are less significant than changes in wind direction over the large spatial extent of the surveyed areas and the topography of the San Joaquin valley. Both local topography (hills, valleys, waterways) and basin topography have impacts. Operational forecast models and re-analysis typically do not resolve winds at a sufficiently small spatial or temporal resolution to be employed directly for the measurements, but they offer some indication of larger scale patterns over the measurements and capture at least basin scale topographical impacts. To this end the most recent high-resolution forecast (horizontal resolution of 5 km, hourly) from WindFinder (www.windfinder.com) was examined daily during measurements and occasional screen dumps were captured. Figure 21 and Figure 22 show two situations from 8 May 2019. The first image from 10:00 shows how 10 m wind direction can vary substantially around the perimeter of the Elk Hills field. This can have an impact on the quality of the measurements since a single average wind applied over the measurement is used to determine the emissions. The second image from 14:00 shows more consistent northerly flow. At the height of the plume the wind direction should be more stable but still differs across the basin. Because inflow to the perimeter is not large both times can be used for measurements. A worse situation arises with westerly or north-westerly winds carrying a large inflow of VOCs into the Elk Hills perimeter from Midway-Sunset and Cymric-McKittrick, or significant gradients in the wind direction and/or variability that causes large uncertainties of the flux. For this reason, the westerly winds have wholly been excluded from the Elk Hills measurements. On other occasions weak or turning winds necessitated excluding measurements. Figure 23 shows an example.

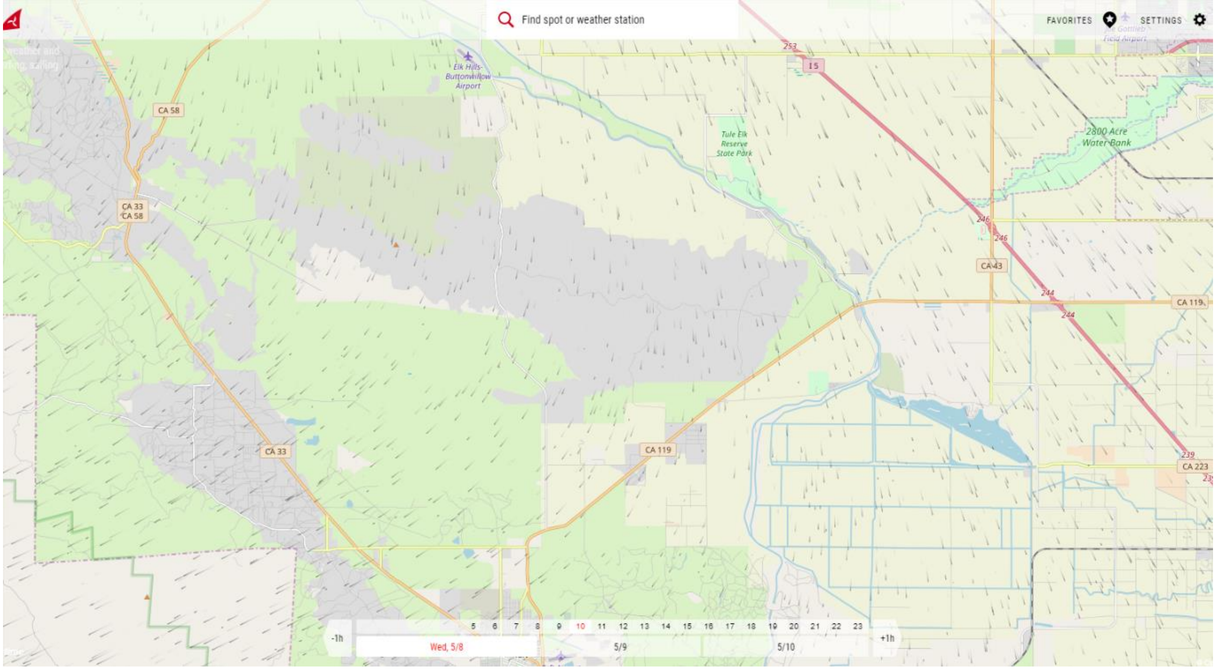

Figure 21. Screen capture of forecast for Elk Hills area, 8 May 2019, 10:00.

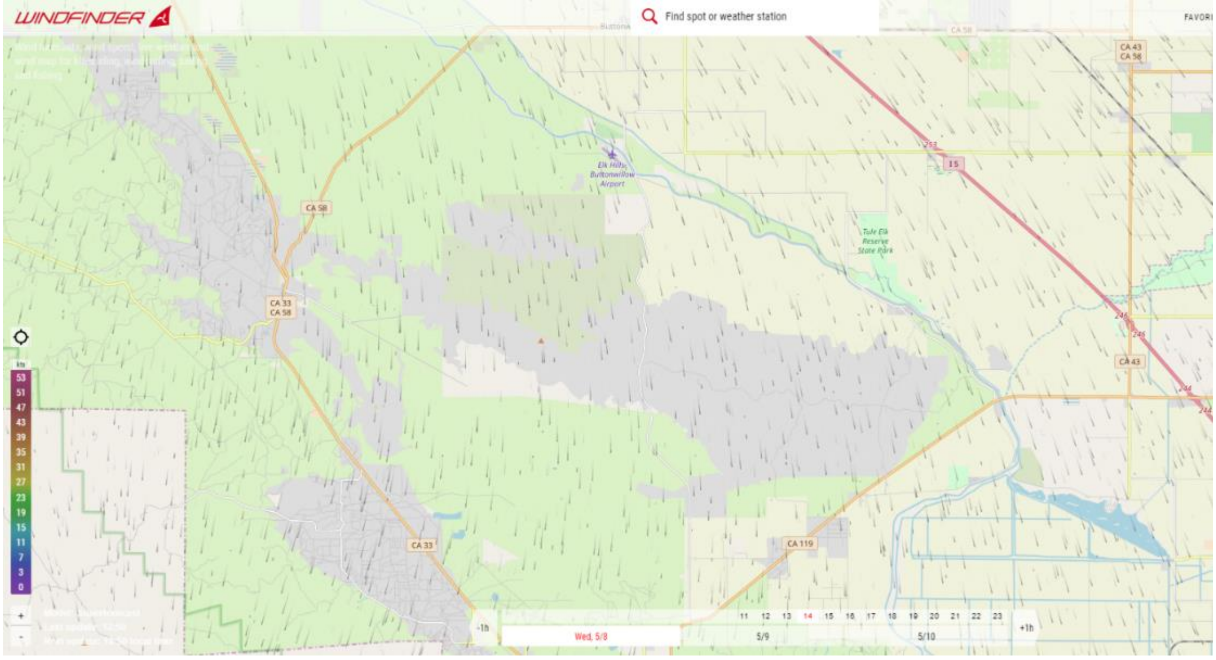

Figure 22. Screen capture of forecast for Elk Hills area, 8 May 2019, 14:00.

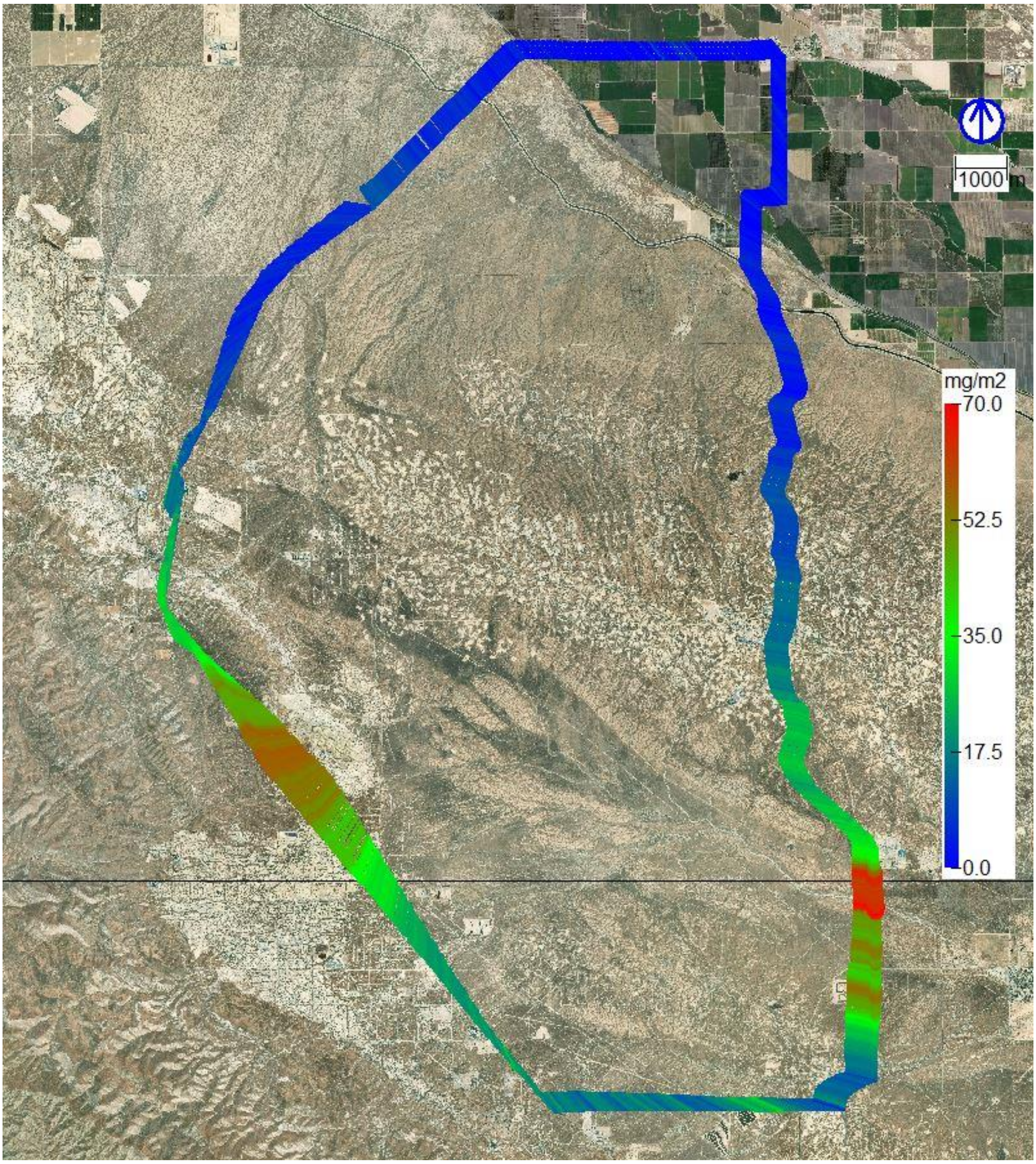

Figure 23 Example of a situation with weak winds and a shift in wind direction during an emission measurement in and around Elk Hills. This traverse was excluded from the measurements. SOF alkane column is shown (mg/m$^2$) with color scale and point size and the line points in the instantaneous wind direction obtained from the LIDAR data.

For some days or times of day LIDAR data was not available for all sites. This was due to distances between survey sites and instrument setup time. In these cases suitable 10 m mast winds were applied with the wind speeds scaled to the appropriate LIDAR profile based on statistical analysis of data when LIDAR was available at the site. Figure 24 shows the relationship between the 2 -100 m LIDAR reference wind and the Bakersfield Meadow Airport (BFL) wind with WNW winds.

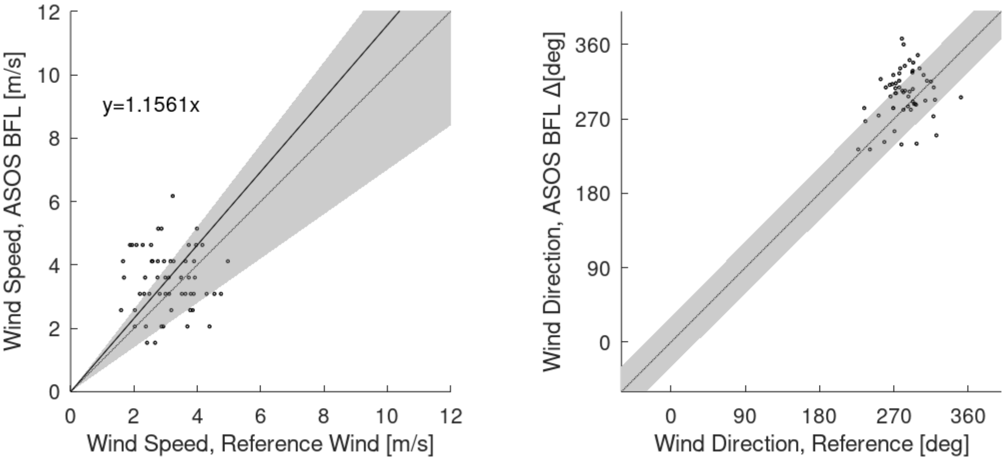

Figure 24. The Bakersfield Meadow Airport (BFL) wind at 10 m versus the LIDAR reference (2 – 100 m) at N. Chester Ave location (5 min average from 9AM to 5PM).

Table 7. Replacement winds when nearby LIDAR data were unavailable

| Date Time | Site | Replacement for LIDAR Data |
|---|---|---|
| 29 April 2019 | All | Bakersfield Meadow Airport (BFL) |

## 5.3 Plume height

The height of the plume influences which wind speed and direction to apply in the flux calculation. In this study we used the average wind speed of the wind LIDAR between ground and 300 m altitude as the main wind speed and direction. This is based on other studies showing a typical vertical mixing speed of 0.5 m/s (Mellqvist, 2009). Given the spatial extent of the oil fields the orthogonal transport distance to the geographic center line leads to plume height estimates above 300 m. For the 2018 data this has been limited to a height of 200 m because the data from over 200 m were less frequently available for the other LIDAR.

## 5.4 Climatology

For the purposes of examining potential impacts of VOC sources on the communities and the representativeness of the measurements on an annual basis, the wind climatology was examined based on data from the Bakersfield airport, Meadows Field, ASOS station  As seen in Figure 25, the survey winds were slightly stronger (3.2 m/s to 2.6 m/s) and more northerly than the preceding annual winds. The higher wind speeds than the annual average (20% higher) may lead to greater emissions from tank storage and open atmospheric sources, produced water ponds for example. Temperatures can also affect emissions, although in this case there were no appreciable differences. The preceding annum at Meadows Field had an average temperature of 19.9 C and during the survey month, 19.7 C.

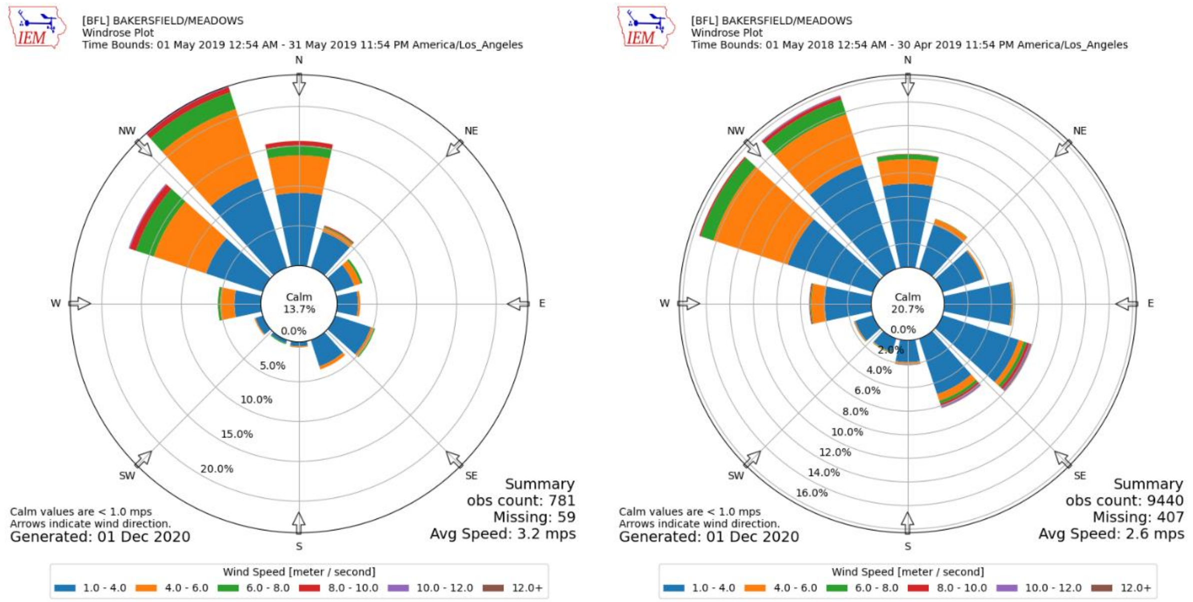

Figure 25. Wind roses for Meadows Field, Bakersfield, May 2019 (left) and annual, May 2018 - May 2019 (right). mps is meters per second.

URL: https://mesonet.agron.iastate.edu/sites/dyn_windrose.phtml?station=BFL&network=CA_ASOS

# 6 Results

Quantitative results for the oil field emission measurements in the San Joaquin Valley are presented in section 6.1 and emission measurements of point sources and other distinct sources are presented in section 6.2. Concentration measurements in communities and along oil field ‘fencelines’ (perimeters) are detailed in Section 6.3 Community monitoring.

SOF measured direct emissions of alkanes, and SkyDOAS measured direct emissions of $SO_2$, $NO_2$ and $H_2CO$. MeFTIR and MWDOAS were used to measure mass concentration ratios of methane to alkanes and BTEX to alkanes at the site fence-lines. These plume mass ratios were combined with the direct alkane flux from SOF measurements to obtain indirect emission estimates of methane and BTEX, respectively.

## 6.1 Emission measurements and gas fluxes – Oil and Gas Fields

Oil and Gas fields were surveyed on a total of 17 days over the period April 27 to May 19, 2019 and 4 days in October 2018. Primary fields were those around Elk Hills, including Elk Hills, Buena Vista, and Midway-Sunset and the more northerly fields McKittrick, Cymric, Belridge and Lost Hills. Also included are the fields closer to Bakersfield to the northeast: Poso Creek, Kern Front and Kern River. For these principal sites, measurements were conducted on multiple days throughout the period, and with more repetitions compared to other sources targeted in the survey. Several smaller fields were also included on a limited number of measurements. The surveyed areas are described in Figures 11 to Figure 15. It should be noted that the areas can comprise several fields and that field boundaries are made rather coarsely and may overlap.

Because of the large extent of the survey emission areas and the shifting winds during the perimeter traverses, the number of measurements fulfilling measurement quality acceptance criteria is greatly reduced compared to standard refinery/small site emission surveys. For sites with few measurements and/or where the winds were less than optimal for the site emissions are still reported; these are indicative of the order of magnitude of the site emissions during the measurements.

Table 8 summarizes the results of the measurements of alkane emissions and methane/alkane ratios for methane emissions (IME) for the major oil and gas fields in the survey. Ratio measurements can be influenced by nearby point sources with different compositions than the field as a whole, however, care has been taken to include as large as area as possible, to minimize the influence of individual sources. Further details are given under the areas' respective section and in the results for identification and measurement of point sources.

Table 8 Results of the alkane and methane emission measurements by SOF and MeFTIR. *Limited number measurements meeting acceptance criteria.

| *Area (fields and associated facilities)* | Days | $N_{meas}$ | Alkane kg/h | $SD_{alkane}$ kg/h | $CH_4$ / Alkane mass concentration ratio | | $CH_4$ kg/h |
|---|---|---|---|---|---|---|---|
| | | | | | 1Q | 3Q | |
| Elk Hills | 8 | 13 | 3470 | 810 | 1.25 | 1.49 | 4820 |
| Poso Creek & Kern Front | 3 | 5 | 440 | 190 | 0.71 | 1.42 | 470 |
| Coles Levee North | 3 | 5 | 250 | 43 | * | * | |
| Cymric & McKittrick | 3 | 7 | 1230 | 480 | 1.06 | 1.35 | 1470 |
| Lost Hills | 4 | 6 | 780 | 310 | 0.38 | 0.46 | 330 |
| Belridge | 2 | 4 | 1480 | 340 | 0.43 | 0.71 | 860 |
| McKittrick | 3 | 4 | 320 | 120 | * | * | |

SkyDOAS measurements were not a primary focus of the campaign since few combustion sources exist in the fields and distances to the field perimeters and private roads preclude closer access to facilities. There was no evidence of emission hot spots and the large-scale measurements of $NO_2$, $SO_2$ and $H_2CO$ were not consistently differentiable from background and/or other interfering sources and as such no results for the fields are reported. BTEX measurements with the exception of point sources were below detectability for fenceline measurements. The point sources measured indicate that BTEX emissions on the whole were less than 1% of the total NMVOC emissions.

### *6.1.1 Elk Hills Area*

The area defined here as Elk Hills includes Asphalto, and the northern part of Buena Vista and northeastern portion of Midway-Sunset by Derby Acres. Figure 26 shows a measurement example. Within this traverse ("box") even Coles Levee North is included, however, wherever possible it has been excluded. Multiple large-scale measurements with SOF, MeFTIR and MWDOAS were carried out around the Elk Hills area over several days in both 2018 and 2019. Figure 27 shows a concentration ratio measurement example. The concentrations of methane and alkanes are integrated along the path and the resulting ratio in this instance was 1.3. Evident in the figure are 2 point sources of methane; one near Derby Acres and the other near McKittrick. The alkane VOCs show slight increases by Derby Acres but not to the same extent as methane. Another consistent point source was in the Buena Vista field near the junction of 119 and Midway Rd. This is not evident in Figure 27 but is covered in Section 6.2.

Emissions of alkanes over these periods were consistently around 3000 kg/h. Results are presented in Table 9. Average alkane emissions were 3500 kg/h over 13 measurements. Ratios of methane to alkanes were consistently greater than one, averaging 1.4 (Table 10). Emissions of methane were 4800 kg/h.

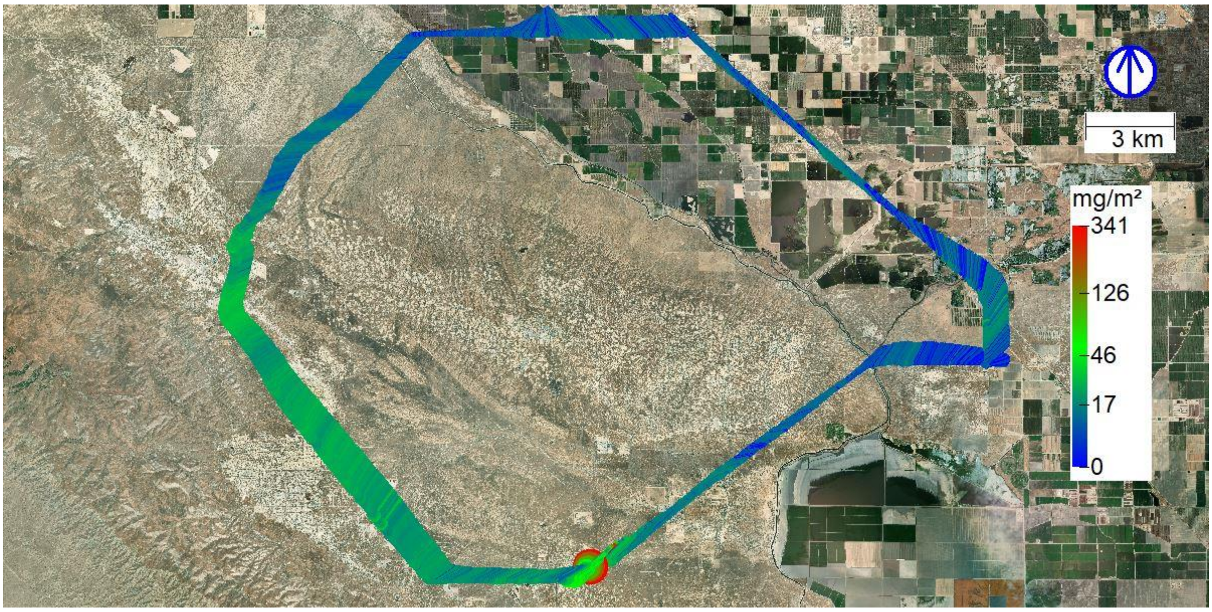

Figure 26. Alkane emission measurement around Elk Hills with northeasterly winds, 1 May 2019, 13:35 – 15:14. Color scale and point size show the SOF alkane column (mg /m$^2$) and the line points in the instantaneous wind direction. NB Color scale is logarithmic.

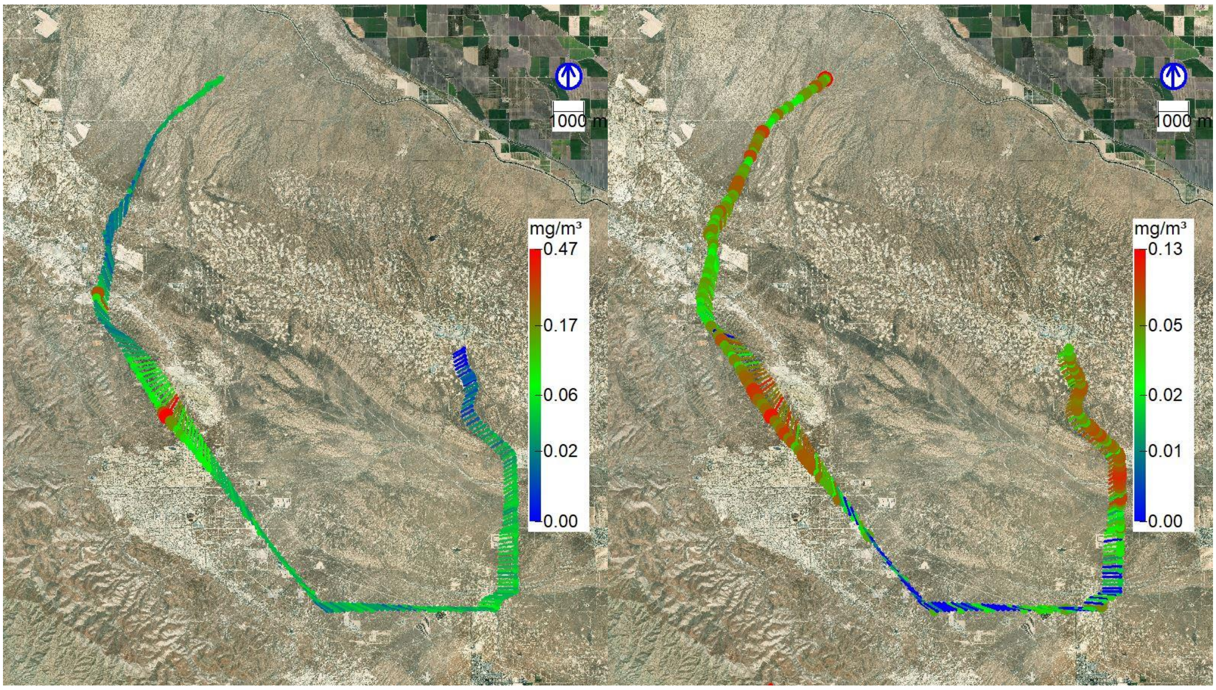

Figure 27. Concentration measurement in and around Elk Hills with varying winds, 8 May 2019, 12:43 – 13:26. Color scale and point size show the methane (left) and alkane (right) concentrations (mg/m$^3$) and the line points in the instantaneous wind direction. NB Color scale is logarithmic. The average integrated mass ratio between $CH_4$ and alkanes was 1.4:1.

Table 9 Alkane emission measurements of the Elk Hills Area.

| Day [yymmdd] | Time span [hhmmss-hhmmss] | N$_{MEAS.}$ | Emission avg [kg/h] | Emission SD [kg/h] | Wind Speed Min-Max [m/s] | Wind Dir Span [deg] |
|---|---|---|---|---|---|---|
| **181001** | 151033-152647 | 1 | 4598 | N/A | 3.1-3.1 | 343-343 |
| **181002** | 104008-112557 | 1 | 3481 | N/A | 5.2-5.2 | 314-314 |
| **181026** | 143410-145956 | 1 | 3362 | N/A | 1.4-1.4 | 343-343 |
| **190427** | 144606-171445 | 3 | 3108 | 327.8 | 4.3-5.3 | 1-352 |
| **190428** | 112912-155401 | 3 | 3632 | 804.8 | 2.7-4.0 | 24-65 |
| **190430** | 143809-150408 | 1 | 3437 | N/A | 3.9-3.9 | 319-319 |
| **190501** | 133528-151429 | 1 | 2576 | N/A | 2.5-2.5 | 41-41 |
| **190508** | 104501-151247 | 2 | 3694 | 1932.6 | 2.2-3.5 | 89-338 |
| **Total # of measurements** | | **13** | **3466.3** | **811.5** | | |
| **Median** | | | **3369.9** | | | |
| **IQR** | | | **2915.3 - 3480.6** | | | |

Table 10 Methane/Alkane mass ratios of the Elk Hills Area from MeFTIR measurements.

| Day [yymmdd] | Time span [hhmmss-hhmmss] | N$_{MEAS.}$ | Mass Ratio avg [%] | Mass Ratio SD [%] | Wind Speed Min-Max [m/s] | Wind Dir Span [deg] |
|---|---|---|---|---|---|---|
| **190508** | 112748-151044 | 3 | 128 | 13.3 | 0.9-3.3 | 0-248 |
| **190511** | 192918-195611 | 1 | 170 | N/A | 3.5-3.5 | 135-135 |
| **Total # of Measurements:** | | **4** | **138.8** | **23.7** | | |
| **Median** | | | **135.0** | | | |
| **IQR** | | | **125.1 - 148.7** | | | |

### 6.1.2 Belridge

Belridge is the northwesternmost field included in the survey, though some smaller fields with few active wells can be found to the west and northwest. No specific targeted measurements were made of Belridge as it was not possible to drive the entire perimeter; however, emissions were occasionally measured as part of boxes around Elk Hills. Figure 28 shows a measurement. For this measurement area few upwind emissions are expected due to a lack of nearby fields in the upwind direction. Observed emissions are assigned to Belridge. Here even the emission traverse is incomplete since the plume for Cymric is entered before the SOF column returns to the zero baseline. Even fewer concentration ratio measurements were available and no point sources were evident in the measurements.

Alkane emissions for Belridge averaged around 1480 kg/h over 4 measurements. The mean methane/alkane ratio was 0.58; methane emissions were 860 kg/h.

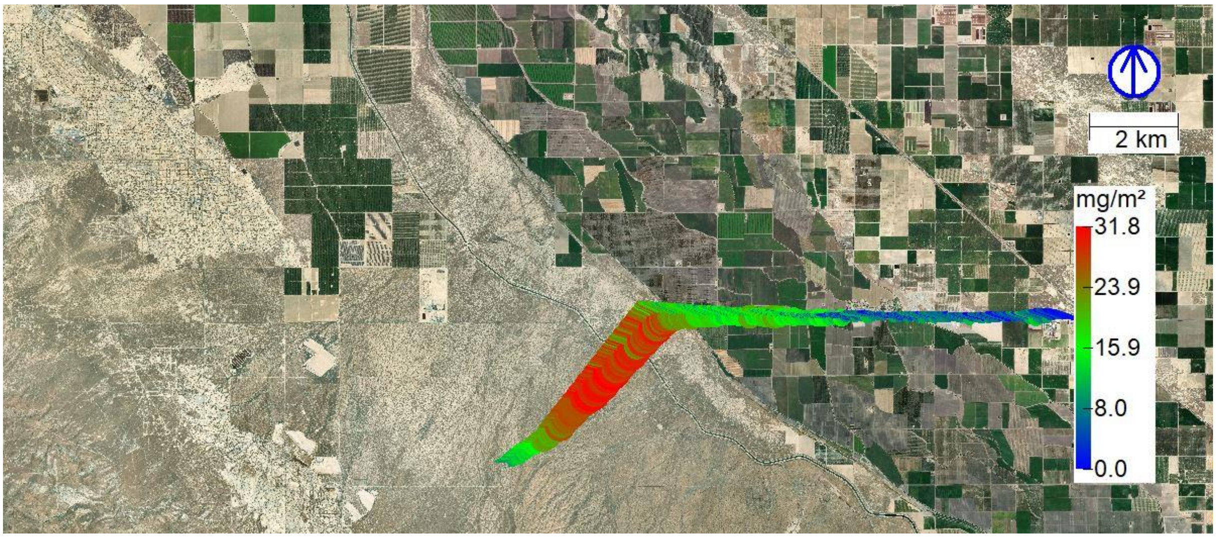

Figure 28. Emission measurement of Belridge with northwesterly winds, 30 April 2019, 13:38 – 13:57. Color scale and point size show the SOF alkane column (mg /m$^2$) and the line points in the instantaneous wind direction. The SOF column down not go to zero in the west because the traverse enters the Cymric plume.

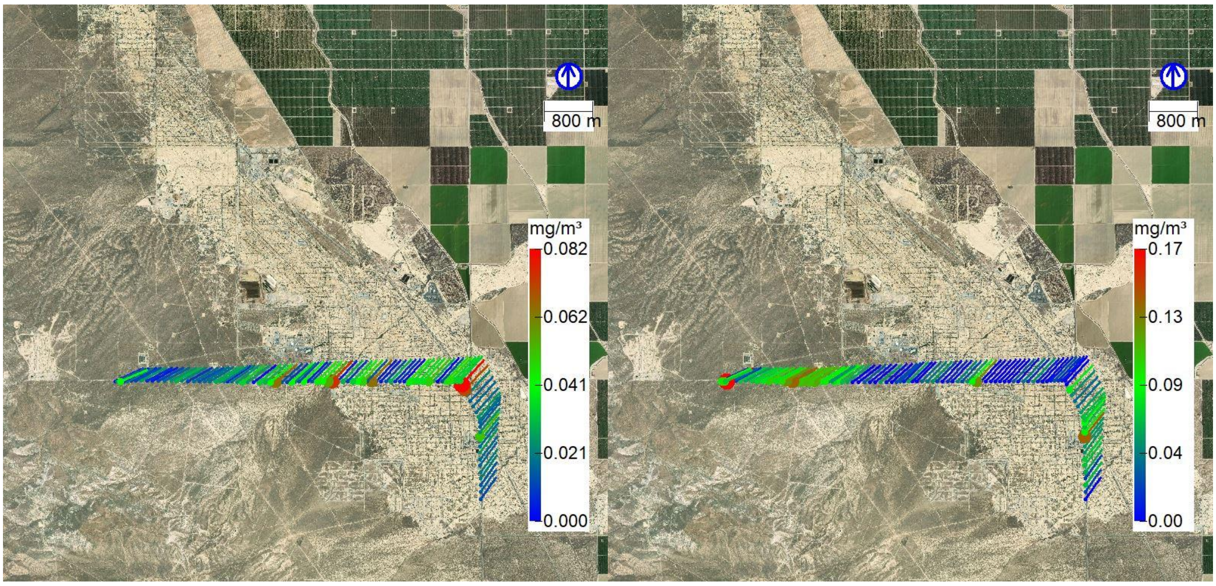

Figure 29. Ratio measurement in and around Belridge North and South fields with northeasterly winds, 4 May 2019, 14:42 – 14:59. Color scale and point size show methane (left) and alkane (right) concentrations (mg/m$^3$) and the lines point in the instantaneous wind direction. The average integrated mass ratio between $CH_4$ and alkanes was 0.58:1.

Table 11 Alkane emission measurements of the Belridge area.

| Day [yymmdd] | Time span [hhmmss-hhmmss] | NMEAS. | Emission avg [kg/h] | Emission SD [kg/h] | Wind Speed Min-Max [m/s] | Wind Dir Span [deg] |
|---|---|---|---|---|---|---|
| **181002** | 144059-152219 | 2 | 1645 | 201.8 | 4.6-4.7 | 332-336 |
| **190430** | 133834-154939 | 2 | 1317 | 446.5 | 3.4-4.0 | 282-287 |
| **Total # of Measurements:** | | **4** | **1481.0** | **340.7** | | |
| **Median** | | | **1567.5** | | | |
| **IQR** | | | **1377.2 - 1671.3** | | | |

Table 12 Methane/Alkane ratios of the Belridge area from MeFTIR measurements.

| Day [yymmdd] | Time span [hhmmss-hhmmss] | NMEAS. | Mass Ratio avg [%] | Mass Ratio SD [%] | Wind Speed Min-Max [m/s] | Wind Dir Span [deg] |
|---|---|---|---|---|---|---|
| **190504** | 144212-145928 | 1 | 53.1 | N/A | 3.8-3.8 | 51-51 |
| **190505** | 150126-151844 | 1 | 32.3 | N/A | 8.4-8.4 | 220-220 |
| **190514** | 233649-021541 | 1 | 89.3 | N/A | 3.0-3.0 | 300-300 |
| **Total # of Measurements:** | | **3** | **58.2** | **28.9** | | |
| **Median** | | | **53.1** | | | |
| **IQR** | | | **42.7 - 71.2** | | | |

### *6.1.3 Coles Levee North*

Coles Levee North is a relatively small area is included only due to the near proximity to Elk Hills and unavoidability of including it in the measurements. There were apparent plumes from a treatment site as well as from the field as a whole. Some of the measurements were made with winds almost parallel to the fields so some accrual of emissions from the methane ‘super emitter’ in the Coles Levee South area is possible. Figure 30 shows an emission measurement of Coles Levee North with west-northwesterly winds. No concentration ratio measurements meeting the acceptance criteria are available. Alkane emissions measured over 3 days averaged 250 kg/h.

Figure 30. Alkane emission measurement of Coles Levee North with westerly winds, 30 April 2019, 16:07 - 16:16. Color scale and point size show the SOF alkane column (mg /m$^2$) and the line points in the instantaneous wind direction.

Table 13 Alkane emission measurements of the Coles Levee North Area.

| Day [yymmdd] | Time span [hhmmss-hhmmss] | $N_{MEAS.}$ | Emission avg [kg/h] | Emission SD [kg/h] | Wind Speed Min-Max [m/s] | Wind Dir Span [deg] |
|---|---|---|---|---|---|---|
| **181002** | 103208-125011 | 2 | 230 | 3.6 | 4.1-4.8 | 314-334 |
| **190427** | 152155-152949 | 1 | 325 | N/A | 5.1-5.1 | 332-332 |
| **190430** | 122338-161655 | 2 | 230 | 11.3 | 3.5-4.0 | 288-293 |
| **Total # of Measurements:** | | **5** | **249.1** | **43.0** | | |
| **Median** | | | **233.0** | | | |
| **IQR** | | | **227.9 - 237.8** | | | |

### 6.1.4 *Cymric and McKittrick*

The area defined here as Cymric and McKittrick includes only the named fields and facilities within their boundaries. All measurements were made in 2019. Measurements were made either as part of the upwind box of Elk Hills or a partial box of Cymric and McKittrick where the western boundary is formed by the western foothills. Figure 31 shows a SOF measurement example of alkane emissions, while Figure 32 displays a concentration measurement of alkanes and methane. Several point and area sources are evident in the figure: in the middle of the Cymric field there are several large facilities and clear point source emissions of methane and alkane VOCs. Unfortunately, emissions from these point sources were not quantified with SOF during this survey.

Emissions of alkanes for the Cymric and McKittrick fields were consistently greater than 1000 kg/h. Results are presented in Table 14. Average alkane emissions were 1230 kg/h over 7 measurements. Ratios of methane to alkanes were consistently greater than one, averaging 1.2 (Table 15). Emissions of methane were 1470 kg/h.

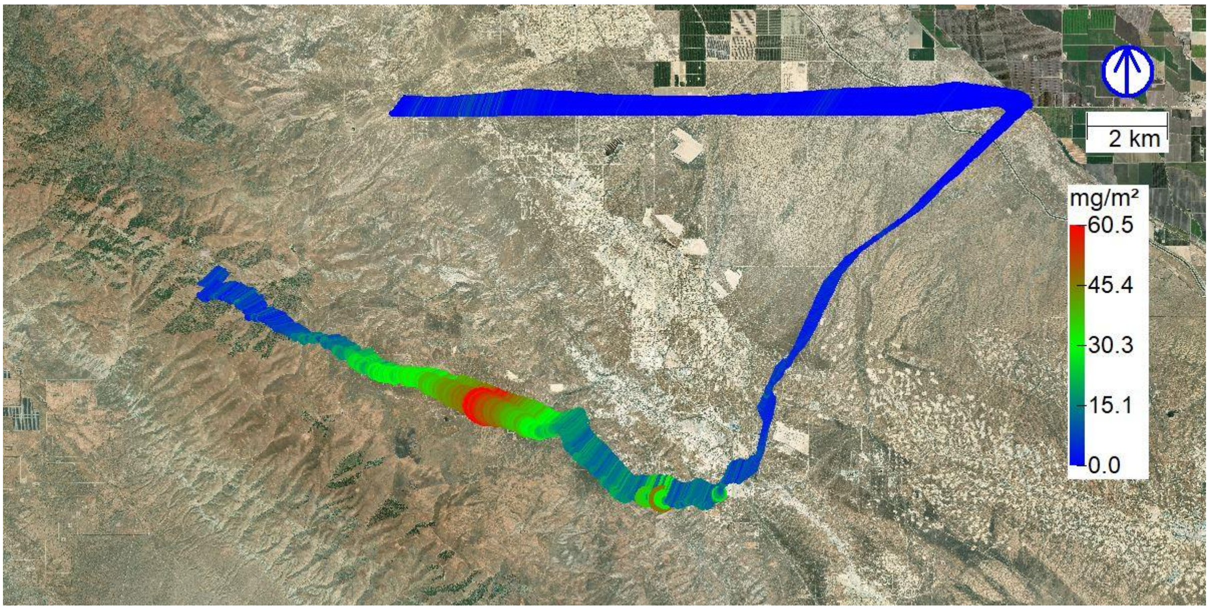

Figure 31. Alkane emission measurement of the Cymric and McKittrick areas with northeasterly winds, 4 May 2019, 13:35 – 15:14. Color scale and point size show the SOF alkane column (mg /m$^2$) and the line points in the instantaneous wind direction.

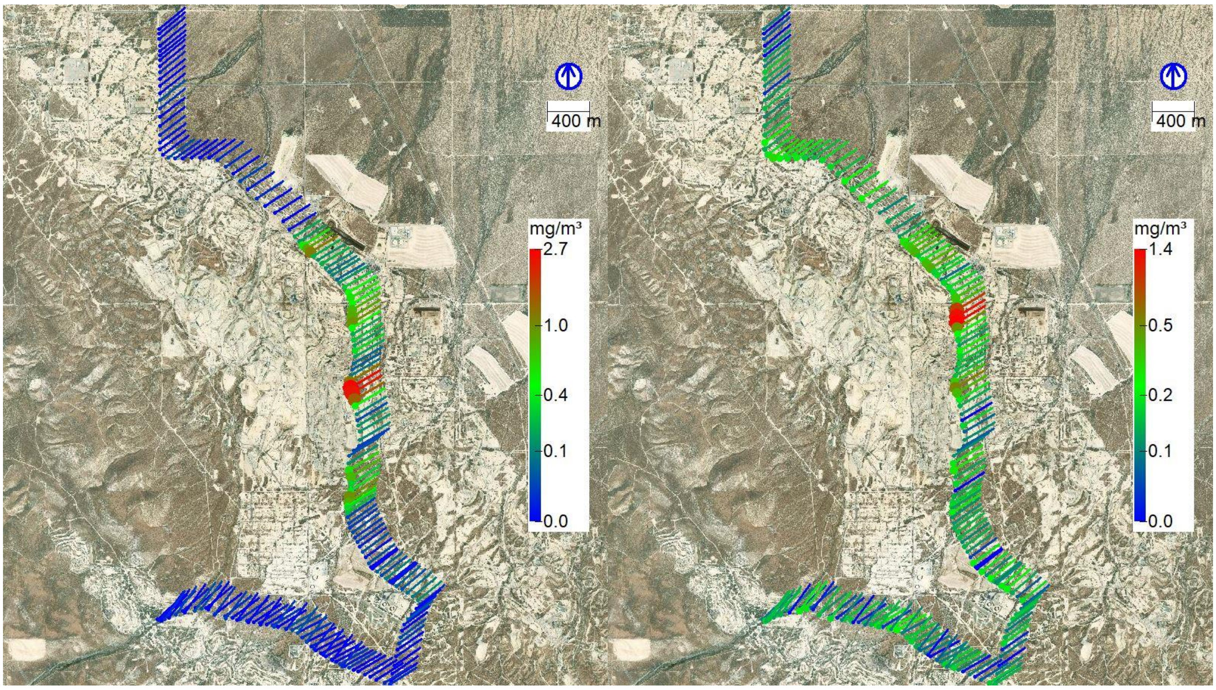

Figure 32. Ratio measurement in and around the Cymric and McKittrick fields with northeasterly winds, 15 May 2019, 15:27 – 16:02. Color scale and point size show methane (left) and alkane (right) concentrations (mg/m$^3$) and the lines point in the instantaneous wind direction. NB Color scale is logarithmic. The typical integrated mass ratio between $CH_4$ and alkanes was 1.2:1.

During one evening measurement BTEX plumes were apparent from an Produced water ponds as well as just south of the town of McKittrick with westerly winds (Figure 33).

Table 14 Alkane emission measurements of the Cymric and McKittrick Fields.

| Day [yymmdd] | Time span [hhmmss-hhmmss] | $N_{MEAS.}$ | Emission avg [kg/h] | Emission SD [kg/h] | Wind Speed Min-Max [m/s] | Wind Dir Span [deg] |
|---|---|---|---|---|---|---|
| **190430** | 132541-153616 | 2 | 893 | 24.0 | 2.2-3.3 | 276-286 |
| **190504** | 120008-173302 | 4 | 1408 | 581.6 | 2.7-3.2 | 24-52 |
| **190508** | 172024-174356 | 1 | 1218 | N/A | 4.2-4.2 | 25-25 |
| **Total # of Measurements:** | | **7** | **1234.1** | **477.8** | | |
| **Median** | | | **1113.8** | | | |
| **IQR** | | | **893.2 - 1483.1** | | | |

Table 15 Methane/Alkane ratios of the Cymric and McKittrick area from MeFTIR measurements.

| Day [yymmdd] | Time span [hhmmss-hhmmss] | $N_{MEAS.}$ | Mass Ratio avg [%] | Mass Ratio SD [%] | Wind Speed Min-Max [m/s] | Wind Dir Span [deg] |
|---|---|---|---|---|---|---|
| **190430** | 152538-154532 | 1 | 140 | N/A | 3.2-3.2 | 284-284 |
| **190504** | 115817-173357 | 4 | 107 | 23.5 | 2.7-3.6 | 31-43 |
| **190505** | 151711-153410 | 1 | 137 | N/A | 9.7-9.7 | 233-233 |
| **190508** | 104514-180632 | 3 | 117 | 16.0 | 2.0-4.2 | 31-356 |
| **190512** | 171927-173129 | 1 | 131 | N/A | 4.6-4.6 | 343-343 |
| **Total # of Measurements:** | | **10** | **118.7** | **20.2** | | |
| **Median** | | | **124.6** | | | |
| **IQR** | | | **106.0 - 134.8** | | | |

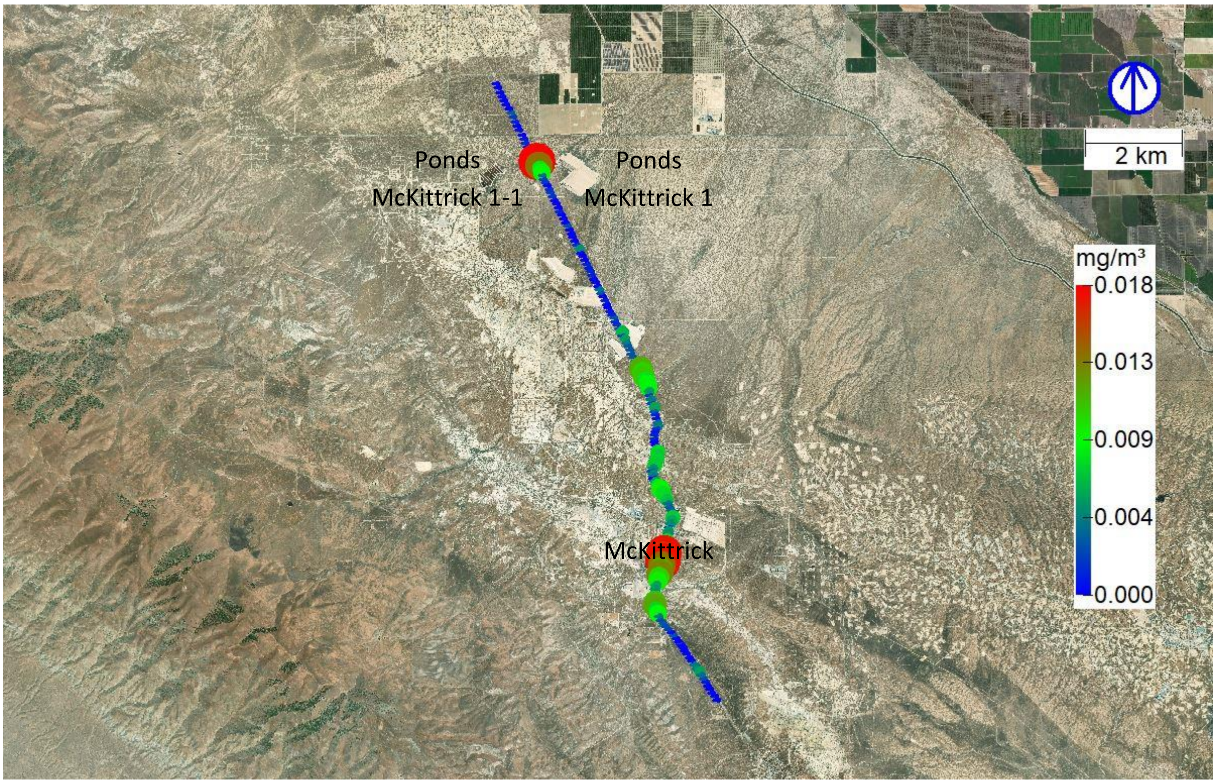

Figure 33. Mobile concentration measurements of BTEX around Cymric-McKittrick, 15 May 2019, 00:19 – 00:25. Color scale and point size show BTEX concentrations (mg/m$^3$) and the lines point in the instantaneous wind direction. Winds were slight and from the west.

### 6.1.5 Poso Creek and Kern Front

All measurements of the Poso Creek and Kern Front fields were made in 2019. Figure 34 shows one such alkane emission measurement with westerly winds. One larger point source is visible in the Kern Front field. Box measurements were made of a sub-area including all but the westernmost part of Poso Creek (see inset, Figure 34) and showed stable inflow to allow determination of emissions for the full Poso Creek and Kern Front fields. Alkane emissions were made over three days and averaged 440 kg/h. Ratio measurements were made over the same days. Figure 35 shows a concentration ratio measurement of Poso Creek (primarily westernmost fields) and Kern Front. These concentration measurements were likely influenced by some of the larger (> 100 kg/h emissions) sources apparent in the JPL Methane Source Finder (https://methane.jpl.nasa.gov). A few distinct plumes can be seen in the methane concentrations; none were observed in the ground level alkane concentrations.

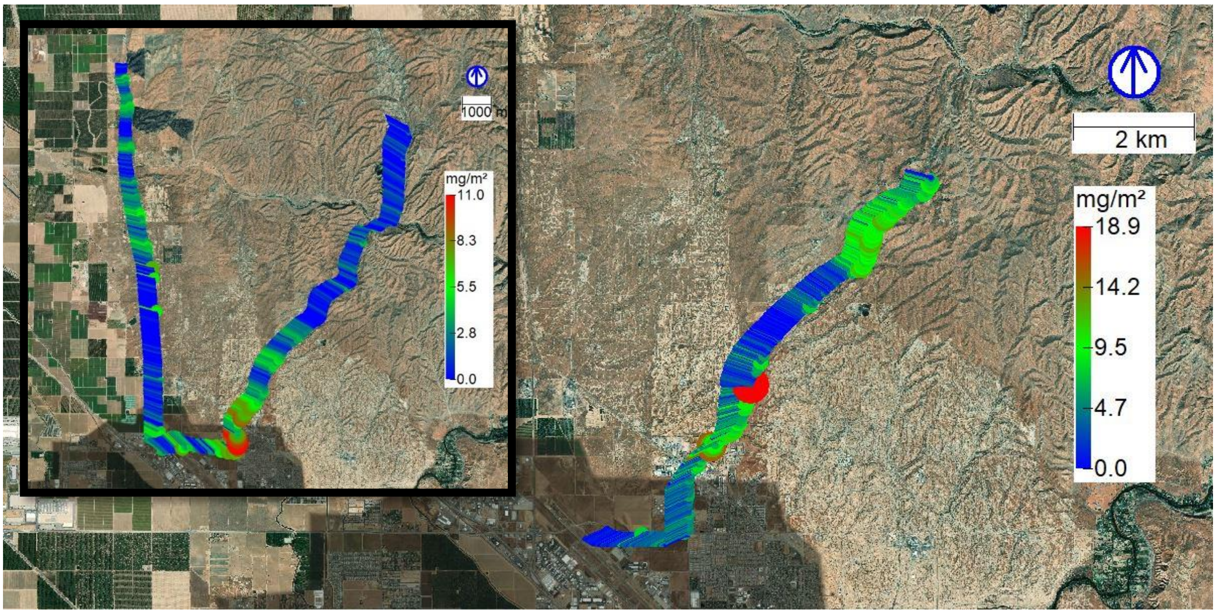

Figure 34. Alkane emission measurement of the Poso Creek and Kern Front areas with westerly winds, 2 May 2019, 12:02 – 12:26. Color scale and point size show the SOF alkane column (mg/m$^2$) and the lines point in the instantaneous wind direction. Inset: Kern Front and Poso Creek E measurement, 3 May 2019.

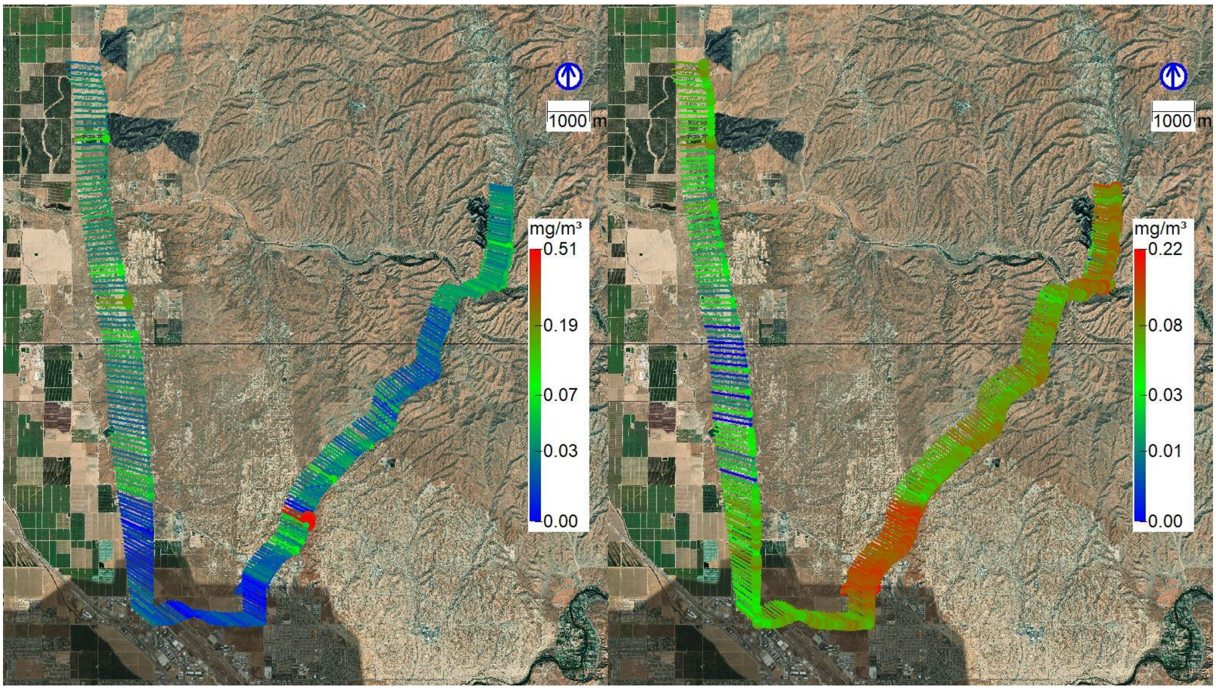

Figure 35. Ratio measurement in and around the Poso Creek and Kern Front fields with westerly winds, 2 May 2019, 14:05 – 15:08. Color scale and point size show methane (left) and alkane (right) concentrations (mg/m$^3$) and the lines point in the instantaneous wind direction. NB Color scale is logarithmic. The average integrated mass ratio between $CH_4$ and alkanes was 1:1.

Table 16 Emission measurements of the Poso Creek and Kern Front Area.

| Day [yymmdd] | Time span [hhmmss-hhmmss] | N<sub>MEAS.</sub> | Emission avg [kg/h] | Emission SD [kg/h] | Wind Speed Min-Max [m/s] | Wind Dir Span [deg] |
|---|---|---|---|---|---|---|
| **190502** | 120219-142854 | 2 | 320 | 81.9 | 3.1-3.4 | 271-274 |
| **190503** | 130308-145032 | 2 | 634 | 122.5 | 4.0-4.3 | 298-298 |
| **190517** | 175914-181821 | 1 | 308 | N/A | 4.8-4.8 | 310-310 |
| **Total # of Measurements:** | | **5** | **443.2** | **189.5** | | |
| **Median** | | | **377.4** | | | |
| **IQR** | | | **308.1 - 547.8** | | | |

Table 17 Methane/Alkane mass ratios of the Poso Creek and Kern Front Area from MeFTIR measurements.

| Day [yymmdd] | Time span [hhmmss-hhmmss] | N<sub>MEAS.</sub> | Mass Ratio avg [%] | Mass Ratio SD [%] | Wind Speed Min-Max [m/s] | Wind Dir Span [deg] |
|---|---|---|---|---|---|---|
| **190502** | 132602-134039 | 1 | 142 | N/A | 2.3-2.3 | 287-287 |
| **190503** | 130235-144234 | 2 | 103 | 56.5 | 3.4-3.8 | 275-299 |
| **190517** | 134102-140019 | 1 | 74.2 | N/A | 1.6-1.6 | 324-324 |
| **Total # of Measurements:** | | **4** | **105.4** | **42.8** | | |
| **Median** | | | **107.9** | | | |
| **IQR** | | | **71.4 - 141.9** | | | |

### *6.1.6 Lost Hills*

Measurements of the Lost Hills field were made in 2018 and 2019. Figure 36 shows one such alkane emission measurement with easterly winds. Alkane emissions were made over four days and averaged 780 kg/h. Ratio measurements were made on two days. Table 18 and Table 19 present the results for the emission measurements and the concentration ratio measurements, respectively.

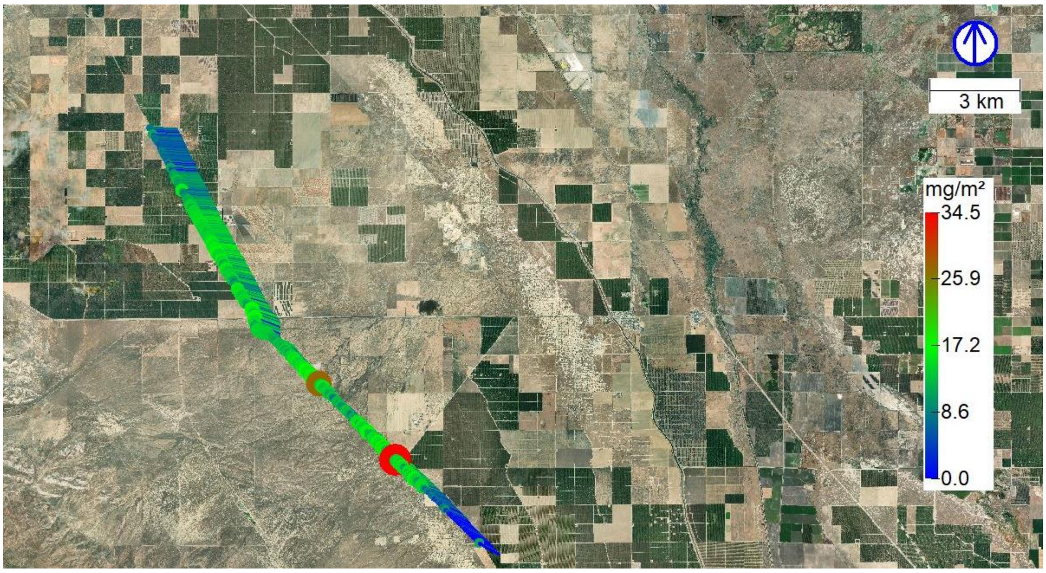

Figure 36. Alkane emission measurement of the Lost Hills Area with easterly winds, 2 May 2019, 12:02 – 12:26. Color scale and point size show the SOF alkane column (mg /m$^2$) and the lines point in the instantaneous wind direction.

Table 18 Alkane emission measurements of the Lost Hills Area.

| Day [yymmdd] | Time span [hhmmss-hhmmss] | N$_{MEAS.}$ | Emission avg [kg/h] | Emission SD [kg/h] | Wind Speed Min-Max [m/s] | Wind Dir Span [deg] |
|---|---|---|---|---|---|---|
| **181002** | 133858-152905 | 2 | 565 | 64.4 | 3.5-4.0 | 0-319 |
| **190504** | 161203-162130 | 1 | 656 | N/A | 4.9-4.9 | 3-3 |
| **190505** | 112735-115232 | 1 | 1378 | N/A | 2.6-2.6 | 35-35 |
| **190511** | 144141-174951 | 2 | 770 | 76.7 | 2.5-3.6 | 111-111 |
| **Total # of Measurements:** | | **6** | **784.1** | **308.1** | | |
| **Median** | | | **686.0** | | | |
| **IQR** | | | **622.3 - 797.0** | | | |

Table 19 Methane/Alkane ratios of the Lost Hills Area from MeFTIR measurements.

| Day [yymmdd] | Time span [hhmmss-hhmmss] | N$_{MEAS.}$ | Mass Ratio avg [%] | Mass Ratio SD [%] | Wind Speed Min-Max [m/s] | Wind Dir Span [deg] |
|---|---|---|---|---|---|---|
| **190505** | 113343-131218 | 2 | 48.0 | 5.8 | 2.8-2.9 | 1-24 |
| **190514** | 214411-235314 | 2 | 36.3 | 5.7 | 3.9-4.0 | 2-307 |
| **Total # of Measurements:** | | **4** | **42.2** | **8.2** | | |
| **Median** | | | **42.1** | | | |
| **IQR** | | | **38.3 - 46.0** | | | |

### 6.1.7 *McKittrick*

In a few instances the McKittrick section could be isolated from the Cymric-McKittrick area as a whole. These measurements are more indicative of the relative emissions of this area due to the uncertain and indistinct boundaries between the fields. Thus, the McKittrick area could be seen as having roughly a fourth of the emissions of the Cymric-McKittrick area as a whole, around 300 kg/h. Figure 37 shows an alkane measurement example. Table 19, Table 20 and

Table 21 present the results for the emission measurements and the concentration ratio measurements. The concentration ratio measurements vary widely due to the vicinity of some sources to the road.

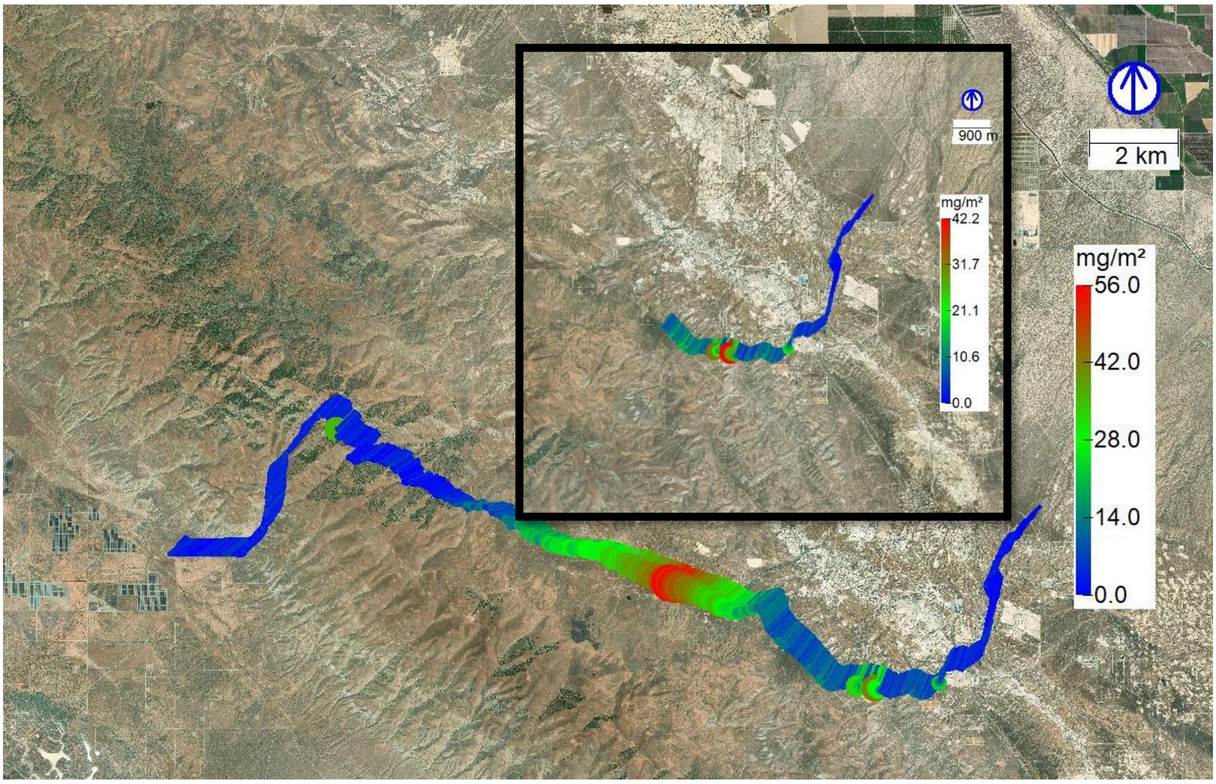

Figure 37. Alkane emission measurement of the McKittrick oil field showing Cymric and McKittrick plumes and just McKittrick (inset), 4 May 2019, 13:22 – 13:38. Color scale and point size show the SOF alkane column (mg /m$^2$) and the lines point in the instantaneous wind direction.

Table 20 Emission measurements of the McKittrick area.

| Day [yymmdd] | Time span [hhmmss-hhmmss] | NMEAS. | Emission avg [kg/h] | Emission SD [kg/h] | Wind Speed Min-Max [m/s] | Wind Dir Span [deg] |
|---|---|---|---|---|---|---|
| **190504** | 114946-133818 | 2 | 297 | 192.2 | 2.8-3.0 | 27-63 |
| **190505** | 152358-152734 | 1 | 315 | N/A | 10.2-10.2 | 245-245 |
| **Total # of Measurements:** | | **3** | **318.0** | **115.2** | | |
| **Median** | | | **338.7** | | | |
| **IQR** | | | **276.4 - 380.3** | | | |

Table 21 Methane/Alkane ratios of the McKittrick area from MeFTIR measurements

| Day [yymmdd] | Time span [hhmmss-hhmmss] | NMEAS. | Mass Ratio avg [%] | Mass Ratio SD [%] | Wind Speed Min-Max [m/s] | Wind Dir Span [deg] |
|---|---|---|---|---|---|---|
| **190428** | 133732-153203 | 3 | 2702 | 2058.7 | 3.2-4.1 | 81-96 |
| **190429** | 191730-203038 | 2 | 137 | 51.8 | 3.6-4.7 | 2-319 |
| **190505** | 181729-182111 | 1 | 147 | N/A | 9.0-9.0 | 305-305 |
| **190508** | 140828-142459 | 1 | 132 | N/A | 3.2-3.2 | 10-10 |
| **Total # of Measurements:** | | **7** | **1236.9** | **1814.3** | | |
| **Median** | | | **173.3** | | | |
| **IQR** | | | **139.4 - 1517.0** | | | |

## 6.2 Emission measurements and gas fluxes – Produced water ponds, concentrated sources and Emission hotspots within O&G fields

Four produced water ponds were surveyed during the study and these are denoted as follows: McKittrick #1, McKittrick #1B East, Taft, and Maricopa. Figure 38 display the locations of these ponds. Details of the measurements are given under their respective sub-headings. During the routine emissions survey measurements, a number of concentrated sources or emissions hotspots within the fields were measured. The designation concentrated source or hotspot is not based on strength of emissions but whether the sources were reliably differentiable from other field sources. Thus, it is not a comprehensive list of surveyed hotspots but only those that could be repeatedly measured due to accessibility and wind. Figure 38 shows the locations of the reported concentrated sources and the produced water ponds.

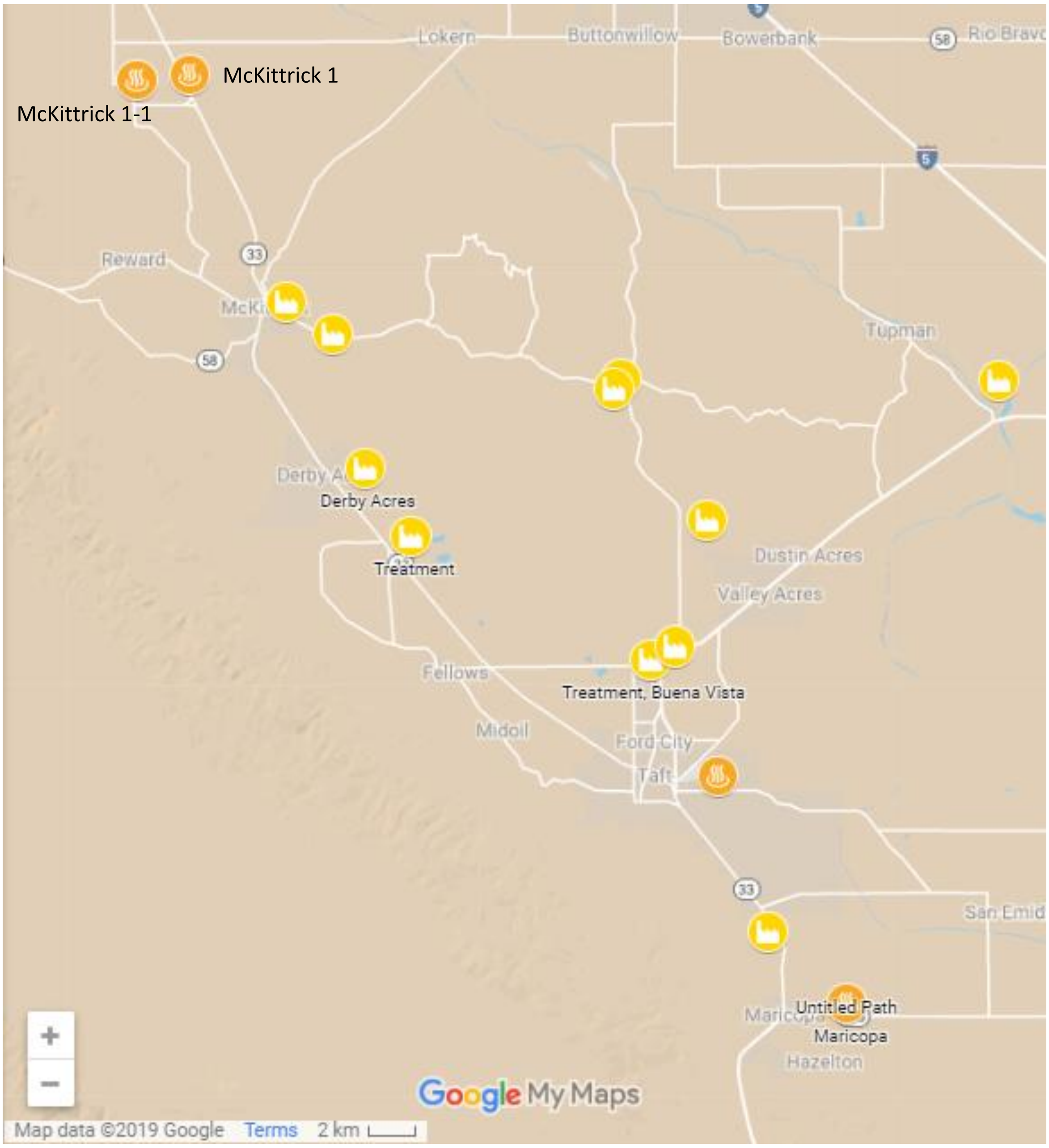

Figure 38. Produced water ponds, distinct sources and emission hotspots within the Elk Hills survey area.

### *6.2.1 Oil and Gas Ponds*

The oil and gas ponds surveyed were small sources of alkane emissions and were inconsequential for methane emissions. The insets of Figure 39 shows example emission measurements of the McKittrick ponds. An exception may be for occasions with very high winds. Although the ponds are covered with netting, high wind speeds may increase emissions disproportionately by increased turbulence near the water air interface.

Table 22 and Table 23 present the results for the emissions and the concentration ratio measurements of McKittrick 1-1, respectively.

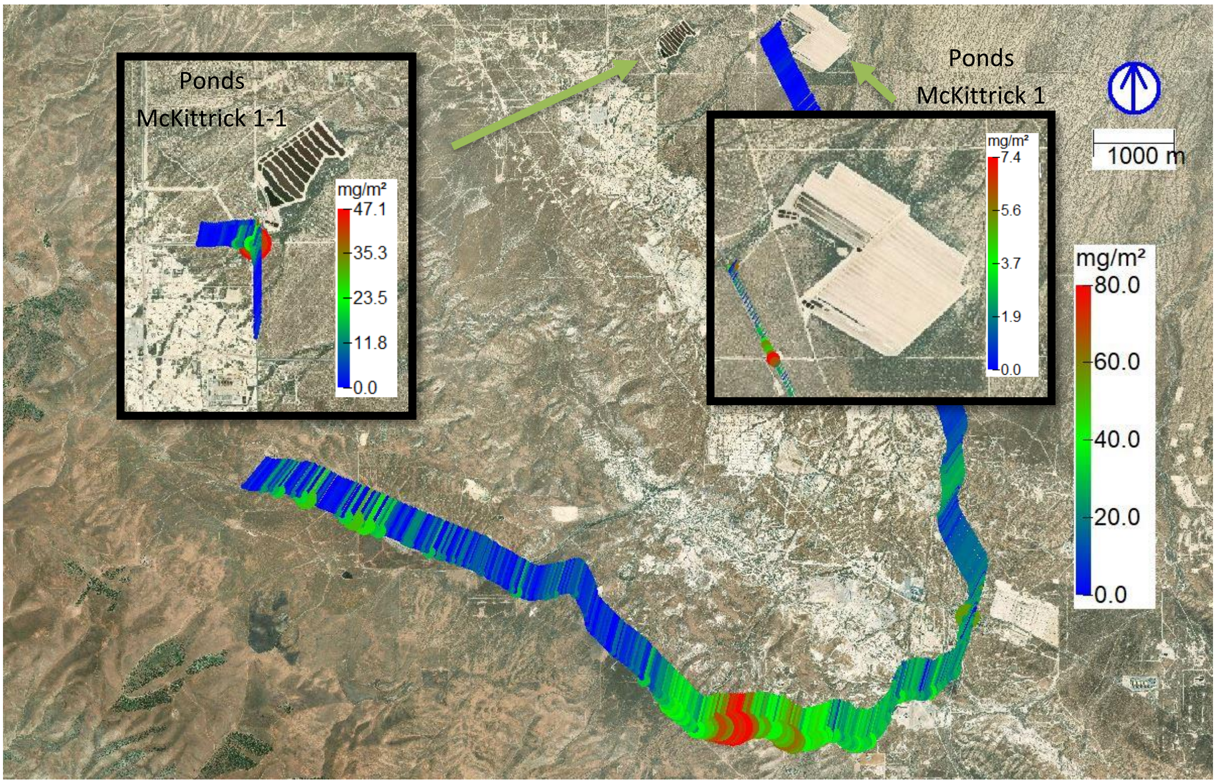

Figure 39. Alkane emission measurement along Highway 33 and 58, 8 May 2019 17:18 – 17:45 with insets showing measurements of McKittrick 1-1 (west of Hwy 33) and McKittrick 1 (east of Hwy 33), 17:05 and 17:20, respectively. Color scale and point size show the SOF alkane column (mg /m$^2$) and the lines point in the instantaneous wind direction.

Table 22 Alkane emission measurements of Produced water ponds McKittrick 1-1.

| Day [yymmdd] | Time span [hhmmss-hhmmss] | $N_{MEAS.}$ | Emission avg [kg/h] | Emission SD [kg/h] | Wind Speed Min-Max [m/s] | Wind Dir Span [deg] |
|---|---|---|---|---|---|---|
| **190508** | 165630-171049 | 3 | 14.7 | 6.0 | 2.5-4.3 | 9-16 |
| **190512** | 174603-174911 | 1 | 11.9 | N/A | 3.9-3.9 | 17-17 |
| **Total # of Measurements:** | | **4** | **14.0** | **5.1** | | |
| **Median** | | | **11.8** | | | |
| **IQR** | | | **11.5 - 14.3** | | | |

Table 23 Methane/Alkane ratios of Produced water ponds McKittrick 1-1.

| Day [yymmdd] | Time span [hhmmss-hhmmss] | $N_{MEAS.}$ | Mass Ratio avg [%] | Mass Ratio SD [%] | Wind Speed Min-Max [m/s] | Wind Dir Span [deg] |
|---|---|---|---|---|---|---|
| **190508** | 165529-200508 | 5 | 59.5 | 59.4 | 2.5-4.5 | 0-19 |
| **190512** | 174544-181806 | 2 | 68.4 | 6.8 | 4.0-4.5 | 8-357 |
| **Total # of Measurements:** | | **7** | **62.0** | **48.8** | | |
| **Median** | | | **63.5** | | | |
| **IQR** | | | **27.6 - 81.9** | | | |

### *6.2.2 Treatment site, 119 & Midway Rd, Buena Vista*

The area just northwest of the intersection of Highway 119 and Midway Road showed large and varying alkane emissions and varying methane alkane ratios. Further investigation of the site showed emissions from tanker trucks (loading activities) along with more continuous emissions. Such activities along with the close proximity of the source to the measurement path resulting in a low plume height explains the large variability. A more confined emission estimate here would require considerably more measurements and knowledge of site activity frequencies. Figure 40 shows an alkane emission measurement of this hot spot along with a second hot spot just at the junction of Elk Hills Road and 119 (6.2.3).

Table 24 and Table 25 present the results for the emissions and the concentration ratio measurements of this source, respectively.

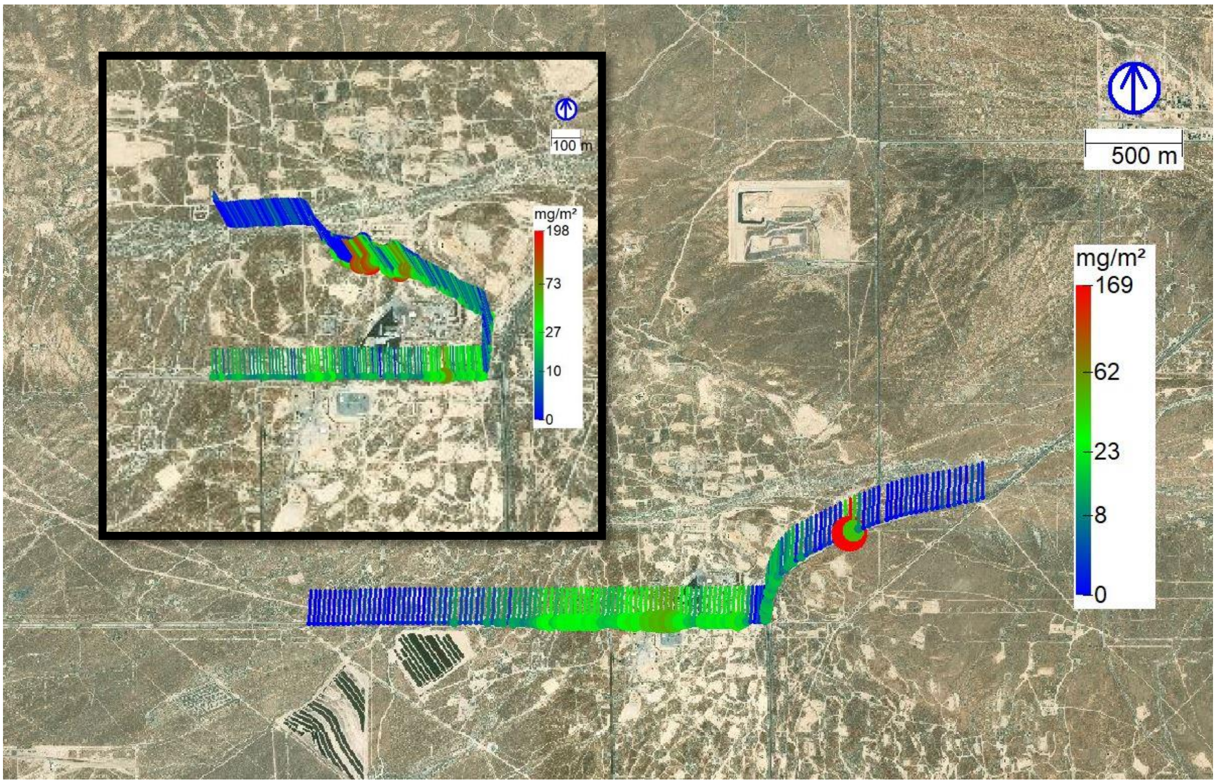

Figure 40. Alkane emission measurement along Highway 119 and Midway Road showing plumes from 2 hot spots, 27 April 2019, 12:02 – 12:26. Color scale and point size show the SOF alkane column (mg /m$^2$) and the lines point in the instantaneous wind direction. Inset: Kern Front and Poso Creek E measurement, 3 May 2019.

Table 24 Alkane emission measurements of Treatment site, Buena Vista, Highway 119 and Midway Road NW.

| Day [yymmdd] | Time span [hhmmss-hhmmss] | $N_{MEAS.}$ | Emission avg [kg/h] | Emission SD [kg/h] | Wind Speed Min-Max [m/s] | Wind Dir Span [deg] |
|---|---|---|---|---|---|---|
| **190427** | 134042-172354 | 5 | 342 | 133.9 | 3.1-5.2 | 4-356 |
| **190428** | 123540-155227 | 4 | 151 | 140.8 | 1.9-3.9 | 33-75 |
| **190430** | 112534-145932 | 2 | 95.3 | 79.6 | 1.4-3.8 | 286-351 |
| **190501** | 140112-154913 | 2 | 348 | 303.4 | 4.1-4.3 | 13-31 |
| **190505** | 155659-161325 | 3 | 349 | 144.5 | 8.5-10.0 | 248-256 |
| **190512** | 150324-165738 | 7 | 116 | 60.2 | 5.0-6.5 | 326-358 |
| **Total # of Measurements:** | | **23** | **219.9** | **161.9** | | |
| **Median** | | | **165.5** | | | |
| **IQR** | | | **96.4 - 334.1** | | | |

Table 25 Methane/Alkane ratios for the Treatment site, Buena Vista, Highway 119 and Midway Road NW.

| Day [yymmdd] | Time span [hhmmss-hhmmss] | $N_{MEAS.}$ | Mass Ratio avg [%] | Mass Ratio SD [%] | Wind Speed Min-Max [m/s] | Wind Dir Span [deg] |
|---|---|---|---|---|---|---|
| **190427** | 190642-190756 | 1 | 0.00 | N/A | 3.9-3.9 | 339-339 |
| **190428** | 123525-154500 | 3 | 576 | 747.7 | 1.9-3.7 | 33-95 |
| **190429** | 221122-222814 | 2 | 232 | 1.3 | 2.9-3.3 | 17-24 |
| **190430** | 220522-122903 | 1 | 0.00 | N/A | 0.0-0.0 | 90-90 |
| **190501** | 140309-140441 | 1 | 226 | N/A | 3.5-3.5 | 56-56 |
| **190505** | 160818-161352 | 2 | 10.5 | 0.4 | 10.0-10.0 | 228-230 |
| **190512** | 161452-165021 | 3 | 136 | 95.1 | 5.8-6.7 | 329-338 |
| **Total # of Measurements:** | | **13** | **219.2** | **378.9** | | |
| **Median** | | | **149.6** | | | |
| **IQR** | | | **10.8 - 225.9** | | | |

### 6.2.3 *Treatment site, Elk Hills Road & 119, Elk Hills*

This source, just NW of the junction of Elk Hills Road & 119 (Figure 40). was also repeatedly measured but much smaller in scope than 6.2.2. The source was only differentiable from its surroundings on two days, 28 and 30 April, and alkane emissions averaged 41 kg/h.

### 6.2.4 *Derby Acres*

The are several sources (treatment and storage) in the near vicinity (< 2 km) of Derby Acres, mostly to the north and east, but also one to the south. Most of the measurements were made downwind on Derby Acres on Highway 33, with the sources upwind. Alkane emissions varied greatly, as did the ratio measurements. The emissions are predominantly methane with a median ratio of more than 4:1 (Table 27). Based on the median alkane emission this indicates methane emissions of more than 600 kg/h.

Table 26 Alkane emission measurements of aggregated sources in the near vicinity, to the north and east of Derby Acres.

| Day [yymmdd] | Time span [hhmmss-hhmmss] | $N_{MEAS.}$ | Emission avg [kg/h] | Emission SD [kg/h] | Wind Speed Min-Max [m/s] | Wind Dir Span [deg] |
|---|---|---|---|---|---|---|
| **190428** | 134316-134655 | 1 | 218 | N/A | 2.7-2.7 | 65-65 |
| **190508** | 113011-113455 | 1 | 922 | N/A | 1.8-1.8 | 72-72 |
| **190512** | 124536-125819 | 2 | 67.5 | 9.8 | 2.8-2.9 | 351-358 |
| **Total # of Measurements:** | | **4** | **318.6** | | | |
| **Median** | | | **146.0** | **408.4** | | |
| **IQR** | | | **70.9 - 393.7** | | | |

Table 27 Methane/Alkane ratios of major sources near Derby Acres.

| Day [yymmdd] | Time span [hhmmss-hhmmss] | $N_{MEAS.}$ | Mass Ratio avg [%] | Mass Ratio SD [%] | Wind Speed Min-Max [m/s] | Wind Dir Span [deg] |
|---|---|---|---|---|---|---|
| **190428** | 125057-153721 | 4 | 2494 | 3908.1 | 2.4-3.8 | 46-108 |
| **190501** | 115851-160953 | 3 | 486 | 138.2 | 3.2-4.0 | 25-341 |
| **190508** | 102429-181611 | 5 | 665 | 738.3 | 1.7-4.3 | 34-354 |
| **190511** | 193756-194524 | 1 | 158 | N/A | 3.4-3.4 | 137-137 |
| **190512** | 125750-191251 | 3 | 242 | 228.4 | 3.4-5.1 | 342-351 |
| **190515** | 133943-163534 | 2 | 501 | 78.4 | 1.6-4.8 | 11-261 |
| **Total # of Measurements:** | | **18** | **924.8** | **1898.4** | | |
| **Median** | | | **427.2** | | | |
| **IQR** | | | **240.7 - 623.0** | | | |

### *6.2.5 Power Generation (Elk Hills Road, main facility)*

The apparent source is located just off Elk Hills road at the location of a power generating facility (Figure 41). Emissions could also emanate from the facilities directly to the west of the plant. Alkane emissions averaged just under 70 kg/h (Table 28). From the concentration ratio measurements (Figure 42), it appears that at least some of the methane sources differ from the NMVOC sources but for the site as a whole the ratios were consistent (Table 29). Methane emissions for this facility were 100 kg/h.

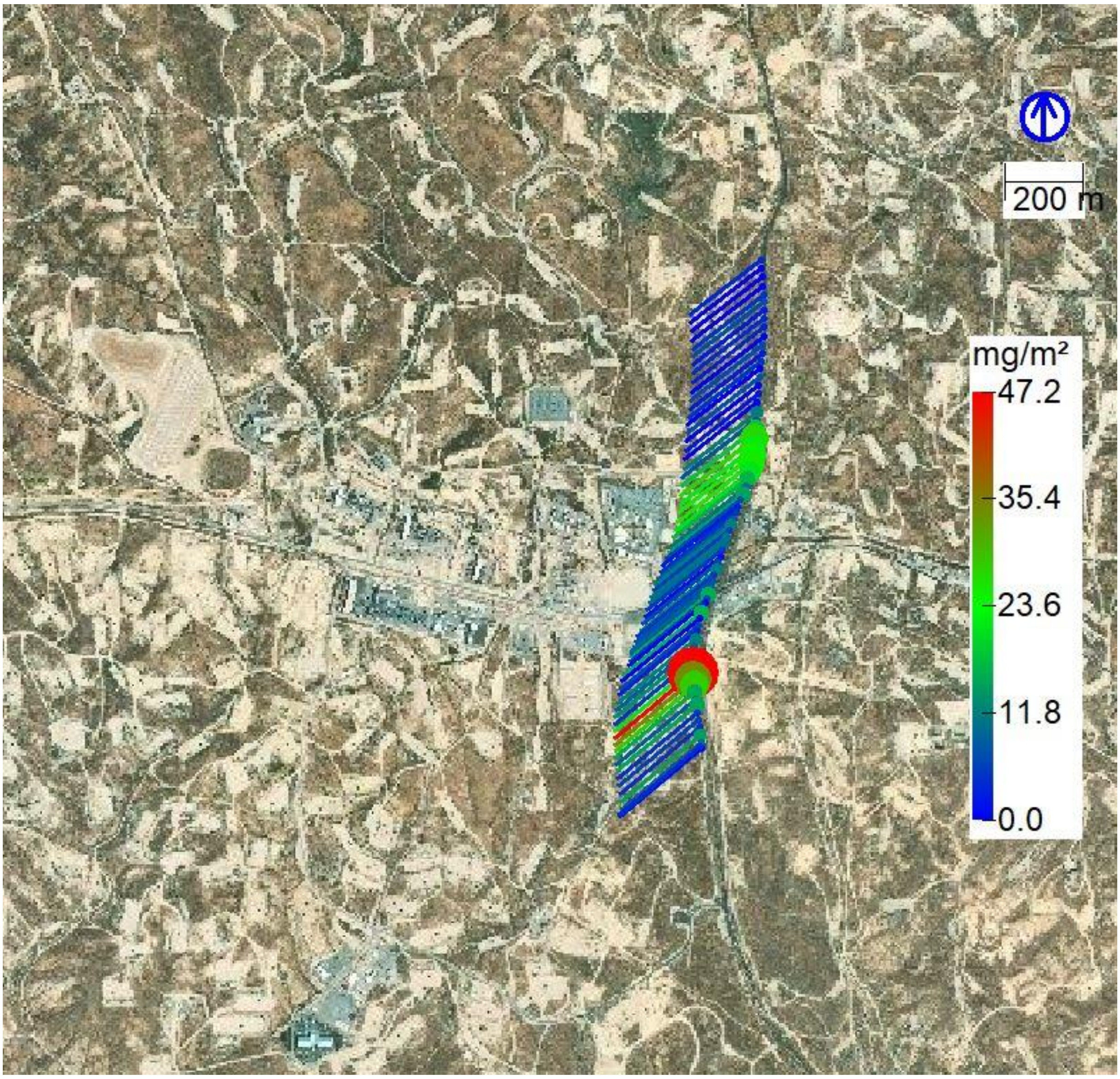

Figure 41. Alkane emission measurement of two sources near the intersection of Elk Hills Rd and Skyline Rd. 5 May 2019, 11:39 – 12:31. Color scale and point size show the SOF alkane column (mg /m$^2$) and the lines point in the instantaneous wind direction.

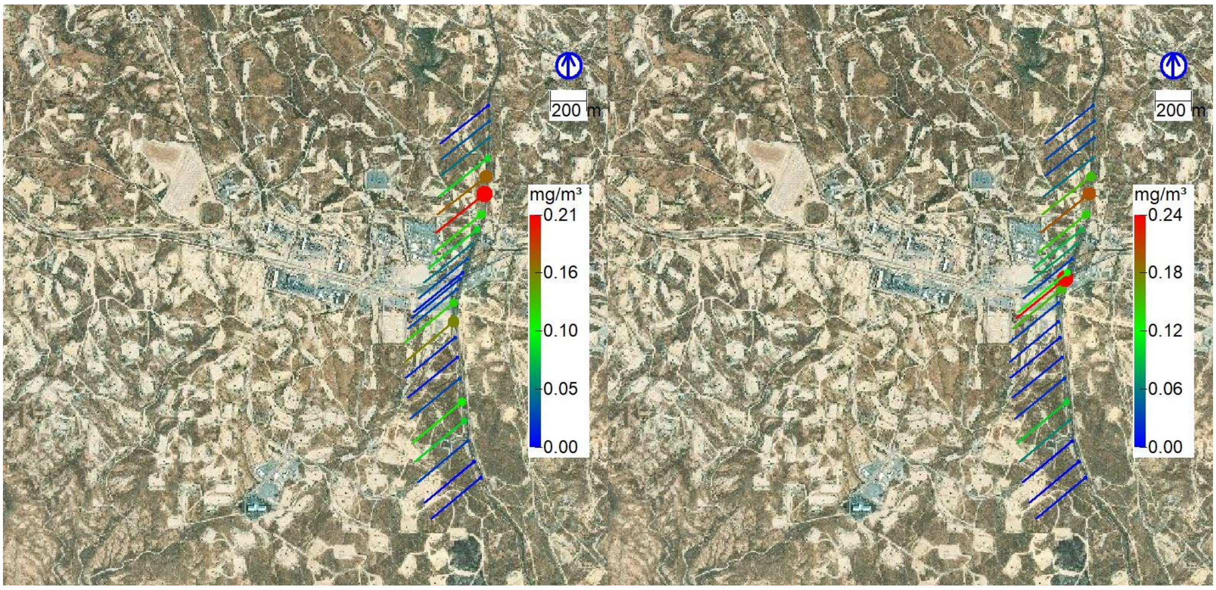

Figure 42. Ratio measurement of methane and alkane for several sources near the intersection of Elk Hills Rd and Skyline Rd. 5 May 2019, 11:39 – 12:31. Color scale and point size show methane (left) and alkane (right) concentrations (mg/m$^3$) and the lines point in the instantaneous wind direction. NB Color scale is logarithmic. The average integrated mass ratio between CH$_4$ and alkanes was 1:1.

Table 28 Alkane emission measurements of power generating facility on Elk Hills Rd.

| Day [yymmdd] | Time span [hhmmss-hhmmss] | $N_{MEAS.}$ | Emission avg [kg/h] | Emission SD [kg/h] | Wind Speed Min-Max [m/s] | Wind Dir Span [deg] |
|---|---|---|---|---|---|---|
| **190505** | 163127-164126 | 3 | 68.7 | 11.7 | 8.6-10.8 | 227-231 |
| **Total # of Measurements:** | | **3** | | | | |
| **Median** | | | **73.5** | | | |
| **IQR** | | | **64.4 - 75.4** | | | |
| **Mean** | | | **68.7** | | | |
| **SD** | | | **11.7** | | | |

Table 29 Methane/Alkane ratios of power generating facility on Elk Hills Rd.

| Day [yymmdd] | Time span [hhmmss-hhmmss] | $N_{MEAS.}$ | Mass Ratio avg [%] | Mass Ratio SD [%] | Wind Speed Min-Max [m/s] | Wind Dir Span [deg] |
|---|---|---|---|---|---|---|
| **190429** | 212335-224851 | 2 | 148 | 15.6 | 3.5-3.8 | 24-32 |
| **Total # of Measurements:** | | **2** | | | | |
| **Median** | | | **147.7** | | | |
| **IQR** | | | **142.2 - 153.2** | | | |
| **Mean** | | | **147.7** | | | |
| **SD** | | | **15.6** | | | |

### *6.2.6 Treatment site (Elk Hills Rd / SkyLine Rd)*

There are two facilities close to the power generation in 6.2.5 separated by Skyline Road with this source likely south of Skyline Road. Again only 3 measurements were made but there was a distinct plume separate from the main facility plume (Figure 41 section 6.2.6). Figure 42(section 6.2.6) shows distinct alkane and methane plumes south of Skyline so there may be no methane emissions directly associated with the measured alkane emissions.

Table 30 Alkane emission measurements of sources southwest of the intersection Elk Hills Rd and Skyline Rd.

| Day [yymmdd] | Time span [hhmmss-hhmmss] | $N_{MEAS.}$ | Emission avg [kg/h] | Emission SD [kg/h] | Wind Speed Min-Max [m/s] | Wind Dir Span [deg] |
|---|---|---|---|---|---|---|
| **190505** | 163049-163938 | 3 | 58.2 | 15.4 | 8.8-10.6 | 228-230 |
| **Total # of Measurements:** | | **3** | | | | |
| **Median** | | | **54.8** | | | |
| **IQR** | | | **49.7 - 64.9** | | | |
| **Mean** | | | **58.2** | | | |
| **SD** | | | **15.4** | | | |

### *6.2.7 Alon Refinery, Bakersfield*

Alkane emissions from the Alon Refinery were measured on two days, 3 May and 18 May 2019. Since the refinery is essentially downwind of oil fields in all directions box measurements were always made. An example is show in Figure 43. Alkane emissions averaged 35 kg/h (Table 31).

Figure 43 Alkane emission measurement of the Alon Refinery, Bakersfield 18 May 2019, 8:00 A.M.

Table 31 Alkane emission measurements of the Alon refinery.

| Day [yymmdd] | Time span [hhmmss-hhmmss] | $N_{MEAS.}$ | Emission avg [kg/h] | Emission SD [kg/h] | Wind Speed Min-Max [m/s] | Wind Dir Span [deg] |
|---|---|---|---|---|---|---|
| **190503** | 162145-163428 | 1 | 41.3 | N/A | 4.3-4.3 | 301-301 |
| **190518** | 080217-095042 | 5 | 34.8 | 10.6 | 1.7-2.1 | 108-216 |
| **Total # of Measurements:** | | **6** | | | | |
| **Median** | | | **37.7** | | | |
| **IQR** | | | **29.6 - 40.9** | | | |
| **Mean** | | | **35.8** | | | |
| **SD** | | | **9.8** | | | |

## 6.3 Community monitoring

One of the objectives in the campaign was to investigate the impacts of various emission sources on Community Scale Air Quality Levels, with special focus on Disadvantaged Communities. This was partly done to assist in and complement current and future community monitoring efforts by CARB. Table 32 shows the measurements locations and dates for community monitoring.

Owing to the time required for emission measurements, there were relatively few dedicated community monitoring measurements. As such these measurements can only be used as an initial indication of possible impacts and all sites require repeated revisits to create reliable statistics over the long-term. Due to the limited number of measurements, gridded concentration maps such as those in *Sub Report A* of this study, cannot be compiled at this time. Concentration maps for each community are presented based on single measurements under their respective sub-sections. It is also important to remember that values presented here are enhancement over background and in many of these communities, background values are strongly influenced by oil fields. This may be particularly relevant for Lost Hills where ‘clean’ background concentrations i.e. upwind of the oil field, were not available.

Methane concentrations, as expected, were high in many of the communities but not accompanied by high concentrations of alkanes or BTEX. In all cases benzene concentrations averaged below detection limits (1 ppb). On occasion benzene could be higher than 1 ppb and occasional plumes of BTEX were observed although seldom with positively identified sources.

Table 32. Summary of all days with community monitoring.

| **Area** | **Date (2019)** |
|---|---|
| Highland Knolls and Meadow view, Bakersfield | 2 May, 17 May |
| Derby Acres | 12 May |
| Lost Hills | 14 May |
| Alon refinery and adjacent communities Quailwood and Park Stockdale | 18 May |
| Port of Stockton | 26 and 27 May |
| Covanta Stanislaus in Patterson | 27 May, unfavorable wind |

### 6.3.1 *Highland Knolls and Meadow View*

These two communities are located on the northeast edge of Bakersfield near Meadows Field airport, in close proximity to the Kern Front and Kern River oil fields and a number of small refineries and other petroleum and gas treatment facilities. Targeted concentration measurements were made on two evenings with northeasterly winds at times when plumes should have been originating from the oil and gas fields, and occasionally while conducting measurements of Kern Front and Kern River. In the evening the measured methane concentrations could be high, up to 7.3 mg/m$^3$ (11 ppm), however, no large plumes of alkane VOCs were observed (Figure 44 and Figure 46). Figure 45 and Figure 47 show BTEX measurements for the same date and time frames. Benzene concentrations are below or near detection limits for both dates, however some plumes of total BTEX were seen. These plumes did not appear to be associated with methane or VOC plumes from the oil fields. One in particular, seen in Figure 45 (Left) at the intersection of Norris Road and Wells Ave, could not be associated with a particular source. There are commercial enterprises (Vape shop) at this location and one block away upwind is a gas station. The field cannot be ruled out as a source either, since the plume may have been transient in nature. In Figure 47, from the larger view two vehicular or commercial sources can be seen, as well as one source northeast of Highland Knolls. In the zoomed perspective (Figure 47, right) the plume also suggests a residential source rather than a source from the oil fields or facilities.

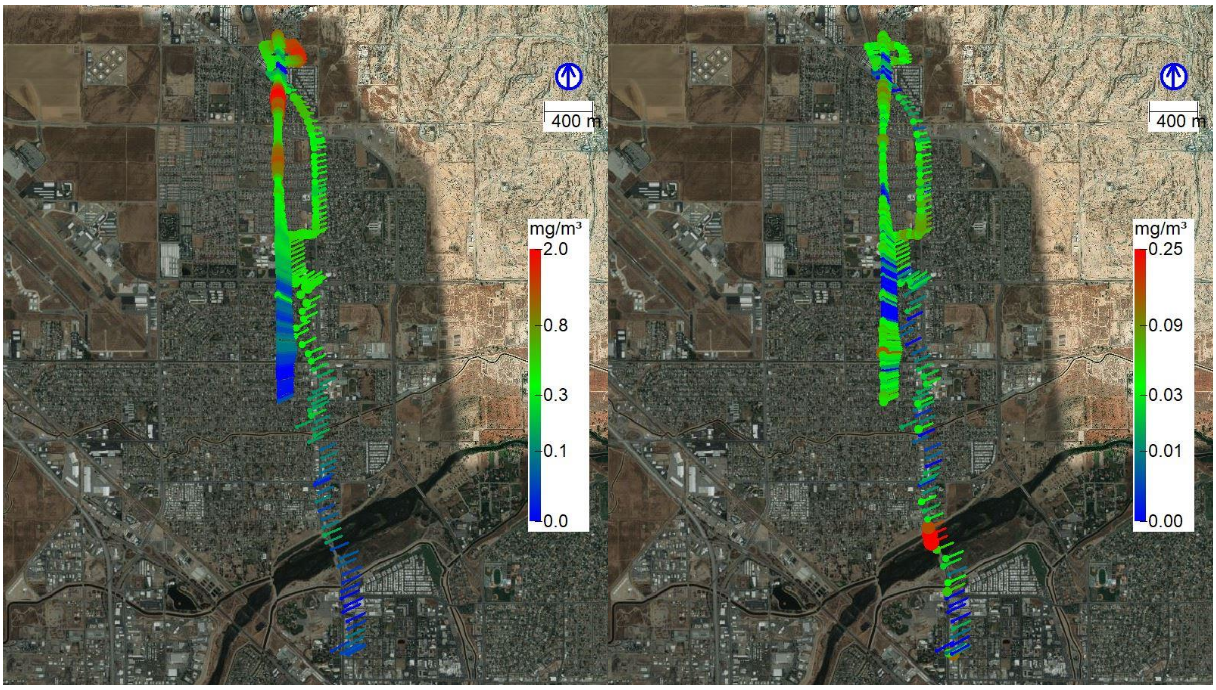

Figure 44. Methane and alkane mobile concentration measurements for community monitoring in the Bakersfield communities of Highland Knolls and Meadow View, 2 May 2019, 22:38 – 23:18. Color scale and point size show methane (left) and alkane (right) concentrations (mg/m$^3$) and the lines point in the instantaneous wind direction. NB Color scale is logarithmic.

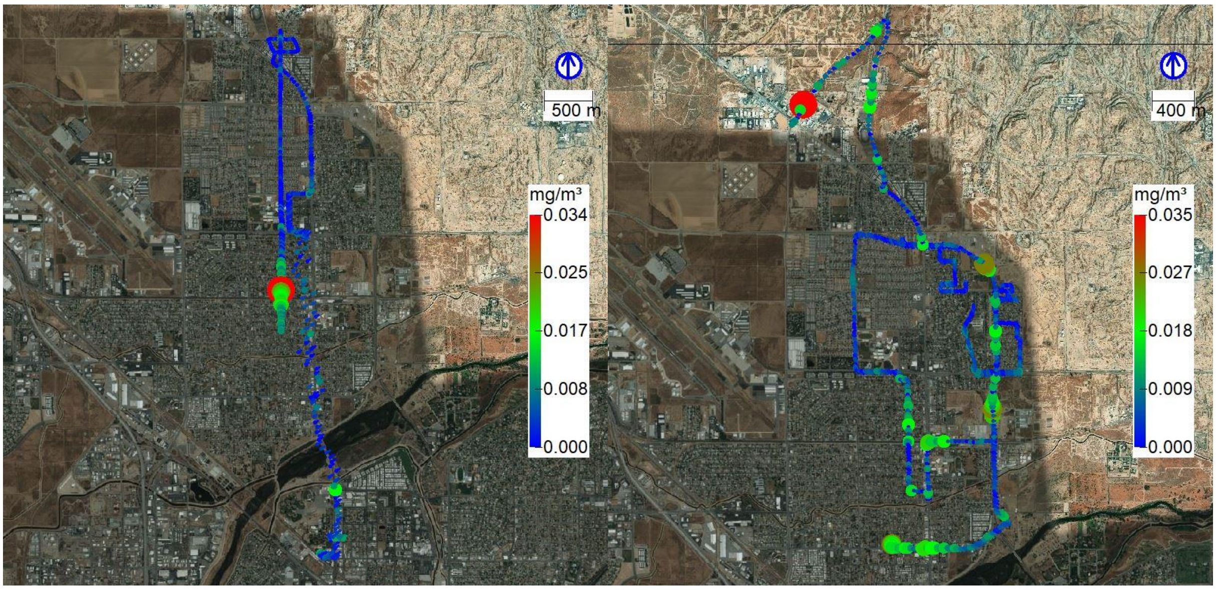

Figure 45. BTEX concentration measurements for community monitoring in the Bakersfield communities of Highland Knolls and Meadow View, 2 May 2019, 22:33 – 23:18 (Left) and 23:31 – 3 May 00:39 (Right). Color scale and point size show BTEX concentrations (mg/m$^3$) and the lines point in the instantaneous wind direction.

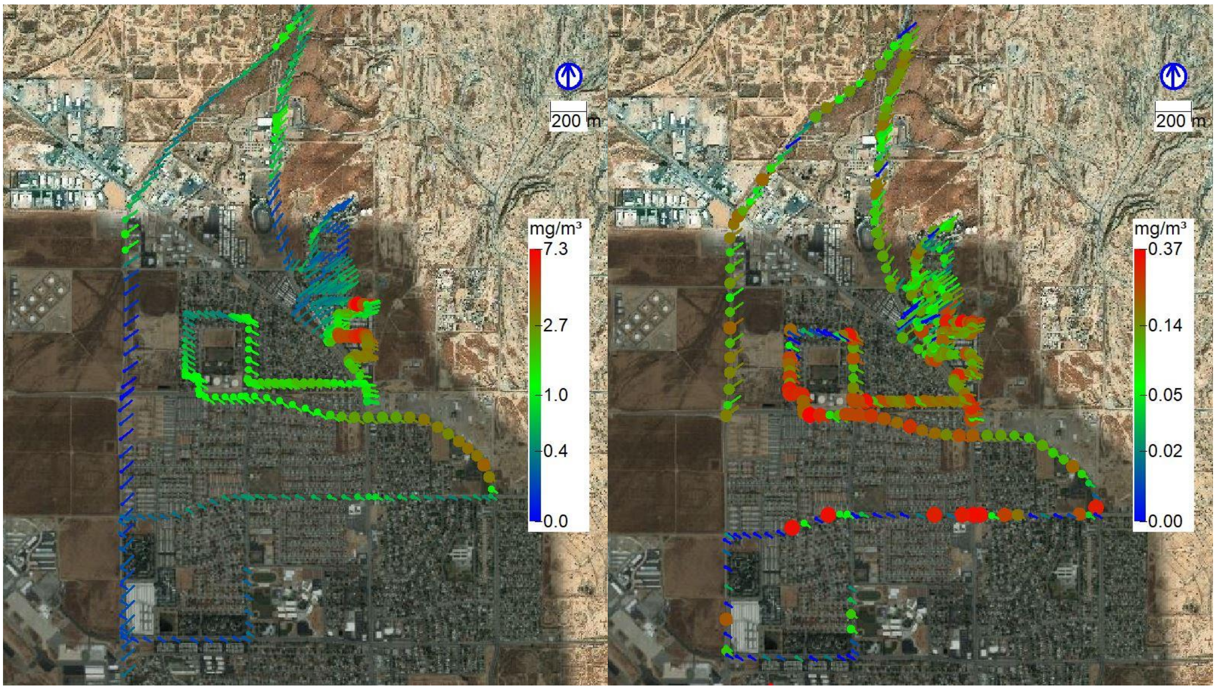

Figure 46. Methane and alkane concentration measurements for community monitoring in the Bakersfield communities of Highland Knolls and Meadow View, 17 May 2019, 21:56 – 23:00. Color scale and point size show methane (left) and alkane (right) concentrations (mg/m$^3$) and the lines point in the instantaneous wind direction. NB Color scale is logarithmic.

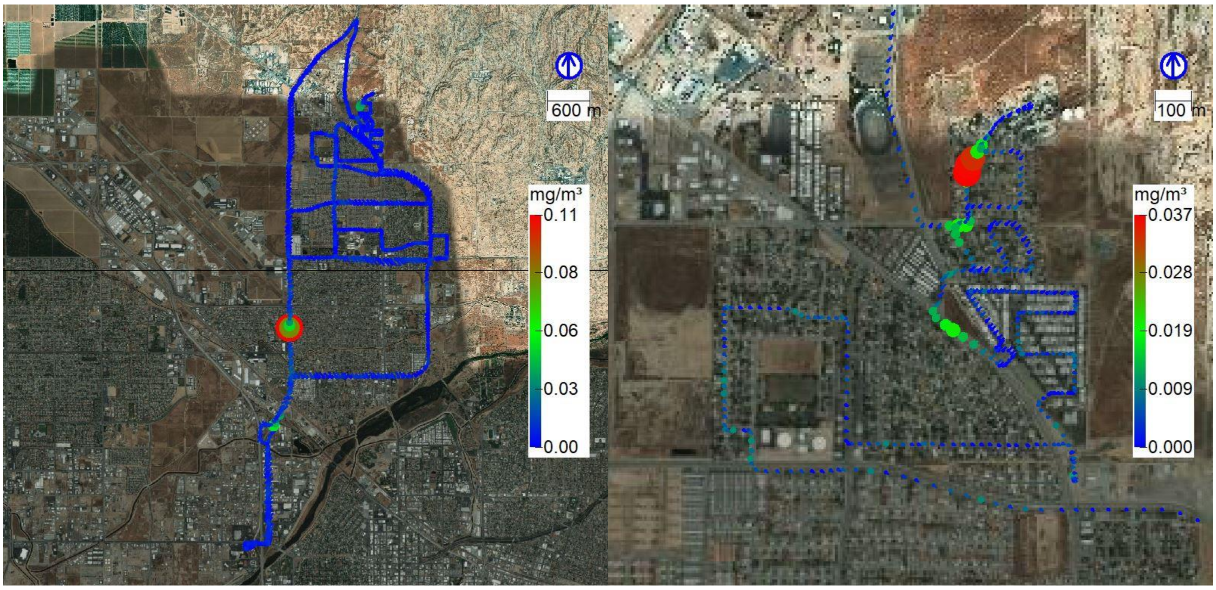

Figure 47. BTEX concentration measurements for community monitoring in the Bakersfield communities of Highland Knolls and Meadow View, 17 May 2019, 21:44 – 23:55. Color scale and point size show BTEX concentrations (mg/m$^3$) and the lines point in the instantaneous wind direction. (Left) Traverse from Central Bakersfield. (Right) Highland Knolls area magnified.

### *6.3.2 Derby Acres*

Derby Acres is located along Hwy 33 north of Taft, between the Midway-Sunset and Elk Hills fields. It was often downwind of several point sources on the hills just to the northeast, see Section 6.2. In contrast to Highland Knolls and Meadow View the measurements were made solely during the day and were conducted more on the outskirts of the residential area. The major part of the emissions is methane, as was noted in Section 6.2, so high VOC concentrations were not expected, and this can be seen in Figure 48.

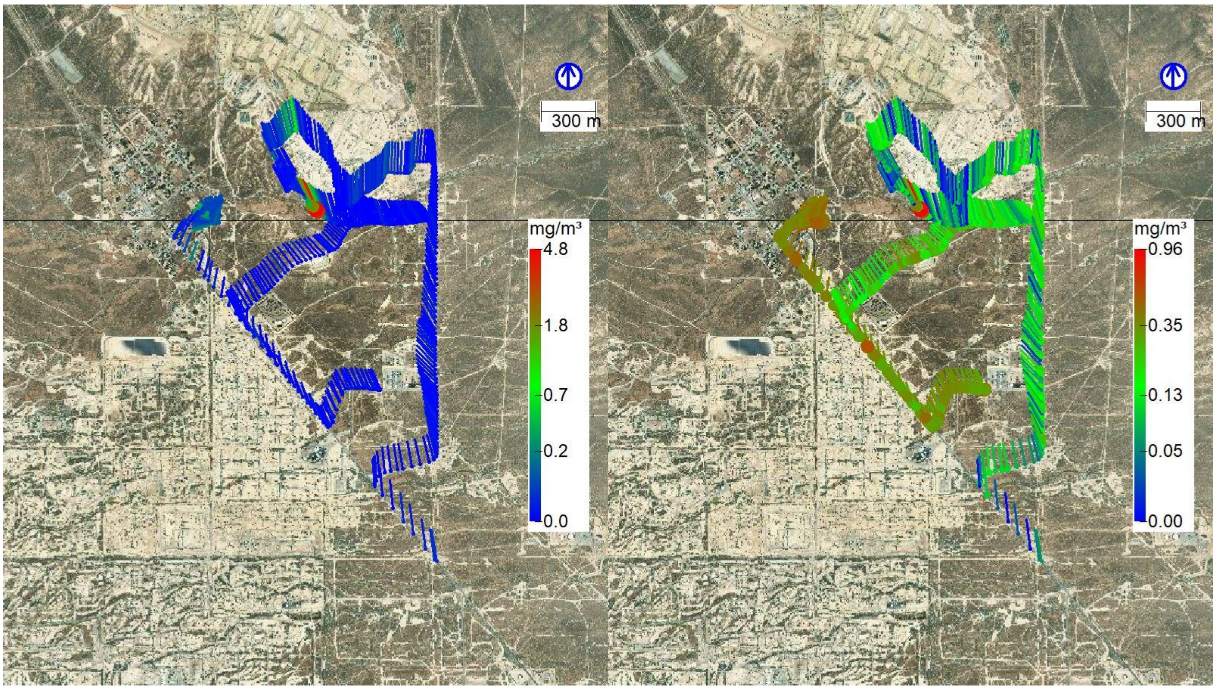

Figure 48. Methane and alkane concentration measurements of in and around Derby Acres, 12 May 2019, 12:35 – 14:01. Color scale and point size show methane (left) and alkane (right) concentrations (mg/m$^3$) and the lines point in the instantaneous wind direction. NB Color scale is logarithmic.

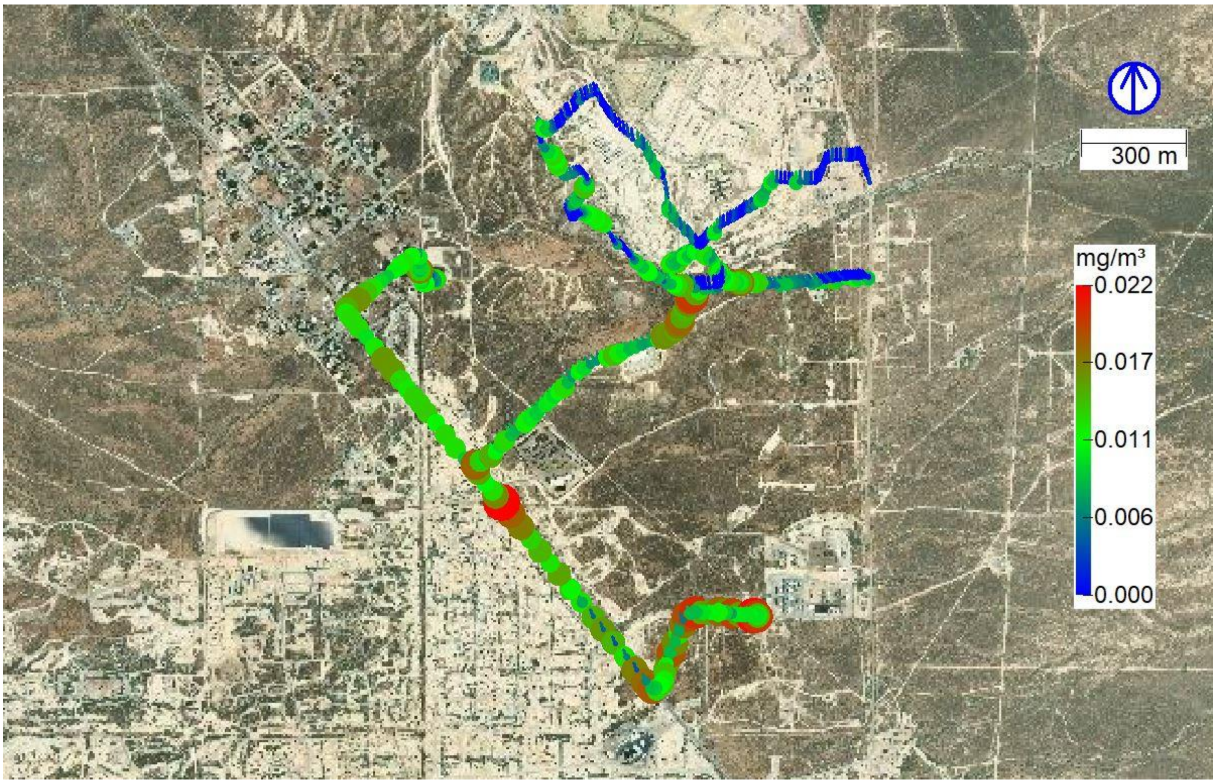

Figure 49. BTEX concentration measurements of in and around Derby Acres, 12 May 2019, 12:35 – 14:01. Color scale and point size show BTEX concentrations (mg/m$^3$) and the lines point in the instantaneous wind direction.

### *6.3.3 Lost Hills*

Lost Hills is situated just at the eastern edge of the Lost Hills field essentially between Lost Hills 1 and 2 (north and south of Hwy 46). Westerly winds should bring oil field plumes in over the community. One treatment facility is located to the southwest at a distance of approximately 1 km from the edge of the residential area. Measurements were made on one evening with westerly winds. No significant plumes of methane or VOCs were observed within the residential areas. However, alkane VOCs were enhanced relative to methane near the waterway (Figure 50).

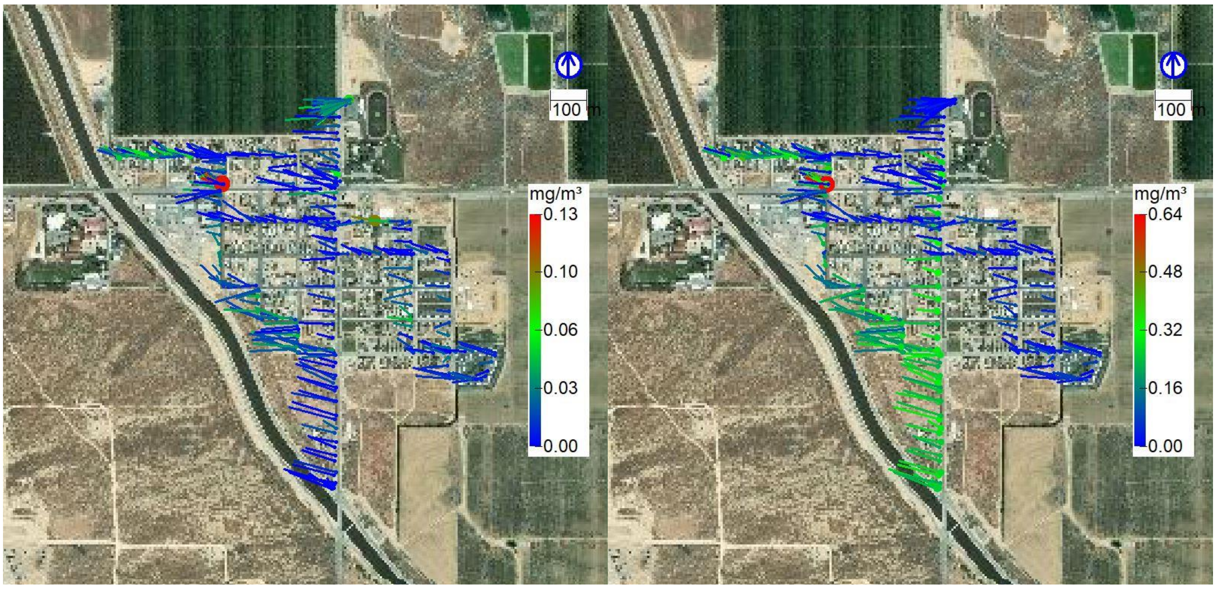

Figure 50. Methane and alkane concentration measurements in Lost Hills, 12 May 2019, 12:35 – 14:01. Color scale and point size show methane (left) and alkane (right) concentrations (mg/m$^3$) and the lines point in the instantaneous wind direction.

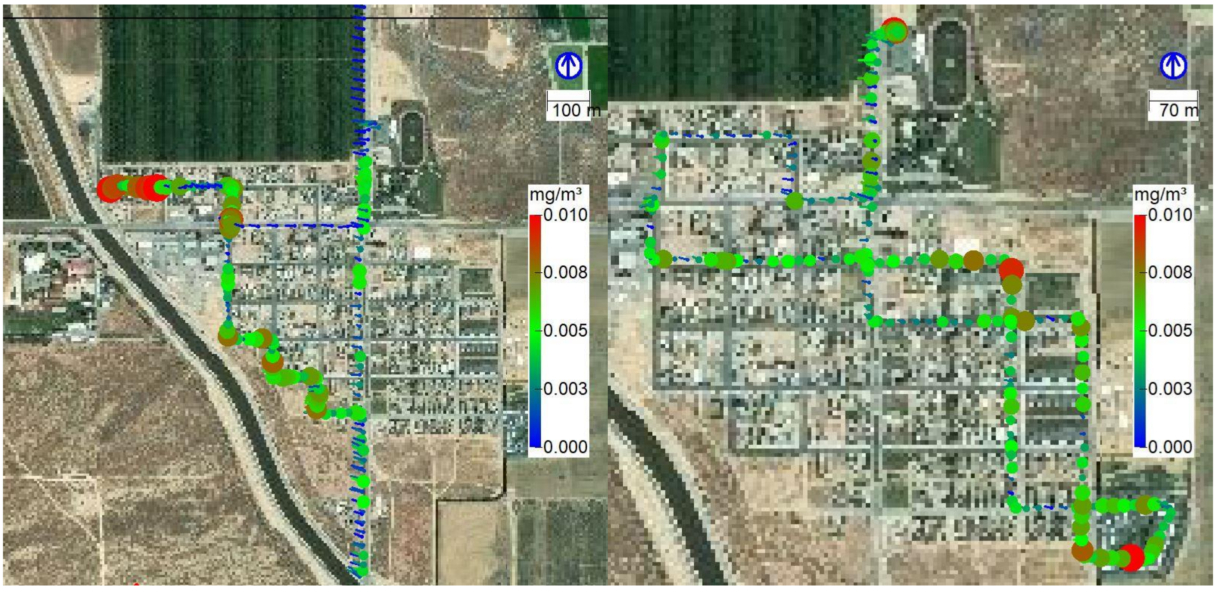

Figure 51. BTEX concentration measurements for community monitoring in Lost Hills, 2 May 2019, 21:55 – 22:42 (Left) and 22:55 – 23:21 (Right). Color scale and point size show BTEX concentrations (mg/m$^3$) and the lines point in the instantaneous wind direction.

### *6.3.4 Port of Stockton Area*

Community monitoring and alkane emission measurements of the Port of Stockton Area were conducted on 26-27 May, 2019. Alkane and ethanol emissions were measured with SOF on both days. Total NMVOC emissions averaged 125 kg/h with approximately 50 kg/h from the ethanol facility. The high levels of ethanol in the plume add some extra uncertainty to these emissions, but for comparison, the measurements at Port of Stockton in the October 2018 survey showed an average alkane emission of 84 kg/h and ethanol 48 kg/h. Ethanol and methane dominate ground level concentrations of VOCs (Figure 52) and the both plumes can easily be traced from the facility to the east end of the port area. There was a residential hotspot of BTEX on the 26 May 2019 (Figure 53).

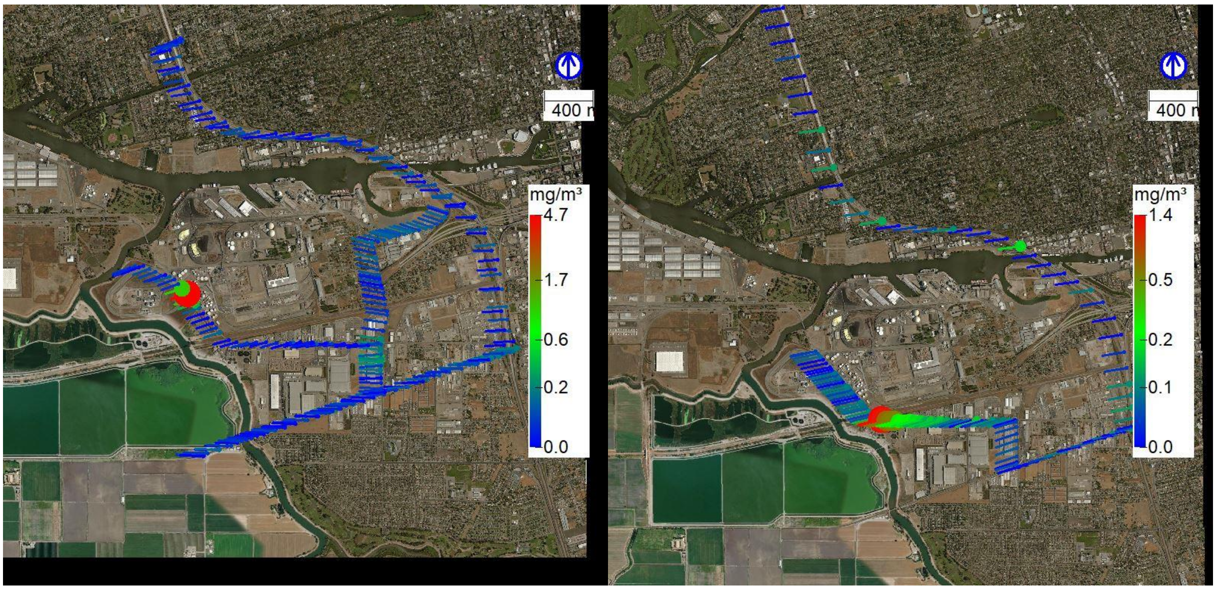

Figure 52. Mobile concentration measurements around the Port of Stockton, 26 May 2019. Color scale and point size show ethanol (left, 17:44 – 18:35) and methane (right, 20:17 – 20:43) concentrations (mg/m$^3$) and the lines point in the instantaneous wind direction. NB Color scale is logarithmic.

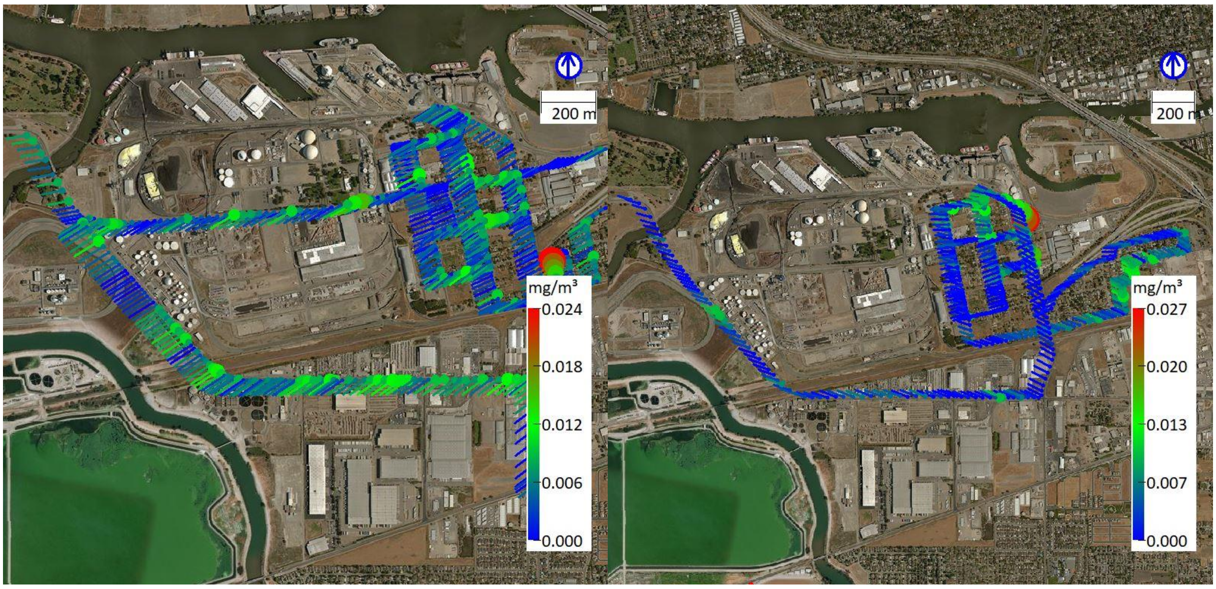

Figure 53. BTEX concentration measurements in and around the Port of Stockton, 26 May 2019, 19:03 – 20:30 (Left) and 27 May 2019, 11:26 – 12:15 (Right). Color scale and point size show BTEX concentrations (mg/m$^3$) and the lines point in the instantaneous wind direction.

### 6.3.5 *Quailwood and Park Stockdale (Bakersfield)*

These two communities are located S-SE of the Alon refinery in Bakersfield, and confined by the Westside Pkwy, Stockdale Hwy and California Ave. Measurements were done on the afternoon of May 18, 2019, with weak NW winds (Figure 54). Insignificant or low concentration enhancements of benzene and BTEX were measured along the refinery fenceline and within the communities, but for an intermittent hot spot near the crossing of California Ave and Real Rd. This plume was likely associated with activity at a nearby gas station or heavy traffic in the road crossing.

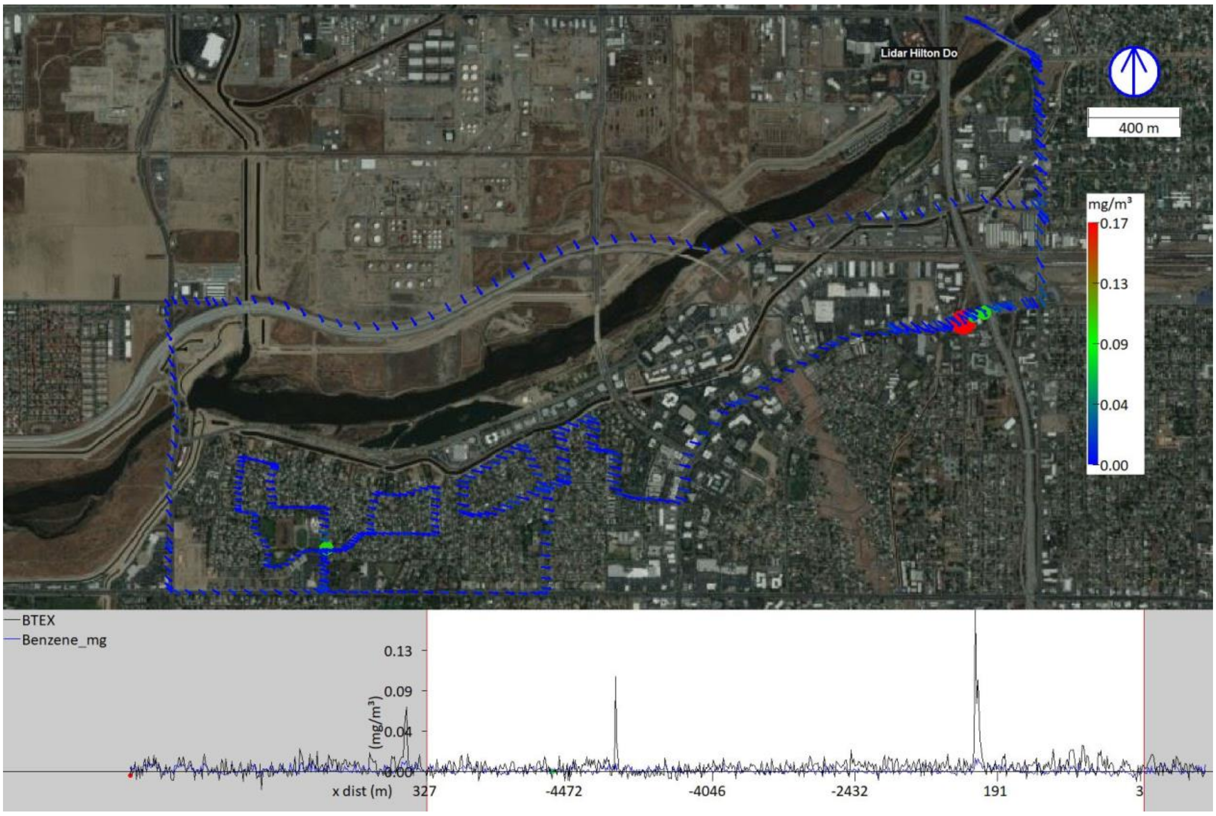

Figure 54. BTEX concentration measurements for community monitoring in the Bakersfield communities of Quailwood and Park Stockdale, 18 May 2019, 13:50 – 14:50. Color scale and point size show BTEX concentrations (mg/m$^3$) and the lines point in the instantaneous wind direction. Benzene concentration is shown in the lower plot as a blue line and total BTEX concentration as a black line.

## Discussion and Conclusions

### 6.4 NMVOC and Methane Emissions

The current study is one of largest diffuse NMVOC emission measurement surveys to date. The area surveyed in this report represents a significant portion of the oil and gas production in California as noted in Section 5.1. Cumulative emissions for the fields, wholly or partially measured, amount to 7600 kg/h NMVOCs and 8000 kg/h methane. Reliable measurements for comparison to the measured NMVOC emissions at this scale are scarce. However, some methane measurements on this scale have been made. The Jet Propulsion Laboratory (JPL) recently made plume measurements of methane sources in California available on-line (URL https://methane.jpl.nasa.gov/, 13 Dec 2019). Though these represent only measurable plumes and not the sum of all diffuse emissions, the total emissions of the sources in the oil and gas sector in Kern County plus two energy sector sources within the survey area (Figure 55) was 10000 kg/h methane. Scientific Aviation, in measurements conducted on 8 May 2019 concurrently with this study, measured methane emissions from the Elk Hills and Cymric and McKittrick fields of 6100 kg/h and 3000 kg/h, respectively. Emissions measured in this study on those days were 4700 kg/h from Elk Hills and 1400 kg/h from Cymric and McKittrick. For the airborne measurements some discrepancy is expected due to uncertainty in field boundaries and possibly not measuring identical areas. Uncertainty is also induced in this study in methane emissions by measuring concentration ratios at the fenceline over these very large areas.

One can also to compare with estimated emission inventories. Total methane emissions as reported in the latest greenhouse gas emissions inventory summary from CARB (2000 – 2017, Last Updated: 11/06/2019) from the industrial oil & gas production and processing sector was 8800 kg/h, of which Kern County and the survey area should account for about 70% of this or around 6200 kg/h, if scaled directly to oil and gas production figures.

Table 33 presents the most recent production data from the fields within the survey area and estimated emissions based on standard emissions factors for Oil & Gas Production as a whole. This is a less rigorous methodology than the CARB data (does not include number of wells, for example) but it is applied to field level data. Based on the emission factors from IPCC, methane emissions for the survey area are projected to be 4600 kg/h. While methane emissions appear to be underestimated from a reporting standpoint to available measurements, measured NMVOC emissions from the area are an order of magnitude higher.

Figure 55. JPL measured methane plumes within the current survey area. Source: Methane Source Finder (https://methane.jpl.nasa.gov/, 13 Dec 2019).

Table 33. 2018 Production and Calculated Emissions derived from standard emission factors, Kern County Oil and Gas Fields. Emission factor sources: *EMEP/EEA air pollutant emission inventory guidebook 2019. **IPCC (Picard, David. 2019. "Fugitive Emissions from Oil and Natural Gas Activities" in *Good Practice Guidance and Uncertainty Management in National Greenhouse Gas Inventories*)

| | Production | | | Calculated Emissions | | | | | |
|---|---|---|---|---|---|---|---|---|---|
| | Oil and Cond. ($10^6$ $m^3$) | Gas ($10^6$ $m^3$) | Ratio $CH_4$: NMVOC | NMVOC (kg/h)* | | | $CH_4$ (kg/h)** | | |
| | | | Vol/Vol Normal TP | Oil | Gas | Total | Oil | Gas | Tot |
| Asphalto | 0.03 | 126.8 | 7.2 | 0.5 | 1.4 | 2.0 | 5 | 36 | 41 |
| Belridge, North | 0.28 | 64.7 | 0.3 | 5.6 | 0.7 | 6.3 | 58 | 18 | 76 |
| Belridge, South | 3.33 | 230.0 | 0.1 | 66.3 | 2.6 | 68.9 | 683 | 65 | 749 |
| Buena Vista | 0.21 | 408.0 | 3.0 | 4.1 | 4.7 | 8.8 | 42 | 116 | 158 |
| Coles Levee, North | 0.01 | 2.9 | 0.3 | 0.3 | 0.0 | 0.3 | 3 | 1 | 4 |
| Coles Levee, South | 0.01 | 13.2 | 2.4 | 0.2 | 0.2 | 0.3 | 2 | 4 | 5 |
| Cymric | 2.06 | 67.3 | 0.0 | 41.1 | 0.8 | 41.9 | 424 | 19 | 443 |
| Elk Hills | 1.36 | 2526 | 2.8 | 27.1 | 28.8 | 56.0 | 280 | 718 | 998 |
| Kern Bluff | 0.01 | 0.0 | 0.0 | 0.1 | 0.0 | 0.1 | 1 | 0 | 1 |
| Kern Front | 0.55 | 1.8 | 0.0 | 11.0 | 0.0 | 11.0 | 113 | 1 | 114 |
| Kern River | 2.61 | 12.9 | 0.0 | 51.9 | 0.1 | 52.1 | 535 | 4 | 539 |
| Lost Hills | 1.54 | 146.6 | 0.1 | 30.6 | 1.7 | 32.3 | 316 | 42 | 357 |
| McKittrick | 0.42 | 31.1 | 0.1 | 8.3 | 0.4 | 8.7 | 86 | 9 | 94 |
| Midway-Sunset | 3.28 | 121.7 | 0.1 | 65.5 | 1.4 | 66.8 | 675 | 35 | 709 |
| Mount Poso | 0.26 | 1.0 | 0.0 | 5.1 | 0.0 | 5.1 | 53 | 0 | 53 |
| Poso Creek | 0.82 | 26.1 | 0.0 | 16.3 | 0.3 | 16.6 | 168 | 7 | 175 |
| Round Mountain | 0.41 | 8.1 | 0.0 | 8.1 | 0.1 | 8.2 | 84 | 2 | 86 |
| **Sum** | **17.2** | **3788.1** | 0.3 | **342.1** | **43.2** | **385.3** | **3527** | **1077** | **4604** |

## 6.5 Community Monitoring and BTEX emissions

As was noted in Section 6.3, concentration mapping measurements did not turn up high levels of BTEX in general or benzene in particular. Exceptions to this were when measuring very close to some of the large point or other distinct VOC sources. Within the communities no suspect field or facility plumes were observed with higher than detectable levels of benzene.

# 7 Acknowledgements

This Report was submitted in fulfilment of 17RD021 "Characterization of Air Toxics and GHG Emission Sources and their Impacts on Community -Scale Air Quality Levels in Disadvantaged Communities" By FluxSense Inc under the sponsorship of the California Air Resources Board. Work was completed as of 13 December 2019.

# 8 References

Bogumil K., et al, 2003. Measurements of molecular absorption spectra with the SCIAMACHY pre-flight model: instrument characterization and reference data for atmospheric remote-sensing in the 230-2380 nm region, *Journal of Photochemistry and Photobiology A: Chemistry*, 157(2-3):167-184 5/5, 2003.

Burrows J.P., A. Richter, A. Dehn, B. Deters, S. Himmelmann, S. Voigt, and J. Orphal, 1999. "Atmospheric remote-sensing reference data from GOME: Part 2. Temperature-dependent absorption cross-sections of $O_3$ in the 231-794 nm range," J. Quant. Spectrosc. Radiat. Transfer 61, 509-517, 1999.

Börjesson, G., Samuelsson, J., Chanton, J., Adolfsson, R., Galle, B., Svensson, B.H., 2009. A national landfill methane budget for Sweden based on field measurements, and an evaluation of IPCC models.Tellus B, 61, 424–435.

DOGGR, 2016. Division of Oil, Gas & Geothermal Resources, at Department of Conservation, CA. http://maps.conservation.ca.gov/doggr/#close .

DOGGR, 2019, Division of Oil, Gas & Geothermal Resources, at Department of Conservation, CA https://maps.conservation.ca.gov/doggr/wellfinder

Downey N., Emery C., Jung J., Sakulyanontvittaya T., Hebert L., Blewitt D., Yarwood G., 2015. Emission reductions and urban ozone responses under more stringent US standards. Atmospheric Environment, 101, pp 209-216, 2015.

Environmental Research & Education Foundation (EREF), 2011. Field comparison of methods for assessment of fugitive emissions from landfills. Available at https://erefdn.org/wp-content/uploads/2015/12/FugitiveEmissions_FinalReport.pdf

Etzkorn T., B. Klotz, S. Sørensen, I.V. Patroescu, I. Barnes, K.H. Becker, and U. Platt, 1999. "Gas-phase absorption cross sections of 24 monocyclic aromatic hydrocarbons in the UV and IR spectral ranges," Atmos. Environ. 33, 525-540, 1999.

European Commission, 2015, Best Available Techniques (BAT) Reference Document for the Refining of Mineral Oil and Gas: Joint Research Centre, Institute for Prospective Technological Studies, ISBN 978-92-79-46198-9 (PDF)ISSN 1831-9424 (online)doi:10.2791/010758, http://eippcb.jrc.ec.europa.eu/reference/BREF/REF_BREF_2015.pdf

Fally S., M. Carleer, and A. C. Vandaele, "UV Fourier transform absorption cross sections of benzene, toluene, meta-, ortho-, and para-xylene," J. Quant. Spectrosc. Radiat. Transfer 110, 766-782, 2009.

Galle, B., J. Samuelsson, B.H. Svensson, G. Börjesson, "Measurements of methane emissions from landfills using a time correlation tracer method based on FTIR absorption spectroscopy." Environ. Sci. Technol. 35: 21–25. 2001.

Griffith D.W.T., Synthetic calibration and quantitative analysis of gas-phase FT-IR spectra. Applied Spectroscopy, 1996. 50(1): p. 59-70.

Johansson, J., et al., 2013a, Quantitative Measurements and Modeling of Industrial Formaldehyde Emissions in the Greater Houston Area during Campaigns in 2009 and 2011, Journal of Geophysical Research – Atmospheres, 2013JD020159R.

Johansson, J., Mellqvist, J., et al., 2013b. Quantification of industrial emissions of VOCs, $NO_2$ and $SO_2$ by SOF and Mobile DOAS during DISCOVER-AQ, AQRP project 13-0051, AQRP report, Dec 7 2013.

Johansson, J. K. E., J. Mellqvist, J. Samuelsson, B. Offerle, B. Lefer, B. Rappenglück, J. Flynn, and G. Yarwood, 2014. Emission measurements of alkenes, alkanes, $SO_2$, and $NO_2$ from stationary sources in Southeast Texas over a 5 year period using SOF and mobile DOAS, Journal of Geophysical Research, 118, doi:10.1002/2013JD020485.

Kihlman, M., 2005a. Application of solar FTIR spectroscopy for quantifying gas emissions, Technical report No. 4L, ISSN 1652-9103, Department of Radio and Space Science, Chalmers University of Technology, Gothenburg, Sweden.

Kihlman, M., J. Mellqvist, and J. Samuelsson (2005b), Monitoring of VOC emissions from three refineries in Sweden and the Oil harbor of Göteborg using the Solar Occultation Flux method, Technical report, ISSN 1653 333X, Department of Radio and Space, Chalmers University of Technology, Gothenburg, Sweden.

Maul J., James & J. Ostrowski, Philip & A. Ublacker, Gregg & Linclau, Bruno & P. Curran, Dennis. (2008). Benzotrifluoride and Derivatives: Useful Solvents for Organic Synthesis and Fluorous Synthesis. 10.1007/3-540-48664-X_4.

Mellqvist, J., et al. (2013a), Pilot study to quantify industrial emissions of VOCs, $NO_2$ and $SO_2$ by SOF and mobile DOAS in the Bay Area, Fluxsense AB, 2013.

Mellqvist, J., et al. (2013b), Pilot study to quantify industrial emissions of VOCs, $NO_2$ and $SO_2$ by SOF and mobile DOAS in the Carson Area, Fluxsense AB, 2013.

Mellqvist, J.  (1999), Application of infrared and UV-visible remote sensing techniques for studying the stratosphere and for estimating anthropogenic emissions, doktorsavhandling, Chalmers tekniska högskola, Göteborg, Sweden, 1999.

Mellqvist, J., Johansson J., Samuelsson J. And Offerle B. (2008a), Emission Measurements of Volatile Organic Compounds with the SOF method in Normandy 2008. available at www.fluxsense.se

Mellqvist, J., Johansson, J., Samuelsson, J., Rivera, C., Lefer, B. and S. Alvarez (2008b), Comparison of Solar Occultation Flux Measurements to the 2006 TCEQ Emission Inventory and Airborne Measurements for the TexAQS II, Project No. 582-5-64594-FY08-06, TCEQ report., Texas. (available at http://www.tceq.state.tx.us/assets/public/implementation/air/am/contracts/reports/da/20081108-comparison_solar_occultation_flux_measurements.pdf)

Mellqvist, J., et al. (2009), Emission Measurements of Volatile Organic Compounds with the SOF method in the Rotterdam Harbor 2008, available at www.fluxsense.se

Mellqvist, J., J. Samuelsson, J. K. E. Johansson, C. Rivera, B. Lefer, S. Alvarez, and J. Jolly (2010), Measurements of industrial emissions of alkenes in Texas using the solar occultation flux method, Journal of Geophysical Research: Atmospheres, 115(D7), doi:10.1029/2008JD011682.

Rinsland, C. P., R. Zander, and P. Demoulin (1991), Ground-based infrared measurements of $HNO_3$ total column abundances: long-term trend and variability. *J. Geophys. Res.*, *96*, 9379–9389.

Rivera, C., Mellqvist, J., Samuelsson, J., Lefer, B., Alvarez, S. & Patel, M. (2010) Quantification of NO2 and SO2 emissions from the Houston Ship Channel and Texas City industrial areas during the 2006 Texas Air Quality Study. Journal of Geophysical Research - Atmospheres 115. DOI: 10.1029/2009JD012675.

Rothman et al. (2003), HITRAN 2000, Journal of Quantitative Spectroscopy and Radiative Transfer, vol. 82, pp. 5-44.

Sharpe, S., et al. (2004), Gas-Phase Databases for Quantitative Infrared Spectroscopy, *Applied Optics*, 58(12).

# Quantification of Ammonia, Methane and Other Gas Emissions from Large Dairies in San Joaquin Valley – Sub Report C

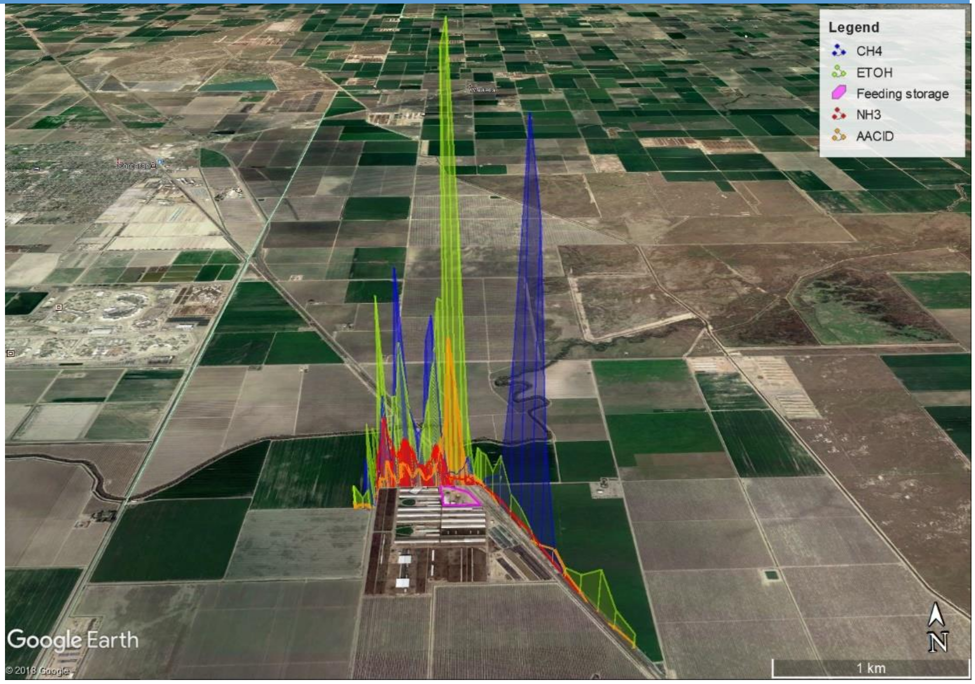

FluxSense

2019

**FINAL REPORT**

Fluxsense

21 May 2020

**Date:** 21 May 2020
**Updated**: 1 December 2020

**Title:** Quantification of ammonia and methane emissions and other gases from large dairies in San Joaquin Valley – Sub report C

**Authors:** Johan Mellqvist[1,3], Jerker Samuelsson[1], Brian Offerle[2], Marianne Ericsson[1], Nathalia Thygesen Vechi[3,4]

[1]FluxSense Inc, 113 W G Street # 757, San Diego, CA 92101
[2]FluxSense AB, Sven Hultins gata 9, SE-41288 Göteborg, Sweden
[3]Chalmers University of Technology, Hörsalsvägen 11, SE-41296, Göteborg, Sweden
[4]Technical University of Denmark, Bygningstorvet, Building 115, Kgs. Lyngby, Denmark

**CARB contract no. 17RD021**
Principal Investigator: Johan Mellqvist,
May 2019, San Joaquin Valley survey
Prepared for the California Air Resources Board
and the California Environmental Protection Agency

[Cover: MeFTIR concentration measurement of ammonia, methane, ethanol and acetic acid, Tulare - California. Image mapped on Google Earth © 2019.]

## DISCLAIMER

The statements and conclusions in this Report are those of the contractor and not necessarily those of the California Air Resources Board. The mention of commercial products, their source, or their use in connection with material reported herein is not to be construed as actual or implied endorsement of such products.

# Executive summary

*Objective*

A two-year study is carried out by FluxSense Inc. on behalf of California Air Resources Board (CARB). The objective is to provide ground-based flux measurements of VOCs, methane, air toxics and ammonia from various sources, e.g. refineries, petrochemical industries, oil storage, port activities, landfills, oil and gas production and Concentrated Animal Feeding Operations (CAFOs). This project complements community monitoring efforts by CARB staff who have measured speciated VOCs and air toxics of concern.

*Background*

This sub-report covers measurements from 12 days of a campaign in May 2019 carried out in the San Joaquin Valley focused on ammonia and methane emissions from dairy cows concentrated feeding operations. It also includes measurements of other gases that can be emitted from this type of activity, for example, ethanol, acetic acid, $NO_x$ and $N_2O$.

The emissions (kg/h) of ammonia were quantified using Solar Occultation Flux (SOF) while MeFTIR (Mobile extractive Fourier Transform Infrared) technique was used to measure ground level concentrations of methane, ammonia, ethanol, acetic acid and $N_2O$. Methane emissions were determined by combining plume concentration ratios of methane to ammonia with the ammonia fluxes that were measured by SOF.

SOF is a proven technique that has been developed at Chalmers University of Technology in Sweden and further developed and applied by FluxSense in over 100 fugitive emission studies around the world. In Europe the SOF technique is considered Best Available Technology (BAT) for measurements of diffuse emissions of VOCs from refineries, and in Sweden it is used in conjunction with tracer correlation and optical gas imaging to annually screen all larger refineries and petrochemical facilities. The estimated uncertainty for SOF emission measurements is typically 30 % for total site emissions. The estimated measurement uncertainties have been verified in several (blind and non-blind) controlled source gas release and in side-by-side measurements with other measurement techniques.

The instruments were operated in the FluxSense mobile laboratory and the measurements were conducted while driving outside the source site fence-lines along public roads. Background columns and concentrations were subtracted by encircling the sites, when possible, or by measuring upwind columns and concentrations, so that only emissions from within the facilities were quantified. Column and concentration measurements are enhancement above background. Wind data were obtained using a Light Detection and Ranging (LIDAR) instrument that measured the wind profile between 10 to 300 m altitude above ground. The emission results are presented as daily and total survey averages. From the combination of the measured column and concentration values the height of the plume could be derived to first order.

*Emission measurements*

Table E.1 summarizes the main results from the campaign, including methane and ammonia emissions from 16 CAFOs located in 3 main regions in the San Joaquin Valley: Bakersfield, Tulare and Merced. The names attributed to the farms are according to their location and the order that they were measured. For most sites, around 7 to 8 transects through the plume were made over 2 to 4 days. For some of the sites only limited repeated measurements were carried out due to the meteorological conditions and they are excluded from the summary statistics but discussed in the report.

Table E.2 shows a summary of the emission factor by facility in g head$^{-1}$ h$^{-1}$, for both methane (49.9 g$CH_4$ head$^{-1}$ h$^{-1}$) and ammonia (11.7 g$NH_3$ head$^{-1}$ h$^{-1}$). Figure ES1 shows the obtained ammonia emission factors.The number of animals were obtained from the San Joaquin Valley Air Pollution Control District (ValleyAir, Personal communication, 2019), corresponding to mature cows, replacement heifers and calves, and calculated in terms of animal unit (here mature animals correspond to one animal unit, heifers to 0.75 and calves to 0.17). The measured emission factors in this study are in line with some studies and higher than other ones, e.g. compared to 10.4 g$NH_3$ head$^{-1}$ h$^{-1}$ and 23 g$CH_4$ head$^{-1}$ h$^{-1}$ (Bjorneberg *et al.*, 2009) and 6.25 g$NH_3$ head$^{-1}$ h$^{-1}$ and 58 g$CH_4$ head$^{-1}$ h$^{-1}$ (Leytem *et al.*, 2011) and 11.8 g$NH_3$ head$^{-1}$ h$^{-1}$ (Kille *et al.*, 2017).

The obtained methane emissions numbers are well correlated with previous airborne measurements performed by Scientific Aviation of the same facilities, although made in other periods of the year. Some of the positive bias observed can be explained by the influence of the sunny weather conditions in which SOF measurements were carried out, and the fact that the survey wind and temperature may differ between studies and from the annual average climatology. Previous studies have shown that similar facilities might have a seasonal variability of ~400% for methane, while for ammonia the variability can be of 1000%, with December and January being the months with lowest emissions and June and July the highest ones (Leifer *et al.*, 2018).

Additionally, measured and inventory estimated methane emissions were compared (Table E.3). The inventory calculations (‘Documentation of California’s 2000-2017 GHG Inventory – Index’) were divided into enteric and manure contributions. For the first, emissions factors were applied according to the animal life stages and for the latter according the different manure managements for the dairy cows and heifers in California. Inventory estimated methane emissions were approximately 30% less than measured emissions.

For ammonia (Table E.4) inventory emissions were estimated only by multiplying the emission factor found in literature (84 lbs/cow/year, US EPA, 2004) by the number of animal units in place. The $NH_3$ inventory estimated emissions were about 50% less compared to measured emissions.

In addition to ammonia and methane, emissions of some other species were observed. Enhanced ethanol concentrations were observed at three sites, and acetic acid at one of these CAFOs. The higher concentrations were correlated with the feeding operation areas, and only found at facilities where favorable wind conditions and nearby road access allowed for close downwind measurements of this part of the farm(s). Some enhanced concentrations of nitrous oxide were detected from fertilized fields adjacent to the farms. Plumes of $NO_2$ were found that were well correlated with a farm south of Bakersfield, however, it was not determined whether the emissions originated from a combustion source or were of biological origin.

Table E.1. Results of the emission measurements based on SOF, SkyDOAS, MeFTIR. Blanks indicate that emissions were below detection limit. ETOH denotes ethanol.

| | | $NH_3$ (kg/h) | | $CH_4$ (kg/h) | | $NH_3$:ETOH (%) | | $NO_2$ (kg/h) | |
|---|---|---|---|---|---|---|---|---|---|
| **CAFO** | **N Transects** | **Avg** | **CI 95%** | **Avg** | **SD** | **Avg** | **CI 95%** | **Avg** | **CI 95%** |
| **SB02** | 7 | 106.8 | 68-146 | 547.5 | 224.9 | | | | |
| **SB03** | 9 | 119.7 | 73-167 | 384.6 | 204.5 | | | | |
| **SB04** | 10 | 61.4 | 42-80 | 214.2 | 148.8 | | | | |
| **SB05** | 8 | 113.5 | 80-152 | 514.0 | 298.7 | | | 23.5 | 15.7-31.3 |
| **NB01** | 7 | 69.8 | 17-122 | 391.9 | 380.8 | | | | |
| **NB02** | 9 | 104.0 | 61-147 | 675.4 | 456.0 | | | | |
| **WT01** | 14 | 70.8 | 48-93 | 196.1 | 165.2 | 26.7 | 21.9-31.5 | | |
| **WT03** | 9 | 157.7 | 121-193 | 388.6 | 194.5 | | | | |
| **WT04** | 7 | 191.5 | 120-263 | 482.8 | 230.8 | 36.2 | 22.5-49.8 | | |
| **WT05** | 6 | 70.3 | 29-111 | 304.3 | 191.6 | 45.5* | 0-137 | | |
| **WT06** | 6 | 120.8 | 57-185 | 259.5 | 192.9 | | | | |
| **WT07** | 8 | 67.0 | 51-83 | 415.1 | 200.2 | | | | |
| **ET01** | 7 | 31.9 | 20-43 | 187.8 | 124.9 | | | | |
| **ET08** | 7 | 60.0 | 48-72 | 292.6 | 134.5 | | | | |
| **SM01** | 7 | 166.0 | 127-204 | 527.2 | 140.4 | | | | |
| **SM02** | 13 | 142.2 | 104-180 | 844.8 | 451.1 | | | | |
| ***Sum*** | ***134*** | ***1653.4*** | | ***6626.4*** | | ***108*** | | | |
| ***Average*** | ***8.4*** | ***103.3*** | | ***414.1*** | ***180.8*** | ***36.1*** | | ***23.5*** | |
| ***Median*** | ***7.5*** | ***105.4*** | | ***390.3*** | | ***36.2*** | | ***23.5*** | |

- The CAFOs were named according to their geographic location in San Joaquin Valley. "SB" stands for South Bakersfield, "NB" for North Bakersfield, "WT" West Tulare, "ET" East Tulare, and finally "SM" for south Merced.

Table E.2. Emission factors, emission per number of animal unit[2], for each facility measured.

| | $NH_3$ (g/head/h) | | $CH_4$ (g/head/h) | |
|---|---|---|---|---|
| **CAFO** | **Avg** | **SD** | **Avg** | **SD** |
| **SB02** | 6.0 | 2.4 | 30.5 | 12.5 |
| **SB03**[1] | 10.5 | 5.4 | 33.8 | 18.0 |
| **SB04** | 10.2 | 4.7 | 37.1 | 25.8 |
| **SB05**[1] | 18.3 | 7.9 | 82.9 | 48.2 |
| **NB01** | 8.8 | 7.2 | 49.3 | 47.9 |
| **NB02** | 12.9 | 7.0 | 83.6 | 56.4 |
| **WT01**[1] | 3.9 | 2.2 | 10.9 | 9.2 |
| **WT03** | 16.7 | 5.0 | 41.2 | 20.6 |
| **WT04** | 15.9 | 7.1 | 41.9 | 20.0 |
| **WT05**[1] | 12.2 | 6.7 | 52.7 | 33.2 |
| **WT06** | 14.6 | 7.4 | 31.3 | 23.3 |
| **WT07**[1] | 15.3 | 4.4 | 95.0 | 45.8 |
| **ET01** | 14.0 | 5.8 | 88.6 | 58.9 |
| **ET08**[1] | 4.1 | 0.9 | 20.0 | 9.2 |
| ***Average*** | ***11.7*** | ***2.2*** | ***49.9*** | ***17.6*** |
| ***Median*** | ***12.5*** | | ***41.4*** | |
| ***CI 95%*** | ***10.4-13.8*** | | ***39.8-81.2*** | |

[1] Farms with a methane collection cover. San Joaquin Valley region denotations: SB – South Bakersfield, NB – North Bakersfield, WT – Western Tulare, ET – Eastern Tulare.

[2] Mature animals correspond to one animal unit, heifers to 0.75 and calves to 0.17.

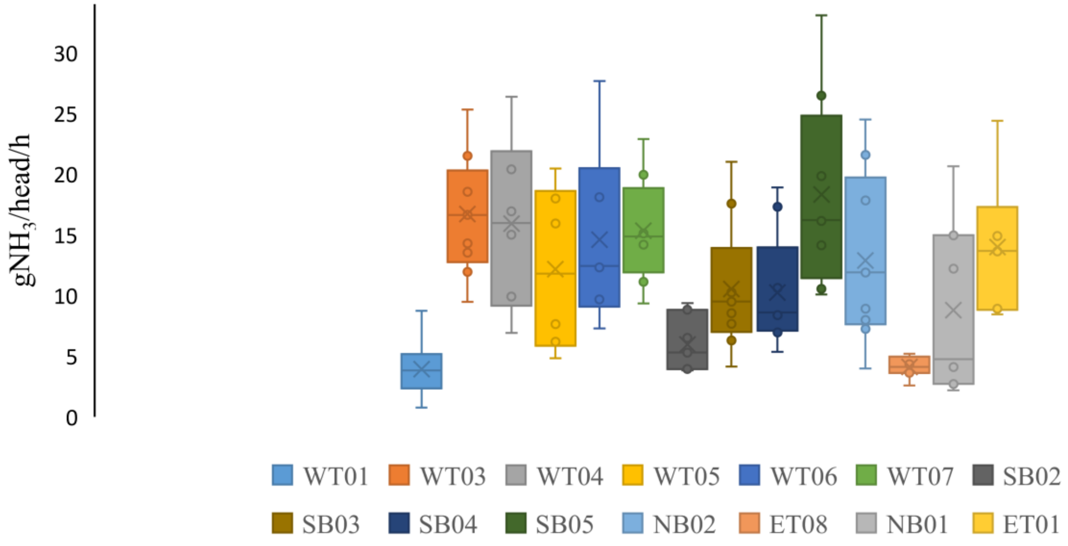

Figure ES 1. Obtained ammonia emission factors. Displayed parameters: the minimum value, 25th percentile, median, mean, 75th percentile, maximum and individual values (circles).

Table E.3. Comparison of measured and inventory[1] CAFO methane emission estimates.

| | Measured | | Inventory[1] estimate |
|---|---|---|---|
| **CAFO** | **$CH_4$ (kg/h)** | **SD (kg/h)** | **$CH_4$ (kg/h)** |
| **SB02** | 547.5 | 224.9 | 430.8 |
| **SB03** | 384.6 | 204.5 | 215.9 |
| **SB04** | 214.2 | 148.8 | 186.3 |
| **SB05** | 514 | 298.7 | 132.3 |
| **NB01** | 391.9 | 380.8 | 254.5 |
| **NB02** | 675.4 | 456 | 295.2 |
| **WT01** | 196.1 | 165.2 | 354.1 |
| **WT03** | 388.6 | 194.5 | 387.0 |
| **WT04** | 482.8 | 230.8 | 436.9 |
| **WT05** | 304.3 | 191.6 | 108.8 |
| **WT06** | 259.5 | 192.9 | 240.3 |
| **WT07** | 415.1 | 200.2 | 87.1 |
| **ET01** | 187.8 | 124.9 | 66.5 |
| **ET08** | 292.6 | 134.5 | 307.9 |

[1] 'Documentation of California's 2000-2017 GHG Inventory - Index'. Available at: https://ww3.arb.ca.gov/cc/inventory/doc/doc_index.php.

Table E.4. Comparison of measured and inventory[2] CAFO ammonia emission estimates.

| NH$_3$ kg/h | | | |
|---|---|---|---|
| **CAFO** | **Measured** | | **Inventory[2] estimate** |
| | **Median** | **CI 95 %** | |
| **SB02** | 95 | 67-45 | 77.4 |
| **SB03** | 108 | 73-167 | 49.1 |
| **SB04** | 50 | 42-80 | 24.9 |
| **SB05** | 101 | 72-154 | 26.8 |
| **NB01** | 38 | 17-122 | 34.3 |
| **NB02** | 96 | 61-147 | 34.9 |
| **WT01** | 69 | 48-93 | 77.7 |
| **WT03** | 157 | 121-193 | 40.7 |
| **WT04** | 195 | 120-262 | 43.8 |
| **WT05** | 68 | 29-111 | 24.9 |
| **WT06** | 103 | 57-165 | 35.7 |
| **WT07** | 65 | 51-83 | 18.9 |
| **ET01** | 29 | 20-43 | 9.2 |
| **ET08** | 60 | 48-72 | 55.6 |

[2] Using a constant EF for dairy cows of 84 lbs/cow/year obtained from 'The National emission inventory - ammonia emissions from animal husbandry operations', (EPA, 2004).

# Acronyms, Units and Definitions

## Acronyms used in this report

| | |
|---|---|
| AFO | Animal Feeding Operations |
| BTEX | Benzene Toluene Ethylbenzene Xylene |
| CARB | California Air Resources Board |
| CAFO | Concentrated Animal Feeding Operations |
| DOAS | Differential Optical Absorption Spectroscopy |
| EF | Emission factor |
| EPA | Environmental Protection Agency |
| ET | East Tulare |
| FTIR | Fourier Transform InfraRed |
| GHG | Greenhouse Gas |
| IME | Indirectly Measured Emission, combining direct emission with plume concentration ratios |
| LIDAR | Light Detection and Ranging |
| MWDOAS | Mobile White cell DOAS |
| MeFTIR | Mobile extractive FTIR |
| NB | North Bakersfield |
| SB | South Bakersfield |
| SM | South Merced |
| SkyDOAS | Scattered Skylight DOAS |
| SOF | Solar Occultation Flux |
| VOC | Volatile organic compound, used interchangeably for non-methane VOC |
| WT | West Tulare |

## Units

| | |
|---|---|
| Air temperature | degrees C |
| Atmospheric Pressure | mbar |
| Relative Humidity | % |
| Wind direction | degrees North |
| Wind speed | m/s |
| Column | $mg/m^2$ |
| Concentration | $mg/m^3$ |
| Flux | kg/h |

## Unit Conversions

1 lbs = 0.4536 kg
1 kg/h = 52.9 lbs/day
1 bbl = 159 l
1 bbl/day = 5.783 kg/h (crude oil)
1 (short) ton = 907.2 kg
1 kton/year = 104 kg/h
1 klbs/year=0.052 kg/h

## TABLE OF CONTENTS

## LIST OF TABLES:

## LIST OF FIGURES

# 1. Objective and introduction

The objectives of this research are to characterize certain statewide GHGs and air toxics emission sources, in order to identify potential sources contributing to air pollution hotspots. This includes quantifying ground-based fluxes of VOCs, methane, air toxics and ammonia from various sources, e.g. refineries, petrochemical industry, oil storage, harbor activities, landfills, oil and gas production and Concentrated Animal Feeding Operations (CAFOs).

This sub report of the study is focused on ammonia and methane emissions from dairy cows in CAFOs in three regions of the San Joaquin Valley: Bakersfield, Tulare and Merced. The results from this study are intended to provide useful screening information, help identify high ammonia and methane CAFOs emissions and improve the efficiency of the mitigation approaches used in some of the farms. The data should also potentially be useful to help CARB develop and improve their models of ammonia and methane emissions from California Central Valley concentrated feedlot operations.

This report covers the sub-set of measurements from a 5-week campaign in May 2019, carried out in the San Joaquin Valley, CA, over the 12 days focused on CAFO measurements.

## 2. Background

Greenhouse gas (GHG) emissions and other biogenic emissions to the atmosphere must drop to combat global climate change, and improve the regional and local air quality. In California, the agricultural sector contributes to 8% of the GHG emissions and approximately 57% of California's anthropogenic $CH_4$ emissions. From this 57 %, 11 MMT $CO_2e$ (million metric tons of carbon dioxide equivalents) per year are attributed to enteric fermentation, and others 10 MMT $CO_2e$ per year to dairy manure management. Even though, the carbon footprint of milk production has been reduced over the years, since the passage of senate bill SB1383, California has been implementing practices to reduce $CH_4$ emissions (Souza *et al.*, 2018). Additionally, research projects have been funded in California to investigate the emissions and new mitigation practices; however, there is still a need to improve the understanding of these emissions.

Furthermore, handling of organic residues rich in nitrogen, especially manure, causes ammonia emissions. Ammonia is an indirect GHG by its contribution to atmospheric $N_2O$ through various transformations (Denmead *et. al.*, 2008; Petersen *et. al.*, 2013), and contributes to eutrophication and particles formation causing environmental and health risks.

Direct measurements of agricultural emissions bring more information to improve inventories, access the emissions dynamics, and evaluate the efficiency of different mitigation strategies. Determination of ammonia emissions from livestock facility is complicated due to the variety and the nature of the factors regulating $NH_3$ volatilization, such as ambient temperature, wind speed, manure composition and pH (Hristov *et al.*, 2011). Ammonia emissions come from manure management, while the main methane sources are enteric fermentation by ruminants and manure management, especially when the manure is treated in the liquid state (VanderZaag *et al.*, 2014). Methane coming from manure management is also highly affected by temperature (Rennie *et al.*, 2018). Even though different pathways produce $NH_3$ and $CH_4$ emissions, both gases are known to scale with animal activity (Miller *et al.*, 2015). Furthermore, $NH_3$ and $CH_4$ emissions have a strong diurnal trend, which is associated with wind speed, temperature, and cattle activity (Leytem *et al.*, 2011).

## 3. Instrumentation and methods

The FluxSense measurement vehicle or “mobile lab” is equipped with four optical instruments for gas monitoring which were used during the survey: SOF (Solar Occultation Flux), SkyDOAS (Differential Optical Absorption Spectroscopy), MeFTIR (Mobile extractive Fourier Transformed Infrared spectrometer) and MWDOAS (Mobile White cell DOAS). The individual measurement methods are described in Table - 1 and the subsections below. The most relevant instruments for this report are SOF and MeFTIR. SOF measures gas columns through the atmosphere by means of light absorption and utilizes infrared light from the direct sun. MeFTIR measures ground-level concentrations of VOCs and methane. SkyDOAS measures scattered ultraviolet light from the sky, and it was used in this report to measure $NO_2$ emissions. MWDOAS measures ground (vehicle roof height, approx. 2 m) concentrations of benzene, toluene, ethylbenzene, and xylene (BTEX) among others.

Table - 1. Summary of FluxSense gas measurement techniques.

| **Method** | **SOF** | **MeFTIR** |
|---|---|---|
| **Compounds** | Alkanes: ($C_nH_{2n+2}$)<br>Alkenes: $C_2H_4$, $C_3H_6$<br>$NH_3$ | $CH_4$, $NH_3$, $N_2O$<br>Alkanes: ($C_nH_{2n+2}$)<br>Alkenes: $C_2H_4$, $C_3H_6$<br>Ethanol ($C_2H_4OH$) |
| **Detection limit Column** | 0.1-5 mg/m$^2$ | 1-10 ppbv |
| **Detection limit Flux*** | 0.2-1 kg/h | 0.2-2 kg/h |
| **Wind Speed Tolerance** | 1.5-12 m/s | |
| **Sampling Time Resolution** | 1-5 s | 5-15 s |
| **Measured Quantity [unit]** | 1) Integrated vertical column mass [mg/m$^2$]<br>2) Mass Flux [kg/h] when combined with wind data | 1) Mass concentration at Vehicle height [mg/m$^3$]<br>2) Alkane and $CH_4$ flux [kg/h] via tracer release |
| **Indirect Quantity [unit]** | | 1) Alkane ratio of ground plume combined with SOF gives plume height information [m]<br>2) Plume concentration ratios combined with SOF flux estimate gives indirect flux estimates of the ratioed compound |
| **Complementary data** | Vehicle GPS-coordinates, Plume wind speed and direction | Vehicle GPS-coordinates<br>Plume wind direction |

*For typical wind conditions at an optimal distance from the source.

Accurate wind data is necessary to compute emission fluxes. A wind LIDAR was used to measure vertical profiles of wind speed and wind direction from 10-300 m height. This was re-located for each measurement day and measurement area to a suitable site within the vicinity (< 5 km radius) of the measured CAFOs.

In order to derive final emission flux estimates, the GPS-tagged gas column measurements by SOF is combined with wind data and integrated across plume transects at the various source locations. Gas mass ratio measurements by MeFTIR are then used to indirectly estimate the methane emissions.

## 3.1. Solar Occultation Flux (SOF)

The SOF method (Mellqvist, 1999, 2009; Kihlman, 2005; Mellqvist, Johansson, Samuelsson and Offerle, 2008; Mellqvist, Johansson, Samuelsson, Rivera, *et al.*, 2008; Mellqvist *et al.*, 2010; Johansson *et al.*, 2014) is based on the recording of broadband infrared spectra of the sun with a Fourier transform infrared spectrometer (FTIR) that is connected to a solar tracker. The latter is a telescope that tracks the sun and reflects the light into the spectrometer independent of the orientation of the vehicle. Using multivariate optimization, it is possible from these solar spectra to retrieve the path-integrated concentrations (referred to as column concentrations), in the unit mg/m$^2$, of various species between the sun and the spectrometer. The system used in this project consists of a custom-built solar tracker, transfer optics and a Bruker IRCube FTIR spectrometer with a spectral resolution of 0.5 cm$^{-1}$, equipped with a dual InSb (Indium Antimonide) / MCT (Mercury Cadmium Telluride) detector. A reference spectrum is taken outside the plume so that atmospheric background concentrations are removed. This means that all measured SOF columns are analyzed relative to the background column concentrations.

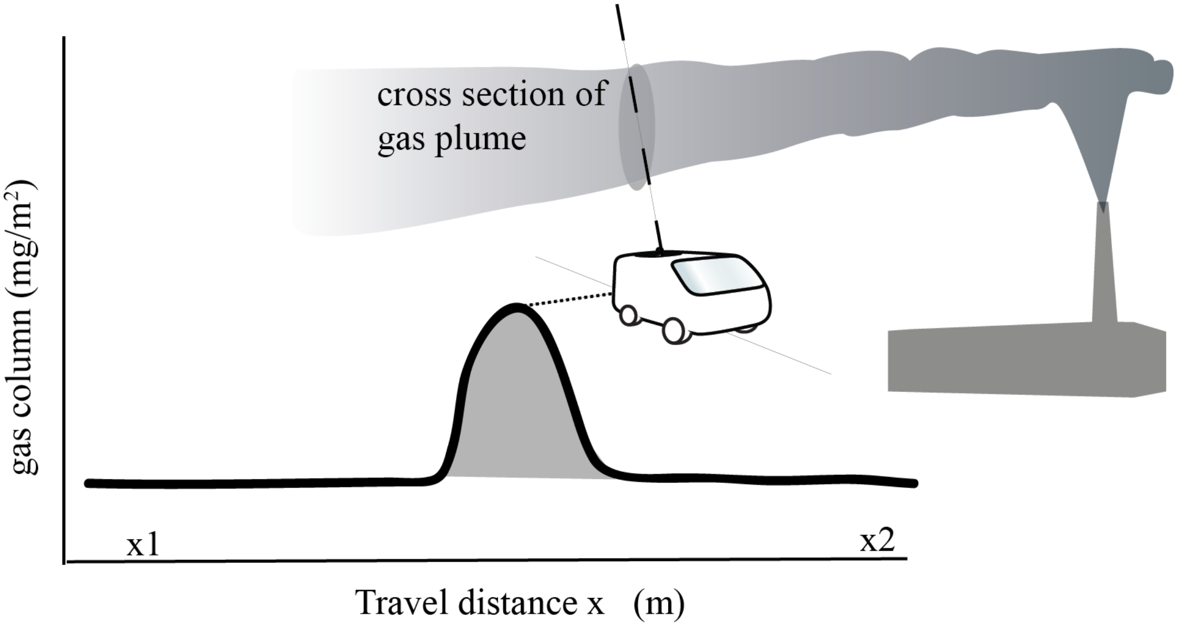

Figure - 1: Schematic of the SOF measurement where the vehicle is driven across the prevailing wind so that the solar beam cuts through the emission plume while the sun is locked into the FTIR spectrometer by the solar tracking device on the roof. The VOC mass (or other compound of interest) is integrated through the plume cross section. See section 4.1 for complete equations.

The system is installed in a measurement vehicle, which allows consecutive column concentration measurements to be performed while driving. The flux of a species in a plume from an industry is measured by collecting spectra while driving the vehicle so that the light path from the sun to the instrument gradually cuts through the whole plume, preferably as orthogonally as possible to the wind direction, see Figure - 1.

For each spectrum, a column concentration of the species is retrieved using custom software (Flux measure). These column concentrations, together with positions recorded with a GPS (Global Positioning System) receiver and the solar angle calculated from the time of the measurements, are used to calculate the area-integrated column of the species in the intersection area between the plume and the light path. The flux other species is then obtained by multiplying this area integrated concentration with the orthogonal wind speed vector component. The IR spectra recorded by the SOF instrument are analyzed in FluxMeasure by fitting a set of spectra from the HITRAN infrared database (Rothman *et al.*, 2003) and the PNNL (Pacific Northwest National Laboratory) database (Sharpe *et al.*, 2004) in a least-squares fitting procedure. Calibration data from the HITRAN database is used to simulate absorption spectra for atmospheric background compounds present in the atmosphere with high enough abundance to have detectable absorption peaks in the wavelength region used by SOF. Spectra, including water vapor, carbon dioxide and methane, are calibrated at the actual pressure and temperature and degraded to the instrumental resolution of the measurements.

For the retrievals, high resolution spectra of ammonia were obtained from the PNNL database and these are degraded to the spectral resolution of the instrument by convolution with the instrument line shape. The uncertainty in the absorption strength of the calibration spectra is about 3.5% for all five species.
In this project, the SOF method was used to measure Ammonia in the alkene mode. The ammonia was measured in the spectral region between 900 and 1000 cm$^{-1}$ using a spectral resolution of 0.5 cm$^{-1}$. The specificity of the measurement mode is good, since the absorption of different species is rather unique in this so called “fingerprint region” and absorption features are often sharp and well separable from each other at 0.5 cm-1 resolution.

SOF is a proven technique employed by FluxSense in over 100 fugitive emission studies around the world. The estimated uncertainty for the SOF emissions measurements is typically 20-30 % for the total site emissions. This uncertainty has been calculated from several controlled release experiments (blind and non-blind) and side-by-side measurements with other measurement techniques.

## 3.2 Mobile extractive FTIR (MeFTIR)

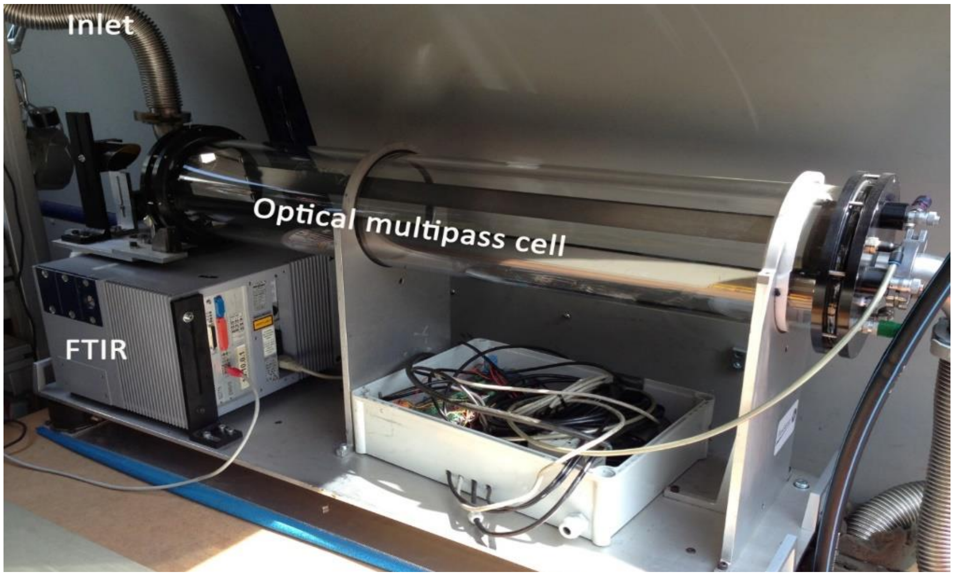

Figure - 2: The MeFTIR instrumentation consisting of a Bruker FTIR spectrometer connected to an optical multi-pass cell.

Mobile Extractive FTIR (MeFTIR) is an optical technique capable of monitoring gas concentrations at ppb-sensitivity in mobile field operations. It is used independently for concentration mapping and flux measurements, but often combined together with simultaneous SOF flux measurements to provide more detailed VOC speciation of plumes and for plume height assessments (Johansson *et al.*, 2013), and methane emissions. The plume height can be estimated by dividing measured columns (mg/m$^2$) with ground concentrations (mg/m$^3$), assuming that the plume is uniformly distributed up to the plume height (and zero above).

The MeFTIR system contains a mid-infrared spectrometer with medium resolution (0.5 cm$^{-1}$). It utilizes an internal glow bar as an infrared radiation source, and by customized optics, this light is transmitted through an optical multi-pass measurement cell with path-length of 68 meters (Figure - 2). The system is mounted on a vibration-dampening platform to allow for real time plume mapping from a mobile platform, such as a vehicle or boat. Additionally, for the ammonia measurements, the inlet and the cell are heated and insulated so that the sample air and cell temperature is above 40 ºC. Heating the sample is desirable since ammonia is a “sticky” gas, therefore heating the inlet and cell minimizes the risk of ammonia adhering to the tubing or cell surface and the residence time in the cell increasing. Internal cell temperature and pressure are averaged each second and logged every minute. Cell temperature variation over the measurement period is presented in Figure - 3.

The transmitted light is detected simultaneously with an InSb-detector in the 2.5–5.5 µm (1800–4000 cm$^{-1}$) region and an MCT detector in the 8.3–14.3 µm (700–1200 cm$^{-1}$) region. Temperature and pressure in the cell are averaged over the duration of each measurement. Atmospheric air is continuously pumped at high flow rate through the optical cell from the outside, taking in plume air from the roof of the vehicle (2.5 m height) through a Teflon tube. A high flow pump is used to ensure that the gas volume in the cell is fully replaced within a few seconds. Spectra are typically recorded with an integration time of 8-12 seconds. A GPS-receiver is used to register the position of the vehicle every second.

The concentration in the spectra is analyzed in real time by fitting a set of calibrated spectra from the HITRAN infrared database (Rothman *et al.*, 2003) and the PNNL database (Sharpe *et al.*, 2004) in a least-squares fitting procedure. Compounds being analyzed include water, methane, CO, $CO_2$ and $N_2O$, ammonia, ethanol and acetic acid. The analysis routines are very similar to the ones for SOF, but less complex because strong absorption by atmospheric trace gases (water, methane, $CO_2$) has less consequence at the shorter path length in the MeFTIR measurement cell.

Concentration measurement by FTIR is a standard technique, and the main uncertainties are associated with the absorption cross sections (typically < 3.5%), spectral retrieval and potential sampling artefacts with an aggregate uncertainty better than 10% in the analysis. The spectral retrieval using FluxMeasure and QESOF (FluxSense custom software) were tested against other open source retrieval methods, and the comparison was within 10% in concentration conversion for the different schemes.

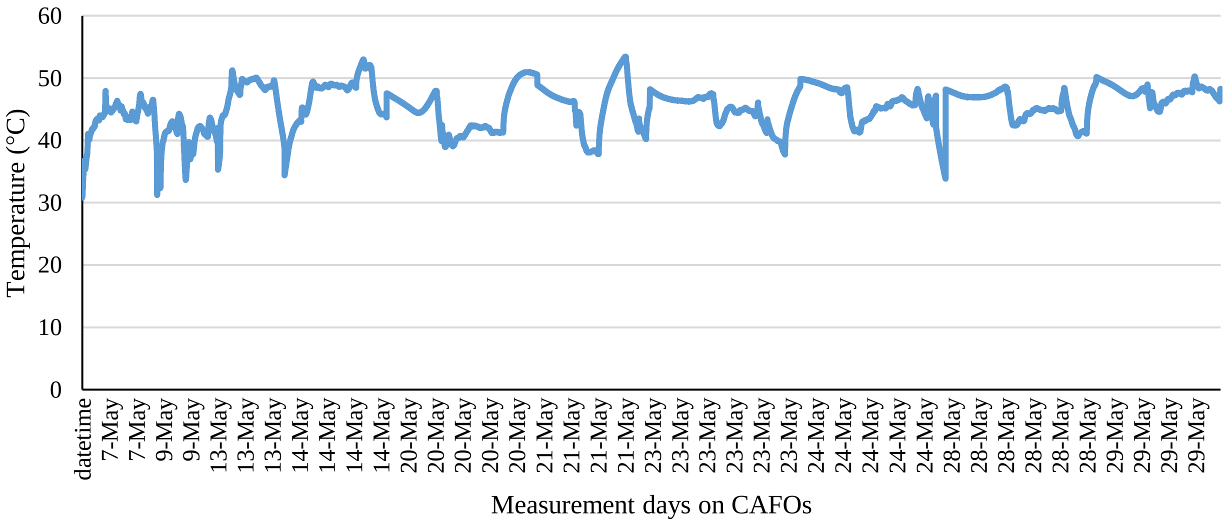

Figure - 3: MeFTIR cell temperature. The figure shows only the days when CAFOs were measured. When mains power was available the heater was kept on during the night.

### 3.3 Wind LIDAR

A wind LIDAR (LIght Detetction and Ranging, Zephyr) was used to measure vertical wind profiles of wind speed and direction, Figure - 4. The LIDAR provided wind profiles in the vertical range of 10 m to up to 300 m above ground. The system records 1-s data, and 5-minute averages were used for flux calculations in this study. The principle of detection is based on the Doppler shift of the infrared pulse that the instrument sends out and retrieves.

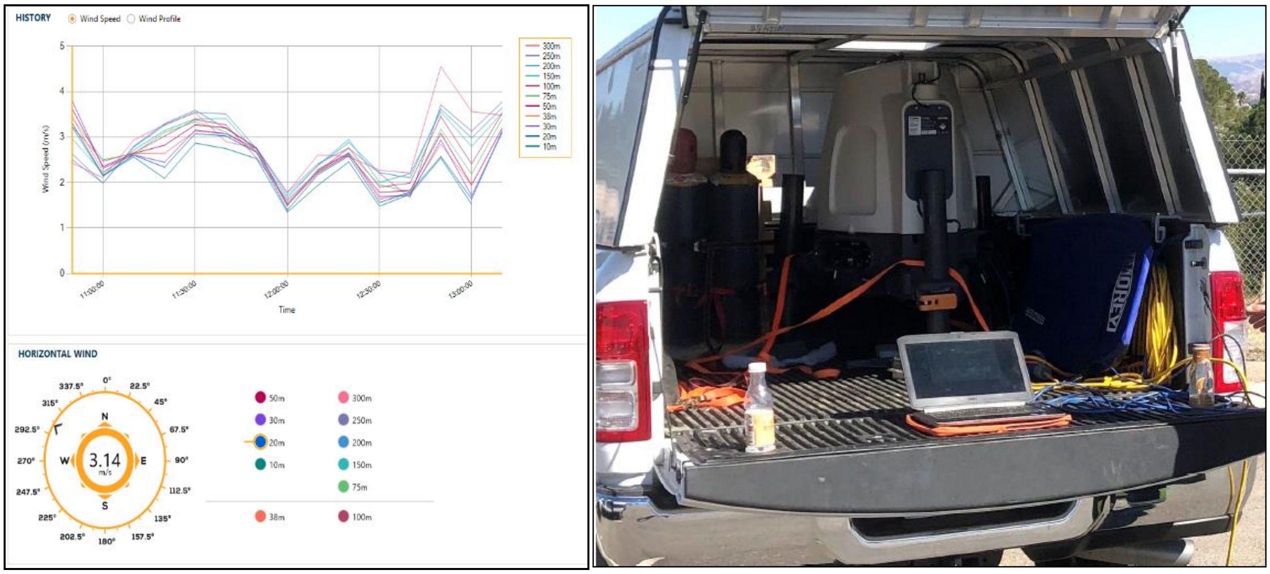

Figure - 4: (a) Data example, LIDAR wind profiler screenshot, (b) Wind measurements with portable wind LIDAR profiler.

### 3.4 Airmar and GPS

A sonic wind meter (Airmar WeatherStation 200 WX) was installed on the roof of the measurement vehicle to complement the other wind measurements and give local ground winds at the vehicle. The wind information from the car-based Airmar was not used for flux calculation since the wind field at street level can be heavily disturbed and turbulent. The Airmar was only used as a real-time aid to keep track of the plume directions when making the gas emission measurements. The Airmar provides wind speed and direction relative to true north (compensating for vehicle position), as well as air temperature, pressure and relative humidity. It also provides GPS positions that may be used as a backup for the other GPS-antenna.

The FluxSense vehicle is equipped with two standard USB GPS-L1 receivers (GlobalSat BU-353S4) connected to the SOF and MeFTIR computers. They are placed horizontally on the roof and by the windscreen for optimal reception. The receivers give the position at a rate of 1 Hz.

# 4. Measurements Methodology

## 4.1. Principal Equations

This report includes two different techniques to measure emission mass fluxes as specified below. The primary method in this project is the direct flux measurements of ammonia from SOF. In the secondary method methane fluxes are measured indirectly from MeFTIR gas mass ratios.

### *4.1.1 Direct flux measurements*

The emission mass flux ($Q$) of species ($j$) measured by SOF for a single transect ($T$) across the plume ($P$) along path ($l$) can be expressed by the following integral (Si-units in gray brackets):

$$Q_T^j[\mathrm{g/s}] = \bar{v}_T[\mathrm{m/s}] \cdot \int_P C_l^j[\mathrm{mg/m^2}] \cdot \cos(\theta_l) \cdot \sin(\alpha_l)\ dl\ [\mathrm{m}]$$

Where,
$\bar{v}_T$ = the average wind speed at plume height for the transect,
$C_l^j$ = the measured slant column densities for the species *j* as measured by SOF or SkyDOAS,
$\theta_l$ = the angles of the light path from zenith ($\cos(\theta_l)$givesverticalcolumns),
$\alpha_l$ = the angles between the wind directions and driving directions
dl = the driving distance across the plume

Note that SOF and SkyDOAS have different light paths, where the SkyDOAS telescope is always looking in the zenith direction while the SOF solar tracker is pointing toward the Sun. Hence, the measured SOF slant column densities will vary with latitude, season and time of day.

To isolate emissions from a specific source, the incoming/upwind background flux must be either insignificant or subtracted. If the source is encircled or "boxed", the integral along *l* is a closed loop and the flux calculations are done with sign. This is taken care of by the FluxSense software.

### *4.1.2 Indirect flux measurements*

The indirectly measured flux (indirectly measured emission, IME) is computed using a combination of SOF and MeFTIR measurements. The inferred mass flux ($\hat{Q}^i$) for species ($i$) are calculated from MeFTIR and ground level gas ratios integrated over the plume ($P$) along path ($l$) are given by (Si-units in gray brackets):

$$\hat{Q}^i[\mathrm{g/s}] = \bar{Q}^j[\mathrm{g/s}] \cdot \frac{1}{k}\sum_k \frac{\int_P N_l^i[\mathrm{\mu g/m^3}]\, dl[\mathrm{m}]}{\int_P N_l^j[\mathrm{\mu g/m^3}]\, dl[\mathrm{m}]}$$

Where,

$\overline{Q}^{j}$ = the average flux of species *j* from multiple transects as measured by SOF,
$N_{l}^{i}$ = the number density concentrations of species *i* as measured by MeFTIR,
$N_{l}^{j}$ = the number density concentrations of species *j* as measured by MeFTIR,
*k* = the number of gas ratio measurements

Note that the IME operates on average values since simultaneous SOF and MeFTIR measurements are generally not performed and because individual gas ratios are more uncertain than the average. Although not necessarily simultaneously measured, SOF and MeFTIR measurements must represent the same source plumes. Note also that gas ratios do not intrinsically depend on complete plume transects (like for direct flux methods) as long as the emission plume is well mixed at the sampling distance. Additionally, it is not necessary that the source of the tracer and measured gas be identical, merely that they are co-located at the measurement distance and uniform in time.

### 4.2. Uncertainties and Error Budget

A summary of the typical performance of the FluxSense measurements is presented in Table - 2. In addition, for each site the statistical error is calculated. It corresponds to the random error but in addition there could be systematic errors. For instance, in the used wind speed due to the errors in estimated height of the plume and spectral calibration errors. The precision statistical error is given by the 95 % Confidence Interval (CI) for the mean, $\bar{x}$, according to:

$$CI = \bar{x} \pm t_{.025}\frac{s}{\sqrt{N}}$$

Here t is Student's T distribution and s corresponds to sample standard deviation:

$$s_x = \sqrt{\frac{\sum_{i=1}^{N}(x-\bar{x})^2}{N-1}}$$

To estimate the error propagation of the ammonia fluxes and ratio concentrations on methane emissions, the standard deviation was calculated as a combination of the two measured standard deviation. According to the equation below.

$$s_{CH4} = \overline{x_{CH4}}.\overline{x_{NH3}}\sqrt{\left(\frac{s_{NH3}}{x_{NH3}}\right)^2 + \left(\frac{s_{CH4}}{x_{CH4}}\right)^2}$$

Table - 2: Performance of FluxSense measurement methods.

| Measurement Parameter | Accuracy | Precision |
|---|---|---|
| SOF column concentrations alkanes, alkenes, $NH_3$ | ±10% | ±5% |
| SkyDOAS column concentrations $NO_2$, | ±10% | ±5% |
| MeFTIR concentrations $CH_4$, VOC, $NH_3$, $N_2O$ | ±10% | ±5% |
| Zephyr ZX 300 | ±0.1 m/s | - |
| GPS position | ±2m | ±2m |
| SOF mass flux, $NH_3$ | 30%-40% | ±10%-30% |
| SkyDOAS mass flux, $NO_2$ | 30%-40% | ±10% |

## 5. Survey Setup

The measurements using SOF and MeFTIR on the CAFOs were carried out for 12 days. For the MWDOAS and SkyDOAS (sharing the same DOAS spectrometer), the measurements were alternated between both instruments according to the weather conditions, resulting in a total of 4 and 6 data days, respectively. The column and concentration ratio measurements were combined with wind data from a Wind LIDAR, in order to quantify the emissions and identify the sources.

The CAFOs were divided into three main regions. The measured facilities were chosen based on a preliminary list provided by CARB, and according to the available roads and weather conditions. The selected survey areas were Bakersfield, Tulare, and Merced (Figure - 5). To organize the farm measurement results, a 2-letter acronym was attributed according to the farms' geographic location in reference to the nearest larger city. The first letter references the cardinal direction (North, South, East, West) from the nearest city (Bakersfield, Tulare, Merced), where the initial of the city name makes up the second letter of the acronym. The nomenclature for each farm was adopted according to the region and the number of farms measured in each sub-region (e.g. for instance NB01 for one farm north of Bakersfield). For clarity Table - 3 shows a comparison between the nomenclature adopted in this report and the one given by CARB (in previous project communications).

All measurements have been subject to quality control and assurance. This means adherence to the standard protocols for the methods, including ocular examination of instruments and measurement data, daily instrument calibration and statistical quality measures in the data treatment. The number of accepted measurements varied substantially from day to day, and from source to source, depending on weather conditions, local measurement conditions (source accessibility, state of the roads, obstacles, etc.) and time-sharing between measurement objects and instruments. Following quality assurance according the SOF method protocol, transects were discarded when the wind speed was lower than 1.5 m/s, if the wind direction and the observed target farm plume location did not match or when there was a large variation on the background or high upwind inflow (Section 6.5). The minimum number of accepted transect to consider a measurement was 5 (Section 6.4).

Statistical estimates of the flux emissions (kg/h) from the various sources were computed for each measurement day and for the entire survey, including the statistical error. It also shows the number of animals used on the factors of the calculation (ValleyAir, personal correspondence, 2019). Mature animals correspond to one animal unit, heifers to 0.75 and calves to 0.17 (Tulare county resource management, 2016). Note that there are numbers missing from the numeric farm sequence in Table - 3 because some farms initially considered during the data treatment were later excluded since they failed to meet the criterion for minimum number of measurements. We have also avoided the GPS coordinates for the farms to anonymize the measurements.

During the measurements in Tulare and Merced, persistent cloud cover and weak winds were challenging for the measurements. Therefore, to follow the quality assurance protocol, some farms and transects were excluded from the final results, see description in the section (6.5).

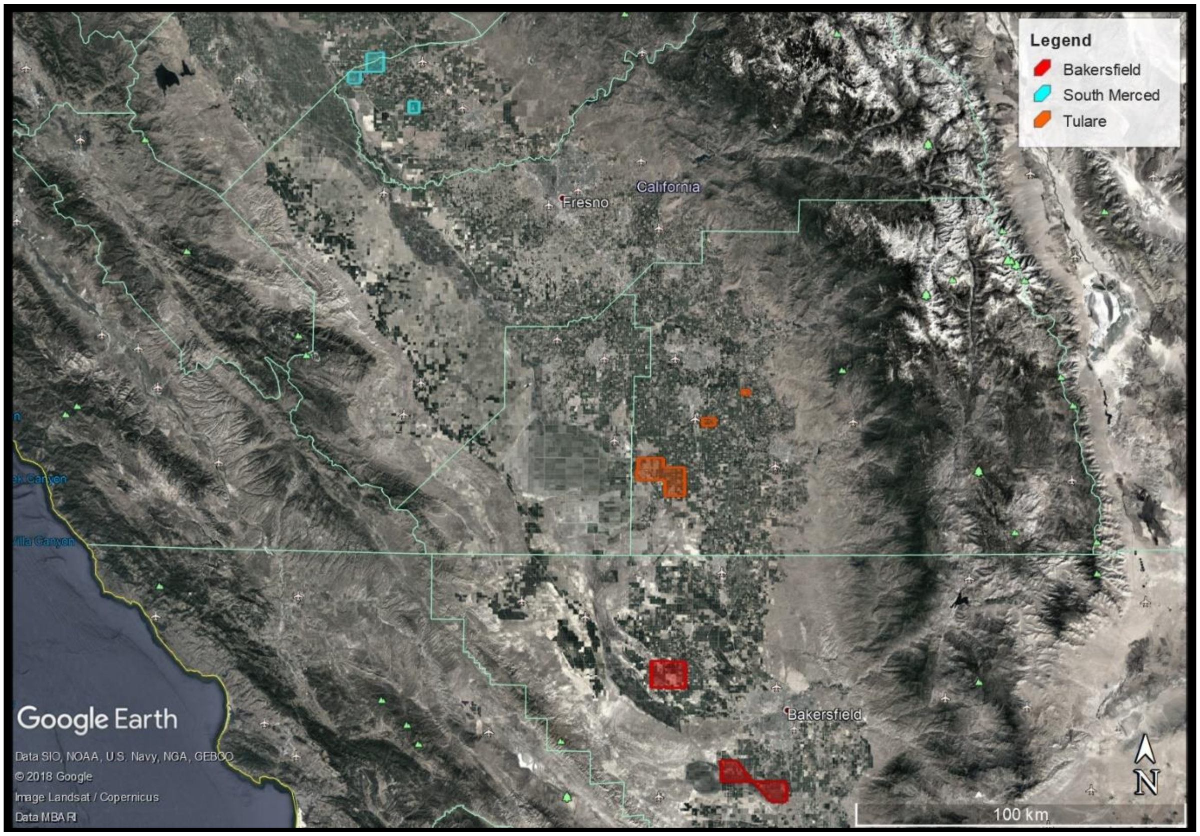

Figure - 5: Three main measurement areas in the San Joaquin valley.

Table - 3: Report and CARB nomenclatures for the CAFOs measured. Animal units (rounded) as obtained from ValleyAir. Here mature animals correspond to one animal unit, heifers to 0.75 and calves to 0.17.

| Report nomenclature CAFOs | No. of Animal Units in place | CARB nomenclature |
|---|---|---|
| NB01 | 7900 | Dairy #1 |
| NB02 | 8080 | - |
| NB04 | - | - |
| NB05 | 7080 | - |
| SB01 | 15650 | Dairy #2 |
| SB02 | 17930 | Dairy #3 |
| SB03 | 11400 | Dairy #4 |
| SB04 | 5780 | - |
| SB05 | 6200 | - |
| WT04 | 11520 | Dairy #6 |
| WT02 | - | Dairy #7 |
| WT01 | 18000 | Dairy #8 |
| WT05 | 5770 | - |
| WT06 | 8280 | - |
| WT07 | 4380 | - |
| ET01 | 2120 | Dairy #9 |
| ET03 | 1200 | - |
| ET05 | 1360 | - |
| ET07 | - | - |
| ET08 | 14640 | Dairy #5 |
| SM01 | - | Dairy #10 |
| SM02 | - | Dairy #11 |
| SM03 | - | Dairy #12 |

* San Joaquin Valley region denotations: SB – South Bakersfield, NB – North Bakersfield, WT – Western Tulare, ET – Eastern Tulare.

## 5.1. Sites

The three main regions Bakersfield, Tulare and Merced were divided into sub-regions: North Bakersfield (NB), South Bakersfield (SB), West Tulare (WT), East Tulare (ET) and South Merced (SM), see Figure - 6 to Figure - 10. The green pins represent the dairies for which survey results were obtained fulfilling the data quality standards. Table - 4 summarizes the measurement days carried out during the campaign.

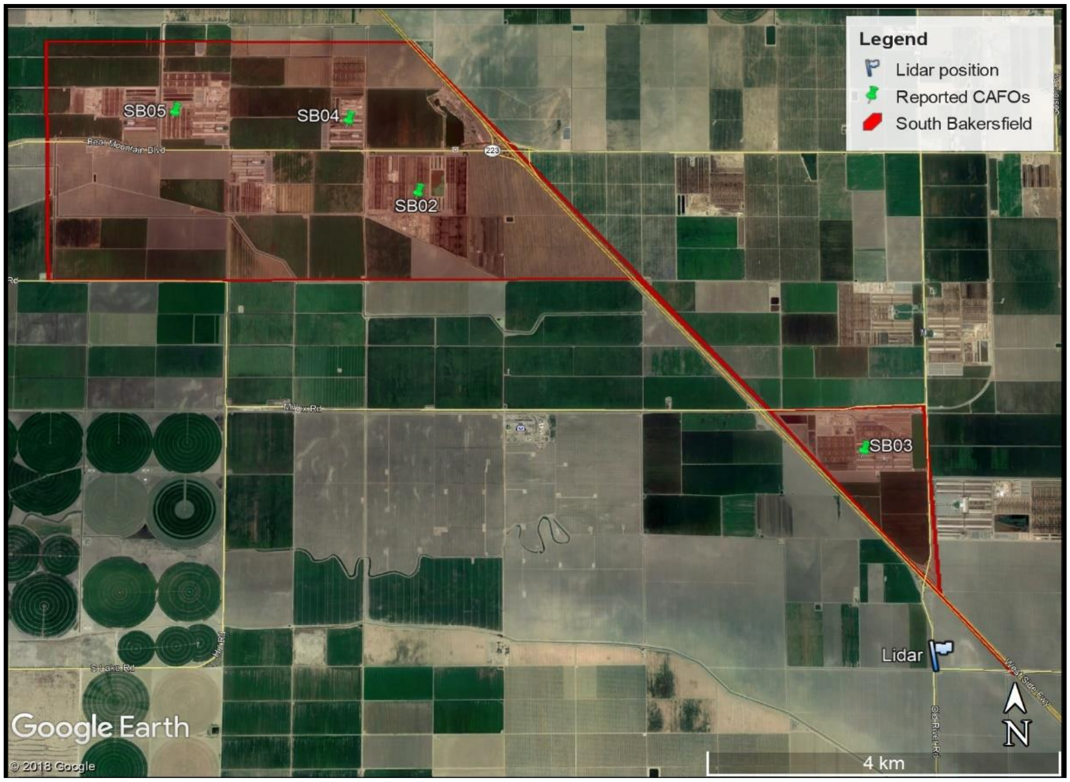

Figure - 6: Survey farms in the South Bakersfield (SB) area.

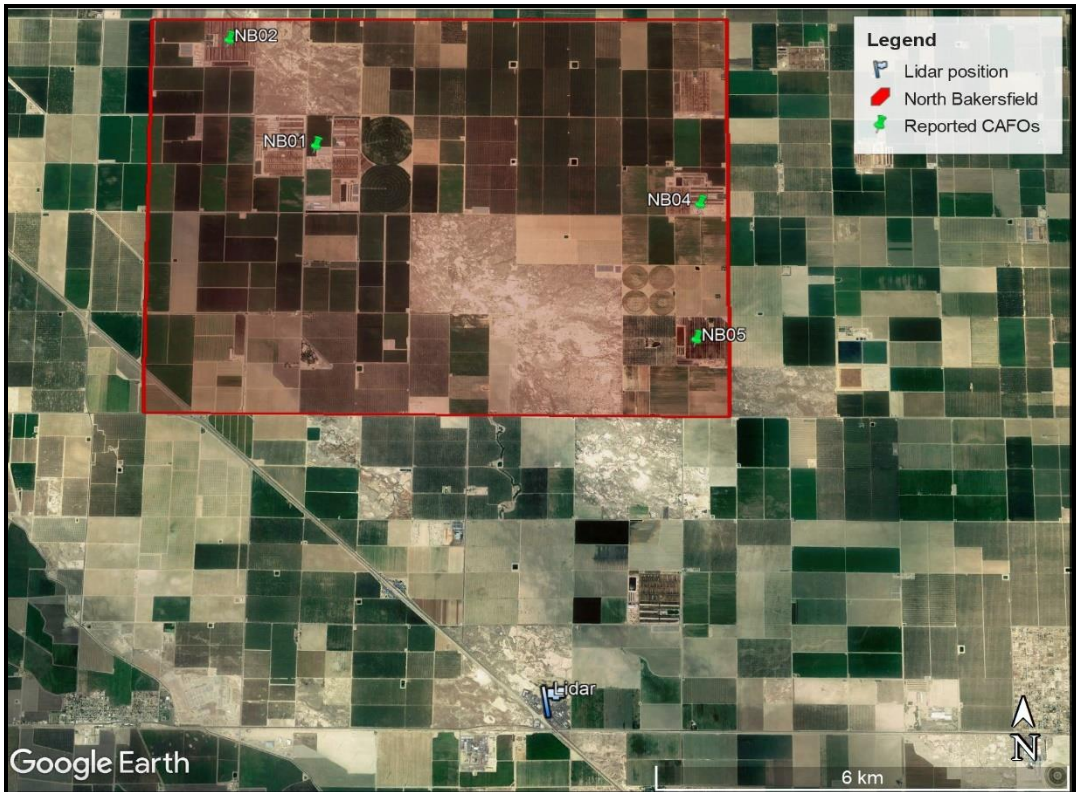

Figure - 7: Survey farms in the North Bakersfield (NB) area.

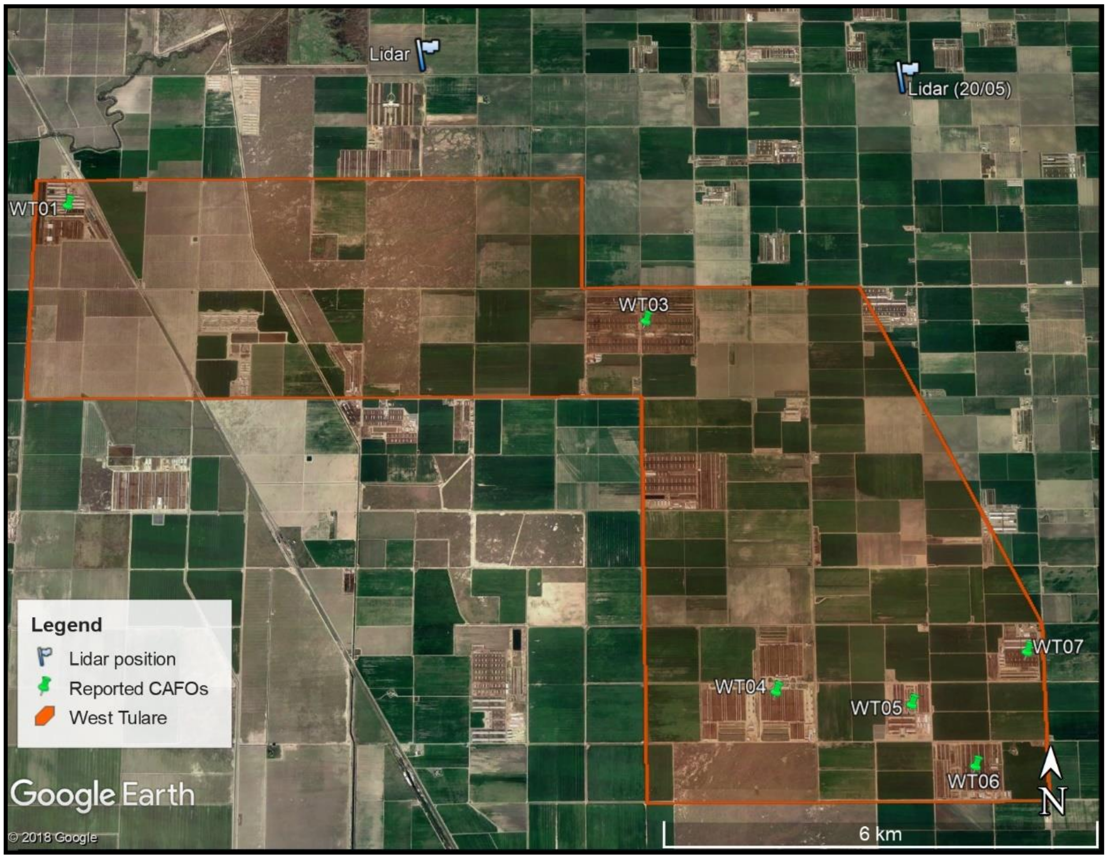

Figure - 8: Survey farms in the West Tulare (WT) area.

Figure - 9: Survey farms in the East Tulare (ET) area.

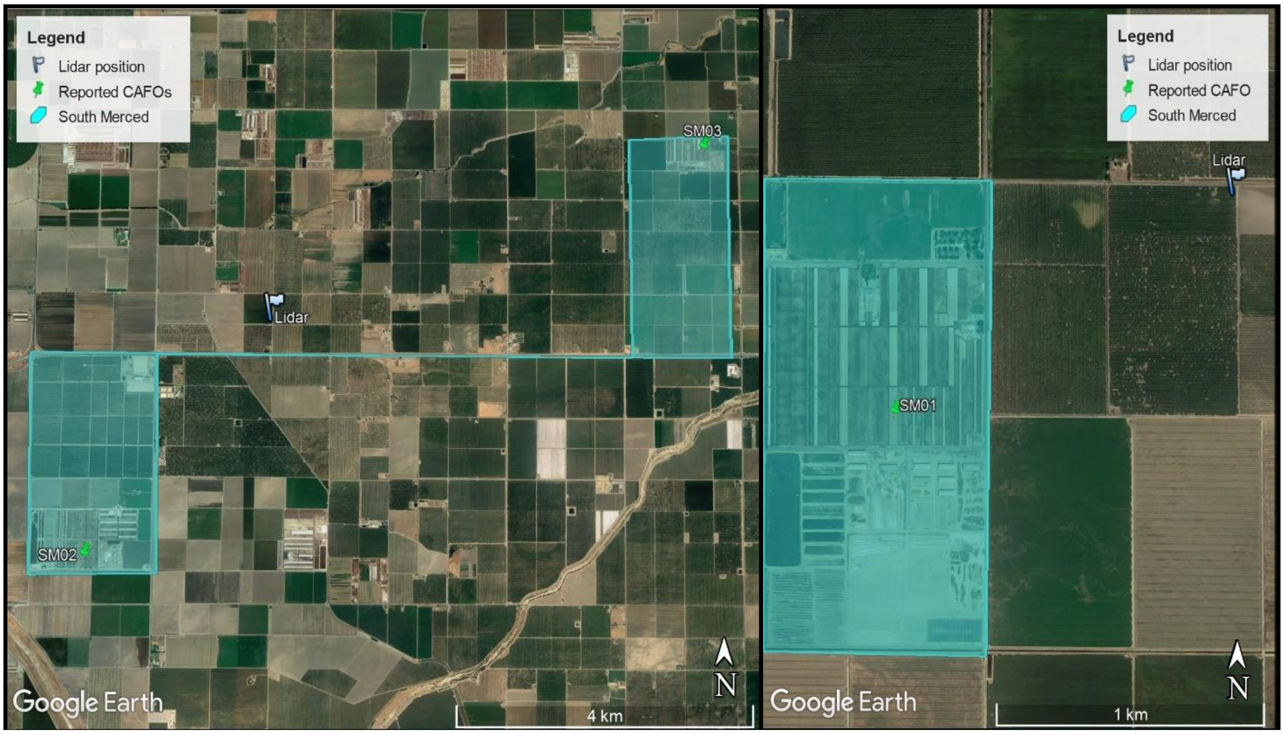

Figure - 10: Survey farms in the South Merced (SM) area.

Table - 4: Measurement days carried out during the campaign. Multiple LIDAR locations on one day separated by the / character.

| Date | Wind LIDAR location | Survey area |
|---|---|---|
| 07-May-2019 | Old river Rd & Herring Rd /<br>Hwy 5 & 58 (@Starbucks) | South Bakersfield/<br>North Bakersfield |
| 09-May-2019 | Hwy 5 & 58 (@Starbucks) | North Bakersfield |
| 13-May-2019 | Old river Rd & Herring Rd | South Bakersfield |
| 14-May-2019 | Old river Rd & Herring Rd | South Bakersfield |
| 20-May-2019 | Rd 88 & Ave 144 | West Tulare |
| 21-May-2019 | E. Academy Avenue & N Mountain View St | East Tulare |
| 23-May-2019 | Avenue 144, 3.7 miles E of Central Valley Hwy | West Tulare |
| 24-May-2019 | Rd 188 & Rd 180/<br>Ave 192 & Rd 128/<br>Avenue 144, 3.7 miles E of Central Valley Hwy | East Tulare/West Tulare |
| 25-May-2019 | Avenue 17 & in between Rd 16 and Rd 15 /<br>Rd 5 & Ave 152 | South Merced |
| 28-May-2019 | Rd 5 & Ave 152 | South Merced |
| 29-May-2019 | Ave 192 & Rd 128/<br>Avenue 144, 3.7 miles E of Central Valley Hwy | East Tulare/West Tulare |

## 5.2. Wind Measurements

For the CAFO's measurements analysis, a wind LIDAR was used as the main wind data source. It was generally assumed that average wind data between ground and to a certain plume mixing height were a good representation for the plume speed and travel direction. The plume mixing height was obtained by either assumption about the vertical mixing (~0.5 m/s) or by combining column and ground concentration measurements, see next section.

San Joaquin valley topography affects the wind conditions and in the Bakersfield area, northwesterly winds are prevalent during the whole year. Therefore, all the measurements in Bakersfield during this survey had NW wind direction. Winds were also characterized mainly light breeze winds (2-4 m/s). Figure - 11 and Figure - 12a show the wind profile for May 13th in the Bakersfield area.

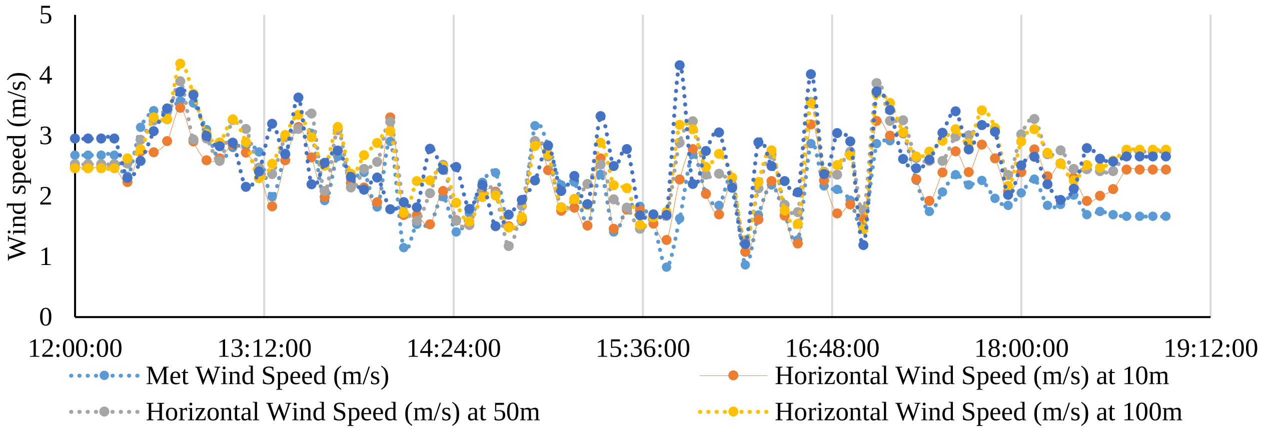

Figure - 11: Wind speed profile for different heights on May 13th, in the Bakersfield area.

In the Tulare and Merced areas, however, not all the days followed the same northwesterly wind pattern and there was an occurrence of moderate breeze. Figure - 13 and Figure - 12b show the measured wind profiles in Tulare for May 24.

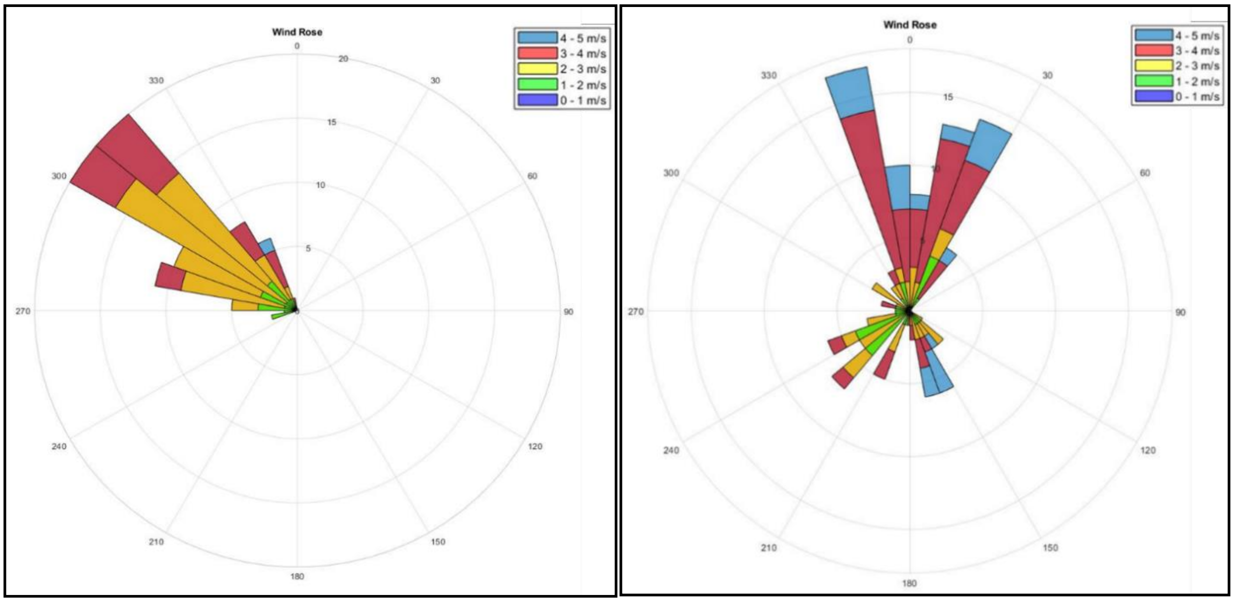

Figure - 12: Wind rose for wind measurements at 100m above ground (a) May 13th, Bakersfield (b) May 24th, Tulare.

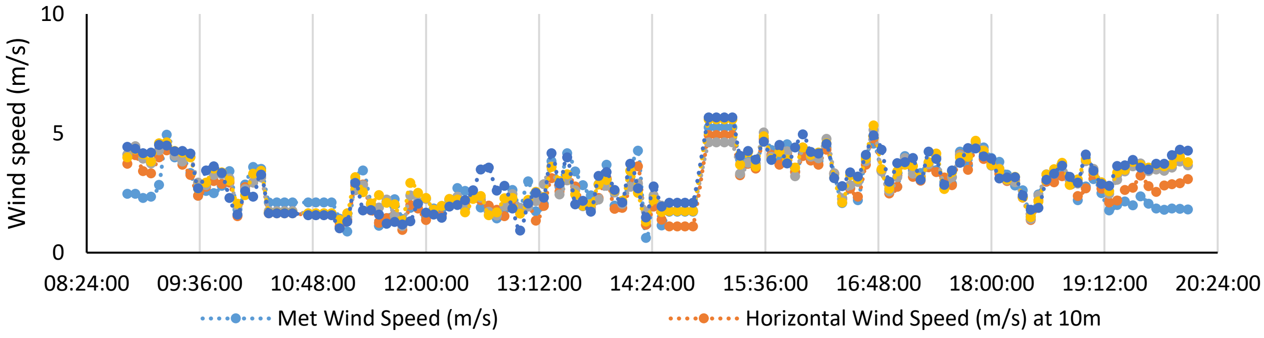

Figure - 13: Wind speed profile for different heights on May 24th, Bakersfield area. The straight-line periods correspond to the LIDAR being shut off for transport between different locations.

### 5.3. Plume height estimation and flux calculation sensitivity

An additional parameter used in the analysis is the plume height. The height of the plume influences which wind speed and direction to apply in the flux calculation. A first-order estimate of the plume mixing height can be retrieved from simultaneous ground concentration measurements and SOF column measurements. The method assumes a homogenous and uniformly distributed plume from ground level to the top of the plume i.e. zero above, and results are used to indicate if the plume is close to ground or aloft. Figure - 14 shows results for the plume height measurements at the different sources and the upper end of the plume (vertical extent) is shown. Another approach is to estimate the plume height by assuming a vertical mixing speed and then calculating the plume height from the plume transport time from the source to the SOF measurement position. Here a vertical mixing speed of 0.5 m/s was used based on LIDAR measurements.

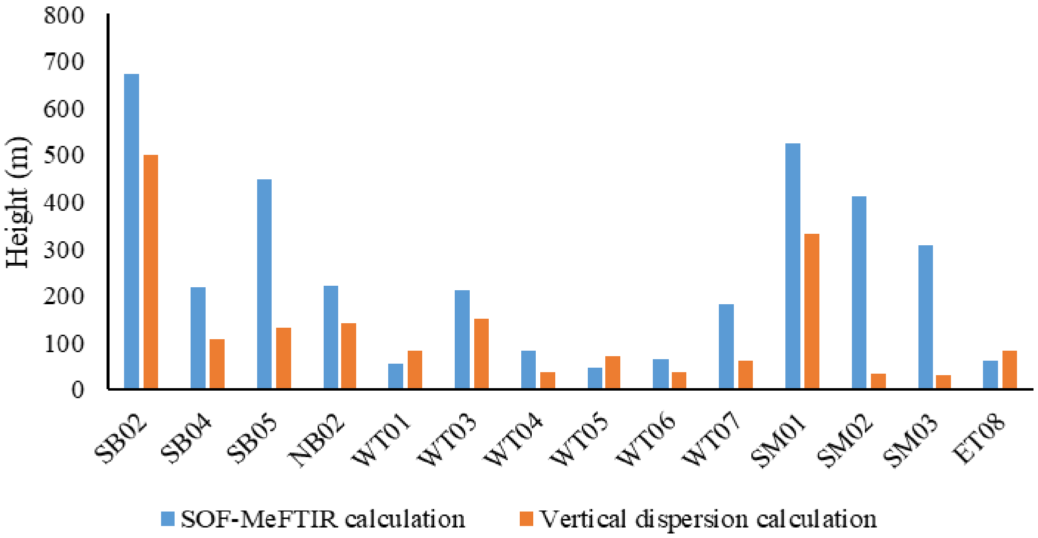

Figure - 14: “Plume height” estimation, used to indicated if the plume is aloft or confined closer to ground.

For some CAFOs the results between the both approaches diverge, but for most locations they follow the same indicative pattern. For the cases SM02 and SM03 wind conditions were atypical, having a moderate breeze at the measurement day, which might have led to reduced ground concentrations due to a more effective dispersion.

Based on these results the average wind from 0-50 m was used for the farms with close to 50 meters plume height estimates, e.g. WT05, ET08, and SM02. For the other farms, mainly winds from 0-100m meters were used. For SB02 and SM01, which were farms at more than 2 km distance from the measurement road, the height of 0-300m was used. Wind attribution for the concentration mapping and ratio measurements is less critical as compared to for the flux estimation, and are important only for source attribution and visualization.

To assess the sensitivity of the flux calculations to deviations from the assumed plume mixing height, wind LIDAR data (5 min average) have been compared for several height intervals. For the entire measurement period and all LIDAR locations, the wind speed average from 0 – 300 m was slightly higher (11.7%) than the wind profile from 0 – 50 m (Figure - 15). The wind direction also had a good correlation between both heights. In other farms, winds ranging from 0-100 m or 0-50 m were also utilized. Even the 0 - 50 m winds differed only slightly from the 0 – 100 m winds with wind speed being a 10 % lower. Wind direction still showed good correlation. These results, with the observed plume being aloft rather than confined close to ground, indicate that uncertainties in the plume height should have only a small effect on the measured fluxes applying the SOF method.

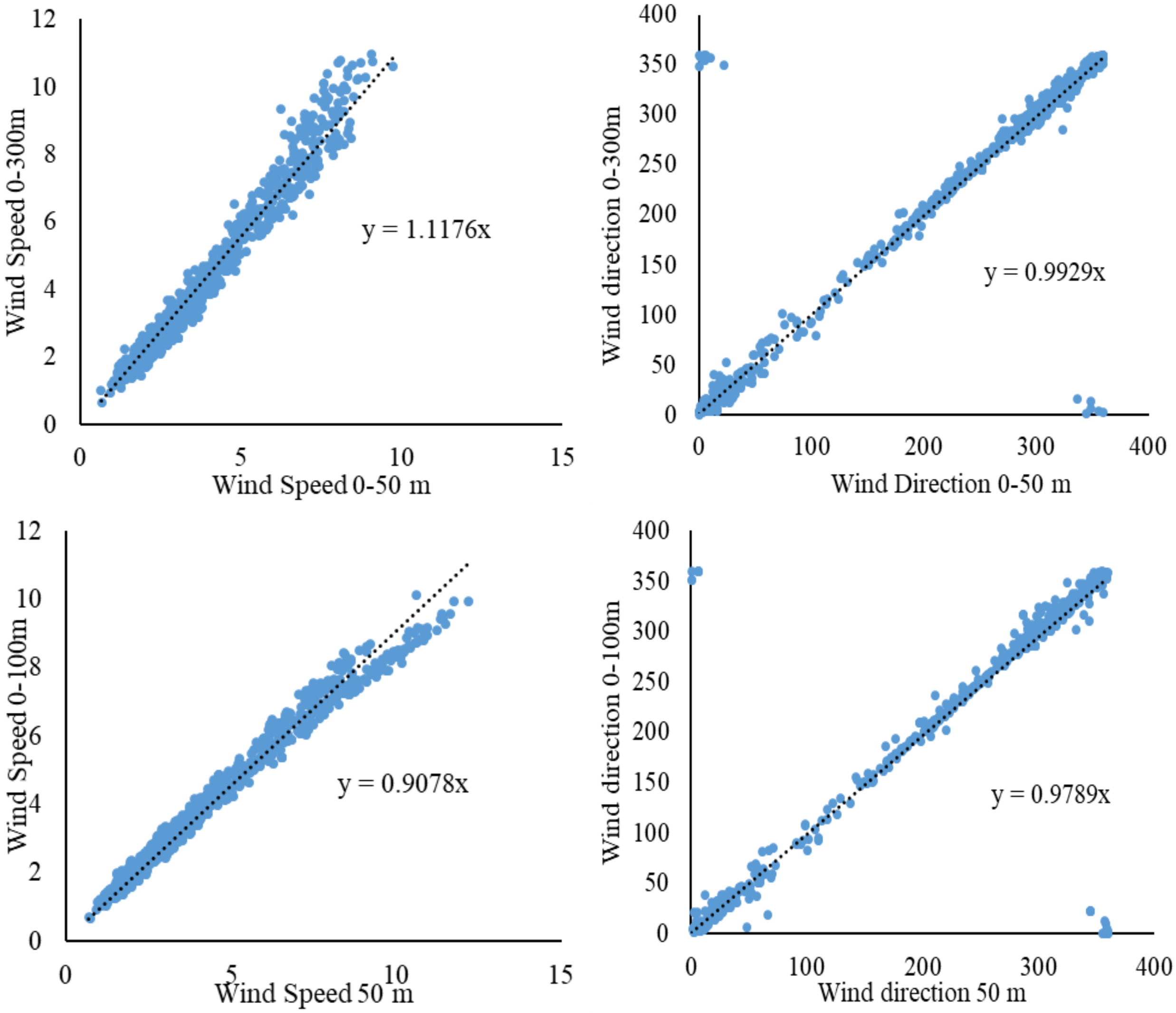

Figure - 15: Correlation of wind profiles ranging different heights for all the measurement days.

## 6. Results

Quantitative results for the emission measurements are divided between the main measurement areas, i.e. the sections 6.1, 6.2 and 6.3 for Bakersfield, Tulare and Merced regions, respectively. Section 6.4 is dedicated to measurements of additional farms which had a limited number of measurement transects, and the last section 6.5 comprises excluded or inconclusive results.

The emission of **ammonia** was measured directly using SOF, while mass concentration ratios of methane to ammonia were obtained using MeFTIR at the fence-line of the sites. These plume mass ratios were combined with the ammonia emission measurements by SOF to obtain indirect emission estimates of methane. The ammonia emissions ranged from 17.3 kg/h to 166 kg/h (Table - 5) for individual farms. These emissions scale with the dairy farm size but also to activities in each farm, and in some cases biases were possibly caused by stronger wind speeds. The emissions from the CAFOs may include contributions from adjacent fields within the measurement perimeter.

For the **methane,** a higher uncertainty is obtained compared to the ammonia results, because they are the result of combining two measurements – the SOF ammonia flux multiplied with the plume concentration ratio of methane to ammonia, see section 4.

**Nitrous oxide** is a gas associated with agricultural sources, both livestock production and soil fertilization. In this survey, $N_2O$ was observed a couple of times with fertilized soils being the apparent source. Significant concentrations of **ethanol** were found on three farms, possibly coming from feed operations. **Acetic acid** was also found in one of the farms together with ethanol and it will be discussed in section 6.2.1.

Measurements by MWDOAS did not indicate any clear aromatic gas plumes and there was no evidence of continuous **BTEX** emissions above the detection limit from the CAFOs. A slight enhancement of **para-cresol** was observed at a few farms, which is a known compound related to farm smell.

The SkyDOAS showed plumes of **$NO_2$** that were well correlated with one of the farms, however, the source origin is unknown.

The nomenclature for emission and concentration graphs in the following result section are described in the caption for Figure - 18.

Table - 5: Survey summary of measured emission data for the included CAFOs. **Limited number of samples* – not included in the summary statistics or summary graphs.

| CAFO | N transects $NH_3$ | $NH_3$ (kg/h) | 95% CI (kg/h) | N transects $CH_4$ | $CH_4$ (kg/h) | SD (kg/h) | $NH_3$ : ETOH (%) | 95% CI (%) | $NO_2$ (kg/h) | 95% CI (kg/h) |
|---|---|---|---|---|---|---|---|---|---|---|
| **SB02** | 7 | 106.8 | 67.7-145.8 | 3 | 547.5 | 224.9 | | | | |
| **SB03** | 9 | 119.7 | 72.6-167 | 3 | 384.6 | 204.5 | | | | |
| **SB04** | 10 | 61.4 | 42.3-80.4 | 9 | 214.2 | 148.8 | | | | |
| **SB05** | 8 | 113.5 | 80.2-152 | 9 | 514.0 | 298.7 | | | 23.5 | 15.7-31.3 |
| **NB01** | 7 | 69.8 | 17-122 | 5 | 391.9 | 380.8 | | | | |
| **NB02** | 9 | 104.0 | 61-147.3 | 4 | 675.4 | 456.0 | | | | |
| *NB04** | *4* | *79.4** | *32.6-126.2* | *6* | *255.0** | - | | | | |
| *NB05** | *4* | *101.9** | *1.5-205* | *4* | *344.0** | - | | | | |
| **WT01** | 14 | 70.8 | 48.2-93.5 | 14 | 196.1 | 165.2 | 26.7 | 21.9-31.5 | | |
| **WT03** | 9 | 157.7 | 121-193 | 11 | 388.6 | 194.5 | | | | |
| **WT04** | 7 | 191.5 | 120-263 | 7 | 482.8 | 230.8 | 36.2 | 22.5-49.8 | | |
| **WT05** | 6 | 70.3 | 29.4-111 | 8 | 304.3 | 191.6 | *45.5** | 0-137 | | |
| **WT06** | 6 | 120.8 | 56.9-184.6 | 6 | 259.5 | 192.9 | | | | |
| **WT07** | 8 | 67.0 | 51-83 | 10 | 415.1 | 200.2 | | | | |
| **ET01** | 7 | 31.9 | 20.2-43.5 | 11 | 187.8 | 124.9 | | | | |
| *ET03** | *3* | *17.7** | *39.6-80.4* | *4* | *35.0** | - | | | | |
| *ET05** | *4* | *20.2** | *2.8-37.6* | *8* | *213.0** | - | | | | |
| *ET07** | *3* | *28.1** | *0-67.9* | *4* | *262.0** | - | | | | |
| **ET08** | 7 | 60.0 | 48.2-71.8 | 7 | 292.6 | 134.5 | | | | |
| **SM01** | 7 | 166.0 | 127-204 | 6 | 527.2.6 | 140.4 | | | | |
| **SM02** | 13 | 142.2 | 104-180 | 13 | 844.8 | 451.1 | | | | |
| *SM03** | *4* | *17.3** | *6.8-27.73* | *6* | *219.0** | - | | | | |
| ***Sum*** | ***134*** | ***1653.4*** | | ***126*** | ***6626.4*** | | | | ***23.5*** | |
| ***Average*** | ***8.4*** | ***103.3*** | | ***7.9*** | ***414.1*** | ***180.8*** | ***36.1*** | | ***23.5*** | |
| ***Median*** | ***7.5*** | ***105.4*** | | ***7.5*** | ***390.3*** | | ***36.2*** | | ***23.5*** | |

Figure - 16 shows a box plot of the ammonia emissions from the reported farms. The graph shows the minimum value observed, 25th percentile, median, mean (“X”), 75th percentile, maximum and individual data points (circles).

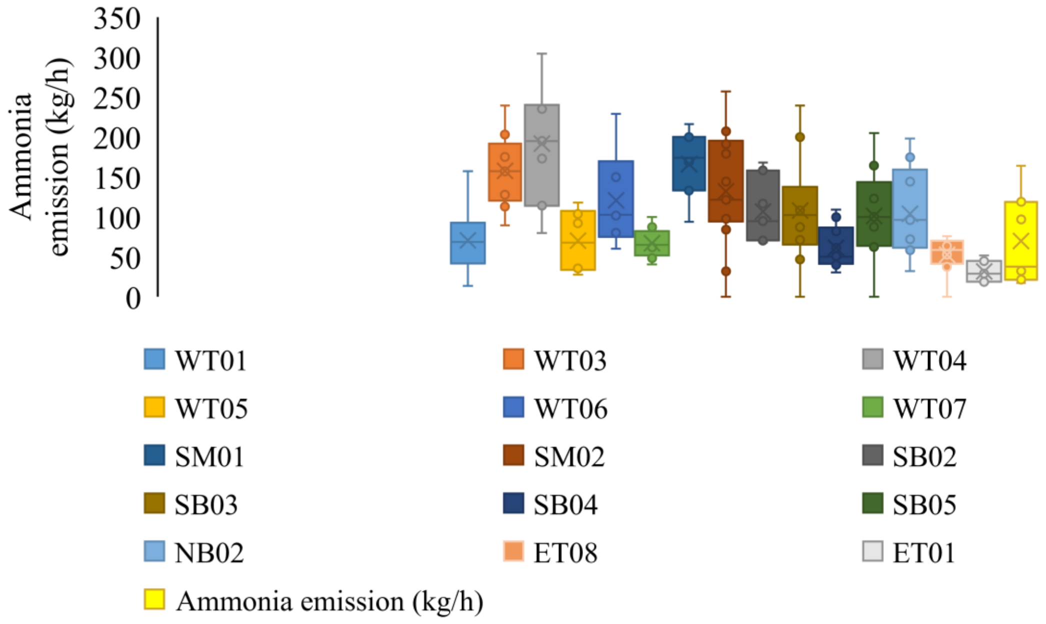

Figure - 16: Overview of ammonia fluxes obtained with SOF. Displayed parameters: the minimum value, 25th percentile, median, mean, 75th percentile, maximum and individual values (circles).

Figure - 17 shows the ammonia to methane ratios, from which the indirect fluxes of methane were calculated together with the data in Figure - 16. The mass ratios are shown as a histogram with frequency on the Y-axis and the $NH_3$:$CH_4$ mass ratio intervals on the X-axis.

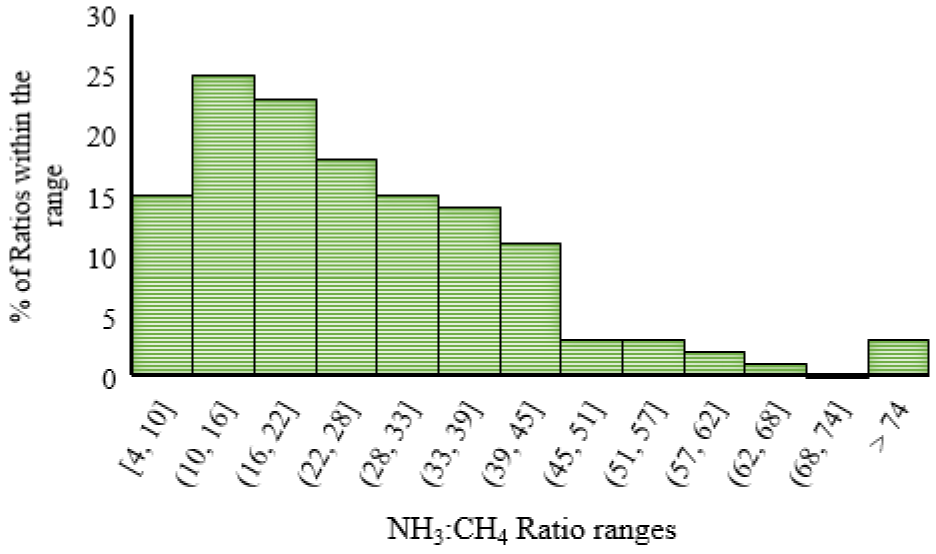

Figure - 17: Histogram of the $NH_3$:$CH_4$ ratios from all farms using MeFTIR.

It can be noted that the mass ratio is lower than 33 % in at least 60 % of the measurements and less than 45 % in about 90 % of the observations - the extreme cases will be discussed later. Due to the prevailing wind conditions, the Bakersfield farms were always measured on the same road and from the same distance. In the other areas, more varying wind speeds and directions allowed measurements from other roads and distances.

## 6.1. CAFOs in the Bakersfield region

Bakersfield area measurements were divided into two subareas, one to the north and one to the south of the city. The measurements were conducted on four days (7, 9, 13 and 14 of May) with good sunny conditions during most of the day and light northwesterly winds. The ammonia emissions of seven CAFOs were obtained.

### *6.1.1. Farm SB02 (South Bakersfield)*

Ammonia emissions from CAFO SB02 were measured on 3 separate days, with a median emission of 95 kg/h (Table - 6). Figure - 18 shows a typical SOF measurement of farm SB02. The farm occupies a large area (1.4 km$^2$) and is operating with open anaerobic lagoons (no cover in place). The mass ratios were measured at a far distance, with approximately 2.3 km from the center of the farm to the measurement roads. Methane emissions were 547 kg/h on average (Table - 7). The methane quantification has a larger uncertainty because it consists of only three transects for the ratios.

Table - 6: Ammonia emissions measured at farm SB02. *Limited number of samples.

| Day [yymmdd] | Time span [hhmmss-hhmmss] | N transects | Emission±SD (kg/h) | Wind speed Min-Max [m/s] | Wind Dir Span [deg] |
|---|---|---|---|---|---|
| **190507** | 114939 -140103 | 4 | 87.7±22.7 | 1.5-2.1 | 305-332 |
| **190513*** | 125512 -130104 | 1 | 168.4 | 3.0 | 319 |
| **190514** | 143550 -152434 | 2 | 114.7±61.4 | 1.9-2.5 | 304-354 |
| **Total # of Meas.** | - | 7 | | | |
| **Median** | | | 94.8 | | |
| **Mean** | - | | 107.0 | - | - |
| **SD** | | | 42.2 | | |
| **95% CI** | | | 67.7-145.8 | | |

Table - 7: $NH_3$:$CH_4$ mass ratio measurements at farm SB02.

| Day [yymmdd] | Timespan [hhmmss-hhmmss] | N transects | Mass Ratio avg ± SD [%] | Wind Speed (m/s) | Wind Dir (deg) | IME $CH_4$ (kg/h) |
|---|---|---|---|---|---|---|
| **190507** | 115050-131947 | 3 | 19.5 ± 2.2 | 1.2-2.1 | 307-352 | |
| **Total # of meas.** | - | **3** | | | | |
| **Median** | - | | 18.5 | | | 512.4 |
| **Mean** | | | 19.5 | | | 547.5 |
| **SD** | | | 2.2 | | | 224.9 |
| **95% CI** | | | 14.1-24.9 | | | |

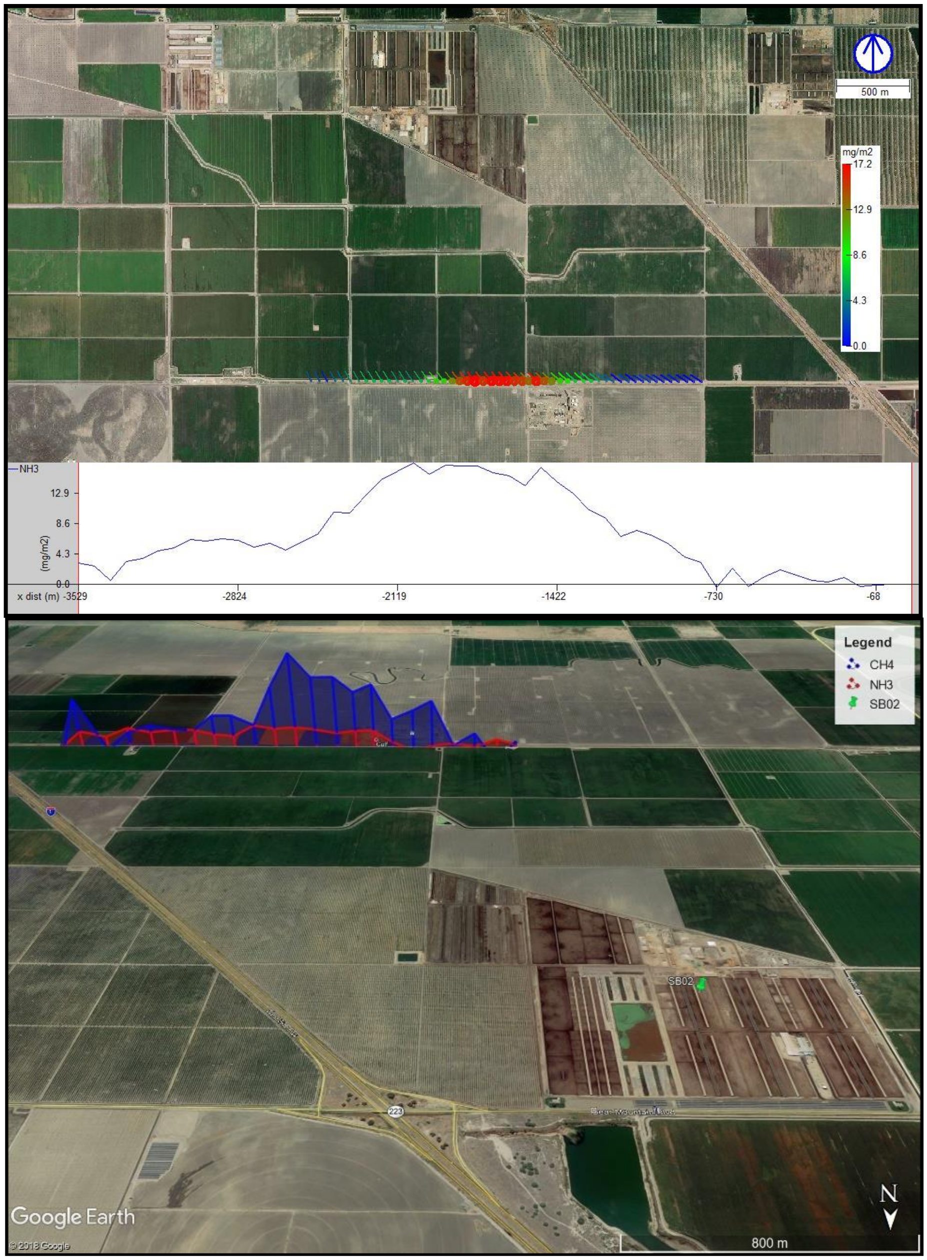

Figure - 18: South Bakersfield CAFO SB02, (Upper) the Ammonia column obtained from SOF, color coded and shown as a diagram below the 2D map.The lines are pointing against the wind. North indicated by the blue arrow, e.g. upward. (Lower) $NH_3$ and $CH_4$ concentrations (MeFTIR), where the height of the curve scales with measured concentration. North indicated by the white arrow and N, e.g. downward.

### *6.1.2. Farm SB03 (South Bakersfield)*

The farm SB03 was measured on three different days. All the ammonia flux measurements were done by “boxing” the farm as showed in Figure - 19, and therefore excluding the contribution of the nearby farms. Median ammonia emissions were 108 kg/h (Table - 8). Concentration plumes measured upwind of the dry lots area, were associated with the digester/lagoons area, and these contained significantly more methane and thus were excluded from the calculation because they do not represent the whole farm contribution. Concentration ratios on the downwind side were, however, more difficult to distinguish from its source, resulting in fewer measurements. The ammonia to methane ratios were around 33%, resulting in methane emissions of 384 kg/h (Table - 9). The farm has a cover system for the anaerobic lagoon, which is intended to reduce methane emissions.

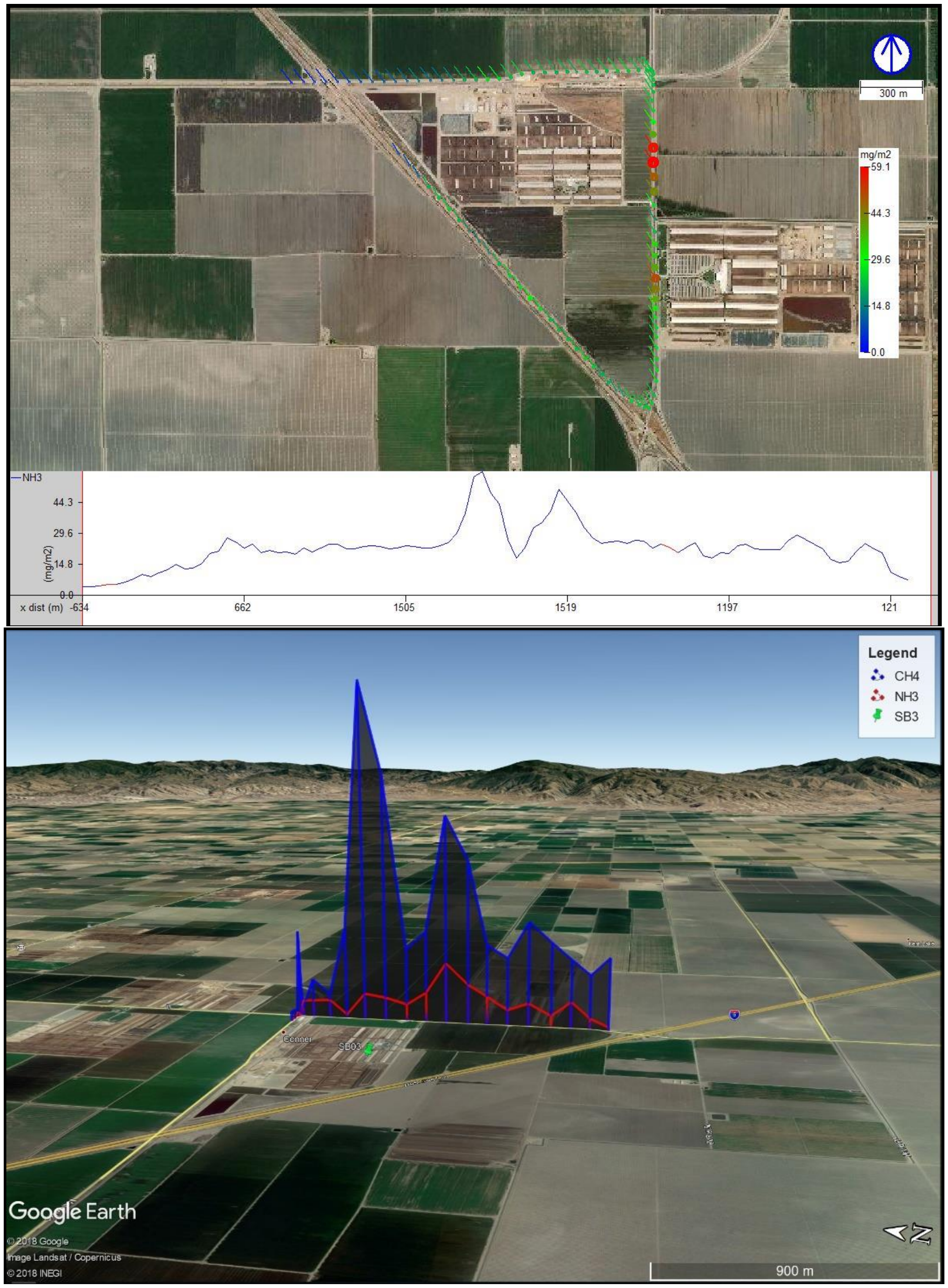

Figure - 19: South Bakersfield CAFO SB03, (Upper) Ammonia column, SOF; (Lower) $NH_3$ and $CH_4$ concentrations, MeFTIR.

Table - 8: Ammonia emissions measured at farm SB03, SOF. *Limited number of samples.

| Day [yymmdd] | Time span [hhmmss-hhmmss] | N transects | Emission±SD (kg/h) | Wind speed Min-Max[m/s] | Wind Dir Span [deg] |
|---|---|---|---|---|---|
| **190507** | 115456 -154659 | 4 | 72.5±17.6 | 1.8-3.0 | 6-328 |
| **190513** | 124516 -165853 | 4 | 167.4±64.5 | 1.8-2.9 | 311-333 |
| **190514*** | 174624 -175129 | 1 | 97.3 | 3.0 | 323 |
| **Total # of Meas** | - | 9 | | | |
| **Median** | | | 108 | | |
| **Mean** | - | | 119.7 | - | - |
| **SD** | | | 61.4 | | |
| **95% CI** | | | 72.6-166.9 | | |

Table - 9 :$NH_3$:$CH_4$ Ratio measurements at farm SB03, MeFTIR.

| Day [yymmdd] | Timespan [hhmmss-hhmmss] | N transects | Mass Ratio avg ± SD [%] | Wind Speed (m/s) | Wind Dir (deg) | IME $CH_4$ (kg/h) |
|---|---|---|---|---|---|---|
| **190507** | 124543-144653 | 3 | 31.1 ± 4.4 | 1.3-2.7 | 256-315 | |
| **Total # of meas** | - | **3** | | | | |
| **Median** | - | | 30 | | | 360.0 |
| **Mean** | | | 31,1 | | | 384.6 |
| **SD** | | | 4.4 | | | 204.5 |
| **95% CI** | | | 20.2-42.1 | | | |

### *6.1.3. Farm SB04 (South Bakersfield)*

The dairy SB04 was measured on the same days as the previously described farm, with a resultant median ammonia emission of 50.2 kg/h (Figure - 20, Table - 10). For the ratios, however, unusual measurements were detected on May 14th. At the start of the measurements, the ammonia to methane ratio was 300%, indicating a large amount of ammonia concentration on the ground. By the end of the measurements, the ratio reduced to 30%, Figure - 21. On the contrary, the ammonia fluxes had the same average as the previous days. These could be a result of non-ordinary activities, even though nothing atypical was observed while driving. Consequently, for the methane estimation, the only reliable ratios were the ones measured on the previous days, three transects (Table - 11), and therefore the uncertainty of the methane emission value is high. Methane flux was 214 kg/h.

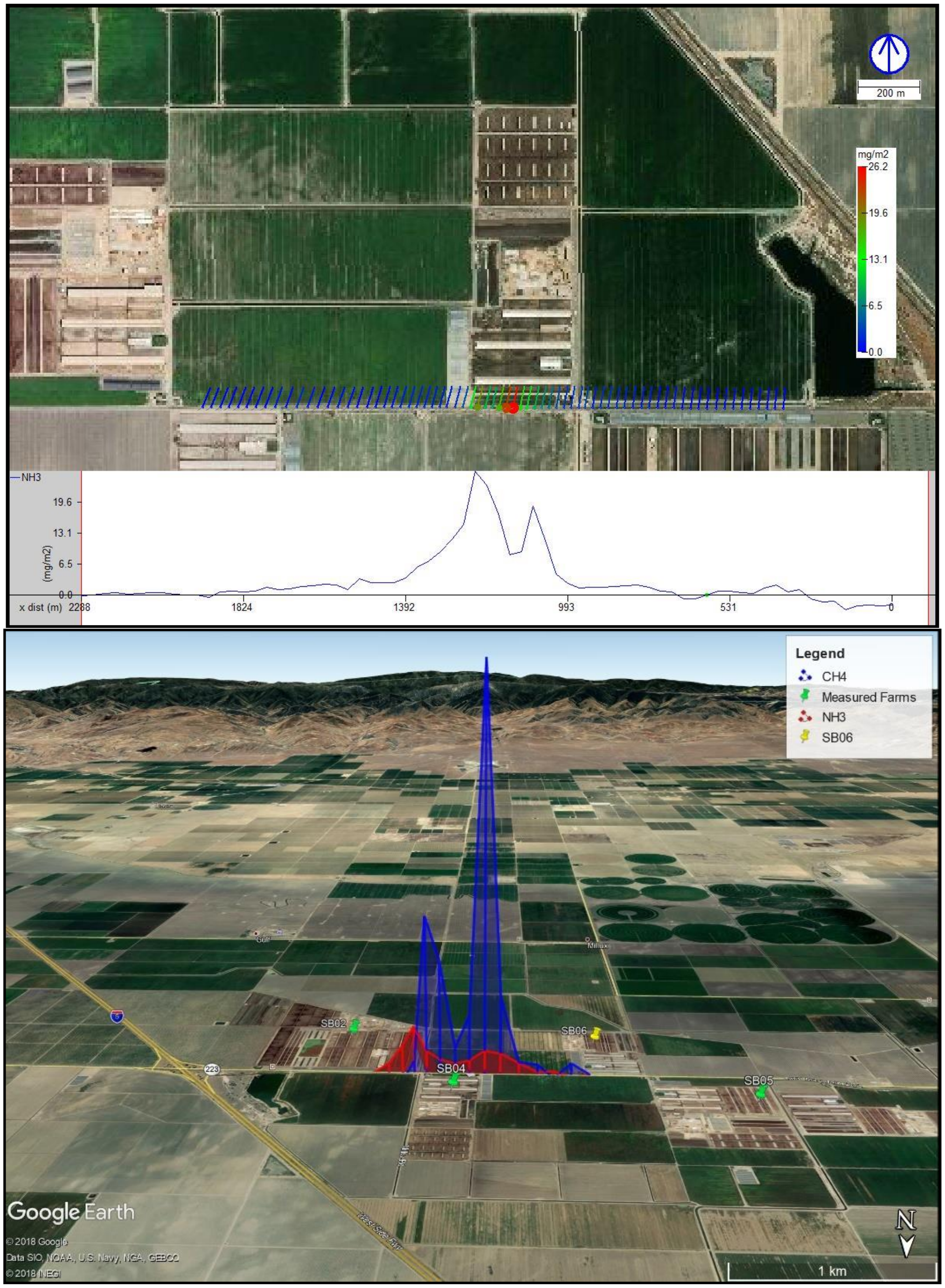

Figure - 20: South Bakersfield CAFO SB04, (Upper) Ammonia column, SOF; (Lower) $NH_3$ and $CH_4$ concentrations, MeFTIR.

Table - 10: Ammonia emissions measured at farm SB04, SOF. *Limited number of samples.

| Day [yymmdd] | Time span [hhmmss-hhmmss] | N transects | Emission±SD (kg/h) | Wind speed Min-Max[m/s] | Wind Dir Span [deg] |
|---|---|---|---|---|---|
| **190507** | 120739 -142359 | 4 | 61.8±31.8 | 1.5-2.5 | 1-352 |
| **190513** | 132110 -132429 | 1 | 82.2 | 3.0 | 354 |
| **190514*** | 133717 -160444 | 5 | 56.8±26.5 | 1.8-3.3 | 4-343 |
| **Total # of Meas** | - | 10 | | | |
| **Median** | | | 50.2 | | |
| **Mean** | - | | 61.4 | - | - |
| **SD** | | | 26.6 | | |
| **95% CI** | | | 42.3 – 80.4 | | |

Table - 11: $NH_3$:$CH_4$ Ratio measurements at farm SB04, MeFTIR. *Limited number of samples.

| Day [yymmdd] | Timespan [hhmmss-hhmmss] | N transects | Mass Ratio avg ± SD [%] | Wind Speed (m/s) | Wind Dir (deg) | IME $CH_4$ (kg/h) |
|---|---|---|---|---|---|---|
| **190507** | 120834-125528 | 2 | 18.2±8.7 | 2.2-2.5 | 3-334 | |
| **190513*** | 132145-132336 | 1 | 14.2 | 3.0 | 334 | |
| **190514** | 133846-175748 | 3 | 40.5±12.1 | 2.5-4.0 | 4-321 | |
| **Total # of meas.** | - | **9** | | | | |
| **Median** | - | | 27.2 | | | 184.6 |
| **Mean** | | | 28.7 | | | 214.2 |
| **SD** | | | 15.5 | | | 148.8 |
| **95% CI** | | | 12.3-45 | | | |

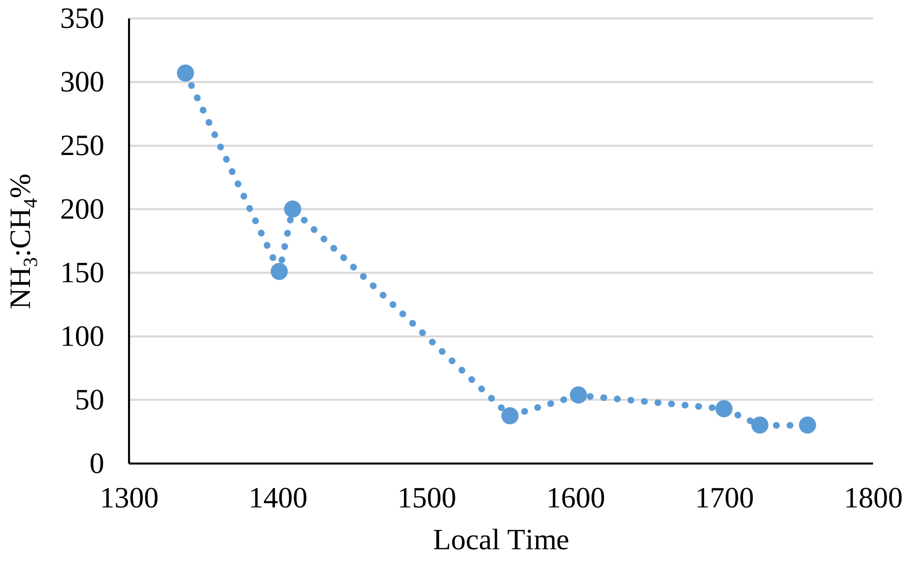

Figure - 21: $NH_3$:$CH_4$ ratios at CAFO SOB04 on May 14th.

### *6.1.4 Farm SB05 (South Bakersfield)*

Two days of measurements on farm SB05 showed an ammonia emission of 100 kg/h (Figure - 22a, Table - 12). This area included two smaller facilities that together cover an area of 1.14 km$^2$, and in one of the dairies, there is a digester. For the ratios (Figure - 22b), an average of 26% was obtained. Methane emissions were 382 kg/h (median) and 514 kg/h on average (Table - 13). Nitrous oxide ($N_2O$) emissions were also apparent (Figure - 22b). Plumes of $NO_2$ (Figure - 22c and Table - 14) were detected on this farm, even though the plumes are well correlated with the facility is not completely clear that the facility is a source of $NO_x$. This emission may be attributed to combustion sources, such as a biogas digester, or to biological emission from upwind of the facility.

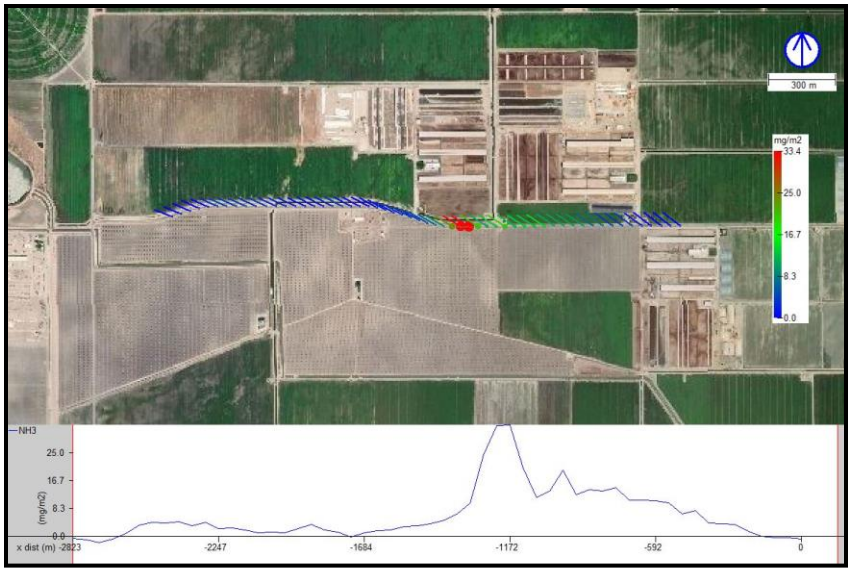

(a)

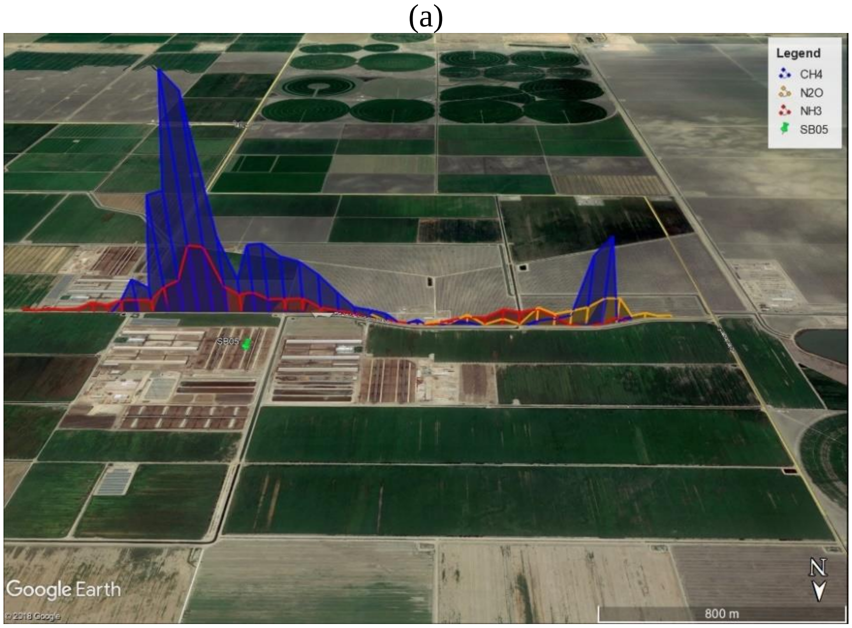

(b)

(c)

Figure - 22: South Bakersfield CAFO SB05, (a) Ammonia column, SOF; (b) $NH_3$, $CH_4$, and $N_2O$ concentrations, MeFTIR (c) $NO_2$ column, SkyDOAS.

Table - 12: Ammonia emissions measured at farm SB05, SOF.

| Day [yymmdd] | Time span [hhmmss-hhmmss] | N transects | Emission±SD (kg/h) | Wind speed Min-Max[m/s] | Wind Dir Span [deg] |
|---|---|---|---|---|---|
| **190507** | 121126 -142140 | 3 | 129.5±32.2 | 1.6-2.3 | 4-320 |
| **190514** | 134113 -160949 | 5 | 104.4±58.7 | 1.8-3.5 | 9-307 |
| **Total # of Meas** | - | 8 | | | |
| **Median** | | | 100 | | |
| **Mean** | - | | 113.5 | - | - |
| **SD** | | | 49.2 | | |
| **95% CI** | | | 72.4 – 154.7 | | |

Table - 13: $NH_3$:$CH_4$ Ratio measurements at farm SB05, MeFTIR

| Day [yymmdd] | Timespan [hhmmss-hhmmss] | N transects | Mass Ratio avg ± SD [%] | Wind Speed (m/s) | Wind Dir (deg) | IME $CH_4$ (kg/h) |
|---|---|---|---|---|---|---|
| **190507** | 121217-142142 | 3 | 11.3±3.9 | 1.7-2.3 | 5-329 | |
| **190513*** | 134123-180246 | 7 | 26.7±4.7 | 1.9-3.4 | 8-313 | |
| **Total # of meas** | - | **10** | | | | |
| **Median** | - | | 26.3 | | | 382.9 |
| **Mean** | | | 22.1 | | | 514 |
| **SD** | | | 8.6 | | | 298.7 |
| **95% CI** | | | 16-28.2 | | | |

Table - 14: $NO_2$ fluxes measured at farm SB05, SkyDOAS.

| Day [yymmdd] | Timespan [hhmmss-hhmmss] | N transects | Emission±SD [kg/h] | Wind Speed Min-Max[m/s] | Wind Dir Span [deg] |
|---|---|---|---|---|---|
| **190514** | 134105 -172634 | 7 | 23.5±8.5 | 1.8-3.3 | 8-333 |
| **Total # of Meas** | - | 7 | | - | - |
| **Median** | - | | 24.7 | - | - |
| **Mean** | | | 23.2 | | |
| **SD** | | | 8.4 | | |
| **95% CI** | | | 15.5-30.9 | | |

### *6.1.5 Farm NB01 (North Bakersfield)*

The CAFO NB01 is located north of Bakersfield, and the area consists of two different dairies with a road in between. Because of the northwesterly prevalent winds on this region and the availability of roads, it was only possible to quantify the facility on the same location all times (Figure - 23).

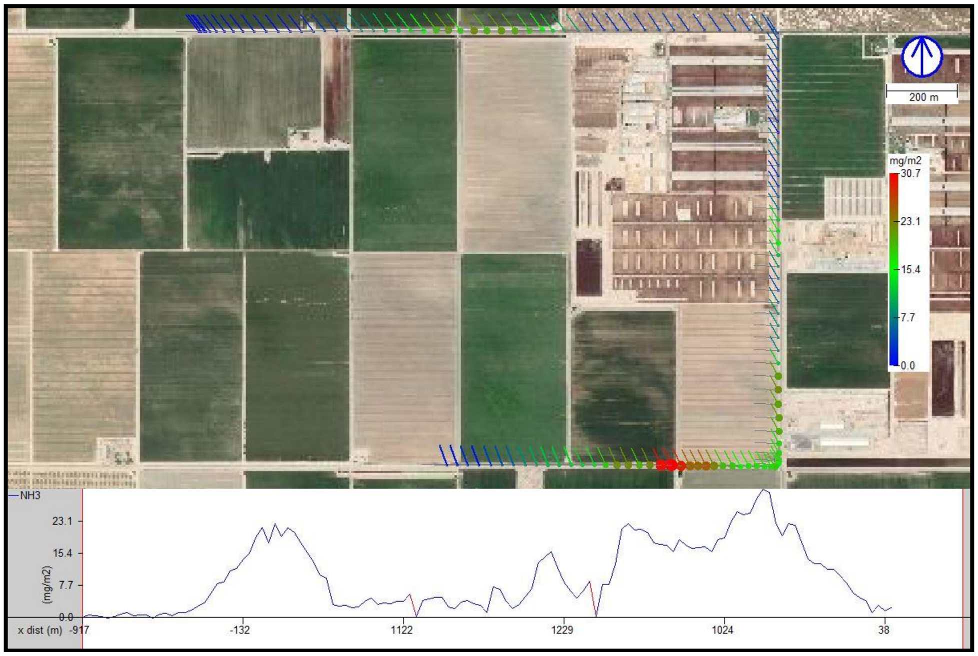

Figure - 23: North Bakersfield CAFO NB01, Ammonia column, SOF.

Table - 15 : $NH_3$:$CH_4$ Ratio measurements at farm NB01, MeFTIR. *Limited number of samples.

| Day [yymmdd] | Timespan [hhmmss-hhmmss] | N transects | Mass Ratio avg ± SD [%] | Wind Speed (m/s) | Wind Dir (deg) | IME $CH_4$ (kg/h) |
|---|---|---|---|---|---|---|
| **190507** | 171416-183403 | 4 | 14.6±8.1 | 2-4.2 | 329-352 | |
| **190509** | 160528-160738 | 1 | 32.2 | 5.7 | 317 | |
| **Total # of meas** | - | **5** | | | | |
| **Median** | - | | 17.6 | | | 214.8 |
| **Mean** | | | 17.8 | | | 391.9 |
| **SD** | | | 11.6 | | | 380.8 |
| **95% CI** | | | 5.9-29.2 | | | |

The median ammonia emission were 38 kg/h (Figure - 23, Figure - 24), with a larger than typical uncertainty (Table - 16). One of the reasons for that might be the higher wind speed on the second day, compared to the first day, which consequently could increase the ammonia flux. For the ratios, 17% ammonia to methane was obtained, resulting in an average methane emission of 392 kg/h (Table - 15). This value is uncertain, and the methane flux obtained when using the median values is 214 kg/h.

Table - 16: Ammonia emissions measured at farm NB01, SOF.

| Day [yymmdd] | Timespan [hhmmss-hhmmss] | N transects | Emission±SD [kg/h] | Wind Speed Min-Max[m/s] | Wind Dir Span [deg] |
|---|---|---|---|---|---|
| **190507** | 170805 -174337 | 2 | 29.9±11.8 | 2.3-3.1 | 329-352 |
| **190509** | 122407 -155557 | 5 | 86.6±60.7 | 3.6-5.4 | 321-343 |
| **Total # of Meas.** | - | 7 | | - | - |
| **Median** | - | | 37.7 | - | - |
| **Mean** | | | 69.8 | | |
| **SD** | | | 57 | | |
| **CI 95%** | | | 17.1-122.6 | | |

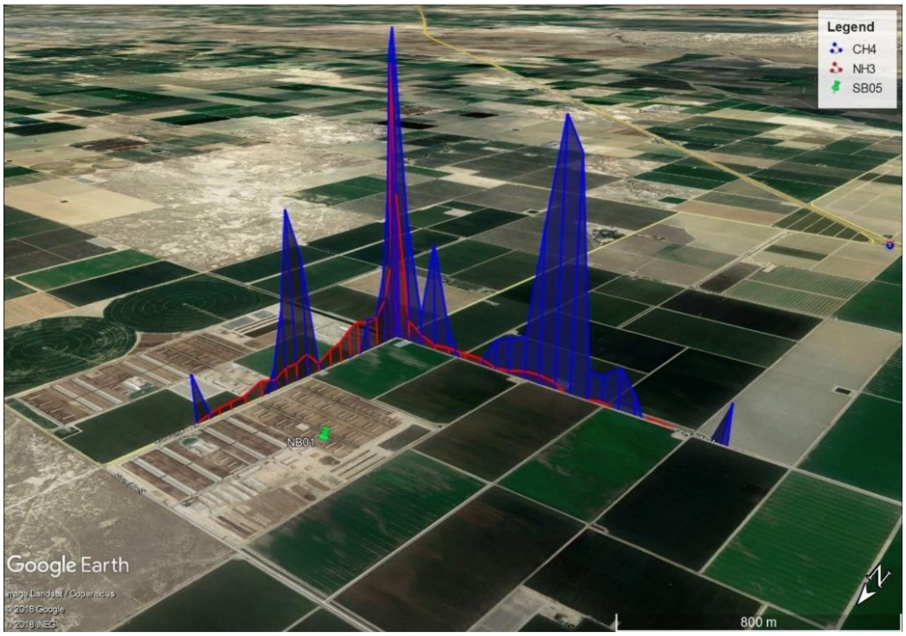

Figure - 24: North Bakersfield CAFO NB01, $NH_3$ and $CH_4$ concentrations, MeFTIR.

### *6.1.6 Farm NB02 (North Bakersfield)*

The dairy NB02 located north from the NB01 facility had a median of 96 kg/h of ammonia (Figure - 25). As for the NB01 measurements, wind speeds and the measured flux was higher on the second day, May 9 (Table - 18). These wind effects will be discussed later in section 7. For the ratios, few measurements were obtained here due to instrument problems. The obtained ratio of 15% were similar to the NB01 farm and this resulted in an average methane emission of 675 kg/h (Table - 17). Once more, these measurements had a high uncertainty, because of the few measurement transects.

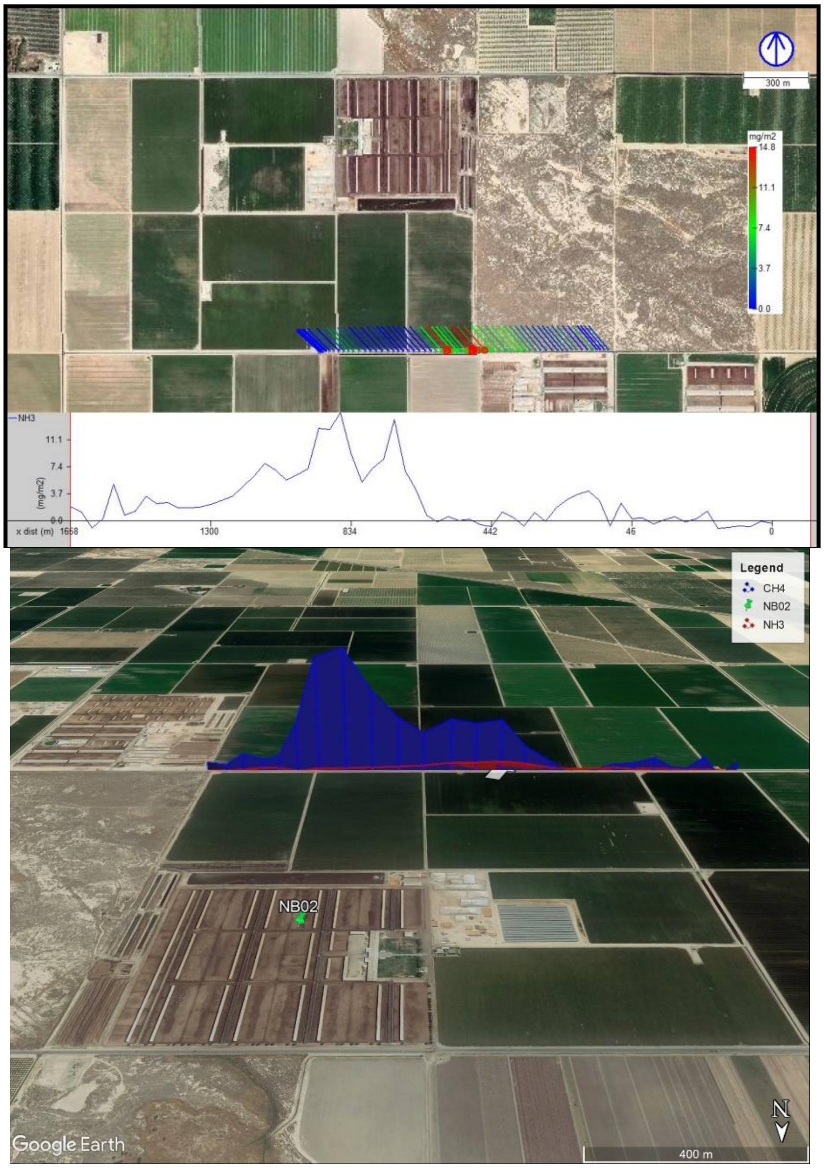

Figure - 25: North Bakersfield CAFO NB02, (Upper) Ammonia column, SOF, (Lower) $NH_3$ and $CH_4$ concentrations, MeFTIR.

Table - 17: $NH_3$:$CH_4$ Ratio measurements at farm NB02, MeFTIR.

| Day [yymmdd] | Timespan [hhmmss-hhmmss] | N transects | Mass Ratio avg ± SD [%] | Wind Speed (m/s) | Wind Dir (deg) | IME $CH_4$ (kg/h) |
|---|---|---|---|---|---|---|
| **190507** | 170354-181801 | 4 | 15.5±6.4 | 2.4-3.9 | 10-328 | |
| **Total # of meas** | - | **4** | | | | |
| **Median** | - | | 14.8 | | | 649.3 |
| **Mean** | | | 15.4 | | | 675.4 |
| **SD** | | | 6.4 | | | 456 |
| **95% CI** | | | 5.5-25.3 | | | |

Table - 18: Ammonia emissions measured at farm NB02, SOF.

| Day [yymmdd] | Timespan [hhmmss-hhmmss] | N transects | Emission±SD [kg/h] | Wind Speed Min-Max [m/s] | Wind Dir Span [deg] |
|---|---|---|---|---|---|
| **190507** | 170222 -175104 | 4 | 62.7±26.2 | 2.3-4.4 | 2-350 |
| **190509** | 121711 -161957 | 5 | 137.2±52.8 | 3.8-6.2 | 313-357 |
| **Total # of Meas** | | 9 | | - | - |
| **Median** | | | 96.1 | - | - |
| **Mean** | | | 104 | | |
| **SD** | | | 56.3 | | |
| **CI 95%** | | | 60.8-147.3 | | |

## 6.2. CAFOs in the Tulare region

Most of the measurements on this campaign were made in Tulare County. This county holds a large number of the dairies in the San Joaquin Valley, with almost 500 thousand dairy cows in 2017 (Monson *et al.*, 2017). For convenience the CAFOs were grouped into West Tulare (WT) and East Tulare (ET). Measurements were made over these two areas for a total of five days. Unlike the period in Bakersfield, there were changing synoptic conditions leading to varying wind direction, as well as periods of rain and persistent cloud cover during the measurement days.

### *6.2.1. Farm WTO1 (West Tulare)*

The WT01 dairy was measured on four days, with one day excluded due to wind inconsistency. The LIDAR was placed five kilometers from the farm. Ammonia emissions were on average 68 kg/h (Table - 19). Due to the layout of the farm (Figure - 26 and Figure - 28) and traversable public roads, it was difficult to measure the ratios from an optimally long distance from the farm. A far sampling distance suppress effects of varying distance (thus varying plume transport time) from the different point sources (such as the digester) within the farm to the sampling location. A too short sampling distance for a widespread farm area can on the other hand lead to bias in the ratio measurements. Care was taken to assure equivalent number of measurements with positive and negative methane bias in the ratio measurements. Similarly, the median is a robust statistic which minimizes the risk of large biases.

The results point to a methane emission of 196 kg/h (Table - 21). Previous measurements by Scientific Aviation found a methane emission of 240 kg/h. Apart from that, the site has a separate composting area south from the facility. The composting area emitted on average 55 kg/h ammonia (Figure - 27). The compost piles were actively being turned during the measurements on May 23. For the ratios in the active composting area, near-field measurements reached 300% of ammonia to methane, while far-field measurements varied from 100 to 30%.

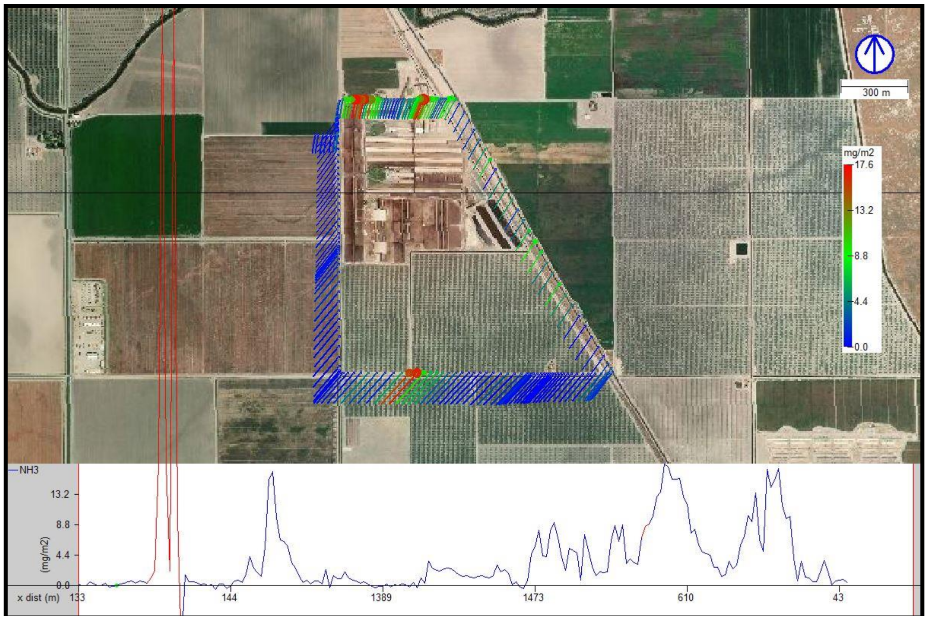

Figure - 26: West Tulare CAFO WT01, Ammonia column, SOF.

Table - 19: Ammonia emissions measured at farm WT01, SOF.

| Day [yymmdd] | Timespan [hhmmss-hhmmss] | N transects | Emission±SD [kg/h] | Wind Speed Min-Max[m/s] | Wind Dir Span [deg] |
|---|---|---|---|---|---|
| **190520** | 130607 -145507 | 4 | 42.6±24.6 | 2.4-3.6 | 288-304 |
| **190523** | 131019 -140823 | 4 | 68.4±23.6 | 3.6-5.2 | 187-214 |
| **190524** | 155346 -165655 | 6 | 91.5±46.4 | 2.8-4.0 | 2-359 |
| **Total # of Meas** | - | 14 | | - | - |
| **Median** | - | | 68.7 | - | - |
| **Mean** | | | 70.8 | | |
| **SD** | | | 39.2 | | |
| **CI 95%** | | | 48.2-93.5 | | |

Table - 20: $NH_3$:Ethanol and $NH_3$:acetic acid ratio measurements for farm WT01, MeFTIR.

| | Ratio $NH_3$: ETOH (%) | Ratio $NH_3$: AACID (%) |
|---|---|---|
| **N meas.** | 7 | 6 |
| **Average** | 26.7 | 175.1 |
| **Median** | 24.5 | 168.5 |
| **SD** | 5.2 | 64.9 |
| **CI 95%** | 21.9-31.5 | 107-243 |

Table - 21: $NH_3$:$CH_4$ Ratio measurements for methane at farm WT01, MeFTIR. *Limited number of samples.

| Day [yymmdd] | Timespan [hhmmss-hhmmss] | N transects | Mass Ratio avg ± SD [%] | Wind Speed (m/s) | Wind Dir (deg) | IME $CH_4$ (kg/h) |
|---|---|---|---|---|---|---|
| **190520*** | 184054 -184636 | 1 | 4.3 | 2.4 | 325 | |
| **190523** | 125721 -135131 | 5 | 40.0±3.4 | 2.7-5.1 | 195-220 | |
| **190524** | 155730 -165929 | 5 | 34.8±31.1 | 2.7-4.0 | 2-355 | |
| **190529** | 113522 -160333 | 3 | 44.1±29.0 | 1.8-4.6 | 38-356 | |
| **Total # of meas** | - | **14** | | | | |
| **Median** | - | | 36.5 | | | 188.1 |
| **Mean** | | | 36.1 | | | 196.1 |
| **SD** | | | 22.9 | | | 165.2 |
| **95% CI** | | | 22.9-49.4 | | | |

For two days of the measurements, peak concentrations of ethanol were detected (from 0.6 to 4.4 mg/$m^3$ peak transect concentrations) in addition to the regularly observed methane and ammonia plumes (Figure - 28, left). The ethanol emissions were correlated with the location of the feeding operations (Figure - 28, right). The fermentation processes from orange peels used for feeding occurring on the feed store produced the observed ethanol. An ammonia to ethanol ratio of 26.7% was obtained, but emissions could not be indirectly estimated because the ethanol source was at a different location and distance than the ammonia source. Acetic acid was also found here, likely coming from the feed store from the same fermentation processes (Figure - 28, Table - 20).

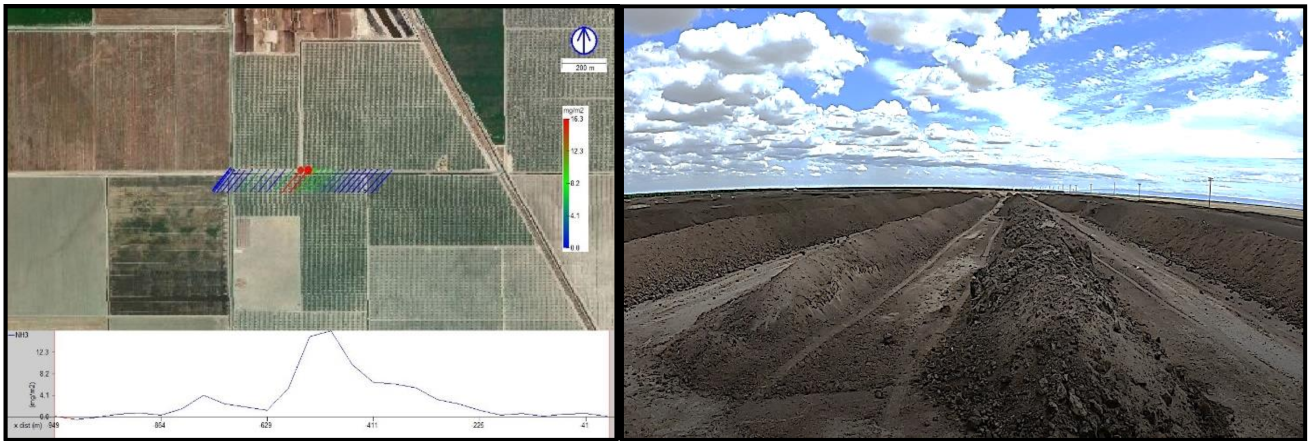

Figure - 27: West Tulare CAFO WT01 Composting area, (Left) Ammonia flux, SOF; (Right) Picture of composting piles;

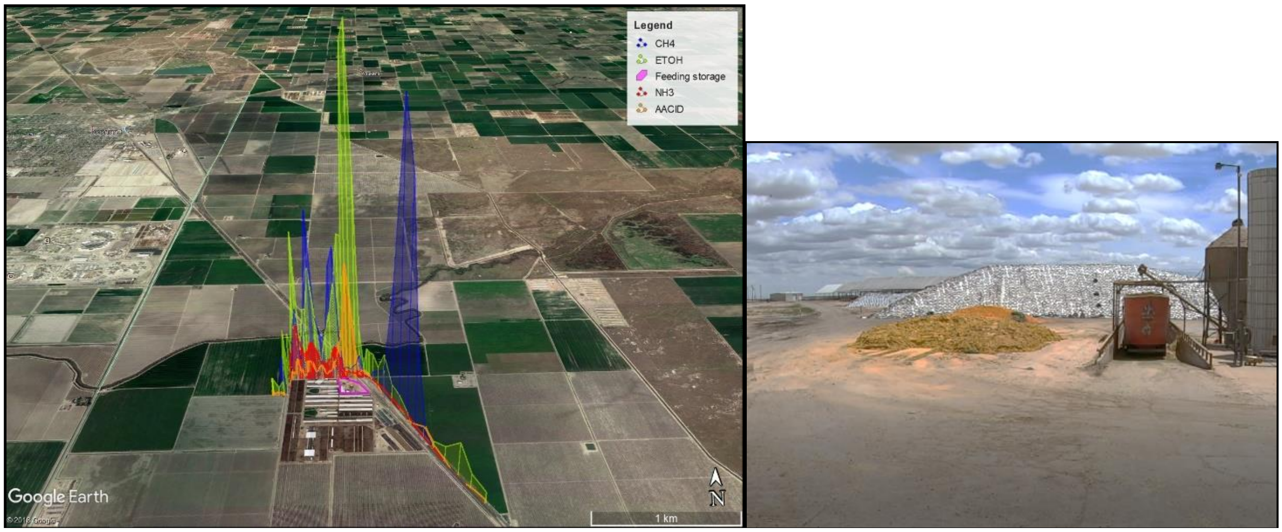

Figure - 28 : West Tulare CAFO WT01, (Left) Concentration measurements, MeFTIR, (Right) picture of orange peels pile, possibly the source for the observed ethanol emission;

### *6.2.2. Farm WT03 (West Tulare)*

West Tulare Farm WT03 had three days of measurements, and the resultant ammonia flux was 157 kg/h (Figure - 29). All the transects were quite confined around this average (Table - 22). Two different wind directions were used for the measurements. The transects do not have upwind measurements, which means that there might be a contribution of other sources to this value, although the sharp plume and well-defined plume edge baseline concentrations do not suggest any major inflow. The $NH_3$:$CH_4$ ratios were on average 43% and had a comparably low standard deviation (Table - 23). The methane emissions on this farm were 388 kg/h (Table - 23).

Table - 22: Ammonia emissions measured at farm WT03, SOF. *Limited number of samples.

| Day [yymmdd] | Timespan [hhmmss-hhmmss] | N transects | Emission±SD [kg/h] | Wind Speed Min-Max[m/s] | Wind Dir Span [deg] |
|---|---|---|---|---|---|
| **190520** | 121533 -181359 | 5 | 154.6±63.8 | 2.6-3.9 | 276-328 |
| **190524** | 173212 -175511 | 3 | 157.9±22.9 | 3.2-4.2 | 0-24 |
| **190529*** | 150422 -150732 | 1 | 175.3 | 3.0 | 355 |
| **Total # of Meas** | - | 9 | | - | - |
| **Median** | - | | 157 | - | - |
| **Mean** | | | 157.7 | | |
| **SD** | | | 46.9 | | |
| **CI 95%** | | | 121.6-193.7 | | |

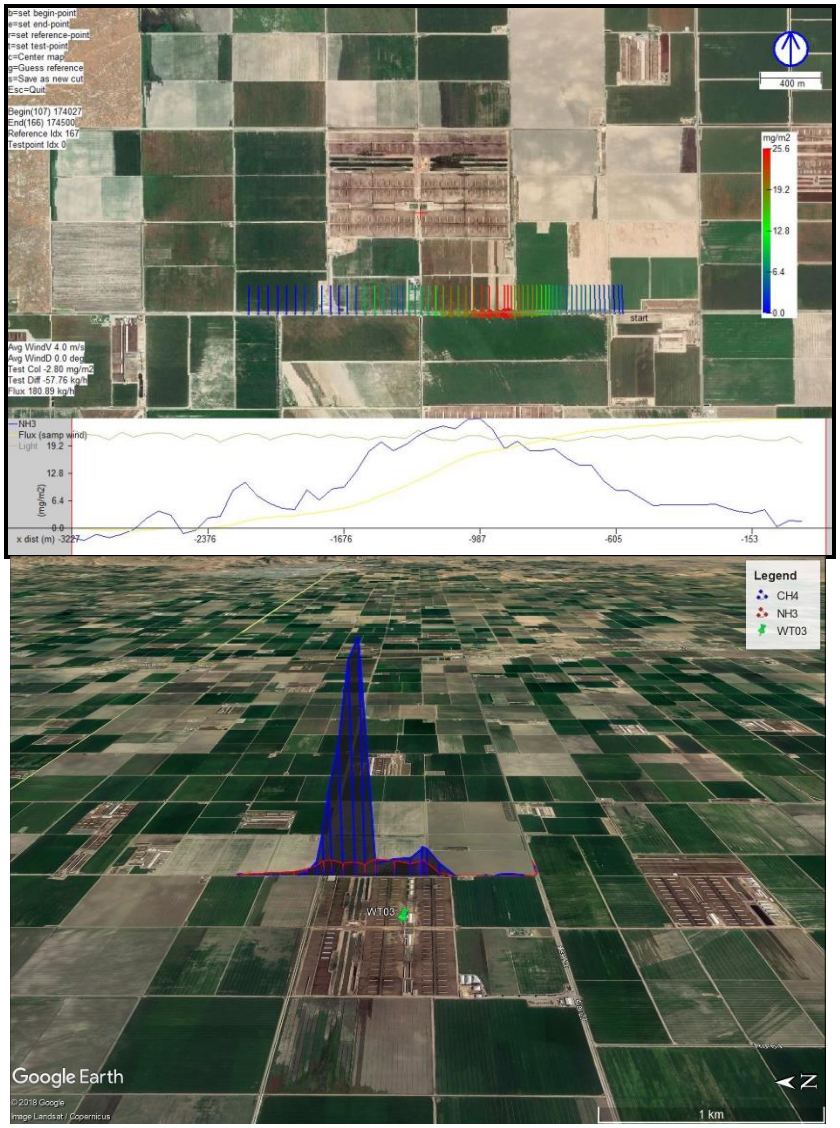

Figure - 29: West Tulare CAFO WT03, (Upper) Ammonia column, SOF; (Lower) $NH_3$ and $CH_4$ concentration, MeFTIR

Table - 23: $NH_3$:$CH_4$ Ratio measurements at farm WT03, MeFTIR.

| Day [yymmdd] | Timespan [hhmmss-hhmmss] | N transects | Mass Ratio avg ± SD [%] | Wind Speed (m/s) | Wind Dir (deg) | IME $CH_4$ (kg/h) |
|---|---|---|---|---|---|---|
| **190520** | 115135 -175736 | 7 | 46.1±11.7 | 1.4-3.8 | 275-327 | |
| **190524** | 173152 -195025 | 2 | 24.3±27.0 | 3.1-3.6 | 21-328 | |
| **190529** | 121516 -124054 | 2 | 38.5±19.7 | 1.8-2.4 | 48-56 | |
| **Total # of meas** | - | **11** | | | | |
| **Median** | - | | 43 | | | 365.1 |
| **Mean** | | | 40.6 | | | 388.6 |
| **SD** | | | 16.3 | | | 194.5 |
| **95% CI** | | | 29.6-51.5 | | | |

### *6.2.3 Farm WT04 (West Tulare)*

The WT04 CAFO was measured on three different days, due to wind conditions and limited road options. The farm had an average ammonia emission of 194 kg/h (Figure - 30, and Table - 24). The high emission value is likely due to its large size, with 11520 animal units. The $NH_3$:$CH_4$ ratios were around 44% and the methane emission totalized 482 kg/h (Table - 26). Previous measurements by Scientific Aviation indicated 670 kg/h of methane emissions on this dairy. Similar to CAFO WT01, ethanol peaks were observed downwind from the farm (0.38 to 2.2 $mg/m^3$), resulting in ammonia to ethanol ratio of 36.2% (Table - 25). Acetic acid was not observed in significant levels at this dairy.

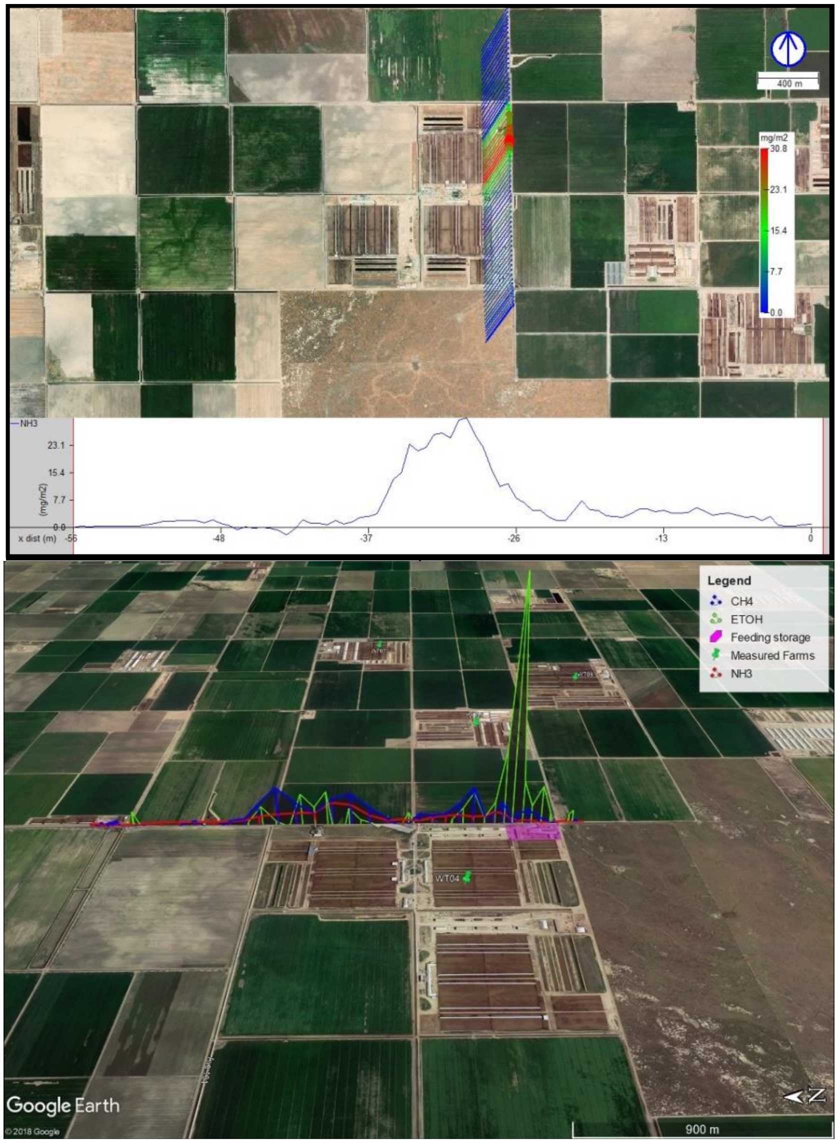

Figure - 30: West Tulare CAFO WT04, (Upper) Ammonia column, SOF; (Lower) $NH_3$, $CH_4$ and Ethanol concentration, MeFTIR

Table - 24: Ammonia emissions measured at farm WT04, SOF.

| Day [yymmdd] | Timespan [hhmmss-hhmmss] | N transects | Emission±SD [kg/h] | Wind Speed Min-Max[m/s] | Wind Dir Span [deg] |
|---|---|---|---|---|---|
| **190523** | 145629 -153826 | 5 | 185.8±90.8 | 5.8-7.2 | 193-213 |
| **190529** | 143047 -145657 | 2 | 206.6±46.4 | 3.1-3.4 | 37-44 |
| **Total # of Meas** | - | 7 |  | - | - |
| **Median** | - |  | 195 | - | - |
| **Mean** |  |  | 191.5 |  |  |
| **SD** |  |  | 71.4 |  |  |
| **CI 95%** |  |  | 120.1-262.9 |  |  |

Table - 25: $NH_3$:Ethanol ratio measurements at farm WT04, MeFTIR.

|  | Ratio $NH_3$: ETOH (%) |
|---|---|
| **Num of Meas** | 6 |
| **Average** | 36.2 |
| **Median** | 35.7 |
| **SD** | 13 |
| **CI 95%** | 22.5 – 49.8 |

Table - 26: $NH_3$:$CH_4$ ratio measurements at farm WT04, MeFTIR. *Limited number of samples.

| Day [yymmdd] | Timespan [hhmmss-hhmmss] | N transects | Mass Ratio avg ± SD [%] | Wind Speed (m/s) | Wind Dir (deg) | IME $CH_4$ (kg/h) |
|---|---|---|---|---|---|---|
| **190523** | 150047-182723 | 6 | 44±10.8 | 6.1-7.1 | 186-245 |  |
| **190529** | 144523-145242* | 1 | 34 | 3.3 | 19 |  |
| **Total # of meas** | - | **11** |  |  |  |  |
| **Median** | - |  | 41.6 |  |  | 468.8 |
| **Mean** |  |  | 39.7 |  |  | 482.8 |
| **SD** |  |  | 10.2 |  |  | 230.8 |
| **95% CI** |  |  | 30.2-49.1 |  |  |  |

### *6.2.4. Farm WT05 (West Tulare)*

Three measurements days at the WT05 farm averaged an ammonia emission of 68 kg/h (Table - 27 and Figure - 31), which is a comparably high emission considering the size of the plant. The proximity to other sources can be one of the reasons to increase the uncertainty on these measurements. The ammonia to methane ratios were around 22% and the methane emission 304 kg/h (Table - 28). An ethanol peak (1 mg/m$^3$) was observed close to the farm feeding storage, only present in two transects.

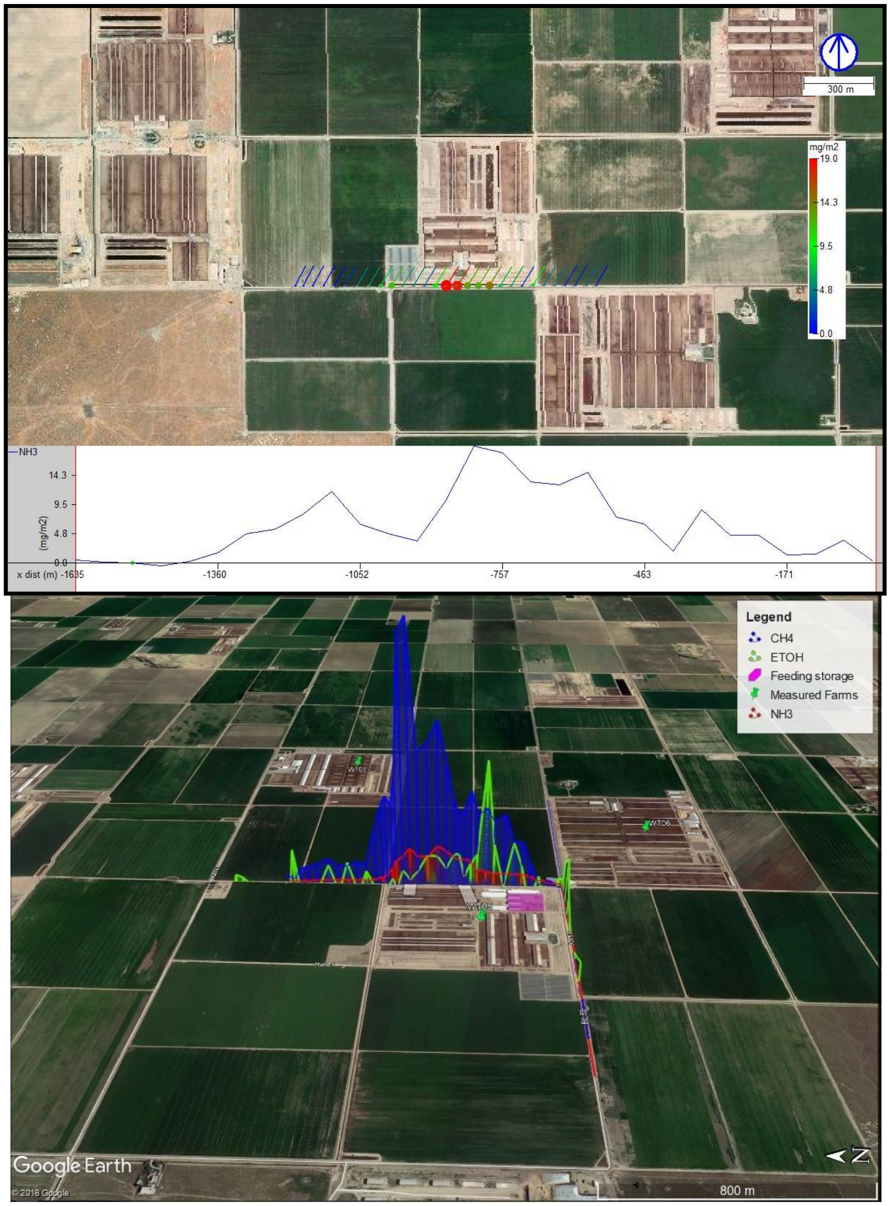

Figure - 31: West Tulare CAFO WT05, (Upper) Ammonia column, SOF (lower) $NH_3$, $CH_4$ and Ethanol concentration MeFTIR;

Table - 27: Ammonia emissions measured at farm WT05, SOF. *Limited number of samples.

| Day [yymmdd] | Timespan [hhmmss-hhmmss] | N transects | Emission±SD [kg/h] | Wind Speed Min-Max[m/s] | Wind Dir Span [deg] |
|---|---|---|---|---|---|
| **190520** | 161433 -163744 | 2 | 39.3±10.9 | 2.5-3.2 | 310-324 |
| **190524*** | 181901 -182038 | 1 | 27.7 | 2.4 | 328 |
| **190529** | 125911 -143042 | 3 | 103.5±15.0 | 2.2-3.4 | 23-46 |
| **Total # of Meas** | - | 6 | | - | - |
| **Median** | - | | 68.1 | - | - |
| **Mean** | | | 70.3 | | |
| **SD** | | | 38.9 | | |
| **CI 95%** | | | 29.4-111 | | |

Table - 28: $NH_3$:$CH_4$ ratio measurements at farm WT05, MeFTIR.

| Day [yymmdd] | Timespan [hhmmss-hhmmss] | N transects | Mass Ratio avg ± SD [%] | Wind Speed (m/s) | Wind Dir (deg) | IME $CH_4$ (kg/h) |
|---|---|---|---|---|---|---|
| **190520** | 160636 -163840 | 3 | 17.6±3.9 | 2.7-3.4 | 313-330 | |
| **190524** | 180932 -184136 | 3 | 24.9±4.2 | 2.3-3.1 | 7-329 | |
| **190529** | 141901 -143130 | 2 | 28.8±10.5 | 3.1-3.3 | 12-37 | |
| **Total # of meas** | - | **8** | | | | |
| **Median** | - | | 21.5 | | | 316.5 |
| **Mean** | | | 23.1 | | | 304.3 |
| **SD** | | | 6.9 | | | 191.6 |
| **95% CI** | | | 15.7-27.3 | | | |

$N_2O$ plumes were observed a couple of times, with fertilized soils being the apparent source. shows a measurement from the fields located between CAFOs WT05 and WT07. Winds were northeasterly at the time, and a peak $N_2O$ concentration of 57 µg/m$^3$ above background was measured. This plume was consistent and measured several times during this day. Since the fields had no apparent ammonia emission, no indirect $N_2O$ emission estimate could be obtained from $N_2O$ : $NH_3$ ratios.

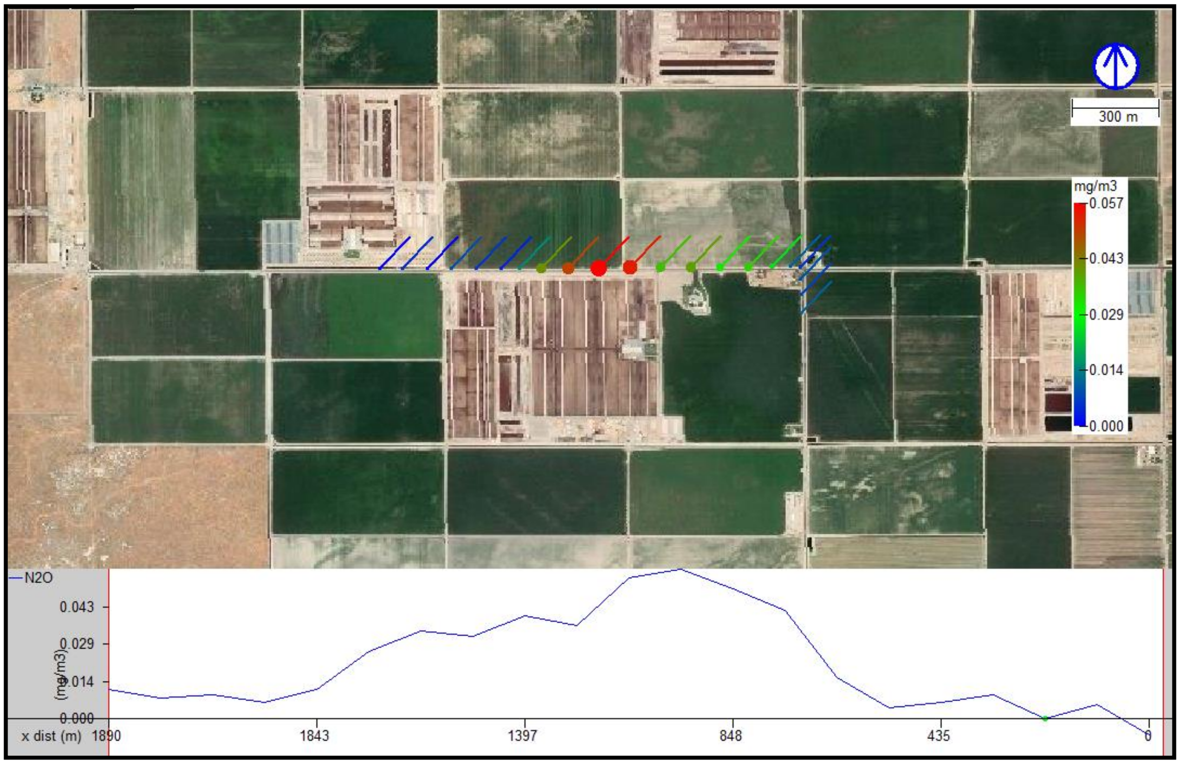

Figure - 32 $N_2O$ plume coming from the fields between CAFOs WT05 and WT07.

### *6.2.5. Farm WT06 (West Tulare)*

The West Tulare dairy WT06 had an ammonia emission of 102 kg/h (median) (Table - 29 and Figure - 33). It was possible to measure this farm in only one day due to the wind conditions and road availability. The ammonia to methane ratios reached 40% and the obtained methane flux of 259 kg/h is uncertain due to the few measurements (Table - 30). The CAFO was measured in moderate wind conditions, which might have contributed to the high emissions.

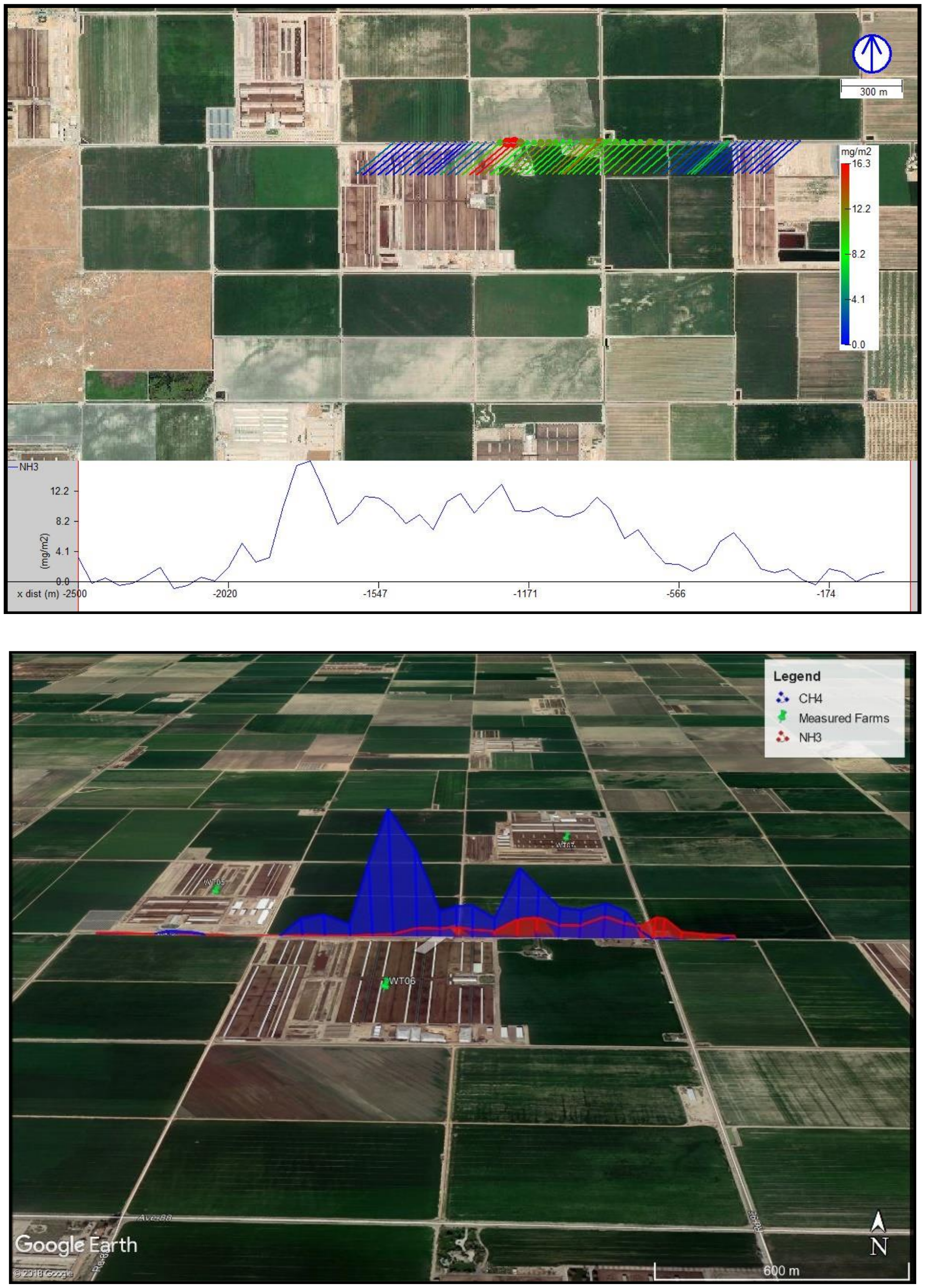

Figure - 33: West Tulare CAFO WT06, (Upper) Ammonia column, SOF;(Lower) $NH_3$ and $CH_4$ concentration MeFTIR.

Table - 29: Ammonia emissions measured at farm WT06, SOF.

| Day [yymmdd] | Timespan [hhmmss-hhmmss] | N transects | Emission±SD [kg/h] | Wind Speed Min-Max[m/s] | Wind Dir Span [deg] |
|---|---|---|---|---|---|
| **190523** | 160148 -165436 | 6 | 120.8±60.9 | 6.4-8.1 | 219-243 |
| **Total # of Meas** | - | 6 | | - | - |
| **Median** | | | 102.9 | | |
| **Mean** | | | 120.8 | | |
| **SD** | | | 60.9 | | |
| **CI 95%** | | | 56.9-184.6 | | |

Table - 30:$NH_3$:$CH_4$ ratio measurements at farm WT06, MeFTIR.

| Day [yymmdd] | Timespan [hhmmss-hhmmss] | N transects | Mass Ratio avg ± SD [%] | Wind Speed (m/s) | Wind Dir (deg) | IME $CH_4$ (kg/h) |
|---|---|---|---|---|---|---|
| **190523** | 160007 -172538 | 6 | 46.6±25.4 | 6.2-8.1 | 209-244 | |
| **Total # of meas** | - | **6** | | | | |
| **Median** | - | | 41.8 | | | 246.1 |
| **Mean** | | | 46.5 | | | 259.5 |
| **SD** | | | 25.4 | | | 192.9 |
| **95% CI** | | | 19.9-73.2 | | | |

### *6.2.6 Farm WT07 (West Tulare)*

West Tulare dairy WT07 was measured on three different days with a total of 67 kg/h of ammonia emissions (Table - 31 and Figure - 34). The ammonia to methane ratios were around 16% and methane emissions on average 415 kg/h (Table - 32). This farm had a digester, hence it was expected to have a comparably lower methane emission. Upwind screening measurements were possible at this site.

Table - 31: Ammonia emissions measured at farm WT07, SOF.

| Day [yymmdd] | Timespan [hhmmss-hhmmss] | N transects | Emission±SD [kg/h] | Wind Speed Min-Max[m/s] | Wind Dir Span [deg] |
|---|---|---|---|---|---|
| **190520** | 155923 -163427 | 3 | 52.5±14.0 | 2.6-3.3 | 291-330 |
| **190523** | 163147 -170129 | 2 | 63.4±0.6 | 7.0-7.4 | 216-236 |
| **190529** | 131322 -142329 | 3 | 84.4±17.2 | 2.1-3.3 | 20-350 |
| **Total # of Meas** | - | 8 | | | - |
| **Median** | - | | 67 | - | - |
| **Mean** | | | 64.9 | | |
| **SD** | | | 19.1 | | |
| **CI 95%** | | | 51-83 | | |

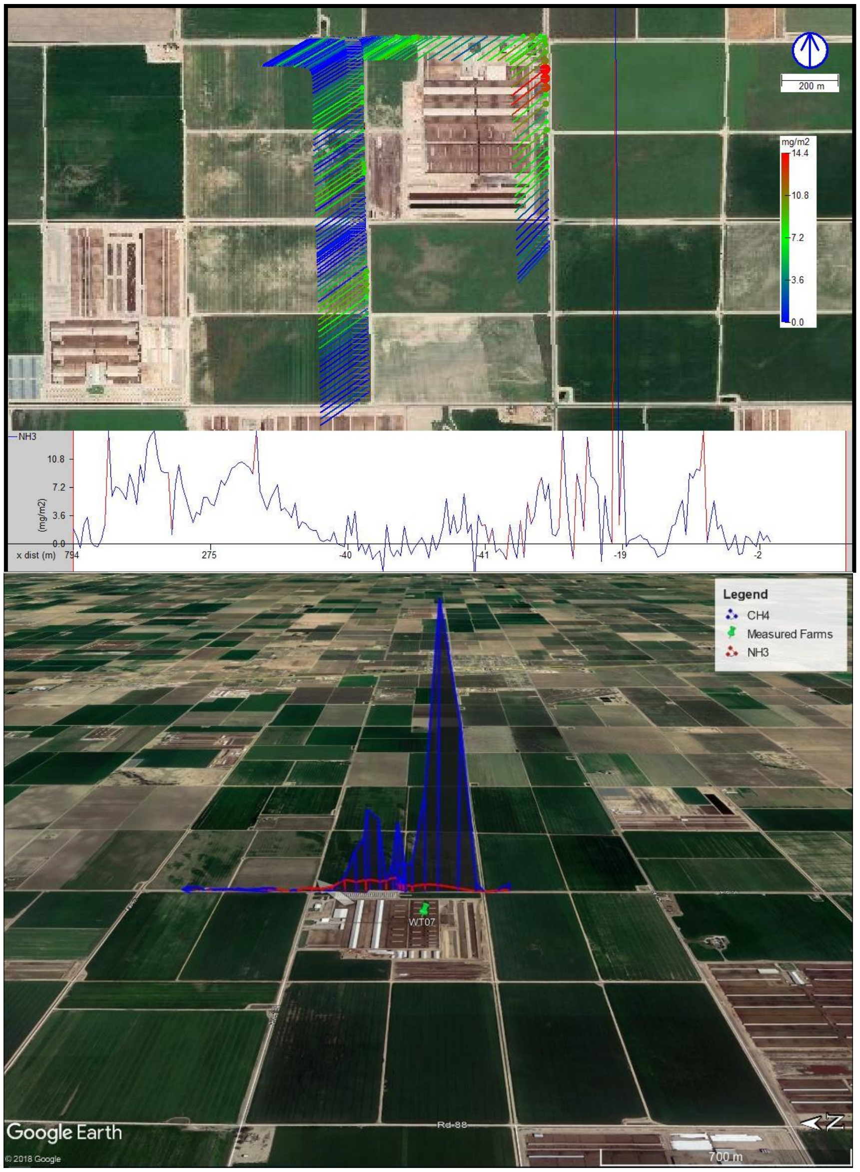

Figure - 34: West Tulare CAFO WT07 (Upper) Ammonia column, SOF; (lower) $NH_3$ and $CH_4$ concentration MeFTIR.

Table - 32: $NH_3$:$CH_4$ ratio measurements at farm WT07, MeFTIR.

| Day [yymmdd] | Timespan [hhmmss-hhmmss] | N transects | Mass Ratio avg ± SD [%] | Wind Speed (m/s) | Wind Dir (deg) | IME $CH_4$ (kg/h) |
|---|---|---|---|---|---|---|
| **190520** | 155111 -162801 | 3 | 21.6±6.2 | 2.2-3.3 | 294-330 | |
| **190523** | 163204 -170716 | 3 | 16.2±2.7 | 4.0-6.9 | 236-270 | |
| **190524** | 191240 -192327 | 2 | 12.6±1.6 | 1.9-2.7 | 344-347 | |
| **190529** | 132640 -141233 | 3 | 14.0±8.4 | 3.4-4.0 | 3-270 | |
| **Total # of meas** | - | **6** | | | | |
| **Median** | - | | 14.6 | | | 444.5 |
| **Mean** | | | 16.2 | | | 415.1 |
| **SD** | | | 6.3 | | | 200.2 |
| **95% CI** | | | 11.7-20.6 | | | |

### *6.2.7. Farm ET01 (East Tulare)*

The farm number one on the east side of Tulare was difficult to measure. This farm combined the difficulty of being surrounded by other farms and inconsistent wind conditions (Figure - 35). The ammonia measurements resulted in 29 kg/h (median) (Table - 33). The ammonia to methane ratios were 17%. Ratios were not measured simultaneously with the emission transects here (Table - 34). The obtained methane emission was 187 kg/h. These measurements included two dairies and they are smaller than the other farms presented before.

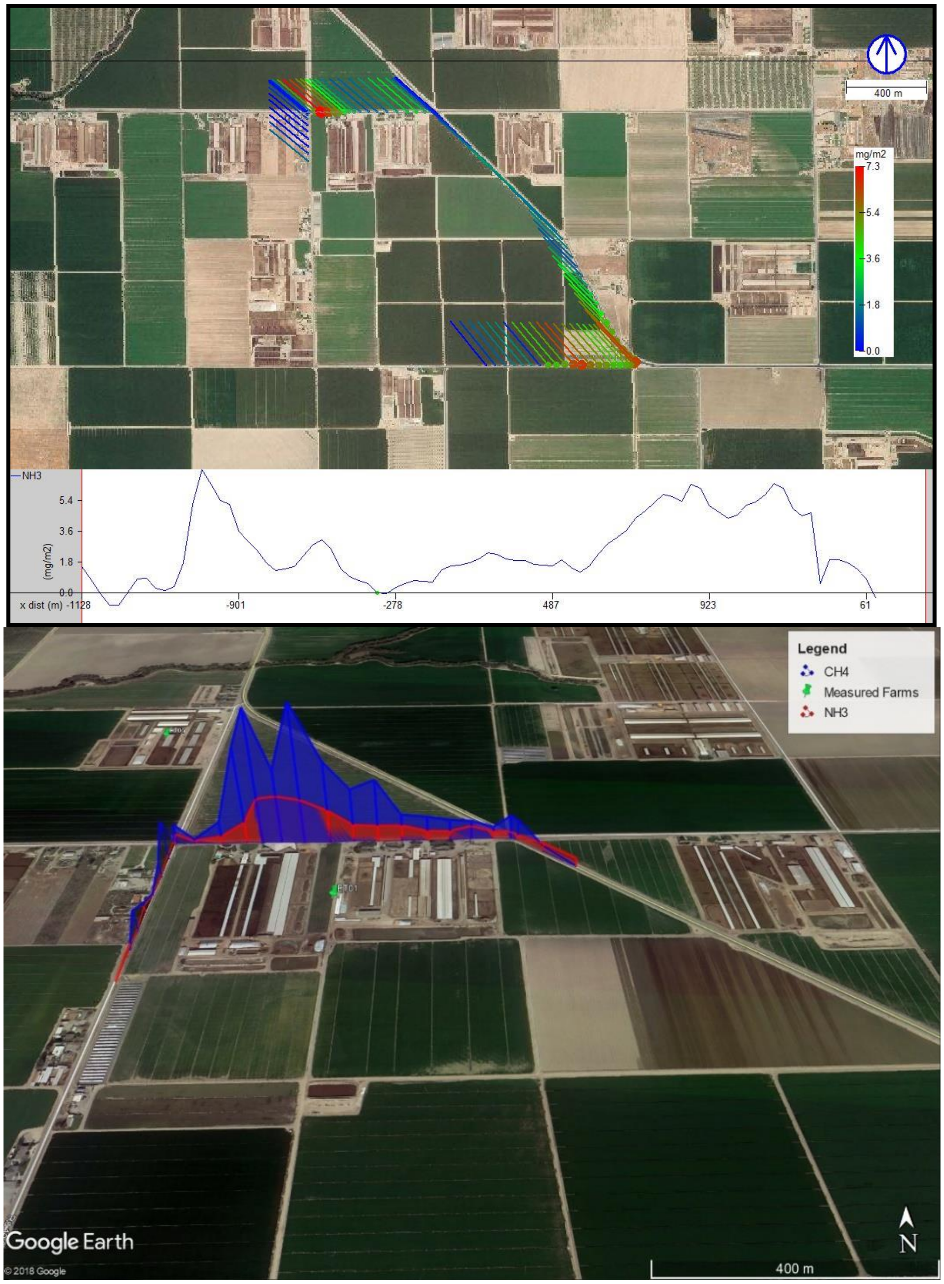

Figure - 35: East Tulare CAFO ET01, (Upper) Ammonia column, SOF (Lower) NH$_3$ and CH$_4$ concentrations, MeFTIR;

Table - 33: Ammonia emissions measured at farm ET01, SOF.

| Day [yymmdd] | Timespan [hhmmss-hhmmss] | N transects | Emission±SD [kg/h] | Wind Speed Min-Max[m/s] | Wind Dir Span [deg] |
|---|---|---|---|---|---|
| **190521*** | 155724 -160358 | 1 | 29.0 | 6.8 | 314 |
| **190524** | 111012 -121310 | 3 | 42.8±10.2 | 1.8-2.3 | 166-214 |
| **190529** | 172116 -181753 | 3 | 21.9±6.1 | 1.7-3.0 | 267-307 |
| **Total # of Meas** | | 7 | | - | - |
| **Median** | | | 29 | | |
| **Mean** | | | 31.9 | | |
| **SD** | | | 12.6 | - | - |
| **CI 95%** | | | 20.2-43.5 | | |

Table - 34: $NH_3$:$CH_4$ ratio measurements at farm ET01, MeFTIR.

| Day [yymmdd] | Timespan [hhmmss-hhmmss] | N transects | Mass Ratio avg ± SD [%] | Wind Speed (m/s) | Wind Dir (deg) | IME $CH_4$ (kg/h) |
|---|---|---|---|---|---|---|
| **190521** | 103538 -170341 | 2 | 17.6±4.6 | 4.5-5.8 | 293-307 | |
| **190524** | 113350 -140008 | 4 | 22.7±12.4 | 1.5-2.6 | 138-318 | |
| **190529** | 175813 -191533 | 5 | 12.3±5.8 | 4.0-4.0 | 270-270 | |
| **Total # of meas** | - | **11** | | | | |
| **Median** | - | | 14.3 | | | 202.9 |
| **Mean** | | | 17 | | | 187.8 |
| **SD** | | | 9.1 | | | 124.9 |
| **95% CI** | | | 10.9-23.1 | | | |

### *6.2.8 Farm ET08 (East Tulare)*

The ET08 dairy was measured only in one day because it was located distant from the other farms. The total emission of ammonia was 60 kg/h (Table - 35, and Figure - 36). The ammonia to methane ratios reached 20% and resulted in a methane emission of 292 kg/h (Table - 36). These measurements were consistent and clear plumes were obtained. This farm had a digester, and according to the concentration measurements, most of the methane contribution was from the digester and the lagoon close to the digester (Figure - 36). Previous measurements by Scientific Aviation showed a methane emission of 541 kg/h.

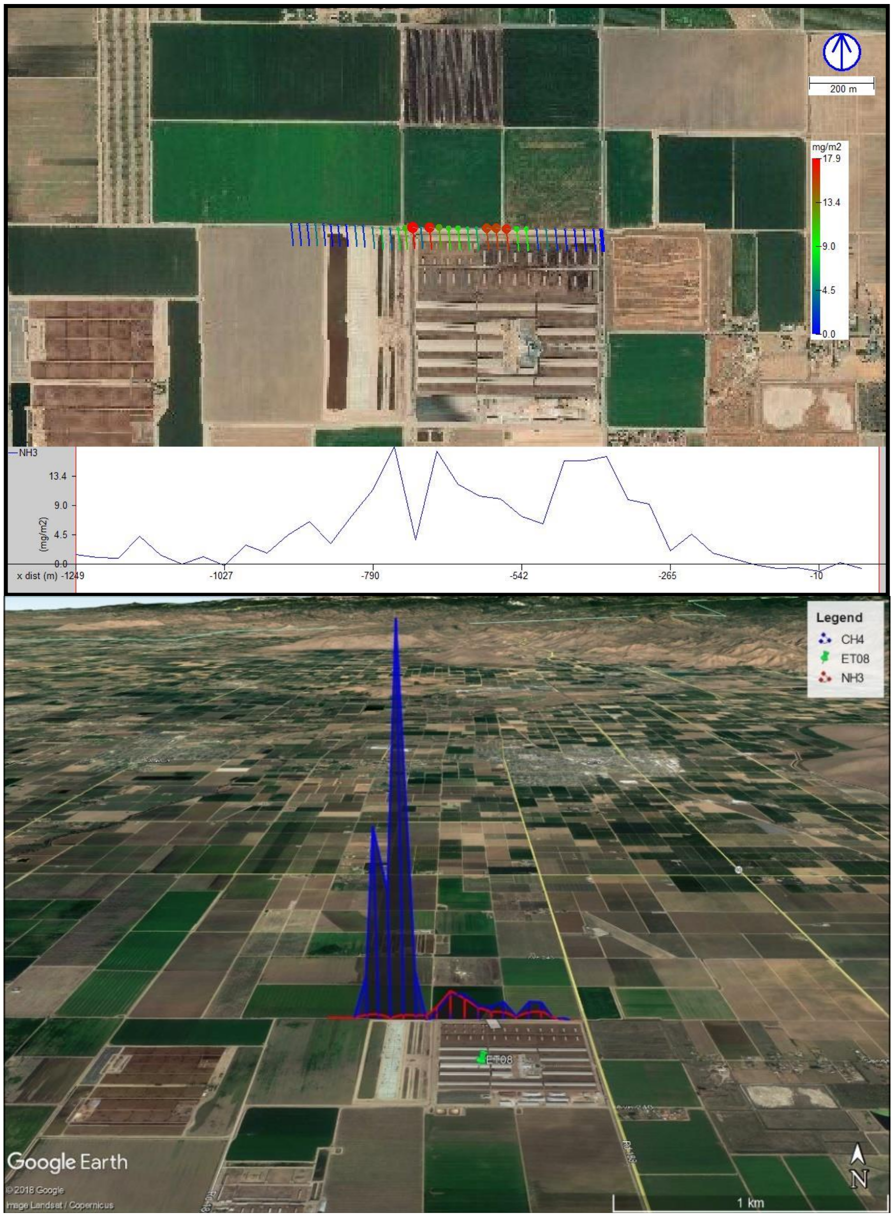

Figure - 36: East Tulare CAFO ET08, (Upper) Ammonia column, SOF, (Lower) $NH_3$ and $CH_4$ concentration measurements, MeFTIR.

Table - 35: Ammonia emissions measured at farm ET08, SOF.

| Day [yymmdd] | Timespan [hhmmss-hhmmss] | N transects | Emission±SD [kg/h] | Wind Speed Min-Max [m/s] | Wind Dir Span [deg] |
|---|---|---|---|---|---|
| **190524** | 091550 -101554 | 7 | 60.1±12.7 | 2.3-4.2 | 161-209 |
| **Total # of Meas** | - | 7 | | - | - |
| **Median** | | | 60 | | |
| **Mean** | | | 60 | | |
| **SD** | | | 12.7 | | |
| **CI 95%** | | | 48.2-71.8 | | |

Table - 36: $NH_3$:$CH_4$ Ratio measurements at farm ET08, MeFTIR.

| Day [yymmdd] | Timespan [hhmmss-hhmmss] | N transects | Mass Ratio avg ± SD [%] | Wind Speed (m/s) | Wind Dir (deg) | IME $CH_4$ (kg/h) |
|---|---|---|---|---|---|---|
| **190524** | 091618 -102153 | 7 | 20.5±8.3 | 2.0-4.2 | 162-207 | |
| **Total # of meas** | - | **7** | | | | |
| **Median** | - | | 17.9 | | | 335.2 |
| **Mean** | | | 20.5 | | | 292.6 |
| **SD** | | | 7.7 | | | 134.5 |
| **95% CI** | | | 12.8-28.2 | | | |

## 6.3. CAFOs in the Merced region

South Merced (optionally north Madera) area was measured on two days in May 2019. Both days had challenging wind conditions. On the first day, moderate wind speeds were observed, while the second day had weak winds. Due to the weaker wind on the second day, most of the measurements of that day were discarded according to the SOF method protocol. The two farms with approved and consistent results are presented below.

### *6.3.1. Farm SM01 (South Merced)*

South Merced farm SM01 was measured on May 25. Good measurements and consistent results were obtained, even though upwind or close by measurements were not possible due to the farm restrictions (Figure - 37 and Table - 37). The ammonia flux obtained was 174 kg/h while the $NH_3$:$CH_4$ ratio of 31.5% resulted in methane emissions of 527 kg/h (Table - 38). Previous measurements by Scientific Aviation showed 700 kg/h of methane emission. As in other farms it was possible to observe that most of the methane contribution came from the anaerobic lagoons while ammonia came from the feedlots (Figure - 37).

Table - 37: Ammonia emissions measured at farm SM01, SOF.

| Day [yymmdd] | Timespan [hhmmss-hhmmss] | N transects | Emission±SD [kg/h] | Wind Speed Min-Max[m/s] | Wind Dir Span [deg] |
|---|---|---|---|---|---|
| **190525** | 122425 -135704 | 7 | 166.3±41.4 | 3.0-3.7 | 297-307 |
| **Total # of Meas** | - | 7 | | - | - |
| **Median** | | | 174 | | |
| **Mean** | | | 166 | | |
| **SD** | | | 41.1 | | |
| **CI 95%** | | | 127-204 | | |

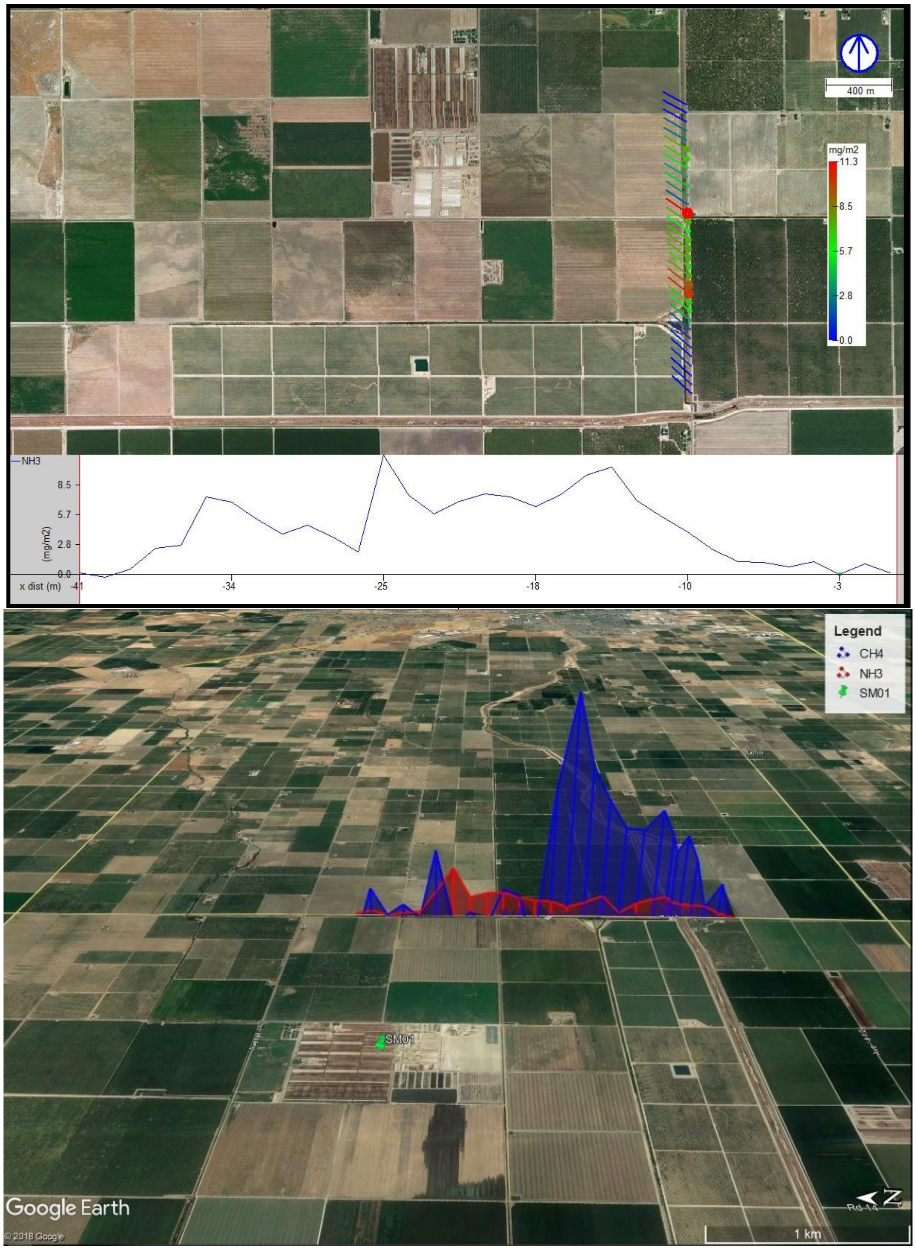

Figure - 37: South Merced CAFO SM01, (Upper) Ammonia flux, SOF; (Lower) $NH_3$:$CH_4$ ratio, MeFTIR.

Table - 38: $NH_3$:$CH_4$ ratio measurements at farm SM01, MeFTIR.

| Day [yymmdd] | Timespan [hhmmss-hhmmss] | N transects | Mass Ratio avg ± SD [%] | Wind Speed (m/s) | Wind Dir (deg) | IME $CH_4$ (kg/h) |
|---|---|---|---|---|---|---|
| **190525** | 122436 -135701 | 6 | 31.5±3.1 | 3.0-3.6 | 297-307 | |
| **Total # of meas** | - | **6** | | | | |
| **Median** | - | | 31 | | | 561 |
| **Mean** | | | 31.5 | | | 527 |
| **SD** | | | 3.1 | | | 140 |
| **95% CI** | | | 27-34.8 | | | |

### *6.3.2. Farm SM02 (South Merced)*

South Merced farm SM02 was measured on 2 days, May 25 with moderate breeze conditions May 28 with light breeze conditions. On the first day, emissions from upwind were detected, these values were attributed to be field emissions because there was no other close by farm (Figure - 38). Additionally, nitrous oxide ground concentrations were observed coming from the soil. The upwind contribution was measured several times and subtracted from the downwind values. Ammonia emissions were comparably high, with an average of 122 kg/h (Table - 39).

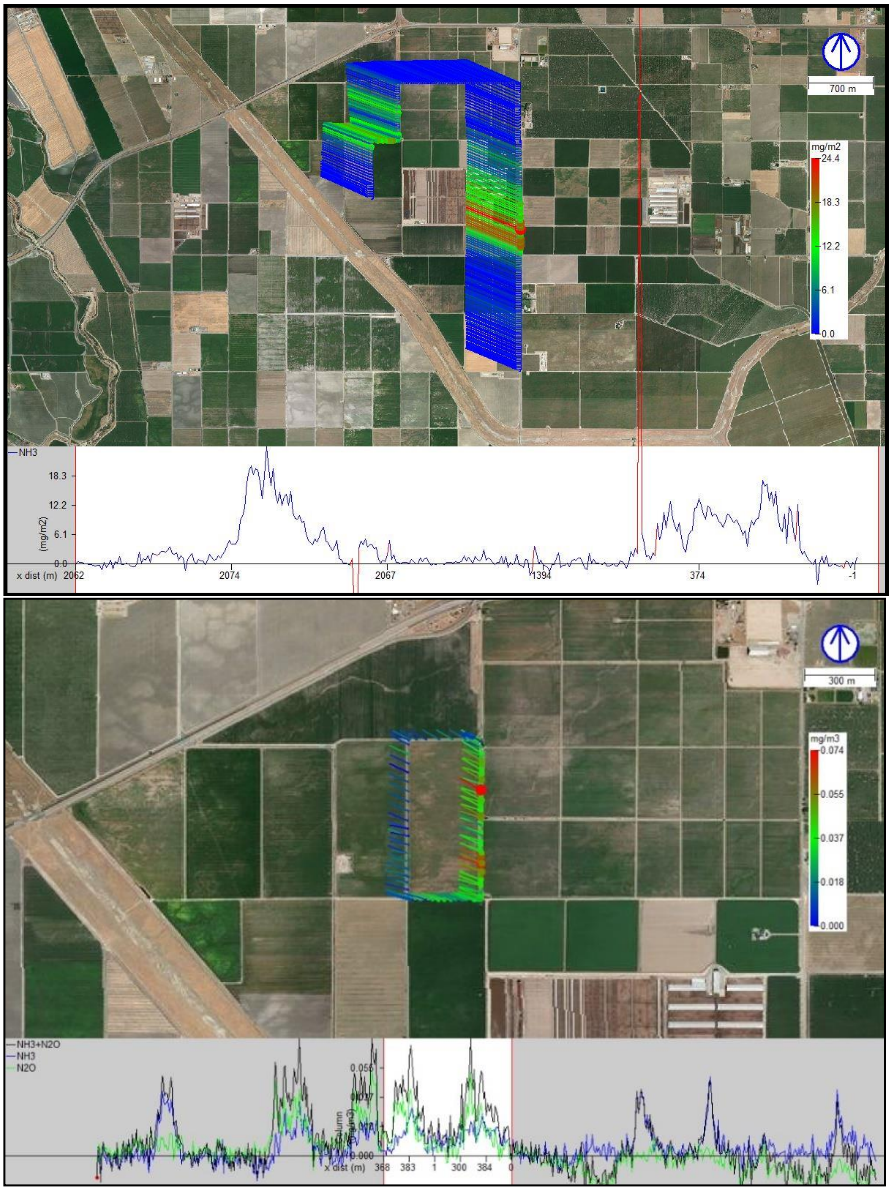

Figure - 38 South Merced CAFO SM02, (Upper) Ammonia column, SOF; (Lower) upwind $NH_3$ and $N_2O$ concentrations, MeFTIR.

Figure – 39: $NH_3$:$CH_4$ ratio concentration downwind of South Merced CAFO SM02.

The $NH_3$ to $CH_4$ ratios were measured only on the first day (Figure – 39). The low $NH_3$:$CH_4$ ratio and high ammonia emission resulted in a high methane emission estimate, averaging 844 kg/h (Table – 40). Previous measurements by Scientific Aviation showed 560 kg/h of methane emission here.

Table - 39: Ammonia emissions measured at farm SM02, SOF.

| Day [yymmdd] | Timespan [hhmmss-hhmmss] | N transects | Emission±SD [kg/h] | Wind Speed Min-Max [m/s] | Wind Dir Span [deg] |
|---|---|---|---|---|---|
| **190525** | 153924 -173316 | 8 | 174±71.9 | 6.4-7.9 | 265-312 |
| **190528** | 142143 -161743 | 5 | 91.8±36.6 | 2.0-3.1 | 10-358 |
| **Total # of Meas** | - | 13 | | - | - |
| **Median** | - | | 122 | - | |
| **Mean** | | | 142 | | |
| **SD** | | | 63 | | |
| **CI 95%** | | | 104-180.5 | | |

Table – 40: $NH_3$:$CH_4$ ratio measurements at farm SM02, MeFTIR.

| Day [yymmdd] | Timespan [hhmmss-hhmmss] | N transects | Mass Ratio avg ± SD [%] | Wind Speed (m/s) | Wind Dir (deg) | IME $CH_4$ (kg/h) |
|---|---|---|---|---|---|---|
| **190525** | 150137-200501 | 12 | 16.8±5.0 | 6.4-7.9 | 265-312 | |
| **190528*** | 153407-154159 | 1 | 21.5 | 2 | 14.5 | |
| **Total # of meas** | - | **13** | | | | |
| **Median** | - | | 16.6 | | | 735 |
| **Mean** | | | 16.8 | | | 844.8 |
| **SD** | | | 5.0 | | | 451.1 |
| **95% CI** | | | 14-19 | | | |

## 6.4 Additional Farms surveyed in the Bakersfield, Tulare and Merced regions

Besides the CAFOs described in the above sections, there were other farms where ammonia fluxes and ratios concentrations were measured, however with few transects/days. Table - 41 shows an overview of these farms. The ET03/05/07 and SM03 farms are small, and consequently lower emissions were observed here (Figure - 40). The NB04 and NB05 farms were measured with moderate wind conditions.

Table - 41: Ammonia emissions and $NH_3$:$CH_4$ concentration ratios measured in 'extra' farms.

| | N transects | $NH_3$ (kg/h) | SD (kg/h) | N transects | Ratio (%) | SD (%) | $CH_4$ (kg/h) |
|---|---|---|---|---|---|---|---|
| **NB04** | 4 | 79 | 29 | 6 | 31 | 15 | 255 |
| **NB05** | 4 | 101 | 65 | 4 | 29 | 1 | 344 |
| **ET03** | 3 | 18 | 8 | 4 | 51 | 6 | 35 |
| **ET05** | 4 | 20 | 11 | 8 | 10 | 3 | 213 |
| **ET07** | 3 | 28 | 16 | 4 | 11 | 11 | 262 |
| **SM03** | 4 | 20 | 6 | 6 | 9 | 3 | 219 |

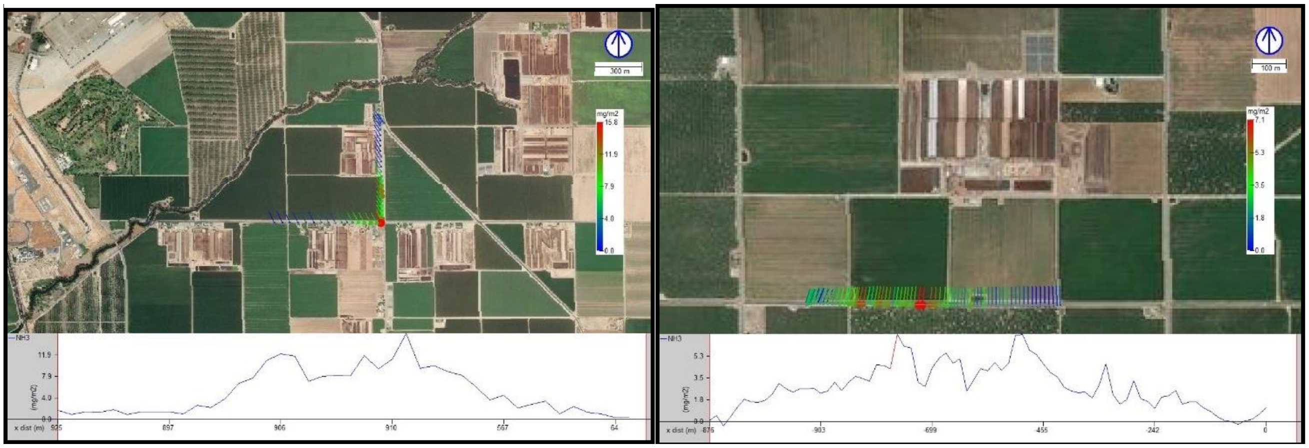

Figure - 40: SOF ammonia column, (Left) South Merced CAFO 03, (Right) East Tulare CAFO 05.

## 6.5. Farms excluded from the overall results

For the CAFO SB01 on the south of Bakersfield, the measurements were inconsistent due to the large upwind flux, which was in some cases larger than the downwind measurement (short term source variations) (Figure - 41, left). The same happened with the SM03 farm, on the first day of measurements (Figure - 41, right). On the second day, the wind direction changed favorably so the emissions were obtained using only that day. For the WT02 dairy, even though some plumes were correlated with the source, the farm operations seemed to be shut down because the barns were empty and the roof slightly damaged (Figure - 42). According to the information obtained from the San

Joaquin Air pollution district, there were only a few heifers on the last inspection of this farm. Additionally, quite low concentrations were observed on the ground, which could be an indication of a distant source rather than contribution from the target farm.

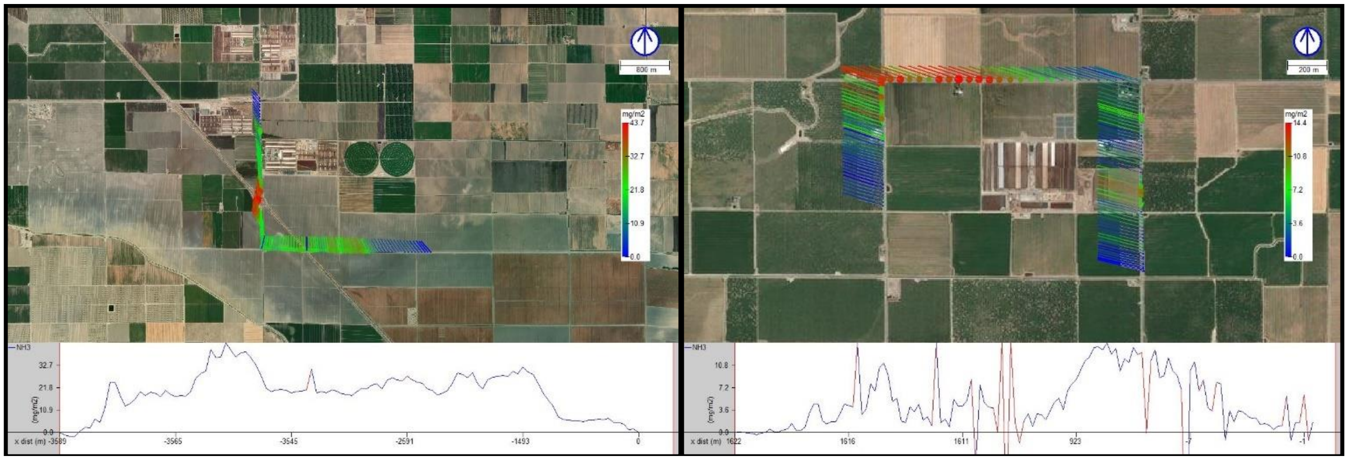

Figure - 41: SOF ammonia column, (Left) South Bakersfield CAFO 01; (Right) S Merced CAFO 03.

Figure - 42: Picture of WT02 CAFO and empty barns.

## 6. Discussion and conclusions

The emissions quantified in the campaign can be compared to inventories, historical data, or emission factors from facilities with similar type of management. Emissions are commonly expressed as emission factors (EF), i.e. emission per animal and hour. Here the number of cows from the studied facilities was obtained from the San Joaquin Valley Air Pollution District (ValleyAir, Personal correspondence, 2019). Emission factors from this study are summarized in Table - 42 and shown in Figure - 43 and Figure - 44 for ammonia and methane, respectively.

Table - 42: Emission factors, emission per number of animal unit[2], for each facility measured.

| **Farm** | **$NH_3$ (g/head/h)** | | **$CH_4$ (g/head/h)** | |
|---|---|---|---|---|
| | **Avg** | **SD** | **Avg** | **SD** |
| **SB02** | 6.0 | 2.4 | 30.5 | 12.5 |
| **SB03[1]** | 10.5 | 5.4 | 33.8 | 18.0 |
| **SB04** | 10.2 | 4.7 | 37.1 | 25.8 |
| **SB05[1]** | 18.3 | 7.9 | 82.9 | 48.2 |
| **NB01** | 8.8 | 7.2 | 49.3 | 47.9 |
| **NB02** | 12.9 | 7.0 | 83.6 | 56.4 |
| **WT01[1]** | 3.9 | 2.2 | 10.9 | 9.2 |
| **WT03** | 16.7 | 5.0 | 41.2 | 20.6 |
| **WT04** | 15.9 | 7.1 | 41.9 | 20.0 |
| **WT05[1]** | 12.2 | 6.7 | 52.7 | 33.2 |
| **WT06** | 14.6 | 7.4 | 31.3 | 23.3 |
| **WT07[1]** | 15.3 | 4.4 | 95.0 | 45.8 |
| **ET01** | 14.0 | 5.8 | 88.6 | 58.9 |
| **ET08[1]** | 4.1 | 0.9 | 20.0 | 9.2 |
| ***Average*** | ***11.7*** | ***2.2*** | ***49.9*** | ***17.6*** |
| ***Median*** | ***12.5*** | | ***41.4*** | |
| ***CI 95%*** | ***10.4-13.8*** | | ***39.8-81.2*** | |

[1] Farms with a methane collection cover.

[2] Mature animals correspond to one animal unit, heifers to 0.75 and calves to 0.17.

The EFs for $NH_3$ ranged between 4 and 18.3 (g$NH_3$/head/h) with an average of 11.5 (g$NH_3$/head/h). These number are high compared to a review paper by (Hristov *et al.* 2011), showing average emissions of 2.45±2.7 (g$NH_3$/head/h) from dairies and double that from beef cows. However, there are other studies that show very similar values to the ones in this study, i.e. (Bjorneberg *et al.* 2009) and (Kille *et al.* 2017) reported average EFs of 10.4 (g$NH_3$/head/h) and 11.4 (g$NH_3$/head/h), respectively.

It should be noted that the ammonia and methane emissions are affected by ambient temperature, wind conditions, solar insolation and diurnal patterns of the animal activity (Leytem et al. 2011; Miller et al. 2015). High temperature increases both methane and ammonia emissions. For methane the temperature is associated with the bacterial activity, while for ammonia emissions, the temperature influences the ammonium($NH_4^+$)-ammonia($NH_3$) equilibrium, and therefore its volatilization (Hristov *et al.*, 2011). Solar radiation can also affect the last, by heating up faster the liquid manure surface as observed in other studies (Miller *et al.*, 2015). Additionally, increasing wind speed rise the ammonia volatilization (Olesen and Sommer, 1993).

The measurements in this study were performed during sunny conditions, at daytime and during the month of May. The average ambient temperature in San Joaquin valley during this month is close to the yearly average (May: 20°C; Annual: 19.4 °C) and therefore the measurements were representative for the annual average emissions wrt to this parameter. The SOF measurements were performed at daytime (9:00 to 18:00). According to modelling by Zhu et al. (2015) this would cause 70 % higher $NH_3$ emissions compared to the average emissions over a 24 h period. For methane the diurnal effects are considerably smaller (Bjorneberg et al, 2009). The wind speeds during the campaign were generally close to the annual average wind speed of 3 m/s, with exceptions for the farms WT06, SM02, NB02, and NB01 for which the wind speeds were twice the average, which potentially increased the measured emissions here. To summarize it appears that the measurements during the campaign were about 70 % higher than the annual average and this is close to the 100% discrepancy observed between emission factor calculations and the measurements. A factor of uncertainty in this study is the number of animals at each farm, used to calculate the emission factors and model the emissions. The animal data were obtained from inspections by the San Joaquin Valley Air Pollution District carried out over several years, and the numbers used on this report are from the last inspection 2017-2019. Since this number can fluctuate during the year it makes the actual number of cows at each farm uncertain in the measured period. In addition, at some farms, emissions upwind or from adjacent crop fields interfered with the measurements, e.g. the measurements at farm SB05.

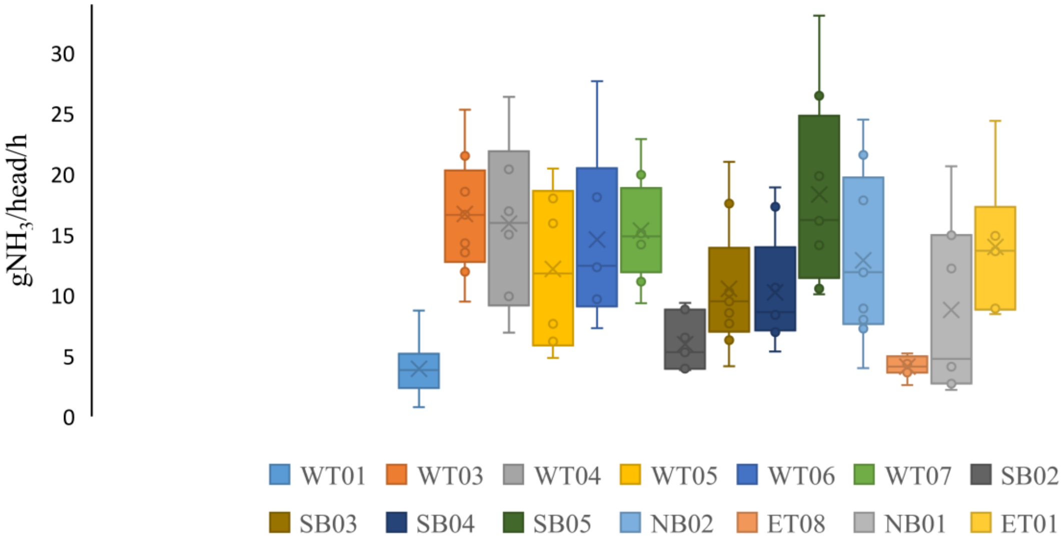

Figure - 43: Ammonia emission factors: minimum, mean (x), median (-), interquartile range, and maximum.

Figure - 44 shows the obtained EFs for methane, ranging between 11 and 95 (gCH$_4$/animal/h) with an average of 50 (gCH$_4$/animal/h). This is consistent with data from literature by (Leytem *et al.* 2011) and (Bjorneberg *et al.* 2009) showing EFs of 58 gCH$_4$/head/h and 23 gCH$_4$/head/h, respectively. The majority of the CAFOs had EF in this range with a few exceptions such as NB02 and WT07. Note that the methane measurements have larger uncertainties than the EFs for NH$_3$ since the former is obtained by combining several measurement steps (methods) with accumulated uncertainty.

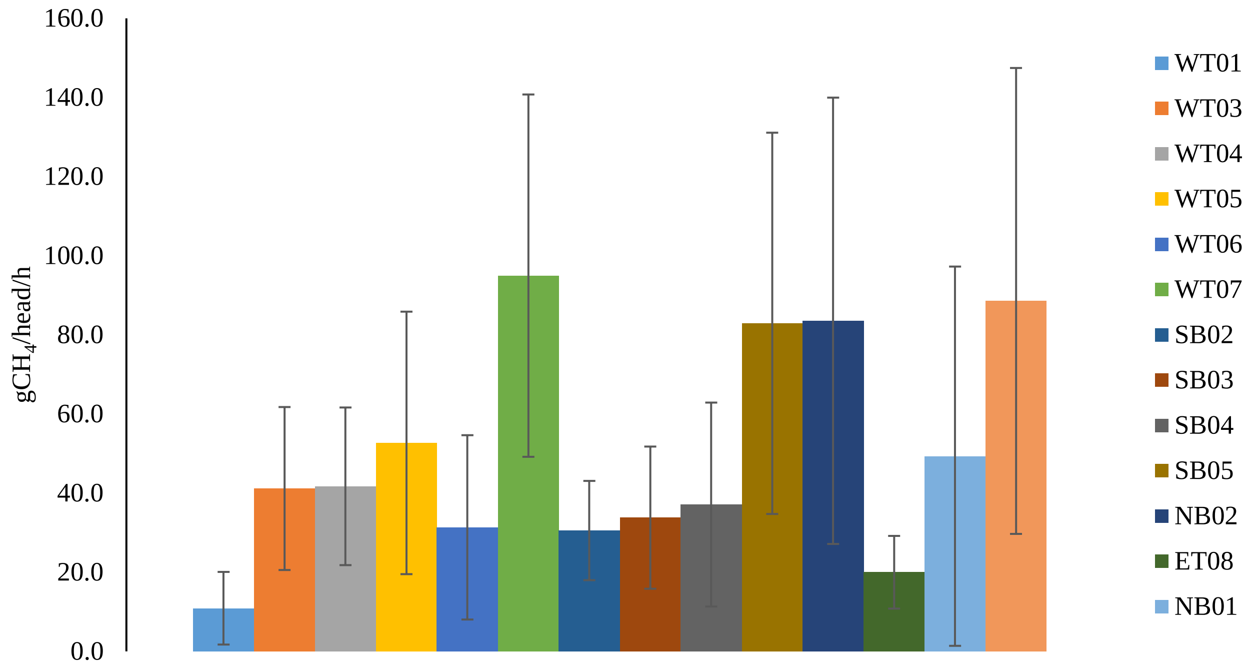

Figure - 44: Methane emission factors, mean and standard deviation.

During the last years, covers have been installed over numerous Californian anaerobic manure lagoons (a.k.a. digester) to be able to collect the methane produced. Comparing the emission factors for farms with and without these covers in place, farms with digesters (WT01, WT07, SB03, SB05, ET08) had a lower median and average methane emission than farms without (Figure - 45). However, the statistical significance of this is questionable due to the low number of sampled farms with digesters.

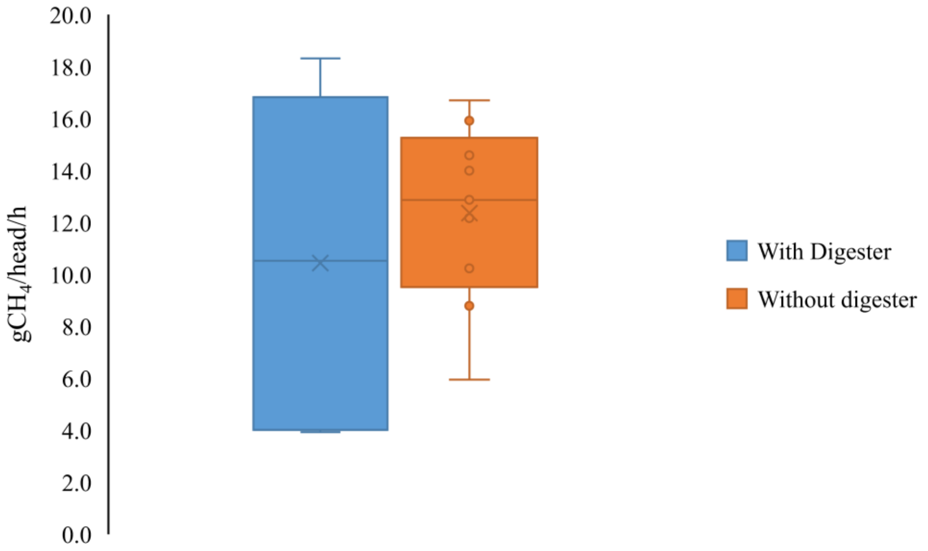

Figure - 45: Classification of methane emission factor on farms with and without digester.

In three of the farms we observed ethanol emissions in proximity to the feeding operation facilities. Similar observations and values have been observed elsewhere (Yuan *et. al.* 2017). In the other farms the measurements were carried out relatively far from the feeding operations and therefore the emission plumes became too diluted to be detected.

Table - 43: Comparison with airborne methane measurements by Scientific Aviation in 2018 and methane obtained from combined SOF and MeFTIR measurements in 2019 by FluxSense at several farms in the San Joaquin valley.

| | **Airborne Flux (kg/h)** | **SOF (kg/h)** |
|---|---|---|
| **WT01** | 240 | 196.1 |
| **WT04** | 670 | 482.8 |
| **ET08** | 541 | 292.6 |
| **SM01** | 727 | 527.2 |
| **SM02** | 560 | 844.3 |

In Table - 43 the methane emission measurements in this study are compared to airborne measurements by Scientific Aviation (CARB, 2019b) in 2018. The latter measurements were made by measuring the concentration of methane in a circle around individual farms, spiraling from approx. 50 m altitude to about 500 m above ground. Note that since the years of the two measurements are different, the numbers of animals and consequently emissions may differ. Seasonal and meteorological differences will also have an impact on observed emissions and induce survey differences. With exception for SM02 the two data sets correlate reasonably well ($R^2$ 0.88) with a scaling factor of 0.7.

In order to benchmark the measurement results, the measured methane and ammonia emissions have been compared with calculated emission data based on published EF data multiplied with number of animals per farm. The emission calculation for methane has been carried out by using EFs from CARB's GHG inventory (CARB, 2019a). The EFs include emission from the cow breathing and from manure management which depends on the type of animal and associated activities that causes the emissions. E.g. for mature cows the activities and their relative contribution to methane emission are (US-EPA, 2017): daily spread — 10%, solid storage — 9%, liquid/slurry — 20%, and anaerobic lagoon — 60%. For replacement heifers the corresponding data are: daily spread — 11%, dry lot — 88%, liquid/slurry — 1%, and pasture — 1% (US-EPA, 2017). For ammonia, the calculation was less sophisticated, simply using a constant EF for Dairy cows of 84 lbs/cow/year from the National emission inventory (EPA, 2004). This EF value corresponds to the national average rather than conditions in California and this might cause discrepancy between the calculations, due to different management practices and yearly temperature conditions. Additionally, as mentioned previously, the inventory is a yearly estimation while the measured emission only represent the season when the measurements took place. The number of cows per farm were obtained from the San Joaquin Valley Air Pollution District (ValleyAir, Personal correspondence, 2019). It is important to highlight that the facilities studied here have more animals than an average farm in these counties (Monson *et al.*, 2017) and larger CAFOs might emit more methane on an animal basis than smaller farms (Thoma *et al.*, 2013), which impact on the inventory comparison.

In Figure - 46 the calculated emissions in kg/h of methane for the individual farms in this study are compared to the actual measurements. The measured methane emission is on average 50% higher but with considerable variability. Again note that possibly varying number of animals at individual farms may induce errors in the inventory emissions compared to the measured emissions. It may be expected that the annual average calculations are lower than the measurements due to the difference in temperature (higher temperature than annual average) during the campaign, as previously discussed.

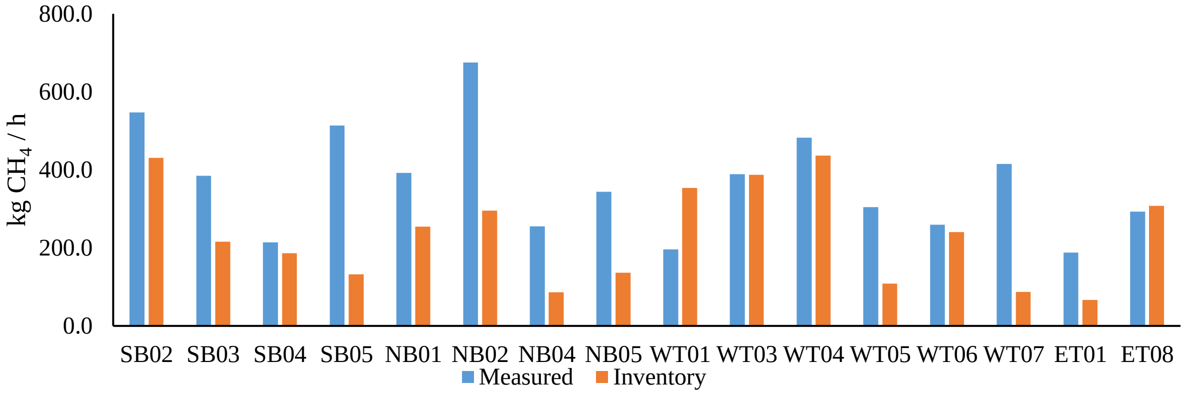

Figure - 46: Methane emissions comparison between measured data and inventory calculations.

Table - 44 shows the measured and calculated inventory $NH_3$ emissions for the individual farms in this study. Measured ammonia emissions are higher than the inventory values and this is consistent with the higher EFs showed in Figure - 43. The difference may also be caused by the fact that the EF used in the calculation is a national average. Figure - 47 displays the relationship between measured and inventory emission factors for ammonia (left) and methane (right).

Table - 44: Comparison of measured ammonia emissions with inventory.

| | kg $NH_3$/h | | |
|---|---|---|---|
| | **Measured 2019** | | **Inventory** |
| | Median | CI 95 % | Estimate |
| **SB02** | 95 | 67-45 | 77.4 |
| **SB03** | 108 | 73-167 | 49.1 |
| **SB04** | 50 | 42-80 | 24.9 |
| **SB05** | 101 | 72-154 | 26.8 |
| **NB01** | 38 | 17-122 | 34.3 |
| **NB02** | 96 | 61-147 | 34.9 |
| **WT01** | 69 | 48-93 | 77.7 |
| **WT03** | 157 | 121-193 | 40.7 |
| **WT04** | 195 | 120-262 | 43.8 |
| **WT05** | 68 | 29-111 | 24.9 |
| **WT06** | 103 | 57-165 | 35.7 |
| **WT07** | 65 | 51-83 | 18.9 |
| **ET01** | 29 | 20-43 | 9.2 |
| **ET08** | 60 | 48-72 | 55.6 |

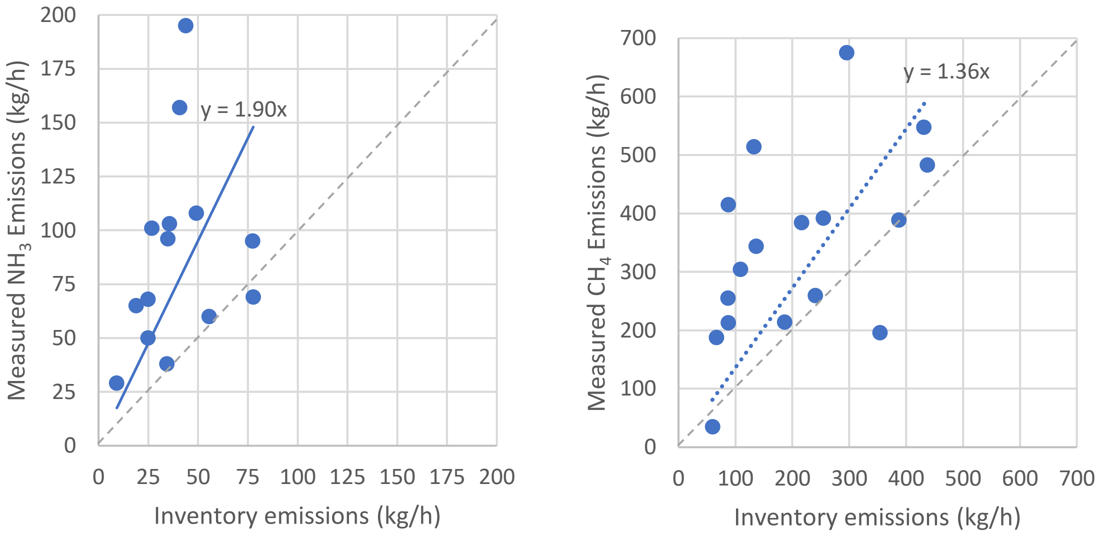

Figure - 47: Relationship between measured and inventoried emissions, 1:1 and linear least squares fit plotted: (left) ammonia (right) methane.

## References

Bjorneberg, D. L. *et al.* (2009) 'Measurement of atmospheric ammonia, methane, and nitrous oxide at a concentrated dairy production facility in southern Idaho using open-path FTIR spctrometry', *Transcations of the American society of agricultural and biological engineers*, 52(5), pp. 1749–1756. doi: 10.13031/2013.29137.

CARB (2019a) 'Documentation of California's 2000-2017 GHG Inventory - Index'. Available at: https://ww3.arb.ca.gov/cc/inventory/doc/doc_index.php.

CARB (2019b) 'Methane research hotspots (AB 1496)'. Available at: https://ww2.arb.ca.gov/our-work/programs/methane/ab1496-research.

EPA (2004) 'National emission inventory—ammonia emissions from animal husbandry operations (Draft Report)', *United States Environmental Protection Agency*, (January 30), pp. D1–D16. Available at: https://www3.epa.gov/ttnchie1/ap42/ch09/related/nh3inventorydraft_jan2004.pdf.

Harper, L. A. *et al.* (2009) 'Ammonia emissions from dairy production in Wisconsin', *Journal of Dairy Science*. Elsevier, 92(5), pp. 2326–2337. doi: 10.3168/jds.2008-1753.

Hristov, A. N. *et al.* (2011) 'Review: Ammonia emissions from dairy farms and beef feedlots', *Canadian Journal of Animal Science*, 91(1), pp. 1–35. doi: 10.4141/CJAS10034.

Johansson, J. *et al.* (2013) 'Quantification of industrial emissions of VOCs, NO2 and SO2 by SOF and Mobile DOAS during DISCOVER-AQ.', (2), pp. 1–71. Available at: http://aqrp.ceer.utexas.edu/projectinfoFY12_13%5C13-005%5C13-005%0AFinal%0AReport.pdf.

Johansson, J. *et al.* (2014) 'Emission measurements of alkenes, alkanes, SO2 and NO2 from stationary sources in southeast Texas over a 5 year period using SOF and Mobile DOAS', *Journal of Geophysical Research*, (x), pp. 1–8. doi: 10.1002/2013JD021350.Received.

Kihlman, M. (2005) *Application of Solar FTIR Spectroscoy for Quantingfying Gas Emissions*. Chalmers University of Technology, Gothenburg, Sweden.

Kille, N. *et al.* (2017) 'The CU mobile Solar Occultation Flux instrument : structure functions and emission rates of NH 3 , NO 2 and C 2 H 6', (September 2014), pp. 373–392. doi: 10.5194/amt-10-373-2017.

Leifer, I. *et al.* (2018) 'Validation of mobile in situ measurements of dairy husbandry emissions by fusion of airborne/surface remote sensing with seasonal context from the Chino Dairy Complex', *Environmental Pollution*. Elsevier Ltd, 242, pp. 2111–2134. doi: 10.1016/j.envpol.2018.03.078.

Leytem, A. B. *et al.* (2011) 'Emissions of Ammonia, Methane, Carbon Dioxide, and Nitrous Oxide from Dairy Cattle Housing and Manure Management Systems', *Journal of Environment Quality*, 40(5), p. 1383. doi: 10.2134/jeq2009.0515.

Mellqvist, J. (1999) *Application of infrared and UV-visible remote sensing techniques for studying th*. Chalmers Tekniska Hogskola.

Mellqvist, J., Johansson, J., Samuelsson, J., Rivera, C., *et al.* (2008) 'Comparison of Solar Occultation Flux Measurements to the 2006 TCEQ Emission I nventory and Airbone Measurements for the TexAQS II, Project No. 582-5-64594-fy08-06, TCEQ report., Texas', *(available at http://www.tceq.state.tx.us/assets/public/implementation/air/am/contracts/reports/da/20081108-comparison_solar_occultation_flux_measurements.pdf)*.

Mellqvist, J., Johansson, J., Samuelsson, J. and Offerle, B. (2008) 'Emission Measurements of Volatile Organic Compounds with the SOF method in Normandy 2008.', *Available at Fluxsense.se*.
Mellqvist, J. (2009) 'Emission Measurements of Volatile Organic Compounds with the SOF method in the Rotterdam Harbor 2008', *Available at www.fluxsense.se*.

Mellqvist, J. *et al.* (2010) 'Measurements of industrial emissions of alkenes in Texas using the solar occultation flux method', *Journal of Geophysical Research*, 115, p. D00F17. doi: 10.1029/2008JD011682.

Miller, D. J. *et al.* (2015) 'Ammonia and methane dairy emission plumes in the San Joaquin Valley of California from individual feedlot to regional scales', pp. 9718–9738. doi: 10.1002/2015JD023241.Received.

Monson, J. *et al.* (2017) 'California Dairy Statistics Annual: 2017 Data', p. 18.

Olesen, J. E. and Sommer, S. G. (1993) 'Modelling effects of wind speed and surface cover on ammonia volatilization from stored pig slurry', *Atmospheric Environment Part A, General Topics*, 27(16), pp. 2567–2574. doi: 10.1016/0960-1686(93)90030-3.

Rennie, T. J. *et al.* (2018) 'Liquid manure storage temperature is affected by storage design and management practices—A modelling assessment', *Agriculture, Ecosystems and Environment*. Elsevier, 260(March), pp. 47–57. doi: 10.1016/j.agee.2018.03.013.

Rothman, L. S. *et al.* (2003) 'The HITRAN molecular spectroscopic database: Edition of 2000 including updates through 2001', *Journal of Quantitative Spectroscopy and Radiative Transfer*, 82(1–4), pp. 5–44. doi: 10.1016/S0022-4073(03)00146-8.

Sharpe, S. W. *et al.* (2004) 'Gas-phase databases for quantitative infrared spectroscopy', *Applied Spectroscopy*, 58(12), pp. 1452–1461. doi: 10.1366/0003702042641281.

Souza, P. *et al.* (2018) 'Dairy research prospectus to achieve California's SB1383 Climate Goals'.

Sun, K. *et al.* (2015) 'Open-path eddy covariance measurements of ammonia fluxes from a beef cattle feedlot', *Agricultural and Forest Meteorology*. Elsevier B.V., 213, pp. 193–202. doi: 10.1016/j.agrformet.2015.06.007.

Thoma, G. *et al.* (2013) 'Regional analysis of greenhouse gas emissions from USA dairy farms: A cradle to farm-gate assessment of the American dairy industry circa 2008', *International Dairy Journal*. Elsevier, 31(1), pp. S29–S40. doi: 10.1016/j.idairyj.2012.09.010.

Tulare county resource management, A. (2016) 'Draft Environmental Impact Report', (January).
US-EPA (2017) 'Annexes to the inventory of U.S. GHG emissions and sinks. U.S. Environmental Protection Agency. Inventory of U.S. Greenhouse gas emissions and sinks: 1990-2015.', (Unfccc), pp. 1–458.

VanderZaag, A. C. *et al.* (2014) 'Measuring methane emissions from two dairy farms: Seasonal and manure-management effects', *Agricultural and Forest Meteorology*. Elsevier B.V., 194, pp. 259–267. doi: 10.1016/j.agrformet.2014.02.003.

Zhu, L. *et al.* (2015) 'Global evaluation of ammonia bidirectional exchange and livestock diurnal variation schemes', *Atmospheric Chemistry and Physics*, 15(22), pp. 12823–12843. doi: 10.5194/acp-15-12823-2015.

# Emission measurements of VOCs and community monitoring in Southern California 2019 - Sub Report D

**2020**

**FINAL REPORT**

FluxSense Inc

17 May 2020

**Date:** 17 May 2020
**Updated**: 1 December 2020

Title: Emission measurements of VOCs and community monitoring in Southern California 2019 - Sub Report D

**Authors:** Johan Mellqvist[1,3], Samuel Brohede[2], Brian Offerle[2], Jerker Samuelsson[1] and Marianne Ericsson[1]

[1]FluxSense Inc, 113 W G Street # 757, San Diego, CA 92101
[2]FluxSense AB, Sven Hultins gata 9, SE-41288 Göteborg, Sweden
[3]Chalmers University of Technology, Hörsalsvägen 11, SE-41296, Göteborg, Sweden

**CARB contract no. 17RD021**
Principal Investigator: Johan Mellqvist,
Prepared for the California Air Resources Board
and the California Environmental Protection Agency

[Cover: Mobile lab measurement at the Frank Bowerman landfill in Southern California]

## DISCLAIMER

## Executive summary

*Objective*

A two-year study is carried out by FluxSense Inc on behalf of California Air Resources Board (CARB). The objective is to provide ground-based flux measurements of VOCs, methane, air toxics and ammonia from various sources, e.g. refineries, petrochemical facilities, oil storage, port activities, landfills, oil and gas production and Concentrated Animal Feeding Operations (CAFOs). The study also characterizes ground concentrations of the above-mentioned species at community scale to provide insights on concentration levels particularly in disadvantaged communities near emission sources and to identify emissions sources and their contributions to observed levels. This project complements community monitoring efforts by CARB staff who have measured speciated VOCs and air toxics of concern.

*Background*

This sub-report consists of measurement results from 10 days in October 2019 carried out in three parts of Southern California CA, i.e. San Diego County Air Basin, Southern South Coast Air Basin around Huntington Beach and northern South Coast Air basin around Northridge. The focus was on screening for potential emission sources of VOC, NOx and SO2 and investigate their magnitude and impact on the neighbouring communities. In the study a variety of sources were studied, including oil and gas production, gas/fuel storage, breweries, landfills, a harbour, and an airport. By coincidence we also measured downwind of several wildfires. This is the 4th sub report in this project and the choice of region and sources partly complements previous reports in which the following source areas were studied: Refineries and ports in Bay area (sub report A), VOC emissions from Oil and Gas production in Central valley (sub report B) and NH3 and CH4 emission from CAFOs (sub report C).

The emission fluxes (kg/h) of alkanes, ammonia, SO2, NO2 and formaldehyde were quantified using Solar Occultation Flux (SOF) and mobile SkyDOAS (Differential Optical Absorption Spectroscopy). MWDOAS (Mobile White Cell DOAS) and MeFTIR (Mobile extractive Fourier Transform Infrared) techniques were used to measure ground level concentrations of alkanes, BTEX and methane, which allowed to indirectly obtain emission fluxes when combined with measured SOF fluxes.

SOF is a proven technique that has been developed at Chalmers University of Technology in Sweden and further developed and applied by FluxSense in over 100 fugitive emission studies around the world. In Europe the SOF technique is considered Best Available Technology (BAT) for measurements of fugitive emission of VOCs from refineries, and in Sweden it is used in conjunction with tracer correlation and optical gas imaging to annually screen all larger refineries and petrochemical facilities. The estimated uncertainty for SOF emission measurements is typically 30 % for total site emissions. The estimated measurement uncertainties have been verified in several (blind and non-blind) controlled source gas release and in side-by-side measurements with other measurement techniques.

The instrument systems above were operated in the FluxSense mobile laboratory and the measurement were conducted while driving outside the source area fence-lines along public roads. Background columns and concentrations were subtracted by encircling the sites, when possible, or by measuring upwind columns and concentrations, so that only emissions from within the facilities were quantified. Wind data were obtained from a Light Detection and

Ranging (LIDAR) instrument that measured the wind profile between 10 to 300 m altitude. From the combination of the measured column and concentration values, the height of the plume could be derived to first order.

*Results and discussion*

Table E.1 shows the main emission results from the campaign in 2019. Here the quantitative results of emission measurements of 18 sites/areas in three regions (San Diego County Air Basin. South part of SCAB and North part of SCAB.) are presented. Altogether, 153 measurement transects were performed during 10 separate days. Relatively few repeats were carried out for each source, however, since the objective was to screen many sources and therefore the uncertainty is higher than the 30% which is usually stated by the used techniques.

The main sources in this study are related to oil and gas production, fuel storage and to landfills, several in close proximity to communities. In Figure E.1 community monitoring of alkane concentration hotspots is shown along the coastline of Huntington Beach and Newport. From these measurements we were able to identify several hotspots related to active oil and gas wells. The main emissions from these were methane and other alkanes while the emissions of aromatic VOCs were small. In addition, general community monitoring in the area confirms this. Measurements of two tank farms in Huntington Beach that were close to residential areas should relatively low VOC emissions, although they caused significant concentrations during the night. The measurements at the landfills shows that these generally emit alkanes, in addition to methane and the CH4 to alkane mass ratio varies between 2 to 14, with a typical value of around 7. However, there are several uncertainty factors involved when determining these ratios from the fence-line and further work is needed here, measuring inside the actual sources. The fact that the alkane emissions from the landfills are strong enough to be measured by SOF, makes this technique promising for future emission studies.

Measurements at the port of San Diego, Figure E.2 and Table E,1, showed significant $NO_2$ and $SO_2$ emissions, 688 kg/h and 265 kg/h, respectively, which appeared to originate from the port activity. Other observations in the study included measuring the influence of Wildfires on the air quality and detecting methane emissions from the CNG buses.

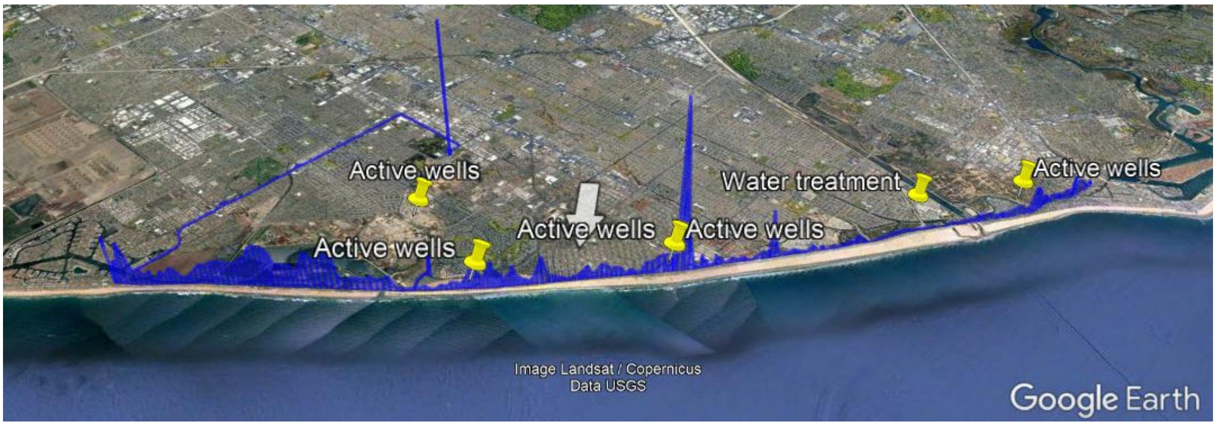

Figure E.1 Community monitoring of Alkane concentration hotspots in NE wind along the coastline of Huntington Beach and Newport, October 30 2019. The wind direction is indicated by the white arrow. Map from Google Earth™, 2020.

Table E.1 Summary of emission flux measurements during the CARB SoCal 2019 survey., n.d.= no detection. *Results based on 3 or fewer measurements should be considered indicative only.

| **Site Name & Region** | ***SOF*** | | ***SkyDOAS*** | | | | ***MeFTIR*** |
|---|---|---|---|---|---|---|---|
| | **Alkanes** | | **$SO_2$** | | **$NO_2$** | | **$CH_4$** |
| | **N** | **Flux** [kg/h] | **N** | **Flux** [kg/h] | **N** | **Flux** [kg/h] | **Flux** [kg/h] |
| **San Diego County** | | | | | | | |
| Mission Valley Tank Farm & Depot | 7 | 27 | 1 | n.d. | 3 | n.d | |
| Otay Landfill | 6 | 47 | | | | | 660 |
| Otay Industry Sites | 6 | 48 | | | | | 135 |
| Miramar Landfill & Airport | 1* | 135 | | | | | 91 |
| Port of San Diego | 4 | 137 | 6 | 265 | 7 | 688 | 92 |
| San Diego Airport | 2* | 5.0 | 2* | 34 | 3* | 26 | |
| **South SCAB** | | | | | | | |
| Highlands Area Facility | 11 | 31 | | | | | 39 |
| Huntington Beach Bolsa Area | 11 | 31 | | | | | 23 |
| Huntington Fuel Depot | 5 | 4.8 | | | | | 0.6 |
| Huntington Toronto Ave Well Site | 7 | 4.3 | | | | | 6.8 |
| Frank Bowerman Landfill | 5 | 46 | | | | | 522 |
| Coyote Canyon Landfill | 5 | n.d. | | | | | |
| **North SCAB** | | | | | | | |
| North Hills Brewery | 1* | 53 | | | | | |
| Irwindale Brewery | 7 | 7.9 | | | | | 5.3 |
| Irwindale Industrial Site 1 | 5 | 7.7 | | | | | |
| Irwindale Industrial Site 2 | 4 | 3.4 | | | | | |
| Placerita Oil Field | 1* | 216 | | | | | 337 |
| **Sum** | **88** | **804** | **9** | **299** | **15** | **715** | **1911** |

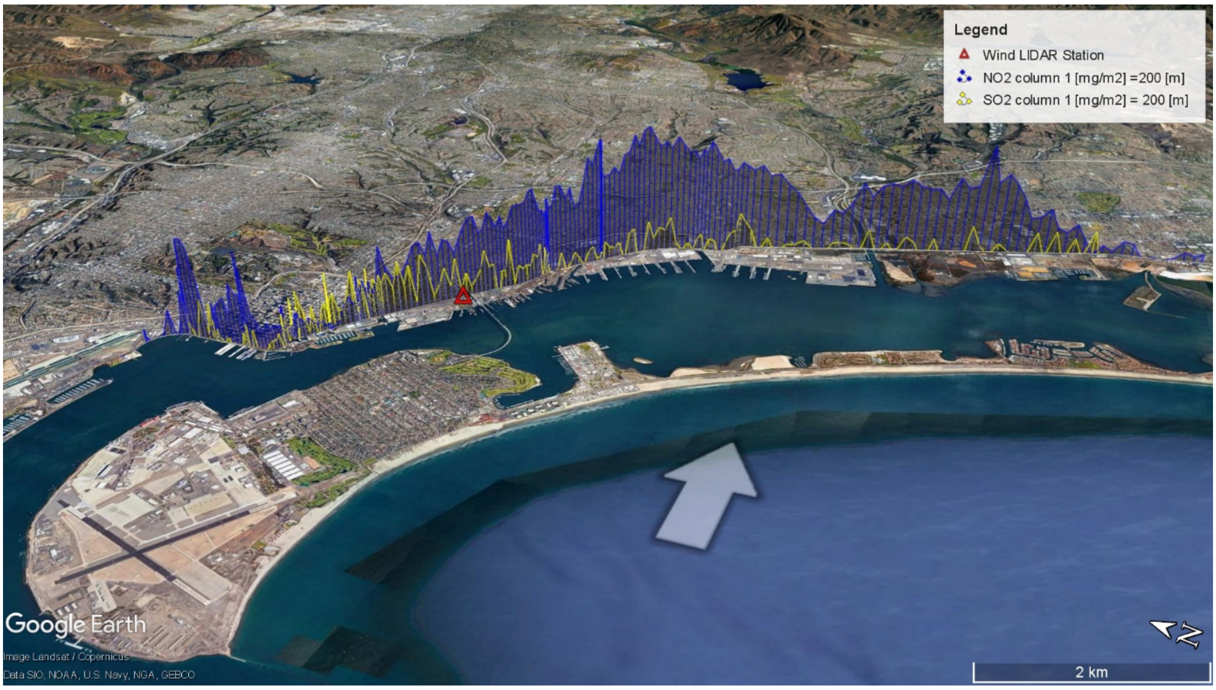

Figure E.2 SkyDOAS columns of $NO_2$ and $SO_2$ downwind the Port of San Diego on October 22 2019. The wind direction is indicated by the white arrow. Map from Google Earth™, 2020.

# Acronyms, Units and Definitions

## Acronyms used in this report

| | |
|---|---|
| BTEX | Sum of Benzene, Toluene, Ethyl Benzene and Xylene |
| CARB | California Air Resources Board |
| DOAS | Differential Optical Absorption Spectroscopy |
| DOGGR | Division of Oil & Gas & Geothermal Resources |
| EF | Emission factor |
| FTIR | Fourier Transform InfraRed |
| IME | Indirectly Measured Emission, combining direct emission with concentration ratios |
| LIDAR | Light Detection and Ranging |
| MWDOAS | Mobile White cell DOAS |
| MeFTIR | Mobile extractive FTIR |
| NMVOC | Non-methane volatile organic compound |
| ROG | Reactive Organic Gases |
| SkyDOAS | Scattered Skylight DOAS |
| SOF | Solar Occultation Flux |
| VOC | Volatile organic compound, used interchangeably for non-methane VOC |
| SCAB | South Coast Air Basin |
| LA | SCAB |

## Units

| | |
|---|---|
| Air temperature | degrees C |
| Atmospheric Pressure | mbar |
| Relative Humidity | % |
| Wind direction | degrees North |
| Wind speed | m/s |
| Column | $mg/m^2$ |
| Concentration | $mg/m^3$ |
| Flux | kg/h |

## Unit Conversions

1 lbs = 0.4536 kg
1 kg/h = 52.9 lbs/day
1 bbl = 159 l
1 bbl/day = 5.783 kg/h (crude oil)
1 (short) ton = 907.2 kg
1 kton/year = 104 kg/h
1 klbs/year=0.052 kg/h

### Definitions

Alkane or Alkanes are considered to be all non-methane alkane species.

# Table of Contents

## List of Figures

## List of Tables

# 1 Objective and Introduction

A two-year study has been carried out with the objective to provide ground-based flux measurements in different regions in California of VOCs, methane, air toxics and ammonia from various sources, e.g. refineries, petrochemical facilities, oil storage, port activities, landfills, oil and gas production and Concentrated Animal Feeding Operations (CAFOs). In addition, the objective was to characterizes ground concentrations of the above-mentioned species at community scale to provide insights on concentration levels particularly in disadvantaged communities near emission sources and to identify emissions sources and their contributions to observed levels.

This sub-report consists of measurement results from a 10 day campaigns in October 2019 in three parts of Southern California CA, i.e. San Diego County Air Basin, Southern South Coast Air Basin (SCAB) around Huntington Beach and northern SCAB around Northridge. The focus was on screening for potential emission sources of VOC, NOx and SO2 and investigate their magnitude and impact on the neighboring communities. In the study a variety of sources were studied, including oil and gas production, gas/fuel storage, breweries, landfills. In addition, we also measured emission from the port and airport of San Diego. This is the 4th sub report in this project and the choice of region and sources partly complements previous reports in which the following source areas were studied: Refineries and ports in Bay area (sub report A), VOC emissions from Oil and Gas production in Central valley (sub report B) and NH3 and CH4 emission from CAFOs (sub report C).

The results from this study should provide useful screening information to identify high-risk communities for prioritizing air pollution mitigation efforts. The data would also be useful to support enforcement efforts to address high BTEX (benzene, toluene, ethylbenzene and xylene) sources, and may be useful to conduct real-world verification of the impact of the oil and gas regulation (effective Jan 1, 2018) on CH4 emissions.

# 2 Background

Industrial volatile organic compounds (VOC) emissions may contribute to significant formation of ground level ozone, which is formed through atmospheric chemical reactions of volatile organic compounds (VOCs) and nitrogen oxides ($NO_x$) in the presence of sunlight, often called photo chemical smog. Elevated ozone concentrations are known to reduce crop yields and constitute a public health concern. Larger metropolitan areas in the US have trouble meeting ozone standards since anthropogenic sources tend to be concentrated in urban areas, including both mobile and stationary sources. For instance, in order to meet current and future more stringent ozone standards in SCAB, reductions in VOC emissions are foreseen [Downey et. al. 2015]. Stationary sources such as refineries, storage depots, petrochemical facilities are the largest point sources of VOC emissions. The emissions are typically dominated by evaporative losses from storage tanks and process equipment, so-called fugitive emissions. Several VOCs are also toxic with direct impact on health. Methane causes climate change. Ammonia emissions cause production of particles of concern for health and climate.

In 2015, the Governor approved Assembly Bill 1496 (AB 1496), which requires the California Air Resources Board (CARB) to monitor and measure high methane emission hotspots within the state using the best available scientific and technical methods. In order to meet the requirements under AB 1496, CARB, in conjunction with the California Energy Commission (CEC), has funded a large-scale statewide aerial methane survey conducted by NASA Jet Propulsion Laboratory (JPL) to detect and identify methane super emitters which may be a large contributor to the regional methane hotspots. CARB has also funded Scientific Aviation to quantify emission fluxes from various methane sources (including super emitters) with airborne measurements. Furthermore, certain emissions from oil and gas facilities, which are also major methane emitters, are known to have potential adverse health effects. Oil and gas operations are located in a variety of areas in California, including densely populated areas and in proximity of disadvantaged communities. In order to meet CARB's mission to protect the public from harmful effects of air pollution, there have been efforts to enhance the community monitoring for air toxics and methane, particularly in the communities near oil and gas facilities, which are primarily disadvantaged communities. The recently approved AB 617 will also require CARB to develop a community monitoring plan to identify disadvantaged communities for community monitoring deployment. It will also require CARB to develop a cumulative impact state strategy to identify communities with high cumulative risk so air districts can develop Community Action Plans.

# 3 Instrumentation and Methods

A Mobile Laboratory was used which is equipped with four instruments for gas monitoring, i.e. SOF (Solar Occultation Flux), SkyDOAS (Differential Optical Absorption Spectroscopy), MeFTIR (Mobile extractive Fourier Transform Infrared) and MWDOAS (Mobile White cell DOAS),see Figure 1.

SOF and SkyDOAS both measure gas columns through the atmosphere by means of light absorption. SOF utilizes infrared light from the direct sun whereas SkyDOAS measures scattered ultraviolet light from the sky. MeFTIR and MWDOAS uses active light sources combined with multi-reflection cells to measure ground level concentrations of alkanes and BTEX, respectively. A wind LIDAR (LIght Detection And Ranging) is generally used to measure vertical profiles of wind speed and wind direction from 50-300 m height. The LIDAR data is combined with data from mobile wind masts and data from meteorological networks.

Figure 1 Internal and external view of the FluxSense mobile lab.

For SOF and SkyDOAS the emission rate is directly obtained by multiplying the measured mass columns across the source plume with the wind speed while the flux measurements by MWDOAS and MeFTIR are measured indirectly through BTEX/alkane ratio measurements combined with the gas flux measurements by SOF and SkyDOAS. The measurements are carried out from a mobile platform making it possible to make measurements in a box (circle) around leaking areas and to discriminate between upwind and downwind concentrations,

The column measurements are combined with wind measurements to estimate the corresponding mass fluxes. The measurement sensitivity for the column varies between 0.1- to 5 mg/m$^2$ (0.5-25 ppb over 100 m) and this results in a lower detectable flux limit of 0.2-2 kg/h for a single isolated source. The estimated uncertainty for SOF emission measurements is typically 30 % for total site emissions. The estimated measurement uncertainties have been verified in several (blind and non-blind) controlled source gas release and in side-by-side measurements with other measurement techniques. For more technical information, see the appendices and reference list.

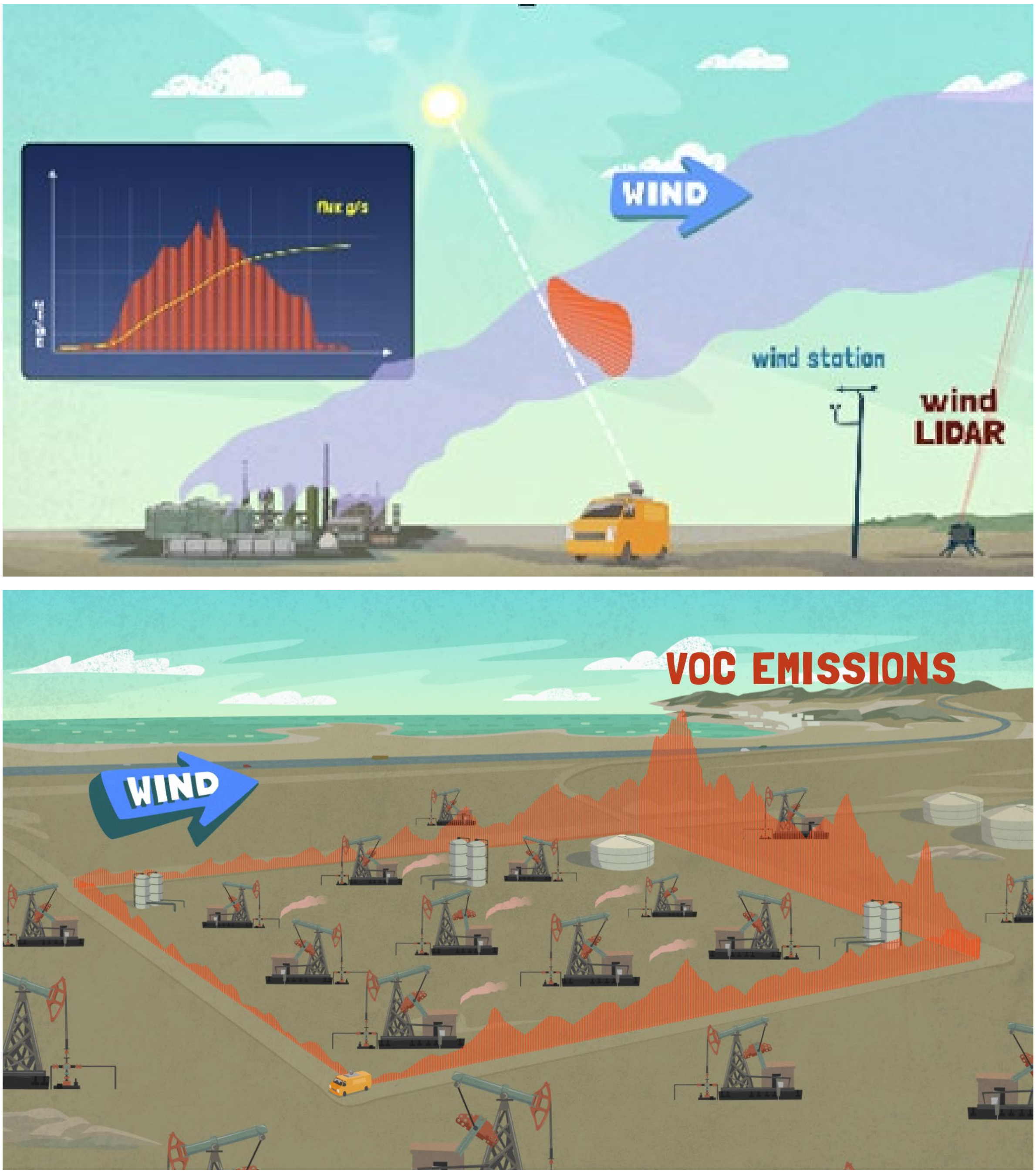

Figure 2 Schematic of the SOF measurement where the vehicle is driven across the prevailing wind so that the solar beam cuts through the emission plume while the sun is locked into the FTIR spectrometer by the solar tracking device on the roof or zenith scattered sky light. The VOC mass (or other compound of interest) is integrated through the plume cross section. Usually the measurements are carried by measuring in a box around the individual sources, in order to subtract the influence of the upwind background concentrations.

Table 1.Summary of FluxSense gas measurement techniques. *For typical wind conditions at an optimal distance from the source.

| **Method** | **SOF** | **Sky DOAS** | **MeFTIR** | **MWDOAS** |
|---|---|---|---|---|
| Compounds | **Alkanes**: ($C_nH_{2n+2}$)<br>**Alkenes:**$C_2H_4$, $C_3H_6$<br>**$NH_3$** | **$SO_2$**<br>**$NO_2$**<br>**$H_2CO$** | **$CH_4$**<br>**Alkanes:** ($C_nH_{2n+2}$)<br>**Alkenes:** $C_2H_4$, $C_3H_6$<br>**$NH_3$**<br>**$N_2O$** (tracer) | **BTEX** |
| Detection limit Column | 0.1-5 $mg/m^2$ | 0.1-5 $mg/m^2$ | 1-10 ppbv | 0.5-3 ppbv |
| Detection limit Flux* | 0.2-1 kg/h | 1 kg/h | 0.2-2 kg/h | 0.2-2 kg/h |
| Wind Speed Tolerance | 1.5-12 m/s | 1.5-12 m/s | | |
| Sampling Time Resolution | 1-5 s | 1-5 s | 5-15 s | 8-10 s |
| Measured Quantity [unit] | Integrated vertical column mass [$mg/m^2$] | Integrated vertical column mass [$mg/m^2$] | Mass concentration at Vehicle height [$mg/m^3$] | Concentration at Vehicle height [$mg/m^3$] |
| Derived Quantity [unit] | Mass Flux [kg/h] | Mass Flux [kg/h] | 1) Alkane and methane mass concentration ratio of ground plume combined with SOF gives mass flux [kg/h] and plume height information [m]<br>2) Alkane and $CH_4$ flux [kg/h] via tracer release | Combined with MeFTIR and SOF gives Mass Flux [kg/h] |
| Complementary data | Vehicle GPS-coordinates, Plume wind speed and direction | Vehicle GPS-coordinates, Plume wind speed and direction | Vehicle GPS-coordinates<br>Plume wind direction | Vehicle GPS-coordinates, Plume wind direction |

# 4 Survey Setup

Mobile measurements with SOF, SkyDOAS, MWDOAS, and MeFTIR were carried out during 10 measurements days in 2019 (Oct 22 to Oct 31) in three different regions:

1. San Diego County Air Basin, see Figure 3
2. South SCAB, see Figure 4
3. North SCAB, see Figure 5

A variety of sources were studied, including oil and gas production, gas/fuel storage, breweries, landfills. In addition, emissions from the port and airport were measured.

The gas measurements were combined with wind data, primarily from a mobile wind LIDAR but also from adjacent stationary meteorological stations, to calculate fluxes and identify sources. During the measurement campaign the wind LIDAR, which was installed on the back of a measurement van, was positioned in proximity to the emission sources.

In Table 2 an overview of the studied areas and emissions sources are shown. From the sources we generally measured the emissions of alkanes, SO2, NO2 and HCHO and performed concentration mapping of alkanes, methane and BTEX. By combining the column and concentration measurements we could obtain indirect fluxes of several species. In the studied areas we also performed general community monitoring of VOC concentrations and in some cases large gas fluxes were measured, for instance from potential wildfires. By coincidence we also measured downwind of several wildfires and these sometimes caused problems in interpretation due to high background concentrations.

Table 2. The measurement areas and source studied.

| Date | Studied areas | Studied emission Sources |
|---|---|---|
| Oct 22 | San Diego Air Basin | Port of San Diego<br>Miramar landfill |
| Oct 23 | San Diego Air Basin | Otay landfill and Mexican Border |
| Oct 23 | San Diego | Miramar landfill, Tank Park and Port of San Diego |
| Oct 25 | North SCAB: San Joaquin Hills | Coyote Canyon Landfill |
| Oct 26 | North SCAB: Santa Clarita<br>Northridge | Placerita Oil Field<br>Sunshine Canyon landfill |
| Oct 27 | North SCAB: Northridge<br>Sun Valley | Brewery<br>Landfill and industries |
| Oct 28 | North SCAB: BrentWood<br>Irvindale | Wildfire<br>Brewery, tank storage |
| Oct 29 | South SCAB: Huntington Beach | Huntington Beach Oilfields |
| Oct 30 | South SCAB: Costa Mesa, Huntington Beach | Franck Bower Landfill<br>Huntington Bolsa Area<br>Huntington fuel depot |
| Oct 31 | South SCAB: Huntington Beach | Huntington Bolsa Area<br>Huntington fuel depot |

Figure 3 Measured areas in the San Diego region during CARB SoCAL survey, October 2019. Map from Google Earth™, 2020.

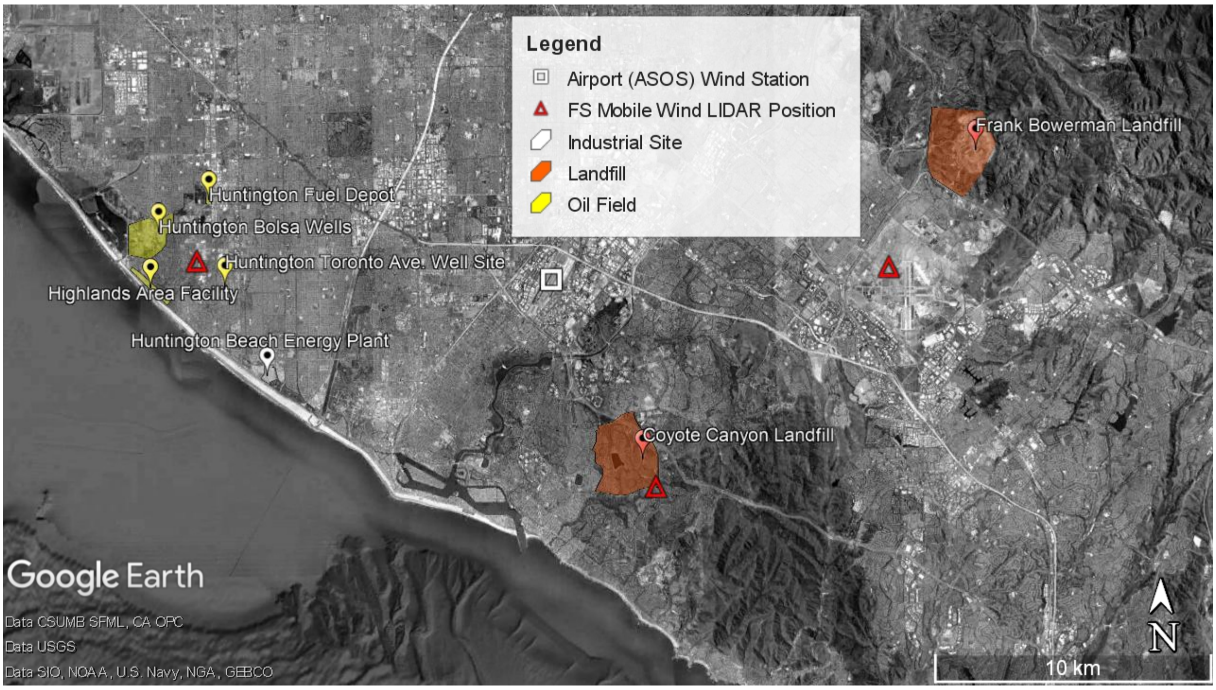

Figure 4 Measured areas in the South SCAB region during CARB SoCAL survey, October 2019. Map from Google Earth™, 2020.

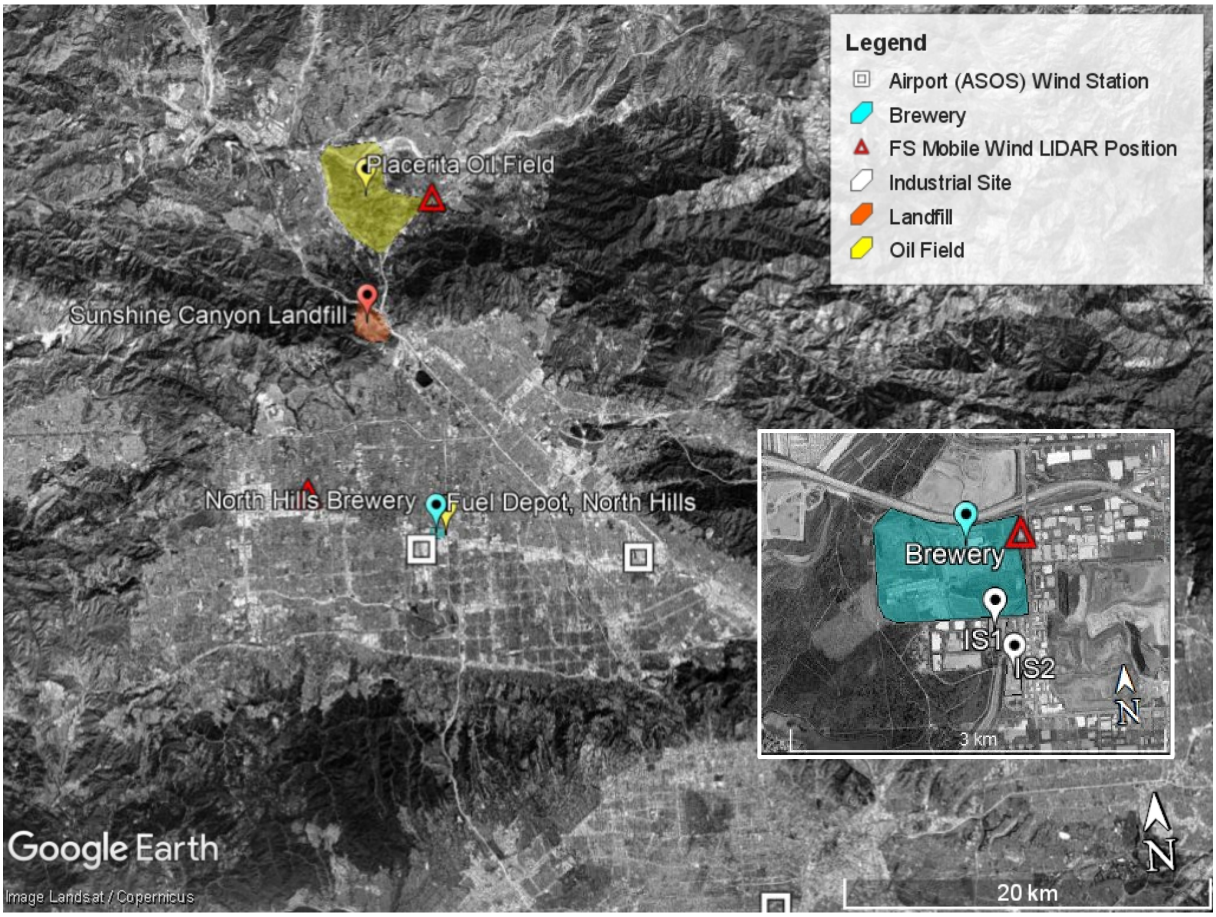

Figure 5 Measured areas in the North SCAB region during CARB SoCAL survey, October 2019. Inset Irwindale industrial sites (IS) and brewery. Map from Google Earth™, 2020.

# 5 Results

A summary of the quantitative results of emission measurements of 18 sites/areas in the three regions (San Diego County Air Basin, South SCAB and North SCAB) is presented in Table 3. All together 153 measurement transects were performed during 10 separate days. We were only able to measure with few repeats on each site, since the objective was to screen many sources in several areas over a limited time frame. The uncertainties are therefore larger than the 30% which is usually stated for SOF measurements.

Table 3 Summary of emission measurements during the CARB SoCal 2019 survey. SOF and SkyDOAS results are reported here as median values of all quality assured transects (N) to reduce sensitivity to outliers, n.d.= no detection. *Results based on 3 or fewer measurements should be considered indicative only.

| **Site Name & Region** | ***SOF*** | | ***SkyDOAS*** | | | | ***MeFTIR*** |
|---|---|---|---|---|---|---|---|
| | **Alkanes** | | **$SO_2$** | | **$NO_2$** | | **$CH_4$** |
| | **N** | **Flux** [kg/h] | **N** | **Flux** [kg/h] | **N** | **Flux** [kg/h] | **Flux** [kg/h] |
| **San Diego County** | | | | | | | |
| Mission Valley Tank Farm & Depot | 7 | 27 | 1 | n.d. | 3 | n.d | |
| Otay Landfill | 6 | 47 | | | | | 660 |
| Otay Industry Sites | 6 | 48 | | | | | 135 |
| Miramar Landfill & Airport | 1* | 135 | | | | | 91 |
| Port of San Diego | 4 | 137 | 6 | 265 | 7 | 688 | 92 |
| San Diego Airport | 2* | 5.0 | 2* | 34 | 3* | 26 | |
| **South SCAB** | | | | | | | |
| Highlands Area Facility | 7 | 31 | | | | | 39 |
| Huntington Beach Bolsa Area | 11 | 31 | | | | | 23 |
| Huntington Fuel Depot | 5 | 4.8 | | | | | 0.6 |
| Huntington Toronto Ave Well Site | 7 | 4.3 | | | | | 6.8 |
| Frank Bowerman Landfill | 5 | 46 | | | | | 522 |
| Coyote Canyon Landfill | 5 | n.d. | | | | | |
| **North SCAB** | | | | | | | |
| North Hills Brewery | 1* | 53 | | | | | |
| Irwindale Brewery | 7 | 7.9 | | | | | 5.3 |
| Irwindale Industrial Site 1 | 5 | 7.7 | | | | | |
| Irwindale Industrial Site 2 | 4 | 3.4 | | | | | |
| Placerita Oil Field | 1* | 216 | | | | | 337 |
| **Sum** | **88** | **804** | **9** | **299** | **15** | **715** | **1911** |

Note that SOF and SkyDOAS provide direct flux measurements while MWDOAS and MeFTIR give indirect fluxes via gas ratio measurements. Ratio measurements can be influenced by nearby point sources with different compositions than the field as a whole, however, care has been taken to include as large as area as possible, to minimize the influence of individual sources. Further details are given under the areas' respective section and in the results for identification and measurement of point sources.

Quantitative results from each region and site are presented in section 5.1, 0 and 5.5. Results in the subsections below are presented as different statistical measures such as averages, standard deviations and medians. Both daily and total survey values are given for each site. Median values are primarily used in this report since it is less sensitivity to outliers than averages. Concentration mapping  in communities and along site ‘fencelines’ (perimeters) are detailed in Section 5.2, 5.4 and 5.6.

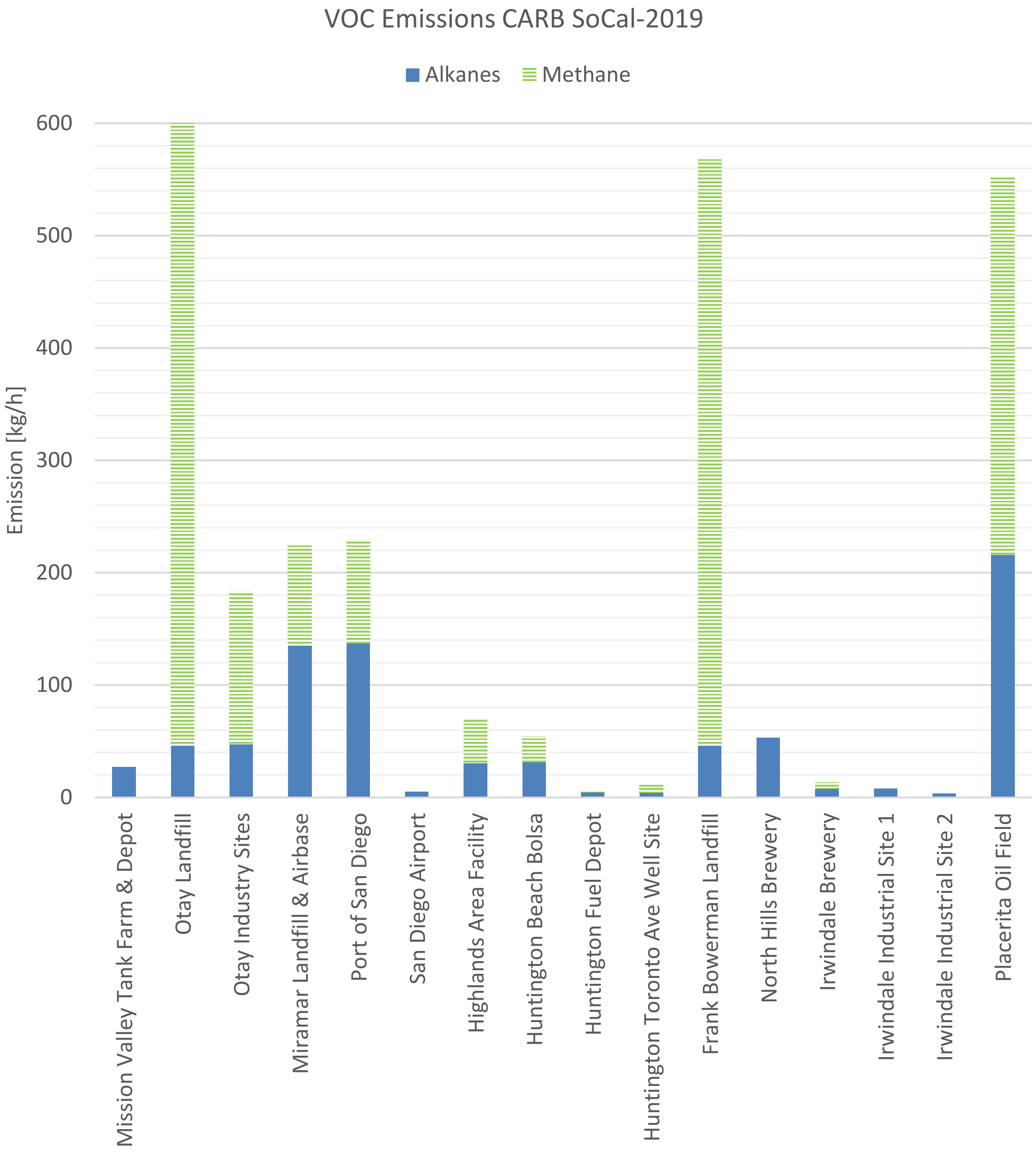

Figure 6 Median values of VOC emissions (Alkanes and Methane) from the sites during the CARB SoCal-2019 survey as measured by the FluxSense SOF, MWDOAS and MeFTIR instruments. Alkane emissions are measured directly while Methane emissions are Indirect fluxes from gas ratios.

## 5.1 Emission measurements and source concentration mapping – San Diego

Measurements in the San Diego county were conducted 22-24 October 2019. Results from six different sites/areas are presented in the subsections below. The sites were either selected in the implementation plan or detected in real-time during measurement and considered interesting.

### *5.1.1 Port of San Diego*

The Port of San Diego includes all emissions sources west of Harbor Drive / Hwy 5 (see green area in Figure 7) and includes various industrial and military sites, ship yards, fuel depots and harbour activities. Measurements were conducted 22 and 24 October 2019 during westerly winds, see examples in Figure 7 - Figure 8. Wind profile data (0-100 m) from the mobile LIDAR located at Cesar Chavez park has been used for flux calculations.

Repeatable, spread out plumes were detected in both SOF and SkyDOAS with no distinct signals from local sources close to the measurement path. This indicates that distant sources on the peninsula and/or off-shore sources are dominating the emissions. Further measurements are needed, including upwind/background sampling in order to investigate this.

The survey median emissions were 137 kg/h of alkanes, 688 kg/h of $NO_2$, 265 kg/h of $SO_2$ and 166 kg/h of HCHO. The measurement of HCHO were close to the detection limit and therefore uncertain. Methane/Alkane ratios of 67% gave an indirect methane emission of 92 kg/h. The emissions of $NO_2$, $SO_2$ and HCHO are most likely from the port activities. Daily results are found in Table 4- Table 8.

Figure 7. SOF alkane columns (blue contour) downwind the Port of San Diego (green area), 22 October 2019. The wind direction is indicated by the white arrow. Map from Google Earth™, 2020.

Figure 8. SkyDOAS columns of $NO_2$ (blue contour), $SO_2$ (orange contour) and HCHO (white contour) downwind the Port of San Diego (green area), 22 October 2019. The wind direction is indicated by the white arrow. Map from Google Earth™, 2020.

Table 4 SOF Alkane emission measurements, Port of San Diego, October 2019

| Day [yymmdd] | Time span [hhmmss-hhmmss] | Num Meas | Emission avg [kg/h] | Emission SD [kg/h] | Wind Speed Min-Max [m/s] | Wind Dir Span [deg] |
|---|---|---|---|---|---|---|
| **191022** | 134916-151237 | 3 | 147 | 27.2 | 4.7-4.8 | 270-271 |
| **191024** | 134635-135802 | 1 | 114 | N/A | 2.9-2.9 | 275-275 |
| **Total # of Meas.** | | **4** | | | | |
| **Median** | | | **137.1** | | | |
| **IQR** | | | **116.0 - 160.3** | | | |
| **Mean** | | | **139.1** | | | |
| **SD** | | | **27.8** | | | |

Table 5 Methane/Alkane mass ratios from MeFTIR measurements, Port of San Diego, October 2019

| Day [yymmdd] | Time span [hhmmss-hhmmss] | Num Meas | Mass Ratio avg [%] | Mass Ratio SD [%] | Wind Speed Min-Max [m/s] | Wind Dir Span [deg] |
|---|---|---|---|---|---|---|
| **191022** | 122511-215241 | 3 | 76.5 | 32.7 | 1.2-5.3 | 262-309 |
| **Total # of Meas.** | | **3** | | | | |
| **Median** | | | **67.1** | | | |
| **IQR** | | | **58.3 - 90.0** | | | |
| **Mean** | | | **76.5** | | | |
| **SD** | | | **32.7** | | | |

Table 6 SkyDOAS NO2 emission measurements, Port of San Diego, October 2019

| Day [yymmdd] | Time span [hhmmss-hhmmss] | Num Meas | Emission avg [kg/h] | Emission SD [kg/h] | Wind Speed Min-Max [m/s] | Wind Dir Span [deg] |
|---|---|---|---|---|---|---|
| **191022** | 131822-160937 | 5 | 809 | 209.8 | 4.3-4.9 | 262-281 |
| **191024** | 142741-160333 | 2 | 555 | 40.1 | 5.1-5.3 | 253-270 |
| **Total # of Meas.** | | **7** | | | | |
| **Median** | | | **688.3** | | | |
| **IQR** | | | **555.2 - 938.8** | | | |
| **Mean** | | | **736.4** | | | |
| **SD** | | | **212.0** | | | |

Table 7 SkyDOAS SO2 emission measurements, Port of San Diego, October 2019

| Day [yymmdd] | Time span [hhmmss-hhmmss] | Num Meas | Emission avg [kg/h] | Emission SD [kg/h] | Wind Speed Min-Max [m/s] | Wind Dir Span [deg] |
|---|---|---|---|---|---|---|
| **191022** | 132328-161225 | 5 | 272 | 161.8 | 4.4-4.9 | 264-271 |
| **191024** | 152737-160349 | 1 | 309 | N/A | 4.9-4.9 | 273-273 |
| **Total # of Meas.** | | **6** | | | | |
| **Median** | | | **264.6** | | | |
| **IQR** | | | **163.6 - 347.0** | | | |
| **Mean** | | | **277.8** | | | |
| **SD** | | | **145.5** | | | |

Table 8 SkyDOAS HCHO emission measurements, Port of San Diego, October 2019

| Day [yymmdd] | Time span [hhmmss-hhmmss] | Num Meas | Emission avg [kg/h] | Emission SD [kg/h] | Wind Speed Min-Max [m/s] | Wind Dir Span [deg] |
|---|---|---|---|---|---|---|
| **191022** | 132216-161225 | 5 | 180 | 61.2 | 4.4-4.9 | 264-271 |
| **191024** | 152737-155513 | 1 | 123 | N/A | 5.1-5.1 | 278-278 |
| **Total # of Meas.** | | **6** | | | | |
| **Median** | | | **166.0** | | | |
| **IQR** | | | **131.2 - 191.5** | | | |
| **Mean** | | | **170.3** | | | |
| **SD** | | | **59.4** | | | |

Concentration mapping of alkanes and BTEX along the coast showed local distinct plumes from various sources, see Figure 9 and Figure 10. The peak concentrations were around 65 µg/m$^3$ of BTEX (of which 21 ug of benzene) and 1300 µg/m$^3$ of alkanes.

Figure 9. MeFTIR alkane concentrations at ground level (blue contour) downwind the Port of San Diego (green area), 22 October 2019. The wind direction is indicated by the white arrow. Map from Google Earth™, 2020.

Figure 10. MWDOAS BTEX concentrations at ground level (blue contour) downwind the Port of San Diego (green area), 22 October 2019. The wind direction is indicated by the white arrow. Map from Google Earth™, 2020.

### 5.1.2 *San Diego Airport*

The San Diego airport was sampled during the San Diego Port measurements, see section 5.1.1. Measurements were conducted 24 October 2019 during westerly winds. Wind profile data (0-100 m) from the mobile LIDAR located at Cesar Chavez park has been used for flux calculations.

A small SOF plume was detected on the downwind side during two transects. SkyDOAS plumes of $NO_2$ and $SO_2$ were also small except for one occasion with was probably related to take-off or landing.

The median emissions were 5 kg/h of alkanes, 26 kg/h of $NO_2$, 34 kg/h of $SO_2$ and 10 kg/h of HCHO. Daily results are found in Table 9- Table 12.

Table 9 SOF Alkane emission measurements, San Diego Airport

| Day [yymmdd] | Time span [hhmmss-hhmmss] | Num Meas | Emission avg [kg/h] | Emission SD [kg/h] | Wind Speed Min-Max [m/s] | Wind Dir Span [deg] |
|---|---|---|---|---|---|---|
| **191024** | 140023-143214 | 2 | 5.0 | 1.6 | 4.3-5.2 | 271-275 |
| **Total # of Meas.** | | **2** | | | | |
| **Median** | | | **5.0** | | | |
| **IQR** | | | **4.4 - 5.6** | | | |
| **Mean** | | | **5.0** | | | |
| **SD** | | | **1.6** | | | |

Table 10 SkyDOAS NO2 emission measurements, San Diego Airport

| Day [yymmdd] | Time span [hhmmss-hhmmss] | Num Meas | Emission avg [kg/h] | Emission SD [kg/h] | Wind Speed Min-Max [m/s] | Wind Dir Span [deg] |
|---|---|---|---|---|---|---|
| **191022** | 151735-152235 | 1 | 22.8 | N/A | 5.7-5.7 | 273-273 |
| **191024** | 135654-143121 | 2 | 95.1 | 97.1 | 4.3-5.1 | 250-275 |
| **Total # of Meas.** | | **3** | | | | |
| **Median** | | | **26.4** | | | |
| **IQR** | | | **24.6 - 95.1** | | | |
| **Mean** | | | **71.0** | | | |
| **SD** | | | **80.3** | | | |

Table 11 SkyDOAS SO2 emission measurements, San Diego Airport

| Day [yymmdd] | Time span [hhmmss-hhmmss] | Num Meas | Emission avg [kg/h] | Emission SD [kg/h] | Wind Speed Min-Max [m/s] | Wind Dir Span [deg] |
|---|---|---|---|---|---|---|
| **191024** | 135654-143109 | 2 | 34.4 | 12.7 | 4.3-5.0 | 250-275 |
| **Total # of Meas.** | | **2** | | | | |
| **Median** | | | **34.4** | | | |
| **IQR** | | | **29.9 - 38.8** | | | |
| **Mean** | | | **34.4** | | | |
| **SD** | | | **12.7** | | | |

Table 12 SkyDOAS HCHO emission measurements, San Diego Airport

| Day [yymmdd] | Time span [hhmmss-hhmmss] | Num Meas | Emission avg [kg/h] | Emission SD [kg/h] | Wind Speed Min-Max [m/s] | Wind Dir Span [deg] |
|---|---|---|---|---|---|---|
| **191022** | 153619-154301 | 1 | 9.7 | N/A | 4.7-4.7 | 272-272 |
| **191024** | 135654-140542 | 1 | 11.0 | N/A | 4.3-4.3 | 275-275 |
| **Total # of Meas.** | | **2** | | | | |
| **Median** | | | **10.3** | | | |
| **IQR** | | | **10.0 - 10.7** | | | |
| **Mean** | | | **10.3** | | | |
| **SD** | | | **0.9** | | | |

### 5.1.3 *Mission Valley Tank Farm & Depot*

A tank farm and fuel depot in Mission Valley (see Figure 11) was measured with SOF and SkyDOAS on 22 and 24 October 2019, see example in Figure 10. Wind profile data (0-100 m) from the mobile LIDAR located just north of the tank park (see Figure 10) has been used for flux calculations.

Repeatable, and distinct SOF signals was detected on the downwind side. SkyDOAS plumes were, however, below the detection limit and could not be differentiated from the background. This is expected since no combustion sources are expected to be found in the tank park.

The survey median emissions were 27 kg/h of alkanes from the tank park and the variability low during the measurement time period. Daily results are found in Table 13.

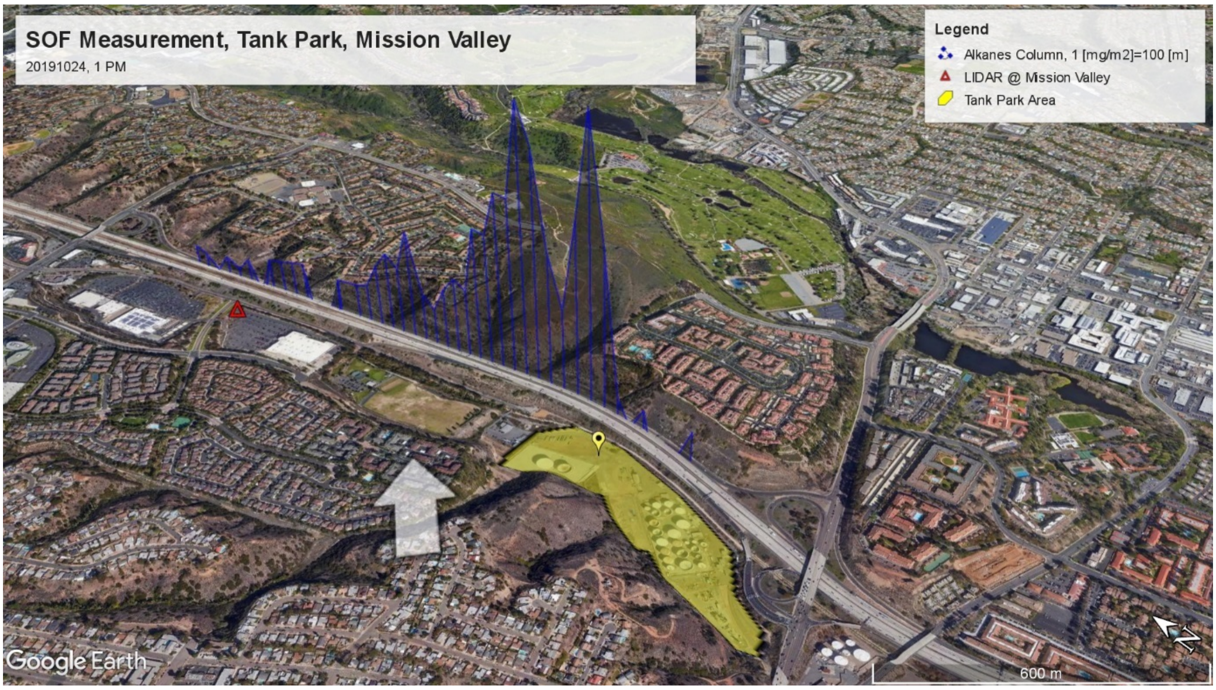

Figure 11. SOF alkane columns (blue contour) downwind the Mission Valley Tank Park (yellow area), 24 October 2019. The wind direction is indicated by the white arrow. Map from Google Earth™, 2020.

Table 13 SOF Alkane emission measurements, Tank Farm, Mission Valley

| Day [yymmdd] | Time span [hhmmss-hhmmss] | Num Meas | Emission avg [kg/h] | Emission SD [kg/h] | Wind Speed Min-Max [m/s] | Wind Dir Span [deg] |
|---|---|---|---|---|---|---|
| **191023** | 102633-102745 | 1 | 27.3 | N/A | 2.6-2.6 | 190-190 |
| **191024** | 121121-132453 | 6 | 26.7 | 3.2 | 2.8-3.5 | 197-352 |
| **Total # of Meas.** | | **7** | | | | |
| **Median** | | | **27.3** | | | |
| **IQR** | | | **25.5 - 28.7** | | | |
| **Mean** | | | **26.7** | | | |
| **SD** | | | **2.9** | | | |

### *5.1.4 Otay Landfill & Industries*

Otay landfill and industries (mainly auto wrecking and car dealers), was measured with SOF and MeFTIR 23 October 2019, see Figure 12. Wind profile data (0-100 m) from the mobile LIDAR located in the south-west corner has been used for flux calculations.

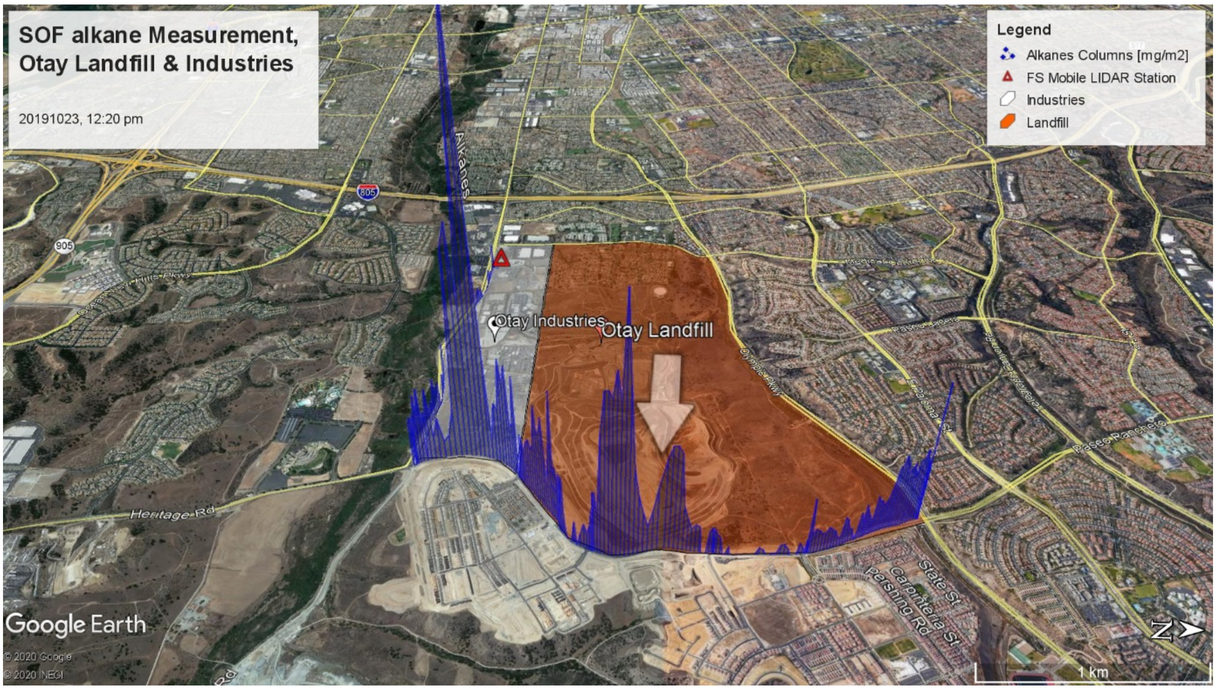

Figure 12. SOF alkane columns (blue contour) at Otay Landfill and Industries, 23 October 2019. The wind direction is indicated by the white arrow. Map from Google Earth™, 2020.

Two separate plumes in both SOF and MeFTIR were detected on the downwind side, one from the actual landfill (hill) and one from the industries south of the landfill. The results from the two parts are reported separately below.

The median emission was 45 kg/h of alkanes from the landfill and 48 kg/h from the industries based on 6 measurement transects, see Table 14 and Table 15.

Table 14 SOF Alkane emission measurements, Otay Landfill

| Day [yymmdd] | Time span [hhmmss-hhmmss] | Num Meas | Emission avg [kg/h] | Emission SD [kg/h] | Wind Speed Min-Max [m/s] | Wind Dir Span [deg] |
|---|---|---|---|---|---|---|
| **191023** | 112022-122314 | 6 | 45.0 | 10.3 | 3.1-4.0 | 273-288 |
| **Total # of Meas.** | | **6** | | | | |
| **Median** | | | **46.5** | | | |
| **IQR** | | | **40.3 - 50.1** | | | |
| **Mean** | | | **45.0** | | | |
| **SD** | | | **10.3** | | | |

Table 15 SOF Alkane emission measurements, Otay Industries

| Day [yymmdd] | Time span [hhmmss-hhmmss] | Num Meas | Emission avg [kg/h] | Emission SD [kg/h] | Wind Speed Min-Max [m/s] | Wind Dir Span [deg] |
|---|---|---|---|---|---|---|
| **191023** | 112251-122526 | 6 | 53.6 | 20.6 | 3.4-4.0 | 269-296 |
| **Total # of Meas.** | | **6** | | | | |
| **Median** | | | **47.6** | | | |
| **IQR** | | | **38.5 - 69.5** | | | |
| **Mean** | | | **53.6** | | | |
| **SD** | | | **20.6** | | | |

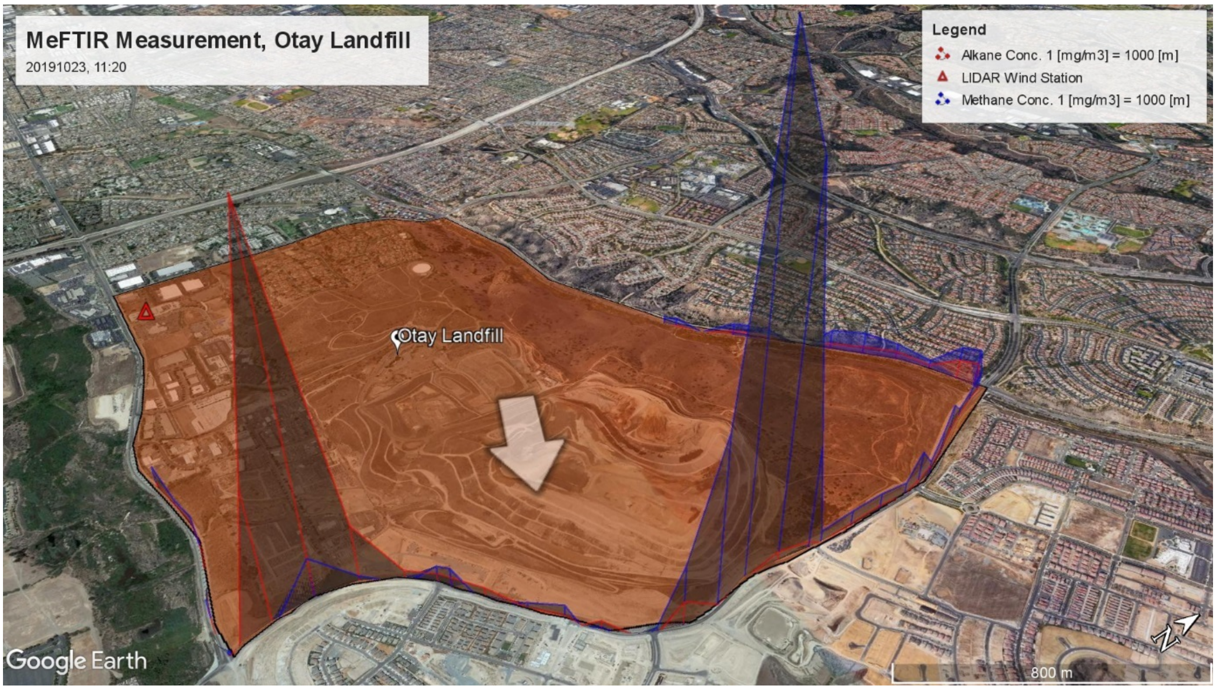

Figure 13. MeFTIR concentrations at ground level of methane (blue contour) and alkanes (red contour) downwind of Otay Landfill and adjacent industries (orange area), 23 October 2019. The wind direction is indicated by the white arrow. Map from Google Earth™, 2020.

A median methane/alkane ratio of 14 in the landfill plumes gave an indirect methane emission of 660 kg/h from the landfill. The alkane concentrations in the MeFTIR measurements were, however, close to the detection limit and the methane emission results must be treated with caution. The methane/alkane ratio in the plume from the industries were much lower, 2.85 which gave an indirect methane emission of 135 kg/h.

Table 16 Methane/Alkane mass ratios from MeFTIR measurements, Otay Landfill, October 2019

| Day [yymmdd] | Time span [hhmmss-hhmmss] | Num Meas | Mass Ratio avg [%] | Mass Ratio SD [%] | Wind Speed Min-Max [m/s] | Wind Dir Span [deg] |
|---|---|---|---|---|---|---|
| **191023** | 112032-122418 | 4 | 1257 | 465.5 | 3.2-3.8 | 273-290 |
| **Total # of Meas.** | | **4** | | | | |
| **Median** | | | **1418.5** | | | |
| **IQR** | | | **1118.0 - 1557.4** | | | |
| **Mean** | | | **1257.0** | | | |
| **SD** | | | **465.5** | | | |

Table 17 Methane/Alkane mass ratios from MeFTIR measurements, Otay Industries, October 2019

| Day [yymmdd] | Time span [hhmmss-hhmmss] | Num Meas | Mass Ratio avg [%] | Mass Ratio SD [%] | Wind Speed Min-Max [m/s] | Wind Dir Span [deg] |
|---|---|---|---|---|---|---|
| **191023** | 111612-121854 | 4 | 274 | 105.5 | 3.1-3.8 | 277-292 |
| **Total # of Meas.** | | **4** | | | | |
| **Median** | | | **284.6** | | | |
| **IQR** | | | **198.4 - 360.4** | | | |
| **Mean** | | | **274.2** | | | |
| **SD** | | | **105.5** | | | |

Concentrations of alkanes and methane in the adjacent communities downwind the landfill/ industries (at the time of the measurement) peaked at 1.2 µg/m$^3$ of alkanes from the industries and 1.8 µg/m$^3$ of methane from the landfill, see example in Figure 13.

### 5.1.5 *Miramar Landfill & Airport*

Miramar Landfill & Airport was measured with SOF and MeFTIR 22 and 24 October 2019, see example in Figure 14. Wind profile data (0-100 m) from the mobile LIDAR located in the south corner (see Figure 14) was used for the flux calculations.

Weak winds and variable background plumes made most of the transects useless for quantification. Only one single SOF measurement fulfilled the quality criteria and gave an emission of 135 kg/h, see Table 18. Further statistics are needed to support this result and to deduce if a separation between the landfill and Airport emissions can be made.

During the MeFTIR concentration mapping 22 August, a huge alkane plume (peaking at around 3.5 µg/m$^3$) was detected in the south part which is probably related to industrial activity, see Figure 14.

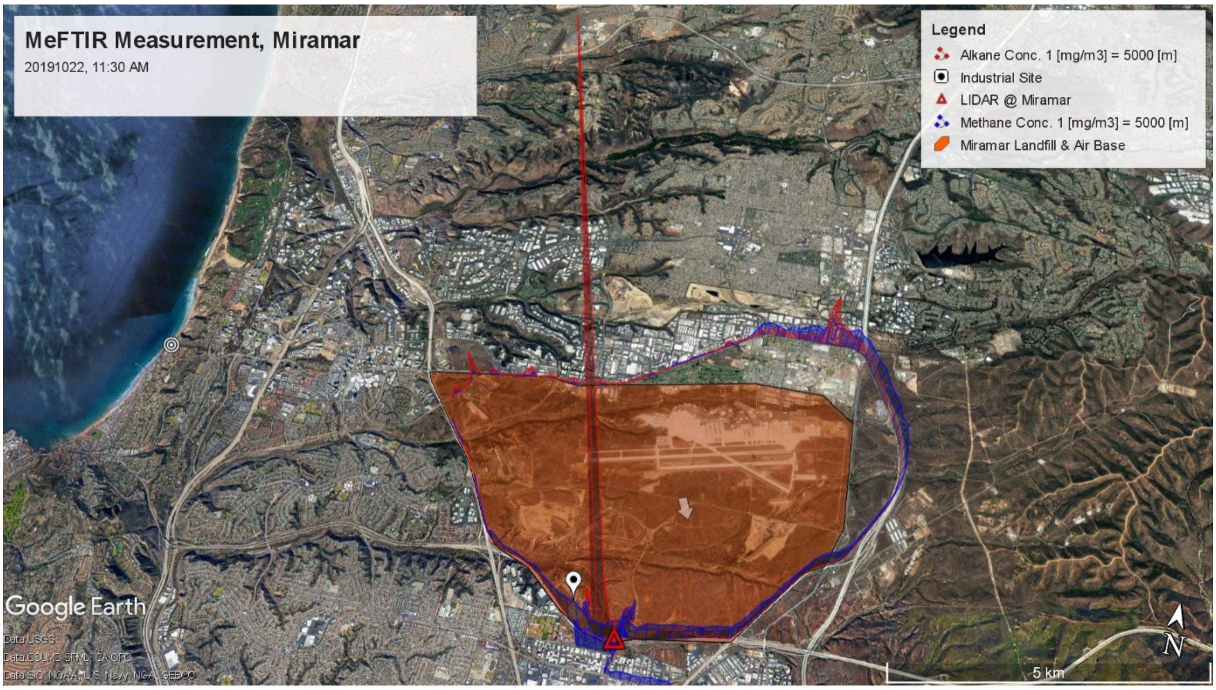

Figure 14. MeFTIR concentrations at ground level of methane (blue contour) and alkanes (red contour) downwind of Otay Landfill and adjacent industries (orange area), 23 October 2019. The wind direction is indicated by the white arrow. Map from Google Earth™, 2020.

Table 18 SOF Alkane emission measurements, Miramar Landfill & Airport, October 2019

| Day [yymmdd] | Time span [hhmmss-hhmmss] | Num Meas | Emission avg [kg/h] | Emission SD [kg/h] | Wind Speed Min-Max [m/s] | Wind Dir Span [deg] |
|---|---|---|---|---|---|---|
| **191024** | 103126-110040 | 1 | 135 | N/A | 2.1-2.1 | 213-213 |
| **Total # of Meas.** | | **1** | | | | |
| **Median** | | | **135.1** | | | |
| **IQR** | | | **135.1 - 135.1** | | | |
| **Mean** | | | **135.1** | | | |
| **SD** | | | **NaN** | | | |

Table 19 Methane/Alkane mass ratios from MeFTIR measurements, Miramar Landfill & Airport, October 2019

| Day [yymmdd] | Time span [hhmmss-hhmmss] | Num Meas | Mass Ratio avg [%] | Mass Ratio SD [%] | Wind Speed Min-Max [m/s] | Wind Dir Span [deg] |
|---|---|---|---|---|---|---|
| **191022** | 111820-121003 | 3 | 73.5 | 25.7 | 0.4-3.0 | 67-247 |
| **Total # of Meas.** | | **3** | | | | |
| **Median** | | | **67.1** | | | |
| **IQR** | | | **59.3 - 84.4** | | | |
| **Mean** | | | **73.5** | | | |
| **SD** | | | **25.7** | | | |

## 5.2 Community Monitoring & Concentration Mapping -San Diego

Measurements in the San Diego county were conducted 22-24 October 2019. Results from concentration mapping in communities that are not related to any specific source are presented in the subsections below. These communities were either selected in the implementation plan or detected in real-time during measurement and considered interesting.

### *5.2.1 Mexican Border*

Measurements along the US-Mexican border and in San Ysidro communities were conducted 23 October 2019. SOF, SkyDOAS and MeFTIR instruments were operated in order to monitor any emissions across the border, along public roads. The wind direction, at the time of the measurements, was from the north-west.

SOF and SkyDOAS measurements showed large-scale plumes and variable background concentrations, which probably emanated from emission sources in the San Diego Port and downtown area which lies directly upwind, see Figure 15 and Figure 16. No quantification could be done due to these variable backgrounds, in-distinct plumes and in-complete plume sampling, but were in order of a few hundred kg per hour. No obvious local sources were found except for maybe something from the Brown Field Airport.

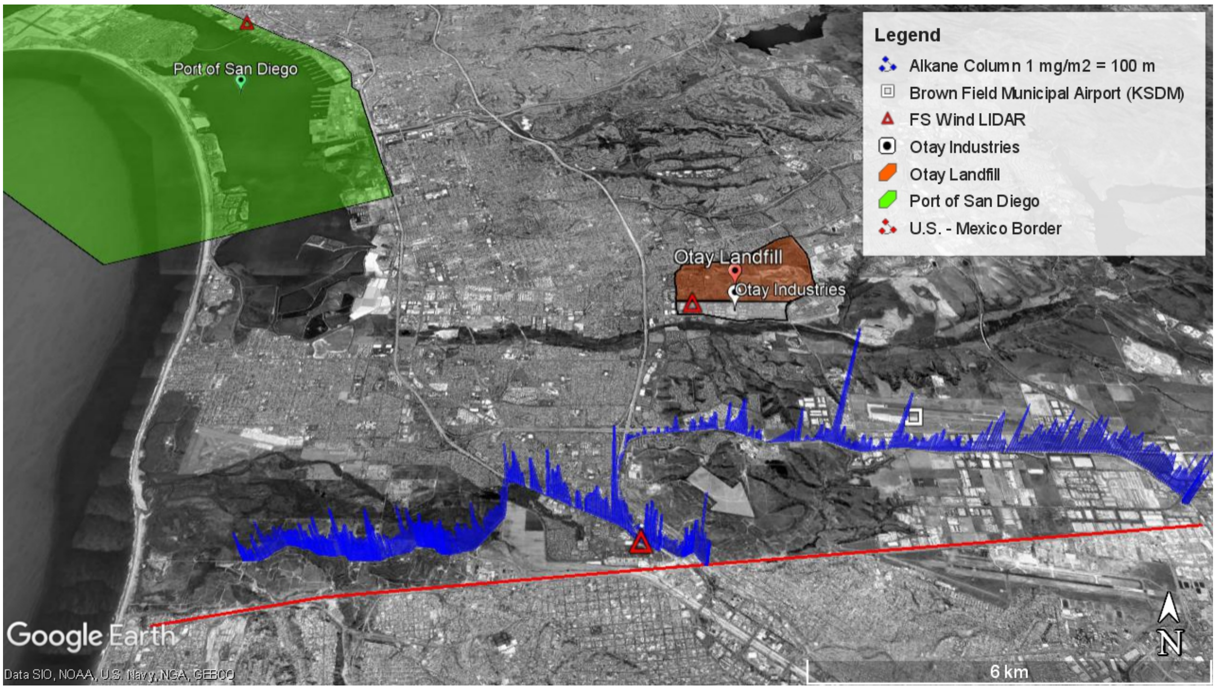

Figure 15. SOF alkane columns (blue contour) along the U.S.- Mexican border (red line), 23 October 2019. The wind direction is indicated by the white arrow. Map from Google Earth™, 2020.

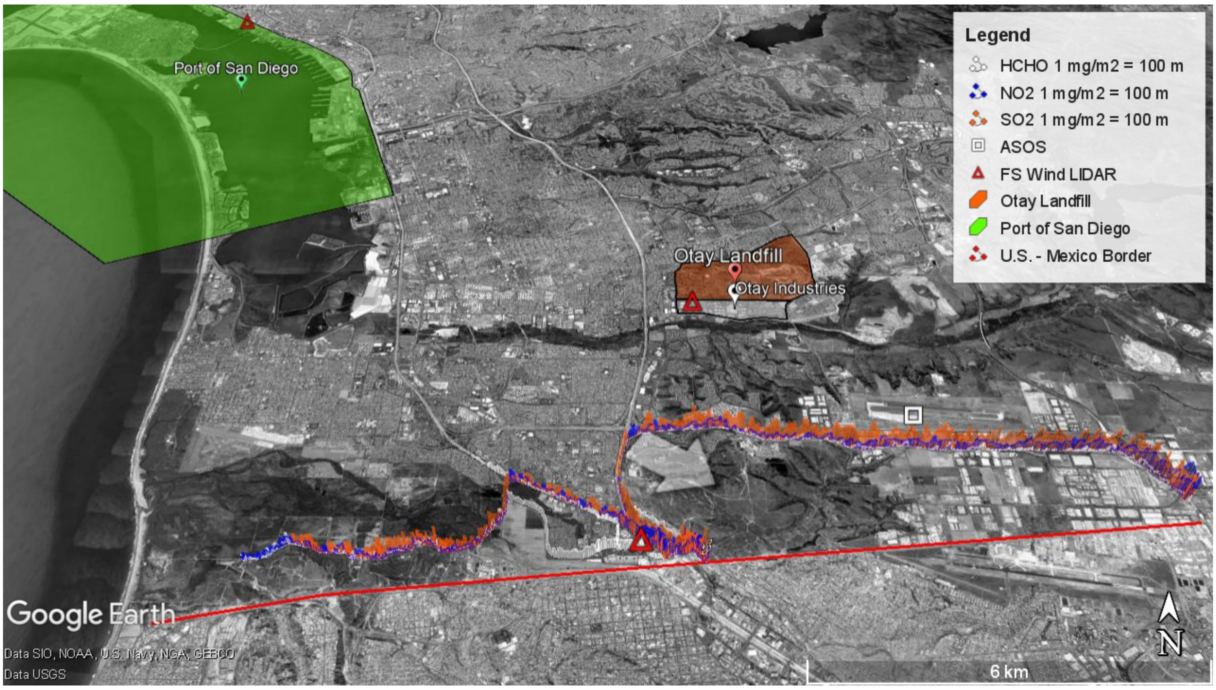

Figure 16. SkyDOAS columns of $NO_2$ (blue contour), $SO_2$ (orange contour) and HCHO (white contour, mostly hidden) along the U.S.- Mexican border (red line), 23 October 2019. The wind direction is indicated by the white arrow. Map from Google Earth™, 2020.

Concentration mapping of alkanes showed an enhancement of around 0.1 mg/m$^3$ at the San Ysidro border crossing, probably related to traffic. Several plumes were also seen along the border on west and east side of San Ysidro, see Figure 17. These plumes are probably related to a combination of distant emission sources from San Diego and local sources, such as the Imperial Beach airport (on the west side) or Brown Field airport (on the east side). Measurements must be made during southerly winds in order to study emissions from Mexico.

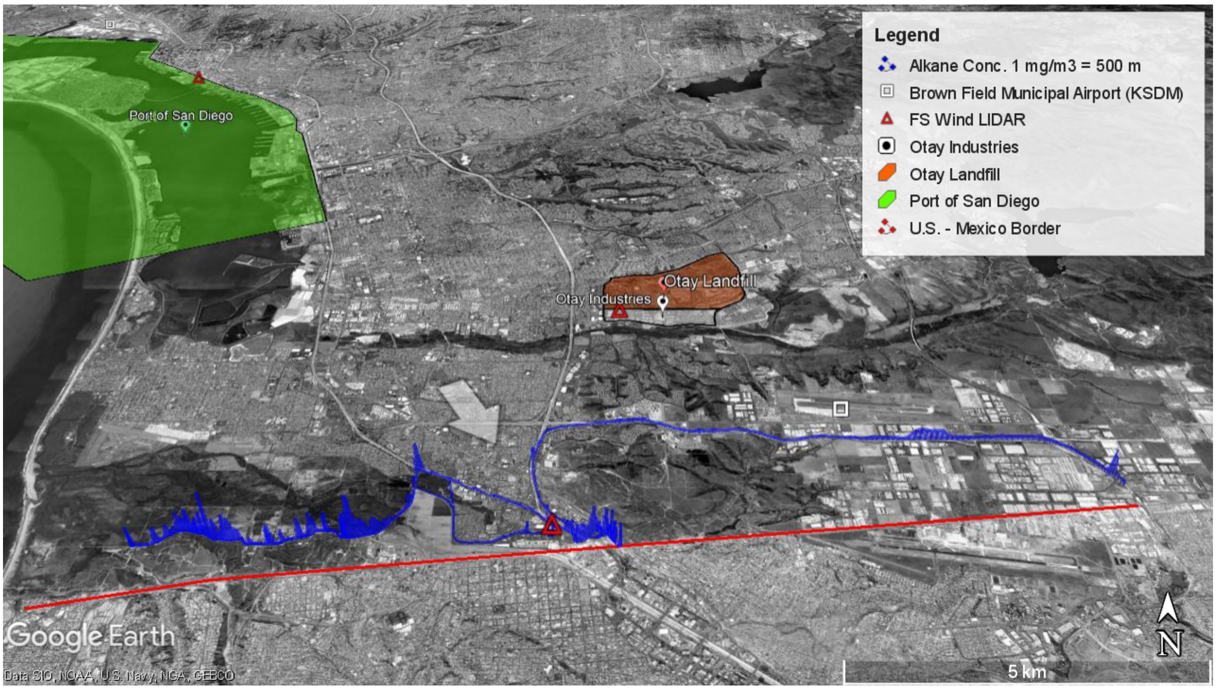

Figure 17. MeFTIR alkane concentrations at ground level (blue contour) along the U.S.- Mexican border (red line), 23 October 2019. The wind direction is indicated by the white arrow. Map from Google Earth™, 2020

## 5.3 Emission measurements and concentration mapping – South SCAB

Measurements in the South SCAB were conducted 29-31 October 2019. Results from six different sites/areas are presented in the subsections below. The sites were either selected in the implementation plan or detected in real-time during measurement and considered interesting.

### *5.3.1 Highlands Area Facility*

The Highlands Area Facility was measured with SOF and MeFTIR 29-31 October 2019 during various wind conditions, see example Figure 18. Wind profile data (0-100 m) from the mobile LIDAR located downtown has been used for flu. x calculations. Drilling activity, with unknown extent and frequency, was ongoing during the measurement period.

Figure 18. SOF alkane columns (blue contour) from Huntington Beach sources, 31 October2019. The figure is a composite of different measurement transect taken between 1:30 pm and 3:30 pm. The wind directions are indicated by the white arrows. Map from Google Earth™, 2020.

The survey median emissions were 31 kg/h of alkanes from the site based on 7 measurement transects, see details in Table 20. Methane/Alkane ratios of 125% gave an indirect methane emission of 39 kg/h, see details in Table 21.

Table 20 SOF Alkane emission measurements, Highlands Area Facility, October 2019

| Day [yymmdd] | Time span [hhmmss-hhmmss] | Num Meas | Emission avg [kg/h] | Emission SD [kg/h] | Wind Speed Min-Max [m/s] | Wind Dir Span [deg] |
|---|---|---|---|---|---|---|
| **191029** | 121134-133624 | 2 | 58.7 | 27.7 | 5.3-5.6 | 159-164 |
| **191030** | 160957-162940 | 2 | 30.2 | 0.9 | 5.4-5.7 | 52-57 |
| **191031** | 125743-132525 | 3 | 30.2 | 1.7 | 3.5-3.9 | 260-272 |
| **Total # of Meas.** | | **7** | | | | |
| **Median** | | | **30.8** | | | |
| **IQR** | | | **29.5 – 39.1** | | | |
| **Mean** | | | **38.3** | | | |
| **SD** | | | **16.6** | | | |

Table 21 Methane/Alkane mass ratios from MeFTIR measurements, Highlands Area Facility, October 2019

| Day [yymmdd] | Time span [hhmmss-hhmmss] | Num Meas | Mass Ratio avg [%] | Mass Ratio SD [%] | Wind Speed Min-Max [m/s] | Wind Dir Span [deg] |
|---|---|---|---|---|---|---|
| **191029** | 123715-184509 | 4 | 106 | 79.3 | 1.3-5.7 | 160-253 |
| **191030** | 161310-173444 | 5 | 147 | 35.5 | 4.7-6.0 | 49-57 |
| **191031** | 124855-154628 | 2 | 237 | 218.7 | 3.5-5.2 | 257-276 |
| **Total # of Meas.** | | **11** | | | | |
| **Median** | | | **125.3** | | | |
| **IQR** | | | **90.3 - 179.7** | | | |
| **Mean** | | | **148.4** | | | |
| **SD** | | | **97.2** | | | |

Results from fence-line concentration mapping of alkanes, methane and BTEX are found in Figure 19 to Figure 21. These measurements indicate very low background concentrations and elevated concentrations of alkanes, methane and BTEX directly downwind the site, peaking at 0.19, 0.64 and 0.18 µg/m$^3$ respectively.

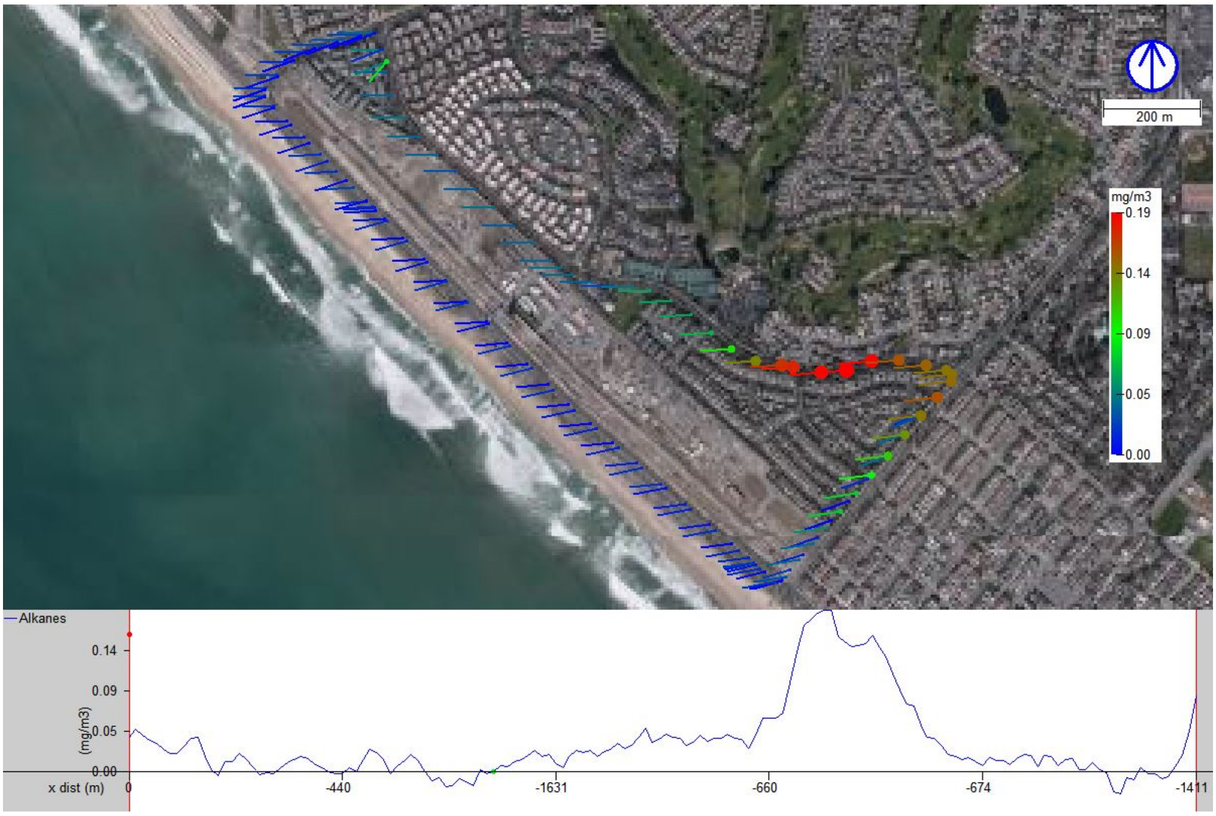

Figure 19 Alkane concentration at the Highlands Area Facility, Oct 31, 12:19-11:39

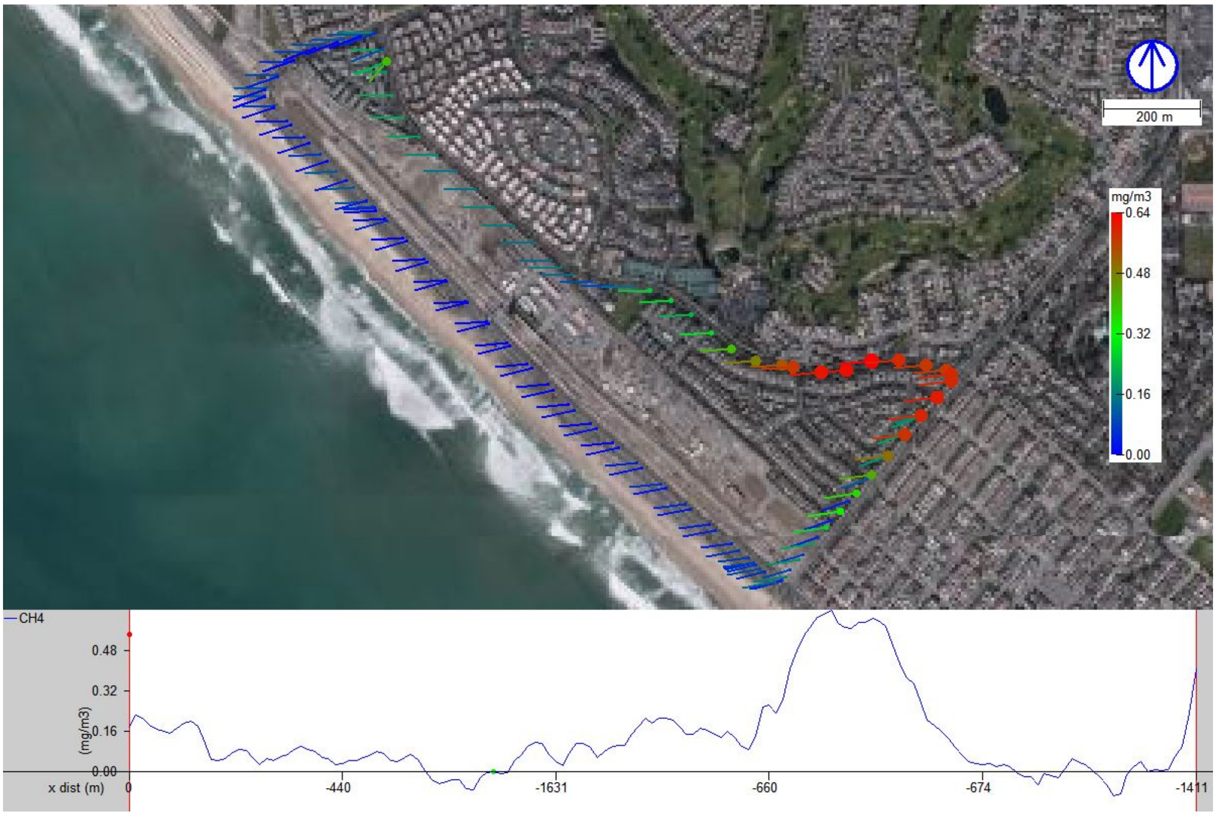

Figure 20 Methane concentration at the Highlands Area Facility l, Oct 30, 13:36-13:44

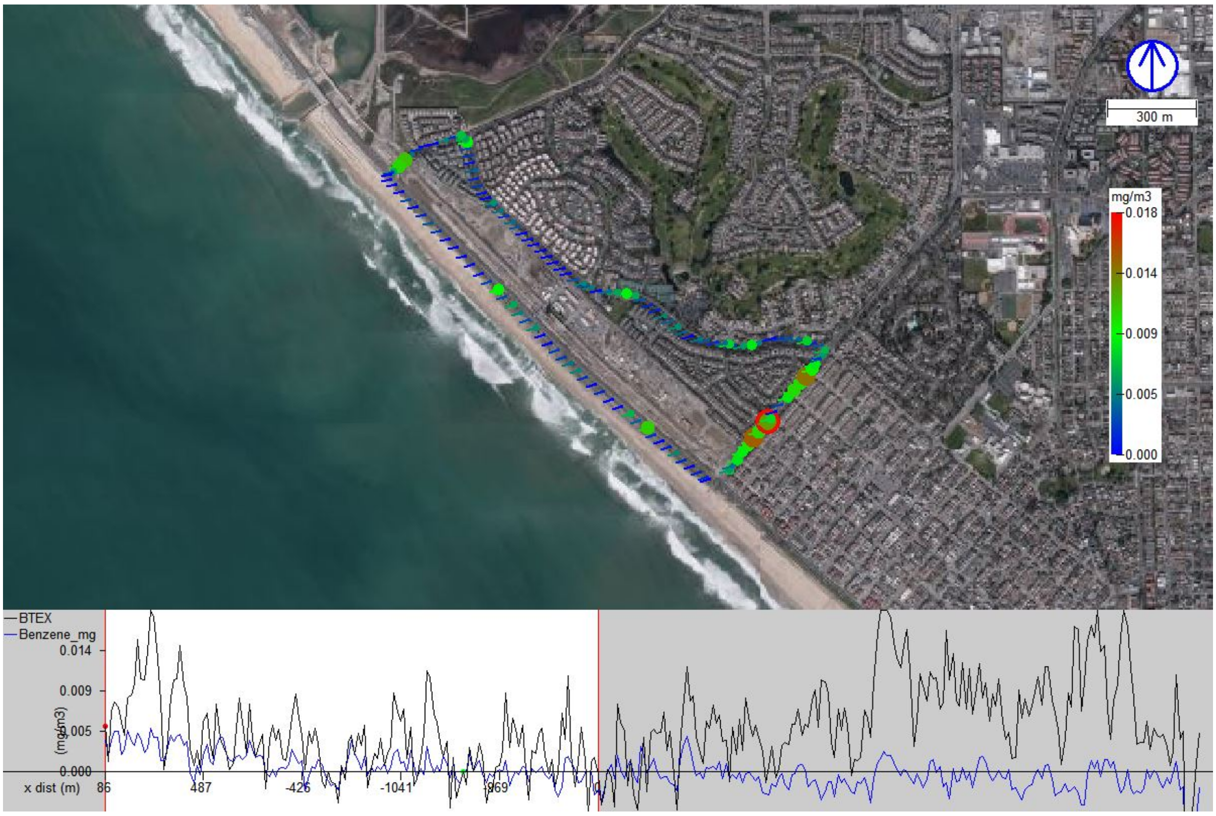

Figure 21 BTEX concentration at the Highlands Area Facility l, Oct 29, 18:35-18:50

### *5.3.2 Huntington Bolsa Area including Copeland and Catalina Wells and Facilities*

The SOFs measurements aggregate measurements from several leases with the Huntington Beach Oil Field, primarily Bolsa, but with some measurements also including Copeland and Catalina. These areas were measured with SOF and MeFTIR 29-31 October 2019 during various wind conditions, see example in Figure 18. Wind profile data (0-100 m) from the mobile LIDAR located downtown has been used for flux calculations.

The survey median emissions were 32 kg/h of alkanes from the site based on 11 measurement transects, see details in Table 22. Methane/Alkane ratios of 72% gave an indirect methane emission of 23 kg/h, see details in Table 23.

Table 22 SOF Alkane emission measurements, Huntington Bolsa Area, October 2019

| Day [yymmdd] | Time span [hhmmss-hhmmss] | Num Meas | Emission avg [kg/h] | Emission SD [kg/h] | Wind Speed Min-Max [m/s] | Wind Dir Span [deg] |
|---|---|---|---|---|---|---|
| **191030** | 164253-165014 | 1 | 74.9 | N/A | 6.1-6.1 | 58-58 |
| **191031** | 110236-155144 | 10 | 34.7 | 21.1 | 1.5-5.2 | 252-321 |
| **Total # of Meas.** | | **11** | | | | |
| **Median** | | | **31.5** | | | |
| **IQR** | | | **23.4 - 58.3** | | | |
| **Mean** | | | **38.4** | | | |
| **SD** | | | **23.4** | | | |

Table 23 Methane/Alkane mass ratios from MeFTIR measurements, Huntington Bolsa, October 2019

| Day [yymmdd] | Time span [hhmmss-hhmmss] | Num Meas | Mass Ratio avg [%] | Mass Ratio SD [%] | Wind Speed Min-Max [m/s] | Wind Dir Span [deg] |
|---|---|---|---|---|---|---|
| **191029** | 105424-190339 | 2 | 60.6 | 13.2 | 0.9-5.3 | 152-247 |
| **191030** | 164451-174627 | 2 | 102 | 5.6 | 5.0-6.2 | 52-58 |
| **191031** | 152848-173608 | 2 | 65.3 | 11.7 | 4.6-4.8 | 256-266 |
| **Total # of Meas.** | | **6** | | | | |
| **Median** | | | **71.8** | | | |
| **IQR** | | | **60.3 - 92.3** | | | |
| **Mean** | | | **76.1** | | | |
| **SD** | | | **22.1** | | | |

Results from fence-line concentration mapping of alkanes, methane and BTEX are found in Figure 22 to Figure 24. These measurements indicate very low background concentrations and elevated concentrations of alkanes, methane and BTEX directly downwind the site, peaking at 0.20, 0.064 and 0.025 µg/m$^3$ respectively.

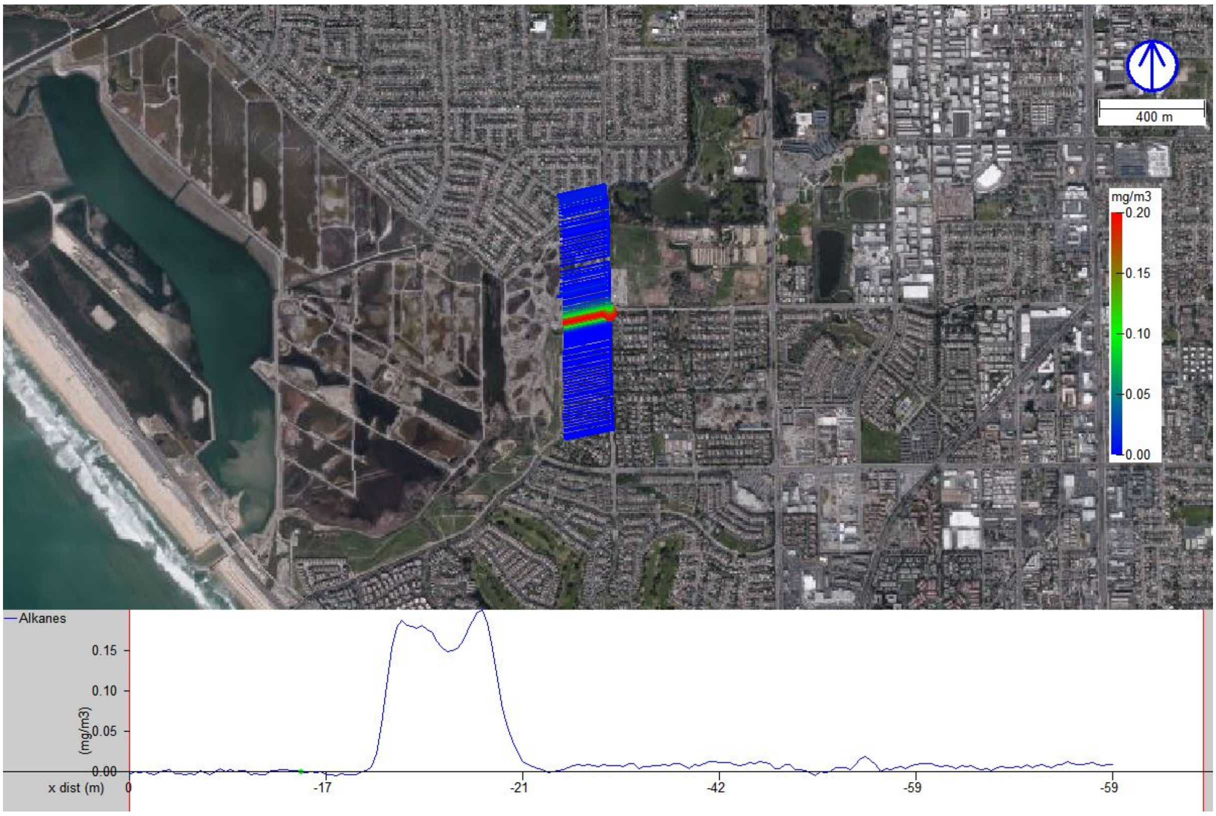

Figure 22 Alkane concentration downwind of the Huntington Bolsa Area, Oct 31, 15:48-15:55

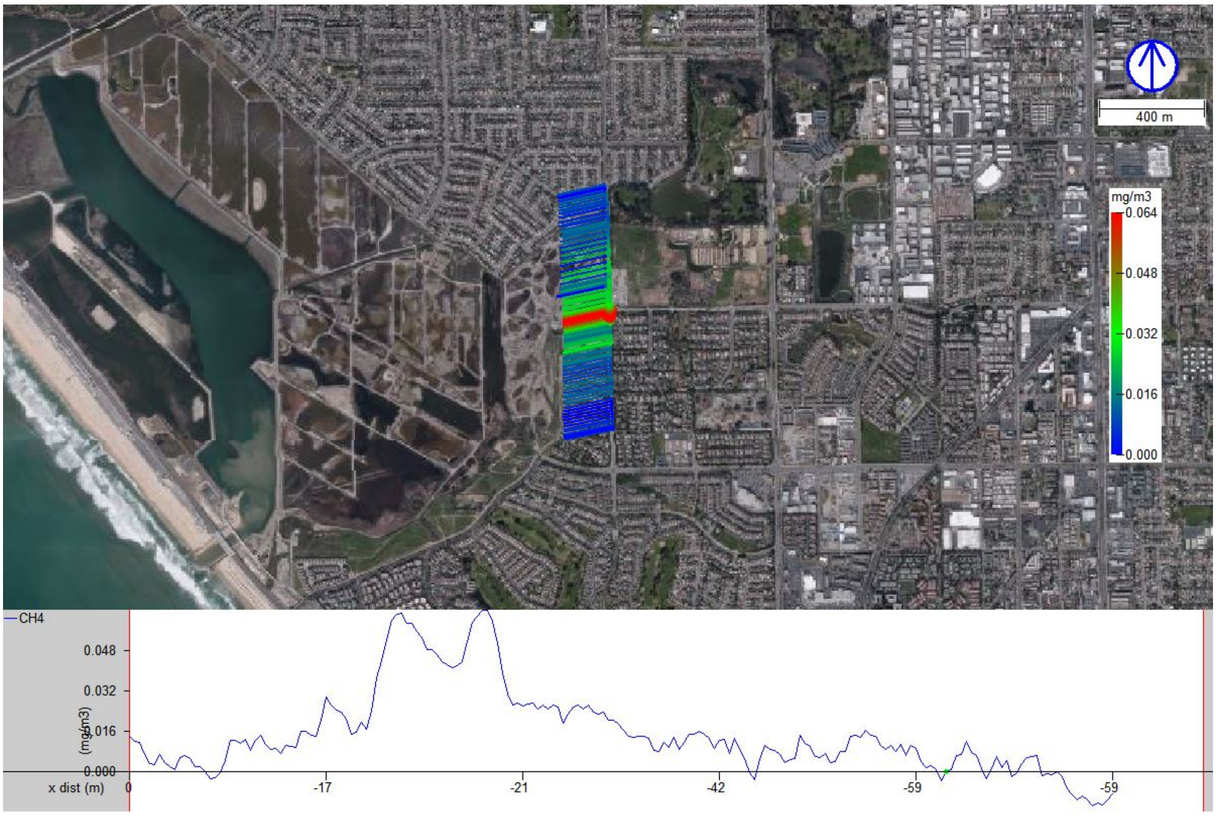

Figure 23 Methane concentration downwind of the Huntington Bolsa Area, Oct 31, 15:48-15:55

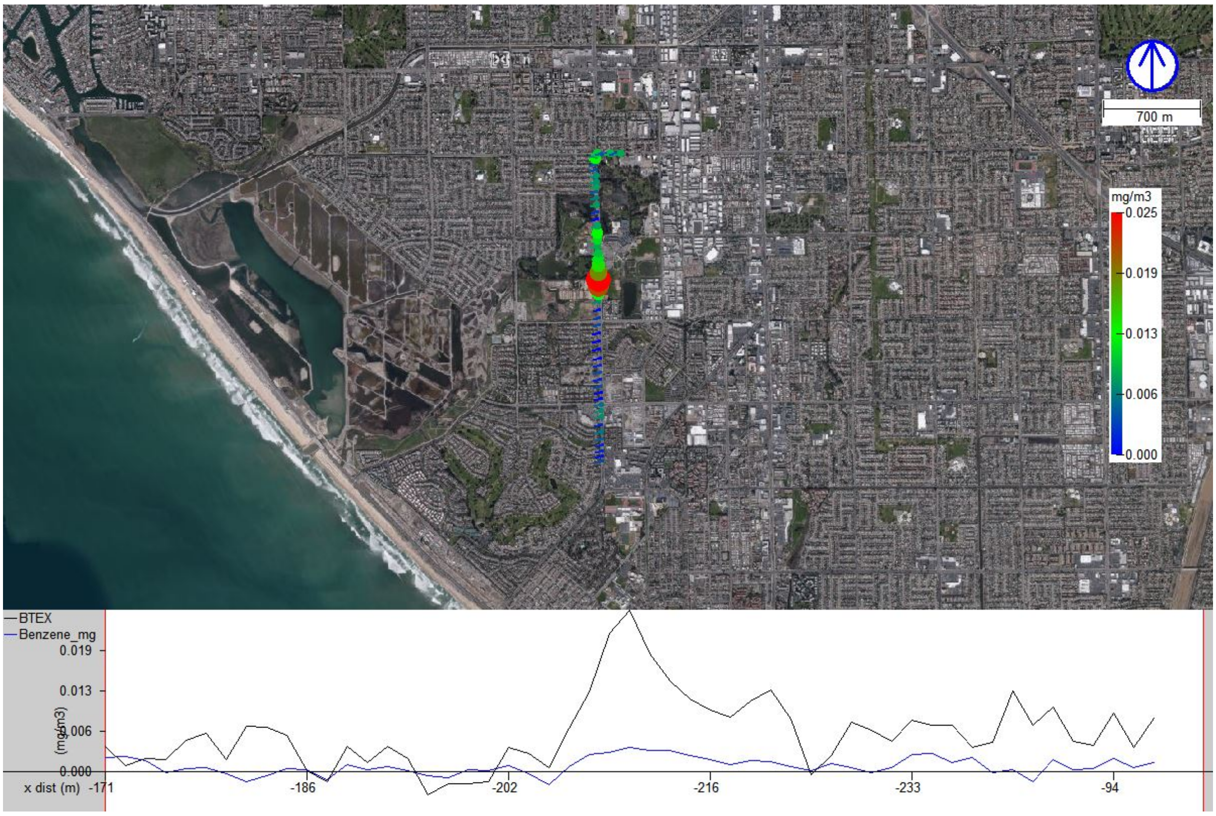

Figure 24 BTEX concentration downwind of the Huntington Bolsa Area, Oct 29, 18:56-19:02

### *5.3.3 Huntington Fuel Depot*

The Huntington Fuel Depot was measured with SOF and MeFTIR 30-31 October 2019 during various wind conditions, see Figure 18. Wind profile data (0-100 m) from the mobile LIDAR located downtown has been used for flux calculations.

Repeatable, and distinct SOF signals were detected on the downwind side, but upwind (background) sources existed most of the time. These have been subtracted in the results below.

The survey median emissions were 5 kg/h of alkanes from the site based on 5 measurement transects, see details in Table 24. Methane/Alkane ratios of 13% gave an indirect methane emission of 0.6 kg/h, see details in Table 25.

Table 24 SOF Alkane emission measurements, Huntington Fuel Depot, October 2019

| Day [yymmdd] | Time span [hhmmss-hhmmss] | Num Meas | Emission avg [kg/h] | Emission SD [kg/h] | Wind Speed Min-Max [m/s] | Wind Dir Span [deg] |
|---|---|---|---|---|---|---|
| **191030** | 153512-153704 | 2 | 3.8 | 1.3 | 5.9-5.9 | 46-47 |
| **191031** | 101955-141453 | 3 | 5.3 | 2.5 | 1.4-4.6 | 252-338 |
| **Total # of Meas.** | | **5** | | | | |
| **Median** | | | **4.8** | | | |
| **IQR** | | | **2.9 - 5.6** | | | |
| **Mean** | | | **4.7** | | | |
| **SD** | | | **2.1** | | | |

Table 25 Methane/Alkane mass ratios from MeFTIR measurements, Huntington Fuel Depot, October 2019

| Day [yymmdd] | Time span [hhmmss-hhmmss] | Num Meas | Mass Ratio avg [%] | Mass Ratio SD [%] | Wind Speed Min-Max [m/s] | Wind Dir Span [deg] |
|---|---|---|---|---|---|---|
| **191030** | 153116-153641 | 1 | 13.4 | N/A | 5.8-5.8 | 49-49 |
| **Total # of Meas.** | | **1** | | | | |
| **Median** | | | **13.4** | | | |
| **IQR** | | | **13.4 - 13.4** | | | |
| **Mean** | | | **13.4** | | | |
| **SD** | | | **NaN** | | | |

Results from fence-line concentration mapping of alkanes, methane and BTEX are found in Figure 25 to Figure 27. These measurements indicate elevated concentrations of alkanes and BTEX (but not for methane) directly downwind the site, peaking at 0.17 and 0.045 µg/m$^3$ respectively.

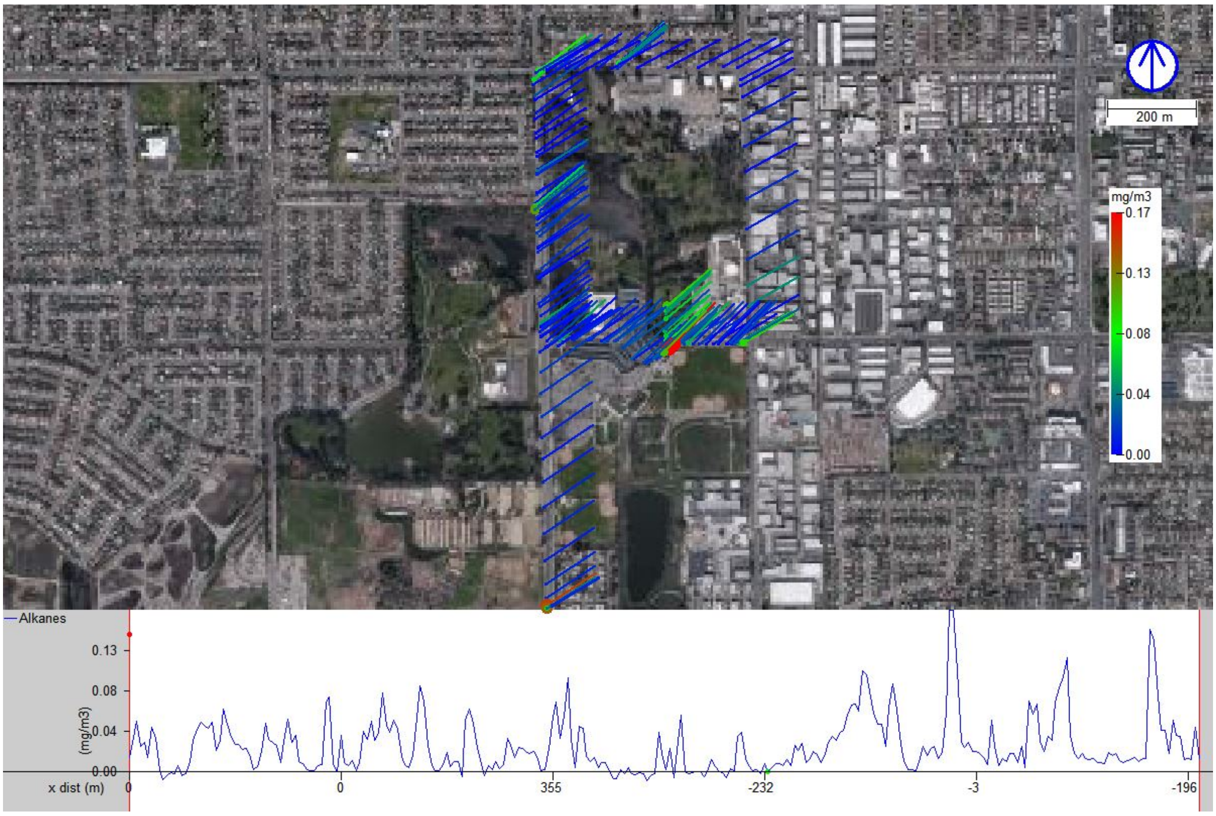

Figure 25 Alkane concentration at Huntington Fuel Depo, Oct 29, 17:38

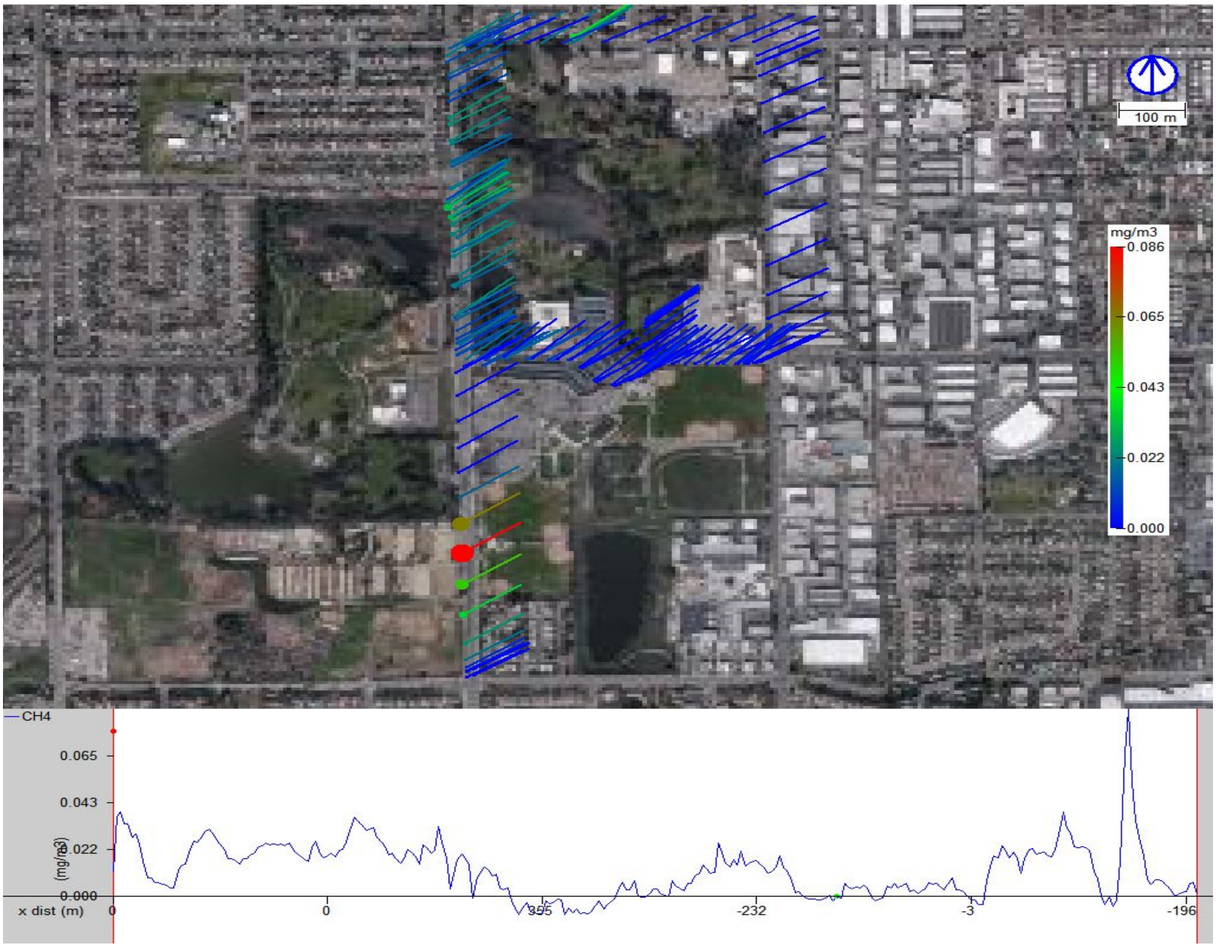

Figure 26 Methane concentration at Huntington Fuel Depo, Oct 29, 17:38

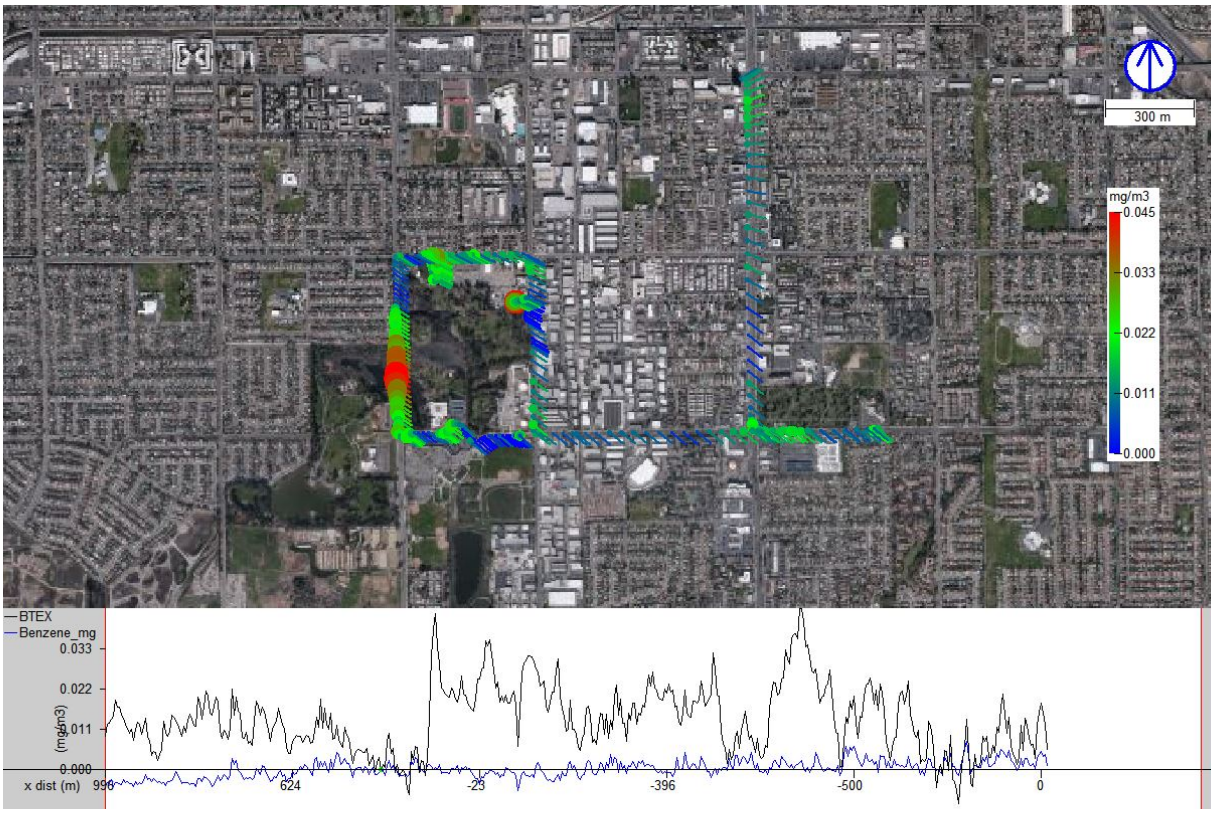

Figure 27 BTEX concentration at Huntington Fuel Depo, Oct 25, 17:04-17:38

### *5.3.4 Huntington Toronto Ave Well Site*

The Huntington Toronto Ave. Well Site was measured with SOF and MeFTIR 29 and 31 October 2019, see Figure 18. Wind profile data (0-100 m) from the mobile LIDAR located downtown has been used for flux calculations.

Repeatable, and distinct SOF signals were detected on the downwind side.

The survey median emissions were 5 kg/h of alkanes from the site based on 7 measurement transects, see details in Table 26. Methane/Alkane ratios of 160% gave an indirect methane emission of 7 kg/h, see details in Table 27.

Table 26 SOF Alkane emission measurements, Huntington Toronto Ave. Well Site, October 2019

| Day [yymmdd] | Time span [hhmmss-hhmmss] | Num Meas | Emission avg [kg/h] | Emission SD [kg/h] | Wind Speed Min-Max [m/s] | Wind Dir Span [deg] |
|---|---|---|---|---|---|---|
| **191029** | 152049-154932 | 3 | 4.8 | 1.7 | 3.5-3.8 | 239-254 |
| **191031** | 134230-135203 | 4 | 5.0 | 2.3 | 4.3-4.8 | 265-272 |
| **Total # of Meas.** | | **7** | | | | |
| **Median** | | | **4.3** | | | |
| **IQR** | | | **3.7 - 5.5** | | | |
| **Mean** | | | **4.9** | | | |
| **SD** | | | **1.9** | | | |

Table 27 Methane/Alkane mass ratios from MeFTIR measurements, Huntington Toronto Ave. Well Site, October 2019

| Day [yymmdd] | Time span [hhmmss-hhmmss] | Num Meas | Mass Ratio avg [%] | Mass Ratio SD [%] | Wind Speed Min-Max [m/s] | Wind Dir Span [deg] |
|---|---|---|---|---|---|---|
| **191029** | 150425-170724 | 4 | 152 | 25.5 | 1.4-3.7 | 235-256 |
| **Total # of Meas.** | | **4** | | | | |
| **Median** | | | **158.4** | | | |
| **IQR** | | | **144.3 - 166.6** | | | |
| **Mean** | | | **152.5** | | | |
| **SD** | | | **25.5** | | | |

Results from fence-line concentration mapping of alkanes, methane and BTEX are found in Figure 28 to Figure 30. These measurements indicate elevated concentrations of alkanes, methane and BTEX directly downwind the site, peaking at 1.3, 2.2 and 0.013 µg/m$^3$ respectively.

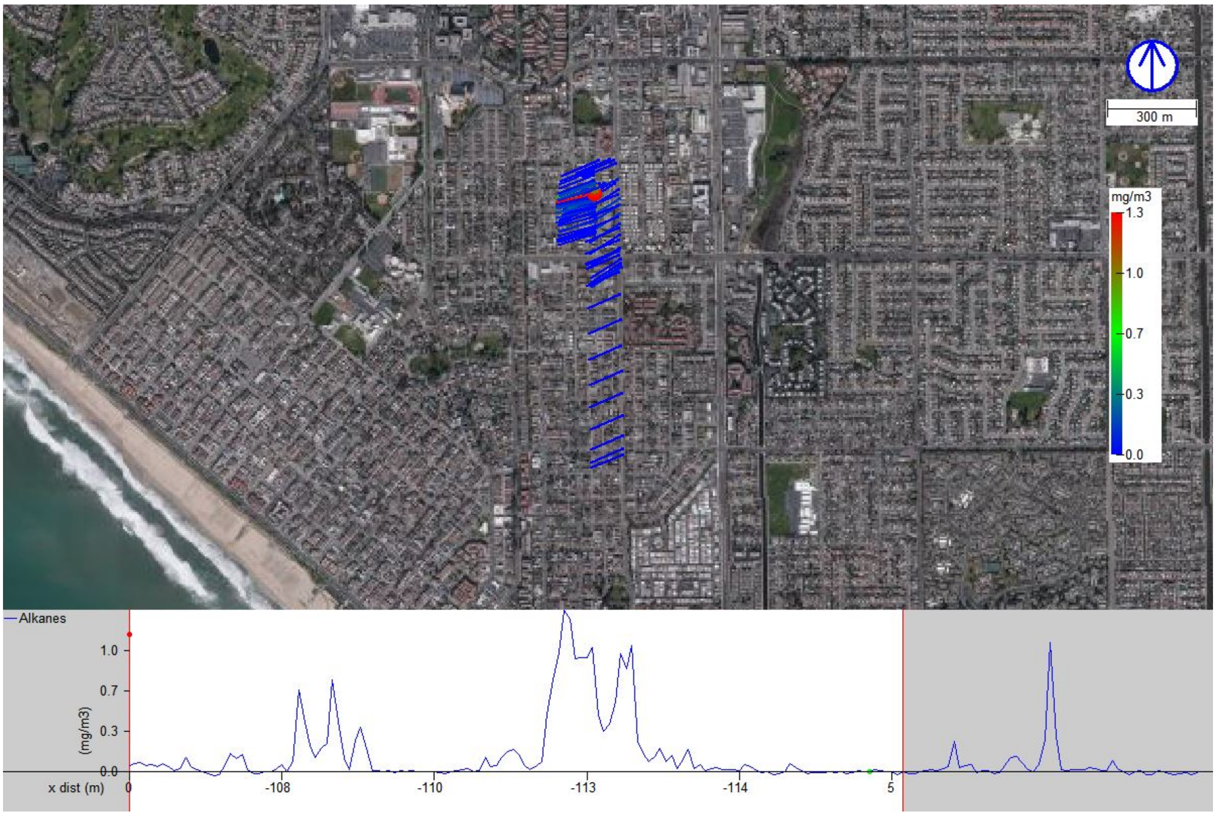

Figure 28 Alkane concentration at Huntington Toronto Ave Well Site, Oct 29, 15:09

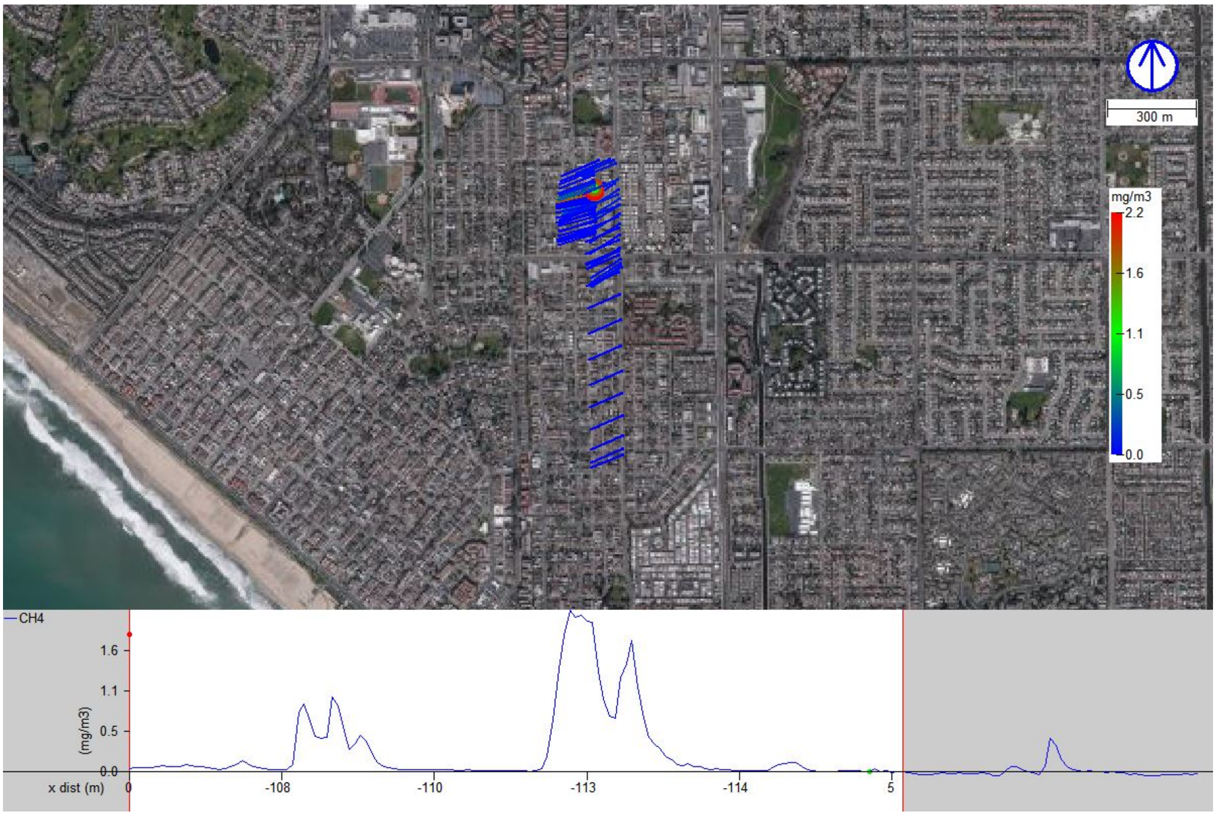

Figure 29 Methane concentration at Huntington Toronto Ave Well Site, Oct 29, 15:09

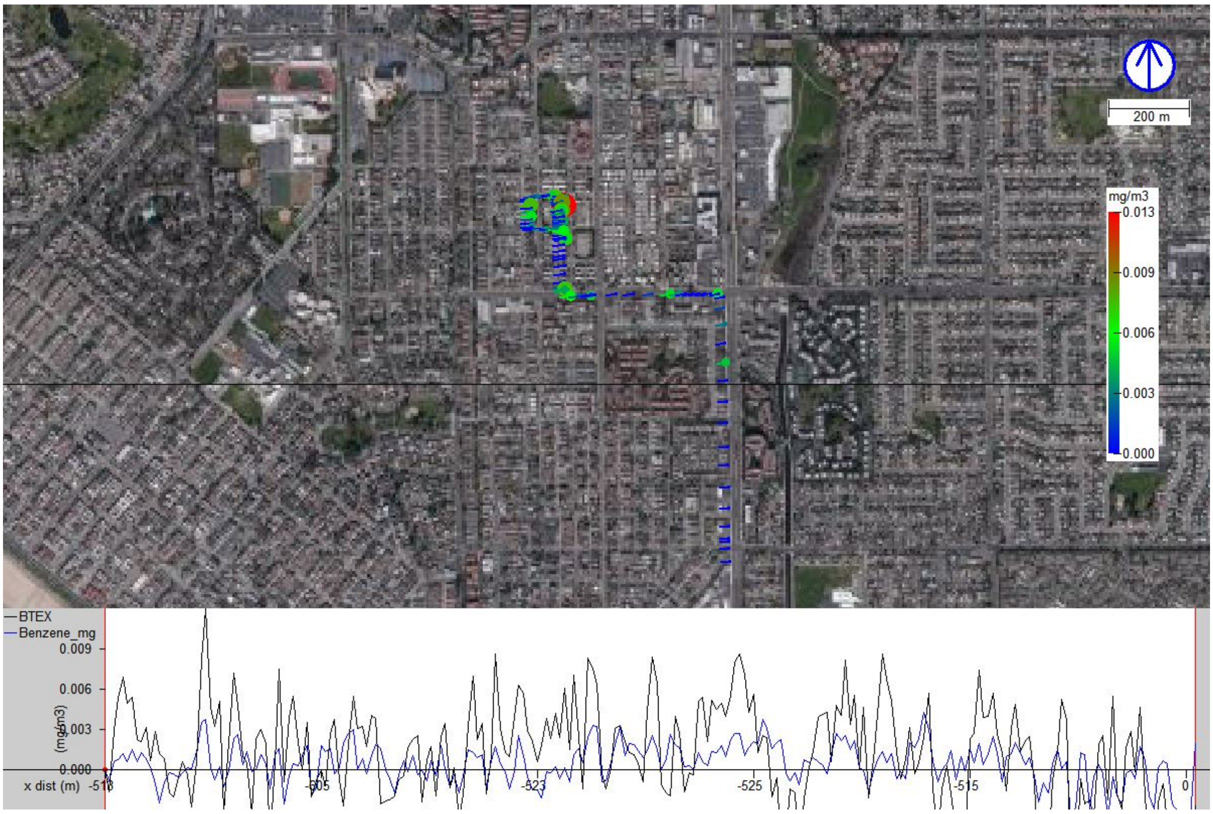

Figure 30 BTEX concentration at Huntington Toronto Ave Well Site, Oct 25, 17:50

### *5.3.5 Frank Bowerman Landfill*

Frank Bowerman landfill, was measured with SOF and MeFTIR 30 October 2019, see Figure 12. Wind profile data (0-100 m) from the mobile LIDAR located at Orange county great park (see Figure 12) used for flux calculations.

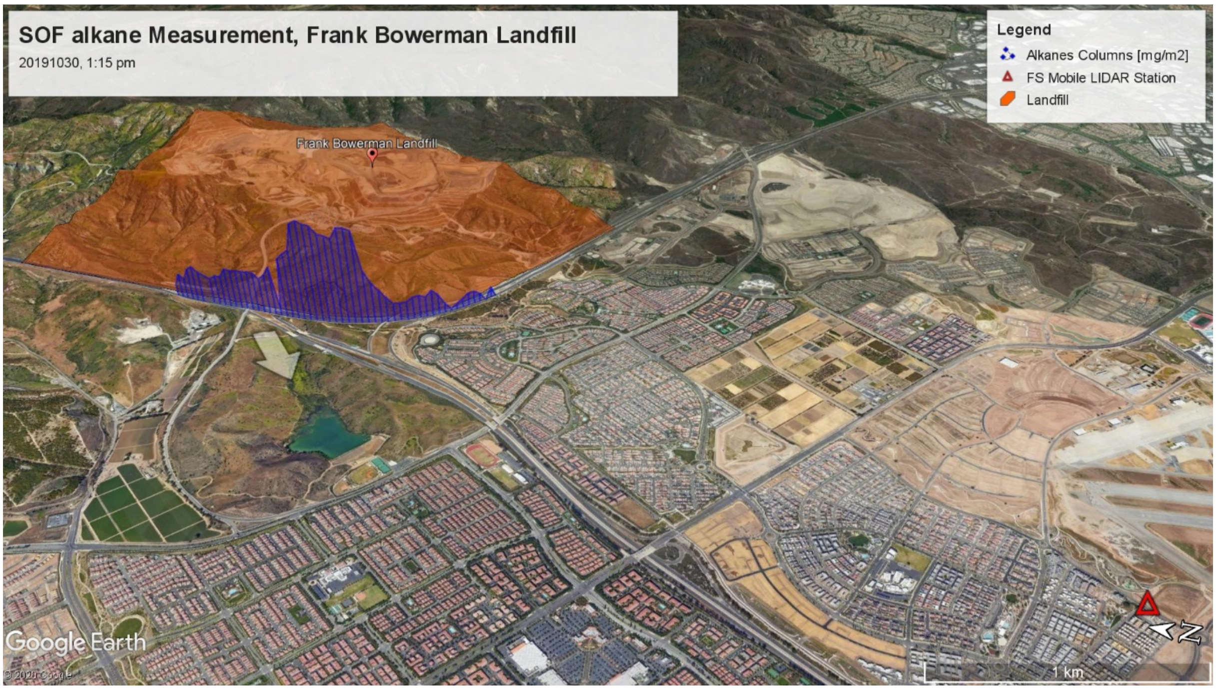

Figure 31 SOF alkane columns (blue contour) at Fran Bowerman Landfill, 30 October 2019. The wind direction is indicated by the white arrow. Map from Google Earth™, 2020.

Distinct plumes downwind the landfill was detected in both SOF and MeFTIR. A clear correlation between alkanes and methane in the MeFTIR concentration measurements was also seen.

The median emission was 46 kg/h of alkanes based on 5 measurement transects, see Table 28. A median methane/alkane ratio of 1100 % (see Table 29) in the landfill plumes gave an indirect methane emission of 522 kg/h from the landfill.

Table 28 SOF Alkane emission measurements, Frank Bowerman Landfill, October 2019

| Day [yymmdd] | Time span [hhmmss-hhmmss] | Num Meas | Emission avg [kg/h] | Emission SD [kg/h] | Wind Speed Min-Max [m/s] | Wind Dir Span [deg] |
|---|---|---|---|---|---|---|
| **191030** | 124530-135716 | 5 | 42.5 | 13.5 | 3.0-6.0 | 36-44 |
| **Total # of Meas.** | | **5** | | | | |
| **Median** | | | **46.4** | | | |
| **IQR** | | | **29.0 - 49.4** | | | |
| **Mean** | | | **42.5** | | | |
| **SD** | | | **13.5** | | | |

Table 29 Methane/Alkane mass ratios from MeFTIR measurements, Frank Bowerman Landfill, October 2019

| Day [yymmdd] | Time span [hhmmss-hhmmss] | Num Meas | Mass Ratio avg [%] | Mass Ratio SD [%] | Wind Speed Min-Max [m/s] | Wind Dir Span [deg] |
|---|---|---|---|---|---|---|
| **191030** | 121032-134102 | 5 | 1142 | 252.7 | 3.2-7.1 | 31-68 |
| **Total # of Meas.** | | **5** | | | | |
| **Median** | | | **1124.3** | | | |
| **IQR** | | | **959.9 - 1236.2** | | | |
| **Mean** | | | **1142.0** | | | |
| **SD** | | | **252.7** | | | |

Results from fence-line concentration mapping of alkanes and methane are found in Figure 32 and Figure 33. These measurements show elevated concentrations of alkanes and methane directly downwind the site, peaking at 0.018 and 0.18 µg/m$^3$ respectively. Clearly, the methane plume is entirely related to the landfill while alkane peaks are also found outside the methane/landfill.

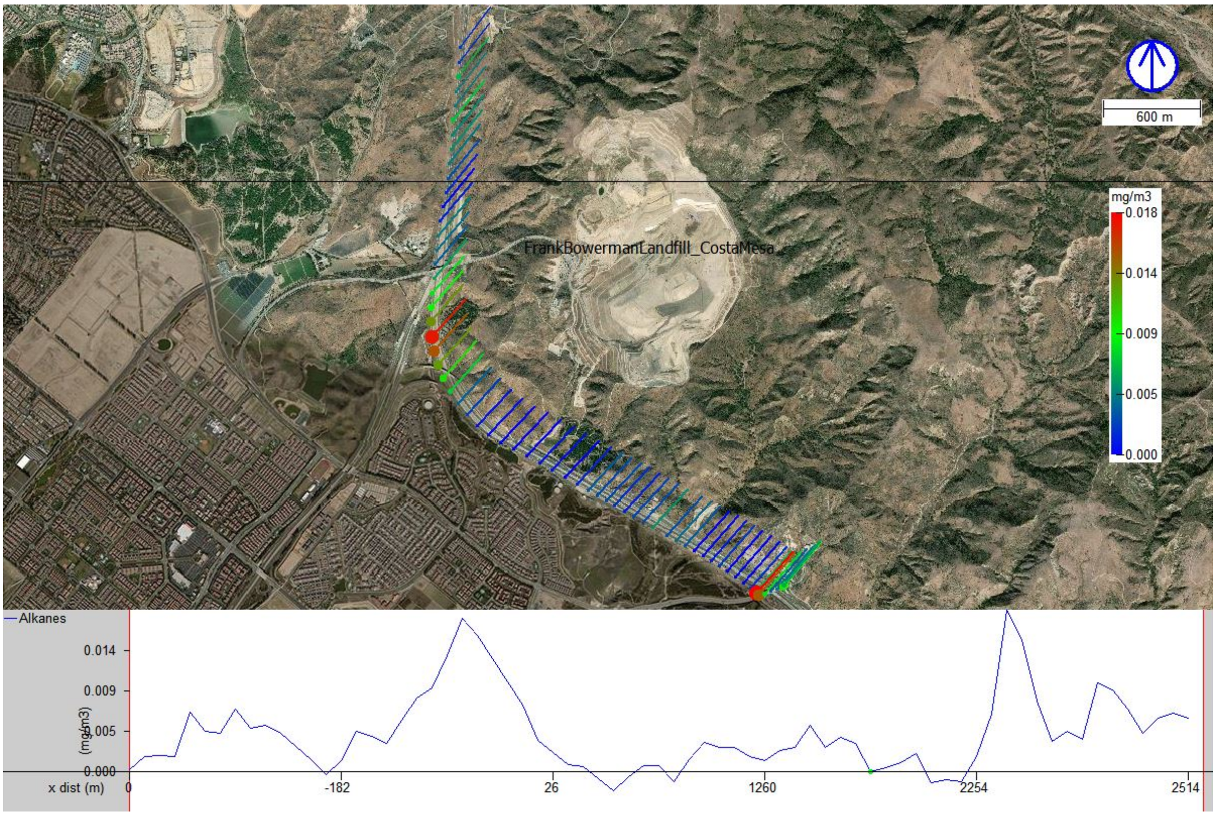

Figure 32 Alkane concentration downwind Frank Bowerman Landfill, Oct 30, 13:36-13:44

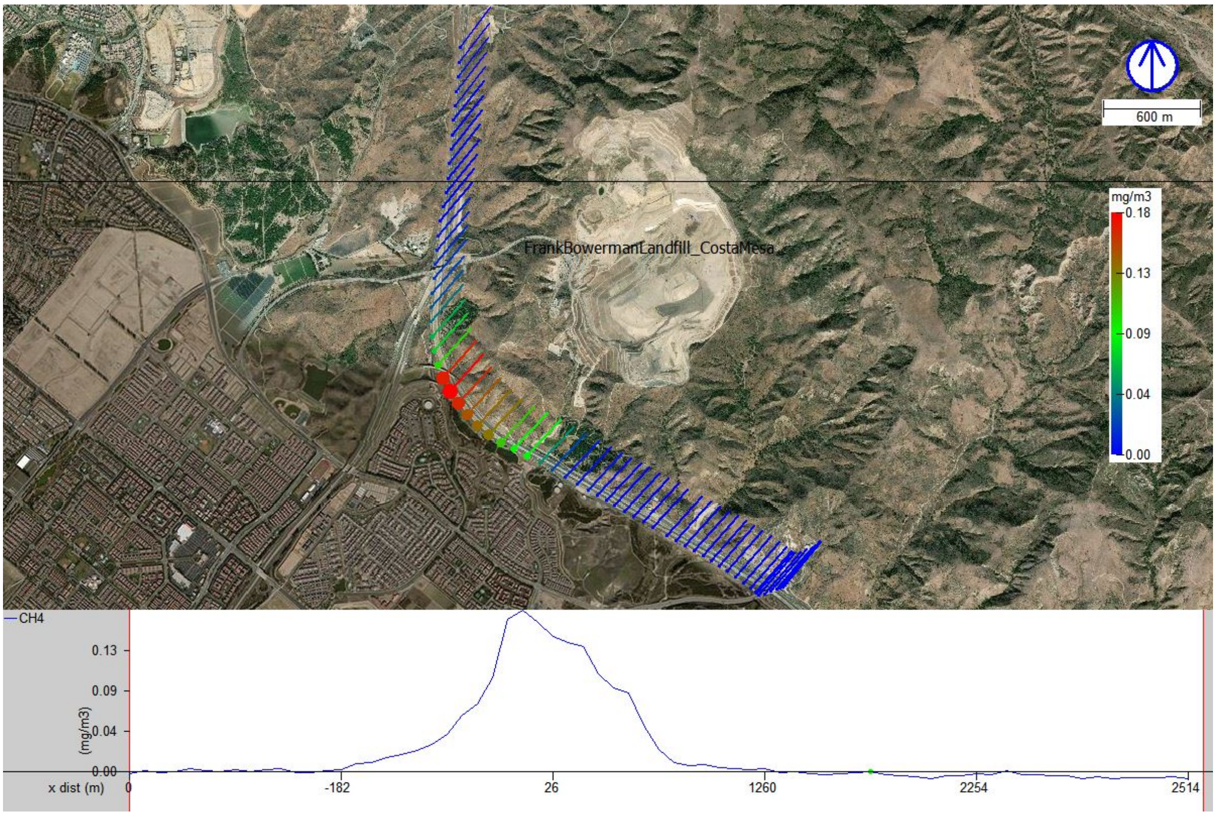

Figure 33 Methane concentration downwind Frank Bowerman Landfill, Oct 30, 13:36-13:44

### *5.3.6 Coyote Canyon Landfill*

The Coyote Canyon landfill, Figure 34, was measured in westerly wind with SOF, MeFTIR and MW-DOAS on 25 October 2019. This was an old landfill, with apparent low gas emissions and the measurements, especially for SOF, were complicated by inflow of background pollutants with varying concentrations. It was therefore not possible to detect any significant emissions of alkanes from the SOF. However, in the concentration measurement higher abundances of both methane and alkane were observed downwind of the landfill compared to upwind, indicating ongoing emissions of both of methane and NMVOCs. However, there was indication BTEX. Example of measurements are shown in Figure 35, Figure 36, Figure 37 and Figure 38.

Figure 34 The Coyote Canyon landfill, Oct 25 12:00.

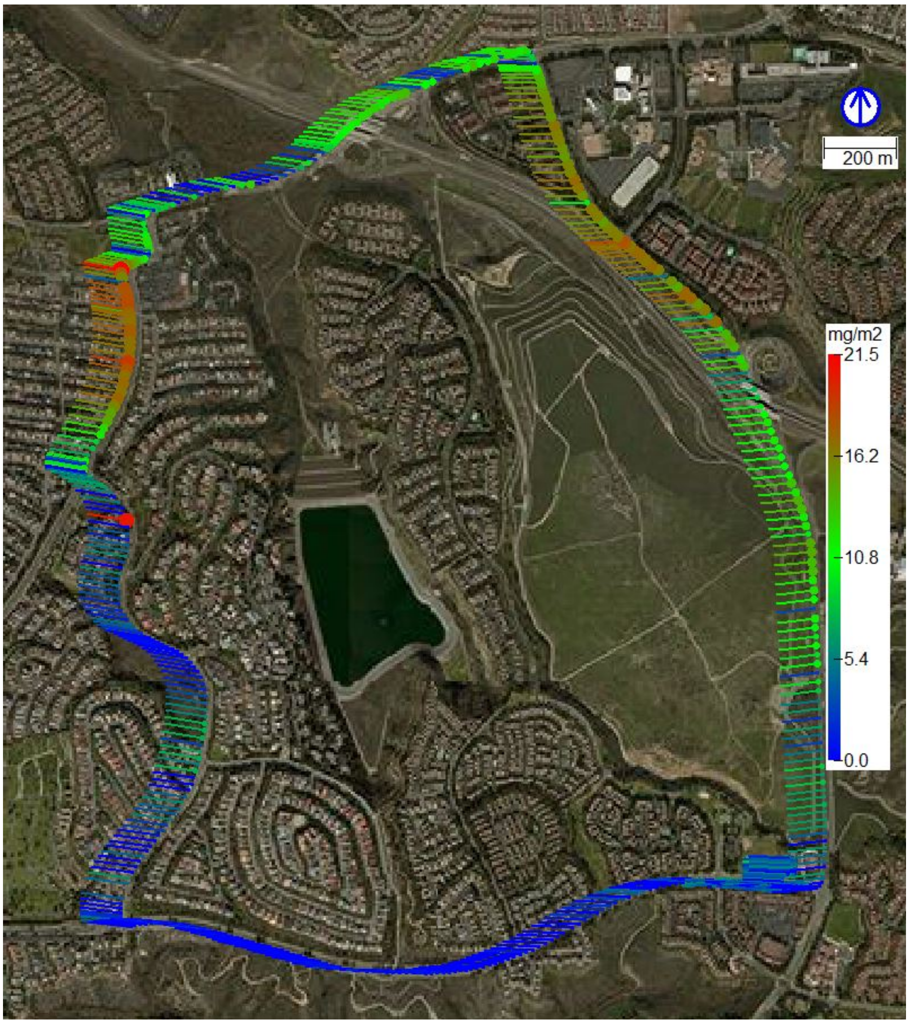

Figure 35 SOF Alkane column measurements downwind Coyote canyon landfill, Oct 25 12:00. .

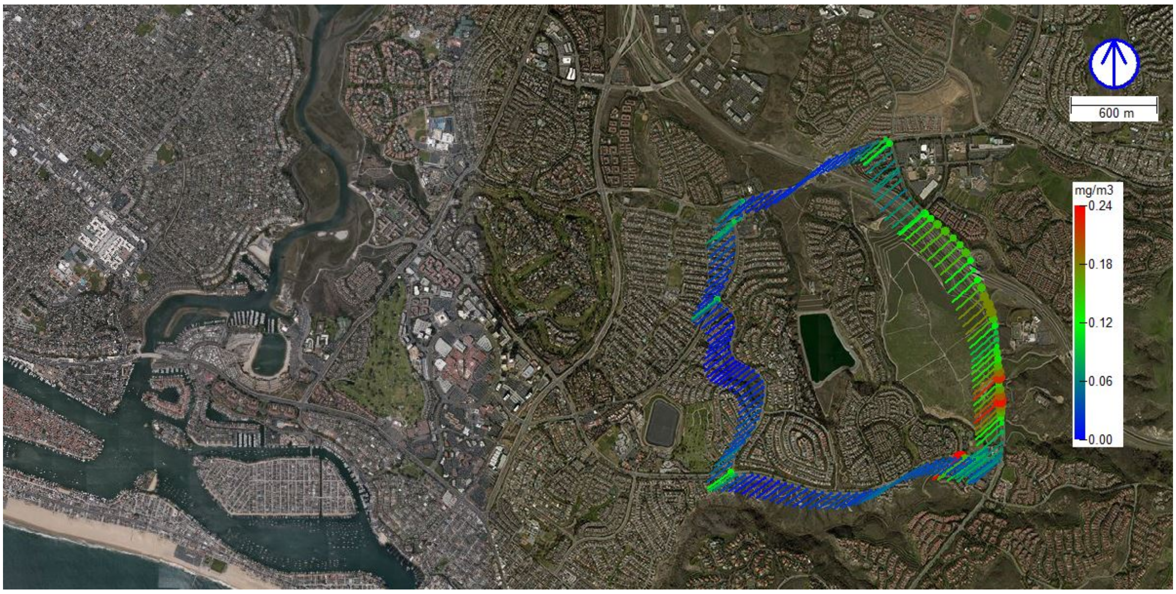

Figure 36 Alkane concentration downwind Coyote Canyon landfill, Oct 25 17:05-17:40.

Figure 37 Methane concentration downwind Coyote Canyon  landfill, Oct 25 17:05-17:40.

1

Figure 38 BTEX concentration downwind Coyote Canyon landfill, Oct 25 17:05-17:40.

## 5.4 Community Monitoring – SCAB South

General concentration mapping was carried out to pin-point concentration hot spots and identify emission sources. In Figure 39 and Figure 40 such measurements are shown for Huntington Beach and Newport . They were carried out in the late afternoon of October 30 in NE wind along the coastline. A number of hotspots were found and potential sources in the vicinity were pinpointed. This included numerous wells and a water treatment facility. These results were compared to the WellFinder database (https://maps.conservation.ca.gov/doggr/wellfinder) which shows active wells in the area, Figure 43 and Figure 44. It can be seen that the hotspots coincide with active wells.

In Figure 41 and Figure 42 similar measurements for BTEX are shown, performed in the early evening. It can be seen that benzene values are below 5 µg/m$^3$ (1.5 ppb) while the total BTEX, usually dominated by toluene, is below 39 µg/m$^3$ (10 ppb).

Figure 39 Alkane concentration measurements in NE wind along the coastline of Huntington Beach and Newport.

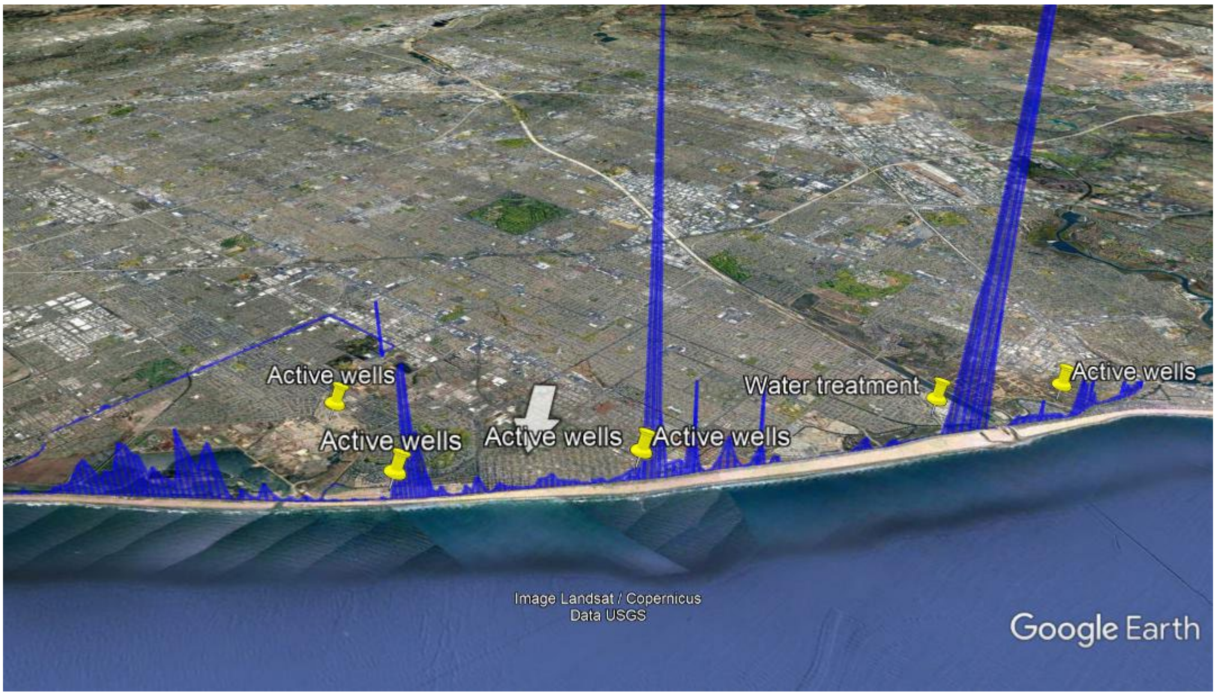

Figure 40 CH4 concentration measurements in NE wind along the coastline of Huntington Beach and Newport.

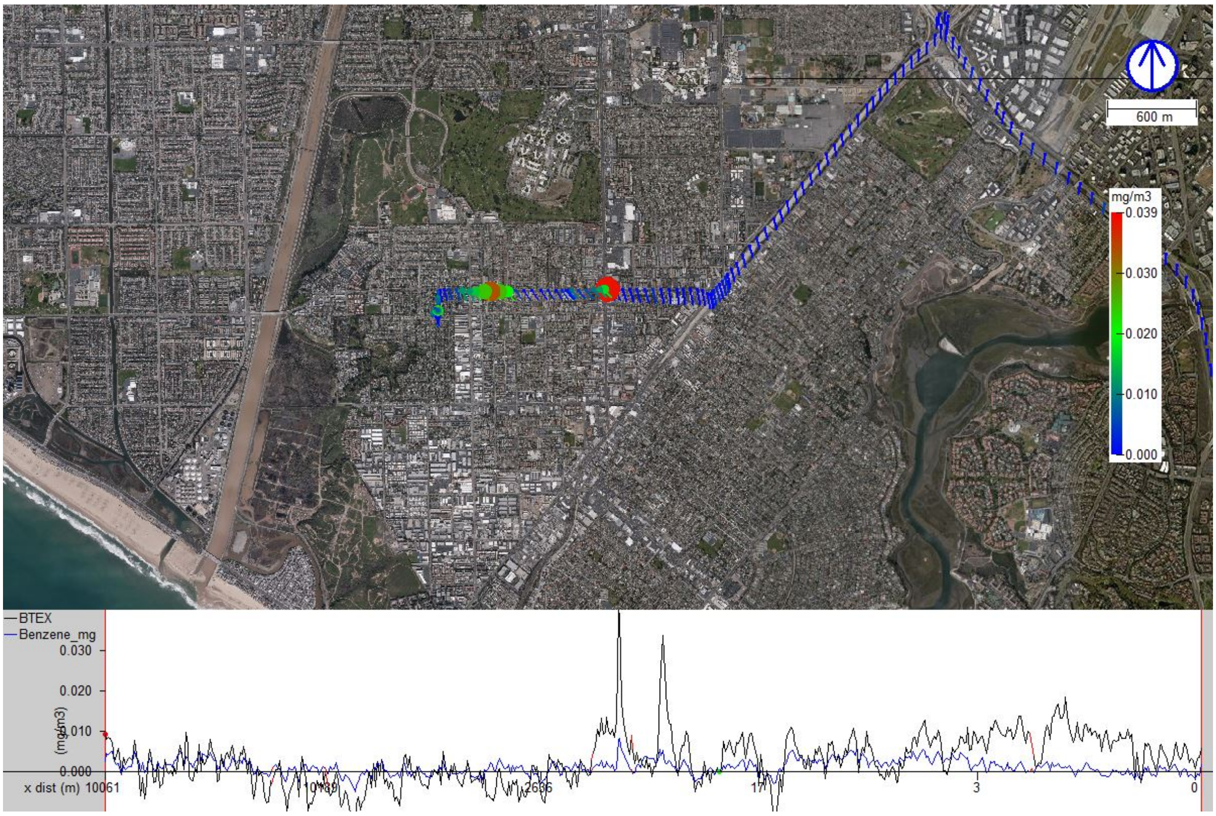

Figure 41 Example of BTEX concentration measurements in mg/m$^3$ near Huntington Beach.

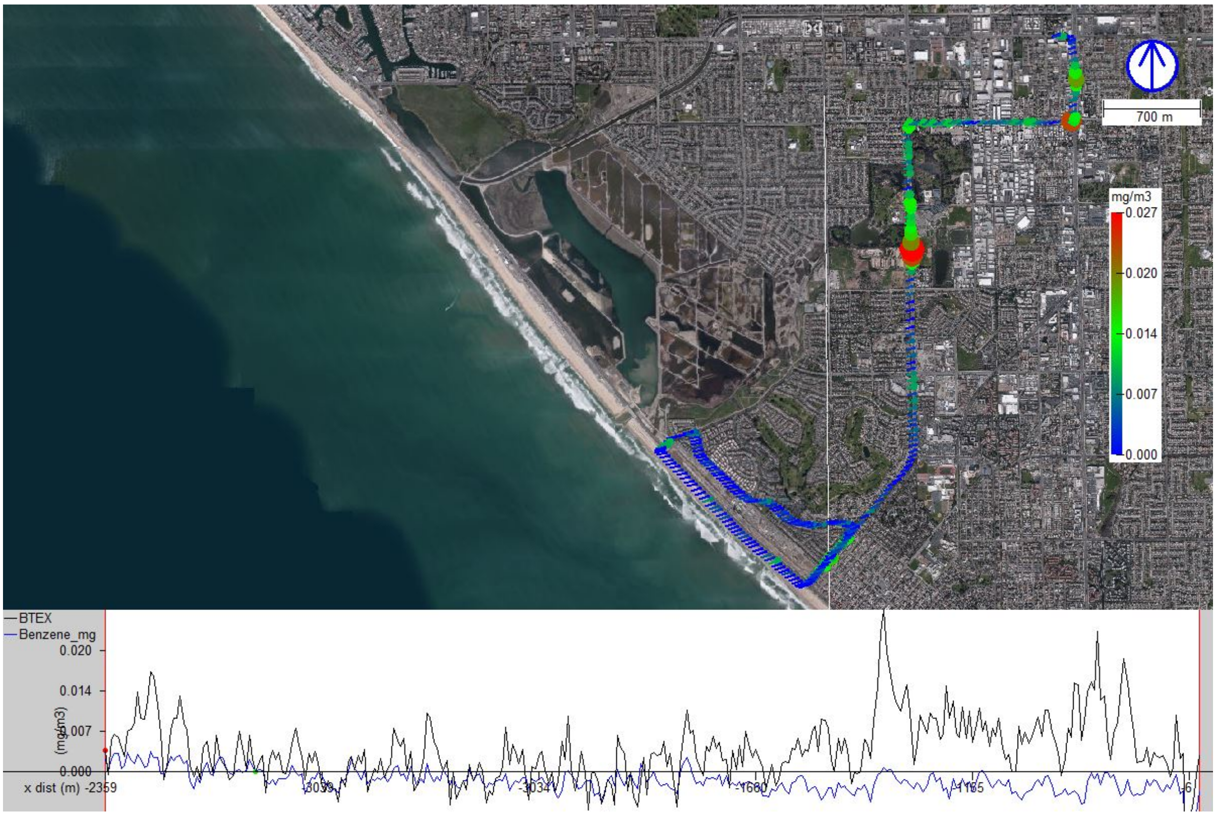

Figure 42 Example of BTEX concentration measurements in mg/m$^3$ near Huntington Beach.

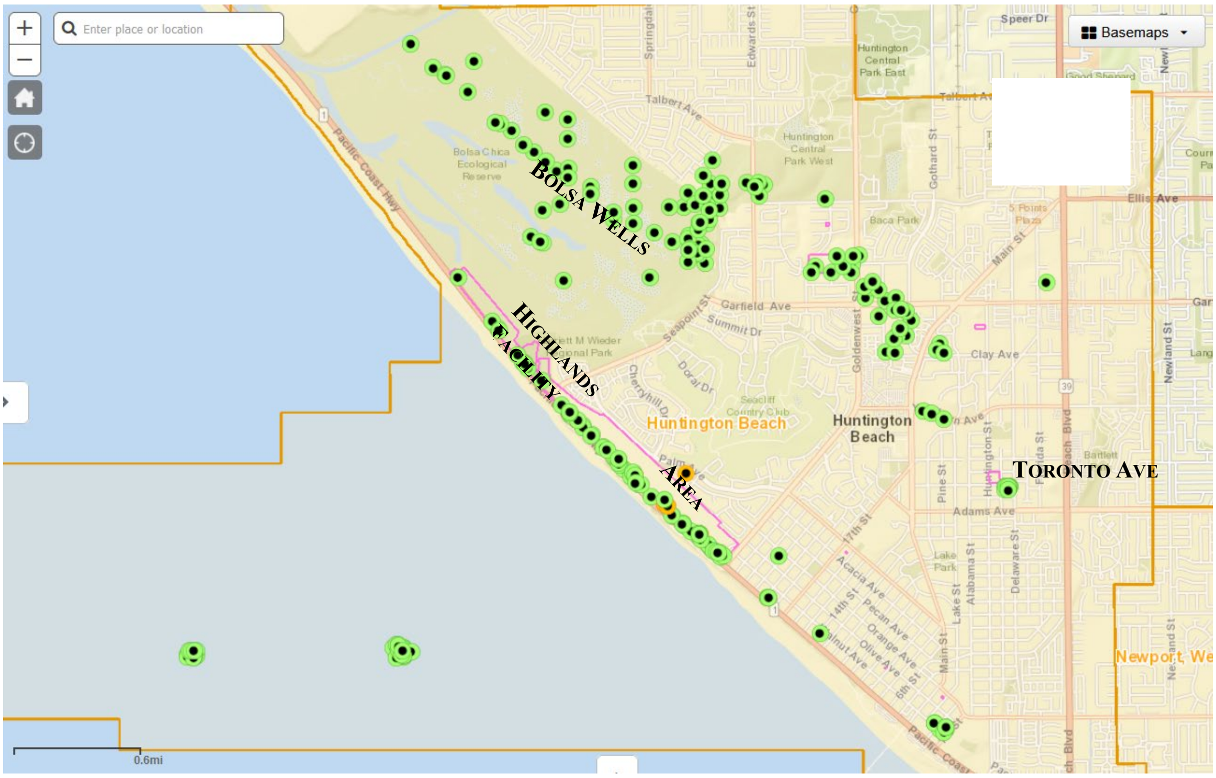

Figure 43 New and active wells in Huntington beach (https://maps.conservation.ca.gov/doggr/wellfinder, November 2020)

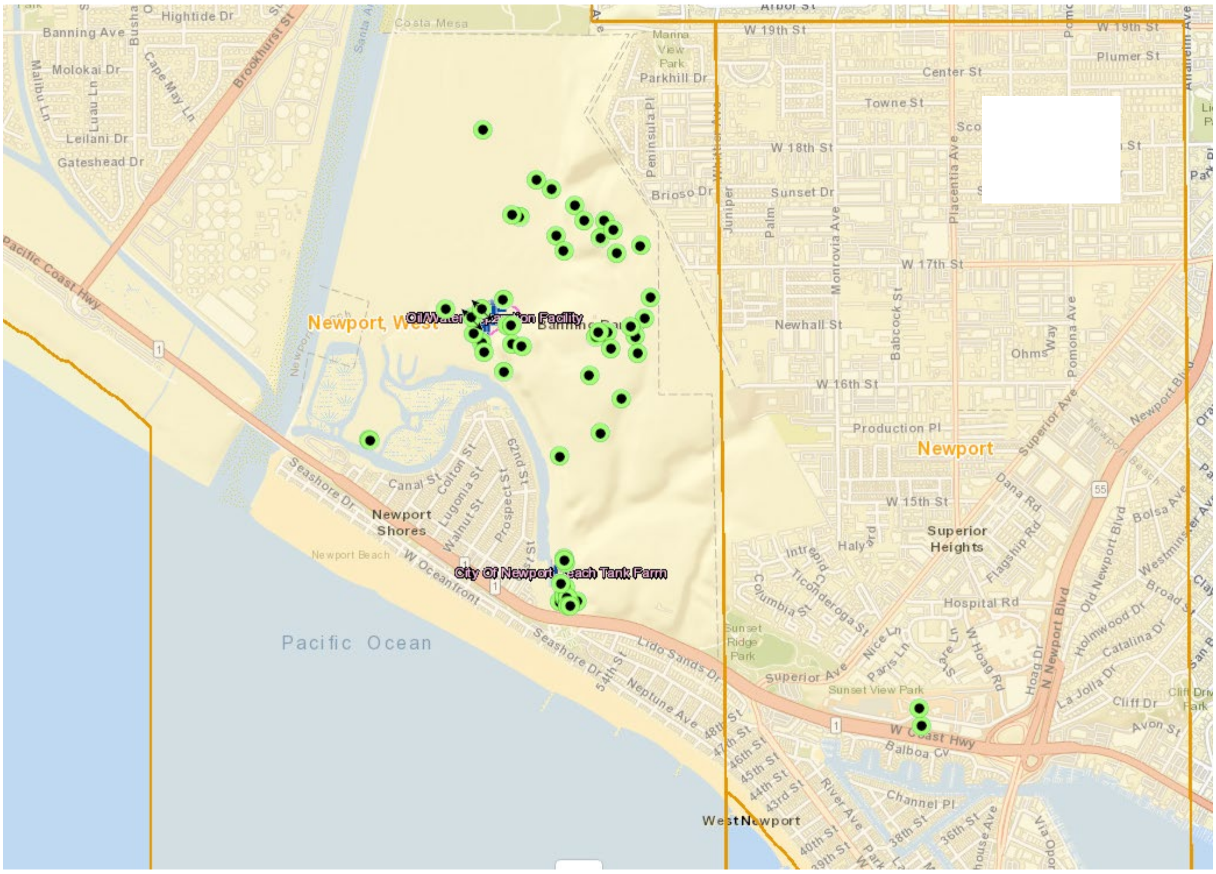

Figure 44 Active wells in Newport beach (https://maps.conservation.ca.gov/doggr/wellfinder, April 2020)

## 5.5 Emission measurements and concentration mapping – SCAB North

Measurements in the South SCAB were conducted 26-28 October 2019. Results from six different sites/areas are presented in the subsections below. The sites were either selected in the implementation plan or detected in real-time during measurement and considered interesting.

### *5.5.1 North Hills Brewery*

North Hills Brewery was measured with SOF and MeFTIR 27 October 2019.

Variable background plumes made most of the transects useless for quantification. Only one single SOF measurement fulfilled the quality criteria and gave an emission of 53 kg/h alkane equivalents, see Table 30. Further statistics are needed to support this result which should be considered indicate only.

Table 30 SOF Alkane emission measurements, North Hills Brewery, October 2019

| Day [yymmdd] | Time span [hhmmss-hhmmss] | Num Meas | Emission avg [kg/h] | Emission SD [kg/h] | Wind Speed Min-Max [m/s] | Wind Dir Span [deg] |
|---|---|---|---|---|---|---|
| **191027** | 121558-122309 | 1 | 53.0 | N/A | 4.3-4.3 | 154-154 |
| **Total # of Meas.** | | **1** | | | | |
| **Median** | | | **53.0** | | | |
| **IQR** | | | **53.0 - 53.0** | | | |
| **Mean** | | | **53.0** | | | |
| **SD** | | | **NaN** | | | |

### *5.5.2 Irwindale Brewery*

The Irwindale was measured with SOF and MeFTIR 28 October 2019, see example in Figure 45. Wind profile data (0-100 m) from the mobile LIDAR located in north-east of the brewery (see Figure 45) has been used for flux calculations.

Repeatable, and distinct SOF signals were detected on the downwind side, but there were also plumes from surrounding oil and gas sources that needed to be considered and subtracted.

The median emissions were 8 kg/h of alkane equivalents from the site based on 7 measurement transects, see details in Table 31. Methane/Alkane ratios of 67% gave an indirect methane emission of 5.3 kg/h, see details in Table 32.

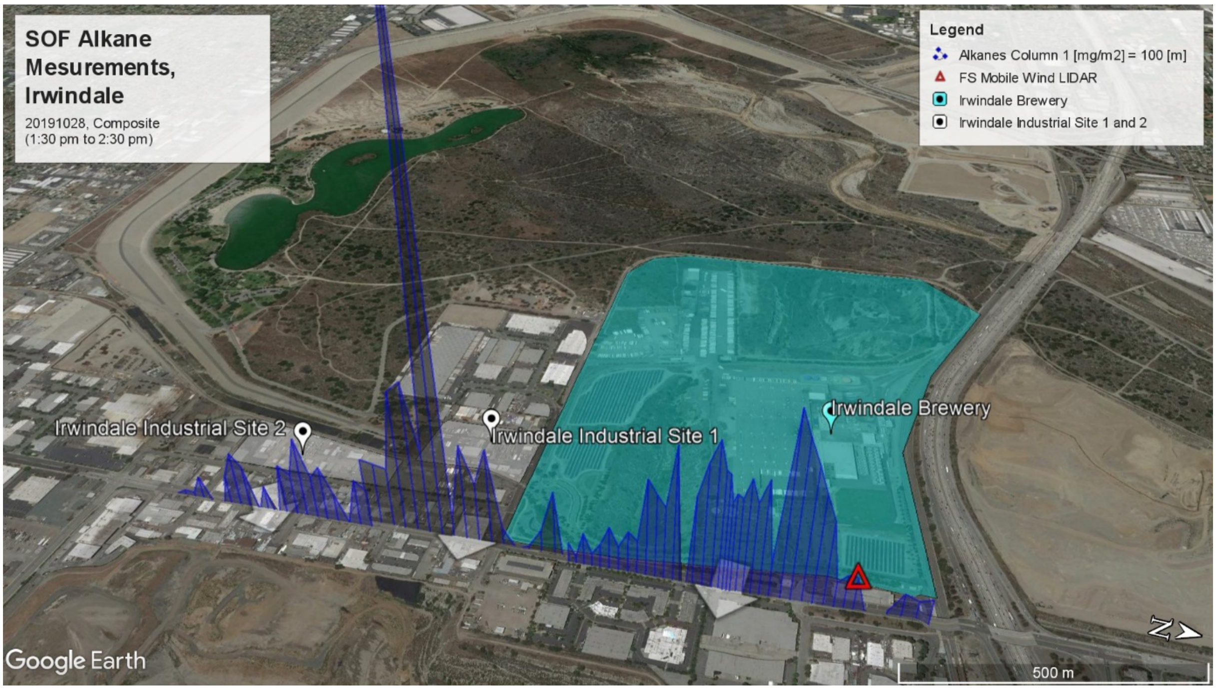

Figure 45 SOF alkane columns (blue contour) from Irwindale Brewery and adjacent industrial sites, 28 October 2019. The figure is a composite of different measurement transect taken between 1:30 pm and 2:30 pm. The wind directions are indicated by the white arrows. Map from Google Earth™, 2020.

Table 31 SOF Alkane emission measurements, Irwindale Brewery, October 2019

| Day [yymmdd] | Time span [hhmmss-hhmmss] | Num Meas | Emission avg [kg/h] | Emission SD [kg/h] | Wind Speed Min-Max [m/s] | Wind Dir Span [deg] |
|---|---|---|---|---|---|---|
| **191028** | 132953-155516 | 7 | 7.7 | 3.7 | 2.0-3.1 | 224-275 |
| **Total # of Meas.** | | **7** | | | | |
| **Median** | | | **7.9** | | | |
| **IQR** | | | **5.3 - 9.0** | | | |
| **Mean** | | | **7.7** | | | |
| **SD** | | | **3.7** | | | |

Table 32 Methane/Alkane mass ratios from MeFTIR measurements, Irwindale Brewery, October 2019

| Day [yymmdd] | Time span [hhmmss-hhmmss] | Num Meas | Mass Ratio avg [%] | Mass Ratio SD [%] | Wind Speed Min-Max [m/s] | Wind Dir Span [deg] |
|---|---|---|---|---|---|---|
| **191028** | 132612-150705 | 5 | 76.7 | 42.8 | 2.0-3.1 | 244-275 |
| **Total # of Meas.** | | **5** | | | | |
| **Median** | | | **67.2** | | | |
| **IQR** | | | **57.1 - 85.3** | | | |
| **Mean** | | | **76.7** | | | |
| **SD** | | | **42.8** | | | |

### *5.5.3 Irwindale Industrial Site 1*

The Irwindale Industrial Site -1 is adjacent to the Irwindale Brewery and was measured with SOF and MeFTIR 28 October 2019, see Figure 45. Wind profile data (0-100 m) from the mobile LIDAR located in north-east of the brewery (see Figure 45) has been used for flux calculations.

Repeatable, and distinct SOF signals were detected on the downwind side, but there were also plumes from surrounding oil and gas sources that needed to be considered and subtracted.

The survey median emissions were 8 kg/h of alkanes from the site based on 5 measurement transects, see details in Table 33. No methane/alkane ratios could be retrieved from this site due to non-detectable plume concentrations.

Table 33 SOF Alkane emission measurements, Irwindale Industrial Site 1, October 2019

| Day [yymmdd] | Time span [hhmmss-hhmmss] | Num Meas | Emission avg [kg/h] | Emission SD [kg/h] | Wind Speed Min-Max [m/s] | Wind Dir Span [deg] |
|---|---|---|---|---|---|---|
| **191028** | 134401-152705 | 5 | 11.3 | 8.0 | 1.8-3.0 | 219-268 |
| **Total # of Meas.** | | **5** | | | | |
| **Median** | | | **7.7** | | | |
| **IQR** | | | **7.5 - 10.9** | | | |
| **Mean** | | | **11.3** | | | |
| **SD** | | | **8.0** | | | |

### *5.5.4 Irwindale Industrial Site 2*

The Irwindale Industrial Site -2 is adjacent to the Irwindale Brewery and was measured with SOF and MeFTIR 28 October 2019, see Figure 45 . Wind profile data (0-100 m) from the mobile LIDAR located in north-east of the brewery (see Figure 45) has been used for flux calculations.

Repeatable, and distinct SOF signals were detected on the downwind side, but there were also plumes from surrounding oil and gas sources that needed to be considered and subtracted.

The survey median emissions were 3 kg/h of alkanes from the site based on 4 measurement transects, see details in Table 34. No methane/alkane ratios could be retrieved from this site due to non-detectable plume concentrations.

Table 34 SOF Alkane emission measurements, Irwindale Industrial Site 2, October 2019

| Day [yymmdd] | Time span [hhmmss-hhmmss] | Num Meas | Emission avg [kg/h] | Emission SD [kg/h] | Wind Speed Min-Max [m/s] | Wind Dir Span [deg] |
|---|---|---|---|---|---|---|
| **191028** | 134703-143236 | 4 | 6.0 | 7.1 | 2.6-3.0 | 235-269 |
| **Total # of Meas.** | | **4** | | | | |
| **Median** | | | **3.4** | | | |
| **IQR** | | | **2.0 - 7.4** | | | |
| **Mean** | | | **6.0** | | | |
| **SD** | | | **7.1** | | | |

### *5.5.5 Placerita Oil Field*

The Placerita Oil Field was measured with SOF and MeFTIR 26 October 2019, see example in Figure 61. Wind profile data (0-100 m) from the mobile LIDAR located in south-east corner of the field (see Figure 46) has been used for flux calculations.

Weak winds and variable background/upwind plumes from surrounding oil fields made it challenging to make quantification from the transects. Only one single SOF measurement fulfilled the quality criteria and gave an emission of 216 kg/h alkane equivalents, see Table 35. Further statistics are needed to support this result which should be considered indicate only.

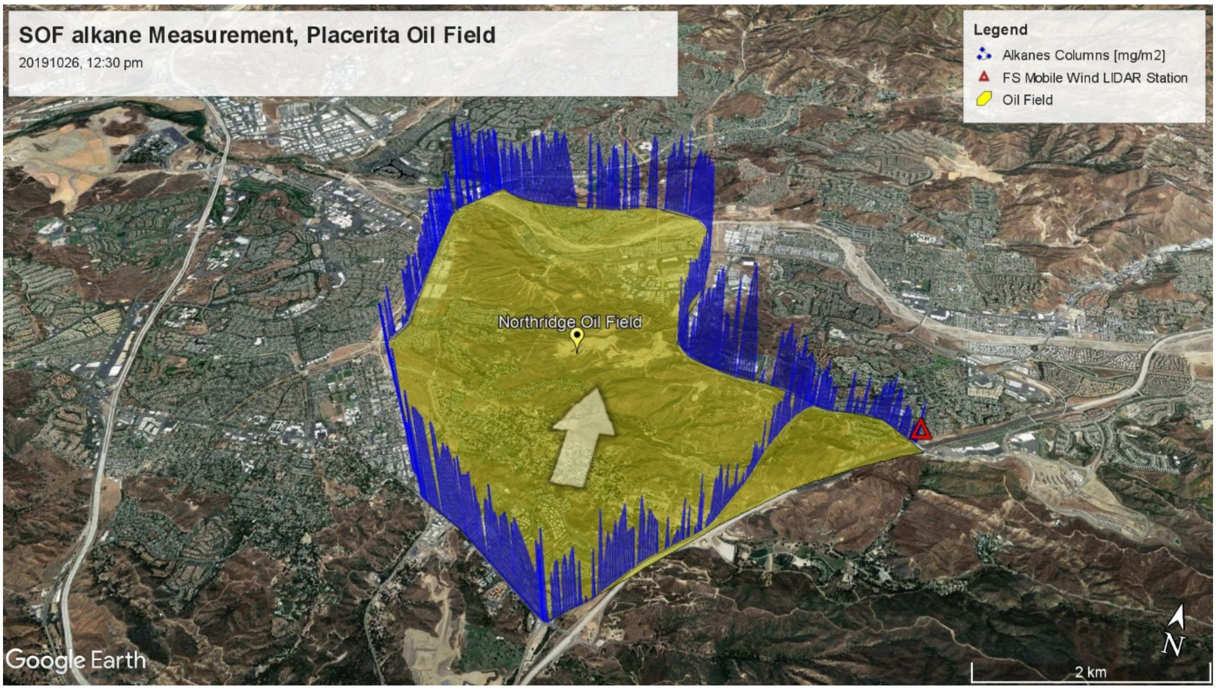

Figure 46 SOF alkane columns (blue contour) at Placerita Oil Field (yellow area), 26 October 2019. The wind direction is indicated by the white arrow. Map from Google Earth™, 2020.

Table 35 SOF Alkane emission measurements, Placerita Oil Field, October 2019

| Day [yymmdd] | Time span [hhmmss-hhmmss] | Num Meas | Emission avg [kg/h] | Emission SD [kg/h] | Wind Speed Min-Max [m/s] | Wind Dir Span [deg] |
|---|---|---|---|---|---|---|
| **191026** | 123055-131324 | 1 | 216 | N/A | 4.8-4.8 | 177-177 |
| **Total # of Meas.** | | **1** | | | | |
| **Median** | | | **216.1** | | | |
| **IQR** | | | **216.1 - 216.1** | | | |
| **Mean** | | | **216.1** | | | |
| **SD** | | | **NaN** | | | |

A median methane/alkane ratio of 156 % (see Table 36) in the downwind plumes gave an indirect methane emission of 337 kg/h from the field, but this is highly uncertain since it's based on a single SOF transect.

Table 36 Methane/Alkane mass ratios from MeFTIR measurements, Placerita Oil Field, October 2019

| Day [yymmdd] | Time span [hhmmss-hhmmss] | Num Meas | Mass Ratio avg [%] | Mass Ratio SD [%] | Wind Speed Min-Max [m/s] | Wind Dir Span [deg] |
|---|---|---|---|---|---|---|
| **191026** | 123215-200438 | 3 | 216 | 153.5 | 2.0-4.3 | 152-173 |
| **Total # of Meas.** | | **3** | | | | |
| | | | | | | |
| **IQR** | | | **128.5 - 273.0** | | | |
| | | | | | | |
| **SD** | | | **153.5** | | | |

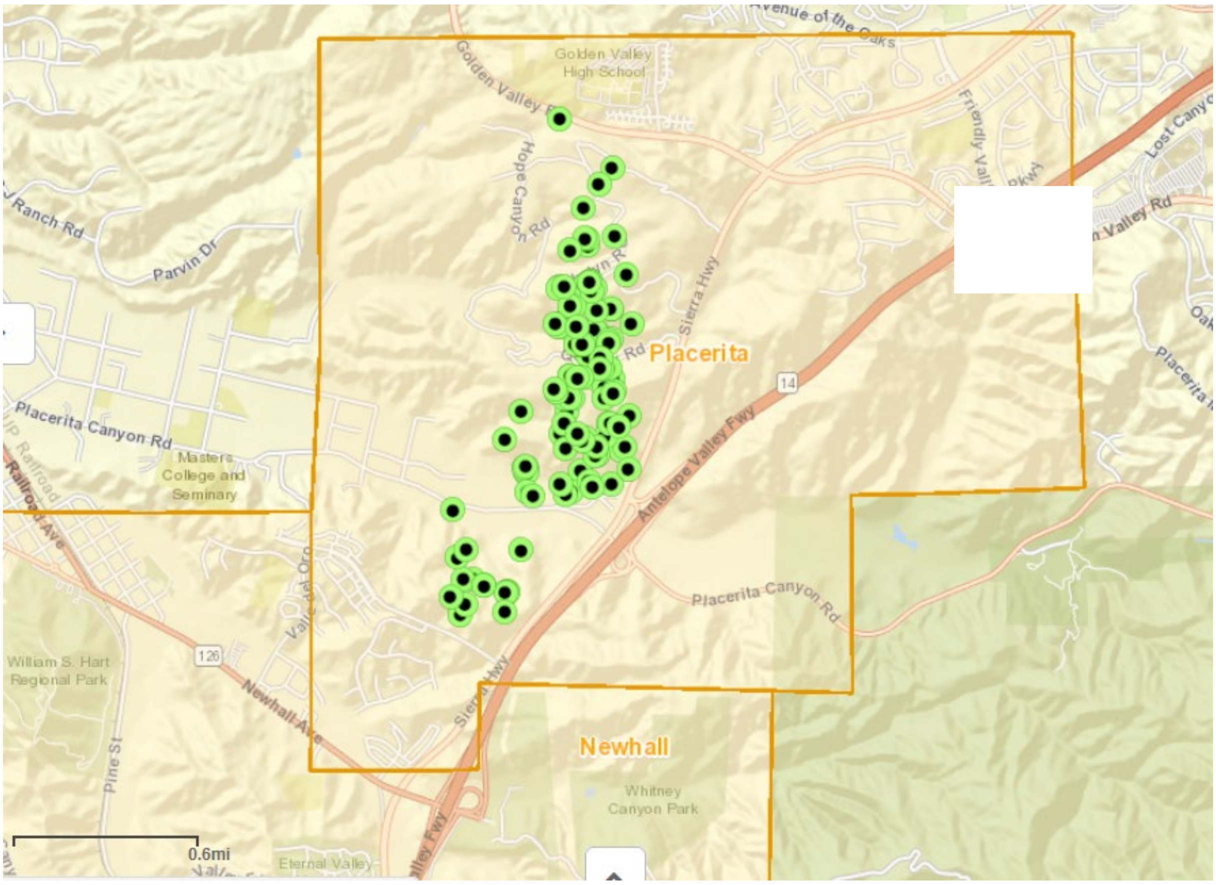

Figure 47 Active wells in the Placerita oil field (https://maps.conservation.ca.gov/doggr/wellfinder, November 2020)

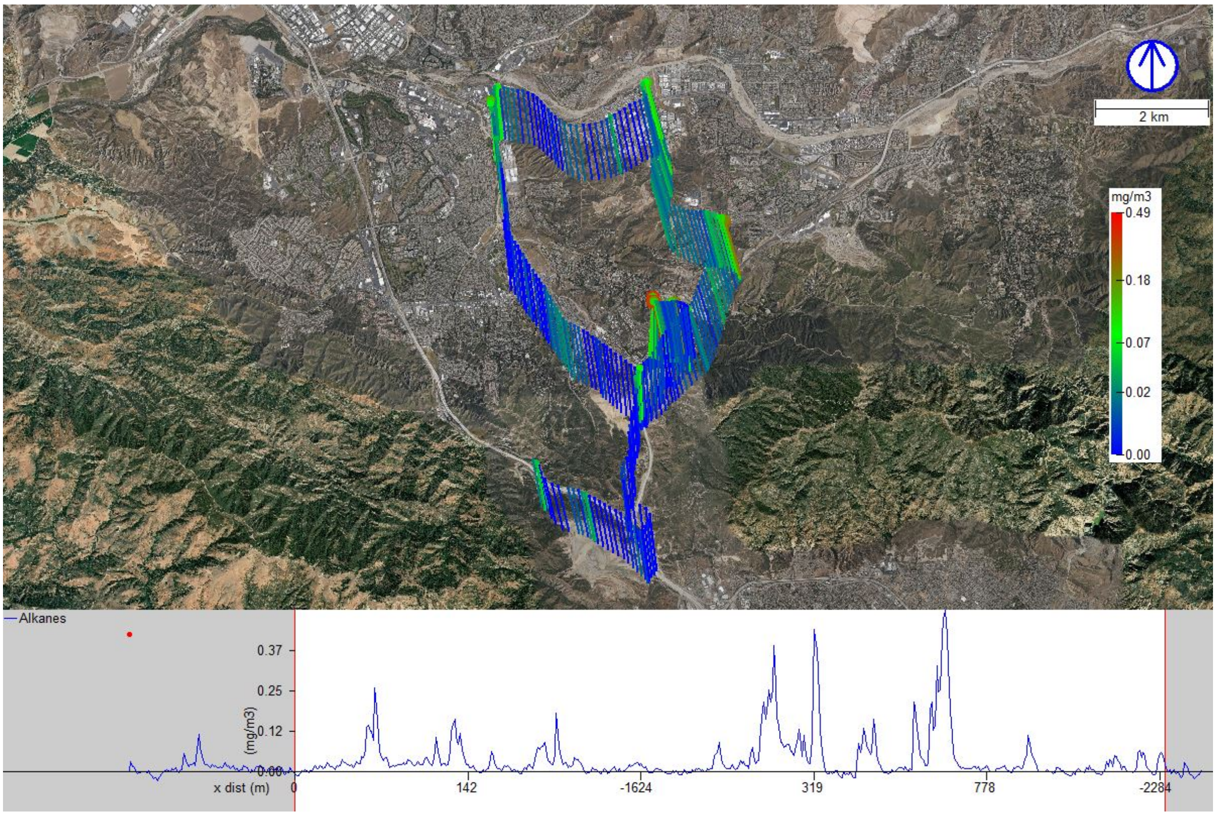

Figure 48 Alkane concentration measurements around the Placerita Oil Field.

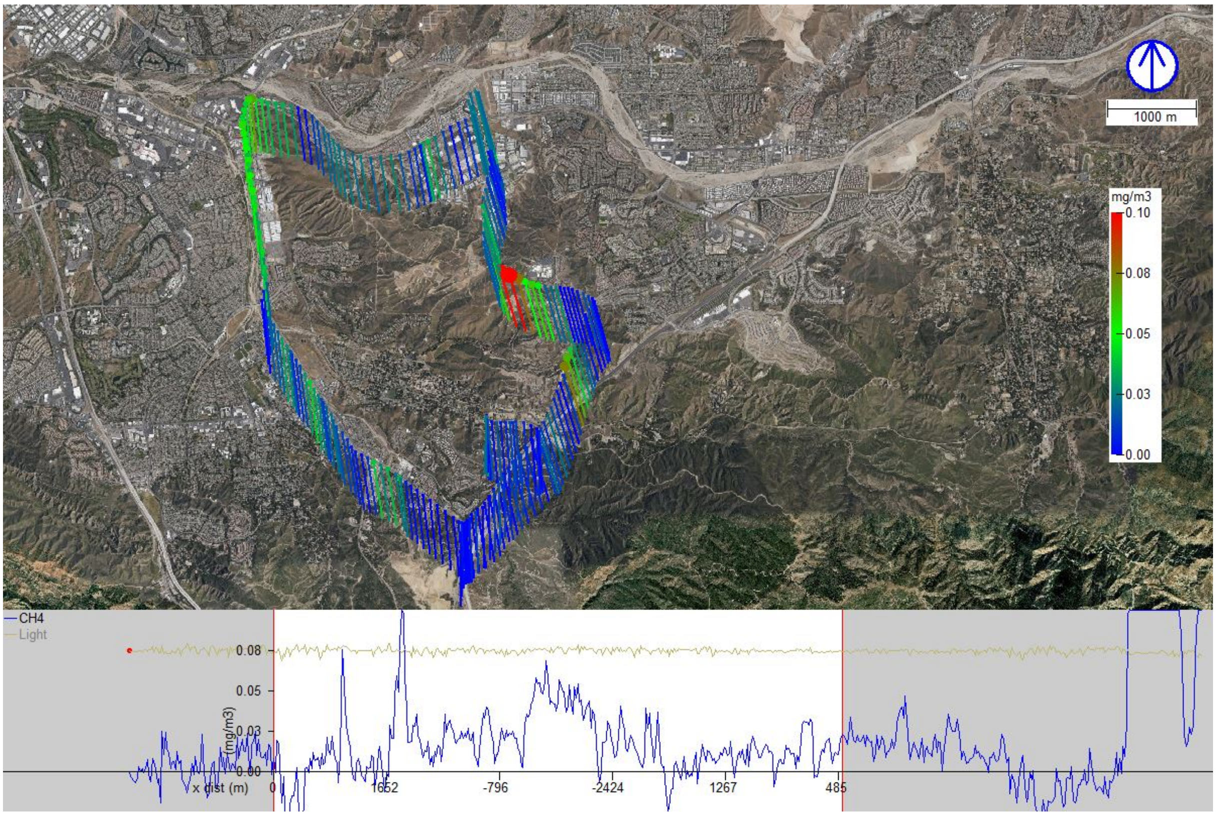

Figure 49 Methane concentration measurements around the Placerita Oil Field.

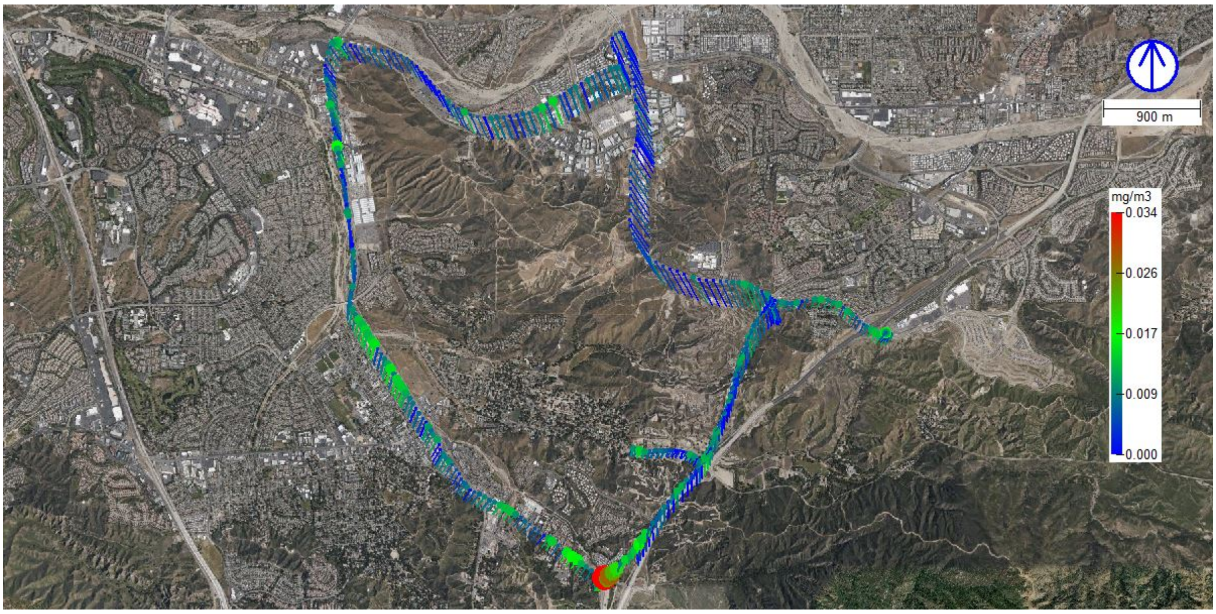

Figure 50 BTEX measurements around the Placerita Oil Field.

Figure 51 Alkane (left) and Methane (right) concentrations downwind of a small tank group in the Placerita Oil Field, Oct 26. The measurements were measured at different times on the same day and the concentrations cannot be compared directly.

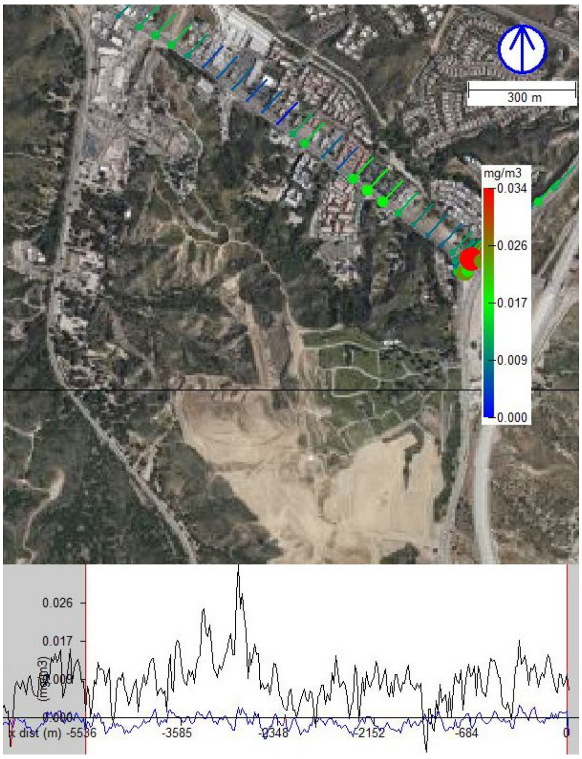

Figure 52 BTEX (on map and black line in plot) and benzene (blue line in plot) concentrations downwind of a small tank group in the Placerita Oil Field, Oct 26. The measurements were measured at different times than the alkane and methane and the concentration cannot be compared directly.

### 5.5.6 *Sunshine Canyon Landfill*

The Sunshine Canyon Landfill was measured with MeFTIR 26 October 2019. This source was however difficult to measure with SOF in southerly wind direction.

MeFTIR measurements, on the other hand, gave distinct results and the median methane/alkane ratio was 680 % (see Table 37) based on three successful transects, Figure 53 and Figure 54. The indirect methane emission is, however, not possible to retrieve due to the absence of SOF alkane measurements.

Table 37 Methane/Alkane mass ratios from MeFTIR measurements, Sunshine Canyon Landfill, October 2019

| Day [yymmdd] | Time span [hhmmss-hhmmss] | Num Meas | Mass Ratio avg [%] | Mass Ratio SD [%] | Wind Speed Min-Max [m/s] | Wind Dir Span [deg] |
|---|---|---|---|---|---|---|
| **191026** | 164119-185935 | 3 | 680 | 152.0 | 2.3-5.3 | 164-169 |
| **Total # of Meas.** | | **3** | | | | |
| **Median** | | | **658.3** | | | |
| **IQR** | | | **599.2 - 750.0** | | | |
| **Mean** | | | **680.0** | | | |
| **SD** | | | **152.0** | | | |

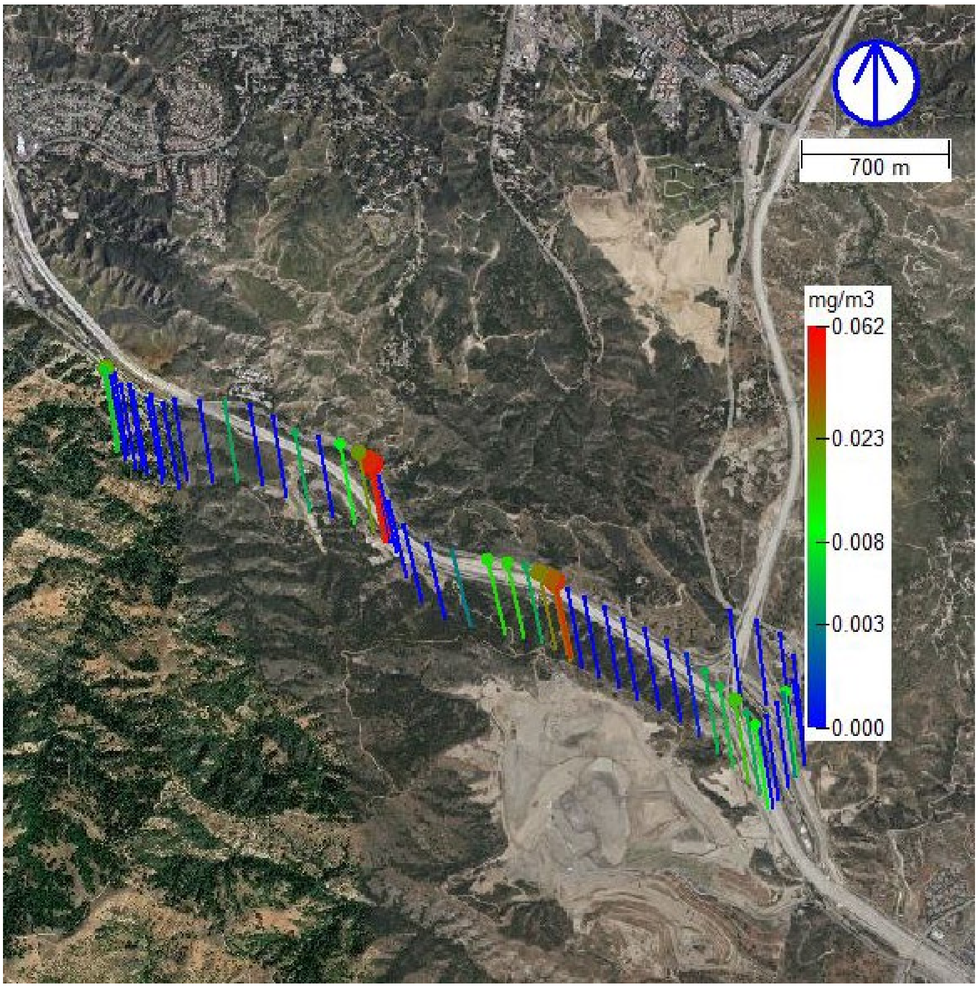

Figure 53 Alkanes concentration downwind of Sunshine Canyon landfill.

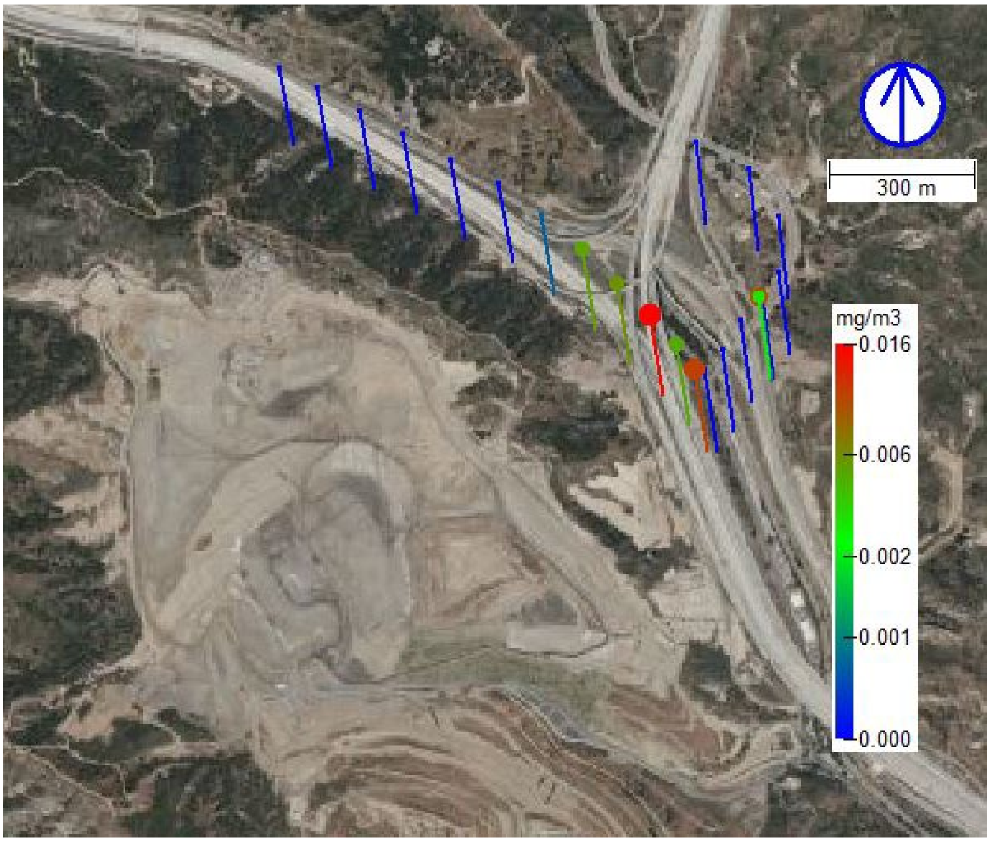

Figure 54  Methane concentration downwind of Sunshine Canyon landfill.

## 5.6 Community Monitoring & Concentration Mapping – SCAB North

### *5.6.1 Irwindale*

Results from concentration mapping of alkanes, methane and BTEX in Irwindale 28 October 2019 are found in Figure 19 to Figure 21. These measurements show enhanced values of alkanes, methane and BTEX downwind the brewery and the industrial sites, peaking at 0.98 µg/m$^3$, 0.6 µg/m$^3$ and 0.053 µg/m$^3$ respectively.

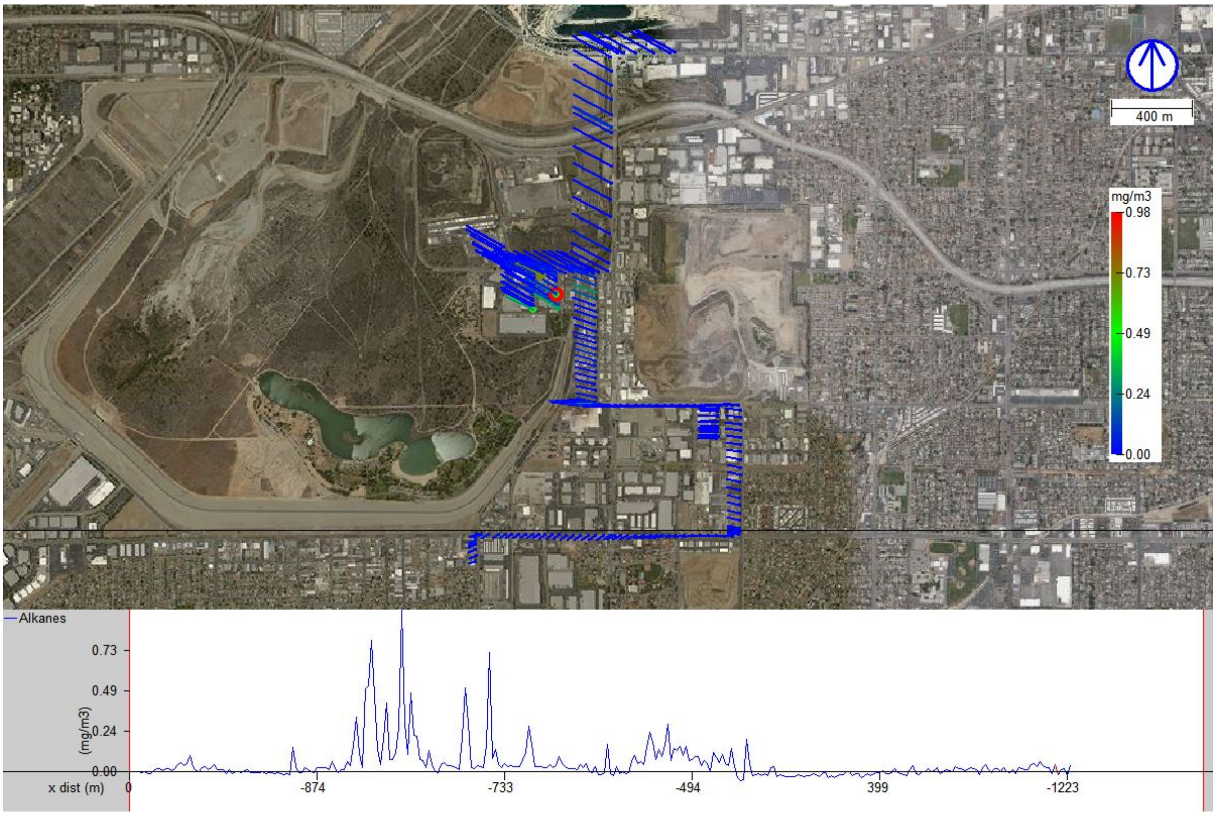

Figure 55 Alkane concentration at Irwindale community, Oct 28, 18:30-19:30

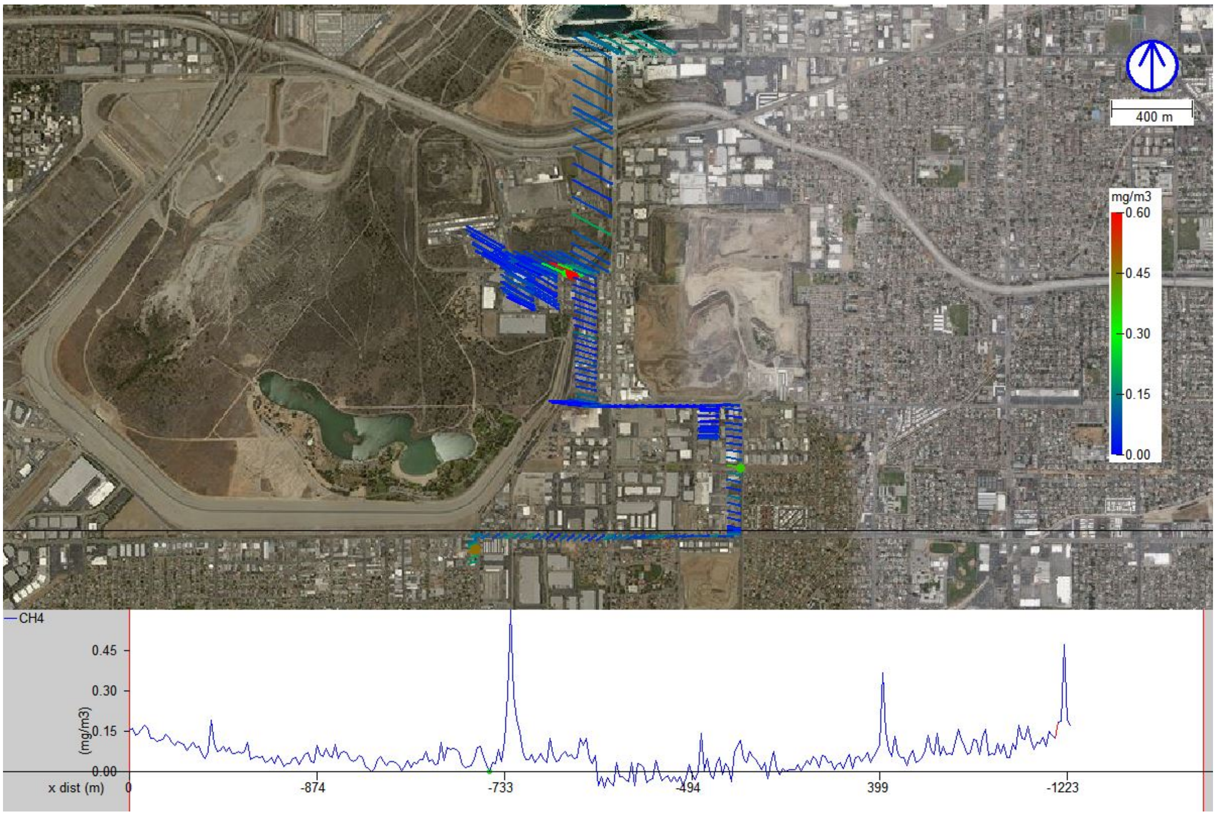

Figure 56 Methane concentration at Irwindale community, Oct 28, 18:30-19:30

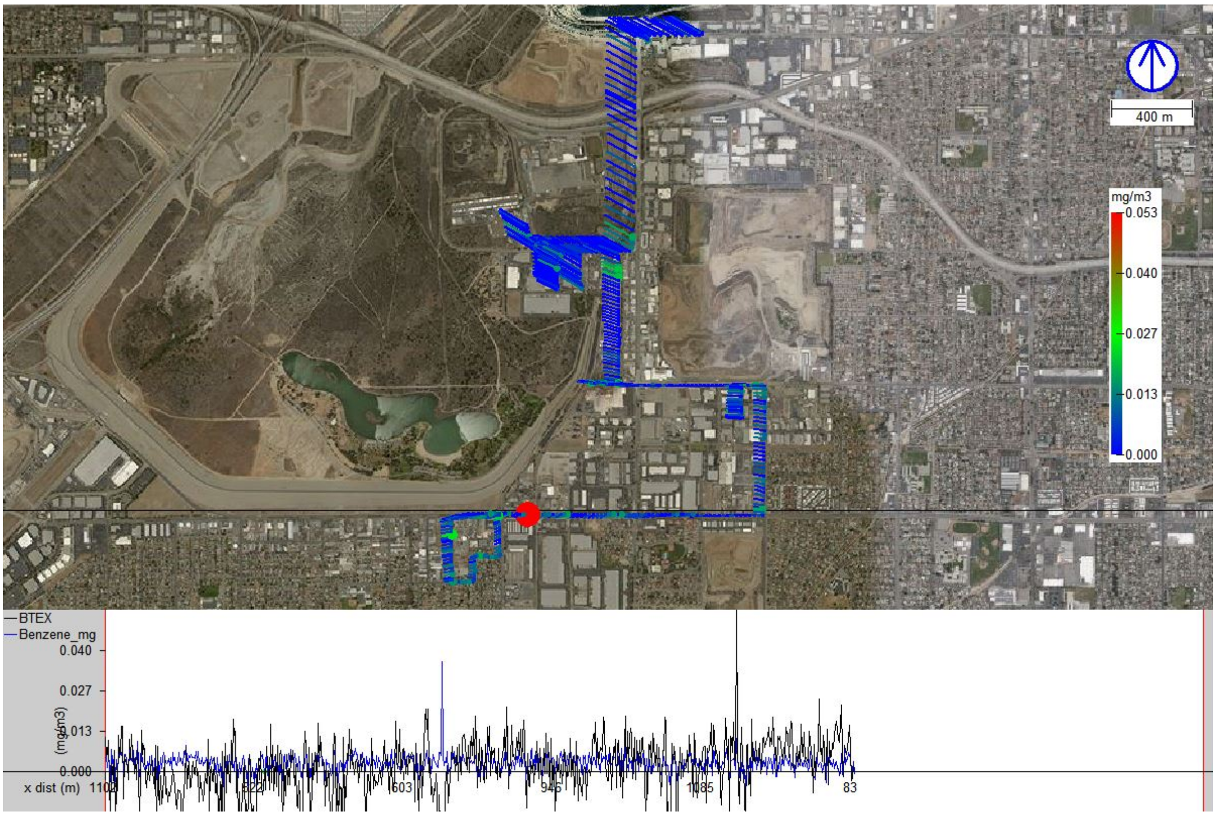

Figure 57 BTEX concentration at Irwindale community, Oct 28, 18:30-19:30

### *5.6.2 Large Scale Mapping (Brentwood to Irwindale)*

A large scale alkane concentration mapping from Brentwood in the east to Irwindale in the east was made 28 October 2019, see Figure 58. The wind came from the north, bringing smoke from a rather large wildfire in the mountains north of Brentwood.

Our interpretation is that the high concentrations in the west (left) correspond to influence of the wildfire while the concentrations in the east (right) around Irwindale originates from a brewery and other activities. The isolated peaks in the middle to the left we believe comes from industries that we passed while the elevated levels in the right part may be caused by wildfires, see correlation with $NH_3$ in Figure 62, but this needs further investigation. The corresponding methane concentrations are shown in Figure 59 and a similar pattern as for the alkanes is shown.

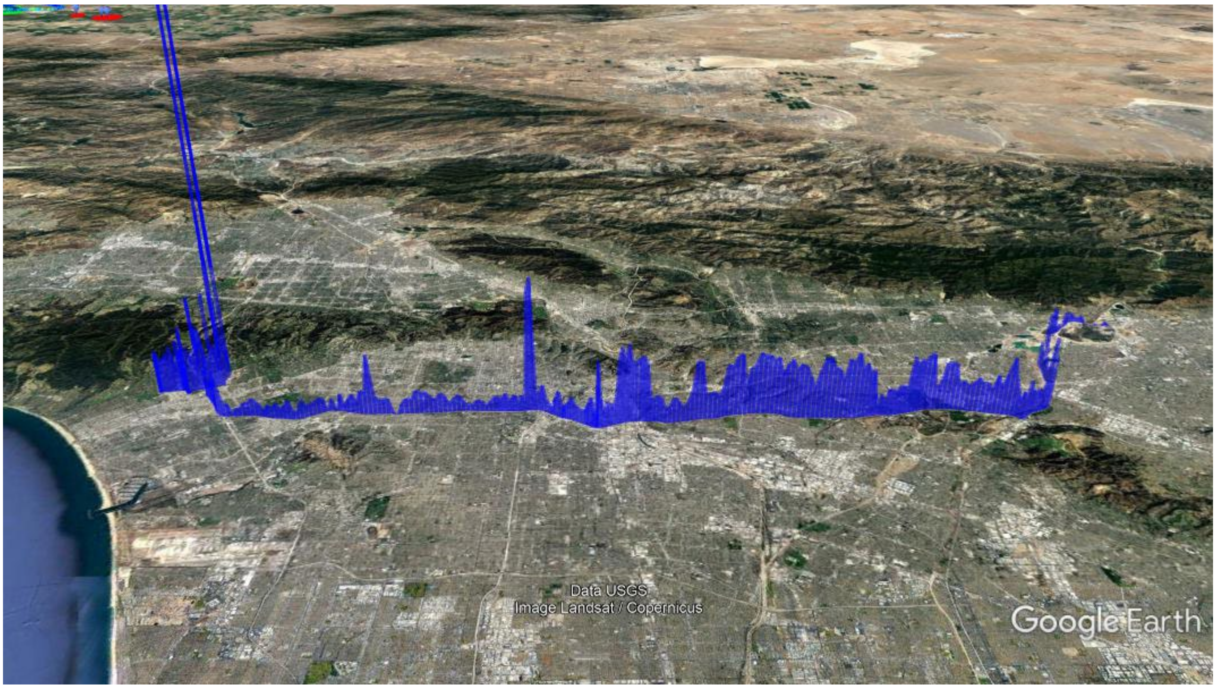

Figure 58 Alkane concentration measured in northern SCAB, from Brentwood to Irwindale, 28 October 2019, 11:18 - 12:57. The maximum scale corresponds to 300 ppb of propane equivalents. The wind blew from the north.

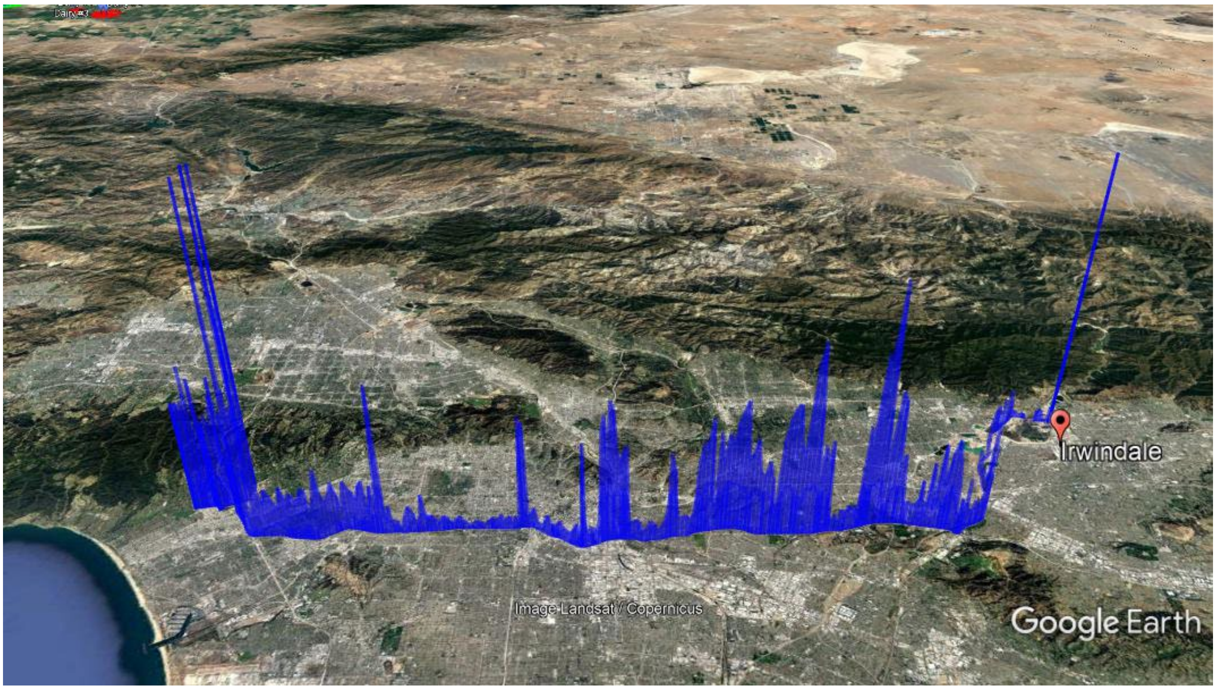

Figure 59 Methane concentration measured in northern SCAB, from Brentwood to Irwindale, 28 October 2019, 11:18 - 12:57. The max scale corresponds to 500 ppb of methane. The wind blew from the north.

## 5.7 Other Observations

### 5.7.1 *CNG buses*

During community monitoring in Northridge we observed that a CNG bus, which is part of the Metro Liner bus system, was leaking significant amounts of methane, with 350 ppb measured 50 m away. This type of emission was not part of the scope of this study but we recommend further studies.

Figure 60 Observation of a methane leak from a CNG Metro Liner bus in Northridge.

### 5.7.2 *Wildfire measurements*

On October 29 there was a wildfire north of Brentwood, Figure 61. The wind was from the NW, a heavy smoke plume came in over Brentwood, and a full evacuation of the area was carried out. There were also several other wildfires further to the north which blew into the SCAB. Figure 62 shows a SOF transect from Brentwood in the west to Irwindale in the east with retrieved $NH_3$ columns culminating in a total flux of 3600 kg/h. The influence of the wildfire smoke is obvious in the left part of the scan (Brentwood), but also in middle of the transect, around downtown LA, and potentially the influence of other wildfires can be seen. Other species such as ethylene and formaldehyde columns correlate well with this. The data also correlates partly with alkane concentration measurements.

Figure 61 Wildfire north of Brentwood on October 28.

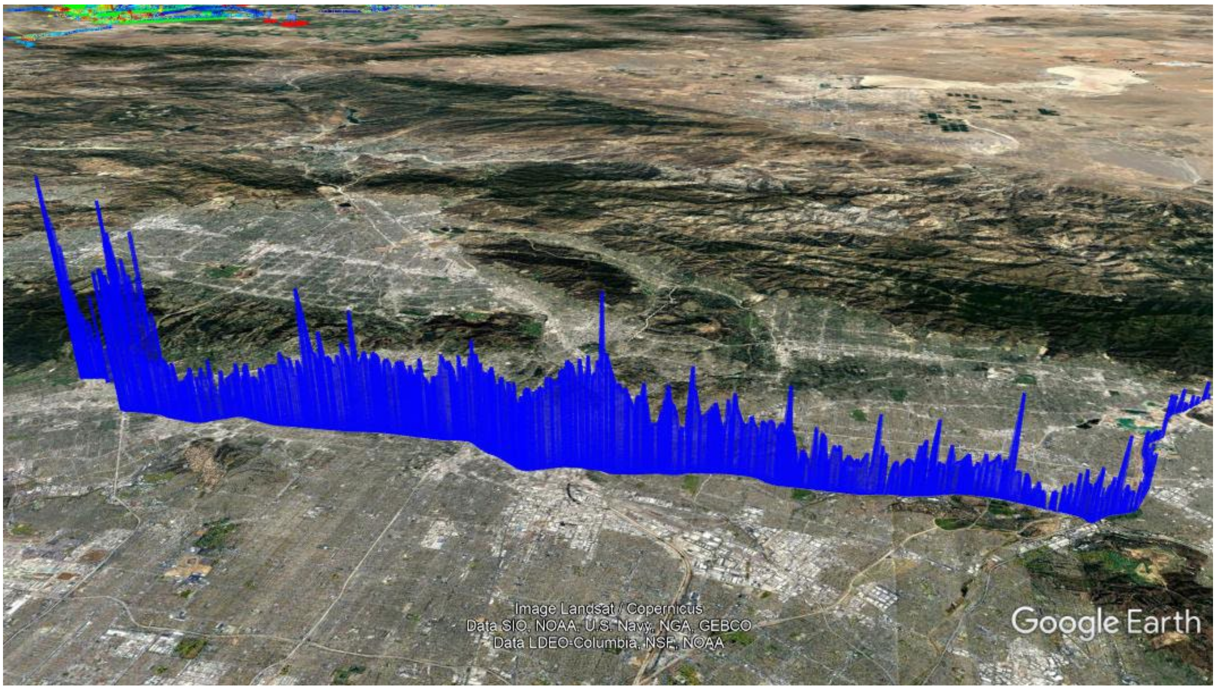

Figure 62 $NH_3$ column measurements in northerly wind. Total flux 3.6 tons/h of $NH_3$.

# 6 Discussion and Conclusions

This study comprises results from 18 sites/areas in three regions (San Diego County Air Basin. South part of SCAB and North part of SCAB.) Altogether, 153 measurement transects were performed during 10 separate days. Relatively few repeats were carried out for each source, however, since the objective was to screen many sources and therefore the uncertainty is higher than the 30% which is usually stated by the used techniques.

The main sources in this study are related to oil and gas production, fuel storage and to landfills, several in close proximity to communities. From community monitoring of alkane concentrations, we were able to identify several hotspots related to active gas wells. The main emissions from these were methane and other alkanes while the emissions of aromatic VOCs were relatively small. In addition, general community monitoring in the area confirms this.
Measurements of two tank farms in Huntington Beach that were close to residential areas showed relatively low VOC emissions, although they contributed to significantly elevated concentrations during the night.

The measurements at the landfills shows that these generally emit alkanes, in addition to methane and the CH4 to alkane mass ratio varies between 2 to 14, with a typical value of around 7. However, there are several uncertainty factors involved when determining these ratios from the fence-line and further work is needed here, measuring inside the actual sources. The fact that the alkane emissions from the landfills are strong enough to be measured by SOF, makes this technique promising for future emission studies.

Measurements at the port of San Diego, showed significant $NO_2$ and $SO_2$ emissions which appeared to originate from the port activity. Other observations in the study included measuring the influence of wildfires on the air quality and detecting methane emissions from the CNG buses.

# 7 Acknowledgements

This Report was submitted in fulfilment of 17RD021 "Characterization of Air Toxics and GHG Emission Sources and their Impacts on Community -Scale Air Quality Levels in Disadvantaged Communities" By FluxSense Inc under the sponsorship of the California Air Resources Board. Work was completed as of 30 April 2020.

# 8 References

Bogumil K., et al, 2003. Measurements of molecular absorption spectra with the SCIAMACHY pre-flight model: instrument characterization and reference data for atmospheric remote-sensing in the 230-2380 nm region, *Journal of Photochemistry and Photobiology A: Chemistry*, 157(2-3):167-184 5/5, 2003.

Burrows J.P., A. Richter, A. Dehn, B. Deters, S. Himmelmann, S. Voigt, and J. Orphal, 1999. "Atmospheric remote-sensing reference data from GOME: Part 2. Temperature-dependent absorption cross-sections of $O_3$ in the 231-794 nm range," J. Quant. Spectrosc. Radiat. Transfer 61, 509-517, 1999.

Börjesson, G., Samuelsson, J., Chanton, J., Adolfsson, R., Galle, B., Svensson, B.H., 2009. A national landfill methane budget for Sweden based on field measurements, and an evaluation of IPCC models.Tellus B, 61, 424–435.

DOGGR, 2016. Division of Oil, Gas & Geothermal Resources, at Department of Conservation, CA. http://maps.conservation.ca.gov/doggr/#close .

DOGGR, 2019, Division of Oil, Gas & Geothermal Resources, at Department of Conservation, CA https://maps.conservation.ca.gov/doggr/wellfinder

Downey N., Emery C., Jung J., Sakulyanontvittaya T., Hebert L., Blewitt D., Yarwood G., 2015. Emission reductions and urban ozone responses under more stringent US standards. Atmospheric Environment, 101, pp 209-216, 2015.

Environmental Research & Education Foundation (EREF), 2011. Field comparison of methods for assessment of fugitive emissions from landfills. Available at https://erefdn.org/wp-content/uploads/2015/12/FugitiveEmissions_FinalReport.pdf

Etzkorn T., B. Klotz, S. Sørensen, I.V. Patroescu, I. Barnes, K.H. Becker, and U. Platt, 1999. "Gas-phase absorption cross sections of 24 monocyclic aromatic hydrocarbons in the UV and IR spectral ranges," Atmos. Environ. 33, 525-540, 1999.

European Commission, 2015, Best Available Techniques (BAT) Reference Document for the Refining of Mineral Oil and Gas: Joint Research Centre, Institute for Prospective Technological Studies, ISBN 978-92-79-46198-9 (PDF)ISSN 1831-9424 (online)doi:10.2791/010758, http://eippcb.jrc.ec.europa.eu/reference/BREF/REF_BREF_2015.pdf

Fally S., M. Carleer, and A. C. Vandaele, "UV Fourier transform absorption cross sections of benzene, toluene, meta-, ortho-, and para-xylene," J. Quant. Spectrosc. Radiat. Transfer 110, 766-782, 2009.

Galle, B., J. Samuelsson, B.H. Svensson, G. Börjesson, "Measurements of methane emissions from landfills using a time correlation tracer method based on FTIR absorption spectroscopy." Environ. Sci. Technol. 35: 21–25. 2001.

Griffith D.W.T., Synthetic calibration and quantitative analysis of gas-phase FT-IR spectra. Applied Spectroscopy, 1996. 50(1): p. 59-70.

Johansson, J., et al., 2013a, Quantitative Measurements and Modeling of Industrial Formaldehyde Emissions in the Greater Houston Area during Campaigns in 2009 and 2011, Journal of Geophysical Research – Atmospheres, 2013JD020159R.

Johansson, J., Mellqvist, J., et al., 2013b. Quantification of industrial emissions of VOCs, $NO_2$ and $SO_2$ by SOF and Mobile DOAS during DISCOVER-AQ, AQRP project 13-0051, AQRP report, Dec 7 2013.

Johansson, J. K. E., J. Mellqvist, J. Samuelsson, B. Offerle, B. Lefer, B. Rappenglück, J. Flynn, and G. Yarwood, 2014. Emission measurements of alkenes, alkanes, $SO_2$, and $NO_2$ from stationary sources in Southeast Texas over a 5 year period using SOF and mobile DOAS, Journal of Geophysical Research, 118, doi:10.1002/2013JD020485.

Kihlman, M., 2005a. Application of solar FTIR spectroscopy for quantifying gas emissions, Technical report No. 4L, ISSN 1652-9103, Department of Radio and Space Science, Chalmers University of Technology, Gothenburg, Sweden.

Kihlman, M., J. Mellqvist, and J. Samuelsson (2005b), Monitoring of VOC emissions from three refineries in Sweden and the Oil harbor of Göteborg using the Solar Occultation Flux method, Technical report, ISSN 1653 333X, Department of Radio and Space, Chalmers University of Technology, Gothenburg, Sweden.

Maul J., James & J. Ostrowski, Philip & A. Ublacker, Gregg & Linclau, Bruno & P. Curran, Dennis. (2008). Benzotrifluoride and Derivatives: Useful Solvents for Organic Synthesis and Fluorous Synthesis. 10.1007/3-540-48664-X_4.

Mellqvist, J., et al. (2013a), Pilot study to quantify industrial emissions of VOCs, $NO_2$ and $SO_2$ by SOF and mobile DOAS in the Bay Area, Fluxsense AB, 2013.

Mellqvist, J., et al. (2013b), Pilot study to quantify industrial emissions of VOCs, $NO_2$ and $SO_2$ by SOF and mobile DOAS in the Carson Area, Fluxsense AB, 2013.

Mellqvist, J. (1999), Application of infrared and UV-visible remote sensing techniques for studying the stratosphere and for estimating anthropogenic emissions, doktorsavhandling, Chalmers tekniska högskola, Göteborg, Sweden, 1999.

Mellqvist, J., Johansson J., Samuelsson J. And Offerle B. (2008a), Emission Measurements of Volatile Organic Compounds with the SOF method in Normandy 2008. available at www.fluxsense.se

Mellqvist, J., Johansson, J., Samuelsson, J., Rivera, C., Lefer, B. and S. Alvarez (2008b), Comparison of Solar Occultation Flux Measurements to the 2006 TCEQ Emission Inventory and Airborne Measurements for the TexAQS II, Project No. 582-5-64594-FY08-06, TCEQ report., Texas. (available at http://www.tceq.state.tx.us/assets/public/implementation/air/am/contracts/reports/da/20081108-comparison_solar_occultation_flux_measurements.pdf)

Mellqvist, J., et al. (2009), Emission Measurements of Volatile Organic Compounds with the SOF method in the Rotterdam Harbor 2008, available at www.fluxsense.se

Mellqvist, J., J. Samuelsson, J. K. E. Johansson, C. Rivera, B. Lefer, S. Alvarez, and J. Jolly (2010), Measurements of industrial emissions of alkenes in Texas using the solar occultation flux method, Journal of Geophysical Research: Atmospheres, 115(D7), doi:10.1029/2008JD011682.

Rinsland, C. P., R. Zander, and P. Demoulin (1991), Ground-based infrared measurements of $HNO_3$ total column abundances: long-term trend and variability. *J. Geophys. Res.*, *96*, 9379–9389.

Rivera, C., Mellqvist, J., Samuelsson, J., Lefer, B., Alvarez, S. & Patel, M. (2010) Quantification of NO2 and SO2 emissions from the Houston Ship Channel and Texas City industrial areas during the 2006 Texas Air Quality Study. Journal of Geophysical Research - Atmospheres 115. DOI: 10.1029/2009JD012675.

Rothman et al. (2003), HITRAN 2000, Journal of Quantitative Spectroscopy and Radiative Transfer, vol. 82, pp. 5-44.

Sharpe, S., et al. (2004), Gas-Phase Databases for Quantitative Infrared Spectroscopy, *Applied Optics*, 58(12).

# 9 APPENDIX I: Instrumentation and Methods

The FluxSense measurement vehicle or "mobile lab" is equipped with four optical instruments for gas monitoring which were used during the survey: SOF (Solar Occultation Flux), SkyDOAS (Differential Optical Absorption Spectroscopy), MeFTIR (Mobile extractive Fourier Transformed Infrared spectrometer) and MWDOAS (Mobile White cell DOAS). The individual measurement methods are described in the subsections below. SOF and SkyDOAS both measure gas columns through the atmosphere by means of light absorption. SOF utilizes infrared light from the direct sun whereas SkyDOAS measures scattered ultraviolet light from the sky. MeFTIR and MWDOAS both measure ground level concentrations (vehicle roof height, approx. 2 m) of alkanes and BTEX (benzene, toluene, ethylbenzene, and xylene) respectively. Accurate wind data is necessary in order to compute gas emission fluxes. Wind information for the survey was derived from several different sources. A wind LIDAR was used to measure vertical profiles of wind speed and wind direction from 10-300 m height. This was re-located for each measurement day and measurement area to a suitable site within the vicinity downwind (ideally with same elevation, no intervening terrain or geographic features) of the measured oil and gas production areas. However due to the large-scale nature of the measurements (for example, the perimeter of Elk Hills is over 60 km with hilly terrain) such requirements could not be met. The LIDAR data was compared with data from several wind masts from fixed met network- and mobile stations to extend the measurements to times when LIDAR was unavailable. This includes measurements begun before LIDAR setup each day and those after shutdown. Figure 63 gives a general overview of the data flow.

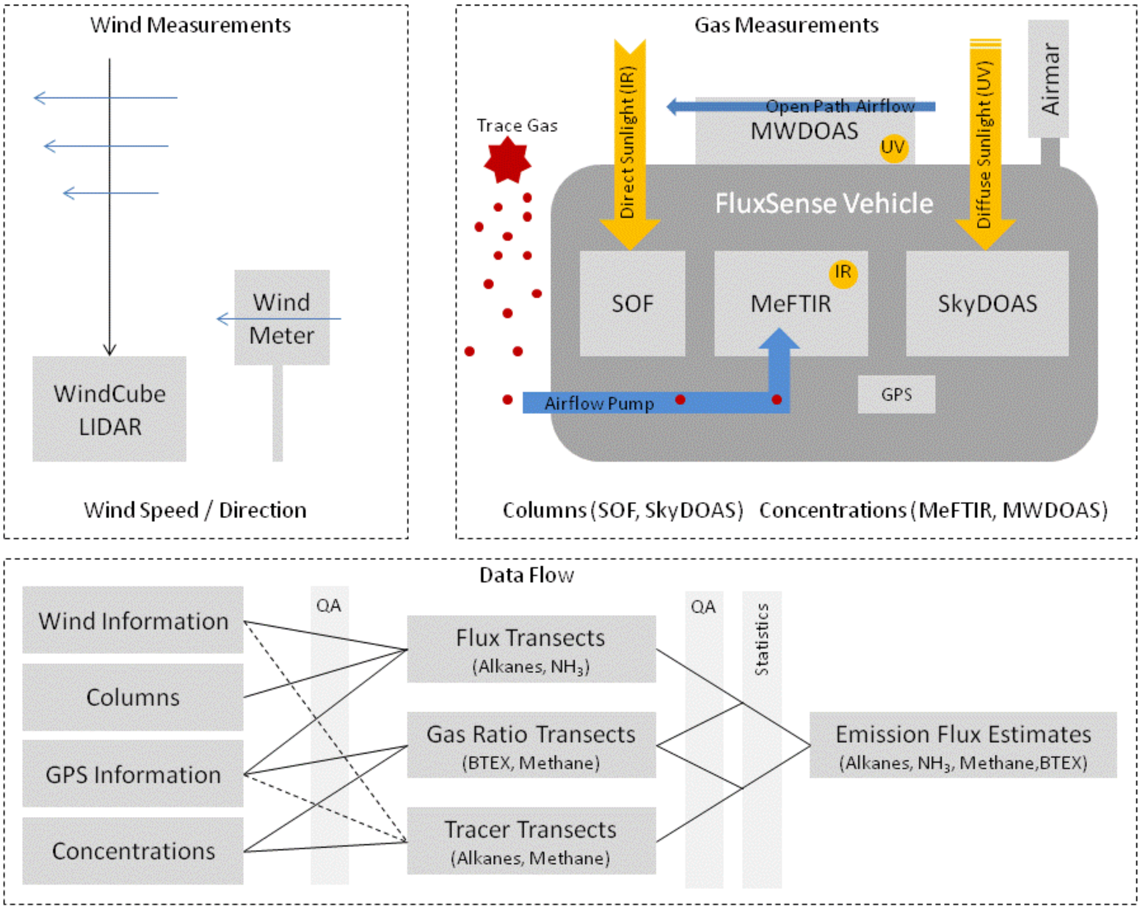

Figure 63 Overview of the FluxSense mobile lab main instruments; SOF, MeFTIR, MWDOAS and SkyDOAS (upper right panel) and wind measurements (upper left panel) and simplified data flow diagram (lower panel). SOF and SkyDOAS are column integrating passive techniques using the Sun as the light source while MeFTIR and SkyDOAS sample local air concentrations using active internal light sources. The data flow describes what information that goes into the flux emission estimates. Direct flux emissions are given from measured columns (SOF and SkyDOAS) of alkanes, $SO_2$ and $NO_2$, while indirectly measured emissions are calculated via gas concentration ratios (MeFTIR and MWDOAS) of BTEX and $CH_4$. All emission flux estimates are based on statistical analysis of measured data. Q.C. = Quality Control, S.A.= Statistical Analysis (see Appendix for details).

In order to derive final emission flux estimates, the GPS-tagged gas column measurements by SOF and SkyDOAS are combined with wind data and integrated across plume transects at the various source locations. Gas mass ratio measurements by MeFTIR and MWDOAS are then used to indirectly estimate the emissions also for methane and BTEX.

Figure 64 Internal and external view of the FluxSense mobile lab.

Table 38 Summary of FluxSense gas measurement techniques. *For typical wind conditions at an optimal distance from the source.

| **Method** | **SOF** | **Sky DOAS** | **MeFTIR** | **MWDOAS** |
|---|---|---|---|---|
| Compounds | **Alkanes**: ($C_nH_{2n+2}$)<br>**Alkenes:**$C_2H_4$, $C_3H_6$<br>**$NH_3$** | **$SO_2$**<br>**$NO_2$**<br>**$H_2CO$** | **$CH_4$**<br>**Alkanes:** ($C_nH_{2n+2}$)<br>**Alkenes:** $C_2H_4$, $C_3H_6$<br>**$NH_3$**<br>**$N_2O$** (tracer) | **BTEX** |
| Detection limit Column | 0.1-5 mg/m$^2$ | 0.1-5 mg/m$^2$ | 1-10 ppbv | 0.5-3 ppbv |
| Detection limit Flux* | 0.2-1 kg/h | 1 kg/h | 0.2-2 kg/h | 0.2-2 kg/h |
| Wind Speed Tolerance | 1.5-12 m/s | 1.5-12 m/s | | |
| Sampling Time Resolution | 1-5 s | 1-5 s | 5-15 s | 8-10 s |
| Measured Quantity [unit] | Integrated vertical column mass [mg/m$^2$] | Integrated vertical column mass [mg/m$^2$] | Mass concentration at Vehicle height [mg/m$^3$] | Concentration at Vehicle height [mg/m$^3$] |
| Derived Quantity [unit] | Mass Flux [kg/h] | Mass Flux [kg/h] | 1) Alkane and methane mass concentration ratio of ground plume combined with SOF gives mass flux [kg/h] and plume height information [m]<br>2) Alkane and $CH_4$ flux [kg/h] via tracer release | Combined with MeFTIR and SOF gives Mass Flux [kg/h] |
| Complementary data | Vehicle GPS-coordinates, Plume wind speed and direction | Vehicle GPS-coordinates, Plume wind speed and direction | Vehicle GPS-coordinates<br>Plume wind direction | Vehicle GPS-coordinates, Plume wind direction |
| | | | | |

## 9.1 The SOF method

The SOF method [Mellqvist 1999, 2008a, 2008b, 2009, 2010; Kihlman 2005a; Johansson 2014] is based on the recording of broadband infrared spectra of the sun with a Fourier transform infrared spectrometer (FTIR) that is connected to a solar tracker. The latter is a telescope that tracks the sun and reflects the light into the spectrometer independent of the orientation of the vehicle. Using multivariate optimization, it is possible from these solar spectra to retrieve the path-integrated concentrations (referred to as column concentrations), in the unit mg/m$^2$, of various species between the sun and the spectrometer. The system used in this project consists of a custom-built solar tracker, transfer optics and a Bruker IRCube FTIR spectrometer with a spectral resolution of 0.5 cm$^{-1}$, equipped with a dual InSb (Indium Antimonide) / MCT (Mercury Cadmium Telluride) detector. A reference spectrum is taken outside the plume so that atmospheric background concentrations are removed. This means that all measured SOF columns are analyzed relative to the background column concentrations. The system is installed in a measurement vehicle which allows consecutive column concentration measurements to be performed while driving. The flux of a species in a plume from an industry is measured by collecting spectra while driving the vehicle so that the light path from the sun to the instrument gradually cuts through the whole plume, preferably as orthogonally as possible to the wind direction.

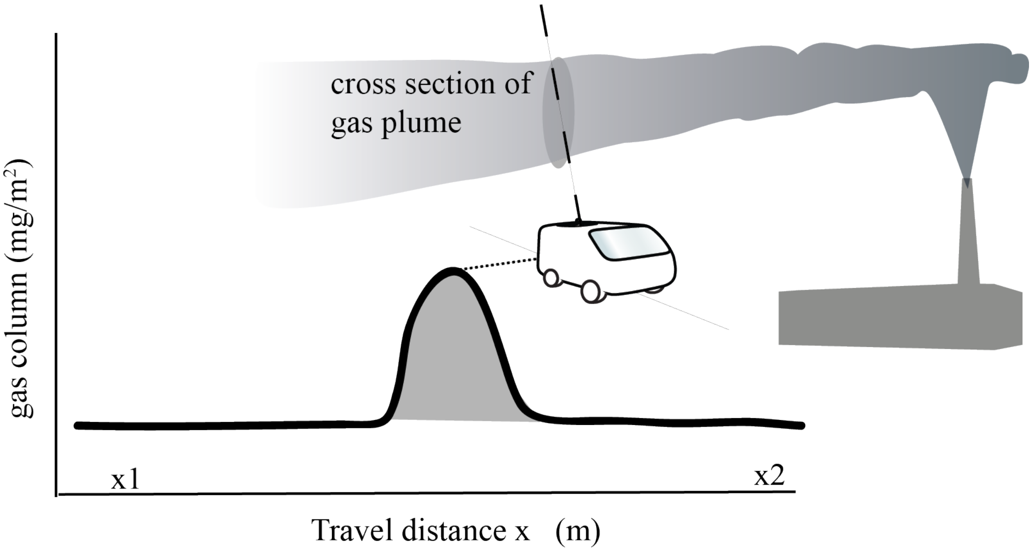

Figure 65 Schematic of the SOF measurement where the vehicle is driven across the prevailing wind so that the solar beam cuts through the emission plume while the sun is locked into the FTIR spectrometer by the solar tracking device on the roof. The VOC mass (or other compound of interest) is integrated through the plume cross section.

For each spectrum a column concentration of the species is retrieved using custom software (QESOF, i.e. *Quantitative evaluation of SOF*) [Kihlman 2005b]. These column concentrations, together with positions recorded with a GPS (Global Positioning System) receiver and the solar angle calculated from the time of the measurements, are used to calculate the area integrated column of the species in the intersection area between the plume and the light path. The flux of the species is then obtained by multiplying this area integrated concentration with the orthogonal wind speed vector component.

The IR spectra recorded by the SOF instrument are analyzed in QESOF by fitting a set of spectra from the HITRAN infrared database [Rothman 2003] and the PNNL (Pacific Northwest National Laboratory) database [Sharpe 2004] in a least-squares fitting procedure. Calibration data from the HITRAN database is used to simulate absorption spectra for atmospheric background compounds present in the atmosphere with high enough abundance to have detectable absorption peaks in the wavelength region used by SOF. Spectra, including water vapor, carbon dioxide and methane, are calibrated at the actual pressure and temperature and degraded to the instrumental resolution of the measurements. The same approach is applied for several retrieval codes for high resolution solar spectroscopy developed within Network for the Detection of Atmospheric Composition Change (NDACC) [Rinsland 1991; Griffith 1996] and QESOF has been tested against these with good agreement, better than 3%. For the retrievals, high resolution spectra of ethylene, propene, propane, n-butane and n-octane were obtained from the PNNL database and these are degraded to the spectral resolution of the instrument by convolution with the instrument line shape. The uncertainty in the absorption strength of the calibration spectra is about 3.5% for all five species.

In this project, the SOF method was used to measure VOCs in two different modes. Most VOCs with C-H-bonds absorb strongly in the 3.3-3.7 μm (2700-3005 $cm^{-1}$) spectral region. This region is mainly used for alkane measurements using a spectral resolution of 8 $cm^{-1}$. Alkenes (including ethylene and propylene) and ammonia are instead measured in the spectral region between 910 and 1000 $cm^{-1}$ using a spectral resolution of 0.5 $cm^{-1}$. In the alkane mode – the IR light absorption is essentially sensitive to the total alkane mass (number of alkane C-H bonds) present in the plume. The absorption structures (cross sections) for the various alkane compounds are rather similar, with the absorption strength scaling to the mass of the alkane species. Hence, the actual mix of alkanes in the plume does not affect the retrieved total alkane mass flux much, although only cross sections from a subset of all alkanes (propane, n-butane and octane) are fitted in the spectral analysis. Typically, the rare event of significant absorption from other species in the plume shows up as elevated residuals and is further investigated in the re-analysis. For the alkene mode the specificity of the measurements is good, since the absorption of different species is rather unique in this so called “fingerprint region” and absorption features are often sharp and well separable from each other at 0.5 $cm^{-1}$ resolution.

SOF is a proven technique employed by FluxSense in over 100 fugitive emission studies around the world. In Europe the SOF technique is considered one of the Best Available Technology [European Commission 2015] for measurements of fugitive emission of VOCs from refineries; and in Sweden it is used together with tracer correlation and optical gas imaging for annual screening of all larger refineries and petrochemical plants. The estimated uncertainty for the SOF emission measurements is typically 30 % for the total site emissions. This uncertainty has been calculated from several controlled release experiments (blind and non-blind) and side-by-side measurements with other measurement techniques.

## 9.2 Mobile SkyDOAS

The principle for Mobile SkyDOAS (Mobile Differential Optical Absorption Spectroscopy) measurements is very similar to that of SOF. Instead of measuring direct sun light in the infrared region, scattered light in the UV and visible region is measured in zenith angle with a telescope connected with an optical fiber to a Czerny-Turner spectrometer with a CCD camera. Column concentrations are retrieved from spectra in a similar way as with the SOF, although absorption is generally weaker. The system that was used for this project consists of a quartz telescope (20 mrad field of view, diameter 7.5 cm) connected with an optical fiber (liquid guide, diameter 3 mm) to a 303 mm focal length Czerny-Turner spectrometer with a 1024 by 255 pixels, thermoelectrically cooled CCD camera, see Figure 66

Figure 66 The mobile SkyDOAS system: Telescope, optical fibre, spectrometer and control computer.

The system was installed in the same measurement vehicle as the SOF system. Plumes were transected in the same way as with the SOF system and the retrieved column concentrations used to calculate fluxes exactly the same way, except that the SkyDOAS measurement direction is always zenith.

In this project, mobile SkyDOAS was used to measure $SO_2$, $NO_2$ and $H_2CO$. $NO_2$ is retrieved in the wavelength region between 324 and 350 nm and $SO_2$ in the region 310-325 nm. $H_2CO$ is measured in the region 322-350 nm. Apart from $SO_2$, $NO_2$ and $H_2CO$ the spectral analysis also includes other atmospheric compounds such as $O_3$ and $O_4$. The rare event of significant absorption from other species in the plume than those included in the spectral fit shows up as elevated residuals and is further investigated in the re-analysis. The absorption line parameters of the retrieved compounds are well established in published databases, stating an uncertainty of 4% (Vandaele *et al.* 1998) for the UV cross section of $NO_2$ and less than 2% for the $SO_2$ cross sections (Bogumil *et al.* 2003).

The DOAS technique was introduced in the 1970's (Platt *et al.* 1979) and has since then become an increasingly important tool in atmospheric research and monitoring both with artificial light sources and in passive mode utilizing the scattered solar light. In recent time the multi axis DOAS technique (scanning passive DOAS) has been applied in tropospheric research for instance measuring formaldehyde (Heckel *et al.* 2005; Pikelnaya *et al.* 2007).

Passive DOAS spectroscopy from mobile platforms has also been quite extensively applied in volcanic gas monitoring (Galle *et al.* 2003) for $SO_2$ flux measurements and for mapping of formaldehyde flux measurements in megacities (Johansson *et al.* 2009), . Mobile SkyDOAS has been used in several studies for measurements of industrial facilities i.e. $SO_2$, $NO_2$ and $H_2CO$ for several campaigns in Texas including $NO_2$ measurements at Longview in 2012 (Johansson *et al.* 2014a; Johansson & Mellqvist 2013). (Rivera 2009) did $SO_2$ measurements on a power plant in Spain for validation purposes. They also made measurements at an industrial conglomerate in Tula in Mexico (Rivera *et al.* 2009a) and measurements of $SO_2$, $NO_2$ and $H_2CO$ during the TexAQS 2006 campaign (Rivera *et al.* 2009b; Rivera *et al.* 2010). There are also groups in both China and Spain working with mobile mini-DOAS.

## 9.3 Mobile extractive FTIR (MeFTIR)

Mobile Extractive FTIR (MeFTIR) [Galle 2001, Börjesson 2009] in combination with tracers has been used to quantify VOC emissions from refinery and petrochemical sources in Europe and in the U.S. Alkanes and alkenes are typically measured, but also methane and other climate gases can be retrieved. MeFTIR is an optical technique capable of monitoring gas concentrations at ppb-sensitivity in mobile field operations. It is used both independently for concentration mapping and flux measurements, but often combined together with simultaneous SOF flux measurements to provide more detailed VOC speciation of plumes and for plume height assessments [Johansson et. al. 2013a]. The plume height can be estimated by dividing measured columns ($mg/m^2$) with ground concentrations ($mg/m^3$), assuming that the plume is evenly distributed up to the plume height (and zero above).

The MeFTIR system contains a mid-infrared spectrometer with medium resolution ($0.5\ cm^{-1}$). It utilizes an internal glow bar as an infrared radiation source, and by customized optics this light is transmitted through an optical multi-pass measurement cell with path-length of 68 meters. The system is mounted on a vibration dampening platform to allow for real time plume mapping from a mobile platform, Additionally, for ammonia measurements, the inlet and the cell are heated and insulated so that the sample air and cell temperature is above 40 ºC. Heating the sample is desirable since ammonia is a “sticky” gas, therefore heating the inlet and cell minimizes the risk of ammonia adhering to the tubing or cell surface and the residence time in the cell increasing. Temperature stability is also necessary to minimize instrumental drift. Internal cell temperature and pressure are sampled each second and logged every minute.

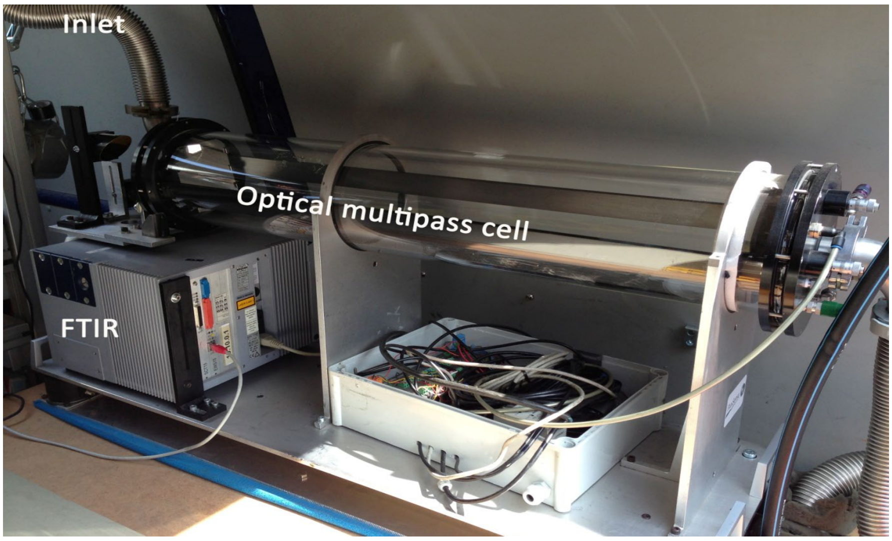

Figure 67 The MeFTIR instrumentation consisting of a Bruker FTIR spectrometer connected to an optical multi-pass cell.

The transmitted light is detected simultaneously with an InSb-detector in the 2.5–5.5 µm (1800–4000 cm$^{-1}$) region and an MCT detector in the 8.3–14.3 µm (700–1200 cm$^{-1}$) region. Temperature and pressure in the cell are averaged over the duration of each measurement. Atmospheric air is continuously pumped at high flow rate through the optical cell from the outside, taking in plume air from the roof of the vehicle (2.5 m height) through a Teflon tube. A high flow pump (> 120 lpm, Vacuubrand ME 8 NT) is used to ensure that the gas volume in the cell (16 l) has a flushing time of less than 8 seconds. Spectra are typically recorded with an integration time of 8-12 seconds. A GPS-receiver is used to register the position of the vehicle every second.

The concentration in the spectra is analyzed in real time by fitting a set of calibrated spectra from the HITRAN infrared database [Rothman 2003] and the PNNL database [Sharpe 2004] in a least-squares fitting procedure. Compounds being analyzed include ethylene, propylene, total alkane mass (based on fitting cross sections of ethane, propane, n-butane, i-pentane, n-octane), water, methane, CO, $CO_2$ and $N_2O$. The analysis routines are very similar to the ones for SOF, but less complex because strong absorption by atmospheric trace gases (water, methane, $CO_2$) has less consequence at the shorter path length in the MeFTIR measurement cell.

The MeFTIR tracer approach has been tested in a so-called gas release "blind test" together with other techniques in U.S. [EREF 2011]. In that test, methane was released from an area-distributed source in four different configurations and flow rates ranging from 1.1-3.3 g/s. At a downwind distance of 400 meters MeFTIR retrieved the fluxes within 6% in 3 cases and 19% in the fourth. This is consistent with other validation experiments, showing a flux estimate accuracy of better than 20%. Concentration measurement by FTIR is a widely used procedure, and the main uncertainties are associated with the absorption cross sections (typically < 3.5%) and spectral retrieval, with an aggregate uncertainty better than 10% in the analysis.

Concentrations are monitored in real time in order to detect emission plumes and to judge whether any interfering sources are being sampled. Unwanted signals from local traffic exhaust or from the measurement vehicle itself could be filtered out by looking at exhaust compound signatures like carbon monoxide concentrations. A stationary source is, on the contrary to any local traffic plumes, characterized by recurrent downwind plumes. Transient and non-repeatable observations are therefore excluded from the results. Furthermore, measurements of ambient concentrations of methane and carbon dioxide (with known atmospheric concentrations) are used for consistency check.

## 9.4 Mobile White Cell DOAS (MW-DOAS)

The ground level mass concentration of benzene, toluene, ethylbenzene, m- and p-xylene (BTEX) was measured using a mobile real-time system: Mobile White cell DOAS (MWDOAS). The MWDOAS system consists of an open, 2.5 m long optical White cell that is mounted on the roof of the measurement vehicle (see). By multiple reflections in the White cell mirror system an overall path length of 210 m is obtained, resulting in low detection limits (ppb). The light from the internal lamp is transmitted through the White cell and then analyzed in a DOAS spectrometer, using the UV wavelength region 255 - 285 nm.

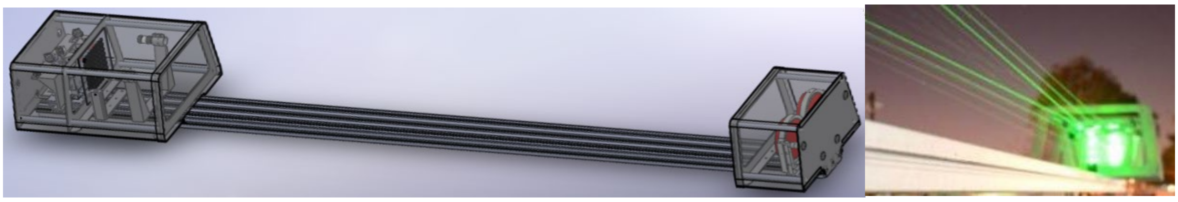

Figure 68 The open path MWDOAS cell having an overall optical path-length of 210 m.

A measurement begins by acquiring a reference spectrum outside the plume, usually upwind of the facility. Spectra are then sampled and averaged continuously while driving through emission plumes. The averaging time is set to around 8 seconds in order to achieve acceptable SNR (see below). This is the lower limit of the temporal sampling between independent measurements, but the spatial sampling is also dependent by the vehicle’s velocity. A typical driving speed for MWDOAS measurements is 10-20 km/h for sufficient plume sampling. The spectra are geo-tagged and evaluated online using the standard DOAS technique, giving information of plume locations and constituents.

The MWDOAS data is later post evaluated and merged with the corresponding MeFTIR data to produce a plume specific BTEX/Alkane mass ratio. The mass ratio of BTEX/Alkanes is then used to calculate the aromatic flux from individual sub areas where alkane fluxes have been measured by SOF, assuming they have the same source. Specific area plumes are ideally probed at several times, and an overall average of all plume transect BTEX/Alkane ratios is then made. The method requires in situ access to the plume of the studied source, and as instrumentation typically are mounted on a truck, highly elevated sources with a strong plume lift like hot flares, chimneys and high process towers will not be possible to survey at close distance.

Table 39 The UV-cross-sections used in the evaluation of the MWDOAS spectra.

| **Chemical compound** | **Origin of reference spectrum** |
|---|---|
| **$O_3$** | [Burrows 1999] |
| **$SO_2$** | [Bogumil 2003] |
| **$O_2$** | [Bogumil 2003] |
| **Toluene** | [Fally 2009] |
| **Benzene** | [Etzkorn 1999] |
| **1,3,5-Trimethylbenzene** | [Etzkorn 1999] |
| **1,2,4-Trimethylbenzene** | [Etzkorn 1999] |
| **Styrene** | [Etzkorn 1999] |
| **Phenol** | [Etzkorn 1999] |
| **p-Xylene** | [Etzkorn 1999] |
| **m-Xylene** | [Etzkorn 1999] |
| **Ethylbenzene** | [Etzkorn 1999] |

The MWDOAS technique has been validated in various surveys by comparison with canister samples acquired at several different locations and which were subsequently analyzed by gas chromatography (GC-FID). The validation shows that the result from MWDOAS lies well within 10% of the result of the certified canister results for BTEX. Due to an absorption cross-section too weak to be used with reliability in the MWDOAS analysis, the ortho isomer of the xylene has been omitted in this comparison. When total xylene is presented in the present survey, the sum of m- and p-xylenes from the MWDOAS measurement is multiplied by 1.32. This number comes from a ratio comparison of xylene isomers in 49 canister samples analyzed by GC/FID and taken from eight refineries and tank parks from two countries. The standard deviation in this comparison was 0.07 and adds a 4.5% uncertainty to the total xylene concentration. Hence, the xylene concentration from MWDOAS is defined as the sum of the measured m- and p-isomers and the inferred o-isomer.

The MWDOAS system has been used in previous campaigns in USA during 2013 with good results. During the 2013 DISCOVER-AQ campaign [Johansson, 2013b] in Houston, Texas, the system was run in parallel to a mobile Proton Transfer Mass spectrometer (PtrMS) lab as a validation check. The results of benzene, toluene and styrene was compared and showed good agreement, with the PtrMS showing slightly elevated benzene concentrations compared to the MWDOAS. The sensitivity of MWDOAS is better than 1 ppb for benzene, better than 3 ppb for toluene, ethylbenzene and m-xylene and 0.5 ppb for p-xylene.

Since the distribution of the BTEX constituents varies with source we will also present the benzene to alkane ratio to facilitate the calculation of benzene flux and identify specific benzene sources.

Unwanted BTEX signals from local traffic exhausts are generally only significant in congestions (at traffic lights etc.) or in confined spaces, e.g. tunnels. Apart from this, large emitters are also occasionally seen elsewhere. They are generally recognized, partly by their typical gasoline composition signature and partly by their transient nature. A stationary BTEX source is, on the other hand, characterized by recurrent downwind plumes. Transient and non-repeatable BTEX observations are therefore excluded from the result. Note that all concentrations are enhancements above the reference/background.

## 9.5 Wind Measurements and Auxiliary Data

### *Wind LIDAR*

A wind LIDAR (LIght Detection and Ranging, Zephyr ZX-300) was used to measure vertical wind profiles of wind speed and direction in 2019. For the wind measurements in 2018 a Leosphere WindCubeV2 was used. The LIDAR provided wind profiles in the vertical range of 10 m to up to 300 m above ground and the measurements are integrated with a sonic anemometer at around 2 m height to provide coverage down to ground level. The system records 1-s data, and 5-minute averages were used for flux calculations in this study. The principle of detection is based on the Doppler shift of the infrared pulse that the instrument sends out and retrieves.

Figure 69 Wind measurements with portable wind LIDAR (10 - 300 m) mounted in pickup. The instrument is integrated with a sonic anemometer at around 2 m height.

### *Airmar (Mobile Weather Station)*

A sonic wind meter (Airmar WeatherStation 200 WX) was installed on the roof of the measurement vehicle to complement the other wind measurements and give local ground winds at the vehicle. The wind information from the car-based Airmar was not used for flux calculation since the wind field at street level can be heavily disturbed and turbulent. The Airmar was only used as a real-time aid to keep track of the plume directions when making the gas emission measurements. The Airmar provides wind speed and direction relative to true north (compensating for vehicle position), as well as air temperature, pressure and relative humidity. It also provides GPS positions that may be used as a backup for the other GPS-antenna.

### ***GPS***

The FluxSense vehicle is equipped with two standard USB GPS-L1 receivers (GlobalSat BU-353S4) hooked up to the SOF and MWDOAS-computers. They are placed horizontally on the roof and by the windscreen for optimal reception. The receivers give the position at a rate of 1 Hz.

# 10 APPENDIX II Measurement Methodology

## 10.1 Principal Equations

This report includes three different techniques to measure emission mass fluxes as specified below. The primary method in this project is the direct flux measurements of alkanes from SOF. In the secondary method BTEX and methane fluxes are measured indirectly from MWDOAS/MeFTIR gas mass ratios.

### *10.1.1 DIRECT FLUX MEASUREMENTS:*

The emission mass flux (*Q*) of species (*j*) measured by SOF for a single transect (*T*) across the plume (*P*) along path (*l*) can be expressed by the following integral (units in gray brackets):

$$Q_T^j[\mathrm{g/s}] = \bar{v}_T[\mathrm{m/s}] \cdot \int_P C_l^j[\mathrm{mg/m^2}] \cdot \cos(\theta_l) \cdot \sin(\alpha_l)\ dl\ [\mathrm{m}]$$

Where,

$\bar{v}_T$ = the average wind speed at plume height for the transect,

$C_l^j$ = the measured slant column densities for the species $j$ as measured by SOF or SkyDOAS,

$\theta_l$ = the angles of the light path from zenith ($\cos(\theta_l)$ gives vertical columns),

$\alpha_l$ = the angles between the wind directions and driving directions

$dl$ = the driving distance across the plume

Note that SOF and SkyDOAS have different light paths, where the SkyDOAS telescope is always looking in the zenith direction while the SOF solar tracker is pointing toward the Sun. Hence, the measured SOF slant column densities will vary with latitude, season and time of day.

To isolate emissions from a specific source, the incoming/upwind background flux must be either insignificant or subtracted. If the source is encircled or "boxed", the integral along *l* is a closed loop and the flux calculations are done with sign. This is taken care of by the FluxSense software.

### *10.1.2 INDIRECT FLUX MEASUREMENTS:*

The indirectly measured flux (indirectly measured emission, IME) is computed using a combination of SOF and MeFTIR/MWDOAS measurements. The inferred mass flux ($\hat{Q}^i$) for species (*i*) are calculated from MeFTIR and/or MWDOAS ground level gas ratios integrated over the plume (*P*) along path (*l*) are given by (Si-units in gray brackets):

$$\hat{Q}^i[\mathrm{g/s}] = \bar{Q}^j[\mathrm{g/s}] \cdot \frac{1}{k}\sum_k \frac{\int_P N_l^i[\mathrm{mg/m^3}]\ dl[\mathrm{m}]}{\int_P N_l^j[\mathrm{mg/m^3}]\ dl[\mathrm{m}]}$$

Where,

$\bar{Q}^j$ = the average flux of species $j$ from multiple transects as measured by SOF,
$N_l^i$ = the number density concentrations of species $i$ as measured by MWDOAS or MeFTIR,
$N_l^j$ = the number density concentrations of species $j$ as measured by MeFTIR,
$k$ = the number of gas ratio measurements

Note that the IME operates on average values since simultaneous SOF, MWDOAS and MeFTIR measurements are generally not performed and because individual gas ratios are more uncertain than the average. Although not necessarily simultaneously measured, SOF and MeFTIR/MWDOAS measurements must represent the same source plumes. Note also that gas ratios do not intrinsically depend on complete plume transects (like for direct flux methods) as long as the emission plume is well mixed at the sampling distance. Additionally, it is not necessary that the source of the tracer and measured gas be identical, merely that they are co-located at the measurement distance and uniform in time.

### *10.1.3 TRACER GAS FLUX MEASUREMENTS:*

The third method to conduct flux measurements is by tracer correlations using only MeFTIR measurements or simultaneous MeFTIR and MWDOAS measurement and a known tracer gas release. Note that this method was not applied during the first campaign in October 2018, although it will be used on later studies. These fluxes are given for each transect (*T*) by the following equation (Si-units in gray brackets):

$$Q_T^j[\mathrm{g/s}] = Q^{tracer}[\mathrm{g/s}]\frac{\int_P N_l^j[\mathrm{mg/m^3}]\,dl[\mathrm{m}]}{\int_P N_l^{tracer}[\mathrm{mg/m^3}]\,dl[\mathrm{m}]}$$

Where,

$Q^{tracer}$ = the release mass flux of the tracer gas from bottle,
$N_l^{tracer}$ = the number density concentrations of the tracer as measured by MeFTIR,
$N_l^j$ = the number density concentrations of species $j$ from MeFTIR or MWDOAS,

Note that tracer gas correlation fluxes do not intrinsically depend on complete plume transects (like for direct flux methods) as long as the emission plume and the tracer gas is well mixed at the sampling distance. Complete plume transects are, however, recommended since the tracer gas release point might not completely match at the sampling distance

## 10.2 Uncertainties and Error Budget

A summary of the typical performance of the FluxSense measurements is presented in Table 40

In addition, for each site the statistical error is calculated. It corresponds to the random error but in addition there could be systematic errors. For instance, in the used wind speed due to the errors in estimated height of the plume and spectral calibration errors. The statistical error is given by the 95 % Confidence Interval (CI) for the mean, $\bar{x}$, according to:

$$CI = \bar{x} \pm t_{.025} \frac{s}{\sqrt{N}}$$

Here t is Student’s T distribution and s corresponds to sample standard deviation:

$$s_x = \sqrt{\frac{\sum_{i=1}^{N} (x - \bar{x})^2}{N - 1}}$$

Table 40 Performance of FluxSense measurement methods.

| Measurement Parameter | Analysis Method | Accuracy | Precision |
|---|---|---|---|
| SOF column concentrations alkanes, alkenes, $NH_3$ | QESOF spectral retrieval | ±10% | ±5% |
| SkyDOAS column concentrations $NO_2$, $SO_2$, $H_2CO$ | DOAS spectral retrieval | ±10% | ±5% |
| MeFTIR concentrations $CH_4$, VOC, $NH_3$, $N_2O$ | QESOF spectral retrieval | ±10% | ±5% |
| MWDOAS concentrations BTEX, Benzene | MWDOAS spectral retrieval | ±10% | ±5% |
| Wind Speed (10 m) | R.M. Young Wind monitor | ±0.3 m/s or 1% | ±0.3 m/s |
| Wind Direction (10 m) | R.M. Young Wind monitor | ±5° | ±3° |
| LIDAR Wind Speed (10-300 m) | Zephyr Zx-3000 Wind LIDAR | ±0.1 m/s | - |
| GPS position | USB GPS receiver | ±2m | ±2m |
| SOF mass flux Alkanes, alkenes, $NH_3$ | SOF-Report flux calculations | 30%-40% 95 CI | ±10%-30% |
| SkyDOAS mass flux $NO_2$, $SO_2$, $H_2CO$ | SkyDOAS flux calculations | ±30% | ±10% |